Tue. May 28, 2019

[E] Poster | P (Space and Planetary Sciences)：P-PS Planetary Sciences

3:30 PM - 5:00 PM JST | 6:30 AM - 8:00 AM UTC | Poster Hall International Exhibition Hall8, Makuhari Messe_1

[P-PS01] Outer Solar System Exploration Today, and Tomorrow

convener:Jun Kimura(Osaka University), Yasumasa Kasaba(Planetary Plasma and Atmospheric Research Center, Tohoku University), Kunio M. Sayanagi(Hampton University)

[PPS01-P01] Critical Role of Entry Probes in Giant Planet Exploration

*Sushil K Atreya[1], Olivier Mousis[2] (1.University of Michigan Ann Arbor, 2.Laboratoire d'Astrophysique de Marseille)

[PPS01-P02] OKEANOS – Jupiter Trojan Asteroid Rendezvous and Landing Experiments Using a Solar Power Sail

*Tatsuaki Okada[1,2], Takahiro Iwata[1], Yoko Kebukawa[3], Motoo Ito[4], Jun Aoki[5], Yosuke Kawai[5], Shoichiro Yokota[5], Yoshifumi Saito[1], Kentaro Terada[5], Michisato Toyoda[5], Hikaru Yabuta[6], Hisayoshi Yurimoto[1,7], Shuji Matsuura[8], Kohji Tsumura[9], Daisuke Yonetoku[10], Tatehiro Mihara[11], Ayako Matsuoka[1], Reiko Nomura[12], Hajime Yano[1], Takayuki Hirai[13], Atsushi Kumamoto[9], Ryosuke Nakamura[14], Stephan Ulamec[15], Ralf Jaumann[15], Jean-Pierre Bibring[16], Noel Grand[17], Cyril Szopa[18], Ernesto Palomba[19], Jorn Helbert[15], Alain Herique[20], Matthias Grott[15], Hans-Ulrich Auster[21], Goester Klingelhoefer[22], Fumi Yoshida[13], Makoto Yoshikawa[1], Jun Matsumoto[1], Toshihiro Chujo[1], Masanori Matsushita[1], Takanao Saiki[1], Hideki Kato[1], Osamu Mori[1], Junichiro Kawaguchi[1] (1.Japan Aerospace Exploration Agency, 2.University of Tokyo, 3.Yokohama National University, 4.Japan Agency for Marine-Earth Science and Technology, 5.Osaka University, 6.Hiroshima University, 7.Hokkaido University, 8.Kwansei Gakuin University, 9.Tohoku University, 10.Kanazawa University, 11.RIKEN, 12.National Astronomical Observatory of Japan, 13.Chiba Institute of Technology, 14.National Institute of Advanced Industrial Science and Technology, 15.German Aerospace Center, 16.Institut d'Astrophysique Spatiale, 17.LISA, 18.LATMOS, 19.INAF-IAPS, 20.IPAG, 21.TU Braunschweig, 22.Leibniz Universität Hannover)

[PPS01-P03] Magnetic field model of Jovian magnetosphere

*Naoya Momoki[1], Hiroaki TOH[1] (1.Division of Earth and Planetary Sciences, Graduate School of Science, Kyoto University)

[PPS01-P04] Enhancement of the Jovian thermospheric temperature above the Great Red Spot based on the infrared spectroscopic data obtained with IRTF/iSHELL

*Ayumu Kambara[1], Hajime Kita[2], Takeshi Sakanoi[1], Yasumasa Kasaba[1], Masato Kagitani[1], Haruna Watanabe[1] (1.Planetary Plasma and Atmospheric Research Center, Graduate School of Science, Tohoku University, 2.Institute of Space and Astronautical Science, Japan Aerospace Exploration Agency)

[PPS01-P05] Pulsation-like variation of Jovian infrared polar emission observed by Subaru 8-m: H3+ and methane emissions

*Yasumasa Kasaba[1], Haruna Watanabe[1], Hajime Kita[2], Chihiro Tao[3], Takeshi Sakanoi[1], Masato Kagitani[1], Orton Glenn[1,4], James Sinclair[4] (1.Planetary Plasma and Atmospheric Research Center, 2.ISAS/JAXA, 3.NICT, 4.NASA/JPL)

[PPS01-P06] Structure of Io plasma torus observed with the Tohoku 60-cm telescope

*Masato Kagitani[1], Fuminori Tsuchiya[1], Kazuo Yoshioka[2], Go Murakami[3], Tomoki Kimura[1], Ryoichi Koga[1], Reina Hikida[4], Takeshi Sakanoi[1] (1.Graduate School of Science, Tohoku University, 2.Graduate School of frontier Science, The University of Tokyo, 3.Institute of Space and Astronautical Science, Japan Aerospace Exploration Agency, 4.Department of Earth and Planetary Science, Graduate School of Science, Tokyo University)

[PPS01-P07] Ion Scale Height Variability in Hisaki Io Torus Observations

*Nicholas McCord Schneider[1], Carl Schmidt[2], Masato Kagitani[3], Yasumasa Kasaba[3], Tomoki Kimura[3], Go Murakami[4], Fuminori Tsuchiya[3], Hajime Kita[3], Reina Hikida[5], Ichiro Yoshikawa[5], Kazuo Yoshioka[5] (1.LASP, University of Colorado Boulder, 2.Boston University, 3.Tohoku University, 4.ISAS/JAXA, 5.University of Tokyo)

[PPS01-P08] Size of the Smallest Particles in Saturn's Rings

*Keiji Ohtsuki[1], Hiroshi Kawamura[1], Naoyuki Hirata[1], Hiroshi Daisaka[2], Hiroshi Kimura[3] (1.Graduate School of Science, Kobe University, 2.Graduate School of Commerce and Management, Hitotsubashi University, 3.Planetary Exploration Research Center, Chiba Institute of Technology)

[PPS01-P09] The Radio & Plasma Wave Investigation (RPWI) for JUICE for the investigation of Jupiter and Icy Moons System: Contributions from Japan

*Yasumasa Kasaba[1], Hiroaki Misawa[1], Fuminori Tsuchiya[1], Atsushi Kumamoto[2], Yuto Katoh[2], Tomoki Kimura[2], Hajime Kita[3], J.-E. Wahlund[4] (1.Planetary Plasma and Atmospheric Research Center, Tohoku University, 2.Department of Geophysics, Tohoku University, 3.ISAS/JAXA, 4.IRF Uppsala, Sweden)

[PPS01-P10] Magnetic field experiment at Jupiter icy moons (JUICE J-MAG) and in-flight alignment calibration

*Ayako Matsuoka[1], Michele Karen Dougherty[2], Patrick Brown[2], Futoshi Takahashi[3], Hisayoshi Shimizu[4], Masaki Matsushima[5] (1.Research Division for Space Plasma, Institute of Space and Astronautical Science, Japan Aerospace Exploration Agency, 2.Imperial College London, 3.Kyushu University, 4.University of Tokyo, 5.Tokyo Institute of Technology)

[PPS01-P11] Science targets of the GAnymede Laser Altimeter (GALA) for the JUICE mission

*Jun Kimura[1], Shunichi Kamata[2], Koji Matsumoto[3], Noriyuki Namiki[3], Keigo Enya[4], Masanori Kobayashi[5], Hiroshi Araki[3], Hirotomo Noda[3], Ko Ishibashi[5], Hauke Hussmann[6], Kay Lingenauber[6] (1.Osaka University, 2.Hokkaido University, 3.National Astronomical Observatory Japan, 4.ISAS/JAXA, 5.Chiba Institute of Technology, 6.German Aerospace Center (DLR), Berlin)

[PPS01-P12] Current status of the antenna developments, the data processing, scientific target for JUICE/SWI JAPAN.

*YASUKO KASAI[1], JUICE SWI Japanese Team (1.National Institute of Information and Communications Technology (NICT))

[E] Poster | P (Space and Planetary Sciences)：P-PS Planetary Sciences

5:15 PM - 6:30 PM JST | 8:15 AM - 9:30 AM UTC | Poster Hall International Exhibition Hall8, Makuhari Messe_1

[P-PS01] Outer Solar System Exploration Today, and Tomorrow

convener:Jun Kimura(Osaka University), Yasumasa Kasaba(Planetary Plasma and Atmospheric Research Center, Tohoku University), Kunio M. Sayanagi(Hampton University)

[PPS01-P01] Critical Role of Entry Probes in Giant Planet Exploration

*Sushil K Atreya[1], Olivier Mousis[2] (1.University of Michigan Ann Arbor, 2.Laboratoire d'Astrophysique de Marseille)

[PPS01-P02] OKEANOS – Jupiter Trojan Asteroid Rendezvous and Landing Experiments Using a Solar Power Sail

*Tatsuaki Okada[1,2], Takahiro Iwata[1], Yoko Kebukawa[3], Motoo Ito[4], Jun Aoki[5], Yosuke Kawai[5], Shoichiro Yokota[5], Yoshifumi Saito[1], Kentaro Terada[5], Michisato Toyoda[5], Hikaru Yabuta[6], Hisayoshi Yurimoto[1,7], Shuji Matsuura[8], Kohji Tsumura[9], Daisuke Yonetoku[10], Tatehiro Mihara[11], Ayako Matsuoka[1], Reiko Nomura[12], Hajime Yano[1], Takayuki Hirai[13], Atsushi Kumamoto[9], Ryosuke Nakamura[14], Stephan Ulamec[15], Ralf Jaumann[15], Jean-Pierre Bibring[16], Noel Grand[17], Cyril Szopa[18], Ernesto Palomba[19], Jorn Helbert[15], Alain Herique[20], Matthias Grott[15], Hans-Ulrich Auster[21], Goester Klingelhoefer[22], Fumi Yoshida[13], Makoto Yoshikawa[1], Jun Matsumoto[1], Toshihiro Chujo[1], Masanori Matsushita[1], Takanao Saiki[1], Hideki Kato[1], Osamu Mori[1], Junichiro Kawaguchi[1] (1.Japan Aerospace Exploration Agency, 2.University of Tokyo, 3.Yokohama National University, 4.Japan Agency for Marine-Earth Science and Technology, 5.Osaka University, 6.Hiroshima University, 7.Hokkaido University, 8.Kwansei Gakuin University, 9.Tohoku University, 10.Kanazawa University, 11.RIKEN, 12.National Astronomical Observatory of Japan, 13.Chiba Institute of Technology, 14.National Institute of Advanced Industrial Science and Technology, 15.German Aerospace Center, 16.Institut d'Astrophysique Spatiale, 17.LISA, 18.LATMOS, 19.INAF-IAPS, 20.IPAG, 21.TU Braunschweig, 22.Leibniz Universität Hannover)

[PPS01-P03] Magnetic field model of Jovian magnetosphere

*Naoya Momoki[1], Hiroaki TOH[1] (1.Division of Earth and Planetary Sciences, Graduate School of Science, Kyoto University)

[PPS01-P04] Enhancement of the Jovian thermospheric temperature above the Great Red Spot based on the infrared spectroscopic data obtained with IRTF/iSHELL

*Ayumu Kambara[1], Hajime Kita[2], Takeshi Sakanoi[1], Yasumasa Kasaba[1], Masato Kagitani[1], Haruna Watanabe[1] (1.Planetary Plasma and Atmospheric Research Center, Graduate School of Science, Tohoku University, 2.Institute of Space and Astronautical Science, Japan Aerospace Exploration Agency)

[PPS01-P05] Pulsation-like variation of Jovian infrared polar emission observed by Subaru 8-m: H3+ and methane emissions

*Yasumasa Kasaba[1], Haruna Watanabe[1], Hajime Kita[2], Chihiro Tao[3], Takeshi Sakanoi[1], Masato Kagitani[1], Orton Glenn[1,4], James Sinclair[4] (1.Planetary Plasma and Atmospheric Research Center, 2.ISAS/JAXA, 3.NICT, 4.NASA/JPL)

[PPS01-P06] Structure of Io plasma torus observed with the Tohoku 60-cm telescope

*Masato Kagitani[1], Fuminori Tsuchiya[1], Kazuo Yoshioka[2], Go Murakami[3], Tomoki Kimura[1], Ryoichi Koga[1], Reina Hikida[4], Takeshi Sakanoi[1] (1.Graduate School of Science, Tohoku University, 2.Graduate School of frontier Science, The University of Tokyo, 3.Institute of Space and Astronautical Science, Japan Aerospace Exploration Agency, 4.Department of Earth and Planetary Science, Graduate School of Science, Tokyo University)

[PPS01-P07] Ion Scale Height Variability in Hisaki Io Torus Observations

*Nicholas McCord Schneider[1], Carl Schmidt[2], Masato Kagitani[3], Yasumasa Kasaba[3], Tomoki Kimura[3], Go Murakami[4], Fuminori Tsuchiya[3], Hajime Kita[3], Reina Hikida[5], Ichiro Yoshikawa[5], Kazuo Yoshioka[5] (1.LASP, University of Colorado Boulder, 2.Boston University, 3.Tohoku University, 4.ISAS/JAXA, 5.University of Tokyo)

[PPS01-P08] Size of the Smallest Particles in Saturn's Rings

*Keiji Ohtsuki[1], Hiroshi Kawamura[1], Naoyuki Hirata[1], Hiroshi Daisaka[2], Hiroshi Kimura[3] (1.Graduate School of Science, Kobe University, 2.Graduate School of Commerce and Management, Hitotsubashi University, 3.Planetary Exploration Research Center, Chiba Institute of Technology)

[PPS01-P09] The Radio & Plasma Wave Investigation (RPWI) for JUICE for the investigation of Jupiter and Icy Moons System: Contributions from Japan

*Yasumasa Kasaba[1], Hiroaki Misawa[1], Fuminori Tsuchiya[1], Atsushi Kumamoto[2], Yuto Katoh[2], Tomoki Kimura[2], Hajime Kita[3], J.-E. Wahlund[4] (1.Planetary Plasma and Atmospheric Research Center, Tohoku University, 2.Department of Geophysics, Tohoku University, 3.ISAS/JAXA, 4.IRF Uppsala, Sweden)

[PPS01-P10] Magnetic field experiment at Jupiter icy moons (JUICE J-MAG) and in-flight alignment calibration

*Ayako Matsuoka[1], Michele Karen Dougherty[2], Patrick Brown[2], Futoshi Takahashi[3], Hisayoshi Shimizu[4], Masaki Matsushima[5] (1.Research Division for Space Plasma, Institute of Space and Astronautical Science, Japan Aerospace Exploration Agency, 2.Imperial College London, 3.Kyushu University, 4.University of Tokyo, 5.Tokyo Institute of Technology)

[PPS01-P11] Science targets of the GAnymede Laser Altimeter (GALA) for the JUICE mission

*Jun Kimura[1], Shunichi Kamata[2], Koji Matsumoto[3], Noriyuki Namiki[3], Keigo Enya[4], Masanori Kobayashi[5], Hiroshi Araki[3], Hirotomo Noda[3], Ko Ishibashi[5], Hauke Hussmann[6], Kay Lingenauber[6] (1.Osaka University, 2.Hokkaido University, 3.National Astronomical Observatory Japan, 4.ISAS/JAXA, 5.Chiba Institute of Technology, 6.German Aerospace Center (DLR), Berlin)

[PPS01-P12] Current status of the antenna developments, the data processing, scientific target for JUICE/SWI JAPAN.

*YASUKO KASAI[1], JUICE SWI Japanese Team (1.National Institute of Information and Communications Technology (NICT))

[E] Poster | P (Space and Planetary Sciences)：P-EM Solar-Terrestrial Sciences, Space Electromagnetism & Space Environment

3:30 PM - 5:00 PM JST | 6:30 AM - 8:00 AM UTC | Poster Hall International Exhibition Hall8, Makuhari Messe_3

[P-EM12] Space Weather and Space Climate

convener:Ryuho Kataoka(National Institute of Polar Research), Antti A Pulkkinen(NASA Goddard Space Flight Center), Kanya Kusano(Institute for Space-Earth Environmental Research, Nagoya University), Kaori Sakaguchi(National Institute of Information and Communications Technology)

[PEM12-P01] Reconnection signatures in solar magnetograms during the solar storms of 4-10 September 2017

*Robert Dean Loper[1,2] (1.Air Force Institute of Technology, Department of Engineering Physics, 2.National Center for Atmospheric Research, High Altitude Observatory)

[PEM12-P02] Statistical Relation between Solar Flares and Coronal Mass Ejections with Respect to Sigmoidal Structures in Active Regions

*Yusuke Kawabata[1,2], Yusuke Iida[3], Takafumi Doi, Sachiko Akiyama[4], Seiji Yashiro[4], Toshifumi Shimizu[2] (1.Earth and Planetary Science, The University of Tokyo, 2.Institute of Space and Astronautical Science, JAXA, 3.Kwansei Gakuin University, 4.The Catholic University of America)

[PEM12-P03] Multi-wavelength Observations of Pre-flare Quasi-periodic Pulsation in the C2.2 Flare on 2012 October 15

*Yung-Chi Yang[1], Ya-Hui Yang[1], Baolin Tan[2], Chengming Tan[2], Y.H. Yan[2] (1.Graduate Institute of Space Science National Central University, 2.Key Laboratory of Solar Activities, National Astronomical Observatories)

[PEM12-P04] Investigation of pre-flare type III solar radio bursts and their potential solar origins

*Shao-Fu Hsieh[1], Ya-Hui Yang[1], Baolin Tan[2], Chengming Tan[2], Y.H. Yan[2] (1.Graduate Institute of Space Science National Central University, 2.Key Laboratory of Solar Activities, National Astronomical Observatories, Chinese Academy of Sciences)

[PEM12-P05] Statistical and observational research of solar flare for constructing total emission spectra prediction model

*Shohei Nishimoto[1], kyoko Watanabe[1], Shinsuke Imada[2], Tomoko Kawate[3], Kyoung-Sun Lee[4] (1.National Defense Academy, 2.Institute for Space-Earth Environmental Research, Nagoya University, 3.Institute Of Space And Astronautical Science, Japan Aerospace Exploration Agency, 4.National Astronomical Observatory of Japan)

[PEM12-P06] Modeling of solar active regions using local linear force-free fields to estimate magnetic twist

*Kento Nakatani[1], Kanya Kusano[1], Sung-Hong Park[1], Leka KD[2] (1.Institute for space-Earth Environmental Research, Nagoya University, 2.North West Reserch Associates)

[PEM12-P07] **Magnetohydrodynamic Simulation of an Erupting Magnetic Flux Rope on February 13 2009: Journey to Coronal Mass Ejection**

*Satoshi Inoue[1], Antonia Savcheva[2] (1.Institute for Space-Earth Environmental Research, Nagoya University, 2.Harvard-Smithsonian Center for Astrophysics)

[PEM12-P08] Investigation of flow structures in the solar interior through the surface magnetic elements' tracking

*Yusuke Iida[1] (1.Kwansei Gakuin University)

[PEM12-P09] High-precision measurement of carbon-14 in tree rings around the onset of the Maunder Minimum

*Hiroko Miyahara[1], Fuyuki Tokanai[2], Toru Moriya[2], Hideyuki Hotta[3] (1.Musashino Art University, 2.Yamagata University, 3.Chiba University)

[PEM12-P10] Examination of ^{10}Be in travertine sediment as a possible tool to reconstruct past solar activity

*Hongyang Xu[1,2], Hiroko Miyahara[2], Kazuho Horiuchi[3], Hiroyuki Matsuzaki[4], Hailong Sun[5], Weijun Luo[5], Xiangmin Zheng[1], Yusuke Suganuma[6,7], Shijie Wang[5], Limin Zhou[1] (1.East China Normal University, 2.Musashino Art University,

3.Hirosaki University, 4.University of Tokyo, 5.Chinese Academy of Sciences, 6.National Institute of Polar Research, 7.The Graduate University for Advanced Studies (SOKENDAI))

[PEM12-P11] Examination of ^{10}Be in travertine sediment as a possible tool to reconstruct past solar activity II

*Hongyang Xu[1,2], Hiroko Miyahara[2], Kazuho Horiuchi[3], Hiroyuki Matsuzaki[4], Hailong Sun[5], Weijun Luo[5], Xiangmin Zheng[1], Yusuke Suganuma[6,7], Shijie Wang[5], Limin Zhou[1] (1.East China Normal University, 2.Musashino Art University, 3.Hirosaki University, 4.University of Tokyo, 5.Chinese Academy of Sciences, 6.National Institute of Polar Research, 7.The Graduate University for Advanced Studies (SOKENDAI))

[PEM12-P12] 1 year of CR observation at Syowa Station in the Antarctic.

*Chihiro Kato[1], Kazuoki Munakata[1], Akira Kadokura[2], Ryuho Kataoka[2], Paul Evenson[3] (1.Shinshu University, 2.National Institute of Polar Research, 3.University of Delaware)

[PEM12-P13] Space weather forecast archives at NICT: handwritten solar activity charts

*Kaori Sakaguchi[1], Daikou Shiota[1], Kaori Fukunaga[1], Katsuhide Marubashi[1], Hiromitsu Ishibashi[1], Yuki Kubo[1], Mamoru Ishii[1] (1.National Institute of Information and Communications Technology)

[PEM12-P14] IMF dependence on solar wind parameters

*Tohru Araki, Yuki Harada[1] (1.Kyoto University)

[PEM12-P15] **Dipole Tilt Effect of Geomagnetic Activity from Low- to High-latitudes**

*Nowada Motoharu[1] (1.Shandong University at Weihai)

[PEM12-P16] A New Prediction Model for Solar Wind-Triggered Magnetospheric Disturbances Based on Potential Learning (Neural Network)

*Ryozo Kitajima[1], Motoharu Nowada[2], Ryotaro Kamimura[3] (1.Seikei University, 2.Shandong University at Weihai, 3.Tokai University)

[PEM12-P17] Real-time magnetosphere simulator for space weather using REProduce Plasma Universe code

*Yasubumi Kubota[1], Aoi Nakamizo[1], Kaori Sakaguchi[1], Mitsue Den[1], Yuki Kubo[1], Tsutomu Nagatsuma[1], Takashi Tanaka[1,2] (1.National Institute of Information and Communications Technology, 2.Kyushu University)

[PEM12-P18] **Simulation of GIC flowing through the power transmission network (187 kV-500 kV) in Japan**

*Nishida Yuichiro[1,6], Yusuke Ebihara[1], Satoko Nakamura[1], Shinichi Watari[2], Kumiko Hashimoto[3], Kentaro Kitamura[4], Takashi Kikuchi[5] (1.Kyoto University Reserch Institute for Sustainable Humanosphere, 2.National Institute of Information and Communications Technology, 3.Kibi International University, 4.National Insutitute of Technology, Tokuyama College, 5.Nagoya University, 6.Kyoto University Department of Electrical Engineering)

[PEM12-P19] Climatological features of the upper atmosphere reproduced by a revised version of a whole atmosphere-ionosphere coupled model GAIA

*Hidekatsu Jin[1], Yasunobu Miyoshi[2], Chihiro Tao[1], Hiroyuki Shinagawa[1], Hitoshi Fujiwara[3] (1.National Institude of Information and Communications Technology, 2.Kyushu University, 3.Seikei University)

[PEM12-P20] Investigation of the thermospheric mass density variations below 200 km

*Hitoshi Fujiwara[1], Yasunobu Miyoshi[2], Masayoshi Utashima[1], Huixin Liu[2] (1.Faculty of Science and Technology, Seikei University, 2.Department of Earth and Planetary Sciences, Faculty of Sciences, Kyushu University)

[PEM12-P21] Low-latitude HF Doppler observations of magnetospheric electric fields during space weather disturbances

*Kumiko K. Hashimoto[1], Takashi Kikuchi[2], Ichiro Tomizawa[3], Keisuke Hosokawa[3], Jaroslav Chum[4] (1.Kibi International University, 2.Nagoya University, 3.University of Electro-Commnunications, 4.Institute of Atmospheric Physics, Prague)

[PEM12-P22] Stratospheric ionization during magnetic storms

*Ryuho Kataoka[1] (1.National Institute of Polar Research)

[PEM12-P23] Calculating propagation time of HF radio wave using ray-tracing method and simple comparison with the observation.

*Ryo Nakao[1], Hiroyuki Nakata[1], Hiroyo Ohya[1], Toshiaki Takano[1], Kornyanat Hozumi[2], Takuya Tsugawa[2], Susumu Saito[3], Mamoru Ishii[2] (1.Graduate School of Engineering, Chiba University, 2.National Institute of imformation and Communications Technology, 3.Electronic Navigation Research Institute)

[PEM12-P24] Why do some probabilistic forecasts lack reliability?

*Yuki Kubo[1] (1.National Institute of Information and Communications Technology)

[PEM12-P25] An estimation method of GEO spacecraft surface charging for a real-time spacecraft risk assessment

*Masao Nakamura[1], Ryota Kawachi[1], Go Takahashi[1], Tsutomu Nagatsuma[2], Mamoru Ishii[2] (1.Osaka Prefecture University, 2.NICT)

[PEM12-P26] A network of HF Doppler sounding systems in Japan

*Keisuke Hosokawa[1], Hiroyuki Nakata[2], Kumiko K. Hashimoto[3], Ichiro Tomizawa[1], Jun Sakai[1], Takashi Kikuchi[4] (1.University of Electro-Communications, 2.Chiba University, 3.Kibi International University, 4.ISEE, Nagoya University)

[E] Poster | P (Space and Planetary Sciences)：P-EM Solar-Terrestrial Sciences, Space Electromagnetism & Space Environment

5:15 PM - 6:30 PM JST | 8:15 AM - 9:30 AM UTC | Poster Hall International Exhibition Hall8, Makuhari Messe_3

[P-EM12] Space Weather and Space Climate

convener:Ryuho Kataoka(National Institute of Polar Research), Antti A Pulkkinen(NASA Goddard Space Flight Center), Kanya Kusano(Institute for Space-Earth Environmental Research, Nagoya University), Kaori Sakaguchi(National Institute of Information and Communications Technology)

[PEM12-P01] Reconnection signatures in solar magnetograms during the solar storms of 4-10 September 2017

*Robert Dean Loper[1,2] (1.Air Force Institute of Technology, Department of Engineering Physics, 2.National Center for Atmospheric Research, High Altitude Observatory)

[PEM12-P02] Statistical Relation between Solar Flares and Coronal Mass Ejections with Respect to Sigmoidal Structures in Active Regions

*Yusuke Kawabata[1,2], Yusuke Iida[3], Takafumi Doi, Sachiko Akiyama[4], Seiji Yashiro[4], Toshifumi Shimizu[2] (1.Earth and Planetary Science, The University of Tokyo, 2.Institute of Space and Astronautical Science, JAXA, 3.Kwansei Gakuin University, 4.The Catholic University of America)

[PEM12-P03] Multi-wavelength Observations of Pre-flare Quasi-periodic Pulsation in the C2.2 Flare on 2012 October 15

*Yung-Chi Yang[1], Ya-Hui Yang[1], Baolin Tan[2], Chengming Tan[2], Y.H. Yan[2] (1.Graduate Institute of Space Science National Central University, 2.Key Laboratory of Solar Activities, National Astronomical Observatories)

[PEM12-P04] Investigation of pre-flare type III solar radio bursts and their potential solar origins

*Shao-Fu Hsieh[1], Ya-Hui Yang[1], Baolin Tan[2], Chengming Tan[2], Y.H. Yan[2] (1.Graduate Institute of Space Science National Central University, 2.Key Laboratory of Solar Activities, National Astronomical Observatories, Chinese Academy of Sciences)

[PEM12-P05] Statistical and observational research of solar flare for constructing total emission spectra prediction model

*Shohei Nishimoto[1], kyoko Watanabe[1], Shinsuke Imada[2], Tomoko Kawate[3], Kyoung-Sun Lee[4] (1.National Defense Academy, 2.Institute for Space-Earth Environmental Research, Nagoya University, 3.Institute Of Space And Astronautical Science, Japan Aerospace Exploration Agency, 4.National Astronomical Observatory of Japan)

[PEM12-P06] Modeling of solar active regions using local linear force-free fields to estimate magnetic twist

*Kento Nakatani[1], Kanya Kusano[1], Sung-Hong Park[1], Leka KD[2] (1.Institute for space-Earth Environmental Research, Nagoya University, 2.North West Reserch Associates)

[PEM12-P07] **Magnetohydrodynamic Simulation of an Erupting Magnetic Flux Rope on February 13 2009: Journey to Coronal Mass Ejection**

*Satoshi Inoue[1], Antonia Savcheva[2] (1.Institute for Space-Earth Environmental Research, Nagoya University, 2.Harvard-Smithsonian Center for Astrophysics)

[PEM12-P08] Investigation of flow structures in the solar interior through the surface magnetic elements' tracking

*Yusuke Iida[1] (1.Kwansei Gakuin University)

[PEM12-P09] High-precision measurement of carbon-14 in tree rings around the onset of the Maunder Minimum

*Hiroko Miyahara[1], Fuyuki Tokanai[2], Toru Moriya[2], Hideyuki Hotta[3] (1.Musashino Art University, 2.Yamagata University, 3.Chiba University)

[PEM12-P10] Examination of ^{10}Be in travertine sediment as a possible tool to reconstruct past solar activity

*Hongyang Xu[1,2], Hiroko Miyahara[2], Kazuho Horiuchi[3], Hiroyuki Matsuzaki[4], Hailong Sun[5], Weijun Luo[5], Xiangmin Zheng[1], Yusuke Suganuma[6,7], Shijie Wang[5], Limin Zhou[1] (1.East China Normal University, 2.Musashino Art University,

3.Hirosaki University, 4.University of Tokyo, 5.Chinese Academy of Sciences, 6.National Institute of Polar Research, 7.The Graduate University for Advanced Studies (SOKENDAI))

[PEM12-P11] Examination of ^{10}Be in travertine sediment as a possible tool to reconstruct past solar activity II

*Hongyang Xu[1,2], Hiroko Miyahara[2], Kazuho Horiuchi[3], Hiroyuki Matsuzaki[4], Hailong Sun[5], Weijun Luo[5], Xiangmin Zheng[1], Yusuke Suganuma[6,7], Shijie Wang[5], Limin Zhou[1] (1.East China Normal University, 2.Musashino Art University, 3.Hirosaki University, 4.University of Tokyo, 5.Chinese Academy of Sciences, 6.National Institute of Polar Research, 7.The Graduate University for Advanced Studies (SOKENDAI))

[PEM12-P12] 1 year of CR observation at Syowa Station in the Antarctic.

*Chihiro Kato[1], Kazuoki Munakata[1], Akira Kadokura[2], Ryuho Kataoka[2], Paul Evenson[3] (1.Shinshu University, 2.National Institute of Polar Research, 3.University of Delaware)

[PEM12-P13] Space weather forecast archives at NICT: handwritten solar activity charts

*Kaori Sakaguchi[1], Daikou Shiota[1], Kaori Fukunaga[1], Katsuhide Marubashi[1], Hiromitsu Ishibashi[1], Yuki Kubo[1], Mamoru Ishii[1] (1.National Institute of Information and Communications Technology)

[PEM12-P14] IMF dependence on solar wind parameters

*Tohru Araki, Yuki Harada[1] (1.Kyoto University)

[PEM12-P15] **Dipole Tilt Effect of Geomagnetic Activity from Low- to High-latitudes**

*Nowada Motoharu[1] (1.Shandong University at Weihai)

[PEM12-P16] A New Prediction Model for Solar Wind-Triggered Magnetospheric Disturbances Based on Potential Learning (Neural Network)

*Ryozo Kitajima[1], Motoharu Nowada[2], Ryotaro Kamimura[3] (1.Seikei University, 2.Shandong University at Weihai, 3.Tokai University)

[PEM12-P17] Real-time magnetosphere simulator for space weather using REProduce Plasma Universe code

*Yasubumi Kubota[1], Aoi Nakamizo[1], Kaori Sakaguchi[1], Mitsue Den[1], Yuki Kubo[1], Tsutomu Nagatsuma[1], Takashi Tanaka[1,2] (1.National Institute of Information and Communications Technology, 2.Kyushu University)

[PEM12-P18] **Simulation of GIC flowing through the power transmission network (187 kV-500 kV) in Japan**

*Nishida Yuichiro[1,6], Yusuke Ebihara[1], Satoko Nakamura[1], Shinichi Watari[2], Kumiko Hashimoto[3], Kentaro Kitamura[4], Takashi Kikuchi[5] (1.Kyoto University Reserch Institute for Sustainable Humanosphere, 2.National Institute of Information and Communications Technology, 3.Kibi International University, 4.National Insutitute of Technology, Tokuyama College, 5.Nagoya University, 6.Kyoto University Department of Electrical Engineering)

[PEM12-P19] Climatological features of the upper atmosphere reproduced by a revised version of a whole atmosphere-ionosphere coupled model GAIA

*Hidekatsu Jin[1], Yasunobu Miyoshi[2], Chihiro Tao[1], Hiroyuki Shinagawa[1], Hitoshi Fujiwara[3] (1.National Institude of Information and Communications Technology, 2.Kyushu University, 3.Seikei University)

[PEM12-P20] Investigation of the thermospheric mass density variations below 200 km

*Hitoshi Fujiwara[1], Yasunobu Miyoshi[2], Masayoshi Utashima[1], Huixin Liu[2] (1.Faculty of Science and Technology, Seikei University, 2.Department of Earth and Planetary Sciences, Faculty of Sciences, Kyushu University)

[PEM12-P21] Low-latitude HF Doppler observations of magnetospheric electric fields during space weather disturbances

*Kumiko K. Hashimoto[1], Takashi Kikuchi[2], Ichiro Tomizawa[3], Keisuke Hosokawa[3], Jaroslav Chum[4] (1.Kibi International University, 2.Nagoya University, 3.University of Electro-Commnunications, 4.Institute of Atmospheric Physics, Prague)

[PEM12-P22] Stratospheric ionization during magnetic storms

*Ryuho Kataoka[1] (1.National Institute of Polar Research)

[PEM12-P23] Calculating propagation time of HF radio wave using ray-tracing method and simple comparison with the observation.

*Ryo Nakao[1], Hiroyuki Nakata[1], Hiroyo Ohya[1], Toshiaki Takano[1], Kornyanat Hozumi[2], Takuya Tsugawa[2], Susumu Saito[3], Mamoru Ishii[2] (1.Graduate School of Engineering, Chiba University, 2.National Institute of imformation and Communications Technology, 3.Electronic Navigation Research Institute)

[PEM12-P24] Why do some probabilistic forecasts lack reliability?

*Yuki Kubo[1] (1.National Institute of Information and Communications Technology)

[PEM12-P25] An estimation method of GEO spacecraft surface charging for a real-time spacecraft risk assessment

*Masao Nakamura[1], Ryota Kawachi[1], Go Takahashi[1], Tsutomu Nagatsuma[2], Mamoru Ishii[2] (1.Osaka Prefecture University, 2.NICT)

[PEM12-P26] A network of HF Doppler sounding systems in Japan

*Keisuke Hosokawa[1], Hiroyuki Nakata[2], Kumiko K. Hashimoto[3], Ichiro Tomizawa[1], Jun Sakai[1], Takashi Kikuchi[4] (1.University of Electro-Communications, 2.Chiba University, 3.Kibi International University, 4.ISEE, Nagoya University)

[E] Poster | P (Space and Planetary Sciences)：P-CG Complex & General

10:45 AM - 12:15 PM JST | 1:45 AM - 3:15 AM UTC | Poster Hall International Exhibition Hall8, Makuhari Messe_1

[P-CG22] Shock responses of planetary materials elucidated from meteorites and dynamic compression experiments

convener:Toshimori Sekine(Center for High Pressure Science and Technology Advanced Research), Takuo Okuchi(Institute for Planetary Materials, Okayama University)

[PCG22-P01] discussion

*Takuo Okuchi[1], Toshimori Sekine[2] (1.Institute for Planetary Materials, Okayama University, 2.Center for High Pressure Science and Technology Advanced Research)

[PCG22-P02] Shock-compressed behavior of quartz by XFEL

*Tomoko Sato[1], Yoshinori Tange[2], Yusuke Seto[3], Toshimori Sekine[4,5], Norimasa Ozaki[4], Toyohito Nishikawa[4], Kohei Miyanishi[4], Kensuke Matsuoka[4], Ryosuke Kodama[4], Tadashi Togashi[2], Yuichi Inubushi[2], Toshinori Yabuuchi[6], Makina Yabashi[6] (1.Hiroshima University, 2.Japan Synchrotron Radiation Research Institute, 3.Kobe University, 4.Osaka University, 5.Center for High Pressure Science &Technology Advanced Research, 6.RIKEN)

[PCG22-P04] Laser-shock experiments of dense polymorphs of Mg_2SiO_4: technical developments using synthetic single crystals

*Narangoo Purevjav[1], Takuo Okuchi[1], Norimasa Ozaki[2], Takayoshi Sano[3], Yuhei Umeda[2], Shintaro Morioka[2], Nobuki Kamimura[2] (1.Institute for Planetary Materials, Okayama University, 2.Graduate School of Engineering, Osaka University, 3.Institute of Laser Engineering, Osaka University)

[PCG22-P05] Richtmyer-Meshkov instability in inhomogeneous density materials and its application to planetary science

*Takayoshi Sano[1] (1.Institute of Laser Engineering, Osaka University)

[PCG22-P06] Impact-induced dehydration reactions of Fe- and Al-hydrates as potential storage, carrier and source of water

*Tsubasa Tobase[1], Toshimori Sekine[1], Ginga Kitahara[2], Makoto Tokuda[2], Akira Yoshiasa[2], Makoto Takafuji[2], Tsutomu Mashimo[2], Nobuaki Kawai[2] (1.HPSTAR, 2.Graduate School of Science and Technology, Kumamoto University)

[PCG22-P07] Crystallization of amorphous $MgSiO_3$ by shock compression

*Akane Arasuna[1], Masayuki Okuno[1], Nobuaki Kawai[2] (1.Kanazawa University, 2.Kumamoto University)

[PCG22-P08] First-principle study of the structural and electronic properties of N-doped $MgAl_2O_4$ spinel

*Chi Pui Tang[1], Pak Kin Leong[1], Toshimori Sekine[2,3] (1.State Key Laboratory of Lunar and Planetary Sciences, Macau University of Science and Technology, 2.Center for High Pressure Science and Technology Advanced Research (HPSTAR) Shanghai Laboratory of HPSTAR, Shanghai, P.R. China, 3.Graduate School of Engineering, Osaka University)

[PCG22-P09] Transparency of shock-compressed single crystal diamond

*Kento Katagiri[1], Norimasa Ozaki[1,2], Kohei Miyanishi[2], Yuhei Umeda[1], Shintaro Morioka[1], Takayoshi Sano[2], Ryosuke Kodama[1,2] (1.Osaka University, 2.Institute of Laser Engineering, Osaka Unversity)

[PCG22-P10] Pb-Pb dating of the NWA 7203 angrite and relationship to its shock metamorphism

*Hideyuki Hayashi[1], Takashi Mikouchi[1], Yuji Sano[1], Martin Bizzarro[2] (1.The university of Tokyo, 2.University of Copenhagen)

[PCG22-P11] Shock recovery of high-pressure phase of SiO_2 using high-power laser

*Tadashi Kondo[1], Hiromoto Kengo[1], Tatsuhiro Sakaiya[1], Hidenori Terasaki[1], Keisuke Shigemori[2], Youichiro Hironaka[2] (1.Department of Earth and Space Science, Graduate School of Science Osaka University, 2.Institute of Laser Engineering, Osaka University)

[PCG22-P12] Hugoniot measurement of calcite under meteorite collision condition

*Fukui Keiya[1], Norimasa Ozaki[1,2], Yuhei Umeda[1], Kohei Miyanishi[3], Kento Katagiri[1], Shintaro Morioka[1], Takayoshi Sano[3], Ryosuke Kodama[1,2,3] (1.Graduate School of Engineering,Osaka univ., 2.PPC, Osaka Univ., 3.ILE, Osaka Univ.)

[PCG22-P13] Direct observation of the transformation toughening of tetragonal stabilized zirconia under shock deformation condition by ns time-resolved XRD.

*Sota Takagi[1,2], Kouhei Ichiyanagi[2,3], Nobuaki Kawai[4], Ryo Fukaya[2], Shunsuke Nozawa[2], Atsushi Kyono[1], Nobumasa Funamori[2], Shin-ichi Adachi[2] (1.University of Tsukuba, 2.KEK PF, 3.Jichi Medical University, 4.Kumamoto University)

[E] Poster | P (Space and Planetary Sciences)：P-CG Complex & General

5:15 PM - 6:30 PM JST | 8:15 AM - 9:30 AM UTC | Poster Hall International Exhibition Hall8, Makuhari Messe_4

[P-CG22] Shock responses of planetary materials elucidated from meteorites and dynamic compression experiments

convener:Toshimori Sekine(Center for High Pressure Science and Technology Advanced Research), Takuo Okuchi(Institute for Planetary Materials, Okayama University)

[PCG22-P01] discussion

*Takuo Okuchi[1], Toshimori Sekine[2] (1.Institute for Planetary Materials, Okayama University, 2.Center for High Pressure Science and Technology Advanced Research)

[PCG22-P02] Shock-compressed behavior of quartz by XFEL

*Tomoko Sato[1], Yoshinori Tange[2], Yusuke Seto[3], Toshimori Sekine[4,5], Norimasa Ozaki[4], Toyohito Nishikawa[4], Kohei Miyanishi[4], Kensuke Matsuoka[4], Ryosuke Kodama[4], Tadashi Togashi[2], Yuichi Inubushi[2], Toshinori Yabuuchi[6], Makina Yabashi[6] (1.Hiroshima University, 2.Japan Synchrotron Radiation Research Institute, 3.Kobe University, 4.Osaka University, 5.Center for High Pressure Science &Technology Advanced Research, 6.RIKEN)

[PCG22-P04] Laser-shock experiments of dense polymorphs of Mg_2SiO_4: technical developments using synthetic single crystals

*Narangoo Purevjav[1], Takuo Okuchi[1], Norimasa Ozaki[2], Takayoshi Sano[3], Yuhei Umeda[2], Shintaro Morioka[2], Nobuki Kamimura[2] (1.Institute for Planetary Materials, Okayama University, 2.Graduate School of Engineering, Osaka University, 3.Institute of Laser Engineering, Osaka University)

[PCG22-P05] Richtmyer-Meshkov instability in inhomogeneous density materials and its application to planetary science

*Takayoshi Sano[1] (1.Institute of Laser Engineering, Osaka University)

[PCG22-P06] Impact-induced dehydration reactions of Fe- and Al-hydrates as potential storage, carrier and source of water

*Tsubasa Tobase[1], Toshimori Sekine[1], Ginga Kitahara[2], Makoto Tokuda[2], Akira Yoshiasa[2], Makoto Takafuji[2], Tsutomu Mashimo[2], Nobuaki Kawai[2] (1.HPSTAR, 2.Graduate School of Science and Technology, Kumamoto University)

[PCG22-P07] Crystallization of amorphous $MgSiO_3$ by shock compression

*Akane Arasuna[1], Masayuki Okuno[1], Nobuaki Kawai[2] (1.Kanazawa University, 2.Kumamoto University)

[PCG22-P08] First-principle study of the structural and electronic properties of N-doped $MgAl_2O_4$ spinel

*Chi Pui Tang[1], Pak Kin Leong[1], Toshimori Sekine[2,3] (1.State Key Laboratory of Lunar and Planetary Sciences, Macau University of Science and Technology, 2.Center for High Pressure Science and Technology Advanced Research (HPSTAR) Shanghai Laboratory of HPSTAR, Shanghai, P.R. China, 3.Graduate School of Engineering, Osaka University)

[PCG22-P09] Transparency of shock-compressed single crystal diamond

*Kento Katagiri[1], Norimasa Ozaki[1,2], Kohei Miyanishi[2], Yuhei Umeda[1], Shintaro Morioka[1], Takayoshi Sano[2], Ryosuke Kodama[1,2] (1.Osaka University, 2.Institute of Laser Engineering, Osaka Unversity)

[PCG22-P10] Pb-Pb dating of the NWA 7203 angrite and relationship to its shock metamorphism

*Hideyuki Hayashi[1], Takashi Mikouchi[1], Yuji Sano[1], Martin Bizzarro[2] (1.The university of Tokyo, 2.University of Copenhagen)

[PCG22-P11] Shock recovery of high-pressure phase of SiO_2 using high-power laser

*Tadashi Kondo[1], Hiromoto Kengo[1], Tatsuhiro Sakaiya[1], Hidenori Terasaki[1], Keisuke Shigemori[2], Youichiro Hironaka[2] (1.Department of Earth and Space Science, Graduate School of Science Osaka University, 2.Institute of Laser Engineering, Osaka University)

[PCG22-P12] Hugoniot measurement of calcite under meteorite collision condition

*Fukui Keiya[1], Norimasa Ozaki[1,2], Yuhei Umeda[1], Kohei Miyanishi[3], Kento Katagiri[1], Shintaro Morioka[1], Takayoshi Sano[3], Ryosuke Kodama[1,2,3] (1.Graduate School of Engineering,Osaka univ., 2.PPC, Osaka Univ., 3.ILE, Osaka Univ.)

[PCG22-P13] Direct observation of the transformation toughening of tetragonal stabilized zirconia under shock deformation condition by ns time-resolved XRD.

*Sota Takagi[1,2], Kouhei Ichiyanagi[2,3], Nobuaki Kawai[4], Ryo Fukaya[2], Shunsuke Nozawa[2], Atsushi Kyono[1], Nobumasa Funamori[2], Shin-ichi Adachi[2] (1.University of Tsukuba, 2.KEK PF, 3.Jichi Medical University, 4.Kumamoto University)

[E] Poster | A (Atmospheric and Hydrospheric Sciences)：A-AS Atmospheric Sciences, Meteorology & Atmospheric Environment

10:45 AM - 12:15 PM JST | 1:45 AM - 3:15 AM UTC | Poster Hall International Exhibition Hall8, Makuhari Messe_2

[A-AS03] Large-scale moisture and organized cloud systems

convener:Hiroaki Miura(The University of Tokyo), Atsushi Hamada(University of Toyama), Satoru Yokoi(Japan Agency for Marine-Earth Science and Technology), Masaki Satoh(Atmosphere and Ocean Research Institute, The University of Tokyo)

[AAS03-P01] Numerical investigation on the shape, terminal velocity, and drag coefficient of a small raindrop by the improved immersed boundary method

*Ong Chia Rui[1], Hiroaki Miura[1] (1.The University of Tokyo)

[AAS03-P02] **A diagnostic study of water vapor during an extreme precipitation event in Yili river valleyA diagnostic study of water vapor during an extreme precipitation event in Yili river valley**

*Jing LiU[1], Yushu Zhou[2], Lianmei Yang[1] (1.Institute of Desert Meteorology,CMA, 2.Institute of Atmospheric Physics,CAS)

[AAS03-P03] **The Study on the Characteristics of Weather and Cloud Types in the Summer and Winter Seasons of the South China Sea**

*Jou Ping Hou[1], Bo-Shiou Wei[1], Li-Zhen Su[1] (1.Chung Cheng Institute of Technology)

[AAS03-P04] **Linkages between the South and East Asian Monsoon water vapor transport during boreal summer**

*Yong Liu[1] (1.Institute of Atmospheric Physics, Beijing , China)

[AAS03-P05] Interannual Modulation of the Local Hadley Circulation on Clouds, Radiation and Diagnostic Fields over the Western North Pacific

*Xinyue Wang[1], Hironobu Iwabuchi[1] (1.Tohoku Univ.)

[AAS03-P06] Seasonal and Regional Variation of Diurnal Cycle of Rainfall over Java Island and the Surrounding Area

*Madam Taqiyya Maulana[1], Takeshi Yamazaki[1] (1.Tohoku University)

[AAS03-P07] **Study on atmospheric circulation characteristics of precipitation anomalies in arid region of Central Asia**

*Lianmei Yang[1], Xuefeng Guan[1] (1.Institute of Desert Meteorology, China Meteorological Administration,)

[AAS03-P08] Mechanisms for northward propagation of boreal summer intraseasonal oscillation

*Kanta Nakae[1], Masaki Satoh[1], Daisuke Takasuka[1] (1.Atmosphere and Ocean Research Institute, The University of Tokyo)

[AAS03-P09] Fractality in the perimeter of tropical clouds observed by Himawari-8 or simulated by a high-resolution model

*Takuya Jinno[1] (1.Graduate School of Science, The University of Tokyo)

[AAS03-P10] **Large-scale deformation of tropical cloud band in the ITCZ detected in NICAM simulations**

*Noriyuki Nishi[1], Atsushi Hamada[4], Yohei Yamada[2], Tomoe Nasuno[2], Reona Satoh[5], Masaki Satoh[3] (1.Faculty of Science, Fukuoka Universtiy, 2.JAMSTEC, 3.AORI, University of Tokyo, 4.Graduate School of Science and Engineering for Education, University of Toyama, 5.Graduate School of Science, Fukuoka University)

[AAS03-P11] **Improvement of single-moment bulk microphysics for super-cooled water clouds over the Southern Ocean in NICAM using Joint simulator and double-moment microphysics**

*Woosub Roh[1], Tatsuya Seiki[2], Masaki Satoh[1], Tempei Hashino[3] (1.AORI, the university of Tokyo, 2.JAMSTEC, 3.Kochi university of technology)

[AAS03-P12] High-cloud property responses to SST change: sensitivity study using a global nonhydrostatic model

*Tomoki Ohno[1], Masaki Satoh[2] (1.Japan Agency for Marine-Earth Science and Technology, 2.Atmosphere and Ocean Research Institute, The University of Tokyo)

[AAS03-P13] Effects of different cloud overlapping parameters on simulated total cloud fraction over the globe and East Asian region

*bo hai Wang[1], hua Zhang[2] (1.Institute of Atmospheric Physics, Chinese Academy of Sciences, 2.State Key Laboratory of Severe Weather, Chinese Academy of Meteorological Sciences)

[E] Poster | A (Atmospheric and Hydrospheric Sciences)：A-AS Atmospheric Sciences, Meteorology & Atmospheric Environment

5:15 PM - 6:30 PM JST | 8:15 AM - 9:30 AM UTC | Poster Hall International Exhibition Hall8, Makuhari Messe_6

[A-AS03] Large-scale moisture and organized cloud systems

convener:Hiroaki Miura(The University of Tokyo), Atsushi Hamada(University of Toyama), Satoru Yokoi(Japan Agency for Marine-Earth Science and Technology), Masaki Satoh(Atmosphere and Ocean Research Institute, The University of Tokyo)

[AAS03-P01] Numerical investigation on the shape, terminal velocity, and drag coefficient of a small raindrop by the improved immersed boundary method

*Ong Chia Rui[1], Hiroaki Miura[1] (1.The University of Tokyo)

[AAS03-P02] **A diagnostic study of water vapor during an extreme precipitation event in Yili river valleyA diagnostic study of water vapor during an extreme precipitation event in Yili river valley**

*Jing LiU[1], Yushu Zhou[2], Lianmei Yang[1] (1.Institute of Desert Meteorology,CMA, 2.Institute of Atmospheric Physics,CAS)

[AAS03-P03] **The Study on the Characteristics of Weather and Cloud Types in the Summer and Winter Seasons of the South China Sea**

*Jou Ping Hou[1], Bo-Shiou Wei[1], Li-Zhen Su[1] (1.Chung Cheng Institute of Technology)

[AAS03-P04] **Linkages between the South and East Asian Monsoon water vapor transport during boreal summer**

*Yong Liu[1] (1.Institute of Atmospheric Physics, Beijing , China)

[AAS03-P05] Interannual Modulation of the Local Hadley Circulation on Clouds, Radiation and Diagnostic Fields over the Western North Pacific

*Xinyue Wang[1], Hironobu Iwabuchi[1] (1.Tohoku Univ.)

[AAS03-P06] Seasonal and Regional Variation of Diurnal Cycle of Rainfall over Java Island and the Surrounding Area

*Madam Taqiyya Maulana[1], Takeshi Yamazaki[1] (1.Tohoku University)

[AAS03-P07] **Study on atmospheric circulation characteristics of precipitation anomalies in arid region of Central Asia**

*Lianmei Yang[1], Xuefeng Guan[1] (1.Institute of Desert Meteorology, China Meteorological Administration,)

[AAS03-P08] Mechanisms for northward propagation of boreal summer intraseasonal oscillation

*Kanta Nakae[1], Masaki Satoh[1], Daisuke Takasuka[1] (1.Atmosphere and Ocean Research Institute, The University of Tokyo)

[AAS03-P09] Fractality in the perimeter of tropical clouds observed by Himawari-8 or simulated by a high-resolution model

*Takuya Jinno[1] (1.Graduate School of Science, The University of Tokyo)

[AAS03-P10] **Large-scale deformation of tropical cloud band in the ITCZ detected in NICAM simulations**

*Noriyuki Nishi[1], Atsushi Hamada[4], Yohei Yamada[2], Tomoe Nasuno[2], Reona Satoh[5], Masaki Satoh[3] (1.Faculty of Science, Fukuoka Universtiy, 2.JAMSTEC, 3.AORI, University of Tokyo, 4.Graduate School of Science and Engineering for Education, University of Toyama, 5.Graduate School of Science, Fukuoka University)

[AAS03-P11] **Improvement of single-moment bulk microphysics for super-cooled water clouds over the Southern Ocean in NICAM using Joint simulator and double-moment microphysics**

*Woosub Roh[1], Tatsuya Seiki[2], Masaki Satoh[1], Tempei Hashino[3] (1.AORI, the university of Tokyo, 2.JAMSTEC, 3.Kochi university of technology)

[AAS03-P12] High-cloud property responses to SST change: sensitivity study using a global nonhydrostatic model

*Tomoki Ohno[1], Masaki Satoh[2] (1.Japan Agency for Marine-Earth Science and Technology, 2.Atmosphere and Ocean Research Institute, The University of Tokyo)

[AAS03-P13] Effects of different cloud overlapping parameters on simulated total cloud fraction over the globe and East Asian region

*bo hai Wang[1], hua Zhang[2] (1.Institute of Atmospheric Physics, Chinese Academy of Sciences, 2.State Key Laboratory of Severe Weather, Chinese Academy of Meteorological Sciences)

[E] Poster | A (Atmospheric and Hydrospheric Sciences)：A-CG Complex & General

10:45 AM - 12:15 PM JST | 1:45 AM - 3:15 AM UTC | Poster Hall International Exhibition Hall8, Makuhari Messe_3

[A-CG32] Global Carbon Cycle Observation and Analysis

convener:Kazuhito Ichii(Chiba University), Prabir Patra(Research Institute for Global Change, JAMSTEC), Forrest M. Hoffman(Oak Ridge National Laboratory), Makoto Saito(National Institute of Environmental Studies)

[ACG32-P01] Regional budgets of 3 major greenhouse gases using inverse modelling of atmospheric data

*Prabir Patra[1], Naveen Chandra[1], Jagat Bisht[1] (1.Japan Agency for Marine-Earth Science and Technology (JAMSTEC))

[ACG32-P02] Analysis of hot summer in 2018

*Kazutaka Murakami[1], Kazuhito Ichii[1,2], Yukio Yoshida[1], Haruki Oshio[1], Makoto Saito[1] (1.National Institute for Environmental Studies, 2.Chiba University)

[ACG32-P03] Updated Data-Driven GPP and NEE Estimation Using Machine Learning Algorithms with Remote Sensing and Flux Data

*Zhiyan Liu[1], Kazuhito Ichii[1], Yusuke Hayasi[1], Riku Kawase[1], Masahito Ueyama[2], Yuji Kominami[3] (1.Chiba University, 2.Osaka Prefecture University, 3.Forest Research and Management Organization)

[ACG32-P04] **Response of a Bornean Rainforest to the Climatic Changes imposed by ENSO during 2009-2016**

*Julie Karine Michelon[1], Tomo'omi Kumagai[2,3], Tetsuya Hiyama[3], Hatsuki Fujinami[3], Kazuho Matsumoto[4], Tomonori Kume[5], Takami Saito[6] (1.Graduate School of Environmental Studies, Nagoya University, 2.Graduate School of Agricultural and Life Sciences, The University of Tokyo, 3.Institute for Space-Earth Environmental Research, Nagoya University, 4.Faculty of Agriculture, University of the Ryukyus, 5.Faculty of Agriculture, Kyushu University, 6.Forest Research and Management Organization)

[ACG32-P05] **Monitoring and Evaluating CO2 Flux in the Grassland Areas of Mongolia**

*Qinxue Wang[1], Tomohiro Okadera[1], Deni Eer[1], Masataka Watanabe[2], Tomohiro Shishime[2], Akihiro Oba[2], Ochirbat Batkhishig[3] (1.National Institute for Environmental Studies, 2.Research and Development Initiative, Chuo University, 3.Institute of Geography and Geoecology, Mongolian Academy of Sciences)

[ACG32-P06] Data-driven monitoring of terrestrial carbon cycle in Mongolia

*ZAYA MART[1], Zhiyan Liu[1], Riku Kawase[1], Kazuhito Ichii[1] (1.Chiba University)

[E] Poster | A (Atmospheric and Hydrospheric Sciences)：A-CG Complex & General

5:15 PM - 6:30 PM JST | 8:15 AM - 9:30 AM UTC | Poster Hall International Exhibition Hall8, Makuhari Messe_13

[A-CG32] Global Carbon Cycle Observation and Analysis

convener:Kazuhito Ichii(Chiba University), Prabir Patra(Research Institute for Global Change, JAMSTEC), Forrest M. Hoffman(Oak Ridge National Laboratory), Makoto Saito(National Institute of Environmental Studies)

[ACG32-P01] Regional budgets of 3 major greenhouse gases using inverse modelling of atmospheric data

*Prabir Patra[1], Naveen Chandra[1], Jagat Bisht[1] (1.Japan Agency for Marine-Earth Science and Technology (JAMSTEC))

[ACG32-P02] Analysis of hot summer in 2018

*Kazutaka Murakami[1], Kazuhito Ichii[1,2], Yukio Yoshida[1], Haruki Oshio[1], Makoto Saito[1] (1.National Institute for Environmental Studies, 2.Chiba University)

[ACG32-P03] Updated Data-Driven GPP and NEE Estimation Using Machine Learning Algorithms with Remote Sensing and Flux Data

*Zhiyan Liu[1], Kazuhito Ichii[1], Yusuke Hayasi[1], Riku Kawase[1], Masahito Ueyama[2], Yuji Kominami[3] (1.Chiba University, 2.Osaka Prefecture University, 3.Forest Research and Management Organization)

[ACG32-P04] **Response of a Bornean Rainforest to the Climatic Changes imposed by ENSO during 2009-2016**

*Julie Karine Michelon[1], Tomo'omi Kumagai[2,3], Tetsuya Hiyama[3], Hatsuki Fujinami[3], Kazuho Matsumoto[4], Tomonori Kume[5], Takami Saito[6] (1.Graduate School of Environmental Studies, Nagoya University, 2.Graduate School of Agricultural and Life Sciences, The University of Tokyo, 3.Institute for Space-Earth Environmental Research, Nagoya University, 4.Faculty of Agriculture, University of the Ryukyus, 5.Faculty of Agriculture, Kyushu University, 6.Forest Research and Management Organization)

[ACG32-P05] **Monitoring and Evaluating CO2 Flux in the Grassland Areas of Mongolia**

*Qinxue Wang[1], Tomohiro Okadera[1], Deni Eer[1], Masataka Watanabe[2], Tomohiro Shishime[2], Akihiro Oba[2], Ochirbat Batkhishig[3] (1.National Institute for Environmental Studies, 2.Research and Development Initiative, Chuo University, 3.Institute of Geography and Geoecology, Mongolian Academy of Sciences)

[ACG32-P06] Data-driven monitoring of terrestrial carbon cycle in Mongolia

*ZAYA MART[1], Zhiyan Liu[1], Riku Kawase[1], Kazuhito Ichii[1] (1.Chiba University)

[E] Poster | H (Human Geosciences)：H-DS Disaster geosciences

3:30 PM - 5:00 PM JST | 6:30 AM - 8:00 AM UTC | Poster Hall International Exhibition Hall8, Makuhari Messe_12

[H-DS09] Landslides and related phenomena

convener:Masahiro Chigira(Disaster Prevention Research Institute, Kyoto University), Gonghui Wang(Disaster Prevention Research Institute, Kyoto University), Fumitoshi Imaizumi(Faculty of Agriculture, Shizuoka University)

[HDS09-P01] **Fluidized landslides triggered by the liquefaction of subsurface volcanic deposits during the 2018 Iburi–Tobu earthquake, Hokkaido**

*Jun Kameda[1], Hiro Kamiya[2], Hirokazu Masumoto[1], Tomonori Morisaki[1], Toru Hiratsuka[2], Chisaki Inaoi (1.Department of Natural History Sciences, Graduate School of Science, Hokkaido University, 2.Department of Earth and Planetary Sciences, School of Science, Hokkaido University)

[HDS09-P02] A comparison between the acoustic signals and seismic signals generated during a dam-break test

★Invited Papers

*Zheng-yi Feng[1], Hao-yang Huang[1], Chia-Ming Chuang[1] (1.Department of Soil and Water Conservation, National Chung Hsing University, Taichung, Taiwan)

[HDS09-P03] Evaluation of factors of safety and landslide risk for a watershed by Scoops3D

*Zheng-yi Feng[1], Chia-Ming Chuang[1], Hao-yang Huang[1] (1.Department of Soil and Water Conservation, National Chung Hsing University, Taichung, Taiwan)

[HDS09-P04] **Fuzzy Clustering Algorithms for Establishing Landslide Susceptibility Map**

*Pei-hsun Tsai[1], Syuan-yi Wang[1], Jie-shin Cheng[1] (1.Chaoyang University of Technology)

[HDS09-P05] **A Study on Landslides and Debris Flows Susceptibility Mapping Using Unmanned Aerial Vehicles**

*Sheng-Jia Liu[1] (1.qwepoi13@gmail.com)

[HDS09-P06] Largescale landslide induced by AD1586 Tensho-Earthquake in Gifu Prefecture, central Japan

*Takahiro Kurimoto[1], Yoshihiko Kariya[2], Kuniyasu Mokudai[3], Ryuji Yamada[4], Takashi Kimura[4] (1.Undergraduate Senshu University, 2.Department of Geography, Senshu University, 3.Japan Geoservice Incorporated, 4.National Research Institute for Earth Science and Disaster Resilience)

[HDS09-P07] Failure Probability of Lushan Landslide, Taiwan

*Wei-Ting Lin[1], Kuang-Tsung Chang[1] (1.National Chung Hsing University)

[HDS09-P08] Interpretation of landslide surface deformation in Kali Gandaki River watershed, Nepal using ALOS-2/PALSAR-2 InSAR image

*Hiroshi, P. Sato[1] (1.College of Humanities and Sciences, Nihon University)

[HDS09-P09] A depth-integrated model for granular flows on the transition of different bed conditions

*Ling-Yi Hsu[1], Chi-Yao Hung[1] (1.National Chung Hsing University)

[HDS09-P10] A viscous granular flow experiment with new refractive index matching material

*Tsai-Jung Lin[1], Chi-Yao Hung[1] (1.National Chung Hsing University)

[HDS09-P11] Sandbox experiments of submarine landslide caused by water film in low permeability layer

*Shogo Kawakita[1], Daisuke Asahina[2], Keiji Kitajima[3], Mitsukazu Nakanishi[3] (1.Graduate School of Science & Technology, Nihon Univ., 2.National Institute of Advanced Industrial Science and Technology, 3.College of Science & Technology, Nihon Univ.)

[HDS09-P12] **Study on Creep Properties of Sand and Cemented Sand**

*JIN-YI YU[1], KUANG-TSUNG CHANG[1] (1.National Chung Hsing University)

[HDS09-P13] The effects of seepage force and the Poisson’s ratio on slope stability

*Hirokazu Fukui[1], Tomomi Terajima[2] (1.Graduate school of Science, Kyoto University, 2.Disaster Prevention Research Institute, Kyoto University)

[HDS09-P14] Study on the factors of seepage erosion

*Szu-Wei Fu[1], Kuang-Tsung Chang[1] (1.National Chung Hsing University)

[HDS09-P15] Deformation of slope models with different orientations of weak planes

*taeyuan tseng[1], Kuang-Tsung Chang[1] (1.National Chung Hsing University)

[E] Poster | H (Human Geosciences)：H-DS Disaster geosciences

5:15 PM - 6:30 PM JST | 8:15 AM - 9:30 AM UTC | Poster Hall International Exhibition Hall8, Makuhari Messe_20

[H-DS09] Landslides and related phenomena

convener:Masahiro Chigira(Disaster Prevention Research Institute, Kyoto University), Gonghui Wang(Disaster Prevention Research Institute, Kyoto University), Fumitoshi Imaizumi(Faculty of Agriculture, Shizuoka University)

[HDS09-P01] **Fluidized landslides triggered by the liquefaction of subsurface volcanic deposits during the 2018 Iburi–Tobu earthquake, Hokkaido**

*Jun Kameda[1], Hiro Kamiya[2], Hirokazu Masumoto[1], Tomonori Morisaki[1], Toru Hiratsuka[2], Chisaki Inaoi (1.Department of Natural History Sciences, Graduate School of Science, Hokkaido University, 2.Department of Earth and Planetary Sciences, School of Science, Hokkaido University)

[HDS09-P02] A comparison between the acoustic signals and seismic signals generated during a dam-break test

★Invited Papers

*Zheng-yi Feng[1], Hao-yang Huang[1], Chia-Ming Chuang[1] (1.Department of Soil and Water Conservation, National Chung Hsing University, Taichung, Taiwan)

[HDS09-P03] Evaluation of factors of safety and landslide risk for a watershed by Scoops3D

*Zheng-yi Feng[1], Chia-Ming Chuang[1], Hao-yang Huang[1] (1.Department of Soil and Water Conservation, National Chung Hsing University, Taichung, Taiwan)

[HDS09-P04] **Fuzzy Clustering Algorithms for Establishing Landslide Susceptibility Map**

*Pei-hsun Tsai[1], Syuan-yi Wang[1], Jie-shin Cheng[1] (1.Chaoyang University of Technology)

[HDS09-P05] **A Study on Landslides and Debris Flows Susceptibility Mapping Using Unmanned Aerial Vehicles**

*Sheng-Jia Liu[1] (1.qwepoi13@gmail.com)

[HDS09-P06] Largescale landslide induced by AD1586 Tensho-Earthquake in Gifu Prefecture, central Japan

*Takahiro Kurimoto[1], Yoshihiko Kariya[2], Kuniyasu Mokudai[3], Ryuji Yamada[4], Takashi Kimura[4] (1.Undergraduate Senshu University, 2.Department of Geography, Senshu University, 3.Japan Geoservice Incorporated, 4.National Research Institute for Earth Science and Disaster Resilience)

[HDS09-P07] Failure Probability of Lushan Landslide, Taiwan

*Wei-Ting Lin[1], Kuang-Tsung Chang[1] (1.National Chung Hsing University)

[HDS09-P08] Interpretation of landslide surface deformation in Kali Gandaki River watershed, Nepal using ALOS-2/PALSAR-2 InSAR image

*Hiroshi, P. Sato[1] (1.College of Humanities and Sciences, Nihon University)

[HDS09-P09] A depth-integrated model for granular flows on the transition of different bed conditions

*Ling-Yi Hsu[1], Chi-Yao Hung[1] (1.National Chung Hsing University)

[HDS09-P10] A viscous granular flow experiment with new refractive index matching material

*Tsai-Jung Lin[1], Chi-Yao Hung[1] (1.National Chung Hsing University)

[HDS09-P11] Sandbox experiments of submarine landslide caused by water film in low permeability layer

*Shogo Kawakita[1], Daisuke Asahina[2], Keiji Kitajima[3], Mitsukazu Nakanishi[3] (1.Graduate School of Science & Technology, Nihon Univ., 2.National Institute of Advanced Industrial Science and Technology, 3.College of Science & Technology, Nihon Univ.)

[HDS09-P12] **Study on Creep Properties of Sand and Cemented Sand**

*JIN-YI YU[1], KUANG-TSUNG CHANG[1] (1.National Chung Hsing University)

[HDS09-P13] The effects of seepage force and the Poisson’s ratio on slope stability

*Hirokazu Fukui[1], Tomomi Terajima[2] (1.Graduate school of Science, Kyoto University, 2.Disaster Prevention Research Institute, Kyoto University)

[HDS09-P14] Study on the factors of seepage erosion

*Szu-Wei Fu[1], Kuang-Tsung Chang[1] (1.National Chung Hsing University)

[HDS09-P15] Deformation of slope models with different orientations of weak planes

*taeyuan tseng[1], Kuang-Tsung Chang[1] (1.National Chung Hsing University)

[E] Poster | H (Human Geosciences)：H-TT Technology & Techniques

3:30 PM - 5:00 PM JST | 6:30 AM - 8:00 AM UTC | Poster Hall International Exhibition Hall8, Makuhari Messe_13

[H-TT18] Development and application of environmental traceability methods

convener:Ichiro Tayasu(Research Institute for Humanity and Nature), Nobuhito Ohte(Department of Social Informatics, Graduate School of Informatics, Kyoto University), Gabriel J Bowen(University of Utah)

[HTT18-P01] Isotopic study on seasonal nitrogen dynamics at Lake Biwa

*Takaaki Ishibashi[1], Ken'ichi Osaka[1], Keisuke Koba[2], Takashi Nakamura[3], Kei Nishida[3] (1.Department of ecosystem study, University of Shiga Prefecture, 2.Center for Ecological Research, Kyoto University, 3.International Research Center for River Basin Environment, University of YAMANASHI)

[HTT18-P02] Relationship between residence time, water quality, and stable isotopes of spring water and groundwater in coastal area of Fukushima prefecture

*Shiho Yabusaki[1], Kazuyoshi Asai[2] (1. Research Institute for Humanity and Nature・Faculty of Symbiotic Systems Science, Fukushima University, 2.Geo Science Laboratory)

[HTT18-P03] Applicability evaluation of CIA due to river and lake

*yusuke hataya[1], SEIKI KAWAGOE[1], Shiho Yabusaki[2], KEN Suzuki[1] (1.fukushima university, 2.Research Institute for Humanity and Nature)

[HTT18-P04] Chemical property analysis of short time scale to determine snowfall source

*Suzuki hiromichi[1], SEIKI KAWAGOE[1], SHO ADACHI[1], Shiho Yabusaki[2] (1.Fukushima University, 2.Research Institute for Humanity and Nature)

[HTT18-P05] Analyzing the origin of surface water in the Saijo Plain, Japan, based on the antimony concentration in the water

*Minoru TOKUMASU[1,2], Ki-Cheol SHIN[3], Yoshihiro YAMADA[4] (1.The United Graduate School of Agricultural Sciences, Ehime University, 2.Saijo City, 3.The Research Institute for Humanity and Nature (RIHN) , 4.Kagawa University, Faculty of Agriculture)

[HTT18-P06] Basic kinetic study on stable isotope ratios of nitrogen compounds: a case study for groundwater in the Kathmandu Valley, Nepal

*Ken Yokozawa[1,2], Kei Nishida[1,3], Takashi Nakamura[1,3], Ken'ichi Osaka[4] (1.University of Yamanashi, 2.Special Graduate Program on River Basin Environmental Science,, 3.ICRE, 4.Department of ecosystem study Univercity of Shiga prefecture)

[HTT18-P07] Usefulness of strontium isotope composition for determining the geographical origin of wasabi and potato

*Takafumi Kamitani[1], Ki-Cheol Shin[2], Sachiko Nakamura[1], Rika Koda[1], Tomoya Oka[1], Noriaki Fushimi[1], Yasuhide Muranaka[1] (1.Shizuoka Institute of Environment and Hygiene, 2.Research Institute for Humanity and Nature)

[HTT18-P08] Reconstruction of sea surface temperature and salinity for the Medieval Climatic Anomaly using a long-lived fossil coral collected at Ishigaki Island, southwestern Japan

*Osamu Abe[1], Maki Morimoto[2], Ryuji Asami[3], Takeshi Nakatsuka[1,4] (1.Graduate School of Environmental Studies, Nagoya University, 2.School of Education, Gifu University, 3.Graduate School of Science, Tohoku University, 4.Research Institute for Humanity and Nature)

[HTT18-P09] Development of the analytical method for sulfur isotope in SO_2 gas

*Masaaki Takahashi[1], Hiroyuki Sase[1], Tsuyoshi Ohizumi[1] (1.Asia Center for Air Pollution Research)

[HTT18-P10] Zinc isotope analysis on human tooth enamel samples to reconstruct diet of the Jomon period.

*Soichiro Kusaka[1], Ki-Cheol Shin[2] (1.Tokai Univ., 2.Research Institute for Humanity and Nature)

[HTT18-P11] Zinc stable isotope analysis of environmental reference materials

*Ki-Cheol Shin[1] (1.Research Institute for Humanity and Nature)

[E] Poster | H (Human Geosciences)：H-TT Technology & Techniques

5:15 PM - 6:30 PM JST | 8:15 AM - 9:30 AM UTC | Poster Hall International Exhibition Hall8, Makuhari Messe_23

[H-TT18] Development and application of environmental traceability methods

convener:Ichiro Tayasu(Research Institute for Humanity and Nature), Nobuhito Ohte(Department of Social Informatics, Graduate School of Informatics, Kyoto University), Gabriel J Bowen(University of Utah)

[HTT18-P01] **Isotopic study on seasonal nitrogen dynamics at Lake Biwa**

*Takaaki Ishibashi[1], Ken'ichi Osaka[1], Keisuke Koba[2], Takashi Nakamura[3], Kei Nishida[3] (1.Department of ecosystem study, University of Shiga Prefecture, 2.Center for Ecological Research, Kyoto University, 3.International Research Center for River Basin Environment, University of YAMANASHI)

[HTT18-P02] Relationship between residence time, water quality, and stable isotopes of spring water and groundwater in coastal area of Fukushima prefecture

*Shiho Yabusaki[1], Kazuyoshi Asai[2] (1. Research Institute for Humanity and Nature・Faculty of Symbiotic Systems Science, Fukushima University, 2.Geo Science Laboratory)

[HTT18-P03] Applicability evaluation of CIA due to river and lake

*yusuke hataya[1], SEIKI KAWAGOE[1], Shiho Yabusaki[2], KEN Suzuki[1] (1.fukushima university, 2.Research Institute for Humanity and Nature)

[HTT18-P04] Chemical property analysis of short time scale to determine snowfall source

*Suzuki hiromichi[1], SEIKI KAWAGOE[1], SHO ADACHI[1], Shiho Yabusaki[2] (1.Fukushima University, 2.Research Institute for Humanity and Nature)

[HTT18-P05] Analyzing the origin of surface water in the Saijo Plain, Japan, based on the antimony concentration in the water

*Minoru TOKUMASU[1,2], Ki-Cheol SHIN[3], Yoshihiro YAMADA[4] (1.The United Graduate School of Agricultural Sciences, Ehime University, 2.Saijo City, 3.The Research Institute for Humanity and Nature (RIHN) , 4.Kagawa University, Faculty of Agriculture)

[HTT18-P06] Basic kinetic study on stable isotope ratios of nitrogen compounds: a case study for groundwater in the Kathmandu Valley, Nepal

*Ken Yokozawa[1,2], Kei Nishida[1,3], Takashi Nakamura[1,3], Ken'ichi Osaka[4] (1.University of Yamanashi, 2.Special Graduate Program on River Basin Environmental Science,, 3.ICRE, 4.Department of ecosystem study Univercity of Shiga prefecture)

[HTT18-P07] Usefulness of strontium isotope composition for determining the geographical origin of wasabi and potato

*Takafumi Kamitani[1], Ki-Cheol Shin[2], Sachiko Nakamura[1], Rika Koda[1], Tomoya Oka[1], Noriaki Fushimi[1], Yasuhide Muranaka[1] (1.Shizuoka Institute of Environment and Hygiene, 2.Research Institute for Humanity and Nature)

[HTT18-P08] Reconstruction of sea surface temperature and salinity for the Medieval Climatic Anomaly using a long-lived fossil coral collected at Ishigaki Island, southwestern Japan

*Osamu Abe[1], Maki Morimoto[2], Ryuji Asami[3], Takeshi Nakatsuka[1,4] (1.Graduate School of Environmental Studies, Nagoya University, 2.School of Education, Gifu University, 3.Graduate School of Science, Tohoku University, 4.Research Institute for Humanity and Nature)

[HTT18-P09] Development of the analytical method for sulfur isotope in SO_2 gas

*Masaaki Takahashi[1], Hiroyuki Sase[1], Tsuyoshi Ohizumi[1] (1.Asia Center for Air Pollution Research)

[HTT18-P10] Zinc isotope analysis on human tooth enamel samples to reconstruct diet of the Jomon period.

*Soichiro Kusaka[1], Ki-Cheol Shin[2] (1.Tokai Univ., 2.Research Institute for Humanity and Nature)

[HTT18-P11] Zinc stable isotope analysis of environmental reference materials

*Ki-Cheol Shin[1] (1.Research Institute for Humanity and Nature)

[E] Poster | H (Human Geosciences)：H-CG Complex & General

1:45 PM - 3:15 PM JST | 4:45 AM - 6:15 AM UTC | Poster Hall International Exhibition Hall8, Makuhari Messe_6

[H-CG28] Implementing Integrated Research for Sustainable Future

convener:Yukio Himiyama(Emeritus Professor, Hokkaido University of Education), Akihiko Kondoh(Center for Environmental Remote Sensing, Chiba University), Takeshi Sakurai(Graduate School of Agricultural and Life Sciences, The University of Tokyo), Kenichi Abe(Research Institute for Humanity and Nature)

[HCG28-P01] **Ground Motion Instrumentation Network and Earthquake Early Warning System for Uttarakhand**

*Pankaj Kumar[1,2], Ashok - Kumar[1,2], Ajay - Gairola[1,2] (1.Indian Institute of Technology Roorkee, India, 2.Earthquake Early Warning Laboratory, Centre of Excellence in Disaster Mitigation & Management, IIT Roorkee)

[HCG28-P02] Linking Socioeconomic and Geographical Model to Analyze Land Use Changes in the Jakarta - Bandung Mega Urban Regions

*Didit Okta Pribadi[1,2] (1.Center for Regional Systems Analysis, Planning and Development (CrestPent) - IPB University, 2.Research Center for Plant Conservation and Botanic Gardens - Indonesian Institute of Sciences)

[HCG28-P03] **Development of an Integrated Model for Evaluation of Pasture Carrying Capacity and its Vulnerability based on Water Resources in Arid and Semi-arid Regions- - - - -A Case Study in Mongolia**

★Invited Papers

*Qinxue Wang[1], Tomohiro Okadera[1], Tadanobu Nakayama[1], Deni Eer[1], Ochirbat Batkhishig[2], Dorjgotov Battogtokh[2], Uudus Bayasaikhan[3] (1.National Institute for Environmental Studies, 2.Institute of Geography and Geoecology, Mongolian Academy of Sciences, 3.School of Arts and Sciences, National University of Mongolia)

[HCG28-P04] Influence of land use histories on vegetation and ecosystem services of restored wetlands in Tumen River basin, China

*CAO GUANGLAN[1], Kazuaki Tsuchiya[1], Weihong Zhu[2], OKURO TOSHIYA[1] (1.The University of Tokyo, 2.Yanbian University)

[HCG28-P05] The spatial flow of freshwater ecosystem services: A case study of Tumen River watershed

*JIAN ZHANG[1], Shizuka hashimoto[1], Kazuaki Tsuchiya[1], Weihong Zhu[2], OKURO TOSHIYA[1] (1.The University of Tokyo, 2.Yanbian University)

[E] Poster | H (Human Geosciences)：H-CG Complex & General

5:15 PM - 6:30 PM JST | 8:15 AM - 9:30 AM UTC | Poster Hall International Exhibition Hall8, Makuhari Messe_25

[H-CG28] Implementing Integrated Research for Sustainable Future

convener:Yukio Himiyama(Emeritus Professor, Hokkaido University of Education), Akihiko Kondoh(Center for Environmental Remote Sensing, Chiba University), Takeshi Sakurai(Graduate School of Agricultural and Life Sciences, The University of Tokyo), Kenichi Abe(Research Institute for Humanity and Nature)

[HCG28-P01] Ground Motion Instrumentation Network and Earthquake Early Warning System for Uttarakhand

*Pankaj Kumar[1,2], Ashok - Kumar[1,2], Ajay - Gairola[1,2] (1.Indian Institute of Technology Roorkee, India, 2.Earthquake Early Warning Laboratory, Centre of Excellence in Disaster Mitigation & Management, IIT Roorkee)

[HCG28-P02] Linking Socioeconomic and Geographical Model to Analyze Land Use Changes in the Jakarta - Bandung Mega Urban Regions

*Didit Okta Pribadi[1,2] (1.Center for Regional Systems Analysis, Planning and Development (CrestPent) - IPB University, 2.Research Center for Plant Conservation and Botanic Gardens - Indonesian Institute of Sciences)

[HCG28-P03] Development of an Integrated Model for Evaluation of Pasture Carrying Capacity and its Vulnerability based on Water Resources in Arid and Semi-arid Regions- - - - -A Case Study in Mongolia

★Invited Papers

*Qinxue Wang[1], Tomohiro Okadera[1], Tadanobu Nakayama[1], Deni Eer[1], Ochirbat Batkhishig[2], Dorjgotov Battogtokh[2], Uudus Bayasaikhan[3] (1.National Institute for Environmental Studies, 2.Institute of Geography and Geoecology, Mongolian Academy of Sciences, 3.School of Arts and Sciences, National University of Mongolia)

[HCG28-P04] Influence of land use histories on vegetation and ecosystem services of restored wetlands in Tumen River basin, China

*CAO GUANGLAN[1], Kazuaki Tsuchiya[1], Weihong Zhu[2], OKURO TOSHIYA[1] (1.The University of Tokyo, 2.Yanbian University)

[HCG28-P05] The spatial flow of freshwater ecosystem services: A case study of Tumen River watershed

*JIAN ZHANG[1], Shizuka hashimoto[1], Kazuaki Tsuchiya[1], Weihong Zhu[2], OKURO TOSHIYA[1] (1.The University of Tokyo, 2.Yanbian University)

[E] Poster | S (Solid Earth Sciences)：S-SS Seismology

3:30 PM - 5:00 PM JST | 6:30 AM - 8:00 AM UTC | Poster Hall International Exhibition Hall8, Makuhari Messe_16

[S-SS06] Nankai Trough Seismogenic Zone Experiment: Logging and sampling the seismogenic megathrust

convener:Kyuichi Kanagawa(Graduate School of Science, Chiba University), Demian M Saffer(Pennsylvania State University), Masataka Kinoshita(Earthquake Research Institute, University of Tokyo)

[SSS06-P01] Crustal structure in the Nankai Trough seismogenic zone based on renewed depth images and seismic attribute analysis

*Kazuya Shiraishi[1], Yasuhiro Yamada[1], Masataka Kinoshita[2], Gaku Kimura[3] (1.Japan Agency for Marine-Earth Science and Technology, 2.Earthquake Research Institute, The University of Tokyo, 3.Tokyo University of Marine Science and Technology)

[SSS06-P02] Along-strike variations in protothrust zone characteristics at the Nankai Trough subduction margin

*Hannah Tilley[1], Gregory F Moore[1], Mikiya Yamashita[2], Shuichi Kodaira[2] (1.University of Hawaii at Manoa, 2.JAMSTEC)

[SSS06-P03] Temporal change in seismic velocity in the Nankai subduction zone from cross-correlation analysis of ambient noise

*Tatsunori Ikeda[1], Takeshi Tsuji[1] (1.Kyushu University)

[SSS06-P04] Strength profile of the Nankai accretionary prism evaluated from drilling parameters

★Invited Papers

*Yohei Hamada[1], Manami Kitamura[2], Takehiro Hirose[1], Yasuhiro Yamada[1], Yoshinori Sanada[1], Takamitsu Sugihara[1], Saneatsu Saito[1], KYAW MOE[1] (1.Japan Agency for Marine-Earth Science and Technology, 2.National Institute of Advanced Industrial Science andTechnology)

[SSS06-P05] Paleotemperature anomalies deduced from thermal-maturity parameters within the décollement, off Cape of Muroto, Japan

*Nana Kamiya[1,2], Takehiro Hirose[2], Yuzuru Yamamoto[2], Yohei Hamada[2], Stephen A Bowden[3], Man-Yin Tsang[4], Kiho Yang[5], Satoshi Tonai[6], Weiren Lin[1,2] (1.Graduate School of Engineering, Kyoto University, 2.JAMSTEC, 3.University of Aberdeen, 4.University of Toronto, 5.Yonsei University, 6.Kochi University)

[SSS06-P06] Modelling thermal maturity of an accretionary wedge

Utsav Mannu[2], *Masataka Kinoshita[1], Taras Gerya[3] (1.Earthquake Research Institute, University of Tokyo, 2.Department of Earth and Climate Science, IISER Pune, 3.Institute of Geophysics, ETH Zürich)

[E] Poster | S (Solid Earth Sciences)：S-SS Seismology

5:15 PM - 6:30 PM JST | 8:15 AM - 9:30 AM UTC | Poster Hall International Exhibition Hall8, Makuhari Messe_28

[S-SS06] Nankai Trough Seismogenic Zone Experiment: Logging and sampling the seismogenic megathrust

convener:Kyuichi Kanagawa(Graduate School of Science, Chiba University), Demian M Saffer(Pennsylvania State University), Masataka Kinoshita(Earthquake Research Institute, University of Tokyo)

[SSS06-P01] Crustal structure in the Nankai Trough seismogenic zone based on renewed depth images and seismic attribute analysis

*Kazuya Shiraishi[1], Yasuhiro Yamada[1], Masataka Kinoshita[2], Gaku Kimura[3] (1.Japan Agency for Marine-Earth Science and Technology, 2.Earthquake Research Institute, The University of Tokyo, 3.Tokyo University of Marine Science and Technology)

[SSS06-P02] Along-strike variations in protothrust zone characteristics at the Nankai Trough subduction margin

*Hannah Tilley[1], Gregory F Moore[1], Mikiya Yamashita[2], Shuichi Kodaira[2] (1.University of Hawaii at Manoa, 2.JAMSTEC)

[SSS06-P03] Temporal change in seismic velocity in the Nankai subduction zone from cross-correlation analysis of ambient noise

*Tatsunori Ikeda[1], Takeshi Tsuji[1] (1.Kyushu University)

[SSS06-P04] Strength profile of the Nankai accretionary prism evaluated from drilling parameters

★Invited Papers

*Yohei Hamada[1], Manami Kitamura[2], Takehiro Hirose[1], Yasuhiro Yamada[1], Yoshinori Sanada[1], Takamitsu Sugihara[1], Saneatsu Saito[1], KYAW MOE[1] (1.Japan Agency for Marine-Earth Science and Technology, 2.National Institute of Advanced Industrial Science andTechnology)

[SSS06-P05] Paleotemperature anomalies deduced from thermal-maturity parameters within the décollement, off Cape of Muroto, Japan

*Nana Kamiya[1,2], Takehiro Hirose[2], Yuzuru Yamamoto[2], Yohei Hamada[2], Stephen A Bowden[3], Man-Yin Tsang[4], Kiho Yang[5], Satoshi Tonai[6], Weiren Lin[1,2] (1.Graduate School of Engineering, Kyoto University, 2.JAMSTEC, 3.University of Aberdeen, 4.University of Toronto, 5.Yonsei University, 6.Kochi University)

[SSS06-P06] Modelling thermal maturity of an accretionary wedge

Utsav Mannu[2], *Masataka Kinoshita[1], Taras Gerya[3] (1.Earthquake Research Institute, University of Tokyo, 2.Department of Earth and Climate Science, IISER Pune, 3.Institute of Geophysics, ETH Zürich)

[E] Poster | S (Solid Earth Sciences)：S-MP Mineralogy & Petrology

10:45 AM - 12:15 PM JST | 1:45 AM - 3:15 AM UTC | Poster Hall International Exhibition Hall8, Makuhari Messe_7

[S-MP29] Oceanic and Continental Subduction Processes

convener:REHMAN Ur Hafiz(Department of Earth and Environmental Sciences, Graduate School of Science and Engineering, Kagoshima University), Tatsuki Tsujimori(Tohoku University), Chin-Ho Tsai(Department of Natural Resources and Environmental Studies, National Dong Hwa University), Kazuaki Okamoto(Faculty of Education, Saitama University)

[SMP29-P01] Zircon U-Pb ages of metasedimentary rocks in the Hakogase (Hida Marginal) area, Fukui Prefecture.

*Atsushi MIYASHITA[1], Tatsuki Tsujimori[2], Daniel Pastor-Galán[3], Yi Keewook[4] (1.Seikei University, 2.Tohoku University, 3.Salamanca University, 4.Korea Basic Science Institue)

[SMP29-P02] Late Permian to Early Triassic back-arc type volcanism in the southern Mongolia volcano-plutonic belt of the Central Asian Orogenic Belt: Implication for timing of the final closure of the Palaeo-Asian Ocean

*Takeshi Imayama[1], Yoichiro Koh[2], Kazumasa Aoki[3], Mototaka Saneyoshi[4], Koshi Yagi[5], Shogo Aoki[4], Yoshihiro Sawada[6], Chiaki Ikawa[5], Tomoya Terada[4], Shinobu Ishigaki[4], Shin Toyoda[3], Khishigjav Tsogtbaatar[7], Buuvei Mainbayar[7] (1.Research Institute of Natural Sciences, Okayama University of Science, 2.Graduate School of Environmental Science, Hokkaido University, 3.Faculty of Science, Okayama University of Science, 4.Faculty of Biosphere - Geosphere Science, Okayama University of Science, 5.Hiruzen Institute for Geology and Chronology, 6.Emeritus Professor of Shimane University, 7.Institute of Paleontology and Geology, Mongolian Academy of Sciences)

[SMP29-P03] Mantle dynamics of slab breakoff constrained from the temporal change of the melting depth estimated from the Cumulate Member of the Ordovician Hayachine-Miyamori Ophiolite

*Takafumi Kimura[1], Kazuhito Ozawa[1] (1.Department of Earth and Planetary Science, The University of Tokyo)

[SMP29-P04] **Evidence of HIMU seamount on the Farallon Plate: Application of *in-situ* Sr-Pb isotope analysis to Franciscan lawsonite-bearing metagreywacke**

*Tomomi Hara[1], Tatsuki Tsujimori[1], Jun-Ichi Kimura[2] (1.Tohoku University, 2.Japan Agency for Marine-Earth Science and Technology)

[SMP29-P05] Boron isotope variations of antigorite serpentinites associated with high-pressure metamorphic rocks: A case study in the Itoigawa–Omi area of the Hida-Gaien Belt, Japan

*Chinatsu Yamada[1], Tatsuki Tsujimori[1], King Chang[2], Jun-Ichi Kimura[2] (1.Tohoku University, 2.Japan Aegency for Marine-Earth Science and Technology)

[SMP29-P06] **Study of zircons structures from the Miocene Shibi-san Granodiorite, Kagoshima Prefecture, Japan**

*Nakabayashi Marimo[1], REHMAN Ur Hafiz[1] (1.Kagoshima University)

[SMP29-P07] **Experimental modeling of eclogite and C-O-H fluid interaction in the subduction zones**

*Nadezda Chertkova[1], Shigeru Yamashita[2], Hiroaki Ohfuji[1], Tetsuo Irifune[1], Hirokazu Kadobayashi[1], Yoshitaka Yamamoto[3] (1.Ehime University, Geodynamics Research Center, 2.Okayama University, Institute for Planetary Materials, 3.National Institute of Advanced Industrial Science and Technology)

[SMP29-P08] Microfabrics of omphacite and garnet in eclogite from the Lanterman Range, northern Victoria Land, Antarctica

*Daeyeong Kim[1], Taehwan Kim[2], Jungmin Kim[3] (1.Division of Polar-Earth Sciences, Korea Polar Research Institute, 2.School of Earth and Environmental Sciences, Seoul National University, 3.Earth and Environmental Sciences, Korea University)

[SMP29-P09] Primordial Apatite from Ophiolite in Taiwan

*Nobuaki Niitsuma[1], Reishi Takashima[2], Yuan Hsi Lee[3] (1.Institute of Geosciences,Shizuoka University, 2.Tohoku University Museum, 3.National Chung-Cheng University, Taiwan)

[SMP29-P10] The evolution of the Cretaceous Jinan Basin in South Korea and the age and tectonic setting for the volcanic rocks in it

*Seung Hwan LEE[1], Chang Whan Oh[1] (1.Department of earth and environmental sciences Chonbuk national university)

[SMP29-P11] GEOCHORONOLOGY AND PETROCHEMISTREY OF LATE PALEOZOIC MAGMATIC ROCKS OF THE MANDAKH AREA, SOUTHEAST MONGOLIA

*Undarmaa Batsaikhan[1], Noriyoshi Tsuchiya[1], Masaoki Uno[1], Yukio Isozaki[2], Uyanga Bold[2], Hikaru Sawada[2] (1.Graduate School of Environmental Studies, Tohoku University, 2.Graduate School of Arts and Sciences The University of Tokyo)

[SMP29-P12] Feedbacks Offshore the Cascadia Margin

*Joan S Gomberg[1] (1.USGS Earthquake Science Center)

[E] Poster | S (Solid Earth Sciences)：S-MP Mineralogy & Petrology

5:15 PM - 6:30 PM JST | 8:15 AM - 9:30 AM UTC | Poster Hall International Exhibition Hall8, Makuhari Messe_32

[S-MP29] Oceanic and Continental Subduction Processes

convener:REHMAN Ur Hafiz(Department of Earth and Environmental Sciences, Graduate School of Science and Engineering, Kagoshima University), Tatsuki Tsujimori(Tohoku University), Chin-Ho Tsai(Department of Natural Resources and Environmental Studies, National Dong Hwa University), Kazuaki Okamoto(Faculty of Education, Saitama University)

[SMP29-P01] Zircon U-Pb ages of metasedimentary rocks in the Hakogase (Hida Marginal) area, Fukui Prefecture.

*Atsushi MIYASHITA[1], Tatsuki Tsujimori[2], Daniel Pastor-Galán[3], Yi Keewook[4] (1.Seikei University, 2.Tohoku University, 3.Salamanca University, 4.Korea Basic Science Institue)

[SMP29-P02] Late Permian to Early Triassic back-arc type volcanism in the southern Mongolia volcano-plutonic belt of the Central Asian Orogenic Belt: Implication for timing of the final closure of the Palaeo-Asian Ocean

*Takeshi Imayama[1], Yoichiro Koh[2], Kazumasa Aoki[3], Mototaka Saneyoshi[4], Koshi Yagi[5], Shogo Aoki[4], Yoshihiro Sawada[6], Chiaki Ikawa[5], Tomoya Terada[4], Shinobu Ishigaki[4], Shin Toyoda[3], Khishigjav Tsogtbaatar[7], Buuvei Mainbayar[7] (1.Research Institute of Natural Sciences, Okayama University of Science, 2.Graduate School of Environmental Science, Hokkaido University, 3.Faculty of Science, Okayama University of Science, 4.Faculty of Biosphere - Geosphere Science, Okayama University of Science, 5.Hiruzen Institute for Geology and Chronology, 6.Emeritus Professor of Shimane University, 7.Institute of Paleontology and Geology, Mongolian Academy of Sciences)

[SMP29-P03] Mantle dynamics of slab breakoff constrained from the temporal change of the melting depth estimated from the Cumulate Member of the Ordovician Hayachine-Miyamori Ophiolite

*Takafumi Kimura[1], Kazuhito Ozawa[1] (1.Department of Earth and Planetary Science, The University of Tokyo)

[SMP29-P04] **Evidence of HIMU seamount on the Farallon Plate: Application of *in-situ* Sr-Pb isotope analysis to Franciscan lawsonite-bearing metagreywacke**

*Tomomi Hara[1], Tatsuki Tsujimori[1], Jun-Ichi Kimura[2] (1.Tohoku University, 2.Japan Agency for Marine-Earth Science and Technology)

[SMP29-P05] Boron isotope variations of antigorite serpentinites associated with high-pressure metamorphic rocks: A case study in the Itoigawa–Omi area of the Hida-Gaien Belt, Japan

*Chinatsu Yamada[1], Tatsuki Tsujimori[1], King Chang[2], Jun-Ichi Kimura[2] (1.Tohoku University, 2.Japan Aegency for Marine-Earth Science and Technology)

[SMP29-P06] **Study of zircons structures from the Miocene Shibi-san Granodiorite, Kagoshima Prefecture, Japan**

*Nakabayashi Marimo[1], REHMAN Ur Hafiz[1] (1.Kagoshima University)

[SMP29-P07] **Experimental modeling of eclogite and C-O-H fluid interaction in the subduction zones**

*Nadezda Chertkova[1], Shigeru Yamashita[2], Hiroaki Ohfuji[1], Tetsuo Irifune[1], Hirokazu Kadobayashi[1], Yoshitaka Yamamoto[3] (1.Ehime University, Geodynamics Research Center, 2.Okayama University, Institute for Planetary Materials, 3.National Institute of Advanced Industrial Science and Technology)

[SMP29-P08] Microfabrics of omphacite and garnet in eclogite from the Lanterman Range, northern Victoria Land, Antarctica

*Daeyeong Kim[1], Taehwan Kim[2], Jungmin Kim[3] (1.Division of Polar-Earth Sciences, Korea Polar Research Institute, 2.School of Earth and Environmental Sciences, Seoul National University, 3.Earth and Environmental Sciences, Korea University)

[SMP29-P09] Primordial Apatite from Ophiolite in Taiwan

*Nobuaki Niitsuma[1], Reishi Takashima[2], Yuan Hsi Lee[3] (1.Institute of Geosciences,Shizuoka University, 2.Tohoku University Museum, 3.National Chung-Cheng University, Taiwan)

[SMP29-P10] The evolution of the Cretaceous Jinan Basin in South Korea and the age and tectonic setting for the volcanic rocks in it

*Seung Hwan LEE[1], Chang Whan Oh[1] (1.Department of earth and environmental sciences Chonbuk national university)

[SMP29-P11] GEOCHORONOLOGY AND PETROCHEMISTREY OF LATE PALEOZOIC MAGMATIC ROCKS OF THE MANDAKH AREA, SOUTHEAST MONGOLIA

*Undarmaa Batsaikhan[1], Noriyoshi Tsuchiya[1], Masaoki Uno[1], Yukio Isozaki[2], Uyanga Bold[2], Hikaru Sawada[2] (1.Graduate School of Environmental Studies, Tohoku University, 2.Graduate School of Arts and Sciences The University of Tokyo)

[SMP29-P12] Feedbacks Offshore the Cascadia Margin

*Joan S Gomberg[1] (1.USGS Earthquake Science Center)

[E] Poster | S (Solid Earth Sciences)：S-MP Mineralogy & Petrology

10:45 AM - 12:15 PM JST | 1:45 AM - 3:15 AM UTC | Poster Hall International Exhibition Hall8, Makuhari Messe_8

[S-MP30] Crust-Mantle Connections

convener:Yoshihiko Tamura(Research Institute for Marine Geodynamics, Japan Agency for Maine-Earth Science and Technology), Osamu Ishizuka(Geological Survey of Japan, AIST), Chris Conway(Geological Survey of Japan)

[SMP30-P01] Secular evolution of proto-Izu-Bonin-Mariana arc volcanism: Constraints from statistical analysis of melt inclusion compositions

*Morihisa Hamada[1], Hikaru Iwamori[1,2], Philipp A. Brandl[3], Takayuki Ushikubo[4], Kenji Shimizu[4], Motoo Ito[4], He Li[5], Ivan P. Savov[6] (1.Department of Solid Earth Geochemistry, Japan Agency for Marine-Earth Science and Technology, 2.Earthquake Research Institute, University of Tokyo, 3.GEOMAR Helmholtz Centre for Ocean Research Kiel, 4.Kochi Institute for Core Sample Research, Japan Agency for Marine-Earth Science and Technology, 5.Institute of Oceanology, Chinese Academy of Sciences, 6.School of Earth and Environment, University of Leeds)

[SMP30-P02] The Jurassic magmatism of protoliths of Mikabu greenstones in SW Japan: zircon U-Pb dating and trace element analysis

*Hikaru Sawada[1], Yukio Isozaki[1], Shogo Aoki[3], Shuhei Sakata[2], Ryo Hasegawa[1], Yasuo Nakamura[1] (1.Department of General Systems Studies, the University of Tokyo, 2.Department of Chemistry, Gakushuin Universtiy, 3.Department of Applied Science, Okayama University of Science)

[SMP30-P03] **Origin of variable CaO/Al_2O_3 in olivine-hosted melt inclusions from Kibblewhite Volcano, Kermadec Arc**

*Yasuhiro Hirai[1], Yoshihiko Tamura[2], Kaj Hoernle[3], Christian Timm[4], Folkmar Hauff[3], Reinhard Werner[3], Takeshi Hanyu[2], Bogdan Vaglarov[2], Qing Chang[2], Takashi Miyazaki[2], Jun-Ichi Kimura[2] (1.Graduate School of Natural Science and Technology, Kanazawa University, Japan, 2.Japan Agency for Marine-Earth Science and Technology (JAMSTEC), Yokosuka, Kanagawa, Japan, 3.GEOMAR Helmholtz Centre for Ocean Research, Kiel, Germany, 4.GNS Science, Lower Hutt, New Zealand)

[SMP30-P04] Ankaramite from Doyo seamount in the Izu-Ogasawara arc: A precursor of continents?

*Yoshihiko Tamura[1], Tomoki Sato[1], Osamu Ishizuka[1,2], Takashi Miyazaki[1], Yasuhiro Hirai[1,3], Mami Takehara[4], Eri Sakamoto[5] (1.JAMSTEC, 2.AIST, 3.Kanazawa Univ., 4.NIPR, 5.NME)

[SMP30-P05] Different Moho reflections adjacent to Minami-Tori Shima and their petrologic origins

*Yoshihiko Tamura[1], Kentaro Kaneda[2], Gou Fujie[1], Akane Ohira[1], Eiichi TAKAZAWA[3], Georges Ceuleneer[4], Katsuyoshi Michibayashi[5], Tomoki Sato[1], Shuichi Kodaira[1], Seiichi Miura[1] (1.Japan Agency for Maine-Earth Science and Technology, 2.Japan Coast Guard, 3.Niigata University, 4.Universite de Toulouse, 5.Nagoya University)

[SMP30-P06] **Melt-rock interaction in plagioclase peridotites from the southern Palawan Ophiolite, Philippines**

*FLORENCE ANNETTE CRUSPERO LABIS[1], BETCHAIDA D PAYOT[1], GABRIEL THEOPHILUS V VALERA[1], JULIUS A PASCO[1], JESLEY MEI A DYCOCO[1] (1.UNIVERSITY OF THE PHILIPPINES)

[SMP30-P07] Intra-oceanic arc magma genesis: a case study from Havre volcano, Kermadec arc

*Chris Conway[1], Kenichiro Tani[2] (1.Geological Survey of Japan, 2.National Museum of Nature and Science)

[E] Poster | S (Solid Earth Sciences)：S-MP Mineralogy & Petrology

5:15 PM - 6:30 PM JST | 8:15 AM - 9:30 AM UTC | Poster Hall International Exhibition Hall8, Makuhari Messe_33

[S-MP30] Crust-Mantle Connections

convener:Yoshihiko Tamura(Research Institute for Marine Geodynamics, Japan Agency for Maine-Earth Science and Technology), Osamu Ishizuka(Geological Survey of Japan, AIST), Chris Conway(Geological Survey of Japan)

[SMP30-P01] Secular evolution of proto-Izu-Bonin-Mariana arc volcanism: Constraints from statistical analysis of melt inclusion compositions

*Morihisa Hamada[1], Hikaru Iwamori[1,2], Philipp A. Brandl[3], Takayuki Ushikubo[4], Kenji Shimizu[4], Motoo Ito[4], He Li[5], Ivan P. Savov[6] (1.Department of Solid Earth Geochemistry, Japan Agency for Marine-Earth Science and Technology, 2.Earthquake Research Institute, University of Tokyo, 3.GEOMAR Helmholtz Centre for Ocean Research Kiel, 4.Kochi Institute for Core Sample Research, Japan Agency for Marine-Earth Science and Technology, 5.Institute of Oceanology, Chinese Academy of Sciences, 6.School of Earth and Environment, University of Leeds)

[SMP30-P02] The Jurassic magmatism of protoliths of Mikabu greenstones in SW Japan: zircon U-Pb dating and trace element analysis

*Hikaru Sawada[1], Yukio Isozaki[1], Shogo Aoki[3], Shuhei Sakata[2], Ryo Hasegawa[1], Yasuo Nakamura[1] (1.Department of General Systems Studies, the University of Tokyo, 2.Department of Chemistry, Gakushuin Universtiy, 3.Department of Applied Science, Okayama University of Science)

[SMP30-P03] **Origin of variable CaO/Al_2O_3 in olivine-hosted melt inclusions from Kibblewhite Volcano, Kermadec Arc**

*Yasuhiro Hirai[1], Yoshihiko Tamura[2], Kaj Hoernle[3], Christian Timm[4], Folkmar Hauff[3], Reinhard Werner[3], Takeshi Hanyu[2], Bogdan Vaglarov[2], Qing Chang[2], Takashi Miyazaki[2], Jun-Ichi Kimura[2] (1.Graduate School of Natural Science and Technology, Kanazawa University, Japan, 2.Japan Agency for Marine-Earth Science and Technology (JAMSTEC), Yokosuka, Kanagawa, Japan, 3.GEOMAR Helmholtz Centre for Ocean Research, Kiel, Germany, 4.GNS Science, Lower Hutt, New Zealand)

[SMP30-P04] Ankaramite from Doyo seamount in the Izu-Ogasawara arc: A precursor of continents?

*Yoshihiko Tamura[1], Tomoki Sato[1], Osamu Ishizuka[1,2], Takashi Miyazaki[1], Yasuhiro Hirai[1,3], Mami Takehara[4], Eri Sakamoto[5] (1.JAMSTEC, 2.AIST, 3.Kanazawa Univ., 4.NIPR, 5.NME)

[SMP30-P05] Different Moho reflections adjacent to Minami-Tori Shima and their petrologic origins

*Yoshihiko Tamura[1], Kentaro Kaneda[2], Gou Fujie[1], Akane Ohira[1], Eiichi TAKAZAWA[3], Georges Ceuleneer[4], Katsuyoshi Michibayashi[5], Tomoki Sato[1], Shuichi Kodaira[1], Seiichi Miura[1] (1.Japan Agency for Maine-Earth Science and Technology, 2.Japan Coast Guard, 3.Niigata University, 4.Universite de Toulouse, 5.Nagoya University)

[SMP30-P06] **Melt-rock interaction in plagioclase peridotites from the southern Palawan Ophiolite, Philippines**

*FLORENCE ANNETTE CRUSPERO LABIS[1], BETCHAIDA D PAYOT[1], GABRIEL THEOPHILUS V VALERA[1], JULIUS A PASCO[1], JESLEY MEI A DYCOCO[1] (1.UNIVERSITY OF THE PHILIPPINES)

[SMP30-P07] Intra-oceanic arc magma genesis: a case study from Havre volcano, Kermadec arc

*Chris Conway[1], Kenichiro Tani[2] (1.Geological Survey of Japan, 2.National Museum of Nature and Science)

[E] Poster | S (Solid Earth Sciences)：S-MP Mineralogy & Petrology

3:30 PM - 5:00 PM JST | 6:30 AM - 8:00 AM UTC | Poster Hall International Exhibition Hall8, Makuhari Messe_18

[S-MP31] Supercontinents and Crustal Evolution

convener:Madhusoodhan Satish-Kumar(Department of Geology, Faculty of Science, Niigata University), Tomokazu Hokada(National Institute of Polar Research), Krishnan Sajeev(Centre for Earth Sciences, Indian Institute of Science), Yasuhito Osanai(Division of Evolution of Earth Environments, Faculty of Social and Cultural Studies, Kyushu University)

[SMP31-P01] Re-examination of metamorphic and geochronologic events in Rayner Complex and Western Rayner Complex in Antarctica

*Tomokazu Hokada[1,2], Sotaro Baba[3], Atsushi Kamei[4], Ippei Kitano[5], Kenji Horie[1,2], Yoshikuni Hiroi[1,6], Yoichi Motoyoshi[1,2], Mami Takehara[1], Kazuyuki Shiraishi[1] (1.National Institute of Polar Research, 2.The Graduate University for Advanced Studies (SOKENDAI), 3.University of the Ryukyus, 4.Shimane University, 5.Kyushu University, 6.Chiba University)

[SMP31-P02] Composition of constituent minerals in corona-bearing and -free mafic gneisses from the Lützow-Holm Complex at Skallen, East Antarctica

*Yuki Mori[1], Takeshi Ikeda[2] (1.Department of Earth and Planetary Sciences, Graduate School of Sciences, Kyushu University, 2.Department of Earth and Planetary Sciences, Faculty of Sciences, Kyushu University)

[SMP31-P03] “Pseudo-concordance” of U-Pb system in zircon at Harvey Nunatak, Napier Complex, East Antarctica

*Mami Takehara[1] (1.National Institute of Polar Research)

[SMP31-P04] Rapid UHT metamorphism and exhumation of the Lützow-Holm Complex in Antarctica

*Yoshikuni Hiroi[1], Tomokazu Hokada[2], Tatsuro Adachi[3], Yasuhito Osanai[3], Yoichi Motoyoshi[2], Kazuyuki Shiraishi[2] (1.Chiba Univ, 2.National Institute of Polar Research, 3.Kyushu University)

[SMP31-P05] Tectonic History of Hiroo Complex and its implication inpaleo-Kuril Arc evolution

*Sreehari Lakshmanan[1], Tsuyoshi Toyoshima[2], Futoshi Nanayama[3] (1.Graduate School of Science and Technology, Niigata University, Niigata, Japan, 2.Department of Geology, Faculty of Science, Niigata Univ. , 3.Geological Survey of Japan, AIST)

[SMP31-P06] **Behaviour of C, O, Sr, Nd and Pb isotopes in high-grade metacarbonate rocks**

*Madhusoodhan Satish-Kumar[1], Akari Imura[1], Momoko Shirakawa[2], Gen Shimoda[3], Kosuke T. Goto[3], M A Sanjeewa P K Malaviarachchi[4] (1.Department of Geology, Faculty of Science, Niigata University, 2.Graduate School of Science and Technology, Niigata University, 3.Geological Survey of Japan, 4.University of Peradeniya, Sri Lanka)

[E] Poster | S (Solid Earth Sciences)：S-MP Mineralogy & Petrology

5:15 PM - 6:30 PM JST | 8:15 AM - 9:30 AM UTC | Poster Hall International Exhibition Hall8, Makuhari Messe_34

[S-MP31] Supercontinents and Crustal Evolution

convener:Madhusoodhan Satish-Kumar(Department of Geology, Faculty of Science, Niigata University), Tomokazu Hokada(National Institute of Polar Research), Krishnan Sajeev(Centre for Earth Sciences, Indian Institute of Science), Yasuhito Osanai(Division of Evolution of Earth Environments, Faculty of Social and Cultural Studies, Kyushu University)

[SMP31-P01] Re-examination of metamorphic and geochronologic events in Rayner Complex and Western Rayner Complex in Antarctica

*Tomokazu Hokada[1,2], Sotaro Baba[3], Atsushi Kamei[4], Ippei Kitano[5], Kenji Horie[1,2], Yoshikuni Hiroi[1,6], Yoichi Motoyoshi[1,2], Mami Takehara[1], Kazuyuki Shiraishi[1] (1.National Institute of Polar Research, 2.The Graduate University for Advanced Studies (SOKENDAI), 3.University of the Ryukyus, 4.Shimane University, 5.Kyushu University, 6.Chiba University)

[SMP31-P02] Composition of constituent minerals in corona-bearing and -free mafic gneisses from the Lützow-Holm Complex at Skallen, East Antarctica

*Yuki Mori[1], Takeshi Ikeda[2] (1.Department of Earth and Planetary Sciences, Graduate School of Sciences, Kyushu University, 2.Department of Earth and Planetary Sciences, Faculty of Sciences, Kyushu University)

[SMP31-P03] “Pseudo-concordance” of U-Pb system in zircon at Harvey Nunatak, Napier Complex, East Antarctica

*Mami Takehara[1] (1.National Institute of Polar Research)

[SMP31-P04] Rapid UHT metamorphism and exhumation of the Lützow-Holm Complex in Antarctica

*Yoshikuni Hiroi[1], Tomokazu Hokada[2], Tatsuro Adachi[3], Yasuhito Osanai[3], Yoichi Motoyoshi[2], Kazuyuki Shiraishi[2] (1.Chiba Univ, 2.National Institute of Polar Research, 3.Kyushu University)

[SMP31-P05] Tectonic History of Hiroo Complex and its implication inpaleo-Kuril Arc evolution

*Sreehari Lakshmanan[1], Tsuyoshi Toyoshima[2], Futoshi Nanayama[3] (1.Graduate School of Science and Technology, Niigata University, Niigata, Japan, 2.Department of Geology, Faculty of Science, Niigata Univ. , 3.Geological Survey of Japan, AIST)

[SMP31-P06] **Behaviour of C, O, Sr, Nd and Pb isotopes in high-grade metacarbonate rocks**

*Madhusoodhan Satish-Kumar[1], Akari Imura[1], Momoko Shirakawa[2], Gen Shimoda[3], Kosuke T. Goto[3], M A Sanjeewa P K Malaviarachchi[4] (1.Department of Geology, Faculty of Science, Niigata University, 2.Graduate School of Science and Technology, Niigata University, 3.Geological Survey of Japan, 4.University of Peradeniya, Sri Lanka)

[E] Poster | S (Solid Earth Sciences)：S-CG Complex & General

3:30 PM - 5:00 PM JST | 6:30 AM - 8:00 AM UTC | Poster Hall International Exhibition Hall8, Makuhari Messe_19

[S-CG49] Hard-Rock Drilling Science: From Continental to Deep Sea Drilling, and Oman Project

convener:Katsuyoshi Michibayashi(Department of Earth and Planetary Sciences, Nagoya University), Eiichi TAKAZAWA(Department of Geology, Faculty of Science, Niigata University), Norikatsu Akizawa(Department of Ocean Floor Geoscience, Atmosphere and Ocean Research Institute, The University of Tokyo)

[SCG49-P01] **Permeability profile in the Oman Drilling Project inferred from resistivity measurements**

*Ikuo Katayama[1], Keishi Okazaki[2], Natsue Abe[2], Ole Ivar Ulven[3], Gilbert Hong[4], Wenlu Zhu[5], Benoit Cordonnier[3], Kohei Hatakeyama[1], Yuya Akamatsu[1], Katsuyoshi Michibayashi[6], Marguerite Godard[7], Peter Kelemen[8], Science Party The Oman Drilling Project Phase 2 (1.Hiroshima University, 2.JAMSTEC, 3.University of Oslo, 4.Seoul National University, 5.University of Maryland, 6.Nagoya University, 7.Universitè Montpellier, 8.Columbia University)

[SCG49-P02] Relationship between alteration intensity and elastic wave velocity of gabbroic rocks from ICDP Hole CM1A, Oman Drilling Project Phase II

*Kosuke Kimura[1], Ikuo Katayama[1], Kohei Hatakeyama[1], Yuya Akamatsu[1], Natsue Abe[2], Keishi Okazaki[2], The Oman Drilling Project Phase II Science Party (1.Hiroshima University, 2.JAMSTEC)

[SCG49-P03] Physical property of the fossilized crust-mantle transition zone from ICDP Oman Drilling Project Hole CM1A and CM2B measured onboard D/V Chikyu

*Keishi Okazaki[1], Natsue Abe[1], Kohei Hatakeyama[2], Yuya Akamatsu[2], Ikuo Katayama[2], Eiichi TAKAZAWA[3], Damon A H Teagle[4], Peter B Kelemen[5], Jude Coggon[4], The Oman Drilling Project Phase 2 Science Party (1.Japan Agency for Marine-Earth Science and Technology, 2.Hiroshima University, 3.Niigata University, 4.University of Southampton, 5.Columbia University)

[SCG49-P04] Microstructures of lower crust gabbros from the Oman Ophiolite: Analyses of the drilled cores of the Oman Drilling Project

*Koki Iida[1], Takahiro Fudai[1], Susumu Umino[1], Yuki Kusano[2] (1.Kanazawa University, 2.Geological Survey of Japan)

[SCG49-P05] Olivine fabric and mineral compositions in the Maqsad area of the Samail massif, the southern Oman ophiolite

*Kaho Takahashi[1], Eiichi TAKAZAWA[2,3], Katsuyoshi Michibayashi[4], Kakihata Yuki[4], Ryoko Senda[5] (1.Graduate School of Science and Technology, Niigata University, 2.Department of Geology, Faculty of Science, Niigata University, 3.JAMSTEC, 4.Nagoya University, 5.Kyushu University)

[SCG49-P06] The evolution of melt inclusions in podiform chromitite in Oman

*Yuan YAO[1], Eiichi TAKAZAWA[2,3], Oman Drilling Project Phase 2 Science Party (1.Graduate School of Sciences& Technology, Niigata University, Japan, 2.Department of Geology, Faculty of Science, Niigata University, Japan, 3.Research and Development Center for Ocean Drilling Science, JAMSTEC, Japan)

[SCG49-P07] Melt/fluid - rock reaction inferred from the Wadi Tayin mantle section in the southern Oman ophiolite

*Keisuke ISHII[1], Eiichi TAKAZAWA[2], Akihiro kuriyama[2], Kyouka Someya[2], Yoshihiko Tamura[3] (1.Graduate School of Science and Technology, Niigata University, 2.Department of Geology, Faculty of Science, Niigata University , 3.R&D Center for Ocean Drilling Science, Japan Agency for Marine-Earth Science and Technology)

[SCG49-P08] Numerical simulations for reaction-induced fracture formation of layered gabbro during hydration process

*Kazuki Yoshida[1], Hiroyuki Shimizu[2], Noriyoshi Tsuchiya[1], Atsushi Okamoto[1], Phase 2 Science Party Oman Drilling Project[3] (1.Tohoku university, 2.Geotechnical Analysis Group, Advanced Analysis Department, Civil Engineering Design Division, Kajima Corporation, 3.Oman Drilling Project Phase 2 Science Party)

[SCG49-P09] X-ray CT images of oceanic lithologies obtained on Oman Drilling Project drillcores during ChikyuOman 2017 and 2018

*Katsuyoshi Michibayashi[1], Peter B Kelemen[2], Margurette Godard[3], Eiichi TAKAZAWA[4], Damon A H Teagle[5], The Oman Drilling Project Science Party[6] (1.Department of Earth and Planetary Sciences, Nagoya University, 2.Columbia University, 3.Université Montpellier, 4.Niigata University, 5.Southampton University, 6.ICDP)

[SCG49-P10] Re-examination of the crystallization process of clinopyroxene oikocrysts in layered gabbros at Hess Deep Rift, EPR

*Akane Yasui[1], Takashi Hoshide[1] (1.Graduate School of International Resource Sciences, Akita University)

[SCG49-P11] Structural petrology of peridotites from the Kalaymyo ophiolite

*Kouhei Asano[1,2], Katsuyoshi Michibayashi[1], Jung-Woo Park[3] (1.Graduate School of Environmental Studies, Nagoya University, 2.Shizuoka University, 3.Seoul National University)

[SCG49-P12] Reevaluation of the origin of mafic layers in the Upper Zone of the Horoman Peridotite

*Yumeto KOGURE[1], Eiichi TAKAZAWA[1] (1.Department of Geology, Faculty of Science, Niigata University)

[SCG49-P13] A structural and petrological study of "Shibukawa ultramafic body" in the Sanbagawa belt, western Shizuoka, Japan

*Hikaru Shioya[1,2], Katsuyoshi Michibayashi[1], Ken-ichi Hirauchi[2] (1.Graduate School of Environmental Studies, Nagoya University, 2.Institute of Geosciences, Shizuoka University)

[E] Poster | S (Solid Earth Sciences)：S-CG Complex & General

5:15 PM - 6:30 PM JST | 8:15 AM - 9:30 AM UTC | Poster Hall International Exhibition Hall8, Makuhari Messe_35

[S-CG49] Hard-Rock Drilling Science: From Continental to Deep Sea Drilling, and Oman Project

convener:Katsuyoshi Michibayashi(Department of Earth and Planetary Sciences, Nagoya University), Eiichi TAKAZAWA(Department of Geology, Faculty of Science, Niigata University), Norikatsu Akizawa(Department of Ocean Floor Geoscience, Atmosphere and Ocean Research Institute, The University of Tokyo)

[SCG49-P01] **Permeability profile in the Oman Drilling Project inferred from resistivity measurements**

*Ikuo Katayama[1], Keishi Okazaki[2], Natsue Abe[2], Ole Ivar Ulven[3], Gilbert Hong[4], Wenlu Zhu[5], Benoit Cordonnier[3], Kohei Hatakeyama[1], Yuya Akamatsu[1], Katsuyoshi Michibayashi[6], Marguerite Godard[7], Peter Kelemen[8], Science Party The Oman Drilling Project Phase 2 (1.Hiroshima University, 2.JAMSTEC, 3.University of Oslo, 4.Seoul National University, 5.University of Maryland, 6.Nagoya University, 7.Universitè Montpellier, 8.Columbia University)

[SCG49-P02] Relationship between alteration intensity and elastic wave velocity of gabbroic rocks from ICDP Hole CM1A, Oman Drilling Project Phase II

*Kosuke Kimura[1], Ikuo Katayama[1], Kohei Hatakeyama[1], Yuya Akamatsu[1], Natsue Abe[2], Keishi Okazaki[2], The Oman Drilling Project Phase II Science Party (1.Hiroshima University, 2.JAMSTEC)

[SCG49-P03] Physical property of the fossilized crust-mantle transition zone from ICDP Oman Drilling Project Hole CM1A and CM2B measured onboard D/V Chikyu

*Keishi Okazaki[1], Natsue Abe[1], Kohei Hatakeyama[2], Yuya Akamatsu[2], Ikuo Katayama[2], Eiichi TAKAZAWA[3], Damon A H Teagle[4], Peter B Kelemen[5], Jude Coggon[4], The Oman Drilling Project Phase 2 Science Party (1.Japan Agency for Marine-Earth Science and Technology, 2.Hiroshima University, 3.Niigata University, 4.University of Southampton, 5.Columbia University)

[SCG49-P04] Microstructures of lower crust gabbros from the Oman Ophiolite: Analyses of the drilled cores of the Oman Drilling Project

*Koki Iida[1], Takahiro Fudai[1], Susumu Umino[1], Yuki Kusano[2] (1.Kanazawa University, 2.Geological Survey of Japan)

[SCG49-P05] Olivine fabric and mineral compositions in the Maqsad area of the Samail massif, the southern Oman ophiolite

*Kaho Takahashi[1], Eiichi TAKAZAWA[2,3], Katsuyoshi Michibayashi[4], Kakihata Yuki[4], Ryoko Senda[5] (1.Graduate School of Science and Technology, Niigata University, 2.Department of Geology, Faculty of Science, Niigata University, 3.JAMSTEC, 4.Nagoya University, 5.Kyushu University)

[SCG49-P06] The evolution of melt inclusions in podiform chromitite in Oman

*Yuan YAO[1], Eiichi TAKAZAWA[2,3], Oman Drilling Project Phase 2 Science Party (1.Graduate School of Sciences& Technology, Niigata University, Japan, 2.Department of Geology, Faculty of Science, Niigata University, Japan, 3.Research and Development Center for Ocean Drilling Science, JAMSTEC, Japan)

[SCG49-P07] Melt/fluid - rock reaction inferred from the Wadi Tayin mantle section in the southern Oman ophiolite

*Keisuke ISHII[1], Eiichi TAKAZAWA[2], Akihiro kuriyama[2], Kyouka Someya[2], Yoshihiko Tamura[3] (1.Graduate School of Science and Technology, Niigata University, 2.Department of Geology, Faculty of Science, Niigata University , 3.R&D Center for Ocean Drilling Science, Japan Agency for Marine-Earth Science and Technology)

[SCG49-P08] Numerical simulations for reaction-induced fracture formation of layered gabbro during hydration process

*Kazuki Yoshida[1], Hiroyuki Shimizu[2], Noriyoshi Tsuchiya[1], Atsushi Okamoto[1], Phase 2 Science Party Oman Drilling Project[3] (1.Tohoku university, 2.Geotechnical Analysis Group, Advanced Analysis Department, Civil Engineering Design Division, Kajima Corporation, 3.Oman Drilling Project Phase 2 Science Party)

[SCG49-P09] X-ray CT images of oceanic lithologies obtained on Oman Drilling Project drillcores during ChikyuOman 2017 and 2018

*Katsuyoshi Michibayashi[1], Peter B Kelemen[2], Margurette Godard[3], Eiichi TAKAZAWA[4], Damon A H Teagle[5], The Oman Drilling Project Science Party[6] (1.Department of Earth and Planetary Sciences, Nagoya University, 2.Columbia University, 3.Université Montpellier, 4.Niigata University, 5.Southampton University, 6.ICDP)

[SCG49-P10] Re-examination of the crystallization process of clinopyroxene oikocrysts in layered gabbros at Hess Deep Rift, EPR

*Akane Yasui[1], Takashi Hoshide[1] (1.Graduate School of International Resource Sciences, Akita University)

[SCG49-P11] Structural petrology of peridotites from the Kalaymyo ophiolite

*Kouhei Asano[1,2], Katsuyoshi Michibayashi[1], Jung-Woo Park[3] (1.Graduate School of Environmental Studies, Nagoya University, 2.Shizuoka University, 3.Seoul National University)

[SCG49-P12] Reevaluation of the origin of mafic layers in the Upper Zone of the Horoman Peridotite

*Yumeto KOGURE[1], Eiichi TAKAZAWA[1] (1.Department of Geology, Faculty of Science, Niigata University)

[SCG49-P13] A structural and petrological study of "Shibukawa ultramafic body" in the Sanbagawa belt, western Shizuoka, Japan

*Hikaru Shioya[1,2], Katsuyoshi Michibayashi[1], Ken-ichi Hirauchi[2] (1.Graduate School of Environmental Studies, Nagoya University, 2.Institute of Geosciences, Shizuoka University)

[E] Poster | B (Biogeosciences)：B-CG Complex & General

3:30 PM - 5:00 PM JST | 6:30 AM - 8:00 AM UTC | Poster Hall International Exhibition Hall8, Makuhari Messe_22

[B-CG06] Earth and Planetary Science Frontiers for Life and Global Environment

convener:Yoshinori Takano(Japan Agency for Marine-Earth Science and Technology (JAMSTEC)), Yohey Suzuki(Graduate School of Science, The University of Tokyo), Shingo Kato(RIKEN), Keisuke Fukushi(Institute of Nature & Environmental Technology, Kanazawa University)

[BCG06-P01] Dynamisms and characteristics of dissolved organic matter (DOM) in deep aquifer: A scope for deep biosphere

*Atsushi Urai[1,2], Yoshinori Takano[2], Naohiko Ohkouchi[2] (1.Department of Science and Technology, Graduate School of Medicine, Science and Technology, Shinshu University, 2.Department of Biogeochemistry, Japan Agency for Marine-Earth Science and Technology)

[BCG06-P02] Correlations of magnetosome-related genes in Nitrospirae genomes to magnetosome geometry and redox stratification in deep-sea environments

*Shinsaku Nakano[1], Shingo Kato[2], Mariko Kouduka[1], Toshitsugu Yamazaki[3], Yohey Suzuki[1] (1.Graduate School of Science, The University of Tokyo, 2.RIKEN, 3.Atmosphere and Ocean Research Institute, The University of Tokyo)

[BCG06-P03] Reconstruction of key ecological responses leading to the most recent dead zone formations in Japan Sea through ancient DNA metabarcodring

*Mariko Kouduka[1], Yohey Suzuki[1] (1.Department of Earth and Planetary Science, The University of Tokyo, 7-3-1 Hongo, Bunkyo-ku, Tokyo, Japan.)

[BCG06-P04] Search for microbial CH_4 production processes in lake sediments and surface water associated with cyanobacterial bloom

*Makoto Matsushita[1], Yoshinori Takano[1], Hiroyuki Imachi[1], Atsushi Urai[2], Ho-Dong Park[3], Hiroki Iwata[3], Naohiko Ohkouchi[1] (1.Japan Agency for Marine-Earth Science and Technology, 2.Department of Science and Technology, Graduate School of Medicine, Science and Technology, Shinshu University, 3.Department of Environmental Sciences, Faculty of Science, Shinshu University)

[BCG06-P05] Did life emerge in a deep-sea metal sulfide chimney? New insights from an archaeal genome and a nanoscale microbe-silicate assemblage

*Hinako Takamiya[1], Hiroki Mukai[2], Mariko Kouduka[1], Shingo Kato[4], Motoo Ito[3], Yohey Suzuki[1] (1.Earth and Planetary Science Graduate School of Science, The University of Tokyo , 2.National Institute of Advanced Industrial Science and Technology, 3.Kochi Institute for Core Sample Research JAMSTEC, 4.RIKEN)

[BCG06-P06] X-ray computed nano-tomography for visualizing microbial cells and their surrounding environments

*Yuki Morono[1], Go-Ichiro Uramoto[2,1], Kentaro Uesugi[3], Nobuhisa Takeuchi[3], Masayuki Uesugi[3], Kengo Kubota[4], Tatsuhiko Hoshino[1], Fumio Inagaki[1] (1.Japan Agency for Marine-Earth Science and Technology, 2.Kochi University, 3.Japan Synchrotron Radiation Research Institute, 4.Tohoku University)

[BCG06-P07] Carbon signatures in amino acids during deep-sea anoxic methanotrophy

*Yoshinori Takano[1] (1.Japan Agency for Marine-Earth Science and Technology (JAMSTEC))

[E] Poster | B (Biogeosciences)：B-CG Complex & General

5:15 PM - 6:30 PM JST | 8:15 AM - 9:30 AM UTC | Poster Hall International Exhibition Hall8, Makuhari Messe_40

[B-CG06] Earth and Planetary Science Frontiers for Life and Global Environment

convener:Yoshinori Takano(Japan Agency for Marine-Earth Science and Technology (JAMSTEC)), Yohey Suzuki(Graduate School of Science, The University of Tokyo), Shingo Kato(RIKEN), Keisuke Fukushi(Institute of Nature & Environmental Technology, Kanazawa University)

[BCG06-P01] Dynamisms and characteristics of dissolved organic matter (DOM) in deep aquifer: A scope for deep biosphere

*Atsushi Urai[1,2], Yoshinori Takano[2], Naohiko Ohkouchi[2] (1.Department of Science and Technology, Graduate School of Medicine, Science and Technology, Shinshu University, 2.Department of Biogeochemistry, Japan Agency for Marine-Earth Science and Technology)

[BCG06-P02] Correlations of magnetosome-related genes in Nitrospirae genomes to magnetosome geometry and redox stratification in deep-sea environments

*Shinsaku Nakano[1], Shingo Kato[2], Mariko Kouduka[1], Toshitsugu Yamazaki[3], Yohey Suzuki[1] (1.Graduate School of Science, The University of Tokyo, 2.RIKEN, 3.Atmosphere and Ocean Research Institute, The University of Tokyo)

[BCG06-P03] Reconstruction of key ecological responses leading to the most recent dead zone formations in Japan Sea through ancient DNA metabarcodring

*Mariko Kouduka[1], Yohey Suzuki[1] (1.Department of Earth and Planetary Science, The University of Tokyo, 7-3-1 Hongo, Bunkyo-ku, Tokyo, Japan.)

[BCG06-P04] Search for microbial CH_4 production processes in lake sediments and surface water associated with cyanobacterial bloom

*Makoto Matsushita[1], Yoshinori Takano[1], Hiroyuki Imachi[1], Atsushi Urai[2], Ho-Dong Park[3], Hiroki Iwata[3], Naohiko Ohkouchi[1] (1.Japan Agency for Marine-Earth Science and Technology, 2.Department of Science and Technology, Graduate School of Medicine, Science and Technology, Shinshu University, 3.Department of Environmental Sciences, Faculty of Science, Shinshu University)

[BCG06-P05] Did life emerge in a deep-sea metal sulfide chimney? New insights from an archaeal genome and a nanoscale microbe-silicate assemblage

*Hinako Takamiya[1], Hiroki Mukai[2], Mariko Kouduka[1], Shingo Kato[4], Motoo Ito[3], Yohey Suzuki[1] (1.Earth and Planetary Science Graduate School of Science, The University of Tokyo , 2.National Institute of Advanced Industrial Science and Technology, 3.Kochi Institute for Core Sample Research JAMSTEC, 4.RIKEN)

[BCG06-P06] X-ray computed nano-tomography for visualizing microbial cells and their surrounding environments

*Yuki Morono[1], Go-Ichiro Uramoto[2,1], Kentaro Uesugi[3], Nobuhisa Takeuchi[3], Masayuki Uesugi[3], Kengo Kubota[4], Tatsuhiko Hoshino[1], Fumio Inagaki[1] (1.Japan Agency for Marine-Earth Science and Technology, 2.Kochi University, 3.Japan Synchrotron Radiation Research Institute, 4.Tohoku University)

[BCG06-P07] Carbon signatures in amino acids during deep-sea anoxic methanotrophy

*Yoshinori Takano[1] (1.Japan Agency for Marine-Earth Science and Technology (JAMSTEC))

[E] Poster | M (Multidisciplinary and Interdisciplinary)：M-IS Intersection

10:45 AM - 12:15 PM JST | 1:45 AM - 3:15 AM UTC | Poster Hall International Exhibition Hall8, Makuhari Messe_10

[M-IS05] New technologies to monitor thunderstorm and severe weather activities

convener:Mitsuteru Sato(Department of Cosmoscience, Hokkaido University), Yukihiro Takahashi(Department of Cosmosciences, Graduate School of Science, Hokkaido University), Hisayuki Kubota(Hokkaido University), Kozo Yamashita(Ashikaga University, Department of Engineering.)

[MIS05-P01] Study on monitoring of thunderstorm activity based on multiple electrostatic measurement

*Kozo Yamashita[1], Kakeru Kanno[1], Mitsuteru Sato[2], Yukihiro Takahashi[2] (1.Ashikaga Univ., 2.Hokkaido Univ.)

[MIS05-P02] **Contribution of Rainfall and Lightning Activities to the Fair Weather Electric Field Evaluated by 3D GEC Model**

*Kittanapat Bandholnopparat[1], Mitsuteru Sato[2], Yukihiro Takahashi[2], Toru Adachi[3], Masashi Kamogawa[5], Yasuhiro Minamoto[5], Akira Kadokura[6], Tomoo Ushio[4] (1.Department of Cosmosciences, Hokkaido University, Sapporo, Japan, 2.Faculty of Science, Hokkaido University, Sapporo, Japan, 3.Meteorological Research Institute, Tsukuba, Japan, 4.Department of Aerospace Engineering, Tokyo Metropolitan University, Hino, Japan, 5.Tokyo Gakugei University, Tokyo, Japan, 6.National Institute of Polar Research, Tokyo, Japan)

[MIS05-P03] A method for locating lightning discharges using tweek atmospherics

*Masafumi Kanno[1], Hiroyo Ohya[2], Kazuo Shiokawa[3], Hiroyuki Nakata[2], Toshiaki Takano[2] (1.Graduate School of Science and Engineering, Chiba University, 2.Graduate School of Engineering, Chiba University, 3.Institute for Space-Earth Environmental Research, Nagoya University)

[MIS05-P04] Monitoring for lightning activities and thunder cloud development over the Tokyo metropolitan area during the 2018 summer

*Jun-Ichi Hamada[1], Jun Matsumoto[1], Kozo Yamashita[2], Masashi Kamogawa[3], Yukihiro Takahashi[4] (1.Faculty of Urban Environmental Sciences, Tokyo Metropolitan University, 2.Department of Engineering, Ashikaga University, 3.Department of Physics, Tokyo Gakugei University, 4.Department of Cosmosciences, Graduate School of Science, Hokkaido University)

[E] Poster | M (Multidisciplinary and Interdisciplinary)：M-IS Intersection

5:15 PM - 6:30 PM JST | 8:15 AM - 9:30 AM UTC | Poster Hall International Exhibition Hall8, Makuhari Messe_42

[M-IS05] New technologies to monitor thunderstorm and severe weather activities

convener:Mitsuteru Sato(Department of Cosmoscience, Hokkaido University), Yukihiro Takahashi(Department of Cosmosciences, Graduate School of Science, Hokkaido University), Hisayuki Kubota(Hokkaido University), Kozo Yamashita(Ashikaga University, Department of Engineering.)

[MIS05-P01] Study on monitoring of thunderstorm activity based on multiple electrostatic measurement

*Kozo Yamashita[1], Kakeru Kanno[1], Mitsuteru Sato[2], Yukihiro Takahashi[2] (1.Ashikaga Univ., 2.Hokkaido Univ.)

[MIS05-P02] **Contribution of Rainfall and Lightning Activities to the Fair Weather Electric Field Evaluated by 3D GEC Model**

*Kittanapat Bandholnopparat[1], Mitsuteru Sato[2], Yukihiro Takahashi[2], Toru Adachi[3], Masashi Kamogawa[5], Yasuhiro Minamoto[5], Akira Kadokura[6], Tomoo Ushio[4] (1.Department of Cosmosciences, Hokkaido University, Sapporo, Japan, 2.Faculty of Science, Hokkaido University, Sapporo, Japan, 3.Meteorological Research Institute, Tsukuba, Japan, 4.Department of Aerospace Engineering, Tokyo Metropolitan University, Hino, Japan, 5.Tokyo Gakugei University, Tokyo, Japan, 6.National Institute of Polar Research, Tokyo, Japan)

[MIS05-P03] A method for locating lightning discharges using tweek atmospherics

*Masafumi Kanno[1], Hiroyo Ohya[2], Kazuo Shiokawa[3], Hiroyuki Nakata[2], Toshiaki Takano[2] (1.Graduate School of Science and Engineering, Chiba University, 2.Graduate School of Engineering, Chiba University, 3.Institute for Space-Earth Environmental Research, Nagoya University)

[MIS05-P04] Monitoring for lightning activities and thunder cloud development over the Tokyo metropolitan area during the 2018 summer

*Jun-Ichi Hamada[1], Jun Matsumoto[1], Kozo Yamashita[2], Masashi Kamogawa[3], Yukihiro Takahashi[4] (1.Faculty of Urban Environmental Sciences, Tokyo Metropolitan University, 2.Department of Engineering, Ashikaga University, 3.Department of Physics, Tokyo Gakugei University, 4.Department of Cosmosciences, Graduate School of Science, Hokkaido University)

[E] Poster | M (Multidisciplinary and Interdisciplinary)：M-GI General Geosciences, Information Geosciences & Simulations

3:30 PM - 5:00 PM JST | 6:30 AM - 8:00 AM UTC | Poster Hall International Exhibition Hall8, Makuhari Messe_28

[M-GI29] Near Surface Investigation and Modeling for Groundwater Resources Assessment and Conservation

convener:Jui-Pin Tsai(National Cheng Kung University, Taiwan), Hwa-Lung Yu(National Taiwan University), Ching-Chung Cheng(National Chiao Tung University Taiwan), Jing-Sen Cai(China University of Geosciences)

[MGI29-P01] Modelling of self-potential signals associated with groundwater flows

*ayaka ishikawa[1], Katsumi Hattori[1] (1.chiba university)

[MGI29-P02] Estimating the Hydraulic Conductivity and Heat Capacity of the Aquifer between the River and Well Site Using Joint Inversion Approach

*Jui-Pin Tsai[1], Chin-Tsai Hsiao[4], Liang-Cheng Chang[2], You-Cheng Chen[2], Chun-Hung Chen[3], Yun-Ta Cheng[3], Jen-Hung Yu[3] (1.National Cheng Kung University, Taiwan , 2.National Chiao Tung University, Taiwan , 3.Water Resources Planning Institute, Water Resources Agency, Taiwan, 4.Department of Information Management, Chung Chou University of Science and Technology)

[MGI29-P03] Evaluation on Soil Permeability Using Electrical Resistant Tomography

*CHIHPING KUO[1], BONIAN SHEN[1], CHIHWEI HUANG[1], YUCHIAO LEE[1], SHENXIANG HUANG[1], YENLIN CHEN[1] (1.Department and Institute of Civil Engineering and Environmental Informatics, Minghsin University of Science and Technology)

[MGI29-P04] The Potential Study of Open Loop System Geothermal Heat Pump in Gifu City, Japan

*Randa Permanda[1], Tomoyuki Ohtani[2] (1.Department of Civil and Environmental Engineering, Gifu University, 2.Department of Civil Engineering, Gifu University)

[MGI29-P05] Application of TL-CHERT Smart Characterization Method to Investigate a Groundwater Contaminated Site

*Tzu-Pin Wang[1,2,5], Yao-Tsung Chen[3], Tien-Hsing Tung[3], Chih-Hung Cheng[2], Jie Wang[4] (1.NCU TW, 2.Geophysical Technology and Engineering Co.,Ltd. R.O.C, 3.Apollo Technology Co.,Ltd. R.O.C., 4.Department of Civil Engineering, Chien Hsin University of Science and Technology, Taoyuan City, Taiwan, 5.Disaster Reduction Research Center, Chien Hsin University of Science and Technology, Taoyuan City, Taiwan)

[MGI29-P06] Data Assimilation in Hydraulic Conductivity Identification using Bayesian Statistical Method

*Shih-Yang Cheng[1], Kuo-Chin Hsu[1] (1.National Cheng Kung Univ.)

[MGI29-P07] Groundwater recharge estimation by using empirical orthogonal function method

Hua-Ting Zeng [1], *Hwa-Lung Yu[1] (1. National Taiwan University)

[MGI29-P08] The Application of Drought Early Warning Index for Regional Hydrological Circumstance Analysis

*Chih Chao Ho[1], Ta Wei Chen[2] (1.Construction and Disaster Prevention Research Center, Feng Chia Univ., 2.Taiwan Hsin-Chu Irrigation Association)

[E] Poster | M (Multidisciplinary and Interdisciplinary)：M-GI General Geosciences, Information Geosciences & Simulations

5:15 PM - 6:30 PM JST | 8:15 AM - 9:30 AM UTC | Poster Hall International Exhibition Hall8, Makuhari Messe_47

[M-GI29] Near Surface Investigation and Modeling for Groundwater Resources Assessment and Conservation

convener:Jui-Pin Tsai(National Cheng Kung University, Taiwan), Hwa-Lung Yu(National Taiwan University), Ching-Chung Cheng(National Chiao Tung University Taiwan), Jing-Sen Cai(China University of Geosciences)

[MGI29-P01] Modelling of self-potential signals associated with groundwater flows

*ayaka ishikawa[1], Katsumi Hattori[1] (1.chiba university)

[MGI29-P02] Estimating the Hydraulic Conductivity and Heat Capacity of the Aquifer between the River and Well Site Using Joint Inversion Approach

*Jui-Pin Tsai[1], Chin-Tsai Hsiao[4], Liang-Cheng Chang[2], You-Cheng Chen[2], Chun-Hung Chen[3], Yun-Ta Cheng[3], Jen-Hung Yu[3] (1.National Cheng Kung University, Taiwan , 2.National Chiao Tung University, Taiwan , 3.Water Resources Planning Institute, Water Resources Agency, Taiwan, 4.Department of Information Management, Chung Chou University of Science and Technology)

[MGI29-P03] Evaluation on Soil Permeability Using Electrical Resistant Tomography

*CHIHPING KUO[1], BONIAN SHEN[1], CHIHWEI HUANG[1], YUCHIAO LEE[1], SHENXIANG HUANG[1], YENLIN CHEN[1] (1.Department and Institute of Civil Engineering and Environmental Informatics, Minghsin University of Science and Technology)

[MGI29-P04] The Potential Study of Open Loop System Geothermal Heat Pump in Gifu City, Japan

*Randa Permanda[1], Tomoyuki Ohtani[2] (1.Department of Civil and Environmental Engineering, Gifu University, 2.Department of Civil Engineering, Gifu University)

[MGI29-P05] Application of TL-CHERT Smart Characterization Method to Investigate a Groundwater Contaminated Site

*Tzu-Pin Wang[1,2,5], Yao-Tsung Chen[3], Tien-Hsing Tung[3], Chih-Hung Cheng[2], Jie Wang[4] (1.NCU TW, 2.Geophysical Technology and Engineering Co.,Ltd. R.O.C, 3.Apollo Technology Co.,Ltd. R.O.C., 4.Department of Civil Engineering, Chien Hsin University of Science and Technology, Taoyuan City, Taiwan, 5.Disaster Reduction Research Center, Chien Hsin University of Science and Technology, Taoyuan City, Taiwan)

[MGI29-P06] Data Assimilation in Hydraulic Conductivity Identification using Bayesian Statistical Method

*Shih-Yang Cheng[1], Kuo-Chin Hsu[1] (1.National Cheng Kung Univ.)

[MGI29-P07] Groundwater recharge estimation by using empirical orthogonal function method

Hua-Ting Zeng [1], *Hwa-Lung Yu[1] (1. National Taiwan University)

[MGI29-P08] The Application of Drought Early Warning Index for Regional Hydrological Circumstance Analysis

*Chih Chao Ho[1], Ta Wei Chen[2] (1.Construction and Disaster Prevention Research Center, Feng Chia Univ., 2.Taiwan Hsin-Chu Irrigation Association)

[E] Poster | M (Multidisciplinary and Interdisciplinary)：M-ZZ Others

1:45 PM - 3:15 PM JST | 4:45 AM - 6:15 AM UTC | Poster Hall International Exhibition Hall8, Makuhari Messe_10

[M-ZZ50] Governance for Trans-boundary Volcanic Disaster

convener:Mayumi Sakamoto(Graduate School of Disaster Resilience and Governance, University of Hyogo), Haruhisa Nakamichi(Sakurajima Volcano Research Center, Disaster Prevention Research Institute, Kyoto University), MASARU ARAKIDA(Asian Disaster Reduction Center)

[MZZ50-P01] Governance for Trans-boundary Volcanic Disaster -a case of 2010 Eyjafjallajökull Eruption-

*Mayumi Sakamoto[1] (1.Graduate School of Disaster Resilience and Governance, University of Hyogo)

[MZZ50-P02] Regional Cooperation against Cross-border Disasters

*MASARU ARAKIDA[1] (1.Asian Disaster Reduction Center)

[MZZ50-P03] Issues of Japan's volcanic disaster prevention system as viewed from overseas alert systems

*Erika Ishimizu[1], Mayumi Sakamoto[1] (1.Graduate School of Disaster Resilience and Governance University of Hyogo)

[E] Poster | M (Multidisciplinary and Interdisciplinary)：M-ZZ Others

5:15 PM - 6:30 PM JST | 8:15 AM - 9:30 AM UTC | Poster Hall International Exhibition Hall8, Makuhari Messe_50

[M-ZZ50] Governance for Trans-boundary Volcanic Disaster

convener:Mayumi Sakamoto(Graduate School of Disaster Resilience and Governance, University of Hyogo), Haruhisa Nakamichi(Sakurajima Volcano Research Center, Disaster Prevention Research Institute, Kyoto University), MASARU ARAKIDA(Asian Disaster Reduction Center)

[MZZ50-P01] Governance for Trans-boundary Volcanic Disaster -a case of 2010 Eyjafjallajökull Eruption-

*Mayumi Sakamoto[1] (1.Graduate School of Disaster Resilience and Governance, University of Hyogo)

[MZZ50-P02] Regional Cooperation against Cross-border Disasters

*MASARU ARAKIDA[1] (1.Asian Disaster Reduction Center)

[MZZ50-P03] Issues of Japan's volcanic disaster prevention system as viewed from overseas alert systems

*Erika Ishimizu[1], Mayumi Sakamoto[1] (1.Graduate School of Disaster Resilience and Governance University of Hyogo)

[E] Poster | P (Space and Planetary Sciences)：P-PS Planetary Sciences

Tue. May 28, 2019 3:30 PM - 5:00 PM JST | Tue. May 28, 2019 6:30 AM - 8:00 AM UTC | Poster Hall International Exhibition Hall8, Makuhari Messe_1

[P-PS01] Outer Solar System Exploration Today, and Tomorrow

convener:Jun Kimura(Osaka University), Yasumasa Kasaba(Planetary Plasma and Atmospheric Research Center, Tohoku University), Kunio M. Sayanagi(Hampton University)

The giant planets provide many keys to understanding planetary processes. They play an important role in shaping our solar system, and the physical and chemical processes they harbor also provide a unique opportunity to study the phenomena relevant for studying Earth and other planets, including exoplanetary systems. In this session, we discuss a wide range of topics encompassing the giant planets and their moons, including their origins, interiors, atmospheres, compositions, surface features, and electromagnetic fields. To advocate for current and future outer planets exploration (Cassini, Juno, New Horizons, JUICE, and beyond), we also call for discussions on future missions to explore giant planet systems, including how to develop better international cooperation. Discussion in this latter category will include progress in developing a solar sail mission concept for observing the Jupiter system and its trojan asteroids.

[PPS01-P01] Critical Role of Entry Probes in Giant Planet Exploration

*Sushil K Atreya[1], Olivier Mousis[2] (1.University of Michigan Ann Arbor, 2.Laboratoire d'Astrophysique de Marseille)

[PPS01-P02] OKEANOS – Jupiter Trojan Asteroid Rendezvous and Landing Experiments Using a Solar Power Sail

*Tatsuaki Okada[1,2], Takahiro Iwata[1], Yoko Kebukawa[3], Motoo Ito[4], Jun Aoki[5], Yosuke Kawai[5], Shoichiro Yokota[5], Yoshifumi Saito[1], Kentaro Terada[5], Michisato Toyoda[5], Hikaru Yabuta[6], Hisayoshi Yurimoto[1,7], Shuji Matsuura[8], Kohji Tsumura[9], Daisuke Yonetoku[10], Tatehiro Mihara[11], Ayako Matsuoka[1], Reiko Nomura[12], Hajime Yano[1], Takayuki Hirai[13], Atsushi Kumamoto[9], Ryosuke Nakamura[14], Stephan Ulamec[15], Ralf Jaumann[15], Jean-Pierre Bibring[16], Noel Grand[17], Cyril Szopa[18], Ernesto Palomba[19], Jorn Helbert[15], Alain Herique[20], Matthias Grott[15], Hans-Ulrich Auster[21], Goester Klingelhoefer[22], Fumi Yoshida[13], Makoto Yoshikawa[1], Jun Matsumoto[1], Toshihiro Chujo[1], Masanori Matsushita[1], Takanao Saiki[1], Hideki Kato[1], Osamu Mori[1], Junichiro Kawaguchi[1] (1.Japan Aerospace Exploration Agency, 2.University of Tokyo, 3.Yokohama National University, 4.Japan Agency for Marine-Earth Science and Technology, 5.Osaka University, 6.Hiroshima University, 7.Hokkaido University, 8.Kwansei Gakuin University, 9.Tohoku University, 10.Kanazawa University, 11.RIKEN, 12.National Astronomical Observatory of Japan, 13.Chiba Institute of Technology, 14.National Institute of Advanced Industrial Science and Technology, 15.German Aerospace Center, 16.Institut d'Astrophysique Spatiale, 17.LISA, 18.LATMOS, 19.INAF-IAPS, 20.IPAG, 21.TU Braunschweig, 22.Leibniz Universität Hannover)

[PPS01-P03] Magnetic field model of Jovian magnetosphere

*Naoya Momoki[1], Hiroaki TOH[1] (1.Division of Earth and Planetary Sciences, Graduate School of Science, Kyoto University)

[PPS01-P04] Enhancement of the Jovian thermospheric temperature above the Great Red Spot based on the infrared spectroscopic data obtained with IRTF/iSHELL

*Ayumu Kambara[1], Hajime Kita[2], Takeshi Sakanoi[1], Yasumasa Kasaba[1], Masato Kagitani[1], Haruna Watanabe[1] (1.Planetary Plasma and Atmospheric Research Center, Graduate School of Science, Tohoku University, 2.Institute of Space and Astronautical Science, Japan Aerospace Exploration Agency)

[PPS01-P05] Pulsation-like variation of Jovian infrared polar emission observed by Subaru 8-m: H3+ and methane emissions

*Yasumasa Kasaba[1], Haruna Watanabe[1], Hajime Kita[2], Chihiro Tao[3], Takeshi Sakanoi[1], Masato Kagitani[1], Orton Glenn[1,4], James Sinclair[4] (1.Planetary Plasma and Atmospheric Research Center, 2.ISAS/JAXA,

3.NICT, 4.NASA/JPL)

[PPS01-P06] Structure of Io plasma torus observed with the Tohoku 60-cm telescope

*Masato Kagitani[1], Fuminori Tsuchiya[1], Kazuo Yoshioka[2], Go Murakami[3], Tomoki Kimura[1], Ryoichi Koga[1], Reina Hikida[4], Takeshi Sakanoi[1] (1.Graduate School of Science, Tohoku University, 2.Graduate School of frontier Science, The University of Tokyo, 3.Institute of Space and Astronautical Science, Japan Aerospace Exploration Agency, 4.Department of Earth and Planetary Science, Graduate School of Science, Tokyo University)

[PPS01-P07] Ion Scale Height Variability in Hisaki Io Torus Observations

*Nicholas McCord Schneider[1], Carl Schmidt[2], Masato Kagitani[3], Yasumasa Kasaba[3], Tomoki Kimura[3], Go Murakami[4], Fuminori Tsuchiya[3], Hajime Kita[3], Reina Hikida[5], Ichiro Yoshikawa[5], Kazuo Yoshioka[5] (1.LASP, University of Colorado Boulder, 2.Boston University, 3.Tohoku University, 4.ISAS/JAXA, 5.University of Tokyo)

[PPS01-P08] Size of the Smallest Particles in Saturn's Rings

*Keiji Ohtsuki[1], Hiroshi Kawamura[1], Naoyuki Hirata[1], Hiroshi Daisaka[2], Hiroshi Kimura[3] (1.Graduate School of Science, Kobe University, 2.Graduate School of Commerce and Management, Hitotsubashi University, 3.Planetary Exploration Research Center, Chiba Institute of Technology)

[PPS01-P09] The Radio & Plasma Wave Investigation (RPWI) for JUICE for the investigation of Jupiter and Icy Moons System: Contributions from Japan

*Yasumasa Kasaba[1], Hiroaki Misawa[1], Fuminori Tsuchiya[1], Atsushi Kumamoto[2], Yuto Katoh[2], Tomoki Kimura[2], Hajime Kita[3], J.-E. Wahlund[4] (1.Planetary Plasma and Atmospheric Research Center, Tohoku University, 2.Department of Geophysics, Tohoku University, 3.ISAS/JAXA, 4.IRF Uppsala, Sweden)

[PPS01-P10] Magnetic field experiment at Jupiter icy moons (JUICE J-MAG) and in-flight alignment calibration

*Ayako Matsuoka[1], Michele Karen Dougherty[2], Patrick Brown[2], Futoshi Takahashi[3], Hisayoshi Shimizu[4], Masaki Matsushima[5] (1.Research Division for Space Plasma, Institute of Space and Astronautical Science, Japan Aerospace Exploration Agency, 2.Imperial College London, 3.Kyushu University, 4.University of Tokyo, 5.Tokyo Institute of Technology)

[PPS01-P11] Science targets of the GAnymede Laser Altimeter (GALA) for the JUICE mission

*Jun Kimura[1], Shunichi Kamata[2], Koji Matsumoto[3], Noriyuki Namiki[3], Keigo Enya[4], Masanori Kobayashi[5], Hiroshi Araki[3], Hirotomo Noda[3], Ko Ishibashi[5], Hauke Hussmann[6], Kay Lingenauber[6] (1.Osaka University, 2.Hokkaido University, 3.National Astronomical Observatory Japan, 4.ISAS/JAXA, 5.Chiba Institute of Technology, 6.German Aerospace Center (DLR), Berlin)

[PPS01-P12] Current status of the antenna developments, the data processing, scientific target for JUICE/SWI JAPAN.

*YASUKO KASAI[1], JUICE SWI Japanese Team (1.National Institute of Information and Communications Technology (NICT))

Critical Role of Entry Probes in Giant Planet Exploration

*Sushil K Atreya[1], Olivier Mousis[2]

1. University of Michigan Ann Arbor, 2. Laboratoire d'Astrophysique de Marseille

Flyby and orbiting spacecraft have explored the giant planets since the early 1970’s. In situ measurements in the troposphere are essential, however, for constraining the models of formation, evolution and interior processes of the giant planets. The models employ abundances and isotopic ratios of key elements, in particular C,N, S, O, He, Ne, Ar, Kr, Xe and D/H, derived from the measurement of their (bulk) reservoir species. That was the scientific rationale for the 1995 Galileo Probe at Jupiter and a Saturn Probe in NASA’s New Frontiers list of candidate missions. Considering that the icy giant planets are distinct from the gas giants, they represent the missing pieces of the puzzle of the formation of the outer solar system, besides being the closest analog for nearly half of the confirmed exoplanets. Thus, their comprehensive exploration with an orbiter-probe spacecraft is essential. The principal focus of this talk is the science, feasibility and implementation strategy of in situ measurements with entry probes at the icy giant planets, Uranus and Neptune, guided by thermochemical models and lessons learned from the Galileo Probe and the ongoing Juno Orbiter. [www.umich.edu/~atreya]

Keywords: Icy Giants, Origin and Evolution, Uranus, Neptune, Entry Probes, Exoplanets

©2019. Japan Geoscience Union. All Right Reserved.

OKEANOS –Jupiter Trojan Asteroid Rendezvous and Landing Experiments Using a Solar Power Sail

*Tatsuaki Okada[1,2], Takahiro Iwata[1], Yoko Kebukawa[3], Motoo Ito[4], Jun Aoki[5], Yosuke Kawai[5], Shoichiro Yokota[5], Yoshifumi Saito[1], Kentaro Terada[5], Michisato Toyoda[5], Hikaru Yabuta[6], Hisayoshi Yurimoto[1,7], Shuji Matsuura[8], Kohji Tsumura[9], Daisuke Yonetoku[10], Tatehiro Mihara[11], Ayako Matsuoka[1], Reiko Nomura[12], Hajime Yano[1], Takayuki Hirai[13], Atsushi Kumamoto[9], Ryosuke Nakamura[14], Stephan Ulamec[15], Ralf Jaumann[15], Jean-Pierre Bibring[16], Noel Grand[17], Cyril Szopa[18], Ernesto Palomba[19], Jorn Helbert[15], Alain Herique[20], Matthias Grott[15], Hans-Ulrich Auster[21], Goester Klingelhoefer[22], Fumi Yoshida[13], Makoto Yoshikawa[1], Jun Matsumoto[1], Toshihiro Chujo[1], Masanori Matsushita[1], Takanao Saiki[1], Hideki Kato[1], Osamu Mori[1], Junichiro Kawaguchi[1]

1. Japan Aerospace Exploration Agency, 2. University of Tokyo, 3. Yokohama National University, 4. Japan Agency for Marine-Earth Science and Technology, 5. Osaka University, 6. Hiroshima University, 7. Hokkaido University, 8. Kwansei Gakuin University, 9. Tohoku University, 10. Kanazawa University, 11. RIKEN, 12. National Astronomical Observatory of Japan, 13. Chiba Institute of Technology, 14. National Institute of Advanced Industrial Science and Technology, 15. German Aerospace Center, 16. Institut d’ Astrophysique Spatiale, 17. LISA, 18. LATMOS, 19. INAF-IAPS, 20. IPAG, 21. TU Braunschweig, 22. Leibniz Universität Hannover

The OKEANOS (Oversize Kite-craft for Exploration and AstroNautics in the Outer Solar system) is a mission under study to rendezvous with and land on a Jupiter Trojan asteroid [1]. The target is a Jupiter Trojan but will be the Saturnian system in the future. It is an engineering mission to demonstrate advanced technologies such as the hybrid thrusting with the enhanced ion engine powered by a 40 x 40 m class large area solar cells to explore the outer solar system cost-effectively. With the new technology, the mission will conduct in-depth scientific measurements for understanding the origin and evolution of the solar system and life. The concept is complementary to NASA Lucy mission [2], multi-flybys to six Jupiter Trojans for understanding the variation of Jupiter Trojans.

Jupiter Trojans are D/P-types enriched in volatiles. They might have experienced almost no or only a low degree of alteration. Their origin and evolution, as well as chemical and physical state still remain unknown. Jupiter Trojans should be a missing link of materials that originate from the inner or the outer solar system by gravity scattering due to migration of giant planets [3]. They are key targets to understand the evolution of astromaterials and the radial distribution of elements and isotopes in the early solar system.

The OKEANOS has been downscaled from the previous proposal [4] due to the severe cost cap. The spacecraft of 1400 kg including a 40 kg lander will be launched in 2027 or later, assisted by gravity of Earth and Jupiter. It will arrive at the target asteroid after a 13-year cruise. 30 kg is allocated for science, 12 kg of which is reserved for international collaboration. Bus instruments such as the optical navigation cameras (ONC-T and -W), LIDAR, and radio science are used for scientific purposes. The lander is like Mascot with uprighting capability on the asteroid surface and 12 kg is allocated for science mission.

During the cruise, science experiments will be carried out from the “deep-space platform”. Measurements of IDPs and magnetic fields will continuously monitor their radial distribution in the solar system and sudden events. The gamma-ray polarimeter will be used for precise positioning of gamma-ray bursts using a very long baseline. Visible to near-infrared telescope will map the zodiacal lights and observe the deep sky under a dust-free condition from outside of the asteroid main belt.

©2019. Japan Geoscience Union. All Right Reserved.

After arrival, global mapping is carried out to characterize the asteroid and select the landing site. The asteroid shape, size, rotation state, and geologic features are imaged by ONC. Gravity is measured by radio tracking and LIDAR. Near-infrared spectroscopy characterizes red or less red patterns, the degree of hydration, mineralogy, and abundance of ices, organics, and brines. Thermal infrared multi-bands inform on thermophysical properties, mineralogy and amorphous phases. A radar probes the surface physical state and also contributes to altimetry. *In situ* experiments with the lander will characterize the footprint and surrounding area by imaging and spectroscopy, followed by measurements of mineralogical, elemental, and organic composition as well as physical, thermal, and magnetic properties at the site. The asteroid surface sample is collected to conduct high-resolution mass spectroscopy (HRMS) based on MULTUM system (infi-TOF type mass spectrometer [5]), especially to determine the isotopic ratios of δD and δ^{15}N and the volatile species contained in the sample. Details will be decided during the critical joint study in 2019. Those experiences will be inherited to future missions.

References: [1] Mori O. et al. (2018) Trans. JSASS Aerospace Tech. Japan, 16, 328-333. [2] Levison H.F. et al. (2016) Lunar Planet. Sci. Conf., 47, #2061. [3] Morbidelli A. et al. (2005) *Nature 435*, 462-466. [4] Okada T. et al. (2018) Planet. Space Sci. 161, 99-106. [6] Toyoda M. et al. (2003) J. Mass Spectrom. 38, 1125-1142.

Keywords: Solar Sail, Trojan, Landing

©2019. Japan Geoscience Union. All Right Reserved.

Magnetic field model of Jovian magnetosphere

*Naoya Momoki[1], Hiroaki TOH[1]

1. Division of Earth and Planetary Sciences, Graduate School of Science, Kyoto University

Europa, Ganymede, Callisto are the Jovian icy satellites called Galilean moons, and are possibly with internal oceans each. While ice is almost an insulator electrically, water including ions has high electrical conductivity, and existence of internal oceans can be verified using electromagnetic (EM) induction methods. In this study, we updated the necessary model of the external magnetic field to the icy satellites for the EM induction studies. Namely, parameters of the Euler potential model of the Jovian magnetosphere (Khurana, 1997) were renewed by adding magnetic data from both Galileo and JUNO spacecrafts.

The configuration of the Jovian current sheet was modeled by Khurana [1992] using three parameters, while the Jovian magnetospheric magnetic field modeled by Khurana [1997] was characterized by 14 parameters. We applied a non-linear optimization technique, i.e., the steepest descent method, to the parameters by newly adding magnetic data from Galileo and Juno spacecrafts. We minimized the root mean squared between the model and the data by exploring the parameter space around several initial sets of the parameters.

As a result, time-varying model parameters for each spacecraft orbit were obtained. Their temporal variation may reflect that of both magnetic field and electric current system in the Jovian magnetosphere.The changes of the parameters can be attributed to the interaction between the Jovian magnetosphere and the solar wind. It, therefore, preferable that the temporal variation of the model parameters is incorporated when the updated magnetic field model of the Jovian magnetosphere is applied to the EM induction studies in search for the internal oceans of the icy satellites.

Keywords: Jupiter, Magnetosphere

©2019. Japan Geoscience Union. All Right Reserved.

Enhancement of the Jovian thermospheric temperature above the Great Red Spot based on the infrared spectroscopic data obtained with IRTF/iSHELL

*Ayumu Kambara[1], Hajime Kita[2], Takeshi Sakanoi[1], Yasumasa Kasaba[1], Masato Kagitani[1], Haruna Watanabe[1]

1. Planetary Plasma and Atmospheric Research Center, Graduate School of Science, Tohoku University, 2. Institute of Space and Astronautical Science, Japan Aerospace Exploration Agency

It is known that the thermospheric temperature of all giant planets including Jupiter is several hundred kelvins higher than that expected from solar heating. At mid- to low-latitudes, although the direct atmospheric heating caused by precipitating particles and the energy transportation from high-latitude auroral region have been considered, it is not enough to explain. Another candidate for the heating is energy transportation by atmospheric waves from the lower atmosphere. Recently, O'Donoghue *et al.* [2016] revealed the heating in the thermosphere above the Great red spot from the intensity ratio of two emission lines (3.383um/3.454um) of the vibrational-rotational spectrum of thermospheic H_3^+ taken by IRTF /SpeX (R~2500) in December 2012. They estimated that the temperature above the Great red spot is 1644±161K, and that on surrounding mid- to low-latitude region is 900±42K. They considered that the reason was the energy transport from the lower atmosphere in the Great red spot region, that is, the propagation of atmospheric gravity waves and acousitic waves generated in the Great red spot, the tropospheric anticyclonic storm, to the thermosphere. However, the infrared spectrum observed SpeX might be contaminated by CH_4 line due to its low-resolution capability.
In this study, we carried out the thermosphere temperature observation in the Jovian mid-latitude region near the Great red spot by IRTF/iSHELL on January 11, 2017. This observation was performed with the iSHELL's Lp1-mode (3.265-3.657um), and the data reduction was performed with NASA's data reduction tool Spextool ver. 5.0.1. Similar to the past study by O'Donoghue *et al.* [2016], we adopted the intensity ratio of two emission lines of H_3^+ (3.3839um/3.4548um), and estimated the temperature precisely distinguished from CH_4 line by iSHELL’s higher wavelength resolution (R~75000). As a result, we estimated the thermospheric temperature above the Great red spot to be 910±132K, and that in the surrounding region to be 583±30K, showing about 300K increase on Great red spot. The estimated temperature was lower than that in O’Donoghue *et al.* [2016], there is possibility that the thermosphere temperature varies in time. However, we confirmed the temperature above Great red spot is higher than that in the surrounding region. This suggests the existence of energy transport from the lower to the upper atmosphere in the Great red spot. In the presentation, we report the result of carefully reduction.

Keywords: Jupiter, Great red spot, Thermosphere

©2019. Japan Geoscience Union. All Right Reserved.

Pulsation-like variation of Jovian infrared polar emission observed by Subaru 8-m: H3+ and methane emissions

*Yasumasa Kasaba[1], Haruna Watanabe[1], Hajime Kita[2], Chihiro Tao[3], Takeshi Sakanoi[1], Masato Kagitani[1], Orton Glenn[1,4], James Sinclair[4]

1. Planetary Plasma and Atmospheric Research Center, 2. ISAS/JAXA, 3. NICT, 4. NASA/JPL

In the Jovian high-latitude region, there are emissions with various wavelengths ranges, morphologies, and time variations. They are important tracers of energy injection carried by auroral particles that precipitate from the magnetosphere. The polar IR emissions excited in the Jovian upper atmosphere, which include the H_3^+ aurora and thermal emissions of hydrocarbons, reflect not only the abundance of emission sources but also the thermal structures. Both are affected by auroral precipitation into the source region. It is known that, in the polar region inner than the auroral oval, the flux of auroral precipitation can have time variations over various scales from years to seconds.

The H_3^+ aurora observed in near infrared is emitted in thermosphere / ionosphere from thermally excited H_3^+ ions above the CH_4 homopause. Auroral precipitation ionized H_2 and produce H_3^+ ions through ion chemistries. In previous observational studies, the shortest timescale of H_3^+ auroral intensity change was ~30 min, but detected by ~16-min step imaging. We performed the temporal imaging observation of the Jovian H_3^+ IR aurora with Subaru/IRCS and the H_3^+ narrow-band filter on 31 January 2015 and 25 May 2016. The adaptive optics enabled us to see the target with high spatial resolution (~0.2 arcsec). From the images obtained with time resolution of ~150 s on 25 May 2016, we detected a patch-like auroral feature pulsating with a period of ~10 min in noon sector of northern polar region. On the other hand, we could not find any periodic variations from the data obtained on 31 January 2015, which was obtained as slit-viewer image for the other study, and whose time intervals of ~10–30 min every several images was not optimized to this research. In addition, the location where the patch-like emissions observed with high intensities on 25 May 2016 were not so bright on 31 January 2015. The patch-like auroral feature that was pulsating during our observation period on 25 May 2016 have been sometimes observed in UV, but not always. Previous UV observations reported some pulsating auroral features with the periods of ~2–11 min in the northern polar region. However, the locations of them are not consistent with the patch-like feature in this study. The pulsation period of the X-ray aurora, which has a hot spot coinciding with our patch-like IR aurora, is 40–50 min. This region is estimated to connect magnetically to out of the magnetopause, and auroral precipitation there can be caused by dayside reconnection between the Jovian magnetospheric field and interplanetary field.

On the other hand, the hydrocarbon polar emission observed in mid-infrared is emitted from the whole stratosphere. From their locations and morphologies, it is estimated to be related with auroral particles penetrating under the homopause. However, the mechanisms of this link (composition change and/or heating by particle precipitations) are not well understood. Previous studies found the intensity time variation of polar CH_4 emission over days and months. We tried to detect the time variation of CH_4 emission intensity by continuous imaging observations of the northern polar region over several tens of minutes on 31 March, 24 and 25 May 2018 with Subaru/COMICS. We obtained the images using the 7.8 μm filter, which is sensitive to the CH_4 thermal emissions occurring in the pressure range of 20–0.5 mbar and 1 μbar in the Jovian upper stratosphere, with time resolution of ~1 min. On all observation days, the polar region was not bright in 7.8 μm. In addition, we could not find clear time variations of polar CH_4 emission intensity during our observation periods, 25, 50 and 60 min on 31 March, 24 and 25 May 2018.

©2019. Japan Geoscience Union. All Right Reserved.

This observation result is consistent to the model estimation by *Kuroda et al.* [2014], which suggested the relaxation time of hydrocarbon thermal emissions in the Jovian upper stratosphere, where is a possible source region of polar CH_4 emission, is at least ~10^5 s (~28 h).

Keywords: Jupiter, polar emission, H3+, CH4, short time variations

©2019. Japan Geoscience Union. All Right Reserved.

Structure of Io plasma torus observed with the Tohoku 60-cm telescope

*Masato Kagitani[1], Fuminori Tsuchiya[1], Kazuo Yoshioka[2], Go Murakami[3], Tomoki Kimura[1], Ryoichi Koga[1], Reina Hikida[4], Takeshi Sakanoi[1]

1. Graduate School of Science, Tohoku University, 2. Graduate School of frontier Science, The University of Tokyo, 3. Institute of Space and Astronautical Science, Japan Aerospace Exploration Agency, 4. Department of Earth and Planetary Science, Graduate School of Science, Tokyo University

Volcanic gases (mainly composed of SO_2, SO and S) originated from jovian satellite Io are ionized by interaction with magnetospheric plasma and then form a donut-shaped region called Io plasma torus. Ion pickup is the most significant energy source on the plasma torus though, distribution of pick-up region and its variability is still unclear. Density profiles of ions along the magnetic field line are determined under condition of diffusive equilibrium. Based on the equilibrium, plasma equator is close to the centrifugal equator though, higher ion anisotropy moves the plasma equator toward the magnetic equator. Measuring ion distribution with enough spatial resolution enables us to derive ion anisotropy which is tightly related to the amount of fresh pickup ion. On this study, we focus on variability of latitudinal structure of Io plasma torus as well as its radial structure using ground-based observation over six month period in 2018. The ground-based observation of sulfur ion emission, [SII] 671.6nm and 673.1nm was made at Haleakala observatory in Hawaii during March through August 2018 using the Tohoku 60-cm telescope (T60). A monochromatic imager with coronagraph attached onto the Cassegrain focus of T60 enables to measure distribution of S^+ with spatial resolution of 0.03 jovian radii (R_J). A digital micro-mirror device DMD was employed to block light from Jupiter disk and Galilean moons. Typical integration time of each frame was 20 minutes and total number of reduced image is 480. We also made observation of neutral sodium cloud extending up to several hundred of R_J as a proxy of supply of neutral particles from Io (Yoneda et al., 2015). Based on observation over the six month, [SII] brightness increases from DOY 80 through 140, then gradually decreases though DOY 230 in 2018. The data reduction of iogenic neutral sodium cloud is still undergoing though, neutral sodium cloud seems to increase from DOY 50 through 135, as [SII] brightness increases. The result suggests that increased volcanic activity from DOY 50-135 caused increase of S+ and brightening of [SII] emission. As for variability of shorter duration, we find [SII] brightening event within a short period (< 2 days) at around 28 through 30 July over a small region (< 30 degrees in longitude). [SII] 671.6 and 673.1 nm emissions are sensitive to cold electron (1-10eV) rather than hot electron (>100eV). Thus, increase of cold electron temperature explains the observed [SII] brightening well as the EUV space telescope Hisaki observed brightening of Io plasma torus associated with injection of hot electron. We also find variation of latitudinal structure of Io plasma torus. Longitudinal peak of S^+ emission at the same system III longitude 279 degree are -0.73, -0.80 and -0.79 R_J on 26, 29 July 7 and August, respectively. The shift of S^+ density peak toward magnetic equator implies higher anisotropy 29 on July and 7 August compared with 26 July. One of the possible explanation of the latitudinal shift of S^+ plasma is an increase of flesh pickup ion which makes higher anisotropy. Further study using Colorado Io Plasma Torus Emission Package (CITEP) will be presented on the presentation to take into account for line-of-sight integration effect of the ground-based observation.

Keywords: Io plasma torus

©2019. Japan Geoscience Union. All Right Reserved.

Ion Scale Height Variability in Hisaki Io Torus Observations

*Nicholas McCord Schneider[1], Carl Schmidt[2], Masato Kagitani[3], Yasumasa Kasaba[3], Tomoki Kimura[3], Go Murakami[4], Fuminori Tsuchiya[3], Hajime Kita[3], Reina Hikida[5], Ichiro Yoshikawa[5], Kazuo Yoshioka[5]

1. LASP, University of Colorado Boulder, 2. Boston University, 3. Tohoku University, 4. ISAS/JAXA, 5. University of Tokyo

Ion temperature is a critical variable in Io plasma torus energetics, but is difficult to derive from remote sensing measurements. The relative importance of hot ions vs. hot electrons in powering the torus emissions remains an open question. Torus brightenings, whether caused by episodic changes in the volcanic supply to the torus or periodic System III/IV enhancements, offer the best chance to search for driving variations in hot electrons or ions. Much attention has been paid to hot electron populations, derivable from detailed spectral modeling, but less work has been done on ion temperature. Ground-based studies have successfully derived $T_{\perp}$ from very high resolution spectra, and $T_{||}$ from scale height measurements in images, both over limited datasets. Schneider et al. 1997 found strong longitudinal variations in $T_{||}$ during a week-long dataset, and anti-correlated System III brightness, but more extended followup datasets have not previously been available.

The Hisaki dataset presents the possibility of an unparalleled opportunity to study long-term and short-term variations in ion temperatures. The instrument is not designed to take images of specific emissions, but its large entrance slit accepts the full height and width of the torus. In the ideal case, each spectral emission feature would appear as an image of the torus at its appropriate position in the spectrum, creating an “overlapogram” (as did the Cassini UVIS instrument). In reality, the emissions are blurred due to instrumental resolution and aberrations, and multiple spectral feature overlap. Furthermore, the changing opening angle of the rotating torus adds a spurious apparent scale height variation which must be removed, with special attention to asymmetries introduced by Jupiter's changing tilt. With allowances for all these effects, we will report on our search for ion temperature variations during the first two years of Hisaki observations, and compare our results to a previous independent study by M. Shishido (M.S. thesis, U. Tohoku).

Keywords: Jupiter, Io, plasma torus, magnetosphere , hisaki, ultraviolet

©2019. Japan Geoscience Union. All Right Reserved.

Size of the Smallest Particles in Saturn's Rings

*Keiji Ohtsuki[1], Hiroshi Kawamura[1], Naoyuki Hirata[1], Hiroshi Daisaka[2], Hiroshi Kimura[3]

1. Graduate School of Science, Kobe University, 2. Graduate School of Commerce and Management, Hitotsubashi University, 3. Planetary Exploration Research Center, Chiba Institute of Technology

Spacecraft and ground-based observations have shown that particles in Saturn's main rings have a power-law distribution roughly between centimeter and ten meters, but sub-centimeter particles appear to be lacking. Recent studies based on Cassini observations suggest that the size of the smallest particles is on the order of millimeters. Cohesive force between particles has been proposed to explain the paucity of sub-centimeter particles, but its strength depends on impact velocity. In order to better understand recent Cassini observations about small ring particles, we examine impact velocity between ring particles using N-body simulation including size distribution. We find that most collisions take place at velocities lower than 0.1 cm per second; even in dense rings where particles' velocity dispersion is enhanced by gravitational wakes, they collide at such low velocities because particles tend to move coherently in the wakes. This velocity is too low to detach sub-centimeter particles that are attached to the surface of large ones due to the cohesive force, explaining their paucity in the main rings. On the other hand, more infrequent high-velocity impacts can release millimeter-sized particles strongly attached to the surface of large ones, explaining the observed free millimeter-sized particles with relatively low abundance. We will discuss implications of our results for the observed size of the smallest particles in Saturn's main rings.

Keywords: Saturn, rings, Cassini

©2019. Japan Geoscience Union. All Right Reserved.

The Radio & Plasma Wave Investigation (RPWI) for JUICE for the investigation of Jupiter and Icy Moons System: Contributions from Japan

*Yasumasa Kasaba[1], Hiroaki Misawa[1], Fuminori Tsuchiya[1], Atsushi Kumamoto[2], Yuto Katoh[2], Tomoki Kimura[2], Hajime Kita[3], J.-E. Wahlund[4]

1. Planetary Plasma and Atmospheric Research Center, Tohoku University, 2. Department of Geophysics, Tohoku University, 3. ISAS/JAXA, 4. IRF Uppsala, Sweden

The Radio & Plasma Wave Investigation (RPWI) for the ESA JUICE mission (launch: 2022, Observations: 2030s) provides an elaborate suite of electromagnetic fields and plasma instruments. RPWI focuses on cold plasma studies and will investigate how the transfer of momentum and energy in the Jovian huge magnetosphere and the electrodynamic coupling with the icy Galilean moons. Remote sensing and direction finding of the Jovian radio emissions will be carried out. This capability is also devoted to the ices and the deep interiors of the icy moons. Investigations of the ice shells will be performed by means of a novel passive ground penetrating radar technique, which utilizes Jovian strong radio emissions as the transmitted signal. On the Ganymede orbit, continuous measurements of the electric field with the JUICE Magnetometer (JMAG) measurements will determine the electric coupling between any ocean, the ionosphere, and the magnetosphere, and provide the constraints on the physical characteristics of the subsurface ocean of Ganymede.
For those objectives, RPWI sensors consist of 4 Langmuir probes (LP-PWI) for determination of the vector electric field up to 1.6 MHz and cold plasma properties (including active measurements by LP sweeps and mutual impedance sounding) up to 1.6 MHz, a tri-axial search coil magnetometer (SCM) for determination of the vector magnetic field up to 20 kHz, and a tri-dipole antenna system (RWI) for monitoring of radio emissions (80 kHz - 45 MHz). From Japan, the RWI preamp and its High Frequency receiver with the onboard software will be provided, based on the modifications from the BepiColombo PWI and Arase PWE developments. Since Arase already shows the good performance in the radiation hard environment around Earth, we have enough confidence for the possible functions and performance on the Jovian hard environment. We will also provide Software Wave-Particle Interaction Analyzer (SWPIA) function to RPWI DPU, for the onboard quantitative detection of electromagnetic field - ion interactions, modifying from the Arase SWPIA which is also activating on the space now.
HF reciever will provide the first highly-resolved information of Jovian radio emissions emitted from Jovian multiple regions including lightning activity and icy moons, by the 3-ch receiver system manufactured by Japan and Sweden connected to the 3-elements 1.25-m E-filed dipole antenna system manufactured by Poland and Japan. Highly matured onboard and ground data processing will also be provided by France and Japan. As a byproduct, reflected Jovian emission can also be expected from the boundary of icy crust and conductive liquid subsurface ocean. Such reflection components could be observed as the Lunar surface reflection of terrestrial auroral kilometric radiation (AKR) seen by Kaguya Lunar Radar Sounder. JUICE has the RIME (Radar for Icy Moons Exploration) instrument, an active radar which emits 9 MHz pulse from 16 m tip-to-tip antenna and tries to detect the ocean under ~10 km icy crust. Since the frequency of Jovian radiation is wider (several 100 kHz to several 10s MHz), RPWI will provide complementary information, including the vertical distributions of conductivity and permittivity in the icy crust.
In the srping 2019, we are manufacturing and testing the Flight Models (FM) which will be shipped in June - July 2019 to Europe. The long road are connected to the first Jupiter and outer planet tour of the

©2019. Japan Geoscience Union. All Right Reserved.

hardware from Japan.

Keywords: Jupiter, JUICE, Radio waves

©2019. Japan Geoscience Union. All Right Reserved.

Magnetic field experiment at Jupiter icy moons (JUICE J-MAG) and in-flight alignment calibration

*Ayako Matsuoka[1], Michele Karen Dougherty[2], Patrick Brown[2], Futoshi Takahashi[3], Hisayoshi Shimizu[4], Masaki Matsushima[5]

1. Research Division for Space Plasma, Institute of Space and Astronautical Science, Japan Aerospace Exploration Agency, 2. Imperial College London, 3. Kyushu University, 4. University of Tokyo, 5. Tokyo Institute of Technology

The magnetometer instrument (J-MAG) is one of the core instruments on the JUICE spacecraft and is critical for resolving prime science objectives of the mission. The importance of a magnetometer instrument on JUICE can be described under following themes. Firstly, the magnetic field drives the plasma processes occurring within the Jupiter system. Understanding such observations allows for a better understanding of dynamical plasma processes, of the generation of aurora and of the various current systems which arise within this rapidly rotating magnetosphere. Secondary, the magnetometer science which is unique to JUICE lies in being able to gain an understanding of the interior structure of the icy moons of Jupiter, specifically those of Ganymede, Callisto and Europa. Of particular interest are knowledge of the depth at which the liquid oceans reside beneath their icy surfaces, the strength of any internal magnetic fields such as at Ganymede and the strength of any induced magnetic fields arising within these oceans.

J-MAG science requirements result in a requirement on the spacecraft to determine accurate knowledge of the orientation of the fluxgate sensors (MAGIBS and MAGOB). Due to the long MAG boom it is not possible to meet J-MAG’ s alignment requirement by mechanical stability alone, therefore the spacecraft includes two orthogonal coils mounted around its body. The coils can be driven with a current which produces a measurable magnetic field vector at the fluxgate sensors. This signal can then be used by the fluxgates to track the variation in the sensor alignment. This technical note describes the results of an analysis using an alignment recovery technique that was developed for the Kaguya mission, applied to the specific case of JUICE, considering the relative positions of the fluxgate sensors with respect to the JACS coils.

We derived equations to calculate the directions of the measurement axes in the frame fixed to the spacecraft, namely alignment angles, from the measurement results of reference magnetic fields generated by JACS. The errors of the alignment angle estimation and their dependence on measurement noise as well as inaccuracy of the coil current intensity are examined. Based on the quantitative results, the requirements to the JACS design and operation to satisfy the requests to the alignment accuracy are determined.

Keywords: Jupiter, Jovian moons, magnetometer

©2019. Japan Geoscience Union. All Right Reserved.

Science targets of the GAnymede Laser Altimeter (GALA) for the JUICE mission

*Jun Kimura[1], Shunichi Kamata[2], Koji Matsumoto[3], Noriyuki Namiki[3], Keigo Enya[4], Masanori Kobayashi[5], Hiroshi Araki[3], Hirotomo Noda[3], Ko Ishibashi[5], Hauke Hussmann[6], Kay Lingenauber[6]

1. Osaka University, 2. Hokkaido University, 3. National Astronomical Observatory Japan, 4. ISAS/JAXA, 5. Chiba Institute of Technology, 6. German Aerospace Center (DLR), Berlin

The JUpiter Icy Moons Explorer (JUICE), led by European Space Agency, has started development toward launch in 2022 (arrival at Jupiter in 2029, and Ganymede orbit insertion in 2032), and we are now developing the GALA instrument onboard JUICE spacecraft collaborating with German Aerospace Center (DLR) and other institutions in Europe. GALA will acquire the key information for understanding the evolution of Jovian icy moons and to play an essential role in the JUICE's purpose: exploration of deep habitat.

Jovian icy moon Ganymede, which is the largest moon in the Solar System and the primary target of the JUICE, can be said to be one of the typical solid bodies along with terrestrial planets in terms of its size and the intrinsic magnetic field originated from the metallic core. However, current knowledge provided by previous explorations is extremely limited since it comes from only several fly-bys. The JUICE will unveil the whole picture of Ganymede by the first orbiting in the history around extra-terrestrial moon. Expected new big picture of the origin and evolution of Ganymede will not only be a key to unveil the origin of diversity among the Solar System bodies, but also contribute to an understanding of exoplanets with a wide diversity.

The GALA will measure a distance between the spacecraft and the surface of icy moons and acquire the topography data (globally for Ganymede, and fly-by region for Europa and Callisto). It will be a first-ever laser altimetry for the icy object. Such information makes surface geologies clear and tremendously improves our understanding of the icy tectonics. By comparing their tectonic styles on the rocky planets/moons, GALA data leads to reconsider the Earth's plate tectonics. In addition, the GALA will confirm a presence/absence of the subsurface ocean by measuring tidal and rotational response, and the gravitational information reflecting the interior structure will be greatly improved. Furthermore, strength and waveform of reflected laser pulse have an information about surface reflectance at the laser wavelength and small-scale roughness. Finally we can see degrees of erosion and space weathering without being affected by illumination condition through GALA measurements.

In order to interpret and understand such measurements, accumulated studies for the Earth over the years will be effectively utilized: e.g., the data for surface topography, roughness and albedo will lead to describe the icy tectonics through the knowledge from terrestrial glaciology and experiments on impact and deformation process. The tidal measurements by GALA will also be a window to see its interior based on our knowledge and experiences cultivated through the past geodetic observations, e.g., the SELENE mission for the terrestrial Moon.

Characterization of the icy moons will be achieved not only from the GALA measurements but also synergy of other scientific instruments onboard JUICE spacecraft, for examples, surface images taken by optical camera (JANUS) will confirm the position of GALA laser footprint to complement the GALA "point" data for precise topographic mapping. A radar sounder (RIME) and a radio science experiment (3GM) probe

©2019. Japan Geoscience Union. All Right Reserved.

the interior structure, especially interior of the icy crust to figure out an occurrence of tectonic features. A visible and infrared imaging spectrometer (MAJIS), an ultraviolet imaging spectrograph (UVS) and a sub-millimeter wave instrument (SWI) will acquire a surface and atmosphere compositional data. A magnetometer (J-MAG) monitors moons' inductive response to the Jovian magnetic field and probes the subsurface ocean with the help of a particle environment package (PEP) and a radio and plasma wave investigation (RPWI). The GALA works closely together with these instruments and plays a leading and a supporting role to clarify the whole picture of Ganymede and other icy moons.

Keywords: Jupiter, Icy moons, Laser altimetry

©2019. Japan Geoscience Union. All Right Reserved.

Current status of the antenna developments, the data processing, scientific target for JUICE/SWI JAPAN.

*YASUKO KASAI[1], [Group] JUICE SWI Japanese Team

1. National Institute of Information and Communications Technology (NICT)

The Submillimetre-Wave Instrument (SWI) is one of the 10 scientific payloads on the JUpiter ICy moon Explorer (JUICE). The main scientific objectives of SWI is to investigate the structure, compositions and dynamics of the middle atmosphere of Jupiter and exosphere of its moons, as well as thermophysical properties if the satellite surfaces. SWI observations will provide pioneering direct measurements of atmospheric compositions in Jupiter system. SWI will performed limb and nadir observations in the frequency region 530-600 and 1075-1275 GHz. Japanese contribution is the development of main- and sub- reflectors, actuators for the instruments, feasibility studies, data processing, and scientific contributions. We present Current status of the antenna developments, the data processing, scientific target for JUICE/SWI JAPAN.

Keywords: Jupiter, Jovian moons, submm instrument, JUICE, SWI

©2019. Japan Geoscience Union. All Right Reserved.

[E] Poster | P (Space and Planetary Sciences)：P-PS Planetary Sciences

Tue. May 28, 2019 5:15 PM - 6:30 PM JST | Tue. May 28, 2019 8:15 AM - 9:30 AM UTC | Poster Hall International Exhibition Hall8, Makuhari Messe_1

[P-PS01] Outer Solar System Exploration Today, and Tomorrow

convener:Jun Kimura(Osaka University), Yasumasa Kasaba(Planetary Plasma and Atmospheric Research Center, Tohoku University), Kunio M. Sayanagi(Hampton University)

The giant planets provide many keys to understanding planetary processes. They play an important role in shaping our solar system, and the physical and chemical processes they harbor also provide a unique opportunity to study the phenomena relevant for studying Earth and other planets, including exoplanetary systems. In this session, we discuss a wide range of topics encompassing the giant planets and their moons, including their origins, interiors, atmospheres, compositions, surface features, and electromagnetic fields. To advocate for current and future outer planets exploration (Cassini, Juno, New Horizons, JUICE, and beyond), we also call for discussions on future missions to explore giant planet systems, including how to develop better international cooperation. Discussion in this latter category will include progress in developing a solar sail mission concept for observing the Jupiter system and its trojan asteroids.

[PPS01-P01] Critical Role of Entry Probes in Giant Planet Exploration

*Sushil K Atreya[1], Olivier Mousis[2] (1.University of Michigan Ann Arbor, 2.Laboratoire d'Astrophysique de Marseille)

[PPS01-P02] OKEANOS – Jupiter Trojan Asteroid Rendezvous and Landing Experiments Using a Solar Power Sail

*Tatsuaki Okada[1,2], Takahiro Iwata[1], Yoko Kebukawa[3], Motoo Ito[4], Jun Aoki[5], Yosuke Kawai[5], Shoichiro Yokota[5], Yoshifumi Saito[1], Kentaro Terada[5], Michisato Toyoda[5], Hikaru Yabuta[6], Hisayoshi Yurimoto[1,7], Shuji Matsuura[8], Kohji Tsumura[9], Daisuke Yonetoku[10], Tatehiro Mihara[11], Ayako Matsuoka[1], Reiko Nomura[12], Hajime Yano[1], Takayuki Hirai[13], Atsushi Kumamoto[9], Ryosuke Nakamura[14], Stephan Ulamec[15], Ralf Jaumann[15], Jean-Pierre Bibring[16], Noel Grand[17], Cyril Szopa[18], Ernesto Palomba[19], Jorn Helbert[15], Alain Herique[20], Matthias Grott[15], Hans-Ulrich Auster[21], Goester Klingelhoefer[22], Fumi Yoshida[13], Makoto Yoshikawa[1], Jun Matsumoto[1], Toshihiro Chujo[1], Masanori Matsushita[1], Takanao Saiki[1], Hideki Kato[1], Osamu Mori[1], Junichiro Kawaguchi[1] (1.Japan Aerospace Exploration Agency, 2.University of Tokyo, 3.Yokohama National University, 4.Japan Agency for Marine-Earth Science and Technology, 5.Osaka University, 6.Hiroshima University, 7.Hokkaido University, 8.Kwansei Gakuin University, 9.Tohoku University, 10.Kanazawa University, 11.RIKEN, 12.National Astronomical Observatory of Japan, 13.Chiba Institute of Technology, 14.National Institute of Advanced Industrial Science and Technology, 15.German Aerospace Center, 16.Institut d'Astrophysique Spatiale, 17.LISA, 18.LATMOS, 19.INAF-IAPS, 20.IPAG, 21.TU Braunschweig, 22.Leibniz Universität Hannover)

[PPS01-P03] Magnetic field model of Jovian magnetosphere

*Naoya Momoki[1], Hiroaki TOH[1] (1.Division of Earth and Planetary Sciences, Graduate School of Science, Kyoto University)

[PPS01-P04] Enhancement of the Jovian thermospheric temperature above the Great Red Spot based on the infrared spectroscopic data obtained with IRTF/iSHELL

*Ayumu Kambara[1], Hajime Kita[2], Takeshi Sakanoi[1], Yasumasa Kasaba[1], Masato Kagitani[1], Haruna Watanabe[1] (1.Planetary Plasma and Atmospheric Research Center, Graduate School of Science, Tohoku University, 2.Institute of Space and Astronautical Science, Japan Aerospace Exploration Agency)

[PPS01-P05] Pulsation-like variation of Jovian infrared polar emission observed by Subaru 8-m: H3+ and methane emissions

*Yasumasa Kasaba[1], Haruna Watanabe[1], Hajime Kita[2], Chihiro Tao[3], Takeshi Sakanoi[1], Masato Kagitani[1], Orton Glenn[1,4], James Sinclair[4] (1.Planetary Plasma and Atmospheric Research Center, 2.ISAS/JAXA,

3.NICT, 4.NASA/JPL)

[PPS01-P06] Structure of Io plasma torus observed with the Tohoku 60-cm telescope

*Masato Kagitani[1], Fuminori Tsuchiya[1], Kazuo Yoshioka[2], Go Murakami[3], Tomoki Kimura[1], Ryoichi Koga[1], Reina Hikida[4], Takeshi Sakanoi[1] (1.Graduate School of Science, Tohoku University, 2.Graduate School of frontier Science, The University of Tokyo, 3.Institute of Space and Astronautical Science, Japan Aerospace Exploration Agency, 4.Department of Earth and Planetary Science, Graduate School of Science, Tokyo University)

[PPS01-P07] Ion Scale Height Variability in Hisaki Io Torus Observations

*Nicholas McCord Schneider[1], Carl Schmidt[2], Masato Kagitani[3], Yasumasa Kasaba[3], Tomoki Kimura[3], Go Murakami[4], Fuminori Tsuchiya[3], Hajime Kita[3], Reina Hikida[5], Ichiro Yoshikawa[5], Kazuo Yoshioka[5] (1.LASP, University of Colorado Boulder, 2.Boston University, 3.Tohoku University, 4.ISAS/JAXA, 5.University of Tokyo)

[PPS01-P08] Size of the Smallest Particles in Saturn's Rings

*Keiji Ohtsuki[1], Hiroshi Kawamura[1], Naoyuki Hirata[1], Hiroshi Daisaka[2], Hiroshi Kimura[3] (1.Graduate School of Science, Kobe University, 2.Graduate School of Commerce and Management, Hitotsubashi University, 3.Planetary Exploration Research Center, Chiba Institute of Technology)

[PPS01-P09] The Radio & Plasma Wave Investigation (RPWI) for JUICE for the investigation of Jupiter and Icy Moons System: Contributions from Japan

*Yasumasa Kasaba[1], Hiroaki Misawa[1], Fuminori Tsuchiya[1], Atsushi Kumamoto[2], Yuto Katoh[2], Tomoki Kimura[2], Hajime Kita[3], J.-E. Wahlund[4] (1.Planetary Plasma and Atmospheric Research Center, Tohoku University, 2.Department of Geophysics, Tohoku University, 3.ISAS/JAXA, 4.IRF Uppsala, Sweden)

[PPS01-P10] Magnetic field experiment at Jupiter icy moons (JUICE J-MAG) and in-flight alignment calibration

*Ayako Matsuoka[1], Michele Karen Dougherty[2], Patrick Brown[2], Futoshi Takahashi[3], Hisayoshi Shimizu[4], Masaki Matsushima[5] (1.Research Division for Space Plasma, Institute of Space and Astronautical Science, Japan Aerospace Exploration Agency, 2.Imperial College London, 3.Kyushu University, 4.University of Tokyo, 5.Tokyo Institute of Technology)

[PPS01-P11] Science targets of the GAnymede Laser Altimeter (GALA) for the JUICE mission

*Jun Kimura[1], Shunichi Kamata[2], Koji Matsumoto[3], Noriyuki Namiki[3], Keigo Enya[4], Masanori Kobayashi[5], Hiroshi Araki[3], Hirotomo Noda[3], Ko Ishibashi[5], Hauke Hussmann[6], Kay Lingenauber[6] (1.Osaka University, 2.Hokkaido University, 3.National Astronomical Observatory Japan, 4.ISAS/JAXA, 5.Chiba Institute of Technology, 6.German Aerospace Center (DLR), Berlin)

[PPS01-P12] Current status of the antenna developments, the data processing, scientific target for JUICE/SWI JAPAN.

*YASUKO KASAI[1], JUICE SWI Japanese Team (1.National Institute of Information and Communications Technology (NICT))

Critical Role of Entry Probes in Giant Planet Exploration

*Sushil K Atreya[1], Olivier Mousis[2]

1. University of Michigan Ann Arbor, 2. Laboratoire d'Astrophysique de Marseille

Flyby and orbiting spacecraft have explored the giant planets since the early 1970’s. In situ measurements in the troposphere are essential, however, for constraining the models of formation, evolution and interior processes of the giant planets. The models employ abundances and isotopic ratios of key elements, in particular C,N, S, O, He, Ne, Ar, Kr, Xe and D/H, derived from the measurement of their (bulk) reservoir species. That was the scientific rationale for the 1995 Galileo Probe at Jupiter and a Saturn Probe in NASA’s New Frontiers list of candidate missions. Considering that the icy giant planets are distinct from the gas giants, they represent the missing pieces of the puzzle of the formation of the outer solar system, besides being the closest analog for nearly half of the confirmed exoplanets. Thus, their comprehensive exploration with an orbiter-probe spacecraft is essential. The principal focus of this talk is the science, feasibility and implementation strategy of in situ measurements with entry probes at the icy giant planets, Uranus and Neptune, guided by thermochemical models and lessons learned from the Galileo Probe and the ongoing Juno Orbiter. [www.umich.edu/~atreya]

Keywords: Icy Giants, Origin and Evolution, Uranus, Neptune, Entry Probes, Exoplanets

©2019. Japan Geoscience Union. All Right Reserved.

OKEANOS –Jupiter Trojan Asteroid Rendezvous and Landing Experiments Using a Solar Power Sail

*Tatsuaki Okada[1,2], Takahiro Iwata[1], Yoko Kebukawa[3], Motoo Ito[4], Jun Aoki[5], Yosuke Kawai[5], Shoichiro Yokota[5], Yoshifumi Saito[1], Kentaro Terada[5], Michisato Toyoda[5], Hikaru Yabuta[6], Hisayoshi Yurimoto[1,7], Shuji Matsuura[8], Kohji Tsumura[9], Daisuke Yonetoku[10], Tatehiro Mihara[11], Ayako Matsuoka[1], Reiko Nomura[12], Hajime Yano[1], Takayuki Hirai[13], Atsushi Kumamoto[9], Ryosuke Nakamura[14], Stephan Ulamec[15], Ralf Jaumann[15], Jean-Pierre Bibring[16], Noel Grand[17], Cyril Szopa[18], Ernesto Palomba[19], Jorn Helbert[15], Alain Herique[20], Matthias Grott[15], Hans-Ulrich Auster[21], Goester Klingelhoefer[22], Fumi Yoshida[13], Makoto Yoshikawa[1], Jun Matsumoto[1], Toshihiro Chujo[1], Masanori Matsushita[1], Takanao Saiki[1], Hideki Kato[1], Osamu Mori[1], Junichiro Kawaguchi[1]

1. Japan Aerospace Exploration Agency, 2. University of Tokyo, 3. Yokohama National University, 4. Japan Agency for Marine-Earth Science and Technology, 5. Osaka University, 6. Hiroshima University, 7. Hokkaido University, 8. Kwansei Gakuin University, 9. Tohoku University, 10. Kanazawa University, 11. RIKEN, 12. National Astronomical Observatory of Japan, 13. Chiba Institute of Technology, 14. National Institute of Advanced Industrial Science and Technology, 15. German Aerospace Center, 16. Institut d’ Astrophysique Spatiale, 17. LISA, 18. LATMOS, 19. INAF-IAPS, 20. IPAG, 21. TU Braunschweig, 22. Leibniz Universität Hannover

The OKEANOS (Oversize Kite-craft for Exploration and AstroNautics in the Outer Solar system) is a mission under study to rendezvous with and land on a Jupiter Trojan asteroid [1]. The target is a Jupiter Trojan but will be the Saturnian system in the future. It is an engineering mission to demonstrate advanced technologies such as the hybrid thrusting with the enhanced ion engine powered by a 40 x 40 m class large area solar cells to explore the outer solar system cost-effectively. With the new technology, the mission will conduct in-depth scientific measurements for understanding the origin and evolution of the solar system and life. The concept is complementary to NASA Lucy mission [2], multi-flybys to six Jupiter Trojans for understanding the variation of Jupiter Trojans.

Jupiter Trojans are D/P-types enriched in volatiles. They might have experienced almost no or only a low degree of alteration. Their origin and evolution, as well as chemical and physical state still remain unknown. Jupiter Trojans should be a missing link of materials that originate from the inner or the outer solar system by gravity scattering due to migration of giant planets [3]. They are key targets to understand the evolution of astromaterials and the radial distribution of elements and isotopes in the early solar system.

The OKEANOS has been downscaled from the previous proposal [4] due to the severe cost cap. The spacecraft of 1400 kg including a 40 kg lander will be launched in 2027 or later, assisted by gravity of Earth and Jupiter. It will arrive at the target asteroid after a 13-year cruise. 30 kg is allocated for science, 12 kg of which is reserved for international collaboration. Bus instruments such as the optical navigation cameras (ONC-T and -W), LIDAR, and radio science are used for scientific purposes. The lander is like Mascot with uprighting capability on the asteroid surface and 12 kg is allocated for science mission.

During the cruise, science experiments will be carried out from the “deep-space platform”. Measurements of IDPs and magnetic fields will continuously monitor their radial distribution in the solar system and sudden events. The gamma-ray polarimeter will be used for precise positioning of gamma-ray bursts using a very long baseline. Visible to near-infrared telescope will map the zodiacal lights and observe the deep sky under a dust-free condition from outside of the asteroid main belt.

©2019. Japan Geoscience Union. All Right Reserved.

After arrival, global mapping is carried out to characterize the asteroid and select the landing site. The asteroid shape, size, rotation state, and geologic features are imaged by ONC. Gravity is measured by radio tracking and LIDAR. Near-infrared spectroscopy characterizes red or less red patterns, the degree of hydration, mineralogy, and abundance of ices, organics, and brines. Thermal infrared multi-bands inform on thermophysical properties, mineralogy and amorphous phases. A radar probes the surface physical state and also contributes to altimetry. *In situ* experiments with the lander will characterize the footprint and surrounding area by imaging and spectroscopy, followed by measurements of mineralogical, elemental, and organic composition as well as physical, thermal, and magnetic properties at the site. The asteroid surface sample is collected to conduct high-resolution mass spectroscopy (HRMS) based on MULTUM system (infi-TOF type mass spectrometer [5]), especially to determine the isotopic ratios of δD and δ^{15}N and the volatile species contained in the sample. Details will be decided during the critical joint study in 2019. Those experiences will be inherited to future missions.

References: [1] Mori O. et al. (2018) Trans. JSASS Aerospace Tech. Japan, 16, 328-333. [2] Levison H.F. et al. (2016) Lunar Planet. Sci. Conf., 47, #2061. [3] Morbidelli A. et al. (2005) *Nature 435*, 462-466. [4] Okada T. et al. (2018) Planet. Space Sci. 161, 99-106. [6] Toyoda M. et al. (2003) J. Mass Spectrom. 38, 1125-1142.

Keywords: Solar Sail, Trojan, Landing

©2019. Japan Geoscience Union. All Right Reserved.

Magnetic field model of Jovian magnetosphere

*Naoya Momoki[1], Hiroaki TOH[1]

1. Division of Earth and Planetary Sciences, Graduate School of Science, Kyoto University

Europa, Ganymede, Callisto are the Jovian icy satellites called Galilean moons, and are possibly with internal oceans each. While ice is almost an insulator electrically, water including ions has high electrical conductivity, and existence of internal oceans can be verified using electromagnetic (EM) induction methods. In this study, we updated the necessary model of the external magnetic field to the icy satellites for the EM induction studies. Namely, parameters of the Euler potential model of the Jovian magnetosphere (Khurana, 1997) were renewed by adding magnetic data from both Galileo and JUNO spacecrafts.

The configuration of the Jovian current sheet was modeled by Khurana [1992] using three parameters, while the Jovian magnetospheric magnetic field modeled by Khurana [1997] was characterized by 14 parameters. We applied a non-linear optimization technique, i.e., the steepest descent method, to the parameters by newly adding magnetic data from Galileo and Juno spacecrafts. We minimized the root mean squared between the model and the data by exploring the parameter space around several initial sets of the parameters.

As a result, time-varying model parameters for each spacecraft orbit were obtained. Their temporal variation may reflect that of both magnetic field and electric current system in the Jovian magnetosphere.The changes of the parameters can be attributed to the interaction between the Jovian magnetosphere and the solar wind. It, therefore, preferable that the temporal variation of the model parameters is incorporated when the updated magnetic field model of the Jovian magnetosphere is applied to the EM induction studies in search for the internal oceans of the icy satellites.

Keywords: Jupiter, Magnetosphere

©2019. Japan Geoscience Union. All Right Reserved.

Enhancement of the Jovian thermospheric temperature above the Great Red Spot based on the infrared spectroscopic data obtained with IRTF/iSHELL

*Ayumu Kambara[1], Hajime Kita[2], Takeshi Sakanoi[1], Yasumasa Kasaba[1], Masato Kagitani[1], Haruna Watanabe[1]

1. Planetary Plasma and Atmospheric Research Center, Graduate School of Science, Tohoku University, 2. Institute of Space and Astronautical Science, Japan Aerospace Exploration Agency

It is known that the thermospheric temperature of all giant planets including Jupiter is several hundred kelvins higher than that expected from solar heating. At mid- to low-latitudes, although the direct atmospheric heating caused by precipitating particles and the energy transportation from high-latitude auroral region have been considered, it is not enough to explain. Another candidate for the heating is energy transportation by atmospheric waves from the lower atmosphere. Recently, O'Donoghue *et al.* [2016] revealed the heating in the thermosphere above the Great red spot from the intensity ratio of two emission lines (3.383um/3.454um) of the vibrational-rotational spectrum of thermospheic H_3^+ taken by IRTF /SpeX (R~2500) in December 2012. They estimated that the temperature above the Great red spot is 1644±161K, and that on surrounding mid- to low-latitude region is 900±42K. They considered that the reason was the energy transport from the lower atmosphere in the Great red spot region, that is, the propagation of atmospheric gravity waves and acousitic waves generated in the Great red spot, the tropospheric anticyclonic storm, to the thermosphere. However, the infrared spectrum observed SpeX might be contaminated by CH_4 line due to its low-resolution capability.
In this study, we carried out the thermosphere temperature observation in the Jovian mid-latitude region near the Great red spot by IRTF/iSHELL on January 11, 2017. This observation was performed with the iSHELL's Lp1-mode (3.265-3.657um), and the data reduction was performed with NASA's data reduction tool Spextool ver. 5.0.1. Similar to the past study by O'Donoghue *et al.* [2016], we adopted the intensity ratio of two emission lines of H_3^+ (3.3839um/3.4548um), and estimated the temperature precisely distinguished from CH_4 line by iSHELL’s higher wavelength resolution (R~75000). As a result, we estimated the thermospheric temperature above the Great red spot to be 910±132K, and that in the surrounding region to be 583±30K, showing about 300K increase on Great red spot. The estimated temperature was lower than that in O’Donoghue *et al.* [2016], there is possibility that the thermosphere temperature varies in time. However, we confirmed the temperature above Great red spot is higher than that in the surrounding region. This suggests the existence of energy transport from the lower to the upper atmosphere in the Great red spot. In the presentation, we report the result of carefully reduction.

Keywords: Jupiter, Great red spot, Thermosphere

©2019. Japan Geoscience Union. All Right Reserved.

Pulsation-like variation of Jovian infrared polar emission observed by Subaru 8-m: H3+ and methane emissions

*Yasumasa Kasaba[1], Haruna Watanabe[1], Hajime Kita[2], Chihiro Tao[3], Takeshi Sakanoi[1], Masato Kagitani[1], Orton Glenn[1,4], James Sinclair[4]

1. Planetary Plasma and Atmospheric Research Center, 2. ISAS/JAXA, 3. NICT, 4. NASA/JPL

In the Jovian high-latitude region, there are emissions with various wavelengths ranges, morphologies, and time variations. They are important tracers of energy injection carried by auroral particles that precipitate from the magnetosphere. The polar IR emissions excited in the Jovian upper atmosphere, which include the H_3^+ aurora and thermal emissions of hydrocarbons, reflect not only the abundance of emission sources but also the thermal structures. Both are affected by auroral precipitation into the source region. It is known that, in the polar region inner than the auroral oval, the flux of auroral precipitation can have time variations over various scales from years to seconds.

The H_3^+ aurora observed in near infrared is emitted in thermosphere / ionosphere from thermally excited H_3^+ ions above the CH_4 homopause. Auroral precipitation ionized H_2 and produce H_3^+ ions through ion chemistries. In previous observational studies, the shortest timescale of H_3^+ auroral intensity change was ~30 min, but detected by ~16-min step imaging. We performed the temporal imaging observation of the Jovian H_3^+ IR aurora with Subaru/IRCS and the H_3^+ narrow-band filter on 31 January 2015 and 25 May 2016. The adaptive optics enabled us to see the target with high spatial resolution (~0.2 arcsec). From the images obtained with time resolution of ~150 s on 25 May 2016, we detected a patch-like auroral feature pulsating with a period of ~10 min in noon sector of northern polar region. On the other hand, we could not find any periodic variations from the data obtained on 31 January 2015, which was obtained as slit-viewer image for the other study, and whose time intervals of ~10–30 min every several images was not optimized to this research. In addition, the location where the patch-like emissions observed with high intensities on 25 May 2016 were not so bright on 31 January 2015. The patch-like auroral feature that was pulsating during our observation period on 25 May 2016 have been sometimes observed in UV, but not always. Previous UV observations reported some pulsating auroral features with the periods of ~2–11 min in the northern polar region. However, the locations of them are not consistent with the patch-like feature in this study. The pulsation period of the X-ray aurora, which has a hot spot coinciding with our patch-like IR aurora, is 40–50 min. This region is estimated to connect magnetically to out of the magnetopause, and auroral precipitation there can be caused by dayside reconnection between the Jovian magnetospheric field and interplanetary field.

On the other hand, the hydrocarbon polar emission observed in mid-infrared is emitted from the whole stratosphere. From their locations and morphologies, it is estimated to be related with auroral particles penetrating under the homopause. However, the mechanisms of this link (composition change and/or heating by particle precipitations) are not well understood. Previous studies found the intensity time variation of polar CH_4 emission over days and months. We tried to detect the time variation of CH_4 emission intensity by continuous imaging observations of the northern polar region over several tens of minutes on 31 March, 24 and 25 May 2018 with Subaru/COMICS. We obtained the images using the 7.8 μm filter, which is sensitive to the CH_4 thermal emissions occurring in the pressure range of 20–0.5 mbar and 1 μbar in the Jovian upper stratosphere, with time resolution of ~1 min. On all observation days, the polar region was not bright in 7.8 μm. In addition, we could not find clear time variations of polar CH_4 emission intensity during our observation periods, 25, 50 and 60 min on 31 March, 24 and 25 May 2018.

©2019. Japan Geoscience Union. All Right Reserved.

This observation result is consistent to the model estimation by *Kuroda et al.* [2014], which suggested the relaxation time of hydrocarbon thermal emissions in the Jovian upper stratosphere, where is a possible source region of polar CH_4 emission, is at least ~10^5 s (~28 h).

Keywords: Jupiter, polar emission, H3+, CH4, short time variations

©2019. Japan Geoscience Union. All Right Reserved.

Structure of Io plasma torus observed with the Tohoku 60-cm telescope

*Masato Kagitani[1], Fuminori Tsuchiya[1], Kazuo Yoshioka[2], Go Murakami[3], Tomoki Kimura[1], Ryoichi Koga[1], Reina Hikida[4], Takeshi Sakanoi[1]

1. Graduate School of Science, Tohoku University, 2. Graduate School of frontier Science, The University of Tokyo, 3. Institute of Space and Astronautical Science, Japan Aerospace Exploration Agency, 4. Department of Earth and Planetary Science, Graduate School of Science, Tokyo University

Volcanic gases (mainly composed of SO_2, SO and S) originated from jovian satellite Io are ionized by interaction with magnetospheric plasma and then form a donut-shaped region called Io plasma torus. Ion pickup is the most significant energy source on the plasma torus though, distribution of pick-up region and its variability is still unclear. Density profiles of ions along the magnetic field line are determined under condition of diffusive equilibrium. Based on the equilibrium, plasma equator is close to the centrifugal equator though, higher ion anisotropy moves the plasma equator toward the magnetic equator. Measuring ion distribution with enough spatial resolution enables us to derive ion anisotropy which is tightly related to the amount of fresh pickup ion. On this study, we focus on variability of latitudinal structure of Io plasma torus as well as its radial structure using ground-based observation over six month period in 2018. The ground-based observation of sulfur ion emission, [SII] 671.6nm and 673.1nm was made at Haleakala observatory in Hawaii during March through August 2018 using the Tohoku 60-cm telescope (T60). A monochromatic imager with coronagraph attached onto the Cassegrain focus of T60 enables to measure distribution of S^+ with spatial resolution of 0.03 jovian radii (R_J). A digital micro-mirror device DMD was employed to block light from Jupiter disk and Galilean moons. Typical integration time of each frame was 20 minutes and total number of reduced image is 480. We also made observation of neutral sodium cloud extending up to several hundred of R_J as a proxy of supply of neutral particles from Io (Yoneda et al., 2015). Based on observation over the six month, [SII] brightness increases from DOY 80 through 140, then gradually decreases though DOY 230 in 2018. The data reduction of iogenic neutral sodium cloud is still undergoing though, neutral sodium cloud seems to increase from DOY 50 through 135, as [SII] brightness increases. The result suggests that increased volcanic activity from DOY 50-135 caused increase of S+ and brightening of [SII] emission. As for variability of shorter duration, we find [SII] brightening event within a short period (< 2 days) at around 28 through 30 July over a small region (< 30 degrees in longitude). [SII] 671.6 and 673.1 nm emissions are sensitive to cold electron (1-10eV) rather than hot electron (>100eV). Thus, increase of cold electron temperature explains the observed [SII] brightening well as the EUV space telescope Hisaki observed brightening of Io plasma torus associated with injection of hot electron. We also find variation of latitudinal structure of Io plasma torus. Longitudinal peak of S^+ emission at the same system III longitude 279 degree are -0.73, -0.80 and -0.79 R_J on 26, 29 July 7 and August, respectively. The shift of S^+ density peak toward magnetic equator implies higher anisotropy 29 on July and 7 August compared with 26 July. One of the possible explanation of the latitudinal shift of S^+ plasma is an increase of flesh pickup ion which makes higher anisotropy. Further study using Colorado Io Plasma Torus Emission Package (CITEP) will be presented on the presentation to take into account for line-of-sight integration effect of the ground-based observation.

Keywords: Io plasma torus

©2019. Japan Geoscience Union. All Right Reserved.

Ion Scale Height Variability in Hisaki Io Torus Observations

*Nicholas McCord Schneider[1], Carl Schmidt[2], Masato Kagitani[3], Yasumasa Kasaba[3], Tomoki Kimura[3], Go Murakami[4], Fuminori Tsuchiya[3], Hajime Kita[3], Reina Hikida[5], Ichiro Yoshikawa[5], Kazuo Yoshioka[5]

1. LASP, University of Colorado Boulder, 2. Boston University, 3. Tohoku University, 4. ISAS/JAXA, 5. University of Tokyo

Ion temperature is a critical variable in Io plasma torus energetics, but is difficult to derive from remote sensing measurements. The relative importance of hot ions vs. hot electrons in powering the torus emissions remains an open question. Torus brightenings, whether caused by episodic changes in the volcanic supply to the torus or periodic System III/IV enhancements, offer the best chance to search for driving variations in hot electrons or ions. Much attention has been paid to hot electron populations, derivable from detailed spectral modeling, but less work has been done on ion temperature. Ground-based studies have successfully derived $T_{\perp}$ from very high resolution spectra, and $T_{||}$ from scale height measurements in images, both over limited datasets. Schneider et al. 1997 found strong longitudinal variations in $T_{||}$ during a week-long dataset, and anti-correlated System III brightness, but more extended followup datasets have not previously been available.

The Hisaki dataset presents the possibility of an unparalleled opportunity to study long-term and short-term variations in ion temperatures. The instrument is not designed to take images of specific emissions, but its large entrance slit accepts the full height and width of the torus. In the ideal case, each spectral emission feature would appear as an image of the torus at its appropriate position in the spectrum, creating an “overlapogram” (as did the Cassini UVIS instrument). In reality, the emissions are blurred due to instrumental resolution and aberrations, and multiple spectral feature overlap. Furthermore, the changing opening angle of the rotating torus adds a spurious apparent scale height variation which must be removed, with special attention to asymmetries introduced by Jupiter's changing tilt. With allowances for all these effects, we will report on our search for ion temperature variations during the first two years of Hisaki observations, and compare our results to a previous independent study by M. Shishido (M.S. thesis, U. Tohoku).

Keywords: Jupiter, Io, plasma torus, magnetosphere , hisaki, ultraviolet

©2019. Japan Geoscience Union. All Right Reserved.

Size of the Smallest Particles in Saturn's Rings

*Keiji Ohtsuki[1], Hiroshi Kawamura[1], Naoyuki Hirata[1], Hiroshi Daisaka[2], Hiroshi Kimura[3]

1. Graduate School of Science, Kobe University, 2. Graduate School of Commerce and Management, Hitotsubashi University, 3. Planetary Exploration Research Center, Chiba Institute of Technology

Spacecraft and ground-based observations have shown that particles in Saturn's main rings have a power-law distribution roughly between centimeter and ten meters, but sub-centimeter particles appear to be lacking. Recent studies based on Cassini observations suggest that the size of the smallest particles is on the order of millimeters. Cohesive force between particles has been proposed to explain the paucity of sub-centimeter particles, but its strength depends on impact velocity. In order to better understand recent Cassini observations about small ring particles, we examine impact velocity between ring particles using N-body simulation including size distribution. We find that most collisions take place at velocities lower than 0.1 cm per second; even in dense rings where particles' velocity dispersion is enhanced by gravitational wakes, they collide at such low velocities because particles tend to move coherently in the wakes. This velocity is too low to detach sub-centimeter particles that are attached to the surface of large ones due to the cohesive force, explaining their paucity in the main rings. On the other hand, more infrequent high-velocity impacts can release millimeter-sized particles strongly attached to the surface of large ones, explaining the observed free millimeter-sized particles with relatively low abundance. We will discuss implications of our results for the observed size of the smallest particles in Saturn's main rings.

Keywords: Saturn, rings, Cassini

©2019. Japan Geoscience Union. All Right Reserved.

The Radio & Plasma Wave Investigation (RPWI) for JUICE for the investigation of Jupiter and Icy Moons System: Contributions from Japan

*Yasumasa Kasaba[1], Hiroaki Misawa[1], Fuminori Tsuchiya[1], Atsushi Kumamoto[2], Yuto Katoh[2], Tomoki Kimura[2], Hajime Kita[3], J.-E. Wahlund[4]

1. Planetary Plasma and Atmospheric Research Center, Tohoku University, 2. Department of Geophysics, Tohoku University, 3. ISAS/JAXA, 4. IRF Uppsala, Sweden

The Radio & Plasma Wave Investigation (RPWI) for the ESA JUICE mission (launch: 2022, Observations: 2030s) provides an elaborate suite of electromagnetic fields and plasma instruments. RPWI focuses on cold plasma studies and will investigate how the transfer of momentum and energy in the Jovian huge magnetosphere and the electrodynamic coupling with the icy Galilean moons. Remote sensing and direction finding of the Jovian radio emissions will be carried out. This capability is also devoted to the ices and the deep interiors of the icy moons. Investigations of the ice shells will be performed by means of a novel passive ground penetrating radar technique, which utilizes Jovian strong radio emissions as the transmitted signal. On the Ganymede orbit, continuous measurements of the electric field with the JUICE Magnetometer (JMAG) measurements will determine the electric coupling between any ocean, the ionosphere, and the magnetosphere, and provide the constraints on the physical characteristics of the subsurface ocean of Ganymede.
For those objectives, RPWI sensors consist of 4 Langmuir probes (LP-PWI) for determination of the vector electric field up to 1.6 MHz and cold plasma properties (including active measurements by LP sweeps and mutual impedance sounding) up to 1.6 MHz, a tri-axial search coil magnetometer (SCM) for determination of the vector magnetic field up to 20 kHz, and a tri-dipole antenna system (RWI) for monitoring of radio emissions (80 kHz - 45 MHz). From Japan, the RWI preamp and its High Frequency receiver with the onboard software will be provided, based on the modifications from the BepiColombo PWI and Arase PWE developments. Since Arase already shows the good performance in the radiation hard environment around Earth, we have enough confidence for the possible functions and performance on the Jovian hard environment. We will also provide Software Wave-Particle Interaction Analyzer (SWPIA) function to RPWI DPU, for the onboard quantitative detection of electromagnetic field - ion interactions, modifying from the Arase SWPIA which is also activating on the space now.
HF reciever will provide the first highly-resolved information of Jovian radio emissions emitted from Jovian multiple regions including lightning activity and icy moons, by the 3-ch receiver system manufactured by Japan and Sweden connected to the 3-elements 1.25-m E-filed dipole antenna system manufactured by Poland and Japan. Highly matured onboard and ground data processing will also be provided by France and Japan. As a byproduct, reflected Jovian emission can also be expected from the boundary of icy crust and conductive liquid subsurface ocean. Such reflection components could be observed as the Lunar surface reflection of terrestrial auroral kilometric radiation (AKR) seen by Kaguya Lunar Radar Sounder. JUICE has the RIME (Radar for Icy Moons Exploration) instrument, an active radar which emits 9 MHz pulse from 16 m tip-to-tip antenna and tries to detect the ocean under ~10 km icy crust. Since the frequency of Jovian radiation is wider (several 100 kHz to several 10s MHz), RPWI will provide complementary information, including the vertical distributions of conductivity and permittivity in the icy crust.
In the srping 2019, we are manufacturing and testing the Flight Models (FM) which will be shipped in June - July 2019 to Europe. The long road are connected to the first Jupiter and outer planet tour of the

©2019. Japan Geoscience Union. All Right Reserved.

hardware from Japan.

Keywords: Jupiter, JUICE, Radio waves

©2019. Japan Geoscience Union. All Right Reserved.

Magnetic field experiment at Jupiter icy moons (JUICE J-MAG) and in-flight alignment calibration

*Ayako Matsuoka[1], Michele Karen Dougherty[2], Patrick Brown[2], Futoshi Takahashi[3], Hisayoshi Shimizu[4], Masaki Matsushima[5]

1. Research Division for Space Plasma, Institute of Space and Astronautical Science, Japan Aerospace Exploration Agency, 2. Imperial College London, 3. Kyushu University, 4. University of Tokyo, 5. Tokyo Institute of Technology

The magnetometer instrument (J-MAG) is one of the core instruments on the JUICE spacecraft and is critical for resolving prime science objectives of the mission. The importance of a magnetometer instrument on JUICE can be described under following themes. Firstly, the magnetic field drives the plasma processes occurring within the Jupiter system. Understanding such observations allows for a better understanding of dynamical plasma processes, of the generation of aurora and of the various current systems which arise within this rapidly rotating magnetosphere. Secondary, the magnetometer science which is unique to JUICE lies in being able to gain an understanding of the interior structure of the icy moons of Jupiter, specifically those of Ganymede, Callisto and Europa. Of particular interest are knowledge of the depth at which the liquid oceans reside beneath their icy surfaces, the strength of any internal magnetic fields such as at Ganymede and the strength of any induced magnetic fields arising within these oceans.

J-MAG science requirements result in a requirement on the spacecraft to determine accurate knowledge of the orientation of the fluxgate sensors (MAGIBS and MAGOB). Due to the long MAG boom it is not possible to meet J-MAG’ s alignment requirement by mechanical stability alone, therefore the spacecraft includes two orthogonal coils mounted around its body. The coils can be driven with a current which produces a measurable magnetic field vector at the fluxgate sensors. This signal can then be used by the fluxgates to track the variation in the sensor alignment. This technical note describes the results of an analysis using an alignment recovery technique that was developed for the Kaguya mission, applied to the specific case of JUICE, considering the relative positions of the fluxgate sensors with respect to the JACS coils.

We derived equations to calculate the directions of the measurement axes in the frame fixed to the spacecraft, namely alignment angles, from the measurement results of reference magnetic fields generated by JACS. The errors of the alignment angle estimation and their dependence on measurement noise as well as inaccuracy of the coil current intensity are examined. Based on the quantitative results, the requirements to the JACS design and operation to satisfy the requests to the alignment accuracy are determined.

Keywords: Jupiter, Jovian moons, magnetometer

©2019. Japan Geoscience Union. All Right Reserved.

Science targets of the GAnymede Laser Altimeter (GALA) for the JUICE mission

*Jun Kimura[1], Shunichi Kamata[2], Koji Matsumoto[3], Noriyuki Namiki[3], Keigo Enya[4], Masanori Kobayashi[5], Hiroshi Araki[3], Hirotomo Noda[3], Ko Ishibashi[5], Hauke Hussmann[6], Kay Lingenauber[6]

1. Osaka University, 2. Hokkaido University, 3. National Astronomical Observatory Japan, 4. ISAS/JAXA, 5. Chiba Institute of Technology, 6. German Aerospace Center (DLR), Berlin

The JUpiter Icy Moons Explorer (JUICE), led by European Space Agency, has started development toward launch in 2022 (arrival at Jupiter in 2029, and Ganymede orbit insertion in 2032), and we are now developing the GALA instrument onboard JUICE spacecraft collaborating with German Aerospace Center (DLR) and other institutions in Europe. GALA will acquire the key information for understanding the evolution of Jovian icy moons and to play an essential role in the JUICE's purpose: exploration of deep habitat.

Jovian icy moon Ganymede, which is the largest moon in the Solar System and the primary target of the JUICE, can be said to be one of the typical solid bodies along with terrestrial planets in terms of its size and the intrinsic magnetic field originated from the metallic core. However, current knowledge provided by previous explorations is extremely limited since it comes from only several fly-bys. The JUICE will unveil the whole picture of Ganymede by the first orbiting in the history around extra-terrestrial moon. Expected new big picture of the origin and evolution of Ganymede will not only be a key to unveil the origin of diversity among the Solar System bodies, but also contribute to an understanding of exoplanets with a wide diversity.

The GALA will measure a distance between the spacecraft and the surface of icy moons and acquire the topography data (globally for Ganymede, and fly-by region for Europa and Callisto). It will be a first-ever laser altimetry for the icy object. Such information makes surface geologies clear and tremendously improves our understanding of the icy tectonics. By comparing their tectonic styles on the rocky planets/moons, GALA data leads to reconsider the Earth's plate tectonics. In addition, the GALA will confirm a presence/absence of the subsurface ocean by measuring tidal and rotational response, and the gravitational information reflecting the interior structure will be greatly improved. Furthermore, strength and waveform of reflected laser pulse have an information about surface reflectance at the laser wavelength and small-scale roughness. Finally we can see degrees of erosion and space weathering without being affected by illumination condition through GALA measurements.

In order to interpret and understand such measurements, accumulated studies for the Earth over the years will be effectively utilized: e.g., the data for surface topography, roughness and albedo will lead to describe the icy tectonics through the knowledge from terrestrial glaciology and experiments on impact and deformation process. The tidal measurements by GALA will also be a window to see its interior based on our knowledge and experiences cultivated through the past geodetic observations, e.g., the SELENE mission for the terrestrial Moon.

Characterization of the icy moons will be achieved not only from the GALA measurements but also synergy of other scientific instruments onboard JUICE spacecraft, for examples, surface images taken by optical camera (JANUS) will confirm the position of GALA laser footprint to complement the GALA "point" data for precise topographic mapping. A radar sounder (RIME) and a radio science experiment (3GM) probe

©2019. Japan Geoscience Union. All Right Reserved.

the interior structure, especially interior of the icy crust to figure out an occurrence of tectonic features. A visible and infrared imaging spectrometer (MAJIS), an ultraviolet imaging spectrograph (UVS) and a sub-millimeter wave instrument (SWI) will acquire a surface and atmosphere compositional data. A magnetometer (J-MAG) monitors moons' inductive response to the Jovian magnetic field and probes the subsurface ocean with the help of a particle environment package (PEP) and a radio and plasma wave investigation (RPWI). The GALA works closely together with these instruments and plays a leading and a supporting role to clarify the whole picture of Ganymede and other icy moons.

Keywords: Jupiter, Icy moons, Laser altimetry

©2019. Japan Geoscience Union. All Right Reserved.

Current status of the antenna developments, the data processing, scientific target for JUICE/SWI JAPAN.

*YASUKO KASAI[1], [Group] JUICE SWI Japanese Team

1. National Institute of Information and Communications Technology (NICT)

The Submillimetre-Wave Instrument (SWI) is one of the 10 scientific payloads on the JUpiter ICy moon Explorer (JUICE). The main scientific objectives of SWI is to investigate the structure, compositions and dynamics of the middle atmosphere of Jupiter and exosphere of its moons, as well as thermophysical properties if the satellite surfaces. SWI observations will provide pioneering direct measurements of atmospheric compositions in Jupiter system. SWI will performed limb and nadir observations in the frequency region 530-600 and 1075-1275 GHz. Japanese contribution is the development of main- and sub- reflectors, actuators for the instruments, feasibility studies, data processing, and scientific contributions. We present Current status of the antenna developments, the data processing, scientific target for JUICE/SWI JAPAN.

Keywords: Jupiter, Jovian moons, submm instrument, JUICE, SWI

©2019. Japan Geoscience Union. All Right Reserved.

[E] Poster | P (Space and Planetary Sciences)：P-EM Solar-Terrestrial Sciences, Space Electromagnetism & Space Environment

Tue. May 28, 2019 3:30 PM - 5:00 PM JST | Tue. May 28, 2019 6:30 AM - 8:00 AM UTC | Poster Hall International Exhibition Hall8, Makuhari Messe_3

[P-EM12] Space Weather and Space Climate

convener:Ryuho Kataoka(National Institute of Polar Research), Antti A Pulkkinen(NASA Goddard Space Flight Center), Kanya Kusano(Institute for Space-Earth Environmental Research, Nagoya University), Kaori Sakaguchi(National Institute of Information and Communications Technology)

We share the latest scientific papers to understand how the solar-terrestrial environment changes in various time scales, and to discuss how we will react via international and interdisciplinary collaborations. More specifically, welcomed papers include space climate studies to reconstruct long-term variations from radio isotopes; cutting-edge observational and modeling studies of the ionosphere, geospace, heliosphere and the sun; simulation and statistical studies to predict the future space weather and space climate; applied science such as operational space weather forecast and mitigation of the social impact due to extreme space hazards.

[PEM12-P01] Reconnection signatures in solar magnetograms during the solar storms of 4-10 September 2017

*Robert Dean Loper[1,2] (1.Air Force Institute of Technology, Department of Engineering Physics, 2.National Center for Atmospheric Research, High Altitude Observatory)

[PEM12-P02] Statistical Relation between Solar Flares and Coronal Mass Ejections with Respect to Sigmoidal Structures in Active Regions

*Yusuke Kawabata[1,2], Yusuke Iida[3], Takafumi Doi, Sachiko Akiyama[4], Seiji Yashiro[4], Toshifumi Shimizu[2] (1.Earth and Planetary Science, The University of Tokyo, 2.Institute of Space and Astronautical Science, JAXA, 3.Kwansei Gakuin University, 4.The Catholic University of America)

[PEM12-P03] Multi-wavelength Observations of Pre-flare Quasi-periodic Pulsation in the C2.2 Flare on 2012 October 15

*Yung-Chi Yang[1], Ya-Hui Yang[1], Baolin Tan[2], Chengming Tan[2], Y.H. Yan[2] (1.Graduate Institute of Space Science National Central University, 2.Key Laboratory of Solar Activities, National Astronomical Observatories)

[PEM12-P04] Investigation of pre-flare type III solar radio bursts and their potential solar origins

*Shao-Fu Hsieh[1], Ya-Hui Yang[1], Baolin Tan[2], Chengming Tan[2], Y.H. Yan[2] (1.Graduate Institute of Space Science National Central University, 2.Key Laboratory of Solar Activities, National Astronomical Observatories, Chinese Academy of Sciences)

[PEM12-P05] Statistical and observational research of solar flare for constructing total emission spectra prediction model

*Shohei Nishimoto[1], kyoko Watanabe[1], Shinsuke Imada[2], Tomoko Kawate[3], Kyoung-Sun Lee[4] (1.National Defense Academy, 2.Institute for Space-Earth Environmental Research, Nagoya University, 3.Institute Of Space And Astronautical Science, Japan Aerospace Exploration Agency, 4.National Astronomical Observatory of Japan)

[PEM12-P06] Modeling of solar active regions using local linear force-free fields to estimate magnetic twist

*Kento Nakatani[1], Kanya Kusano[1], Sung-Hong Park[1], Leka KD[2] (1.Institute for space-Earth Environmental Research, Nagoya University, 2.North West Reserch Associates)

[PEM12-P07] Magnetohydrodynamic Simulation of an Erupting Magnetic Flux Rope on February 13 2009: Journey to Coronal Mass Ejection

*Satoshi Inoue[1], Antonia Savcheva[2] (1.Institute for Space-Earth Environmental Research, Nagoya University, 2.Harvard-Smithsonian Center for Astrophysics)

[PEM12-P08] Investigation of flow structures in the solar interior through the surface magnetic elements' tracking

*Yusuke Iida[1] (1.Kwansei Gakuin University)

[PEM12-P09] High-precision measurement of carbon-14 in tree rings around the onset of the Maunder Minimum

*Hiroko Miyahara[1], Fuyuki Tokanai[2], Toru Moriya[2], Hideyuki Hotta[3] (1.Musashino Art University, 2.Yamagata University, 3.Chiba University)

[PEM12-P10] Examination of ^{10}Be in travertine sediment as a possible tool to reconstruct past solar activity

*Hongyang Xu[1,2], Hiroko Miyahara[2], Kazuho Horiuchi[3], Hiroyuki Matsuzaki[4], Hailong Sun[5], Weijun Luo[5], Xiangmin Zheng[1], Yusuke Suganuma[6,7], Shijie Wang[5], Limin Zhou[1] (1.East China Normal University, 2.Musashino Art University, 3.Hirosaki University, 4.University of Tokyo, 5.Chinese Academy of Sciences, 6.National Institute of Polar Research, 7.The Graduate University for Advanced Studies (SOKENDAI))

[PEM12-P11] Examination of ^{10}Be in travertine sediment as a possible tool to reconstruct past solar activity II

*Hongyang Xu[1,2], Hiroko Miyahara[2], Kazuho Horiuchi[3], Hiroyuki Matsuzaki[4], Hailong Sun[5], Weijun Luo[5], Xiangmin Zheng[1], Yusuke Suganuma[6,7], Shijie Wang[5], Limin Zhou[1] (1.East China Normal University, 2.Musashino Art University, 3.Hirosaki University, 4.University of Tokyo, 5.Chinese Academy of Sciences, 6.National Institute of Polar Research, 7.The Graduate University for Advanced Studies (SOKENDAI))

[PEM12-P12] 1 year of CR observation at Syowa Station in the Antarctic.

*Chihiro Kato[1], Kazuoki Munakata[1], Akira Kadokura[2], Ryuho Kataoka[2], Paul Evenson[3] (1.Shinshu University, 2.National Institute of Polar Research, 3.University of Delaware)

[PEM12-P13] Space weather forecast archives at NICT: handwritten solar activity charts

*Kaori Sakaguchi[1], Daikou Shiota[1], Kaori Fukunaga[1], Katsuhide Marubashi[1], Hiromitsu Ishibashi[1], Yuki Kubo[1], Mamoru Ishii[1] (1.National Institute of Information and Communications Technology)

[PEM12-P14] IMF dependence on solar wind parameters

*Tohru Araki, Yuki Harada[1] (1.Kyoto University)

[PEM12-P15] **Dipole Tilt Effect of Geomagnetic Activity from Low- to High-latitudes**

*Nowada Motoharu[1] (1.Shandong University at Weihai)

[PEM12-P16] A New Prediction Model for Solar Wind-Triggered Magnetospheric Disturbances Based on Potential Learning (Neural Network)

*Ryozo Kitajima[1], Motoharu Nowada[2], Ryotaro Kamimura[3] (1.Seikei University, 2.Shandong University at Weihai, 3.Tokai University)

[PEM12-P17] Real-time magnetosphere simulator for space weather using REProduce Plasma Universe code

*Yasubumi Kubota[1], Aoi Nakamizo[1], Kaori Sakaguchi[1], Mitsue Den[1], Yuki Kubo[1], Tsutomu Nagatsuma[1], Takashi Tanaka[1,2] (1.National Institute of Information and Communications Technology, 2.Kyushu University)

[PEM12-P18] **Simulation of GIC flowing through the power transmission network (187 kV-500 kV) in Japan**

*Nishida Yuichiro[1,6], Yusuke Ebihara[1], Satoko Nakamura[1], Shinichi Watari[2], Kumiko Hashimoto[3], Kentaro Kitamura[4], Takashi Kikuchi[5] (1.Kyoto University Reserch Institute for Sustainable Humanosphere, 2.National Institute of Information and Communications Technology, 3.Kibi International University, 4.National Insutitute of Technology, Tokuyama College, 5.Nagoya University, 6.Kyoto University Department of Electrical Engineering)

[PEM12-P19] Climatological features of the upper atmosphere reproduced by a revised version of a whole atmosphere-ionosphere coupled model GAIA

*Hidekatsu Jin[1], Yasunobu Miyoshi[2], Chihiro Tao[1], Hiroyuki Shinagawa[1], Hitoshi Fujiwara[3] (1.National Institude of Information and Communications Technology, 2.Kyushu University, 3.Seikei University)

[PEM12-P20] Investigation of the thermospheric mass density variations below 200 km

*Hitoshi Fujiwara[1], Yasunobu Miyoshi[2], Masayoshi Utashima[1], Huixin Liu[2] (1.Faculty of Science and Technology, Seikei University, 2.Department of Earth and Planetary Sciences, Faculty of Sciences, Kyushu University)

[PEM12-P21] Low-latitude HF Doppler observations of magnetospheric electric fields during space weather disturbances

*Kumiko K. Hashimoto[1], Takashi Kikuchi[2], Ichiro Tomizawa[3], Keisuke Hosokawa[3], Jaroslav Chum[4] (1.Kibi International University, 2.Nagoya University, 3.University of Electro-Commnunications, 4.Institute of Atmospheric Physics, Prague)

[PEM12-P22] Stratospheric ionization during magnetic storms

*Ryuho Kataoka[1] (1.National Institute of Polar Research)

[PEM12-P23] Calculating propagation time of HF radio wave using ray-tracing method and simple comparison with the observation.

*Ryo Nakao[1], Hiroyuki Nakata[1], Hiroyo Ohya[1], Toshiaki Takano[1], Kornyanat Hozumi[2], Takuya Tsugawa[2], Susumu Saito[3], Mamoru Ishii[2] (1.Graduate School of Engineering, Chiba University, 2.National Institute of imformation and Communications Technology, 3.Electronic Navigation Research Institute)

[PEM12-P24] Why do some probabilistic forecasts lack reliability?

*Yuki Kubo[1] (1.National Institute of Information and Communications Technology)

[PEM12-P25] An estimation method of GEO spacecraft surface charging for a real-time spacecraft risk assessment

*Masao Nakamura[1], Ryota Kawachi[1], Go Takahashi[1], Tsutomu Nagatsuma[2], Mamoru Ishii[2] (1.Osaka Prefecture University, 2.NICT)

[PEM12-P26] A network of HF Doppler sounding systems in Japan

*Keisuke Hosokawa[1], Hiroyuki Nakata[2], Kumiko K. Hashimoto[3], Ichiro Tomizawa[1], Jun Sakai[1], Takashi Kikuchi[4] (1.University of Electro-Communications, 2.Chiba University, 3.Kibi International University, 4.ISEE, Nagoya University)

Reconnection signatures in solar magnetograms during the solar storms of 4-10 September 2017

*Robert Dean Loper[1,2]

1. Air Force Institute of Technology, Department of Engineering Physics, 2. National Center for Atmospheric Research, High Altitude Observatory

Solar flare forecasting is limited to active region classification and historical correlation, due largely to our lack of understanding of magnetic reconnection as a driving mechanism for solar flares and coronal mass ejections. Photospheric observations indicate magnetic field changes during solar flares, brought about during magnetic reconnection and related to magnetic field helicity on the solar surface. While the neutral point of the reconnection event associated with a flare usually occurs in the solar corona, some signs of the magnetic field changes should manifest as low as the photosphere. This study utilizes data from SDO HMI and Space-Weather HMI Active Regions Patches (SHARPS) to analyze full vector field component data in the photospheric magnetic field during several magnetic reconnection events during the space weather events of 4-10 September 2017.

Keywords: solar atmosphere, sunspots, magnetogram, solar flares

©2019. Japan Geoscience Union. All Right Reserved.

Statistical Relation between Solar Flares and Coronal Mass Ejections with Respect to Sigmoidal Structures in Active Regions

*Yusuke Kawabata[1,2], Yusuke Iida[3], Takafumi Doi, Sachiko Akiyama[4], Seiji Yashiro[4], Toshifumi Shimizu[2]

1. Earth and Planetary Science, The University of Tokyo, 2. Institute of Space and Astronautical Science, JAXA, 3. Kwansei Gakuin University, 4. The Catholic University of America

We will report statistical dependences among features of coronal mass ejections (CMEs), solar flares, and sigmoidal structures in soft-X-ray images (Kawabata et al. 2018). We applied analysis methods to all the features in the same way in order to investigate the reproducibility of the correlations among them, which may be found from previous statistical studies. Samples of 211 M-class and X-class flares, observed between 2006 and 2015 by the Hinode/X-ray telescope, Solar and Heliospheric Observatory/Large Angle and Spectrometric Coronagraph, and Geostationary Operational Environmental Satellite, were examined statistically. Five kinds of analysis were performed: Occurrence rate analysis, linear-correlation analysis, association analysis, the Kolmogorov–Smirnov test, and the Anderson–Darling test. These give three main results. First, the sigmoidal structure and long-duration events (LDEs) have a stronger dependence on CME occurrence than large X-ray-class events in on-disk events. Second, for the limb events, a significant dependence exists between LDEs and CME occurrence, and between X-ray-class events and CME occurrence. Third, 32.4% of on-disk flare events have sigmoidal structure and are not accompanied by CMEs. However, the occurrence probability of CMEs without sigmoidal structure is very small, 8.8%, in on-disk events. While the first and second results are consistent with previous studies, we provide for the first time a difference between the on-disk and limb events. The third result, that non-sigmoidal regions produce fewer eruptive events, is also different from previous results. We suggest that sigmoidal structures in soft X-ray images will be a helpful feature for CME prediction in on-disk flare events.

Keywords: Sun, Solar flares, Coronal mass ejections, Sigmoid

©2019. Japan Geoscience Union. All Right Reserved.

Multi-wavelength Observations of Pre-flare Quasi-periodic Pulsation in the C2.2 Flare on 2012 October 15

*Yung-Chi Yang[1], Ya-Hui Yang[1], Baolin Tan[2], Chengming Tan[2], Y.H. Yan[2]

1. Graduate Institute of Space Science National Central University, 2. Key Laboratory of Solar Activities, National Astronomical Observatories

Quasi-periodic pulsation (QPP) is thought to be the nature of solar flares, which can be observed during and before flares in various wavelengths, such as the radio, microwave, SXR, and EUV. In this study, we analyze a pre-flare QPP event on 2012 October 15 and its association with the following C2.2 flare based on the radio data in the ranges of 2.81-2.85 GHz and 2.91-2.95 GHz from Solar Broadband Radio Spectrometer (SBRS), EUV images from AIA multi-wavelength observations, and wavelet analysis. Our result show that the main period of the radio QPP is ~800 s which is similar to the period of ~13.5 min obtained in SXR by Tan et al. (2016). Moreover, we analyze several localized areas in the flare-eruptive AR 11593 to search for the possible regions responsible for the occurrence of pre-flare QPP. We find that the footpoints of brightening loops in 211 Åshow the quasi-periodic behavior of ~850 s. It is thus suggested that the pre-flare QPP with a period of 13-15 min can be manifested in both of the thermal (SXR, EUV) and nonthermal (radio) radiation processes. The relationship between the pre-flare QPP and the subsequent C2.2 flare will also be discussed.

Keywords: sun, solar flares, solar oscillation

©2019. Japan Geoscience Union. All Right Reserved.

Investigation of pre-flare type III solar radio bursts and their potential solar origins

*Shao-Fu Hsieh[1], Ya-Hui Yang[1], Baolin Tan[2], Chengming Tan[2], Y.H. Yan[2]

1. Graduate Institute of Space Science National Central University, 2. Key Laboratory of Solar Activities, National Astronomical Observatories, Chinese Academy of Sciences

Type III solar radio bursts are characterized as the fast-drifting radio emissions in a dynamic spectrogram, which is believed to be produced by the propagating electron beams and often accompanied with the solar flares or magnetic reconnection. Studying the type III radio bursts in high-frequency range before flares would be important for understanding the trigger of energy release although it is rarely reported previously. Here we present two pre-flare type III burst events found in the range of 2.6-3.8 GHz at Solar Broadband Radio Spectrometer (SBRS). By comparing with the SDO/AIA multi-wavelength observations in flare active regions, the pre-flare type III radio bursts have good temporal correlations with the increases of EUV emissions. Furthermore, we find that one event is related to the EUV brightening with 1-min delay, implying the existence of plasma heating before energy release. The other event has a simultaneous EUV jet with a speed of ~700 km/s indicating the occurrence of magnetic reconnection. We suppose both pre-flare events are associated with small-scale energy release via magnetic reconnection.

Keywords: sun, solar flares, solar radio bursts

©2019. Japan Geoscience Union. All Right Reserved.

Statistical and observational research of solar flare for constructing total emission spectra prediction model

*Shohei Nishimoto[1], kyoko Watanabe[1], Shinsuke Imada[2], Tomoko Kawate[3], Kyoung-Sun Lee[4]

1. National Defense Academy, 2. Institute for Space-Earth Environmental Research, Nagoya University, 3. Institute Of Space And Astronautical Science, Japan Aerospace Exploration Agency, 4. National Astronomical Observatory of Japan

Impulsive energy release phenomena such as solar flares, sometimes affect to the solar-terrestrial environment. Usually, we use soft X-ray flux (GOES class) as the index of flare scale. However, the magnitude of effect to the solar-terrestrial environment is not proportional to this scale. Therefore, it is considered that the GOES class is not optimal parameter for predicting the Sudden Ionospheric Disturbance (SID). To identify the relationship between solar flare phenomena and influence to the solar-terrestrial environment, we need to understand the full spectra of solar flares in detail.
There is the solar flare irradiance model named the Flare Irradiance Spectral Model (FISM) (Chamberlin et al., 2006, 2007, 2008). FISM is the most used model, and can estimate solar flare spectra with high wavelength and temporal resolution. However, this model can not express the time evolution of emitted plasma during the solar flare, and has low accuracy on short wavelength that might strongly affect to the total flare spectra. Therefore, individual SID phenomenon can not be reproduced.
In this work, in order to solve the problems of FISM, we performed statistical analysis on observational data during the solar flares. From This study, we tried to find the parameters that control the solar flare emission spectra. We selected solar flare events larger than M-class from the Hinode flare catalogue (Watanabe et al., 2012). First, we focused on the EUV emission observed by the SDO/EVE. We examined the intensities and time evolutions of five EUV lines (Fe XX, Fe XVIII, Fe XVI, Fe VIII, and He II) for 54 flare events. As a result, we found positive correlation between the “GOES class” and the “EUV peak flux” for all Fe lines. Moreover, we found that hotter lines peaked earlier than cooler lines. On the other hand, He II line data have poor correlation with GOES X-ray data. Furthermore, we considered that the geometrical features of solar flares effect to those time evolutions. We measured flare ribbon length for 33 flare events observed by SDO/AIA, and found positive correlation between the “flare duration” and the “ribbon length”. From the statistical research of these observational data, we found that the time evolution of EUV emission can be explained by the X-ray emission.
Then, we tried to identify parameters that determine the solar flare spectra by comparing the flare emissions derived from physical based numerical model of solar flare with the actual observational data. Consequently, we used numerical simulation same as Imada et al.(2015). This numerical model can reproduce the movement and ionization of the plasma in the flare loop.
In this presentation, we will show some results of numerical simulation, and discuss the parameters for total solar flare emission spectra by comparing of simulation results, observational data and FISM.

Keywords: Space Weather, Solar Flare

©2019. Japan Geoscience Union. All Right Reserved.

Modeling of solar active regions using local linear force-free fields to estimate magnetic twist

*Kento Nakatani[1], Kanya Kusano[1], Sung-Hong Park[1], Leka KD[2]

1. Institute for space-Earth Environmental Research, Nagoya University, 2. North West Reserch Associates

The prediction of solar flares is an important issue for space weather forecasting. Although solar flares are believed to be caused by the magnetohydrodynamic (MHD) instability in solar active regions, the method for accurately evaluating the stability of solar magnetic field is not yet established. Recently, Ishiguro & Kusano (2017) proposed that a new instability called the Double Arc Instability (DAI) plays a role of initial driver of solar flares and the critical parameter for this instability can be used to evaluate the stability of active regions. The parameter can be derived by the integration of the magnetic twist as the function of magnetic flux. One way for it is given by the nonlinear force-free field (NLFFF) extrapolation using the photospheric vector magnetic field data. However, the NLFFF extrapolation demands heavy computation and it sometimes cannot well work as a model of solar coronal magnetic field because the force-free condition is limited on the photosphere. Therefore, in order to improve the efficiency and applicability of the flare prediction using , it may be required to develop a method to approximately but much quickly capture the overall features of magnetic field in solar active regions, especially in the flare triggering region. From this point of view, we try to develop a method to extract the characteristic feature of magnetic field in solar active regions using the linear force-free field (LFFF) model. For this objective, we compare the several methods to accurately capture the structure of using LFFF. In this study, we report the result of the analysis for the solar active region NOAA 11429.

Keywords: Space weather, solar , twist, force-free, photosphere, active region

©2019. Japan Geoscience Union. All Right Reserved.

Magnetohydrodynamic Simulation of an Erupting Magnetic Flux Rope on February 13 2009: Journey to Coronal Mass Ejection

*Satoshi Inoue[1], Antonia Savcheva[2]

1. Institute for Space-Earth Environmental Research, Nagoya University, 2. Harvard-Smithsonian Center for Astrophysics

We performed a magnetohydrodynamic (MHD) simulation of a solar eruption launched from solar active region 11012 on February 13, 2009. We in particular concentrated on the evolution of the magnetic flux rope (MFR) leading a coronal mass ejection. We first extrapolated the pre-eruptive magnetic flux ropes using a flux insertion method, in which the MFRs can be extrapolated from the normal component of the magnetic field (Bz) observed by SOHO/MDI and Extreme-Ultra Violet (EUV) images observed by the STEREO satellite. The extrapolated magnetic field reproduced the sigmoidal magnetic structure observed in EUV image well. Next we performed the MHD simulation using the extrapolated magnetic field.

The resulting simulation showed the dramatic eruption of the magnetic flux rope under which the current sheet and the post-flare loops are formed. This is well explained by the standard CSHKP flare model. The evolution of the MFR did not show simple dynamics, rather it showed very complicated dynamics through a magnetic reconnection. We found, during the eruption, that the coherent MFR is created through the reconnection of multiple pre-existing MFRs. Magnetic reconnection plays a role in producing the coherent, erupting MFR and supplying further twist into it. Furthermore we found that the footpoints of the erupting MFR moves along or away from the polarity inversion line, as seen in two-ribbon flares. The locations of both the footpoints of the MFR correspond to those of dimming regions observed in EUV images. Since the location and shape of the post-flare loops obtained from the simulation is reproduced in the observations, we can confirm the reliability of our simulation.

Keywords: Solar Flare, Solar Eruption, Magnetohydrodynamics

©2019. Japan Geoscience Union. All Right Reserved.

Investigation of flow structures in the solar interior through the surface magnetic elements' tracking

*Yusuke Iida[1]

1. Kwansei Gakuin University

We investigate the correlation of meridional flow and rotation velocity in the solar interior by tracking huge number of the surface magnetic elements.

As reported in JpGU2017 meeting, we found that the meridional flow velocity from the magnetic elements' tracking depends positively on their flux and size. We discussed that it may come from that the larger magnetic elements are rooted in the deeper solar interior. We further investigate this issue by correlating the meridional flow velocity and rotation velocity.

We use line-of-sight magnetograms obtained by SDO/HMI in July 2016. Time cadence is 45 seconds, in which the travel distance of magnetic element is smaller than 1 pixel. The magnetograms are transposed from the Earth-view coordinate to the Stonyhurst coordinate. We use the data within 75 degree from the disk center. Magnetic field strength is converted with an assumption that magnetic field is vertical to the surface and interpolated with a cubic spline interpolation.

We detected approximately 8,000 elements in each magnetogram and 4.5x108 displacements in our data set. The meridional flow and rotation velocity on magnetic flux are investigated. The rotation velocity shows negative dependence on the flux at the latitude within 45 degree while it shows weekly positive dependence at the latitude higher than 45 degree. This result is consistent with the depth dependence of rotation velocity obtained by previous helioseismology researches.

Keywords: Sun, Bigdata, Turbulence

©2019. Japan Geoscience Union. All Right Reserved.

High-precision measurement of carbon-14 in tree rings around the onset of the Maunder Minimum

*Hiroko Miyahara[1], Fuyuki Tokanai[2], Toru Moriya[2], Hideyuki Hotta[3]

1. Musashino Art University, 2. Yamagata University, 3. Chiba University

It is well known that the Sun indicates long-term variations at time scales of a few hundred years to a few millennia. It sometimes brings the grand minima, at which period the sunspots disappear for more than several decades. The detailed process of such long-lasting disappearance of sunspots, however, remains unclear. We therefore have been trying to reconstruct solar cycles around the onset of grand minima based on high-precision measurement of carbon-14 in tree rings. In this paper, we report on our preliminary result on the measurement of carbon-14 around the onset of the Maunder Minimum.

Keywords: solar cycle, grand minima, cosmogenic nuclide

©2019. Japan Geoscience Union. All Right Reserved.

Examination of ^{10}Be in travertine sediment as a possible tool to reconstruct past solar activity

*Hongyang Xu[1,2], Hiroko Miyahara[2], Kazuho Horiuchi[3], Hiroyuki Matsuzaki[4], Hailong Sun[5], Weijun Luo[5], Xiangmin Zheng[1], Yusuke Suganuma[6,7], Shijie Wang[5], Limin Zhou[1]

1. East China Normal University, 2. Musashino Art University, 3. Hirosaki University, 4. University of Tokyo, 5. Chinese Academy of Sciences, 6. National Institute of Polar Research, 7. The Graduate University for Advanced Studies (SOKENDAI)

In this study, we explore the possibility of using travertine sediment for reconstructing the past solar activity. We obtained an annual ^{10}Be record from travertine deposit from the modern period and compared with the neutron monitor data. We discuss a possible methodology to calibrate the climatological impact on ^{10}Be deposition and to obtain the signal of past solar and cosmic-ray variations.

Keywords: Beryllium-10, cosmogenic nuclide, solar activity, endogenic travertine

©2019. Japan Geoscience Union. All Right Reserved.

Examination of ^{10}Be in travertine sediment as a possible tool to reconstruct past solar activity II

*Hongyang Xu[1,2], Hiroko Miyahara[2], Kazuho Horiuchi[3], Hiroyuki Matsuzaki[4], Hailong Sun[5], Weijun Luo[5], Xiangmin Zheng[1], Yusuke Suganuma[6,7], Shijie Wang[5], Limin Zhou[1]

1. East China Normal University, 2. Musashino Art University, 3. Hirosaki University, 4. University of Tokyo, 5. Chinese Academy of Sciences, 6. National Institute of Polar Research, 7. The Graduate University for Advanced Studies (SOKENDAI)

We have been examining the potential of ^{10}Be in travertine sediment as a tool to reconstruct past solar and cosmic-ray variations. In this paper, we compare the ^{10}Be profile in the travertine layers from the rainy and dry seasons, and discuss the nature of ^{10}Be deposition at the two seasons.

Keywords: Beryllium-10, cosmogenic nuclide, solar activity, endogenic travertine

©2019. Japan Geoscience Union. All Right Reserved.

1 year of CR observation at Syowa Station in the Antarctic.

*Chihiro Kato[1], Kazuoki Munakata[1], Akira Kadokura[2], Ryuho Kataoka[2], Paul Evenson[3]

1. Shinshu University, 2. National Institute of Polar Research, 3. University of Delaware

CR observation has been carried out for 1 year at Syowa Station in the Antarctic. There was no serious unavailability of data during the whole year. It is now concluded that this station can contribute to a space weather study as one of the CR monitoring station of Global Muon Detector Network (GMDN). We report observed data and its stability as GMDN.

Keywords: Cosmic Rays, Space Weather

©2019. Japan Geoscience Union. All Right Reserved.

Space weather forecast archives at NICT: handwritten solar activity charts

*Kaori Sakaguchi[1], Daikou Shiota[1], Kaori Fukunaga[1], Katsuhide Marubashi[1], Hiromitsu Ishibashi[1], Yuki Kubo[1], Mamoru Ishii[1]

1. National Institute of Information and Communications Technology

About 40 years ago from 1978 to 1999, at Hiraiso Branch, Radio Research Laboratory; present Space Environment Laboratory of National Institute for Information and Communication Technology (NICT) in Japan, space environment data had been recorded in "solar activity chart" by hand for the operation of the radio wave warning service. The charts were created based on URSIgram codes, which were developed to facilitate the rapid exchange of information by telex in periods when internet was not available. Based on the exchanged codes, sunspots transitions and solar flare occurrences on the solar surface, these effects on shortwave propagation, geomagnetic disturbance, and cosmic ray flux over Japan were written in the solar activity charts together with comments and sketch by recorders. One chart was created for each Bertel’ s solar rotation number between No. 1974 and No. 2254, corresponding to sunspot cycles 21 and 22. We realized that the data exchange is almost only once a day from each observation point and charts was accumulation of the available data in real-time at that time.It might be quite difficult to decide future forecast from such a limited real-time data set. Currently, we are digitizing the solar activities charts and the data shown there. In this poster, we present examples of solar activity charts and possible real-time data set and time delay, as well as the verifying result of the solar flare / geomagnetism storm forecast at the time.

Keywords: Space Weather Archive, URSIgram

©2019. Japan Geoscience Union. All Right Reserved.

IMF dependence on solar wind parameters

*Tohru Araki, Yuki Harada[1]

1. Kyoto University

We studied IMF dependence upon solar wind parameters using OMNI hourly values.

Figure below is a plot of the total force (B), horizontal component (Bxy) in the ecliptic plane and vertical component (Bz) of IMF versus the solar wind density (Nsw). The IMF is averaged over 0.2/cc bin of Nsw. Data number in each bin is also plotted. The data period here is 1979-1981 (maximum SSN phase).

The figure shows (1) that B, Bxy and Bz slowly decrease with decreasing Nsw and (2) that when Nsw approaches further to zero. B and Bxy begin to increase and converges to the same finite value (about 10 nT here) while Bz converges to zero. The property (2) suggests that IMF converges to a typical spiral pattern when solar wind density converges to zero.

Two other data periods, 1999-2001 (SSN maximum) and 2007-2009 (SSN minimum) are examined. IMF observed by MAVEN orbiting Mars is also studied for the period, 2014-2018. The results of the analysis are roughly consistent with the description above. We also checked IMF dependence on solar wind velocity

Keywords: IMF, solar wind density, solar wind melocity

©2019. Japan Geoscience Union. All Right Reserved.

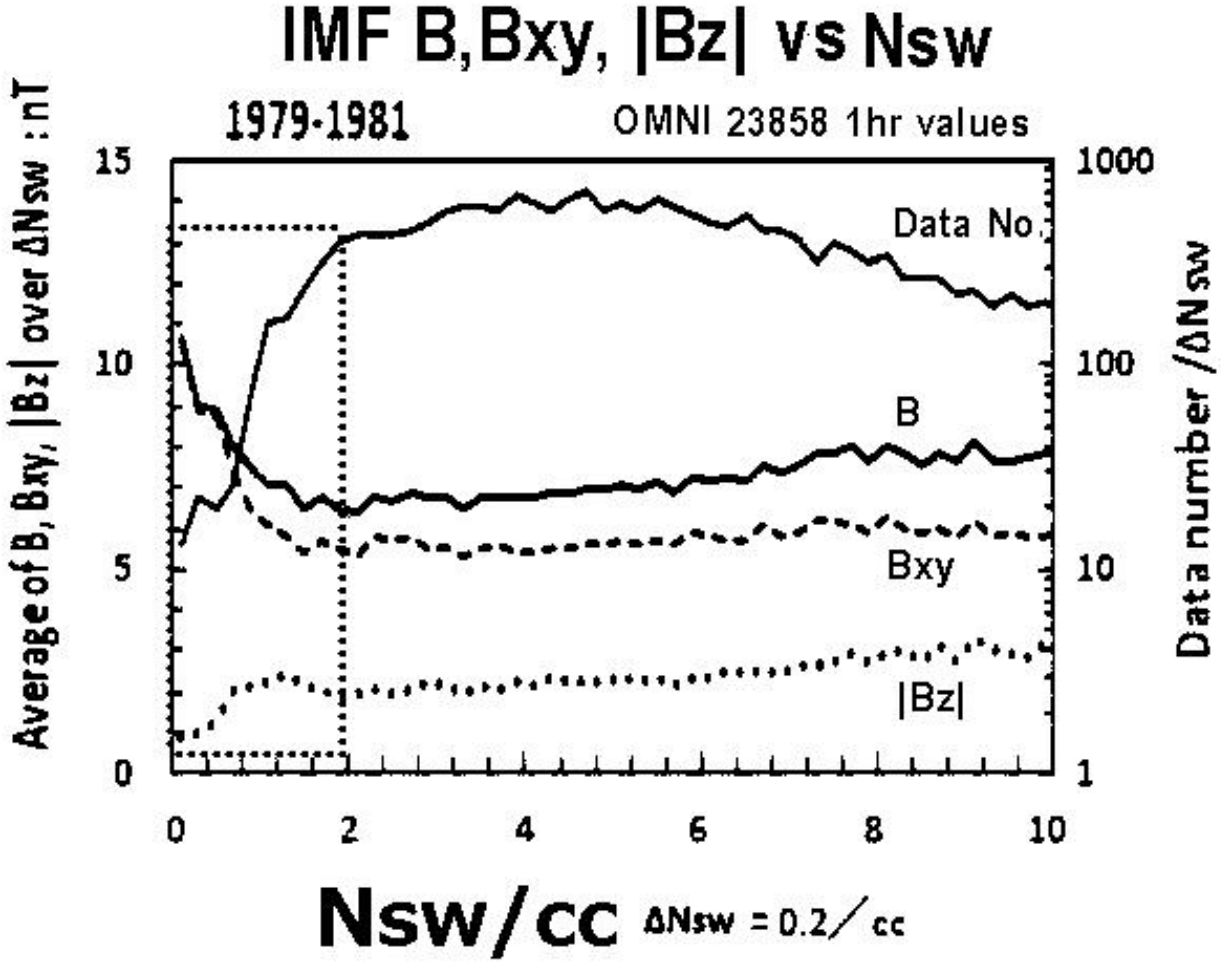

©2019. Japan Geoscience Union. All Right Reserved.

Dipole Tilt Effect of Geomagnetic Activity from Low- to High-latitudes

*Nowada Motoharu[1]

1. Shandong University at Weihai

Geomagnetic activity is dominantly impacted by the orientation of the Interplanetary Magnetic Field (IMF). However, when trying to address why the variations of geomagnetic activity are “semi-annual”, and are greater at equinoxes than at solstices, only IMF control of geomagnetic activity is not enough. This is because these variations are strongly dependent on the Earth’s dipole tilt; the dipole tilt is smaller at the equinoxes than at the solstices. Primitive studies assumed that magnetic reconnection occurs only at the subsolar point of dayside magnetopause. In their studies, the dipole tilt effect was not considered, but only the magnetic field direction between the IMF and the magnetosphere at the subsolar point was discussed in their studies. After them, geomagnetic variations where both dipole tilt effect and IMF direction are taken into account have been investigated. Based on a large database of IMF and AL/AU, we examined the relationship between the IMF clock angle and AL/AU at various dipole tilts. For both positive and negative dipole tilts, geomagnetic activity decrease as the clock angle moves away from 180˚. The AL/AU indices also tend to become smaller for larger dipole tilts. This dipole tilt dependence enhances the semi-annual variation of high-latitude geomagnetic activity.
It also remains unclear how degree energy input rate from solar wind to ring current (dD_{st}^{*}/dt) depends on dipole tilt under various interplanetary magnetic field (IMF) orientation and whether or not ring current development also follows this dipole tilt dependence. We tried to statistically investigate the dependence of dipole tilt and IMF clock angles on low- and middle-latitude geomagnetic activity (D_{st}^{*}), which is a proxy of ring current development, and solar wind energy input rate to ring current (dD_{st}^{*}/dt) over one solar cycle (1978 - 1988). D_{st}^{*} was calculated with the solar wind dynamic pressure and original D_{st} index, and the dipole tilt angle was defined as function of the day of year and universal time. The (dD_{st}^{*}/dt) values were obtained based on the solar wind electric field under the southward IMF conditions. Under positive and negative dipole tilts, the (dD_{st}^{*}/dt) values under low dipole tilt are negatively larger than those in case of high dipole tilt. Further peaks at 180˚ of the IMF clock angle are seen in most of the dipole tilt cases. However, the D_{st}^{*} index shows neither a peak at 180˚ of the IMF clock angle nor particular dipole tilt dependence in case of negative dipole tilt angles. This result suggests that low- and middle latitude geomagnetic activity (ring current development) does not necessarily show dipole tilt dependence and a one-to-one correlation with solar wind energy input rate to ring current (dD_{st}^{*}/dt).

Keywords: Geomagnetic activity (Dst*), Solar wind energy input rate to ring current (dDst*/dt), Semiannual variation , Dipole tilt effect, Interplanetary magnetic field and clock angel, Magnetic reconnection

©2019. Japan Geoscience Union. All Right Reserved.

A New Prediction Model for Solar Wind-Triggered Magnetospheric Disturbances Based on Potential Learning (Neural Network)

*Ryozo Kitajima[1], Motoharu Nowada[2], Ryotaro Kamimura[3]

1. Seikei University, 2. Shandong University at Weihai, 3. Tokai University

Nowadays, it becomes so important in saving our economic activity, and preventing the disasters caused by terrestrial electromagnetic effects to predict a scale and the duration of the geomagnetic disturbances based on in-situ solar wind observations. Recently, one of the notable techniques for the predictions of the magnetospheric disturbances is Neural Network (NN). However, most of these studies are focused on the reproduction of the behaviors of the index values, which represent the geomagnetic disturbances (e.g, D_{st} and AE), by inputting the solar wind parameters measured by the satellites. In our study, we apply a novel neural network model of ‘Potential Learning (PL)’.
Basically, Neural Networks (NNs) are models which imitate the information processing in the nervous system of brain. The nerve is made of cells as referred to as “neurons”, which specializes the information processing. NNs consist of “artificial” neurons, and can process information by learning. Therefore, using NNs, we can obtain some characteristics of the data inputted. The PL is a new kind of the NNs. A feature of the PL is to make a network that can understand the input variables based on learning by “input potentialities”, which are indices as calculated with the variances derived from the input variables. If using this PL, we can specify what input variable(s) is (are) potentially important and influential for a phenomenon.
In this study, introducing the PL technique, we try to specify which solar wind parameter plays an essential role in causing the geomagnetic disturbances. Although the conventional PL, where we used, had automatically selected the variables of interest, we develop a “improved” PL in this study so that the variables can manually be selected. We benchmark this new algorithm using the 4 polar magnetic storm cases occurred under the southward Interplanetary Magnetic Field (IMF)-B_z conditions, and advisedly set the maximum potentiality for the IMF-B_z, so that the IMF-B_z component is the most possible solar wind parameter to cause the geomagnetic disturbances. We note “second” solar wind parameter(s) to possibly cause the magnetospheric disturbances, following the IMF-B_z component. After testing our new technique to actual storm events, we might distinguish the magnetospheric disturbances into two different types, that is, the geomagnetic disturbances driven by “IMF-dominant” and “combination of IMF with solar wind plasma (dynamic pressure)”. The advantages to adopt this new algorithm to space weather, and more detailed results will be discussed in this presentation.

Keywords: Predictions of Geomagnetic Activity, Neural Network Considered Potential Learning, Development of Space Weather

©2019. Japan Geoscience Union. All Right Reserved.

Real-time magnetosphere simulator for space weather using REProduce Plasma Universe code

*Yasubumi Kubota[1], Aoi Nakamizo[1], Kaori Sakaguchi[1], Mitsue Den[1], Yuki Kubo[1], Tsutomu Nagatsuma[1], Takashi Tanaka[1,2]

1. National Institute of Information and Communications Technology, 2. Kyushu University

Surface charging of artificial satellite is one of risks caused by dynamical variations of space environment. It occurs when a satellite exposes high energy electrons around 10 keV created by plasma injection accompanied with substorm. Therefore we want to predict timing and electron energy of plasma injection using magnetosphere-ionosphere coupling global MHD simulation. Now we are developing a real-time numerical simulator for space weather forecast using magnetosphere-ionosphere coupling global MHD simulation called REPPU (REProduce Plasma Universe) code. The feature of the simulation code is highly robust to extreme solar wind parameters because the unstructured grid system has no singular point and is able to calculate in the uniform accuracy over the whole region. We use the real-time solar wind data formatted in the GSM coordinate system observed by DSCOVR spacecraft. Magnetic-dipole axis is fixed to z-direction in our simulation. Therefore daily variation of magnetic-dipole axis is not reproduced. Instead, we convert the input direction of the solar wind velocity and magnetic field into that which tilts including daily variation of magnetic dipole axis in x-z plane. In the method the solar wind structure is not exact. However we can relatively reproduce the magnetosphere response including daily variation of the magnetic-dipole axis against solar wind. The resolution is 7682 grids in the horizontal direction and 240 grids in the radial direction.
In this presentation, we compare the simulation results with the CPCP, AE index, and plasma variations observed by geostationary orbit satellites. Density and temperature of plasma injection derived from MHD simulation tends to estimate larger and smaller values than observation respectively because the MHD simulation does not include kinetic heating effects. We have to interpret MHD simulation results for prediction of electron density and temperature. We will discuss how to interpret electron density and temperature between observation and MHD simulation.

Keywords: global MHD simulation, surface charging

©2019. Japan Geoscience Union. All Right Reserved.

Simulation of GIC flowing through the power transmission network (187 kV-500 kV) in Japan

*Nishida Yuichiro[1,6], Yusuke Ebihara[1], Satoko Nakamura[1], Shinichi Watari[2], Kumiko Hashimoto[3], Kentaro Kitamura[4], Takashi Kikuchi[5]

1. Kyoto University Reserch Institute for Sustainable Humanosphere, 2. National Institute of Information and Communications Technology, 3. Kibi International University, 4. National Insutitute of Technology, Tokuyama College, 5. Nagoya University, 6. Kyoto University Department of Electrical Engineering

The energy released from the sun can enhance electric currents in Earth’ s magnetosphere, which induces an electric field on the ground surface. This electric field, called a geomagnetically induced electric field (GIE), gives rise to geomagnetically induced current (GIC) flowing in a transmission line. Japan is situated at geomagnetically low latitudes, but the potential risk is probably non-zero because a large-amplitude of GIC, as high as 129 A, was recorded in the Japanese power grid during the Halloween storm in October 2003. To evaluate the potential risk of the Japanese power grid properly, we modeled the Japanese power grid with high voltage class over 187 kV on the basis of publicly available data. The model consists of 602 nodes and 763 paths. The uniform GIE imposed on Japan was estimated on the basis of the geoelectric field observed in April 2018 at Kakioka Magnetic Observatory. We applied the uniform GIE on the model. The calculated GIC is roughly in agreement with that measured at 4 substations in Japan. For the westmost substation, a disagreement was found when we considered only the highest class of the power grid (500 kV), which may imply that the lower voltage class of the grid (<500 kV) may have some contribution to the GIC in Japan. We discuss the general tendency of the GIC flowing in the Japanese power grid, and prediction capability of the currently available model.

©2019. Japan Geoscience Union. All Right Reserved.

Simulation of GIC flowing through the power transmission network (187 kV-500 kV) in Japan

Yuichiro Nishida
Yusuke Ebihara
Satoko Nakamura
Shin-Ichi Watari
Kumiko Hashimoto
Kentaro Kitamura
Takashi Kikuchi

Abstract

The energy released from the sun can enhance electric currents in Earth's magnetosphere, which induces an electric field on the ground surface. This electric field, called a geomagnetically induced electric field (GIE), gives rise to geomagnetically induced current (GIC) flowing in a transmission line. Japan is situated at geomagnetically low latitudes, but the potential risk is probably non-zero because a large-amplitude of GIC, as high as 129 A, was recorded in the Japanese power grid during the Halloween storm in October 2003. To evaluate the potential risk of the Japanese power grid properly, we modeled the Japanese power grid with high voltage class over 187 kV on the basis of publicly available data. The model consists of 602 nodes and 763 paths. The uniform GIE imposed on Japan was estimated on the basis of the geoelectric field observed in April 2018 at Kakioka Magnetic Observatory. We applied the uniform GIE on the model. The calculated GIC is roughly in agreement with that measured at 4 substations in Japan. For the westmost substation, a disagreement was found when we considered only the highest class of the power grid (500 kV), which may imply that the lower voltage class of the grid (<500 kV) may have some contribution to the GIC in Japan. We discuss the general tendency of the GIC flowing in the Japanese power grid, and prediction capability of the currently available model.

©2019. Japan Geoscience Union. All Right Reserved.

Climatological features of the upper atmosphere reproduced by a revised version of a whole atmosphere-ionosphere coupled model GAIA

*Hidekatsu Jin[1], Yasunobu Miyoshi[2], Chihiro Tao[1], Hiroyuki Shinagawa[1], Hitoshi Fujiwara[3]

1. National Institude of Information and Communications Technology, 2. Kyushu University, 3. Seikei University

Temporal and spatial variations in the ionospheric electron density and thermospheric mass density could have significant impacts on radio communications between ground and space, and particle and atmospheric drag environments around satellites. Origins of such upper atmospheric variations are not only in the solar atmosphere through the emissions of solar radiation, high-speed plasma gas and high-energy particles, but also in the Earth’ s lower atmosphere, where meteorological phenomena could give rise to atmospheric waves propagating upward. In order to nowcast and forecast the upper atmospheric variations and disturbances, a whole atmospheric model, GAIA, has been developed, which combines a whole atmospheric GCM, an ionospheric model and an electrodynamics model in a self-consistent manner.

So far, for the purpose of its validation, we have compared climatological features of thermosphere and ionosphere reproduced by GAIA with those from ionospheric observation and observation-based empirical models. The comparison indicates that the model and observations are generally in good agreements, but in some condition such as at solar maximum there are significant disagreements in the ionospheric electron density distribution. In order to improve the accuracy of the model, we have made several updates such as ion chemical processes, energetics, parameterization, and so on. We also have introduced magnetospheric effects into the model, such as electrodynamics coupling with magnetosphere and particle precipitation. In this presentation, we discuss how the upper atmospheric model can improve its accuracy and how they can be validated.

Keywords: space weather, whole atmosphere, ionosphere, simulation, thermosphere, assimilation

©2019. Japan Geoscience Union. All Right Reserved.

Investigation of the thermospheric mass density variations below 200 km

*Hitoshi Fujiwara[1], Yasunobu Miyoshi[2], Masayoshi Utashima[1], Huixin Liu[2]

1. Faculty of Science and Technology, Seikei University, 2. Department of Earth and Planetary Sciences, Faculty of Sciences, Kyushu University

Since both the effects from the lower atmosphere and in-situ forcing are significant in the thermospheric region between 100 and 200 km altitude, the thermosphere in the region shows complex variations depending on various conditions. In addition, observations of the thermosphere (neutral atmosphere) between 100 and 200 km are very few compared to the upper thermosphere (above 300 km) and the ionosphere. These make it difficult to improve reliability of empirical and numerical models. Observations from Low Earth Orbit (LOE) satellites would be essential for building up available data sets in the thermospheric region between 100 and 200 km altitude. We will introduce our research project to investigate the thermospheric mass density variations in the 100-200 km altitude region with the LOE satellite, e.g., Tsubame (SLATS), data and a whole atmosphere GCM.

Keywords: thermosphere, mass density, Low Earth Orbit (LOE) satellite, GCM

©2019. Japan Geoscience Union. All Right Reserved.

Low-latitude HF Doppler observations of magnetospheric electric fields during space weather disturbances

*Kumiko K. Hashimoto[1], Takashi Kikuchi[2], Ichiro Tomizawa[3], Keisuke Hosokawa[3], Jaroslav Chum[4]

1. Kibi International University, 2. Nagoya University, 3. University of Electro-Commnunications, 4. Institute of Atmospheric Physics, Prague

Ionospheric electric fields penetrated from the magnetosphere to the low latitude ionosphere have been observed as geomagnetic disturbances caused by ionospheric currents, such as the equatorial electrojet (EEJ) at the dayside equator. The ionospheric currents are too weak to be a detector of the electric field at low latitudes on the dayside and even at the equator on the nightside. The HF Doppler (HFD) sounder is another powerful tool for observations of the electric filed at low latitudes on both the day- and night-sides. We have shown that the electric fields of the geomagnetic sudden commencements (SC) are composed of the preliminary impulse followed by the main impulse, of which directions are opposite to each other and both electric fields are opposite on the day- to night-sides (Kikuchi et al. 2016 JGR). We have also shown that the substorm electric fields are composed of the growth phase followed by expansion phase overshielding electric fields, of which directions are opposite to each other (Hashimoto et al., 2017). In this paper, we show that the HFD sounder is capable of detecting stormtime electric fields and that the electric fields are found to decay rather rapidly over one hour during the main phase with the time scale of a few hours. Combining with the equatorial magnetometer data, we would be able to estimate the decaying rate of the HFD electric fields, which helps obtain the stormtime electric fields quantitatively from the HFD data. We discuss advantages of widely separated HFD sounder operations and cooperations with SuperDARN as well as with magnetometer networks.

Keywords: HF Doppler observation, ionosphere electric field, magnetospheric electric field, geomagnetic storm, equatorial electrojet

©2019. Japan Geoscience Union. All Right Reserved.

Stratospheric ionization during magnetic storms

*Ryuho Kataoka[1]

1. National Institute of Polar Research

Transient mesospheric ionization was detected at an altitude of 65-70 km during the auroral breakup that occurred from 2220 to 2226 UT on June 30, 2017. During this event, the footprint of the Arase satellite was located within the field of view of the all-sky imagers at Syowa Station in the Antarctic. Auroral observations at Syowa Station revealed the dominant precipitation of relatively soft electrons during the auroral breakup. A corresponding spike in cosmic noise absorption was also observed at Syowa Station, while the Arase satellite observed a flux enhancement of >100 keV electrons and a broadband noise without detecting chorus waves or electromagnetic ion cyclotron waves. A general-purpose Monte Carlo particle transport simulation code was used to quantitatively evaluate the ionization in the middle atmosphere. Results of this study indicate that the precipitation of energetic electrons of >100 keV, rather than X-rays from the auroral electrons, played a dominant role in the transient and deep (65-70 km) mesospheric ionization during the observed auroral breakup. Based on the above results of Kataoka et al. (2019), we further discuss a possible role of X-rays to ionize the stratosphere during magnetic storms.

Reference:
Kataoka et al. (2019), Earth, Planets and Space, 71, 9, https://doi.org/10.1186/s40623-019-0989-7

©2019. Japan Geoscience Union. All Right Reserved.

Calculating propagation time of HF radio wave using ray-tracing method and simple comparison with the observation.

*Ryo Nakao[1], Hiroyuki Nakata[1], Hiroyo Ohya[1], Toshiaki Takano[1], Kornyanat Hozumi[2], Takuya Tsugawa[2], Susumu Saito[3], Mamoru Ishii[2]

1. Graduate School of Engineering, Chiba University, 2. National Institute of imformation and Communications Technology, 3. Electronic Navigation Research Institute

To provide the information of nowcast of radio propagation, we have started a project, HF-START (HF simulator Targeting for All user's Regional Telecommunications). In this project, a simulator that is able to predict propagation of HF radio waves is constructed by ray-tracing calculation.
Using this simulator, we have examined whether HF radio wave travels between any two points. In this calculation, the electron density, which is necessary to calculate reflection index is determined by International Reference Ionosphere (IRI).In this project, HF receivers have been installed at Chiba University (Chiba, 35.62N, 140.10E), Sarobetu (Hokkaido, 45.16N, 141.74E), Numata (Gunma, 36.62N, 139.02E), Yamagawa (Kagoshima, 31.20N, 130.61), Ogimi (Okinawa, 26.68, 128.15E) for observing HF radio wave transmitted from radioNIKKEI (Nagara, Chiba, 35.46N, 140.20E) to confirm the results of the ray-tracing calculation. In the ray-tracing calculation, therefore, we set the same locations of the transmitter and receivers as the observatories of HF-START. As a result of simple comparison between the ray-tracing results and the observation, it is found that there was a difference of the propagation time between the ray-tracing results and the observations. It is possible that the radio wave propagation between radioNIKKEI and Ciba University is not ground wave but sky wave that is reflected by ionosphere. As for further calculation, we plan to use the electron density distributions determined by GAIA and GNSS tomography in the ray-tracing calculation.

©2019. Japan Geoscience Union. All Right Reserved.

Why do some probabilistic forecasts lack reliability?

*Yuki Kubo[1]

1. National Institute of Information and Communications Technology

One of the important attributes to be satisfied for the probabilistic forecast system is reliability. However, some probabilistic forecast systems lack reliability. Why do some probabilistic forecasts lack reliability? We investigate a condition for a probabilistic binary forecast to be reliable in this work. We mathematically prove that a necessary, but not sufficient, condition for achieving a reliable probabilistic forecast is maximizing the Peirce skill score (PSS) at the threshold probability of the climatological base rate. The condition is confirmed by using artificially synthesized forecast-outcome pair data and previously published probabilistic solar flare forecast models. The condition gives a partial answer as to why some probabilistic forecast systems lack reliability, because the system, which does not satisfy the proved condition, can never be reliable. The result implies that those who want to develop a reliable probabilistic forecast system must adjust or train the system so as to maximize PSS near the threshold probability of the climatological base rate.

Keywords: Probabilistic forecast, Reliability

©2019. Japan Geoscience Union. All Right Reserved.

An estimation method of GEO spacecraft surface charging for a real-time spacecraft risk assessment

*Masao Nakamura[1], Ryota Kawachi[1], Go Takahashi[1], Tsutomu Nagatsuma[2], Mamoru Ishii[2]

1. Osaka Prefecture University, 2. NICT

Spacecraft anomalies are often induced by electrostatic discharges due to surface charging. Some spacecraft charging simulation software is developed by space agencies and research institutes and used for spacecraft designs and charging analysis. However these simulations cannot be used for a real-time estimation because they need hours or days to calculate the surface potential for a given plasma environment. Therefore we develop a quick estimation method of GEO spacecraft surface charging for the Space Environment Customized Risk Estimation for Spacecraft (SECURES) of the space weather forecast Project for Solar-Terrestrial Environment Prediction (PSTEP). We estimate the surface potentials by interpolation using lookup tables of the pre-simulated surface potentials for combinations of plasma temperatures and densities. We study fitting functions used in the interpolation and how to make the lookup tables for the good estimation. Then we can real-time estimate the surface potentials of the target GEO spacecraft when the on-orbit plasma environment is predicted or observed. The spacecraft risk assessment can be accomplished by additional information about the experimental discharging differential potential of the surface materials.

Keywords: Spacecraft surface charging, Space weather, Spacecraft risk assessment

©2019. Japan Geoscience Union. All Right Reserved.

A network of HF Doppler sounding systems in Japan

*Keisuke Hosokawa[1], Hiroyuki Nakata[2], Kumiko K. Hashimoto[3], Ichiro Tomizawa[1], Jun Sakai[1], Takashi Kikuchi[4]

1. University of Electro-Communications, 2. Chiba University, 3. Kibi International University, 4. ISEE, Nagoya University

Since 2003, a network observation of HF Doppler sounding has been conducted in Japan for remote-sensing the atmospheric, ionospheric and magnetospheric processes. Currently, 1 transmitting station (Tx) and 7 receiving stations (Rx) are operative by a collaborative effort of four difference universities. The main transmitting station is located at Chofu, Tokyo, Japan in the Campus of University of Electro-Communications (JG2XA). JG2XA transmits continuous waves at 5006 kHz and 8006 kHz with a transmitting power of 200 W. By receiving this JG2XA signal at 7 Rx stations (Sugadaira, Oarai, Kure, Kashima, Iitate, Fujisawa and Sugito) we derive the Doppler shift imposed during the propagation and reflection in the ionosphere. In particular, the Doppler shift data can be used to detect vertical motion of the ionospheric F region with a temporal resolution of 10 s. At some stations, we also have observed signals from Radio Nikkei 1 (JOZ at 3925 kHz, JOZ2 at 6055 kHz, and JOZ3 at 9595 kHz) transmitted from Nagara, Chiba, Japan, which allows us to observe the vertical motion of the ionosphere at several altitude levels. The data obtained from this experiment since 2003 are all available at http://gwave.cei.uec.ac.jp/~hfd. Not only quick-look plots but also several types of digital data (raw wave form and Doppler shift data) can be retrieved from this database. The experiment covers various ionospheric phenomena in the Magnetosphere-Ionospheric (M-I) coupling system, such as sporadic E-layer (Es), medium-scale traveling ionospheric disturbances (MSTIDs), large-scale traveling ionospheric disturbances (LSTIDs), global-scale electric field variation, geomagnetic pulsations, and sudden commencement (SC). The data can also be used for the studies of vertical coupling between the lower atmosphere and ionosphere, for example, observations of ionospheric variation after large earthquakes, volcanic eruptions and typhoons. To facilitate analyses of the phenomena listed above, it is desired to observe a wider area in latitude and longitude. For this purpose we plan to extend the network covering the entire ionosphere over Japan in the near future. In the presentation, we will give a brief introduction to the experiments and online database, and then discuss the future direction of the studies of atmosphere, ionosphere and magnetosphere using the HF Doppler sounding in a framework of international collaborations.

Keywords: HF Doppler experiment, Ionosphere

©2019. Japan Geoscience Union. All Right Reserved.

[E] Poster | P (Space and Planetary Sciences)：P-EM Solar-Terrestrial Sciences, Space Electromagnetism & Space Environment

Tue. May 28, 2019 5:15 PM - 6:30 PM JST | Tue. May 28, 2019 8:15 AM - 9:30 AM UTC | Poster Hall International Exhibition Hall8, Makuhari Messe_3

[P-EM12] Space Weather and Space Climate

convener:Ryuho Kataoka(National Institute of Polar Research), Antti A Pulkkinen(NASA Goddard Space Flight Center), Kanya Kusano(Institute for Space-Earth Environmental Research, Nagoya University), Kaori Sakaguchi(National Institute of Information and Communications Technology)

We share the latest scientific papers to understand how the solar-terrestrial environment changes in various time scales, and to discuss how we will react via international and interdisciplinary collaborations. More specifically, welcomed papers include space climate studies to reconstruct long-term variations from radio isotopes; cutting-edge observational and modeling studies of the ionosphere, geospace, heliosphere and the sun; simulation and statistical studies to predict the future space weather and space climate; applied science such as operational space weather forecast and mitigation of the social impact due to extreme space hazards.

[PEM12-P01] Reconnection signatures in solar magnetograms during the solar storms of 4-10 September 2017

*Robert Dean Loper[1,2] (1.Air Force Institute of Technology, Department of Engineering Physics, 2.National Center for Atmospheric Research, High Altitude Observatory)

[PEM12-P02] Statistical Relation between Solar Flares and Coronal Mass Ejections with Respect to Sigmoidal Structures in Active Regions

*Yusuke Kawabata[1,2], Yusuke Iida[3], Takafumi Doi, Sachiko Akiyama[4], Seiji Yashiro[4], Toshifumi Shimizu[2] (1.Earth and Planetary Science, The University of Tokyo, 2.Institute of Space and Astronautical Science, JAXA, 3.Kwansei Gakuin University, 4.The Catholic University of America)

[PEM12-P03] Multi-wavelength Observations of Pre-flare Quasi-periodic Pulsation in the C2.2 Flare on 2012 October 15

*Yung-Chi Yang[1], Ya-Hui Yang[1], Baolin Tan[2], Chengming Tan[2], Y.H. Yan[2] (1.Graduate Institute of Space Science National Central University, 2.Key Laboratory of Solar Activities, National Astronomical Observatories)

[PEM12-P04] Investigation of pre-flare type III solar radio bursts and their potential solar origins

*Shao-Fu Hsieh[1], Ya-Hui Yang[1], Baolin Tan[2], Chengming Tan[2], Y.H. Yan[2] (1.Graduate Institute of Space Science National Central University, 2.Key Laboratory of Solar Activities, National Astronomical Observatories, Chinese Academy of Sciences)

[PEM12-P05] Statistical and observational research of solar flare for constructing total emission spectra prediction model

*Shohei Nishimoto[1], kyoko Watanabe[1], Shinsuke Imada[2], Tomoko Kawate[3], Kyoung-Sun Lee[4] (1.National Defense Academy, 2.Institute for Space-Earth Environmental Research, Nagoya University, 3.Institute Of Space And Astronautical Science, Japan Aerospace Exploration Agency, 4.National Astronomical Observatory of Japan)

[PEM12-P06] Modeling of solar active regions using local linear force-free fields to estimate magnetic twist

*Kento Nakatani[1], Kanya Kusano[1], Sung-Hong Park[1], Leka KD[2] (1.Institute for space-Earth Environmental Research, Nagoya University, 2.North West Reserch Associates)

[PEM12-P07] Magnetohydrodynamic Simulation of an Erupting Magnetic Flux Rope on February 13 2009: Journey to Coronal Mass Ejection

*Satoshi Inoue[1], Antonia Savcheva[2] (1.Institute for Space-Earth Environmental Research, Nagoya University, 2.Harvard-Smithsonian Center for Astrophysics)

[PEM12-P08] Investigation of flow structures in the solar interior through the surface magnetic elements' tracking

*Yusuke Iida[1] (1.Kwansei Gakuin University)

[PEM12-P09] High-precision measurement of carbon-14 in tree rings around the onset of the Maunder Minimum

*Hiroko Miyahara[1], Fuyuki Tokanai[2], Toru Moriya[2], Hideyuki Hotta[3] (1.Musashino Art University, 2.Yamagata University, 3.Chiba University)

[PEM12-P10] Examination of ^{10}Be in travertine sediment as a possible tool to reconstruct past solar activity

*Hongyang Xu[1,2], Hiroko Miyahara[2], Kazuho Horiuchi[3], Hiroyuki Matsuzaki[4], Hailong Sun[5], Weijun Luo[5], Xiangmin Zheng[1], Yusuke Suganuma[6,7], Shijie Wang[5], Limin Zhou[1] (1.East China Normal University, 2.Musashino Art University, 3.Hirosaki University, 4.University of Tokyo, 5.Chinese Academy of Sciences, 6.National Institute of Polar Research, 7.The Graduate University for Advanced Studies (SOKENDAI))

[PEM12-P11] Examination of ^{10}Be in travertine sediment as a possible tool to reconstruct past solar activity II

*Hongyang Xu[1,2], Hiroko Miyahara[2], Kazuho Horiuchi[3], Hiroyuki Matsuzaki[4], Hailong Sun[5], Weijun Luo[5], Xiangmin Zheng[1], Yusuke Suganuma[6,7], Shijie Wang[5], Limin Zhou[1] (1.East China Normal University, 2.Musashino Art University, 3.Hirosaki University, 4.University of Tokyo, 5.Chinese Academy of Sciences, 6.National Institute of Polar Research, 7.The Graduate University for Advanced Studies (SOKENDAI))

[PEM12-P12] 1 year of CR observation at Syowa Station in the Antarctic.

*Chihiro Kato[1], Kazuoki Munakata[1], Akira Kadokura[2], Ryuho Kataoka[2], Paul Evenson[3] (1.Shinshu University, 2.National Institute of Polar Research, 3.University of Delaware)

[PEM12-P13] Space weather forecast archives at NICT: handwritten solar activity charts

*Kaori Sakaguchi[1], Daikou Shiota[1], Kaori Fukunaga[1], Katsuhide Marubashi[1], Hiromitsu Ishibashi[1], Yuki Kubo[1], Mamoru Ishii[1] (1.National Institute of Information and Communications Technology)

[PEM12-P14] IMF dependence on solar wind parameters

*Tohru Araki, Yuki Harada[1] (1.Kyoto University)

[PEM12-P15] **Dipole Tilt Effect of Geomagnetic Activity from Low- to High-latitudes**

*Nowada Motoharu[1] (1.Shandong University at Weihai)

[PEM12-P16] A New Prediction Model for Solar Wind-Triggered Magnetospheric Disturbances Based on Potential Learning (Neural Network)

*Ryozo Kitajima[1], Motoharu Nowada[2], Ryotaro Kamimura[3] (1.Seikei University, 2.Shandong University at Weihai, 3.Tokai University)

[PEM12-P17] Real-time magnetosphere simulator for space weather using REProduce Plasma Universe code

*Yasubumi Kubota[1], Aoi Nakamizo[1], Kaori Sakaguchi[1], Mitsue Den[1], Yuki Kubo[1], Tsutomu Nagatsuma[1], Takashi Tanaka[1,2] (1.National Institute of Information and Communications Technology, 2.Kyushu University)

[PEM12-P18] **Simulation of GIC flowing through the power transmission network (187 kV-500 kV) in Japan**

*Nishida Yuichiro[1,6], Yusuke Ebihara[1], Satoko Nakamura[1], Shinichi Watari[2], Kumiko Hashimoto[3], Kentaro Kitamura[4], Takashi Kikuchi[5] (1.Kyoto University Reserch Institute for Sustainable Humanosphere, 2.National Institute of Information and Communications Technology, 3.Kibi International University, 4.National Insutitute of Technology, Tokuyama College, 5.Nagoya University, 6.Kyoto University Department of Electrical Engineering)

[PEM12-P19] Climatological features of the upper atmosphere reproduced by a revised version of a whole atmosphere-ionosphere coupled model GAIA

*Hidekatsu Jin[1], Yasunobu Miyoshi[2], Chihiro Tao[1], Hiroyuki Shinagawa[1], Hitoshi Fujiwara[3] (1.National Institude of Information and Communications Technology, 2.Kyushu University, 3.Seikei University)

[PEM12-P20] Investigation of the thermospheric mass density variations below 200 km

*Hitoshi Fujiwara[1], Yasunobu Miyoshi[2], Masayoshi Utashima[1], Huixin Liu[2] (1.Faculty of Science and Technology, Seikei University, 2.Department of Earth and Planetary Sciences, Faculty of Sciences, Kyushu University)

[PEM12-P21] Low-latitude HF Doppler observations of magnetospheric electric fields during space weather disturbances

*Kumiko K. Hashimoto[1], Takashi Kikuchi[2], Ichiro Tomizawa[3], Keisuke Hosokawa[3], Jaroslav Chum[4] (1.Kibi International University, 2.Nagoya University, 3.University of Electro-Commnunications, 4.Institute of Atmospheric Physics, Prague)

[PEM12-P22] Stratospheric ionization during magnetic storms

*Ryuho Kataoka[1] (1.National Institute of Polar Research)

[PEM12-P23] Calculating propagation time of HF radio wave using ray-tracing method and simple comparison with the observation.

*Ryo Nakao[1], Hiroyuki Nakata[1], Hiroyo Ohya[1], Toshiaki Takano[1], Kornyanat Hozumi[2], Takuya Tsugawa[2], Susumu Saito[3], Mamoru Ishii[2] (1.Graduate School of Engineering, Chiba University, 2.National Institute of imformation and Communications Technology, 3.Electronic Navigation Research Institute)

[PEM12-P24] Why do some probabilistic forecasts lack reliability?

*Yuki Kubo[1] (1.National Institute of Information and Communications Technology)

[PEM12-P25] An estimation method of GEO spacecraft surface charging for a real-time spacecraft risk assessment

*Masao Nakamura[1], Ryota Kawachi[1], Go Takahashi[1], Tsutomu Nagatsuma[2], Mamoru Ishii[2] (1.Osaka Prefecture University, 2.NICT)

[PEM12-P26] A network of HF Doppler sounding systems in Japan

*Keisuke Hosokawa[1], Hiroyuki Nakata[2], Kumiko K. Hashimoto[3], Ichiro Tomizawa[1], Jun Sakai[1], Takashi Kikuchi[4] (1.University of Electro-Communications, 2.Chiba University, 3.Kibi International University, 4.ISEE, Nagoya University)

Reconnection signatures in solar magnetograms during the solar storms of 4-10 September 2017

*Robert Dean Loper[1,2]

1. Air Force Institute of Technology, Department of Engineering Physics, 2. National Center for Atmospheric Research, High Altitude Observatory

Solar flare forecasting is limited to active region classification and historical correlation, due largely to our lack of understanding of magnetic reconnection as a driving mechanism for solar flares and coronal mass ejections. Photospheric observations indicate magnetic field changes during solar flares, brought about during magnetic reconnection and related to magnetic field helicity on the solar surface. While the neutral point of the reconnection event associated with a flare usually occurs in the solar corona, some signs of the magnetic field changes should manifest as low as the photosphere. This study utilizes data from SDO HMI and Space-Weather HMI Active Regions Patches (SHARPS) to analyze full vector field component data in the photospheric magnetic field during several magnetic reconnection events during the space weather events of 4-10 September 2017.

Keywords: solar atmosphere, sunspots, magnetogram, solar flares

©2019. Japan Geoscience Union. All Right Reserved.

Statistical Relation between Solar Flares and Coronal Mass Ejections with Respect to Sigmoidal Structures in Active Regions

*Yusuke Kawabata[1,2], Yusuke Iida[3], Takafumi Doi, Sachiko Akiyama[4], Seiji Yashiro[4], Toshifumi Shimizu[2]

1. Earth and Planetary Science, The University of Tokyo, 2. Institute of Space and Astronautical Science, JAXA, 3. Kwansei Gakuin University, 4. The Catholic University of America

We will report statistical dependences among features of coronal mass ejections (CMEs), solar flares, and sigmoidal structures in soft-X-ray images (Kawabata et al. 2018). We applied analysis methods to all the features in the same way in order to investigate the reproducibility of the correlations among them, which may be found from previous statistical studies. Samples of 211 M-class and X-class flares, observed between 2006 and 2015 by the Hinode/X-ray telescope, Solar and Heliospheric Observatory/Large Angle and Spectrometric Coronagraph, and Geostationary Operational Environmental Satellite, were examined statistically. Five kinds of analysis were performed: Occurrence rate analysis, linear-correlation analysis, association analysis, the Kolmogorov–Smirnov test, and the Anderson–Darling test. These give three main results. First, the sigmoidal structure and long-duration events (LDEs) have a stronger dependence on CME occurrence than large X-ray-class events in on-disk events. Second, for the limb events, a significant dependence exists between LDEs and CME occurrence, and between X-ray-class events and CME occurrence. Third, 32.4% of on-disk flare events have sigmoidal structure and are not accompanied by CMEs. However, the occurrence probability of CMEs without sigmoidal structure is very small, 8.8%, in on-disk events. While the first and second results are consistent with previous studies, we provide for the first time a difference between the on-disk and limb events. The third result, that non-sigmoidal regions produce fewer eruptive events, is also different from previous results. We suggest that sigmoidal structures in soft X-ray images will be a helpful feature for CME prediction in on-disk flare events.

Keywords: Sun, Solar flares, Coronal mass ejections, Sigmoid

©2019. Japan Geoscience Union. All Right Reserved.

Multi-wavelength Observations of Pre-flare Quasi-periodic Pulsation in the C2.2 Flare on 2012 October 15

*Yung-Chi Yang[1], Ya-Hui Yang[1], Baolin Tan[2], Chengming Tan[2], Y.H. Yan[2]

1. Graduate Institute of Space Science National Central University, 2. Key Laboratory of Solar Activities, National Astronomical Observatories

Quasi-periodic pulsation (QPP) is thought to be the nature of solar flares, which can be observed during and before flares in various wavelengths, such as the radio, microwave, SXR, and EUV. In this study, we analyze a pre-flare QPP event on 2012 October 15 and its association with the following C2.2 flare based on the radio data in the ranges of 2.81-2.85 GHz and 2.91-2.95 GHz from Solar Broadband Radio Spectrometer (SBRS), EUV images from AIA multi-wavelength observations, and wavelet analysis. Our result show that the main period of the radio QPP is ~800 s which is similar to the period of ~13.5 min obtained in SXR by Tan et al. (2016). Moreover, we analyze several localized areas in the flare-eruptive AR 11593 to search for the possible regions responsible for the occurrence of pre-flare QPP. We find that the footpoints of brightening loops in 211 Åshow the quasi-periodic behavior of ~850 s. It is thus suggested that the pre-flare QPP with a period of 13-15 min can be manifested in both of the thermal (SXR, EUV) and nonthermal (radio) radiation processes. The relationship between the pre-flare QPP and the subsequent C2.2 flare will also be discussed.

Keywords: sun, solar flares, solar oscillation

©2019. Japan Geoscience Union. All Right Reserved.

Investigation of pre-flare type III solar radio bursts and their potential solar origins

*Shao-Fu Hsieh[1], Ya-Hui Yang[1], Baolin Tan[2], Chengming Tan[2], Y.H. Yan[2]

1. Graduate Institute of Space Science National Central University, 2. Key Laboratory of Solar Activities, National Astronomical Observatories, Chinese Academy of Sciences

Type III solar radio bursts are characterized as the fast-drifting radio emissions in a dynamic spectrogram, which is believed to be produced by the propagating electron beams and often accompanied with the solar flares or magnetic reconnection. Studying the type III radio bursts in high-frequency range before flares would be important for understanding the trigger of energy release although it is rarely reported previously. Here we present two pre-flare type III burst events found in the range of 2.6-3.8 GHz at Solar Broadband Radio Spectrometer (SBRS). By comparing with the SDO/AIA multi-wavelength observations in flare active regions, the pre-flare type III radio bursts have good temporal correlations with the increases of EUV emissions. Furthermore, we find that one event is related to the EUV brightening with 1-min delay, implying the existence of plasma heating before energy release. The other event has a simultaneous EUV jet with a speed of ~700 km/s indicating the occurrence of magnetic reconnection. We suppose both pre-flare events are associated with small-scale energy release via magnetic reconnection.

Keywords: sun, solar flares, solar radio bursts

©2019. Japan Geoscience Union. All Right Reserved.

Statistical and observational research of solar flare for constructing total emission spectra prediction model

*Shohei Nishimoto[1], kyoko Watanabe[1], Shinsuke Imada[2], Tomoko Kawate[3], Kyoung-Sun Lee[4]

1. National Defense Academy, 2. Institute for Space-Earth Environmental Research, Nagoya University, 3. Institute Of Space And Astronautical Science, Japan Aerospace Exploration Agency, 4. National Astronomical Observatory of Japan

Impulsive energy release phenomena such as solar flares, sometimes affect to the solar-terrestrial environment. Usually, we use soft X-ray flux (GOES class) as the index of flare scale. However, the magnitude of effect to the solar-terrestrial environment is not proportional to this scale. Therefore, it is considered that the GOES class is not optimal parameter for predicting the Sudden Ionospheric Disturbance (SID). To identify the relationship between solar flare phenomena and influence to the solar-terrestrial environment, we need to understand the full spectra of solar flares in detail.
There is the solar flare irradiance model named the Flare Irradiance Spectral Model (FISM) (Chamberlin et al., 2006, 2007, 2008). FISM is the most used model, and can estimate solar flare spectra with high wavelength and temporal resolution. However, this model can not express the time evolution of emitted plasma during the solar flare, and has low accuracy on short wavelength that might strongly affect to the total flare spectra. Therefore, individual SID phenomenon can not be reproduced.
In this work, in order to solve the problems of FISM, we performed statistical analysis on observational data during the solar flares. From This study, we tried to find the parameters that control the solar flare emission spectra. We selected solar flare events larger than M-class from the Hinode flare catalogue (Watanabe et al., 2012). First, we focused on the EUV emission observed by the SDO/EVE. We examined the intensities and time evolutions of five EUV lines (Fe XX, Fe XVIII, Fe XVI, Fe VIII, and He II) for 54 flare events. As a result, we found positive correlation between the “GOES class” and the “EUV peak flux” for all Fe lines. Moreover, we found that hotter lines peaked earlier than cooler lines. On the other hand, He II line data have poor correlation with GOES X-ray data. Furthermore, we considered that the geometrical features of solar flares effect to those time evolutions. We measured flare ribbon length for 33 flare events observed by SDO/AIA, and found positive correlation between the “flare duration” and the “ribbon length”. From the statistical research of these observational data, we found that the time evolution of EUV emission can be explained by the X-ray emission.
Then, we tried to identify parameters that determine the solar flare spectra by comparing the flare emissions derived from physical based numerical model of solar flare with the actual observational data. Consequently, we used numerical simulation same as Imada et al.(2015). This numerical model can reproduce the movement and ionization of the plasma in the flare loop.
In this presentation, we will show some results of numerical simulation, and discuss the parameters for total solar flare emission spectra by comparing of simulation results, observational data and FISM.

Keywords: Space Weather, Solar Flare

©2019. Japan Geoscience Union. All Right Reserved.

Modeling of solar active regions using local linear force-free fields to estimate magnetic twist

*Kento Nakatani[1], Kanya Kusano[1], Sung-Hong Park[1], Leka KD[2]

1. Institute for space-Earth Environmental Research, Nagoya University, 2. North West Reserch Associates

The prediction of solar flares is an important issue for space weather forecasting. Although solar flares are believed to be caused by the magnetohydrodynamic (MHD) instability in solar active regions, the method for accurately evaluating the stability of solar magnetic field is not yet established. Recently, Ishiguro & Kusano (2017) proposed that a new instability called the Double Arc Instability (DAI) plays a role of initial driver of solar flares and the critical parameter for this instability can be used to evaluate the stability of active regions. The parameter can be derived by the integration of the magnetic twist as the function of magnetic flux. One way for it is given by the nonlinear force-free field (NLFFF) extrapolation using the photospheric vector magnetic field data. However, the NLFFF extrapolation demands heavy computation and it sometimes cannot well work as a model of solar coronal magnetic field because the force-free condition is limited on the photosphere. Therefore, in order to improve the efficiency and applicability of the flare prediction using , it may be required to develop a method to approximately but much quickly capture the overall features of magnetic field in solar active regions, especially in the flare triggering region. From this point of view, we try to develop a method to extract the characteristic feature of magnetic field in solar active regions using the linear force-free field (LFFF) model. For this objective, we compare the several methods to accurately capture the structure of using LFFF. In this study, we report the result of the analysis for the solar active region NOAA 11429.

Keywords: Space weather, solar , twist, force-free, photosphere, active region

©2019. Japan Geoscience Union. All Right Reserved.

Magnetohydrodynamic Simulation of an Erupting Magnetic Flux Rope on February 13 2009: Journey to Coronal Mass Ejection

*Satoshi Inoue[1], Antonia Savcheva[2]

1. Institute for Space-Earth Environmental Research, Nagoya University, 2. Harvard-Smithsonian Center for Astrophysics

We performed a magnetohydrodynamic (MHD) simulation of a solar eruption launched from solar active region 11012 on February 13, 2009. We in particular concentrated on the evolution of the magnetic flux rope (MFR) leading a coronal mass ejection. We first extrapolated the pre-eruptive magnetic flux ropes using a flux insertion method, in which the MFRs can be extrapolated from the normal component of the magnetic field (Bz) observed by SOHO/MDI and Extreme-Ultra Violet (EUV) images observed by the STEREO satellite. The extrapolated magnetic field reproduced the sigmoidal magnetic structure observed in EUV image well. Next we performed the MHD simulation using the extrapolated magnetic field.

The resulting simulation showed the dramatic eruption of the magnetic flux rope under which the current sheet and the post-flare loops are formed. This is well explained by the standard CSHKP flare model. The evolution of the MFR did not show simple dynamics, rather it showed very complicated dynamics through a magnetic reconnection. We found, during the eruption, that the coherent MFR is created through the reconnection of multiple pre-existing MFRs. Magnetic reconnection plays a role in producing the coherent, erupting MFR and supplying further twist into it. Furthermore we found that the footpoints of the erupting MFR moves along or away from the polarity inversion line, as seen in two-ribbon flares. The locations of both the footpoints of the MFR correspond to those of dimming regions observed in EUV images. Since the location and shape of the post-flare loops obtained from the simulation is reproduced in the observations, we can confirm the reliability of our simulation.

Keywords: Solar Flare, Solar Eruption, Magnetohydrodynamics

©2019. Japan Geoscience Union. All Right Reserved.

Investigation of flow structures in the solar interior through the surface magnetic elements' tracking

*Yusuke Iida[1]

1. Kwansei Gakuin University

We investigate the correlation of meridional flow and rotation velocity in the solar interior by tracking huge number of the surface magnetic elements.

As reported in JpGU2017 meeting, we found that the meridional flow velocity from the magnetic elements' tracking depends positively on their flux and size. We discussed that it may come from that the larger magnetic elements are rooted in the deeper solar interior. We further investigate this issue by correlating the meridional flow velocity and rotation velocity.

We use line-of-sight magnetograms obtained by SDO/HMI in July 2016. Time cadence is 45 seconds, in which the travel distance of magnetic element is smaller than 1 pixel. The magnetograms are transposed from the Earth-view coordinate to the Stonyhurst coordinate. We use the data within 75 degree from the disk center. Magnetic field strength is converted with an assumption that magnetic field is vertical to the surface and interpolated with a cubic spline interpolation.

We detected approximately 8,000 elements in each magnetogram and 4.5x108 displacements in our data set. The meridional flow and rotation velocity on magnetic flux are investigated. The rotation velocity shows negative dependence on the flux at the latitude within 45 degree while it shows weekly positive dependence at the latitude higher than 45 degree. This result is consistent with the depth dependence of rotation velocity obtained by previous helioseismology researches.

Keywords: Sun, Bigdata, Turbulence

©2019. Japan Geoscience Union. All Right Reserved.

High-precision measurement of carbon-14 in tree rings around the onset of the Maunder Minimum

*Hiroko Miyahara[1], Fuyuki Tokanai[2], Toru Moriya[2], Hideyuki Hotta[3]

1. Musashino Art University, 2. Yamagata University, 3. Chiba University

It is well known that the Sun indicates long-term variations at time scales of a few hundred years to a few millennia. It sometimes brings the grand minima, at which period the sunspots disappear for more than several decades. The detailed process of such long-lasting disappearance of sunspots, however, remains unclear. We therefore have been trying to reconstruct solar cycles around the onset of grand minima based on high-precision measurement of carbon-14 in tree rings. In this paper, we report on our preliminary result on the measurement of carbon-14 around the onset of the Maunder Minimum.

Keywords: solar cycle, grand minima, cosmogenic nuclide

©2019. Japan Geoscience Union. All Right Reserved.

Examination of ^{10}Be in travertine sediment as a possible tool to reconstruct past solar activity

*Hongyang Xu[1,2], Hiroko Miyahara[2], Kazuho Horiuchi[3], Hiroyuki Matsuzaki[4], Hailong Sun[5], Weijun Luo[5], Xiangmin Zheng[1], Yusuke Suganuma[6,7], Shijie Wang[5], Limin Zhou[1]

1. East China Normal University, 2. Musashino Art University, 3. Hirosaki University, 4. University of Tokyo, 5. Chinese Academy of Sciences, 6. National Institute of Polar Research, 7. The Graduate University for Advanced Studies (SOKENDAI)

In this study, we explore the possibility of using travertine sediment for reconstructing the past solar activity. We obtained an annual ^{10}Be record from travertine deposit from the modern period and compared with the neutron monitor data. We discuss a possible methodology to calibrate the climatological impact on ^{10}Be deposition and to obtain the signal of past solar and cosmic-ray variations.

Keywords: Beryllium-10, cosmogenic nuclide, solar activity, endogenic travertine

©2019. Japan Geoscience Union. All Right Reserved.

Examination of ^{10}Be in travertine sediment as a possible tool to reconstruct past solar activity II

*Hongyang Xu[1,2], Hiroko Miyahara[2], Kazuho Horiuchi[3], Hiroyuki Matsuzaki[4], Hailong Sun[5], Weijun Luo[5], Xiangmin Zheng[1], Yusuke Suganuma[6,7], Shijie Wang[5], Limin Zhou[1]

1. East China Normal University, 2. Musashino Art University, 3. Hirosaki University, 4. University of Tokyo, 5. Chinese Academy of Sciences, 6. National Institute of Polar Research, 7. The Graduate University for Advanced Studies (SOKENDAI)

We have been examining the potential of ^{10}Be in travertine sediment as a tool to reconstruct past solar and cosmic-ray variations. In this paper, we compare the ^{10}Be profile in the travertine layers from the rainy and dry seasons, and discuss the nature of ^{10}Be deposition at the two seasons.

Keywords: Beryllium-10, cosmogenic nuclide, solar activity, endogenic travertine

©2019. Japan Geoscience Union. All Right Reserved.

1 year of CR observation at Syowa Station in the Antarctic.

*Chihiro Kato[1], Kazuoki Munakata[1], Akira Kadokura[2], Ryuho Kataoka[2], Paul Evenson[3]

1. Shinshu University, 2. National Institute of Polar Research, 3. University of Delaware

CR observation has been carried out for 1 year at Syowa Station in the Antarctic. There was no serious unavailability of data during the whole year. It is now concluded that this station can contribute to a space weather study as one of the CR monitoring station of Global Muon Detector Network (GMDN). We report observed data and its stability as GMDN.

Keywords: Cosmic Rays, Space Weather

©2019. Japan Geoscience Union. All Right Reserved.

Space weather forecast archives at NICT: handwritten solar activity charts

*Kaori Sakaguchi[1], Daikou Shiota[1], Kaori Fukunaga[1], Katsuhide Marubashi[1], Hiromitsu Ishibashi[1], Yuki Kubo[1], Mamoru Ishii[1]

1. National Institute of Information and Communications Technology

About 40 years ago from 1978 to 1999, at Hiraiso Branch, Radio Research Laboratory; present Space Environment Laboratory of National Institute for Information and Communication Technology (NICT) in Japan, space environment data had been recorded in "solar activity chart" by hand for the operation of the radio wave warning service. The charts were created based on URSIgram codes, which were developed to facilitate the rapid exchange of information by telex in periods when internet was not available. Based on the exchanged codes, sunspots transitions and solar flare occurrences on the solar surface, these effects on shortwave propagation, geomagnetic disturbance, and cosmic ray flux over Japan were written in the solar activity charts together with comments and sketch by recorders. One chart was created for each Bertel’ s solar rotation number between No. 1974 and No. 2254, corresponding to sunspot cycles 21 and 22. We realized that the data exchange is almost only once a day from each observation point and charts was accumulation of the available data in real-time at that time.It might be quite difficult to decide future forecast from such a limited real-time data set. Currently, we are digitizing the solar activities charts and the data shown there. In this poster, we present examples of solar activity charts and possible real-time data set and time delay, as well as the verifying result of the solar flare / geomagnetism storm forecast at the time.

Keywords: Space Weather Archive, URSIgram

©2019. Japan Geoscience Union. All Right Reserved.

IMF dependence on solar wind parameters

*Tohru Araki, Yuki Harada[1]

1. Kyoto University

We studied IMF dependence upon solar wind parameters using OMNI hourly values.

Figure below is a plot of the total force (B), horizontal component (Bxy) in the ecliptic plane and vertical component (Bz) of IMF versus the solar wind density (Nsw). The IMF is averaged over 0.2/cc bin of Nsw. Data number in each bin is also plotted. The data period here is 1979-1981 (maximum SSN phase).

The figure shows (1) that B, Bxy and Bz slowly decrease with decreasing Nsw and (2) that when Nsw approaches further to zero. B and Bxy begin to increase and converges to the same finite value (about 10 nT here) while Bz converges to zero. The property (2) suggests that IMF converges to a typical spiral pattern when solar wind density converges to zero.

Two other data periods, 1999-2001 (SSN maximum) and 2007-2009 (SSN minimum) are examined. IMF observed by MAVEN orbiting Mars is also studied for the period, 2014-2018. The results of the analysis are roughly consistent with the description above. We also checked IMF dependence on solar wind velocity

Keywords: IMF, solar wind density, solar wind melocity

©2019. Japan Geoscience Union. All Right Reserved.

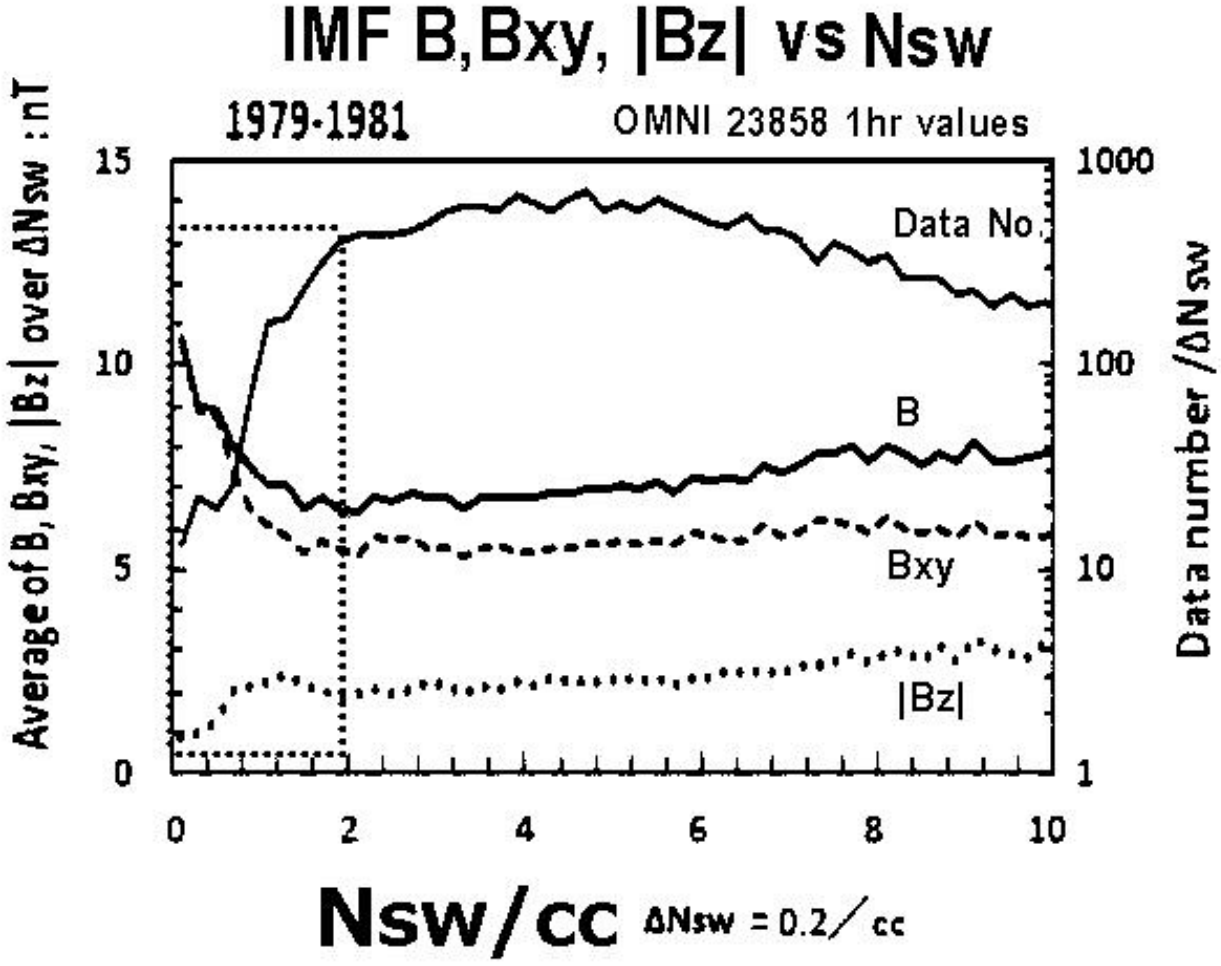

©2019. Japan Geoscience Union. All Right Reserved.

Dipole Tilt Effect of Geomagnetic Activity from Low- to High-latitudes

*Nowada Motoharu[1]

1. Shandong University at Weihai

Geomagnetic activity is dominantly impacted by the orientation of the Interplanetary Magnetic Field (IMF). However, when trying to address why the variations of geomagnetic activity are “semi-annual”, and are greater at equinoxes than at solstices, only IMF control of geomagnetic activity is not enough. This is because these variations are strongly dependent on the Earth’s dipole tilt; the dipole tilt is smaller at the equinoxes than at the solstices. Primitive studies assumed that magnetic reconnection occurs only at the subsolar point of dayside magnetopause. In their studies, the dipole tilt effect was not considered, but only the magnetic field direction between the IMF and the magnetosphere at the subsolar point was discussed in their studies. After them, geomagnetic variations where both dipole tilt effect and IMF direction are taken into account have been investigated. Based on a large database of IMF and AL/AU, we examined the relationship between the IMF clock angle and AL/AU at various dipole tilts. For both positive and negative dipole tilts, geomagnetic activity decrease as the clock angle moves away from 180˚. The AL/AU indices also tend to become smaller for larger dipole tilts. This dipole tilt dependence enhances the semi-annual variation of high-latitude geomagnetic activity.
It also remains unclear how degree energy input rate from solar wind to ring current (dD_{st}^{*}/dt) depends on dipole tilt under various interplanetary magnetic field (IMF) orientation and whether or not ring current development also follows this dipole tilt dependence. We tried to statistically investigate the dependence of dipole tilt and IMF clock angles on low- and middle-latitude geomagnetic activity (D_{st}^{*}), which is a proxy of ring current development, and solar wind energy input rate to ring current (dD_{st}^{*}/dt) over one solar cycle (1978 - 1988). D_{st}^{*} was calculated with the solar wind dynamic pressure and original D_{st} index, and the dipole tilt angle was defined as function of the day of year and universal time. The (dD_{st}^{*}/dt) values were obtained based on the solar wind electric field under the southward IMF conditions. Under positive and negative dipole tilts, the (dD_{st}^{*}/dt) values under low dipole tilt are negatively larger than those in case of high dipole tilt. Further peaks at 180˚ of the IMF clock angle are seen in most of the dipole tilt cases. However, the D_{st}^{*} index shows neither a peak at 180˚ of the IMF clock angle nor particular dipole tilt dependence in case of negative dipole tilt angles. This result suggests that low- and middle latitude geomagnetic activity (ring current development) does not necessarily show dipole tilt dependence and a one-to-one correlation with solar wind energy input rate to ring current (dD_{st}^{*}/dt).

Keywords: Geomagnetic activity (Dst*), Solar wind energy input rate to ring current (dDst*/dt), Semiannual variation , Dipole tilt effect, Interplanetary magnetic field and clock angel, Magnetic reconnection

©2019. Japan Geoscience Union. All Right Reserved.

A New Prediction Model for Solar Wind-Triggered Magnetospheric Disturbances Based on Potential Learning (Neural Network)

*Ryozo Kitajima[1], Motoharu Nowada[2], Ryotaro Kamimura[3]

1. Seikei University, 2. Shandong University at Weihai, 3. Tokai University

Nowadays, it becomes so important in saving our economic activity, and preventing the disasters caused by terrestrial electromagnetic effects to predict a scale and the duration of the geomagnetic disturbances based on in-situ solar wind observations. Recently, one of the notable techniques for the predictions of the magnetospheric disturbances is Neural Network (NN). However, most of these studies are focused on the reproduction of the behaviors of the index values, which represent the geomagnetic disturbances (e.g, D_{st} and AE), by inputting the solar wind parameters measured by the satellites. In our study, we apply a novel neural network model of ‘Potential Learning (PL)’.
Basically, Neural Networks (NNs) are models which imitate the information processing in the nervous system of brain. The nerve is made of cells as referred to as “neurons”, which specializes the information processing. NNs consist of “artificial” neurons, and can process information by learning. Therefore, using NNs, we can obtain some characteristics of the data inputted. The PL is a new kind of the NNs. A feature of the PL is to make a network that can understand the input variables based on learning by “input potentialities”, which are indices as calculated with the variances derived from the input variables. If using this PL, we can specify what input variable(s) is (are) potentially important and influential for a phenomenon.
In this study, introducing the PL technique, we try to specify which solar wind parameter plays an essential role in causing the geomagnetic disturbances. Although the conventional PL, where we used, had automatically selected the variables of interest, we develop a “improved” PL in this study so that the variables can manually be selected. We benchmark this new algorithm using the 4 polar magnetic storm cases occurred under the southward Interplanetary Magnetic Field (IMF)-B_z conditions, and advisedly set the maximum potentiality for the IMF-B_z, so that the IMF-B_z component is the most possible solar wind parameter to cause the geomagnetic disturbances. We note “second” solar wind parameter(s) to possibly cause the magnetospheric disturbances, following the IMF-B_z component. After testing our new technique to actual storm events, we might distinguish the magnetospheric disturbances into two different types, that is, the geomagnetic disturbances driven by “IMF-dominant” and “combination of IMF with solar wind plasma (dynamic pressure)”. The advantages to adopt this new algorithm to space weather, and more detailed results will be discussed in this presentation.

Keywords: Predictions of Geomagnetic Activity, Neural Network Considered Potential Learning, Development of Space Weather

©2019. Japan Geoscience Union. All Right Reserved.

Real-time magnetosphere simulator for space weather using REProduce Plasma Universe code

*Yasubumi Kubota[1], Aoi Nakamizo[1], Kaori Sakaguchi[1], Mitsue Den[1], Yuki Kubo[1], Tsutomu Nagatsuma[1], Takashi Tanaka[1,2]

1. National Institute of Information and Communications Technology, 2. Kyushu University

Surface charging of artificial satellite is one of risks caused by dynamical variations of space environment. It occurs when a satellite exposes high energy electrons around 10 keV created by plasma injection accompanied with substorm. Therefore we want to predict timing and electron energy of plasma injection using magnetosphere-ionosphere coupling global MHD simulation. Now we are developing a real-time numerical simulator for space weather forecast using magnetosphere-ionosphere coupling global MHD simulation called REPPU (REProduce Plasma Universe) code. The feature of the simulation code is highly robust to extreme solar wind parameters because the unstructured grid system has no singular point and is able to calculate in the uniform accuracy over the whole region. We use the real-time solar wind data formatted in the GSM coordinate system observed by DSCOVR spacecraft. Magnetic-dipole axis is fixed to z-direction in our simulation. Therefore daily variation of magnetic-dipole axis is not reproduced. Instead, we convert the input direction of the solar wind velocity and magnetic field into that which tilts including daily variation of magnetic dipole axis in x-z plane. In the method the solar wind structure is not exact. However we can relatively reproduce the magnetosphere response including daily variation of the magnetic-dipole axis against solar wind. The resolution is 7682 grids in the horizontal direction and 240 grids in the radial direction.
In this presentation, we compare the simulation results with the CPCP, AE index, and plasma variations observed by geostationary orbit satellites. Density and temperature of plasma injection derived from MHD simulation tends to estimate larger and smaller values than observation respectively because the MHD simulation does not include kinetic heating effects. We have to interpret MHD simulation results for prediction of electron density and temperature. We will discuss how to interpret electron density and temperature between observation and MHD simulation.

Keywords: global MHD simulation, surface charging

©2019. Japan Geoscience Union. All Right Reserved.

Simulation of GIC flowing through the power transmission network (187 kV-500 kV) in Japan

*Nishida Yuichiro[1,6], Yusuke Ebihara[1], Satoko Nakamura[1], Shinichi Watari[2], Kumiko Hashimoto[3], Kentaro Kitamura[4], Takashi Kikuchi[5]

1. Kyoto University Reserch Institute for Sustainable Humanosphere, 2. National Institute of Information and Communications Technology, 3. Kibi International University, 4. National Insutitute of Technology, Tokuyama College, 5. Nagoya University, 6. Kyoto University Department of Electrical Engineering

The energy released from the sun can enhance electric currents in Earth’ s magnetosphere, which induces an electric field on the ground surface. This electric field, called a geomagnetically induced electric field (GIE), gives rise to geomagnetically induced current (GIC) flowing in a transmission line. Japan is situated at geomagnetically low latitudes, but the potential risk is probably non-zero because a large-amplitude of GIC, as high as 129 A, was recorded in the Japanese power grid during the Halloween storm in October 2003. To evaluate the potential risk of the Japanese power grid properly, we modeled the Japanese power grid with high voltage class over 187 kV on the basis of publicly available data. The model consists of 602 nodes and 763 paths. The uniform GIE imposed on Japan was estimated on the basis of the geoelectric field observed in April 2018 at Kakioka Magnetic Observatory. We applied the uniform GIE on the model. The calculated GIC is roughly in agreement with that measured at 4 substations in Japan. For the westmost substation, a disagreement was found when we considered only the highest class of the power grid (500 kV), which may imply that the lower voltage class of the grid (<500 kV) may have some contribution to the GIC in Japan. We discuss the general tendency of the GIC flowing in the Japanese power grid, and prediction capability of the currently available model.

©2019. Japan Geoscience Union. All Right Reserved.

Simulation of GIC flowing through the power transmission network (187 kV-500 kV) in Japan

Yuichiro Nishida
Yusuke Ebihara
Satoko Nakamura
Shin-Ichi Watari
Kumiko Hashimoto
Kentaro Kitamura
Takashi Kikuchi

Abstract

The energy released from the sun can enhance electric currents in Earth's magnetosphere, which induces an electric field on the ground surface. This electric field, called a geomagnetically induced electric field (GIE), gives rise to geomagnetically induced current (GIC) flowing in a transmission line. Japan is situated at geomagnetically low latitudes, but the potential risk is probably non-zero because a large-amplitude of GIC, as high as 129 A, was recorded in the Japanese power grid during the Halloween storm in October 2003. To evaluate the potential risk of the Japanese power grid properly, we modeled the Japanese power grid with high voltage class over 187 kV on the basis of publicly available data. The model consists of 602 nodes and 763 paths. The uniform GIE imposed on Japan was estimated on the basis of the geoelectric field observed in April 2018 at Kakioka Magnetic Observatory. We applied the uniform GIE on the model. The calculated GIC is roughly in agreement with that measured at 4 substations in Japan. For the westmost substation, a disagreement was found when we considered only the highest class of the power grid (500 kV), which may imply that the lower voltage class of the grid (<500 kV) may have some contribution to the GIC in Japan. We discuss the general tendency of the GIC flowing in the Japanese power grid, and prediction capability of the currently available model.

©2019. Japan Geoscience Union. All Right Reserved.

Climatological features of the upper atmosphere reproduced by a revised version of a whole atmosphere-ionosphere coupled model GAIA

*Hidekatsu Jin[1], Yasunobu Miyoshi[2], Chihiro Tao[1], Hiroyuki Shinagawa[1], Hitoshi Fujiwara[3]

1. National Institude of Information and Communications Technology, 2. Kyushu University, 3. Seikei University

Temporal and spatial variations in the ionospheric electron density and thermospheric mass density could have significant impacts on radio communications between ground and space, and particle and atmospheric drag environments around satellites. Origins of such upper atmospheric variations are not only in the solar atmosphere through the emissions of solar radiation, high-speed plasma gas and high-energy particles, but also in the Earth’ s lower atmosphere, where meteorological phenomena could give rise to atmospheric waves propagating upward. In order to nowcast and forecast the upper atmospheric variations and disturbances, a whole atmospheric model, GAIA, has been developed, which combines a whole atmospheric GCM, an ionospheric model and an electrodynamics model in a self-consistent manner.

So far, for the purpose of its validation, we have compared climatological features of thermosphere and ionosphere reproduced by GAIA with those from ionospheric observation and observation-based empirical models. The comparison indicates that the model and observations are generally in good agreements, but in some condition such as at solar maximum there are significant disagreements in the ionospheric electron density distribution. In order to improve the accuracy of the model, we have made several updates such as ion chemical processes, energetics, parameterization, and so on. We also have introduced magnetospheric effects into the model, such as electrodynamics coupling with magnetosphere and particle precipitation. In this presentation, we discuss how the upper atmospheric model can improve its accuracy and how they can be validated.

Keywords: space weather, whole atmosphere, ionosphere, simulation, thermosphere, assimilation

©2019. Japan Geoscience Union. All Right Reserved.

Investigation of the thermospheric mass density variations below 200 km

*Hitoshi Fujiwara[1], Yasunobu Miyoshi[2], Masayoshi Utashima[1], Huixin Liu[2]

1. Faculty of Science and Technology, Seikei University, 2. Department of Earth and Planetary Sciences, Faculty of Sciences, Kyushu University

Since both the effects from the lower atmosphere and in-situ forcing are significant in the thermospheric region between 100 and 200 km altitude, the thermosphere in the region shows complex variations depending on various conditions. In addition, observations of the thermosphere (neutral atmosphere) between 100 and 200 km are very few compared to the upper thermosphere (above 300 km) and the ionosphere. These make it difficult to improve reliability of empirical and numerical models. Observations from Low Earth Orbit (LOE) satellites would be essential for building up available data sets in the thermospheric region between 100 and 200 km altitude. We will introduce our research project to investigate the thermospheric mass density variations in the 100-200 km altitude region with the LOE satellite, e.g., Tsubame (SLATS), data and a whole atmosphere GCM.

Keywords: thermosphere, mass density, Low Earth Orbit (LOE) satellite, GCM

©2019. Japan Geoscience Union. All Right Reserved.

Low-latitude HF Doppler observations of magnetospheric electric fields during space weather disturbances

*Kumiko K. Hashimoto[1], Takashi Kikuchi[2], Ichiro Tomizawa[3], Keisuke Hosokawa[3], Jaroslav Chum[4]

1. Kibi International University, 2. Nagoya University, 3. University of Electro-Commnunications, 4. Institute of Atmospheric Physics, Prague

Ionospheric electric fields penetrated from the magnetosphere to the low latitude ionosphere have been observed as geomagnetic disturbances caused by ionospheric currents, such as the equatorial electrojet (EEJ) at the dayside equator. The ionospheric currents are too weak to be a detector of the electric field at low latitudes on the dayside and even at the equator on the nightside. The HF Doppler (HFD) sounder is another powerful tool for observations of the electric filed at low latitudes on both the day- and night-sides. We have shown that the electric fields of the geomagnetic sudden commencements (SC) are composed of the preliminary impulse followed by the main impulse, of which directions are opposite to each other and both electric fields are opposite on the day- to night-sides (Kikuchi et al. 2016 JGR). We have also shown that the substorm electric fields are composed of the growth phase followed by expansion phase overshielding electric fields, of which directions are opposite to each other (Hashimoto et al., 2017). In this paper, we show that the HFD sounder is capable of detecting stormtime electric fields and that the electric fields are found to decay rather rapidly over one hour during the main phase with the time scale of a few hours. Combining with the equatorial magnetometer data, we would be able to estimate the decaying rate of the HFD electric fields, which helps obtain the stormtime electric fields quantitatively from the HFD data. We discuss advantages of widely separated HFD sounder operations and cooperations with SuperDARN as well as with magnetometer networks.

Keywords: HF Doppler observation, ionosphere electric field, magnetospheric electric field, geomagnetic storm, equatorial electrojet

©2019. Japan Geoscience Union. All Right Reserved.

Stratospheric ionization during magnetic storms

*Ryuho Kataoka[1]

1. National Institute of Polar Research

Transient mesospheric ionization was detected at an altitude of 65-70 km during the auroral breakup that occurred from 2220 to 2226 UT on June 30, 2017. During this event, the footprint of the Arase satellite was located within the field of view of the all-sky imagers at Syowa Station in the Antarctic. Auroral observations at Syowa Station revealed the dominant precipitation of relatively soft electrons during the auroral breakup. A corresponding spike in cosmic noise absorption was also observed at Syowa Station, while the Arase satellite observed a flux enhancement of >100 keV electrons and a broadband noise without detecting chorus waves or electromagnetic ion cyclotron waves. A general-purpose Monte Carlo particle transport simulation code was used to quantitatively evaluate the ionization in the middle atmosphere. Results of this study indicate that the precipitation of energetic electrons of >100 keV, rather than X-rays from the auroral electrons, played a dominant role in the transient and deep (65-70 km) mesospheric ionization during the observed auroral breakup. Based on the above results of Kataoka et al. (2019), we further discuss a possible role of X-rays to ionize the stratosphere during magnetic storms.

Reference:
Kataoka et al. (2019), Earth, Planets and Space, 71, 9, https://doi.org/10.1186/s40623-019-0989-7

©2019. Japan Geoscience Union. All Right Reserved.

Calculating propagation time of HF radio wave using ray-tracing method and simple comparison with the observation.

*Ryo Nakao[1], Hiroyuki Nakata[1], Hiroyo Ohya[1], Toshiaki Takano[1], Kornyanat Hozumi[2], Takuya Tsugawa[2], Susumu Saito[3], Mamoru Ishii[2]

1. Graduate School of Engineering, Chiba University, 2. National Institute of imformation and Communications Technology, 3. Electronic Navigation Research Institute

To provide the information of nowcast of radio propagation, we have started a project, HF-START (HF simulator Targeting for All user's Regional Telecommunications). In this project, a simulator that is able to predict propagation of HF radio waves is constructed by ray-tracing calculation.
Using this simulator, we have examined whether HF radio wave travels between any two points. In this calculation, the electron density, which is necessary to calculate reflection index is determined by International Reference Ionosphere (IRI).In this project, HF receivers have been installed at Chiba University (Chiba, 35.62N, 140.10E), Sarobetu (Hokkaido, 45.16N, 141.74E), Numata (Gunma, 36.62N, 139.02E), Yamagawa (Kagoshima, 31.20N, 130.61), Ogimi (Okinawa, 26.68, 128.15E) for observing HF radio wave transmitted from radioNIKKEI (Nagara, Chiba, 35.46N, 140.20E) to confirm the results of the ray-tracing calculation. In the ray-tracing calculation, therefore, we set the same locations of the transmitter and receivers as the observatories of HF-START. As a result of simple comparison between the ray-tracing results and the observation, it is found that there was a difference of the propagation time between the ray-tracing results and the observations. It is possible that the radio wave propagation between radioNIKKEI and Ciba University is not ground wave but sky wave that is reflected by ionosphere. As for further calculation, we plan to use the electron density distributions determined by GAIA and GNSS tomography in the ray-tracing calculation.

©2019. Japan Geoscience Union. All Right Reserved.

Why do some probabilistic forecasts lack reliability?

*Yuki Kubo[1]

1. National Institute of Information and Communications Technology

One of the important attributes to be satisfied for the probabilistic forecast system is reliability. However, some probabilistic forecast systems lack reliability. Why do some probabilistic forecasts lack reliability? We investigate a condition for a probabilistic binary forecast to be reliable in this work. We mathematically prove that a necessary, but not sufficient, condition for achieving a reliable probabilistic forecast is maximizing the Peirce skill score (PSS) at the threshold probability of the climatological base rate. The condition is confirmed by using artificially synthesized forecast-outcome pair data and previously published probabilistic solar flare forecast models. The condition gives a partial answer as to why some probabilistic forecast systems lack reliability, because the system, which does not satisfy the proved condition, can never be reliable. The result implies that those who want to develop a reliable probabilistic forecast system must adjust or train the system so as to maximize PSS near the threshold probability of the climatological base rate.

Keywords: Probabilistic forecast, Reliability

©2019. Japan Geoscience Union. All Right Reserved.

An estimation method of GEO spacecraft surface charging for a real-time spacecraft risk assessment

*Masao Nakamura[1], Ryota Kawachi[1], Go Takahashi[1], Tsutomu Nagatsuma[2], Mamoru Ishii[2]

1. Osaka Prefecture University, 2. NICT

Spacecraft anomalies are often induced by electrostatic discharges due to surface charging. Some spacecraft charging simulation software is developed by space agencies and research institutes and used for spacecraft designs and charging analysis. However these simulations cannot be used for a real-time estimation because they need hours or days to calculate the surface potential for a given plasma environment. Therefore we develop a quick estimation method of GEO spacecraft surface charging for the Space Environment Customized Risk Estimation for Spacecraft (SECURES) of the space weather forecast Project for Solar-Terrestrial Environment Prediction (PSTEP). We estimate the surface potentials by interpolation using lookup tables of the pre-simulated surface potentials for combinations of plasma temperatures and densities. We study fitting functions used in the interpolation and how to make the lookup tables for the good estimation. Then we can real-time estimate the surface potentials of the target GEO spacecraft when the on-orbit plasma environment is predicted or observed. The spacecraft risk assessment can be accomplished by additional information about the experimental discharging differential potential of the surface materials.

Keywords: Spacecraft surface charging, Space weather, Spacecraft risk assessment

©2019. Japan Geoscience Union. All Right Reserved.

A network of HF Doppler sounding systems in Japan

*Keisuke Hosokawa[1], Hiroyuki Nakata[2], Kumiko K. Hashimoto[3], Ichiro Tomizawa[1], Jun Sakai[1], Takashi Kikuchi[4]

1. University of Electro-Communications, 2. Chiba University, 3. Kibi International University, 4. ISEE, Nagoya University

Since 2003, a network observation of HF Doppler sounding has been conducted in Japan for remote-sensing the atmospheric, ionospheric and magnetospheric processes. Currently, 1 transmitting station (Tx) and 7 receiving stations (Rx) are operative by a collaborative effort of four difference universities. The main transmitting station is located at Chofu, Tokyo, Japan in the Campus of University of Electro-Communications (JG2XA). JG2XA transmits continuous waves at 5006 kHz and 8006 kHz with a transmitting power of 200 W. By receiving this JG2XA signal at 7 Rx stations (Sugadaira, Oarai, Kure, Kashima, Iitate, Fujisawa and Sugito) we derive the Doppler shift imposed during the propagation and reflection in the ionosphere. In particular, the Doppler shift data can be used to detect vertical motion of the ionospheric F region with a temporal resolution of 10 s. At some stations, we also have observed signals from Radio Nikkei 1 (JOZ at 3925 kHz, JOZ2 at 6055 kHz, and JOZ3 at 9595 kHz) transmitted from Nagara, Chiba, Japan, which allows us to observe the vertical motion of the ionosphere at several altitude levels. The data obtained from this experiment since 2003 are all available at http://gwave.cei.uec.ac.jp/~hfd. Not only quick-look plots but also several types of digital data (raw wave form and Doppler shift data) can be retrieved from this database. The experiment covers various ionospheric phenomena in the Magnetosphere-Ionospheric (M-I) coupling system, such as sporadic E-layer (Es), medium-scale traveling ionospheric disturbances (MSTIDs), large-scale traveling ionospheric disturbances (LSTIDs), global-scale electric field variation, geomagnetic pulsations, and sudden commencement (SC). The data can also be used for the studies of vertical coupling between the lower atmosphere and ionosphere, for example, observations of ionospheric variation after large earthquakes, volcanic eruptions and typhoons. To facilitate analyses of the phenomena listed above, it is desired to observe a wider area in latitude and longitude. For this purpose we plan to extend the network covering the entire ionosphere over Japan in the near future. In the presentation, we will give a brief introduction to the experiments and online database, and then discuss the future direction of the studies of atmosphere, ionosphere and magnetosphere using the HF Doppler sounding in a framework of international collaborations.

Keywords: HF Doppler experiment, Ionosphere

©2019. Japan Geoscience Union. All Right Reserved.

[E] Poster | P (Space and Planetary Sciences)：P-CG Complex & General

Tue. May 28, 2019 10:45 AM - 12:15 PM JST | Tue. May 28, 2019 1:45 AM - 3:15 AM UTC | Poster Hall International Exhibition Hall8, Makuhari Messe_1

[P-CG22] Shock responses of planetary materials elucidated from meteorites and dynamic compression experiments

convener:Toshimori Sekine(Center for High Pressure Science and Technology Advanced Research), Takuo Okuchi(Institute for Planetary Materials, Okayama University)

Impact phenomena had played essential roles in the process of planetary evolution. Recent analytical and experimental developments reveal a new prospective on the effects of shock-compression process for planetary materials. For deeper understanding of such shock effects, it is necessary to evaluate the detailed shock conditions from the observations of naturally-shocked planetary materials, and to compare them with the results on the planetary materials experienced a wide range of known shock conditions. Several metastable phases, that have not been known before, have recently been identified in shocked meteorites. They suggest that the shock state is often not in equilibrium and that it is more complicated process than ever thought. Experimental techniques including laser-driven shock compression and x-ray free electron laser diagnostics have been progressed to successfully simulate a wide range of shock conditions. The recent results indicate that shocked grains are fractured and rotated at relatively low pressures, and that they are subsequently transformed into denser phases or melts, or their mixtures at pressures of a few 100s GPa. Understanding of such shock dynamics requires another prospect, which is qualitatively different from the static high pressure and high temperature consensus. Therefore, it is timely to have an international symposium on dynamics of planetary materials.

[PCG22-P01] discussion

*Takuo Okuchi[1], Toshimori Sekine[2] (1.Institute for Planetary Materials, Okayama University, 2.Center for High Pressure Science and Technology Advanced Research)

[PCG22-P02] Shock-compressed behavior of quartz by XFEL

*Tomoko Sato[1], Yoshinori Tange[2], Yusuke Seto[3], Toshimori Sekine[4,5], Norimasa Ozaki[4], Toyohito Nishikawa[4], Kohei Miyanishi[4], Kensuke Matsuoka[4], Ryosuke Kodama[4], Tadashi Togashi[2], Yuichi Inubushi[2], Toshinori Yabuuchi[6], Makina Yabashi[6] (1.Hiroshima University, 2.Japan Synchrotron Radiation Research Institute, 3.Kobe University, 4.Osaka University, 5.Center for High Pressure Science &Technology Advanced Research, 6.RIKEN)

[PCG22-P04] Laser-shock experiments of dense polymorphs of Mg_2SiO_4: technical developments using synthetic single crystals

*Narangoo Purevjav[1], Takuo Okuchi[1], Norimasa Ozaki[2], Takayoshi Sano[3], Yuhei Umeda[2], Shintaro Morioka[2], Nobuki Kamimura[2] (1.Institute for Planetary Materials, Okayama University, 2.Graduate School of Engineering, Osaka University, 3.Institute of Laser Engineering, Osaka University)

[PCG22-P05] Richtmyer-Meshkov instability in inhomogeneous density materials and its application to planetary science

*Takayoshi Sano[1] (1.Institute of Laser Engineering, Osaka University)

[PCG22-P06] Impact-induced dehydration reactions of Fe- and Al-hydrates as potential storage, carrier and source of water

*Tsubasa Tobase[1], Toshimori Sekine[1], Ginga Kitahara[2], Makoto Tokuda[2], Akira Yoshiasa[2], Makoto Takafuji[2], Tsutomu Mashimo[2], Nobuaki Kawai[2] (1.HPSTAR, 2.Graduate School of Science and Technology, Kumamoto University)

[PCG22-P07] Crystallization of amorphous $MgSiO_3$ by shock compression

*Akane Arasuna[1], Masayuki Okuno[1], Nobuaki Kawai[2] (1.Kanazawa University, 2.Kumamoto University)

[PCG22-P08] First-principle study of the structural and electronic properties of N-doped $MgAl_2O_4$ spinel

*Chi Pui Tang[1], Pak Kin Leong[1], Toshimori Sekine[2,3] (1.State Key Laboratory of Lunar and Planetary Sciences, Macau University of Science and Technology, 2.Center for High Pressure Science and Technology Advanced Research (HPSTAR) Shanghai Laboratory of HPSTAR, Shanghai, P.R. China, 3.Graduate School of Engineering, Osaka University)

[PCG22-P09] Transparency of shock-compressed single crystal diamond

*Kento Katagiri[1], Norimasa Ozaki[1,2], Kohei Miyanishi[2], Yuhei Umeda[1], Shintaro Morioka[1], Takayoshi Sano[2], Ryosuke Kodama[1,2] (1.Osaka University, 2.Institute of Laser Engineering, Osaka Unversity)

[PCG22-P10] Pb-Pb dating of the NWA 7203 angrite and relationship to its shock metamorphism

*Hideyuki Hayashi[1], Takashi Mikouchi[1], Yuji Sano[1], Martin Bizzarro[2] (1.The university of Tokyo, 2.University of Copenhagen)

[PCG22-P11] Shock recovery of high-pressure phase of SiO_2 using high-power laser

*Tadashi Kondo[1], Hiromoto Kengo[1], Tatsuhiro Sakaiya[1], Hidenori Terasaki[1], Keisuke Shigemori[2], Youichiro Hironaka[2] (1.Department of Earth and Space Science, Graduate School of Science Osaka University, 2.Institute of Laser Engineering, Osaka University)

[PCG22-P12] Hugoniot measurement of calcite under meteorite collision condition

*Fukui Keiya[1], Norimasa Ozaki[1,2], Yuhei Umeda[1], Kohei Miyanishi[3], Kento Katagiri[1], Shintaro Morioka[1], Takayoshi Sano[3], Ryosuke Kodama[1,2,3] (1.Graduate School of Engineering,Osaka univ., 2.PPC, Osaka Univ., 3.ILE, Osaka Univ.)

[PCG22-P13] Direct observation of the transformation toughening of tetragonal stabilized zirconia under shock deformation condition by ns time-resolved XRD.

*Sota Takagi[1,2], Kouhei Ichiyanagi[2,3], Nobuaki Kawai[4], Ryo Fukaya[2], Shunsuke Nozawa[2], Atsushi Kyono[1], Nobumasa Funamori[2], Shin-ichi Adachi[2] (1.University of Tsukuba, 2.KEK PF, 3.Jichi Medical University, 4.Kumamoto University)

discussion

*Takuo Okuchi[1], Toshimori Sekine[2]

1. Institute for Planetary Materials, Okayama University, 2. Center for High Pressure Science and Technology Advanced Research

We discuss natural and experimendal evidences on impact phenomena, which had played essential roles in the process of early planetary evolution. Recent analytical and experimenotal developments reveal a new prospective on the effects of shock-compression process of planetary materials. For deeper understanding of such shock effects, it is necessary to evaluate the detailed shock conditions from the observations of naturally-shocked planetary materials, as well as to compare them with the results of shock-compression experiments of these materials obtained at laboratory conditions.

Keywords: discussion

©2019. Japan Geoscience Union. All Right Reserved.

Shock-compressed behavior of quartz by XFEL

*Tomoko Sato[1], Yoshinori Tange[2], Yusuke Seto[3], Toshimori Sekine[4,5], Norimasa Ozaki[4], Toyohito Nishikawa[4], Kohei Miyanishi[4], Kensuke Matsuoka[4], Ryosuke Kodama[4], Tadashi Togashi[2], Yuichi Inubushi[2], Toshinori Yabuuchi[6], Makina Yabashi[6]

1. Hiroshima University, 2. Japan Synchrotron Radiation Research Institute, 3. Kobe University, 4. Osaka University, 5. Center for High Pressure Science &Technology Advanced Research, 6. RIKEN

We have conducted x-ray diffraction measurement (XRD) with femtosecond x-ray pulses generated by the x-ray free electron laser (XFEL) to observe lattice dynamics and phase transformation of single-crystal quartz under high strain-rate shock compression (~10^9 s^{-1}) and high pressure. Single-crystal quartz samples were shock-compressed by high-power short- and long-pulse lasers. In the short-pulse experiments, the lattice was reduced to 15% and 1.5% in the direction parallel and perpendicular to the compression axis, respectively. The sample was uniaxially compressed over its known Hugoniot elastic limit. In the long-pulse experiments, three different states were observed. Polycrystalline stishovite appeared at first, and elastically compressed state and a topotaxially transformed new phase were observed successively.

Keywords: Shock compression, in-situ X-ray diffraction, quartz

©2019. Japan Geoscience Union. All Right Reserved.

Laser-shock experiments of dense polymorphs of Mg_2SiO_4: technical developments using synthetic single crystals

*Narangoo Purevjav[1], Takuo Okuchi[1], Norimasa Ozaki[2], Takayoshi Sano[3], Yuhei Umeda[2], Shintaro Morioka[2], Nobuki Kamimura[2]

1. Institute for Planetary Materials, Okayama University, 2. Graduate School of Engineering, Osaka University, 3. Institute of Laser Engineering, Osaka University

Mg_2SiO_4 polymorphs (α-phase as forsterite, β-phase as wadsleyite, and γ-phase as ringwoodite) are the major constituents of our Earth's mantle and also for Earth-like planets. Thus studying these polymorphs at extreme pressure and temperature conditions will lead to understanding their changes of chemical and physical properties at extremely high pressure and temperature conditions, such as those occurring during the giant impacts phenomena of such planets at their final stage of accretion. Shock compression of forsterite has been studied up to ~ 1000 GPa by using polycrystalline and single crystal samples [1-3]. The studies have reported contradicting results for the shock compression of forsterite. Sekine et al (2016) reported that there are several phase transformations in the liquid state of Mg_2SiO_4 at > 270 GPa, while other two studies were reported no phase transformation [1, 3]. Thus it is interesting to see how the Hugonoit relations of Mg_2SiO_4 polymorphs will come up at different pressure and temperature conditions. However, Hugoniot relations of wadsleyite and ringwoodite have not been studied well. Especially, there is any data on the densest polymorph ringwoodite. Shock compression of wadsleyite was carried out up to 200 GPa by using polycrystalline samples [4]. In addition, there are no studies by using single crystal samples for both wadsleyite and ringwoodite. To newly conduct such studies, the denser polymorph of Mg_2SiO_4 are needed to be synthesized and grown at their relevant conditions of deep mantle corresponding to the 15 –21 GPa and 1000 –1500 ˚C in the laboratory. Most importantly, the synthesized minerals must be chemically, physically and optically homogenous and should have suitable sizes for the laser-shock experiments. Here, by utilizing the results of our previous efforts for growing such quality of single crystals, we made possible to obtain Hugoniot relation of wadsleyite and ringwoodite by laser-shock compression. Their crystals were synthesized and grown by using a scaled-up Kawai-type cell by together with applying our pre-established a slow-cooling method at their relevant conditions [5]. Recovered crystals were up to 1 mm in sizes and confirmed to be chemically homogenous and free from twinning, cracks, and inclusions. The crystals were then doubly polished separately down to 100 mm in thickness and with an area of > 500 mm. They were assembled to form targets which are optimized for the laser-shock experiments. laser-shock experiments at GEKKO XII were conducted at Institute of Laser Engineering, Osaka University. The crystals are optical to give very clean VISAR (Velocity Interferometer System for Any Reflector) images. The details of our technical developments will be discussed on the poster.

[1] Root, T., Townsend, J. L., Davies, E., Lemke, R. W., Bliss, D. E., Fratanduono, D. E., et al. (2018). *Geophys. Res. Lett.*, **45**:3865. [2] Sekine, T., Ozaki, N., Miyanishi, K., Asaumi, Y., Kimura, T., Albertazzi, B. et al. (2016). *Sci. Adv.*, **2**:e1600157. [3] Bolis, R. M., Morard, G., Vinci, T., Ravasio, A., Bambrink, E. et al. (2016). *Geophys. Res. Lett.*, **43**:9475. [4] Mosenfelder, J. L., Asimow, P. D. and Ahrens, T. J. (2007). *J. Geophys. Res.*, **112**:B06208. [5] Okuchi, T., Purevjav, N., Tomioka, N., Lin, J. F., Kuribayashi, T. et al. (2015). *Am. Mineral.*, **100**:1483.

Keywords: laser-shock compression, Mg2SiO4 polymorphs

©2019. Japan Geoscience Union. All Right Reserved.

©2019. Japan Geoscience Union. All Right Reserved.

Richtmyer-Meshkov instability in inhomogeneous density materials and its application to planetary science

*Takayoshi Sano[1]

1. Institute of Laser Engineering, Osaka University

Richtmyer-Meshkov instability (RMI) is a hydrodynamic interfacial instability, which occurs by the interaction between a shock wave and corrugated density jump. Because of the corrugation of the interface, the surface profiles of the transmitted and reflected shocks are also rippled. The RMI is driven by the vorticity left by these rippled shocks at the interface and in the fluid. In this study, we consider shock propagation in inhomogeneous density materials (e.g., uniform density materials with small round voids) and the turbulent growth of the interface. For these cases, the vorticity distribution and turbulent motion are much more complicated than the standard RMI cases. Then the spatial fluctuation of pressure or temperature could be significantly large after the shock passage. Using two-dimensional hydrodynamic simulations, we will examine the dependence of the pressure fluctuation on the density inhomogeneity. As the application of this numerical study, we will discuss about the shock propagation in meteorites with large density fluctuation.

Keywords: shock waves, Richtmyer-Meshkov instability

©2019. Japan Geoscience Union. All Right Reserved.

Impact-induced dehydration reactions of Fe- and Al-hydrates as potential storage, carrier and source of water

*Tsubasa Tobase[1], Toshimori Sekine[1], Ginga Kitahara[2], Makoto Tokuda[2], Akira Yoshiasa[2], Makoto Takafuji[2], Tsutomu Mashimo[2], Nobuaki Kawai[2]

1. HPSTAR, 2. Graduate School of Science and Technology, Kumamoto University

Hydrous minerals have been known to play an important role to preserve and carry water because a mechanism is required for water to reach the inner planets such as Earth far beyond the snow line that defines the boundary between water ice and vapor. In order to understand the detailes, we need to know the stability at high temperature and high pressure and impact resistance for possible hydrous minerals. Fe- and Al-hydrates (FeOOH and AlOOH) have been reported to be stable under static high temperature and static high pressure. In addition, they are observed in some meteorites and the surface on Mars. Although there are some data available on clay minerals and serpentine, those Fe- and Al-hydrates are considered to be present in the Earth’ s deep lower mantle according to the recent studies.

We have investigated the impact resistibility through shock recovery techniques. Our peak shock pressures are 24 GPa and 31 GPa for the recovered Fe- and Al-hydrates, respectively, where they displayed significant dehydration. We set various range of sample porosity and peak shock pressure to investing the dehydration reaction. These impact conditions correspond to impact velocities of 2.6 km/s and 4.9 km/s if we assume face to face impacts between carbonaceous chondrite such as Murchison. These are within a range of velocity for possible meteoritic collisions, and we need to know the relationship between impact condition and degree of dehydration. Using TG/DTA analyses of samples we estimated the relationship. The phase changes by impact dehydration are investigated by XRD, XAFS and Raman spectroscopy. We also try to understand dynamical void formation process by dehydration that can occur during adiabatic quenching through observation of void distribution in the recovered samples.

In our previous research for shock recovery experiments of hydrous minerals, we observed heterogenous temperature rise in dehydration process. We tried to confirm whether heterogeneous temperature rise occurs even in Fe- and Al-hydrates by comparison with the results between previously reported hydrous minerals. We will be able to select most possible candidate by comparing the thermal stability and impact resistibility among them.

Keywords: Shock recovered experiments, hydrous mineral, dynamic water loss, Powder x-ray diffraction

©2019. Japan Geoscience Union. All Right Reserved.

Crystallization of amorphous $MgSiO_3$ by shock compression

*Akane Arasuna[1], Masayuki Okuno[1], Nobuaki Kawai[2]

1. Kanazawa University, 2. Kumamoto University

Structural change of synthesized amorphous $MgSiO_3$ by shock compression up to 22.2 GPa has been investigated using XRD and IR analyses. The obtained result provides information for elucidating of the collision behavior of $MgSiO_3$ contained in cosmic dust.

Amorphous $MgSiO_3$ sample was prepared by an aqueous solution of TEOS, Magnesium Nitrate Hexahydrate, and ethanol with ammonia as a catalyst. As-prepared sample was heated at 700 C˚ to dehydrate excess water. TG curve of this sample indicated that the sample contained about 8.8 wt% of water molecules and hydroxyl groups.

A powdered heated (original) sample was put in an aluminum tubes and pressed at 20 kN for 10 minutes to obtain samples for shock compression experiment. These samples were compressed at 13.6, 17.2, and 22.2 GPa using a single-stage propellant gun at Kumamoto University.

XRD pattern of the pressed sample showed no crystalline peak as same as the original sample. However, the XRD pattern of thesample compressed at 13.6 GPa showed the weak crystalline peaks at around 2θ = 28, 31, 35-36˚. These peaks became intense with increasing shock pressure. Crystalline peaks observed in the XRD pattern for the sample of 22.2 GPa were attributed to those of enstatite. However, some peaks was due to the formation of Mg_2SiO_4. IR spectra for the compressed samples showed the similar trend as the result of XRD analysis. But IR analysis indicated that the sample contains water molecules even after the shock compression at 22.2 GPa. Water molecules probably present in the remaining amorphous part. Crystallization of sample by shock compression has not been reported in shock experiments for other crystalline and non-crystalline silicates. The crystallization of our samples at low pressure may be due to the simple chain structure of enstatite. Also, high shock temperature which generated by friction due to the porosity of the sample may promote this crystallization.

Keywords: MgSiO3, amorphous , shock compression, enstatite

©2019. Japan Geoscience Union. All Right Reserved.

First-principle study of the structural and electronic properties of N-doped $MgAl_2O_4$ spinel

*Chi Pui Tang[1], Pak Kin Leong[1], Toshimori Sekine[2,3]

1. State Key Laboratory of Lunar and Planetary Sciences, Macau University of Science and Technology, 2. Center for High Pressure Science and Technology Advanced Research (HPSTAR) Shanghai Laboratory of HPSTAR, Shanghai, P.R. China, 3. Graduate School of Engineering, Osaka University

On basis of the first principle calculation, we report a possible nitrogen doped structure of $MgAl_2O_4$ spinel. The structural and electronic properties (include the band structure, density of states and phonon) of spinel ($MgAl_2O_4$) and N-doped spinel ($MgAl_2O_{3.5}N_{0.5}$) compounds are performed using density functional theory (DFT). The density and space group of two crystal cells are 3.47 g/cm^3 (Fd3m) for $MgAl_2O_4$ and 3.38 g/cm^3 (R3m) for $MgAl_2O_{3.5}N_{0.5}$, respectively. The calculated direct band gaps at the Γ-point are about 5.13 eV for $MgAl_2O_4$ and 4.24 eV for $MgAl_2O_{3.5}N_{0.5}$, respectively. The projected density of states (PDOS) shows that the tops of the valence bands are built up from ~93% of *p*(O) states and ~60% of *p*(N) + ~32% of *p*(O) states (for $MgAl_2O_4$ and $MgAl_2O_{3.5}N_{0.5}$, respectively). In the phonon analysis, the lowest frequency of $MgAl_2O_{3.5}N_{0.5}$ is redshifted to 36.6 cm^{-1} ($MgAl_2O_4$ is 39.8 cm^{-1}) caused by the N-doped. We also calculate their cohesive energy in the pressure range of 0-150 GPa. We found that the cohesive energy of $MgAl_2O_{3.5}N_{0.5}$ is lower than $MgAl_2O_4$ at the pressure higher than ~115 GPa, it implies that $MgAl_2O_{3.5}N_{0.5}$ is more stable than $MgAl_2O_4$ at high pressure. Finally, we suggest that nitrogen atom would replace the oxygen of spinel in the depths of the earth. The results imply the deep mantle may storage a considerable amount of nitrogen.

Keywords: First principle calculation, Density functional theory, Spinel

©2019. Japan Geoscience Union. All Right Reserved.

Transparency of shock-compressed single crystal diamond

*Kento Katagiri[1], Norimasa Ozaki[1,2], Kohei Miyanishi[2], Yuhei Umeda[1], Shintaro Morioka[1], Takayoshi Sano[2], Ryosuke Kodama[1,2]

1. Osaka University, 2. Institute of Laser Engineering, Osaka Unversity

Carbon is one of the most prominent elements in nature and it is abundant in the Earth and many other planets. Diamond, a metastable phase of carbon, is naturally synthesized in deep inside of the Earth where substances are isotropically pressured. Diamond is known for its many unique properties such as high hardness, low compressibility, small thermal expansion coefficient, and transparency. Since it is important to understand how substances behave under high pressure, properties of compressed diamond have been measured in a wide range of pressures up to 5 TPa. However, the transparency of diamond under pressure has not been fully elucidated. Here, we report the measurment of the pressure dependency of the absorption coefficient of laser shock compressed single crystalline diamond. A high-intensity laser was utilized to shock compress the diamond sample along its <100> direction, and velocity interferometer systems for any reflector (VISARs) were used to determine the absorption coefficient and pressure. It was found that single crystalline diamond remains largely transparent to the probe laser for VISAR (λ =532 nm) up to 140 GPa. The pressure dependence of the refractive index will also be discussed.

This experiment was conducted under the joint research of the Institute of Laser Engineering, Osaka University. This work was supported in part by JSPS KAKENHI grant No. 16H02246 and No. 16H01119. The part of work was also supported by Genesis Research Institute, Inc. (Konpon-ken, TOYOTA).

Keywords: Shock-compression, High intensity laser, Diamond, Transparency, Refractive index

©2019. Japan Geoscience Union. All Right Reserved.

Pb-Pb dating of the NWA 7203 angrite and relationship to its shock metamorphism

*Hideyuki Hayashi[1], Takashi Mikouchi[1], Yuji Sano[1], Martin Bizzarro[2]

1. The university of Tokyo, 2. University of Copenhagen

Introduction: Angrite is one of the oldest basaltic achondrites in the early solar system which is depleted in volatile elements and enriched in refractory elements (e.g., Keil, 2012). Almost all angrites show either a quenched or slowly-cooled texture. The crystallization ages of quenched angrites are older (ca. 4564 Ma) than those of slowly-cooled samples (ca. 4558 Ma). One of the most striking mineralogical characteristics about angrites is the lack of shock metamorphism. Thus, quenched angrites can be good time anchors to connect absolute and relative ages, because the age differences between two systems can be ignored due to fast cooling and furthermore there is no chronological reset by shock metamorphism. However, NWA 1670 and NWA 7203 are known to show evidence for shock (Mikouchi et al., 2003; Hayashi et al., 2018), and especially we found that NWA 7203 exhibited remarkable shock metamorphic textures. The Pb-Pb dating of angrites has been done only for angrites without shock textures, indicating the obtained ages are crystallization ages. Pb-Pb age is relatively easy to be reset by shock heating. Therefore, Pb-Pb age of NWA 1670 or especially NWA 7203 may be reset by shock heating. However, there is no study which measured Pb-Pb dating of NWA 1670 or NWA 7203. In this study, we measured Pb isotopic ratios of silico-apatite in NWA 7203 by Nano-SIMS, and discussed the Pb-Pb age of NWA 7203.

Sample: We used NWA 7203 for this study. NWA 7203 is an angrite meteorite showing a quenched texture. NWA 7203 consists of a dendritic texture of olivine and anorthite, and pyroxene fills gaps of the dendrites. Grain size exhibits large variations from fine grains (~1 μm) to coarse grains (>100 μm). This is not a typical characteristic of quenched angrites. NWA 7203 is composed mainly of olivine, pyroxene and anorthite, and the accessory minerals are troilite, ulvospinel and silico-apatite.

Methods: Observation was carried out on thin sections by optical microscope and BSE images of FE-EPMA. Mineral phases were identified by micro-Raman spectroscopic analysis. Pb-Pb dating of NWA 7203 was carried out by measuring Pb isotope ratios of silico-apatites using Nano-SIMS at AORI, Univ. of Tokyo. Measurement conditions were 300 pA for primary ions and $^{16}O^-$ for ion sources. Pre-sputtering was performed for 8 minutes in the range of 10 x 10 μm. In the SIMS measurement, raster diameter of 3 x 3 μm and analysis time of 60 seconds were applied for two magnetic fields, respectively, and repeated for 30 cycles. For the standard, NIST SRM 610 was used.

Result and discussion: Pb isotopic ratios of silico-apatite in the NWA 7203 angrite were obtained. We obtained a weighted approximate straight line for each plot and found the Pb-Pb age to be 4551 ±17 Ma. These plots are relatively variable. This is probably because Pb isotopic ratios were disturbed by shock metamorphism. In fact, the Pb-Pb age of silico-apatite grains that are at least 200 μm away from the shock veins was found to be 4560 ±16 Ma. It is considered that the Pb isotopic ratios of these silico-apatite grains are relatively undisturbed as they are linearly aligned. This age coincides with the crystallization age of other quenched angrites within the error range. Takenouchi et al. (2019) measured the Ar-Ar ages of NWA 7203 and found that it has two plateau ages of 3800 ±440 Ma and 2300 ±140 Ma, and concluded that the shock metamorphism of NWA 7203 occurred at 2300 ±140 Ma. From this result, it is considered that the Pb-Pb age of NWA 7203 is not completely reset, but slightly disturbed.

©2019. Japan Geoscience Union. All Right Reserved.

Keywords: NWA 7203, Angrite, Pb-Pb dating, Shock metamorphism, Parent body

©2019. Japan Geoscience Union. All Right Reserved.

Shock recovery of high-pressure phase of SiO_2 using high-power laser

*Tadashi Kondo[1], Hiromoto Kengo[1], Tatsuhiro Sakaiya[1], Hidenori Terasaki[1], Keisuke Shigemori[2], Youichiro Hironaka[2]

1. Department of Earth and Space Science, Graduate School of Science Osaka University, 2. Institute of Laser Engineering, Osaka University

High-pressure phases in meteorites provide us the important information of shock history in natural materials. Experimental approach to reproduce such high-pressure phase have been studied intensively mainly by light-gas gun so far, though shock condition with impact velocity beyond 10km/s is difficult. Recent technical progress of high-intensity laser as a tool of shock experiment realize the recovery of samples with shock condition above 10km/s(Nagaki et al.,2016). However, the limited shock duration time of about 10 nsec has been too short to drive structural conversion to high-pressure form in single crystal sample. In this study, we explored recovery condition of high-pressure phase of SiO_2 using finely ground samples of quartz, cristobalite and fused silica as starting materials. Laser shock experiments were performed using GXII hyper laser at Institute of Laser Engineering, Osaka University. The whole sample retaining relative locations in the recovered box made of aluminum was quenched without significant scattering in each run. The sectioned sample at shocked center were examined by optical microscope, micro-focused X-ray diffraction and SEM-EDS. We will report the characteristic feature of top portion of sample, which shows layered structure with different metamorphism, and distribution of grass and stishovite phase found in the samples shocked above 100GPa, which have still a residual stress to 10GPa in the ambient condition. We will discuss the dependence of the initial state of crystal to recover the high-pressure phase in shocked samples in nsec.

Keywords: shocked quartz, high-intensity laser, recovery experiments

©2019. Japan Geoscience Union. All Right Reserved.

Hugoniot measurement of calcite under meteorite collision condition

*Fukui Keiya[1], Norimasa Ozaki[1,2], Yuhei Umeda[1], Kohei Miyanishi[3], Kento Katagiri[1], Shintaro Morioka[1], Takayoshi Sano[3], Ryosuke Kodama[1,2,3]

1. Graduate School of Engineering,Osaka univ., 2. PPC, Osaka Univ., 3. ILE, Osaka Univ.

Volatile substances inside planetary materialsare generated and released as gas under the extreme condition caused by collision phenomenon that is thought to contribute greatly to the formation of the planetary atmosphere [1]. Particularly the degassing reaction of carbonate, may generate CO or CO_2as greenhouse gas and affect the temperature of the planetary surface. A typical planetary mineral as carbonate of calcite ($CaCO_3$) is expected degassing above 3300 K at pressure of 150 GPa along the Hugoniot[2].
In the previous study, the experimental investigations for the shock-degassing reaction were carried out only below the impact pressure of 100 GPa. Also, we have not understood when the degassing reaction of calcite occur on a compressed state or a released state [3]
In natural, typical meteorite impacts exceed 10 km/s in impact velocity, and can generate at the pressure above 150 GPa. The purpose of this research is to understand the impact compression characteristics of calcite under the meteorite collision condition.

This experiment was conducted in Shock Drive Laser (Gekko XII) atInstitute for Laser Engineering, Osaka University. The target consists of polypropylene as an ablator aluminum as a piston, quartz as a standard material, and calcite as a sample from laser side. The impact pressures and temperatures were estimated by the measured shock wave velocity using Velocity interferometer system for any reflector (VISAR) and self-emission intensity using radiance thermometer (SOP).
As a result of this experiments, we obtained the Hugoniot date at the puressure from 200 GPa to 1 Tpa at the temperature above 5000 K. The detailed results will be shown as this presentation.
Acknowledgements

This experiment was conducted on the joint research of the Institute of Laser Engineering, Osaka University. This work was supported in part by JSPS KAKENHI grant No. 16H02246 and No. 16H01119. The part of work was also supported by Genesis Research Institute, Inc. (Konpon-ken, TOYOTA).

REFERENCES

[1] T. Matsui and Y.Abe: Nature, 319, 303 - 319 (1986).

[2] B.Ivanov and A. Deutsch: Physics of the Earth and Planetary Interiors, 129, 131-143 (2002).

[3] K.Kawaragi et al.: Earth and Planetary Science Letters, 282, 56 - 64 (2009).

Keywords: Laser-Shock-compression, hugoniot, calcite, degassing

©2019. Japan Geoscience Union. All Right Reserved.

Direct observation of the transformation toughening of tetragonal stabilized zirconia under shock deformation condition by ns time-resolved XRD.

*Sota Takagi[1,2], Kouhei Ichiyanagi[2,3], Nobuaki Kawai[4], Ryo Fukaya[2], Shunsuke Nozawa[2], Atsushi Kyono[1], Nobumasa Funamori[2], Shin-ichi Adachi[2]

1. University of Tsukuba, 2. KEK PF, 3. Jichi Medical University, 4. Kumamoto University

The enhancement of strength and toughness was found in oxide-doped tetragonal stabilized zirconia, with the suggestion that the absorption of energy during the martensitic transformation contribute to the increment [Gravie et al., 1975; Gupta et al., 1977]. Using transmission electron microscopy (TEM), in recovery sample, it was observed that the stress-induced transformation from stabilized tetragonal phase to monoclinic phase can be occurred around the crack tip [Porter et al., 1977], and the transformation-toughening model were devised [McMeeking et al., 1982; Hannink et al., 2000]. In high-pressure experiments, the phase transformation behavior of tetragonal stabilized zirconia has not been clarified in both static and shock compression because a lack of in-situ observation [Ohtaka et al., 1988; Grady et al., 1992]. We tried to observe the behavior of tetragonal stabilized zirconia under shock compression condition using time-resolved XRD method.We performed the experiments at NW14A beamline at PF-AR (Photon Factory Advanced Ring), High Energy Accelerator Research Organization (KEK), Japan. Nd:glass laser with the wavelength of 1064 nm, pulse energy of 16 J, pulse width of 12 ns was used for shock-driving source. The laser beam was focused by optical lens to the size of 500 μm × 500 μm on the sample surface. For TR-XRD experiments, the synchrotron X-ray pulse of PF-AR was used as a probe source. The energy, the pulse width, and the size on the sample were 15.68 keV, about 100 ps, and 450 μm (H) ×250 μm (W), respectively. The irradiation timing between laser pulse and X-ray pulse on the sample surface were controlled by delay generator at ns time scale. The targets consisted of an 25 um PET film ablator with Al coated on the surface and 50 um polycrystalline 3 mol% yttria doped tetragonal stabilized zirconia.
The XRD change were observed up to 35 ns after shock compression started. Before shock, the (101), (002), (110), (102), (112), (200) diffraction of tetragonal phase were observed. 6.5 ns after shock, the diffraction from compression region appeared with maximum compression of 6%. No phase transition occurred at compression states. At release states (~11.4 ns), on the other hand, the (-111), (111), (022), (-221) diffraction peaks of monoclinic phase were appeared. We will discuss the detail of the experimental results and the transformation toughening mechanism.

Keywords: Synchrotron X-ray, Time-resolved XRD, Laser-induced shock wave, Tetragonal stabilized zirconia

©2019. Japan Geoscience Union. All Right Reserved.

[E] Poster | P (Space and Planetary Sciences)：P-CG Complex & General

Tue. May 28, 2019 5:15 PM - 6:30 PM JST | Tue. May 28, 2019 8:15 AM - 9:30 AM UTC | Poster Hall International Exhibition Hall8, Makuhari Messe_4

[P-CG22] Shock responses of planetary materials elucidated from meteorites and dynamic compression experiments

convener:Toshimori Sekine(Center for High Pressure Science and Technology Advanced Research), Takuo Okuchi(Institute for Planetary Materials, Okayama University)

Impact phenomena had played essential roles in the process of planetary evolution. Recent analytical and experimental developments reveal a new prospective on the effects of shock-compression process for planetary materials. For deeper understanding of such shock effects, it is necessary to evaluate the detailed shock conditions from the observations of naturally-shocked planetary materials, and to compare them with the results on the planetary materials experienced a wide range of known shock conditions. Several metastable phases, that have not been known before, have recently been identified in shocked meteorites. They suggest that the shock state is often not in equilibrium and that it is more complicated process than ever thought. Experimental techniques including laser-driven shock compression and x-ray free electron laser diagnostics have been progressed to successfully simulate a wide range of shock conditions. The recent results indicate that shocked grains are fractured and rotated at relatively low pressures, and that they are subsequently transformed into denser phases or melts, or their mixtures at pressures of a few 100s GPa. Understanding of such shock dynamics requires another prospect, which is qualitatively different from the static high pressure and high temperature consensus. Therefore, it is timely to have an international symposium on dynamics of planetary materials.

[PCG22-P01] discussion

*Takuo Okuchi[1], Toshimori Sekine[2] (1.Institute for Planetary Materials, Okayama University, 2.Center for High Pressure Science and Technology Advanced Research)

[PCG22-P02] Shock-compressed behavior of quartz by XFEL

*Tomoko Sato[1], Yoshinori Tange[2], Yusuke Seto[3], Toshimori Sekine[4,5], Norimasa Ozaki[4], Toyohito Nishikawa[4], Kohei Miyanishi[4], Kensuke Matsuoka[4], Ryosuke Kodama[4], Tadashi Togashi[2], Yuichi Inubushi[2], Toshinori Yabuuchi[6], Makina Yabashi[6] (1.Hiroshima University, 2.Japan Synchrotron Radiation Research Institute, 3.Kobe University, 4.Osaka University, 5.Center for High Pressure Science &Technology Advanced Research, 6.RIKEN)

[PCG22-P04] Laser-shock experiments of dense polymorphs of Mg_2SiO_4: technical developments using synthetic single crystals

*Narangoo Purevjav[1], Takuo Okuchi[1], Norimasa Ozaki[2], Takayoshi Sano[3], Yuhei Umeda[2], Shintaro Morioka[2], Nobuki Kamimura[2] (1.Institute for Planetary Materials, Okayama University, 2.Graduate School of Engineering, Osaka University, 3.Institute of Laser Engineering, Osaka University)

[PCG22-P05] Richtmyer-Meshkov instability in inhomogeneous density materials and its application to planetary science

*Takayoshi Sano[1] (1.Institute of Laser Engineering, Osaka University)

[PCG22-P06] Impact-induced dehydration reactions of Fe- and Al-hydrates as potential storage, carrier and source of water

*Tsubasa Tobase[1], Toshimori Sekine[1], Ginga Kitahara[2], Makoto Tokuda[2], Akira Yoshiasa[2], Makoto Takafuji[2], Tsutomu Mashimo[2], Nobuaki Kawai[2] (1.HPSTAR, 2.Graduate School of Science and Technology, Kumamoto University)

[PCG22-P07] Crystallization of amorphous $MgSiO_3$ by shock compression

*Akane Arasuna[1], Masayuki Okuno[1], Nobuaki Kawai[2] (1.Kanazawa University, 2.Kumamoto University)

[PCG22-P08] First-principle study of the structural and electronic properties of N-doped $MgAl_2O_4$ spinel

*Chi Pui Tang[1], Pak Kin Leong[1], Toshimori Sekine[2,3] (1.State Key Laboratory of Lunar and Planetary Sciences, Macau University of Science and Technology, 2.Center for High Pressure Science and Technology Advanced Research (HPSTAR) Shanghai Laboratory of HPSTAR, Shanghai, P.R. China, 3.Graduate School of Engineering, Osaka University)

[PCG22-P09] Transparency of shock-compressed single crystal diamond

*Kento Katagiri[1], Norimasa Ozaki[1,2], Kohei Miyanishi[2], Yuhei Umeda[1], Shintaro Morioka[1], Takayoshi Sano[2], Ryosuke Kodama[1,2] (1.Osaka University, 2.Institute of Laser Engineering, Osaka Unversity)

[PCG22-P10] Pb-Pb dating of the NWA 7203 angrite and relationship to its shock metamorphism

*Hideyuki Hayashi[1], Takashi Mikouchi[1], Yuji Sano[1], Martin Bizzarro[2] (1.The university of Tokyo, 2.University of Copenhagen)

[PCG22-P11] Shock recovery of high-pressure phase of SiO_2 using high-power laser

*Tadashi Kondo[1], Hiromoto Kengo[1], Tatsuhiro Sakaiya[1], Hidenori Terasaki[1], Keisuke Shigemori[2], Youichiro Hironaka[2] (1.Department of Earth and Space Science, Graduate School of Science Osaka University, 2.Institute of Laser Engineering, Osaka University)

[PCG22-P12] Hugoniot measurement of calcite under meteorite collision condition

*Fukui Keiya[1], Norimasa Ozaki[1,2], Yuhei Umeda[1], Kohei Miyanishi[3], Kento Katagiri[1], Shintaro Morioka[1], Takayoshi Sano[3], Ryosuke Kodama[1,2,3] (1.Graduate School of Engineering,Osaka univ., 2.PPC, Osaka Univ., 3.ILE, Osaka Univ.)

[PCG22-P13] Direct observation of the transformation toughening of tetragonal stabilized zirconia under shock deformation condition by ns time-resolved XRD.

*Sota Takagi[1,2], Kouhei Ichiyanagi[2,3], Nobuaki Kawai[4], Ryo Fukaya[2], Shunsuke Nozawa[2], Atsushi Kyono[1], Nobumasa Funamori[2], Shin-ichi Adachi[2] (1.University of Tsukuba, 2.KEK PF, 3.Jichi Medical University, 4.Kumamoto University)

discussion

*Takuo Okuchi[1], Toshimori Sekine[2]

1. Institute for Planetary Materials, Okayama University, 2. Center for High Pressure Science and Technology Advanced Research

We discuss natural and experimendal evidences on impact phenomena, which had played essential roles in the process of early planetary evolution. Recent analytical and experimenotal developments reveal a new prospective on the effects of shock-compression process of planetary materials. For deeper understanding of such shock effects, it is necessary to evaluate the detailed shock conditions from the observations of naturally-shocked planetary materials, as well as to compare them with the results of shock-compression experiments of these materials obtained at laboratory conditions.

Keywords: discussion

©2019. Japan Geoscience Union. All Right Reserved.

Shock-compressed behavior of quartz by XFEL

*Tomoko Sato[1], Yoshinori Tange[2], Yusuke Seto[3], Toshimori Sekine[4,5], Norimasa Ozaki[4], Toyohito Nishikawa[4], Kohei Miyanishi[4], Kensuke Matsuoka[4], Ryosuke Kodama[4], Tadashi Togashi[2], Yuichi Inubushi[2], Toshinori Yabuuchi[6], Makina Yabashi[6]

1. Hiroshima University, 2. Japan Synchrotron Radiation Research Institute, 3. Kobe University, 4. Osaka University, 5. Center for High Pressure Science &Technology Advanced Research, 6. RIKEN

We have conducted x-ray diffraction measurement (XRD) with femtosecond x-ray pulses generated by the x-ray free electron laser (XFEL) to observe lattice dynamics and phase transformation of single-crystal quartz under high strain-rate shock compression (~10^9 s^{-1}) and high pressure. Single-crystal quartz samples were shock-compressed by high-power short- and long-pulse lasers. In the short-pulse experiments, the lattice was reduced to 15% and 1.5% in the direction parallel and perpendicular to the compression axis, respectively. The sample was uniaxially compressed over its known Hugoniot elastic limit. In the long-pulse experiments, three different states were observed. Polycrystalline stishovite appeared at first, and elastically compressed state and a topotaxially transformed new phase were observed successively.

Keywords: Shock compression, in-situ X-ray diffraction, quartz

©2019. Japan Geoscience Union. All Right Reserved.

Laser-shock experiments of dense polymorphs of Mg_2SiO_4: technical developments using synthetic single crystals

*Narangoo Purevjav[1], Takuo Okuchi[1], Norimasa Ozaki[2], Takayoshi Sano[3], Yuhei Umeda[2], Shintaro Morioka[2], Nobuki Kamimura[2]

1. Institute for Planetary Materials, Okayama University, 2. Graduate School of Engineering, Osaka University, 3. Institute of Laser Engineering, Osaka University

Mg_2SiO_4 polymorphs (α-phase as forsterite, β-phase as wadsleyite, and γ-phase as ringwoodite) are the major constituents of our Earth's mantle and also for Earth-like planets. Thus studying these polymorphs at extreme pressure and temperature conditions will lead to understanding their changes of chemical and physical properties at extremely high pressure and temperature conditions, such as those occurring during the giant impacts phenomena of such planets at their final stage of accretion. Shock compression of forsterite has been studied up to ~ 1000 GPa by using polycrystalline and single crystal samples [1-3]. The studies have reported contradicting results for the shock compression of forsterite. Sekine et al (2016) reported that there are several phase transformations in the liquid state of Mg_2SiO_4 at > 270 GPa, while other two studies were reported no phase transformation [1, 3]. Thus it is interesting to see how the Hugonoit relations of Mg_2SiO_4 polymorphs will come up at different pressure and temperature conditions. However, Hugoniot relations of wadsleyite and ringwoodite have not been studied well. Especially, there is any data on the densest polymorph ringwoodite. Shock compression of wadsleyite was carried out up to 200 GPa by using polycrystalline samples [4]. In addition, there are no studies by using single crystal samples for both wadsleyite and ringwoodite. To newly conduct such studies, the denser polymorph of Mg_2SiO_4 are needed to be synthesized and grown at their relevant conditions of deep mantle corresponding to the 15 –21 GPa and 1000 –1500 ˚C in the laboratory. Most importantly, the synthesized minerals must be chemically, physically and optically homogenous and should have suitable sizes for the laser-shock experiments. Here, by utilizing the results of our previous efforts for growing such quality of single crystals, we made possible to obtain Hugoniot relation of wadsleyite and ringwoodite by laser-shock compression. Their crystals were synthesized and grown by using a scaled-up Kawai-type cell by together with applying our pre-established a slow-cooling method at their relevant conditions [5]. Recovered crystals were up to 1 mm in sizes and confirmed to be chemically homogenous and free from twinning, cracks, and inclusions. The crystals were then doubly polished separately down to 100 mm in thickness and with an area of > 500 mm. They were assembled to form targets which are optimized for the laser-shock experiments. laser-shock experiments at GEKKO XII were conducted at Institute of Laser Engineering, Osaka University. The crystals are optical to give very clean VISAR (Velocity Interferometer System for Any Reflector) images. The details of our technical developments will be discussed on the poster.

[1] Root, T., Townsend, J. L., Davies, E., Lemke, R. W., Bliss, D. E., Fratanduono, D. E., et al. (2018). *Geophys. Res. Lett.*, **45**:3865. [2] Sekine, T., Ozaki, N., Miyanishi, K., Asaumi, Y., Kimura, T., Albertazzi, B. et al. (2016). *Sci. Adv.*, **2**:e1600157. [3] Bolis, R. M., Morard, G., Vinci, T., Ravasio, A., Bambrink, E. et al. (2016). *Geophys. Res. Lett.*, **43**:9475. [4] Mosenfelder, J. L., Asimow, P. D. and Ahrens, T. J. (2007). *J. Geophys. Res.*, **112**:B06208. [5] Okuchi, T., Purevjav, N., Tomioka, N., Lin, J. F., Kuribayashi, T. et al. (2015). *Am. Mineral.*, **100**:1483.

Keywords: laser-shock compression, Mg2SiO4 polymorphs

©2019. Japan Geoscience Union. All Right Reserved.

©2019. Japan Geoscience Union. All Right Reserved.

Richtmyer-Meshkov instability in inhomogeneous density materials and its application to planetary science

*Takayoshi Sano[1]

1. Institute of Laser Engineering, Osaka University

Richtmyer-Meshkov instability (RMI) is a hydrodynamic interfacial instability, which occurs by the interaction between a shock wave and corrugated density jump. Because of the corrugation of the interface, the surface profiles of the transmitted and reflected shocks are also rippled. The RMI is driven by the vorticity left by these rippled shocks at the interface and in the fluid. In this study, we consider shock propagation in inhomogeneous density materials (e.g., uniform density materials with small round voids) and the turbulent growth of the interface. For these cases, the vorticity distribution and turbulent motion are much more complicated than the standard RMI cases. Then the spatial fluctuation of pressure or temperature could be significantly large after the shock passage. Using two-dimensional hydrodynamic simulations, we will examine the dependence of the pressure fluctuation on the density inhomogeneity. As the application of this numerical study, we will discuss about the shock propagation in meteorites with large density fluctuation.

Keywords: shock waves, Richtmyer-Meshkov instability

©2019. Japan Geoscience Union. All Right Reserved.

Impact-induced dehydration reactions of Fe- and Al-hydrates as potential storage, carrier and source of water

*Tsubasa Tobase[1], Toshimori Sekine[1], Ginga Kitahara[2], Makoto Tokuda[2], Akira Yoshiasa[2], Makoto Takafuji[2], Tsutomu Mashimo[2], Nobuaki Kawai[2]

1. HPSTAR, 2. Graduate School of Science and Technology, Kumamoto University

Hydrous minerals have been known to play an important role to preserve and carry water because a mechanism is required for water to reach the inner planets such as Earth far beyond the snow line that defines the boundary between water ice and vapor. In order to understand the detailes, we need to know the stability at high temperature and high pressure and impact resistance for possible hydrous minerals. Fe- and Al-hydrates (FeOOH and AlOOH) have been reported to be stable under static high temperature and static high pressure. In addition, they are observed in some meteorites and the surface on Mars. Although there are some data available on clay minerals and serpentine, those Fe- and Al-hydrates are considered to be present in the Earth’ s deep lower mantle according to the recent studies.

We have investigated the impact resistibility through shock recovery techniques. Our peak shock pressures are 24 GPa and 31 GPa for the recovered Fe- and Al-hydrates, respectively, where they displayed significant dehydration. We set various range of sample porosity and peak shock pressure to investing the dehydration reaction. These impact conditions correspond to impact velocities of 2.6 km/s and 4.9 km/s if we assume face to face impacts between carbonaceous chondrite such as Murchison. These are within a range of velocity for possible meteoritic collisions, and we need to know the relationship between impact condition and degree of dehydration. Using TG/DTA analyses of samples we estimated the relationship. The phase changes by impact dehydration are investigated by XRD, XAFS and Raman spectroscopy. We also try to understand dynamical void formation process by dehydration that can occur during adiabatic quenching through observation of void distribution in the recovered samples.

In our previous research for shock recovery experiments of hydrous minerals, we observed heterogenous temperature rise in dehydration process. We tried to confirm whether heterogeneous temperature rise occurs even in Fe- and Al-hydrates by comparison with the results between previously reported hydrous minerals. We will be able to select most possible candidate by comparing the thermal stability and impact resistibility among them.

Keywords: Shock recovered experiments, hydrous mineral, dynamic water loss, Powder x-ray diffraction

©2019. Japan Geoscience Union. All Right Reserved.

Crystallization of amorphous $MgSiO_3$ by shock compression

*Akane Arasuna[1], Masayuki Okuno[1], Nobuaki Kawai[2]

1. Kanazawa University, 2. Kumamoto University

Structural change of synthesized amorphous $MgSiO_3$ by shock compression up to 22.2 GPa has been investigated using XRD and IR analyses. The obtained result provides information for elucidating of the collision behavior of $MgSiO_3$ contained in cosmic dust.

Amorphous $MgSiO_3$ sample was prepared by an aqueous solution of TEOS, Magnesium Nitrate Hexahydrate, and ethanol with ammonia as a catalyst. As-prepared sample was heated at 700 C˚ to dehydrate excess water. TG curve of this sample indicated that the sample contained about 8.8 wt% of water molecules and hydroxyl groups.

A powdered heated (original) sample was put in an aluminum tubes and pressed at 20 kN for 10 minutes to obtain samples for shock compression experiment. These samples were compressed at 13.6, 17.2, and 22.2 GPa using a single-stage propellant gun at Kumamoto University.

XRD pattern of the pressed sample showed no crystalline peak as same as the original sample. However, the XRD pattern of thesample compressed at 13.6 GPa showed the weak crystalline peaks at around 2θ = 28, 31, 35-36˚. These peaks became intense with increasing shock pressure. Crystalline peaks observed in the XRD pattern for the sample of 22.2 GPa were attributed to those of enstatite. However, some peaks was due to the formation of Mg_2SiO_4. IR spectra for the compressed samples showed the similar trend as the result of XRD analysis. But IR analysis indicated that the sample contains water molecules even after the shock compression at 22.2 GPa. Water molecules probably present in the remaining amorphous part. Crystallization of sample by shock compression has not been reported in shock experiments for other crystalline and non-crystalline silicates. The crystallization of our samples at low pressure may be due to the simple chain structure of enstatite. Also, high shock temperature which generated by friction due to the porosity of the sample may promote this crystallization.

Keywords: MgSiO3, amorphous , shock compression, enstatite

©2019. Japan Geoscience Union. All Right Reserved.

First-principle study of the structural and electronic properties of N-doped $MgAl_2O_4$ spinel

*Chi Pui Tang[1], Pak Kin Leong[1], Toshimori Sekine[2,3]

1. State Key Laboratory of Lunar and Planetary Sciences, Macau University of Science and Technology, 2. Center for High Pressure Science and Technology Advanced Research (HPSTAR) Shanghai Laboratory of HPSTAR, Shanghai, P.R. China, 3. Graduate School of Engineering, Osaka University

On basis of the first principle calculation, we report a possible nitrogen doped structure of $MgAl_2O_4$ spinel. The structural and electronic properties (include the band structure, density of states and phonon) of spinel ($MgAl_2O_4$) and N-doped spinel ($MgAl_2O_{3.5}N_{0.5}$) compounds are performed using density functional theory (DFT). The density and space group of two crystal cells are 3.47 g/cm^3 (Fd3m) for $MgAl_2O_4$ and 3.38 g/cm^3 (R3m) for $MgAl_2O_{3.5}N_{0.5}$, respectively. The calculated direct band gaps at the Γ-point are about 5.13 eV for $MgAl_2O_4$ and 4.24 eV for $MgAl_2O_{3.5}N_{0.5}$, respectively. The projected density of states (PDOS) shows that the tops of the valence bands are built up from ~93% of *p*(O) states and ~60% of *p*(N) + ~32% of *p*(O) states (for $MgAl_2O_4$ and $MgAl_2O_{3.5}N_{0.5}$, respectively). In the phonon analysis, the lowest frequency of $MgAl_2O_{3.5}N_{0.5}$ is redshifted to 36.6 cm^{-1} ($MgAl_2O_4$ is 39.8 cm^{-1}) caused by the N-doped. We also calculate their cohesive energy in the pressure range of 0-150 GPa. We found that the cohesive energy of $MgAl_2O_{3.5}N_{0.5}$ is lower than $MgAl_2O_4$ at the pressure higher than ~115 GPa, it implies that $MgAl_2O_{3.5}N_{0.5}$ is more stable than $MgAl_2O_4$ at high pressure. Finally, we suggest that nitrogen atom would replace the oxygen of spinel in the depths of the earth. The results imply the deep mantle may storage a considerable amount of nitrogen.

Keywords: First principle calculation, Density functional theory, Spinel

©2019. Japan Geoscience Union. All Right Reserved.

Transparency of shock-compressed single crystal diamond

*Kento Katagiri[1], Norimasa Ozaki[1,2], Kohei Miyanishi[2], Yuhei Umeda[1], Shintaro Morioka[1], Takayoshi Sano[2], Ryosuke Kodama[1,2]

1. Osaka University, 2. Institute of Laser Engineering, Osaka Unversity

Carbon is one of the most prominent elements in nature and it is abundant in the Earth and many other planets. Diamond, a metastable phase of carbon, is naturally synthesized in deep inside of the Earth where substances are isotropically pressured. Diamond is known for its many unique properties such as high hardness, low compressibility, small thermal expansion coefficient, and transparency. Since it is important to understand how substances behave under high pressure, properties of compressed diamond have been measured in a wide range of pressures up to 5 TPa. However, the transparency of diamond under pressure has not been fully elucidated. Here, we report the measurment of the pressure dependency of the absorption coefficient of laser shock compressed single crystalline diamond. A high-intensity laser was utilized to shock compress the diamond sample along its <100> direction, and velocity interferometer systems for any reflector (VISARs) were used to determine the absorption coefficient and pressure. It was found that single crystalline diamond remains largely transparent to the probe laser for VISAR (λ =532 nm) up to 140 GPa. The pressure dependence of the refractive index will also be discussed.

This experiment was conducted under the joint research of the Institute of Laser Engineering, Osaka University. This work was supported in part by JSPS KAKENHI grant No. 16H02246 and No. 16H01119. The part of work was also supported by Genesis Research Institute, Inc. (Konpon-ken, TOYOTA).

Keywords: Shock-compression, High intensity laser, Diamond, Transparency, Refractive index

©2019. Japan Geoscience Union. All Right Reserved.

Pb-Pb dating of the NWA 7203 angrite and relationship to its shock metamorphism

*Hideyuki Hayashi[1], Takashi Mikouchi[1], Yuji Sano[1], Martin Bizzarro[2]

1. The university of Tokyo, 2. University of Copenhagen

Introduction: Angrite is one of the oldest basaltic achondrites in the early solar system which is depleted in volatile elements and enriched in refractory elements (e.g., Keil, 2012). Almost all angrites show either a quenched or slowly-cooled texture. The crystallization ages of quenched angrites are older (ca. 4564 Ma) than those of slowly-cooled samples (ca. 4558 Ma). One of the most striking mineralogical characteristics about angrites is the lack of shock metamorphism. Thus, quenched angrites can be good time anchors to connect absolute and relative ages, because the age differences between two systems can be ignored due to fast cooling and furthermore there is no chronological reset by shock metamorphism. However, NWA 1670 and NWA 7203 are known to show evidence for shock (Mikouchi et al., 2003; Hayashi et al., 2018), and especially we found that NWA 7203 exhibited remarkable shock metamorphic textures. The Pb-Pb dating of angrites has been done only for angrites without shock textures, indicating the obtained ages are crystallization ages. Pb-Pb age is relatively easy to be reset by shock heating. Therefore, Pb-Pb age of NWA 1670 or especially NWA 7203 may be reset by shock heating. However, there is no study which measured Pb-Pb dating of NWA 1670 or NWA 7203. In this study, we measured Pb isotopic ratios of silico-apatite in NWA 7203 by Nano-SIMS, and discussed the Pb-Pb age of NWA 7203.

Sample: We used NWA 7203 for this study. NWA 7203 is an angrite meteorite showing a quenched texture. NWA 7203 consists of a dendritic texture of olivine and anorthite, and pyroxene fills gaps of the dendrites. Grain size exhibits large variations from fine grains (~1 μm) to coarse grains (>100 μm). This is not a typical characteristic of quenched angrites. NWA 7203 is composed mainly of olivine, pyroxene and anorthite, and the accessory minerals are troilite, ulvospinel and silico-apatite.

Methods: Observation was carried out on thin sections by optical microscope and BSE images of FE-EPMA. Mineral phases were identified by micro-Raman spectroscopic analysis. Pb-Pb dating of NWA 7203 was carried out by measuring Pb isotope ratios of silico-apatites using Nano-SIMS at AORI, Univ. of Tokyo. Measurement conditions were 300 pA for primary ions and $^{16}O^-$ for ion sources. Pre-sputtering was performed for 8 minutes in the range of 10 x 10 μm. In the SIMS measurement, raster diameter of 3 x 3 μm and analysis time of 60 seconds were applied for two magnetic fields, respectively, and repeated for 30 cycles. For the standard, NIST SRM 610 was used.

Result and discussion: Pb isotopic ratios of silico-apatite in the NWA 7203 angrite were obtained. We obtained a weighted approximate straight line for each plot and found the Pb-Pb age to be 4551 ±17 Ma. These plots are relatively variable. This is probably because Pb isotopic ratios were disturbed by shock metamorphism. In fact, the Pb-Pb age of silico-apatite grains that are at least 200 μm away from the shock veins was found to be 4560 ±16 Ma. It is considered that the Pb isotopic ratios of these silico-apatite grains are relatively undisturbed as they are linearly aligned. This age coincides with the crystallization age of other quenched angrites within the error range. Takenouchi et al. (2019) measured the Ar-Ar ages of NWA 7203 and found that it has two plateau ages of 3800 ±440 Ma and 2300 ±140 Ma, and concluded that the shock metamorphism of NWA 7203 occurred at 2300 ±140 Ma. From this result, it is considered that the Pb-Pb age of NWA 7203 is not completely reset, but slightly disturbed.

©2019. Japan Geoscience Union. All Right Reserved.

Keywords: NWA 7203, Angrite, Pb-Pb dating, Shock metamorphism, Parent body

©2019. Japan Geoscience Union. All Right Reserved.

Shock recovery of high-pressure phase of SiO_2 using high-power laser

*Tadashi Kondo[1], Hiromoto Kengo[1], Tatsuhiro Sakaiya[1], Hidenori Terasaki[1], Keisuke Shigemori[2], Youichiro Hironaka[2]

1. Department of Earth and Space Science, Graduate School of Science Osaka University, 2. Institute of Laser Engineering, Osaka University

High-pressure phases in meteorites provide us the important information of shock history in natural materials. Experimental approach to reproduce such high-pressure phase have been studied intensively mainly by light-gas gun so far, though shock condition with impact velocity beyond 10km/s is difficult. Recent technical progress of high-intensity laser as a tool of shock experiment realize the recovery of samples with shock condition above 10km/s(Nagaki et al.,2016). However, the limited shock duration time of about 10 nsec has been too short to drive structural conversion to high-pressure form in single crystal sample. In this study, we explored recovery condition of high-pressure phase of SiO_2 using finely ground samples of quartz, cristobalite and fused silica as starting materials. Laser shock experiments were performed using GXII hyper laser at Institute of Laser Engineering, Osaka University. The whole sample retaining relative locations in the recovered box made of aluminum was quenched without significant scattering in each run. The sectioned sample at shocked center were examined by optical microscope, micro-focused X-ray diffraction and SEM-EDS. We will report the characteristic feature of top portion of sample, which shows layered structure with different metamorphism, and distribution of grass and stishovite phase found in the samples shocked above 100GPa, which have still a residual stress to 10GPa in the ambient condition. We will discuss the dependence of the initial state of crystal to recover the high-pressure phase in shocked samples in nsec.

Keywords: shocked quartz, high-intensity laser, recovery experiments

©2019. Japan Geoscience Union. All Right Reserved.

Hugoniot measurement of calcite under meteorite collision condition

*Fukui Keiya[1], Norimasa Ozaki[1,2], Yuhei Umeda[1], Kohei Miyanishi[3], Kento Katagiri[1], Shintaro Morioka[1], Takayoshi Sano[3], Ryosuke Kodama[1,2,3]

1. Graduate School of Engineering,Osaka univ., 2. PPC, Osaka Univ., 3. ILE, Osaka Univ.

Volatile substances inside planetary materialsare generated and released as gas under the extreme condition caused by collision phenomenon that is thought to contribute greatly to the formation of the planetary atmosphere [1]. Particularly the degassing reaction of carbonate, may generate CO or CO_2as greenhouse gas and affect the temperature of the planetary surface. A typical planetary mineral as carbonate of calcite ($CaCO_3$) is expected degassing above 3300 K at pressure of 150 GPa along the Hugoniot[2].
In the previous study, the experimental investigations for the shock-degassing reaction were carried out only below the impact pressure of 100 GPa. Also, we have not understood when the degassing reaction of calcite occur on a compressed state or a released state [3]
In natural, typical meteorite impacts exceed 10 km/s in impact velocity, and can generate at the pressure above 150 GPa. The purpose of this research is to understand the impact compression characteristics of calcite under the meteorite collision condition.

This experiment was conducted in Shock Drive Laser (Gekko XII) atInstitute for Laser Engineering, Osaka University. The target consists of polypropylene as an ablator aluminum as a piston, quartz as a standard material, and calcite as a sample from laser side. The impact pressures and temperatures were estimated by the measured shock wave velocity using Velocity interferometer system for any reflector (VISAR) and self-emission intensity using radiance thermometer (SOP).
As a result of this experiments, we obtained the Hugoniot date at the puressure from 200 GPa to 1 Tpa at the temperature above 5000 K. The detailed results will be shown as this presentation.
Acknowledgements

This experiment was conducted on the joint research of the Institute of Laser Engineering, Osaka University. This work was supported in part by JSPS KAKENHI grant No. 16H02246 and No. 16H01119. The part of work was also supported by Genesis Research Institute, Inc. (Konpon-ken, TOYOTA).

REFERENCES

[1] T. Matsui and Y.Abe: Nature, 319, 303 - 319 (1986).

[2] B.Ivanov and A. Deutsch: Physics of the Earth and Planetary Interiors, 129, 131-143 (2002).

[3] K.Kawaragi et al.: Earth and Planetary Science Letters, 282, 56 - 64 (2009).

Keywords: Laser-Shock-compression, hugoniot, calcite, degassing

©2019. Japan Geoscience Union. All Right Reserved.

Direct observation of the transformation toughening of tetragonal stabilized zirconia under shock deformation condition by ns time-resolved XRD.

*Sota Takagi[1,2], Kouhei Ichiyanagi[2,3], Nobuaki Kawai[4], Ryo Fukaya[2], Shunsuke Nozawa[2], Atsushi Kyono[1], Nobumasa Funamori[2], Shin-ichi Adachi[2]

1. University of Tsukuba, 2. KEK PF, 3. Jichi Medical University, 4. Kumamoto University

The enhancement of strength and toughness was found in oxide-doped tetragonal stabilized zirconia, with the suggestion that the absorption of energy during the martensitic transformation contribute to the increment [Gravie et al., 1975; Gupta et al., 1977]. Using transmission electron microscopy (TEM), in recovery sample, it was observed that the stress-induced transformation from stabilized tetragonal phase to monoclinic phase can be occurred around the crack tip [Porter et al., 1977], and the transformation-toughening model were devised [McMeeking et al., 1982; Hannink et al., 2000]. In high-pressure experiments, the phase transformation behavior of tetragonal stabilized zirconia has not been clarified in both static and shock compression because a lack of in-situ observation [Ohtaka et al., 1988; Grady et al., 1992]. We tried to observe the behavior of tetragonal stabilized zirconia under shock compression condition using time-resolved XRD method.We performed the experiments at NW14A beamline at PF-AR (Photon Factory Advanced Ring), High Energy Accelerator Research Organization (KEK), Japan. Nd:glass laser with the wavelength of 1064 nm, pulse energy of 16 J, pulse width of 12 ns was used for shock-driving source. The laser beam was focused by optical lens to the size of 500 μm × 500 μm on the sample surface. For TR-XRD experiments, the synchrotron X-ray pulse of PF-AR was used as a probe source. The energy, the pulse width, and the size on the sample were 15.68 keV, about 100 ps, and 450 μm (H) ×250 μm (W), respectively. The irradiation timing between laser pulse and X-ray pulse on the sample surface were controlled by delay generator at ns time scale. The targets consisted of an 25 um PET film ablator with Al coated on the surface and 50 um polycrystalline 3 mol% yttria doped tetragonal stabilized zirconia.
The XRD change were observed up to 35 ns after shock compression started. Before shock, the (101), (002), (110), (102), (112), (200) diffraction of tetragonal phase were observed. 6.5 ns after shock, the diffraction from compression region appeared with maximum compression of 6%. No phase transition occurred at compression states. At release states (~11.4 ns), on the other hand, the (-111), (111), (022), (-221) diffraction peaks of monoclinic phase were appeared. We will discuss the detail of the experimental results and the transformation toughening mechanism.

Keywords: Synchrotron X-ray, Time-resolved XRD, Laser-induced shock wave, Tetragonal stabilized zirconia

©2019. Japan Geoscience Union. All Right Reserved.

[E] Poster | A (Atmospheric and Hydrospheric Sciences)：A-AS Atmospheric Sciences, Meteorology & Atmospheric Environment

Tue. May 28, 2019 10:45 AM - 12:15 PM JST | Tue. May 28, 2019 1:45 AM - 3:15 AM UTC | Poster Hall International Exhibition Hall8, Makuhari Messe_2

[A-AS03] Large-scale moisture and organized cloud systems

convener:Hiroaki Miura(The University of Tokyo), Atsushi Hamada(University of Toyama), Satoru Yokoi(Japan Agency for Marine-Earth Science and Technology), Masaki Satoh(Atmosphere and Ocean Research Institute, The University of Tokyo)

Water vapor plays a significant role in regulating the global atmospheric circulation, especially in the troposphere. The overturning circulation is directly driven by the longwave radiative cooling of water vapor and the latent heating/cooling through microphysical processes to balance it. This global circulation is composed of diverse atmospheric phenomena with various spatial and temporal scales. Developments of some significant turbulent motions such as 3D isotropic turbulence in clouds, stratocumulus and cumulus convection, squall lines and tropical cyclones, and the Madden-Julian oscillation, are essentially associated with moisture anomaly in each scale. Moisture is accumulated relatively slowly in larger horizontal scales, but is consumed relatively quickly in smaller ones. This significant scale gaps between the accumulation and consumption may be one of the causes of the long-lasting difficulty in developing the theory of the moist atmosphere. The aim of this session is to share the recent researches about the relationships between moisture and organized cloud systems in wider spatial and temporal scales to enhance collaborations between modeling, observational, and theoretical approaches in tackling this challenging task. Research results relating to the Years of the Maritime Continent (YMC) and Radiative-Convective Equilibrium Model Intercomparison Project (RCEMPI) are welcome.

[AAS03-P01] Numerical investigation on the shape, terminal velocity, and drag coefficient of a small raindrop by the improved immersed boundary method

*Ong Chia Rui[1], Hiroaki Miura[1] (1.The University of Tokyo)

[AAS03-P02] **A diagnostic study of water vapor during an extreme precipitation event in Yili river valleyA diagnostic study of water vapor during an extreme precipitation event in Yili river valley**

*Jing LiU[1], Yushu Zhou[2], Lianmei Yang[1] (1.Institute of Desert Meteorology,CMA, 2.Institute of Atmospheric Physics,CAS)

[AAS03-P03] **The Study on the Characteristics of Weather and Cloud Types in the Summer and Winter Seasons of the South China Sea**

*Jou Ping Hou[1], Bo-Shiou Wei[1], Li-Zhen Su[1] (1.Chung Cheng Institute of Technology)

[AAS03-P04] **Linkages between the South and East Asian Monsoon water vapor transport during boreal summer**

*Yong Liu[1] (1.Institute of Atmospheric Physics, Beijing , China)

[AAS03-P05] Interannual Modulation of the Local Hadley Circulation on Clouds, Radiation and Diagnostic Fields over the Western North Pacific

*Xinyue Wang[1], Hironobu Iwabuchi[1] (1.Tohoku Univ.)

[AAS03-P06] Seasonal and Regional Variation of Diurnal Cycle of Rainfall over Java Island and the Surrounding Area

*Madam Taqiyya Maulana[1], Takeshi Yamazaki[1] (1.Tohoku University)

[AAS03-P07] **Study on atmospheric circulation characteristics of precipitation anomalies in arid region of Central Asia**

*Lianmei Yang[1], Xuefeng Guan[1] (1.Institute of Desert Meteorology, China Meteorological Administration,)

[AAS03-P08] Mechanisms for northward propagation of boreal summer intraseasonal oscillation

*Kanta Nakae[1], Masaki Satoh[1], Daisuke Takasuka[1] (1.Atmosphere and Ocean Research Institute, The University of Tokyo)

[AAS03-P09] Fractality in the perimeter of tropical clouds observed by Himawari-8 or simulated by a high-resolution model

*Takuya Jinno[1] (1.Graduate School of Science, The University of Tokyo)

[AAS03-P10] **Large-scale deformation of tropical cloud band in the ITCZ detected in NICAM simulations**

*Noriyuki Nishi[1], Atsushi Hamada[4], Yohei Yamada[2], Tomoe Nasuno[2], Reona Satoh[5], Masaki Satoh[3] (1.Faculty of Science, Fukuoka Universtiy, 2.JAMSTEC, 3.AORI, University of Tokyo, 4.Graduate School of Science and Engineering for Education, University of Toyama, 5.Graduate School of Science, Fukuoka University)

[AAS03-P11] **Improvement of single-moment bulk microphysics for super-cooled water clouds over the Southern Ocean in NICAM using Joint simulator and double-moment microphysics**

*Woosub Roh[1], Tatsuya Seiki[2], Masaki Satoh[1], Tempei Hashino[3] (1.AORI, the university of Tokyo, 2.JAMSTEC, 3.Kochi university of technology)

[AAS03-P12] High-cloud property responses to SST change: sensitivity study using a global nonhydrostatic model

*Tomoki Ohno[1], Masaki Satoh[2] (1.Japan Agency for Marine-Earth Science and Technology, 2.Atmosphere and Ocean Research Institute, The University of Tokyo)

[AAS03-P13] Effects of different cloud overlapping parameters on simulated total cloud fraction over the globe and East Asian region

*bo hai Wang[1], hua Zhang[2] (1.Institute of Atmospheric Physics, Chinese Academy of Sciences, 2.State Key Laboratory of Severe Weather, Chinese Academy of Meteorological Sciences)

Numerical investigation on the shape, terminal velocity, and drag coefficient of a small raindrop by the improved immersed boundary method

*Ong Chia Rui[1], Hiroaki Miura[1]

1. The University of Tokyo

The cloud microphysical processes play a crucial part in controlling the water cycle, cloud formation, and radiation transfer in the atmosphere. These process are parameterized in a numerical weather prediction model by empirical formulae. In particular, empirical formulae for the prediction of the terminal velocity, drag coefficient, and shape of a free-falling water droplet are used widely in the parameterizations. Despite that the model accuracy is sensitive to the microphysics parameterizations to a considerable extent, these formulae are only verified by experiments which are conducted at room temperature and standard atmospheric pressure or linear theories in an ideal condition. The validity of the parameterizations is therefore questionable under general conditions and the accuracy of the numerical prediction may be affected.
In this work, a new numerical tool, the immersed boundary method, is proposed as an alternative way to investigate the terminal velocity, drag coefficient, and shape of an axisymmetric free-falling raindrop. This improved immersed boundary method for water droplet simulations is applied to verify those commonly used empirical formulae under different conditions. The largest size of the free-falling raindrop in this work is 0.5 mm. To first verify the reliability and robustness of this new method the terminal velocity and drag coefficient obtained from axisymmetric raindrop simulations at standard pressure and temperature fit well with the experimental data. Further simulation results of an axisymmetric free-falling raindrop of diameters of 0.025, 0.01, and 0.5 mm at different altitudes assuming a fixed lapse rate show that the variation of the shape of the raindrop is negligibly small, and there is a significant discrepancy between the numerical results and some of the widely used empirical formulae. The discrepancy is larger at higher altitudes for small raindrops. This is because of the assumption of the fixed drag coefficient in the derivation of those empirical formulae. A new parameterization with better accuracy for terminal velocity aloft of raindrops with diameter smaller than 0.5 mm is proposed. A further sensitivity test of a 0.5 mm free-falling axisymmetric raindrop with different surface tension coefficients are performed and the numerical results suggest that the change in the shape and terminal velocity is negligible with respect to aerosols.

Keywords: Cloud Microphysis, Immersed boundary method, Terminal velocity

©2019. Japan Geoscience Union. All Right Reserved.

A diagnostic study of water vapor during an extreme precipitation event in Yili river valleyA diagnostic study of water vapor during an extreme precipitation event in Yili river valley

*Jing LiU[1], Yushu Zhou[2], Lianmei Yang[1]

1. Institute of Desert Meteorology,CMA, 2. Institute of Atmospheric Physics,CAS

An extreme precipitation events was happened during 31 July to 1 August, 2016 at Yili river valley which multi-stations breakthrough extreme precipitation’ s value. Based on calculation of water vapor transport stream function and the non-divergent (rotational) components, potential function and divergent (irrotational) components, the water vapor transport budget and water vapor transport trajectories for the Yili river valley using the conventional detection,1° x 1° NCEP/NCAR reanalysis, HYSPLIT model based on Lagrangian method, Ground-based GPS observation precipitable water vapor data(GPS-PWV) , the large-scale water vapor transport and convergence characteristics were analyzed during the heavy rainfall period. The results showed that: (1) The Indian, the Pacific and the Atlantic ocean all contributed to the water supply during the heavy rain period, and Indian summer monsoon circulation, the south China sea summer monsoon circulation at low latitudes and Atlantic ocean’ s east airflow at mid-latitude were constituted the water vapor transmission channel, which the Indian Ocean southwest water vapor transport mainly concentrated in the lower troposphere, and middle troposphere water vapor transport was given priority to the west flow of the Atlantic ocean and low trough itself; the valley was in the convergence area of water vapor flux during the heavy rain, and the convergence and uplift of the terrain to the West opening caused vertical motion development provided a favorable dynamic convergence mechanism for the occurrence of local heavy rain.(2) The 3000 m water vapor transmission trajectory included the westward and eastward path at bottom layer and the northward path at middle troposphere as complement of water vapor for the lower troposphere through the vertical motion, the southward path at lower troposphere which water vapor come from the Arabian sea,and the mid-latitude water vapor transport of the westward path was the most powerful ; The 5000 m water vapor transmission trajectory was dominated by the westward path and the low trough itself;(3) During the precipitation period, the water vapor was concentrated in the lower troposphere which transported to the upper level through vertical movement, and the water vapor was positive at the middle and upper layers contrasted with negative at the lower layer. south boundary of water vapor inflow was rapidly increasing at the lower layer while the middle and higher layer water vapor inflow derived from the western boundary during the heavy rainfall period;(4)Yili river valley GPS-PWV jumped caused by the southwest airflow front of low trough before the rainfall happened and steadily maintain the high value influenced by India southwest monsoon during the heavy rainfall period. The large-scale water vapor transport convergence enhancement corresponding local GPS-PWV increased, suggested that the water vapor supply in local heavy rain event was at least associated with the water vapor transport and convergence of hemisphere scale.

Keywords: torrential rain, transfer of water vapor, lagrange trajectory, ground-based GPS

©2019. Japan Geoscience Union. All Right Reserved.

The Study on the Characteristics of Weather and Cloud Types in the Summer and Winter Seasons of the South China Sea

*Jou Ping Hou[1], Bo-Shiou Wei[1], Li-Zhen Su[1]

1. Chung Cheng Institute of Technology

The South China Sea is vast with a tropical maritime climate near the equator and a subtropical climate in the north. Therefore, although it is winter, there are still deep convective and strong precipitation systems in the South China Sea. In summer, thermal convection is strong, sometimes typhoons pass; Dongsha Island and Taiping Island are located in the north and south of the South China Sea. The weather in the region is bound to be significantly affected by various weather systems in the South China Sea. We selected the winter of December 2017 and the summer of June 2018 to study it. The Dongsha Island and Taiping Island areas were subjected to research on the northeast monsoon and tropical convection. The dual island observation and satellite data were combined with numerical models to analyze the mutual interaction between the thermal and dynamic processes in the South China Sea. To enhance the understanding of the weather evolution mechanism in the South China Sea, in order to further clarify the various cloud-phase characteristics of the monsoon circulation and thermal convection in the South China Sea. The results show that the change of northeast monsoon intensity obviously affects the interaction of air-sea in the South China Sea, enhances the intensity of precipitation, and changes the amount and height of the stratus cumulus in the sea. In addition, the northeast monsoon circulation may interact with the surrounding terrain of the South China Sea, thus induces local deep convection. In the summer, the southwest monsoon will be enhanced and thermal convection is very strong. The intensity and life cycle of the typhoon can be maintained when it passes this area.

Keywords: Dongsha Island, Taiping Island, Air-Sea interaction, Deep Convection

©2019. Japan Geoscience Union. All Right Reserved.

Linkages between the South and East Asian Monsoon water vapor transport during boreal summer

*Yong Liu[1]

1. Institute of Atmospheric Physics, Beijing , China

This study provides a water vapor transport (WVT) perspective on the linkages between the South and East Asian summer monsoons (SASM and EASM) and indicates two robustly coupled modes of the vertical integrated WVT (VIWVT) over the two monsoons that accounts for above 90% of the total squared covariance fraction. The first coupled mode (SVD1 mode) depicts a meridional linkage between the meridional dipole VIWVT anomalies over both the SASM and EASM. While the second coupled mode (SVD2 mode) illustrates a zonal connection of an anomalous cyclonic/anticyclone VIWVT over the SASM and a zonal wave-like VIWVT over the EASM. The SVD1 mode is linked through the anomalous subtropical High over the western North Pacific (WNPSH) and primarily associated with the transition phase of El Niñ o/La Niña (ENSO) and simultaneous Indian Ocean Basin mode (IOBM) SST warming/cooling. The meridional connection of the VIWVT in the SVD1 mode experienced a clear intensification since the late-1970s that may be attributed to the strengthened impacts of the ENSO/IOBM on the EASM and SASM after the late-1970s. The SVD2 mode is connected by the Circumglobal teleconnection (CGT) pattern and related to the developing phase of ENSO and summer north Atlantic tripole (NAT) SST anomalies. The zonal VIWVT connection in SVD2 mode is strongly modulated by the SASM-CGT connections and reveals significant weakening since the late-1970s but re-intensifies after the early-1990s. This may be associated with the weakened ENSO-SASM relationship after the late-1970s and interdecadal decreasing of the all Indian summer rainfall since the early-1990s.

Keywords: Water vapor transport, South and East Asian summer monsoon, linkage, interdecadal change

©2019. Japan Geoscience Union. All Right Reserved.

Interannual Modulation of the Local Hadley Circulation on Clouds, Radiation and Diagnostic Fields over the Western North Pacific

*Xinyue Wang[1], Hironobu Iwabuchi[1]

1. Tohoku Univ.

Variation of the local Hadley cell (HC) northern boundary over the western North Pacific, and its interannual imprints on the tropospheric clouds and atmospheric fields are examined with observation and reanalysis data for the winter season from December 1982 to February 2016. The poleward shift of the local HC subsiding edge is marked by anomalous rising motion, large-scale decreased static stability, and corresponding increases of the midlevel cloud amount over the climatological sinking zone around 30N. These responses primarily locate over the continental and coastal areas instead of the open oceans. Concomitant with the increasing cloud fraction, a net negative top-of-atmosphere radiation anomaly is identified, and the main contributor is suggested to be the cumulus congestus, whose top pressures are in a range of 440–680 hPa, and optical thicknesses in a range of 23–60. Interactions between this specific cloud type and the vertical moist instability, and their constrains on the precipitation field is further discussed.

Keywords: Regional Hadley cell, Cloud and radiation, Precipitation pattern

©2019. Japan Geoscience Union. All Right Reserved.

Seasonal and Regional Variation of Diurnal Cycle of Rainfall over Java Island and the Surrounding Area

*Madam Taqiyya Maulana[1], Takeshi Yamazaki[1]

1. Tohoku University

The seasonality and regional variability of diurnal cycle of rainfall (DCR) over Java Island and the surrounding area (coastal region of the Java Sea and the Indian Ocean) are analyzed through satellite observations. This study focus on the area where the studies of the seasonality of DCR over Indonesian Maritime Continent (IMC) are still limited. The DCR is a prominent phenomenon over IMC which is important for aviation industry and related to heavy precipitation events that cause hydro-meteorological disasters.

In this study, **we investigate seasonal and regional variation of DCR (the phase and the amplitude)** through satellite observations. High resolution (spatial and temporal) rainfall estimate is needed to capture feature of DCR over the study area which is difficult to obtain from ground observation. We **mainly employ the high-resolution dataset of Global Satellite Mapping of Precipitation (GSMaP) reanalysis (GSMaP_RNL) and near real time (GSMaP_NRT).** The analysis of DCR seasonal variability is based on investigation throughout boreal winter (December-January-February), boreal spring (March-April-May), boreal summer (June-July-August), and boreal autumn (September-October-November) from 2008-2018 (GSMaP_NRT) and 2009-2014 (GSMaP_RNL).

The results show that hourly data of GSMaP_RNL and GSMaP_NRT with 0.1˚ spatial resolution are able to depict the detailed features of the seasonality and regional variability of DCRover Java Island and surrounding areas. **The comparison between GSMaP_RNL and GSMaP_NRT shows that GSMaP_NRT represents significant time lag of DCR phase over off shore region. GSMaP_NRT shows that the offshore region of the Java Sea is dominated by noon-afternoon rainfall while GSMaP_RNL shows morning rainfall.** However, both of GSMaP_RNL and GSMaP_NRT show similar pattern on phase and amplitude of DCR. Phase of DCR indicates the time when maximum rainfall occurs, while amplitudes indicates the magnitude of DCR. In general, both of GSMaP_RNL and GSMaP_NRT composites, show that the land region with wider landmass area (West Java and western part of East Java) is dominated by evening phase while narrow landmass area (Central Java and eastern part of Java Island) is dominated by late afternoon phase. A large magnitude of the DCR is concentrated inland. The Java Sea has a higher amplitude of DCR compared to the Indian Ocean and the coastal region. The amplitude over the coastal region of the Indian Ocean is higher than over the Indian Ocean and the coastal area of the Java Sea.

Both of rainfall estimates capture inhomogeneous seasonal shifting phase of DCR over this region. The remarkable seasonal shifting phase occurs along the coastal area of the Java Sea. Though, phase shifting over inland of a wide landmass area and the coastal region of the Indian Ocean is not significant. Inhomogeneous seasonal shifting phase of DCR indicated interactions between local circulations, which affected by the topography (e.g. terrain and shape of the coastline), and large circulations (background wind, synoptic conditions, etc.). The analysis of wind profile from reanalysis data confirms the seasonal change of interactions between large and small circulations that caused seasonal shifting phase of DCR.

Keywords: Diurnal cycle of rainfall (DCR), Seasonal variability, Regional variability, Shifting Phase, GSMaP

©2019. Japan Geoscience Union. All Right Reserved.

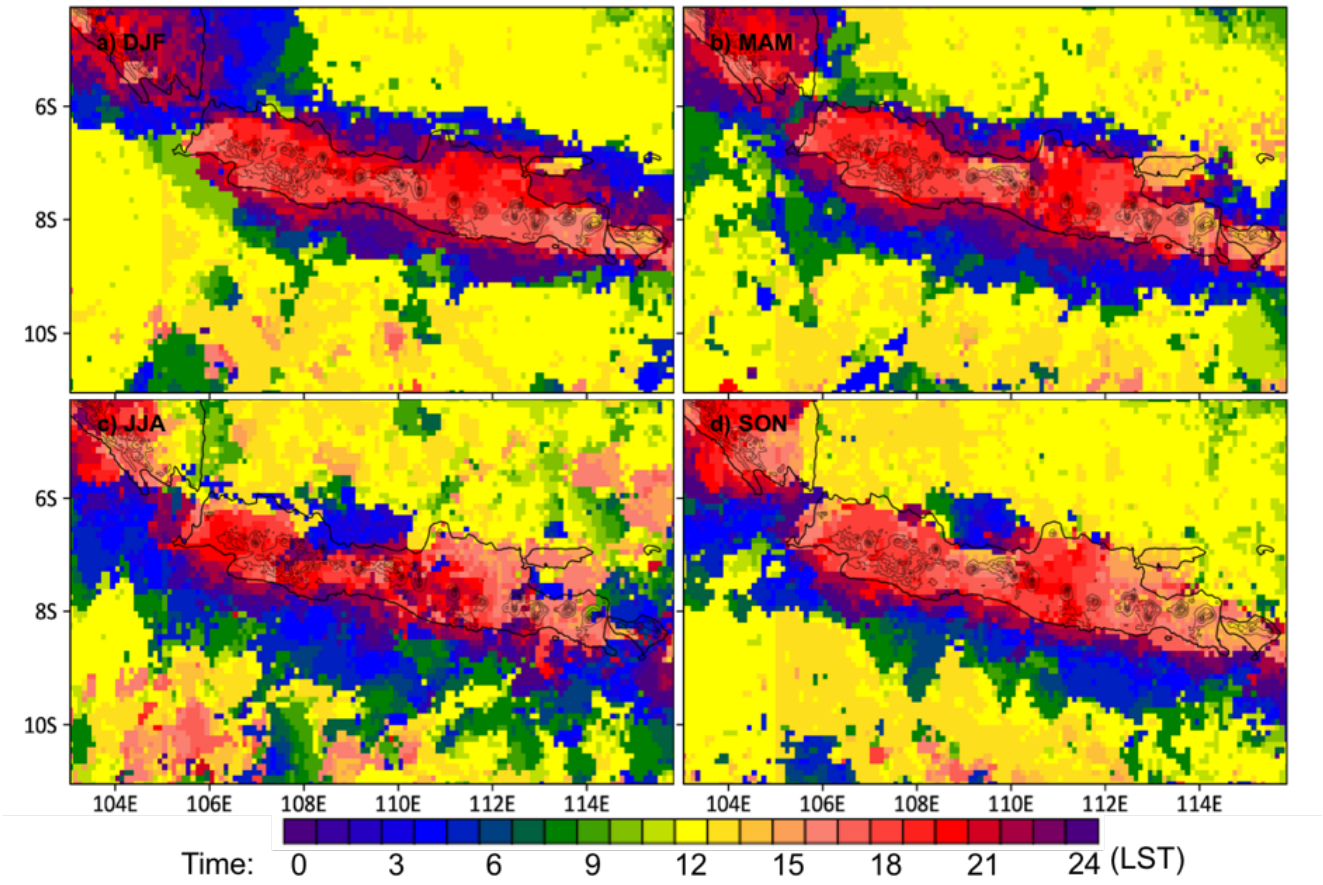

©2019. Japan Geoscience Union. All Right Reserved.

Study on atmospheric circulation characteristics of precipitation anomalies in arid region of Central Asia

*Lianmei Yang[1], Xuefeng Guan[1]

1. Institute of Desert Meteorology, China Meteorological Administration,

As climate transition zone between Mediterranean climate region and East Asian monsoon region, arid region of Central Asia (including five Central Asian countries and Xinjiang province of China) which is influenced by high, middle and low latitude circulations has different synoptic-climatic characteristics from that of Europe and East Asia while its climate characteristics also varies greatly within the region. Central Asia has unique and complicated topography and ecosystem patterns like deserts, oasis, glaciers and basins, forming a highly representative meteorological disaster-breeding environment under the influence of multiple-background, multiple-factor and multiple-scale. This area has abundant solar-heat energy, large evaporation and dramatic temperature changes. Besides, its precipitation is scarce and has extremely uneven distribution with high value in the western and middle parts of Tianshan Mountains. Over the last one hundred years, Central Asia has experienced a warm and wet trend. Central Asia low value system together with the high, middle and low latitude circulation systems linked by West Asia westerly jet stream have contributed to the interdecadal and interannual variations of precipitation in Xinjiang. However, due to the insufficient construction of integrated meteorological observation network, the studies concerning regional featured circulation system, regularity and mechanism of disastrous weathers, high resolution regional numerical model, impacts of land-atmosphere interaction on regional weather and climate change prediction are still inadequate. Correspondingly, to carry out those studies has essential scientific significance and strategic value for the sustainable social and economic development in Silk Road Economic Belt.

Keywords: Arid region of Central Asia, synoptic-climatic characteristics, precipitation anomaly, atmospheric circulation, water vapor

©2019. Japan Geoscience Union. All Right Reserved.

Mechanisms for northward propagation of boreal summer intraseasonal oscillation

*Kanta Nakae[1], Masaki Satoh[1], Daisuke Takasuka[1]

1. Atmosphere and Ocean Research Institute, The University of Tokyo

The 20-90-day Intraseasonal Oscillation (ISO) is one of the dominant modes of tropical variability. In boreal summer northward propagation (NP), which occurs on ISO time scales, originates near the equator and extends to India and western North Pacific Ocean. Understanding the NP of the boreal summer ISO (BSISO) is of vital importance to extended-range weather prediction. Hence, several mechanisms of the NP have been examined. However, they are still incompletely understood. The purpose of this study is to investigate the importance of vertical shear and sea surface temperature (SST) for the NP of the BSISO. In order to obtain a basic structure of the BSISO, we have conducted JJA-perpetual experiments using the Non-hydrostatic Icosahedral Atmospheric Model (NICAM) with a 56-km horizontal mesh.
Although the perpetual experiment has strong Indian monsoon over Arabian sea due to the bias of surface temperature on land, it is found that the NP of the BSISO from Indian Ocean (IO) has two abovementioned mechanisms. One warm SST anomaly north of convection destabilize the lower troposphere, while another tilted vertical shear can generate positive barotropic vorticity to the north of convection. In order to assess the effect of the former mechanism, we made an experiment using fix SST (SSTFIX) obtained from CTL experiment. SSTFIX experiment reproduces the NP of the BSISO from IO, although the amplitude became lower. Therefore, it suggests that the NP of the BSISO from IO doesn’t need warm SST anomaly. To Improve the bias related to basic state like vertical shear, we conducted an experiment using nudging method for surface temperature on land (LNDADJ). In LNDADJ experiment the NP of the BSISO from IO isn’t reproduced due to reduction of column water vapor over Bay of Bengal. Thus, tilted vertical shear can just begin the NP. On the other hand, it is suggested that the NP needs SST and column water vapor to maintain its strength.

Keywords: Boreal summer intraseasonal oscillation, Asian monsoon, Northward propagation

©2019. Japan Geoscience Union. All Right Reserved.

Fractality in the perimeter of tropical clouds observed by Himawari-8 or simulated by a high-resolution model

*Takuya Jinno[1]

1. Graduate School of Science, The University of Tokyo

Cloud clusters show a wide variety of shape and size, and their spatial pattern is often taken up as a typical example of fractal. However, the methods of studying fractal are in an early stage of development. In this study, we conducted fractal analysis on the perimeter of tropical clouds using satellite observation and cloud-resolving simulation of sub-kilometer resolution. We evaluated fractal dimension as a function of spatial scale (transient fractal dimension) and quantified the characteristic spatial scale of the pattern from the scale where self-similarity breaks down. From the observational data from HIMAWARI-8, It is shown that the self-similarity of the cloud perimeter persists only in the spatial scale range from 2 km up to 30 km. The limit of the self-similarity is suggested to be the characteristic scale of the pattern formation of tropical clouds. The cloud-resolving simulation data with NICAM also shows finite-size self-similarity. However, the profile of the transient fractal dimension changed with integration time far more rapidly than HIMAWARI-8 observation, and it lost its self-similarity at the end of the 48-hour simulation. This process is suggested to reflect the increase of stratiform cloud in the upper-troposphere as an adjustment to the transition of spatial resolution.

Keywords: fractal, HIMAWARI-8, cloud-resolving model

©2019. Japan Geoscience Union. All Right Reserved.

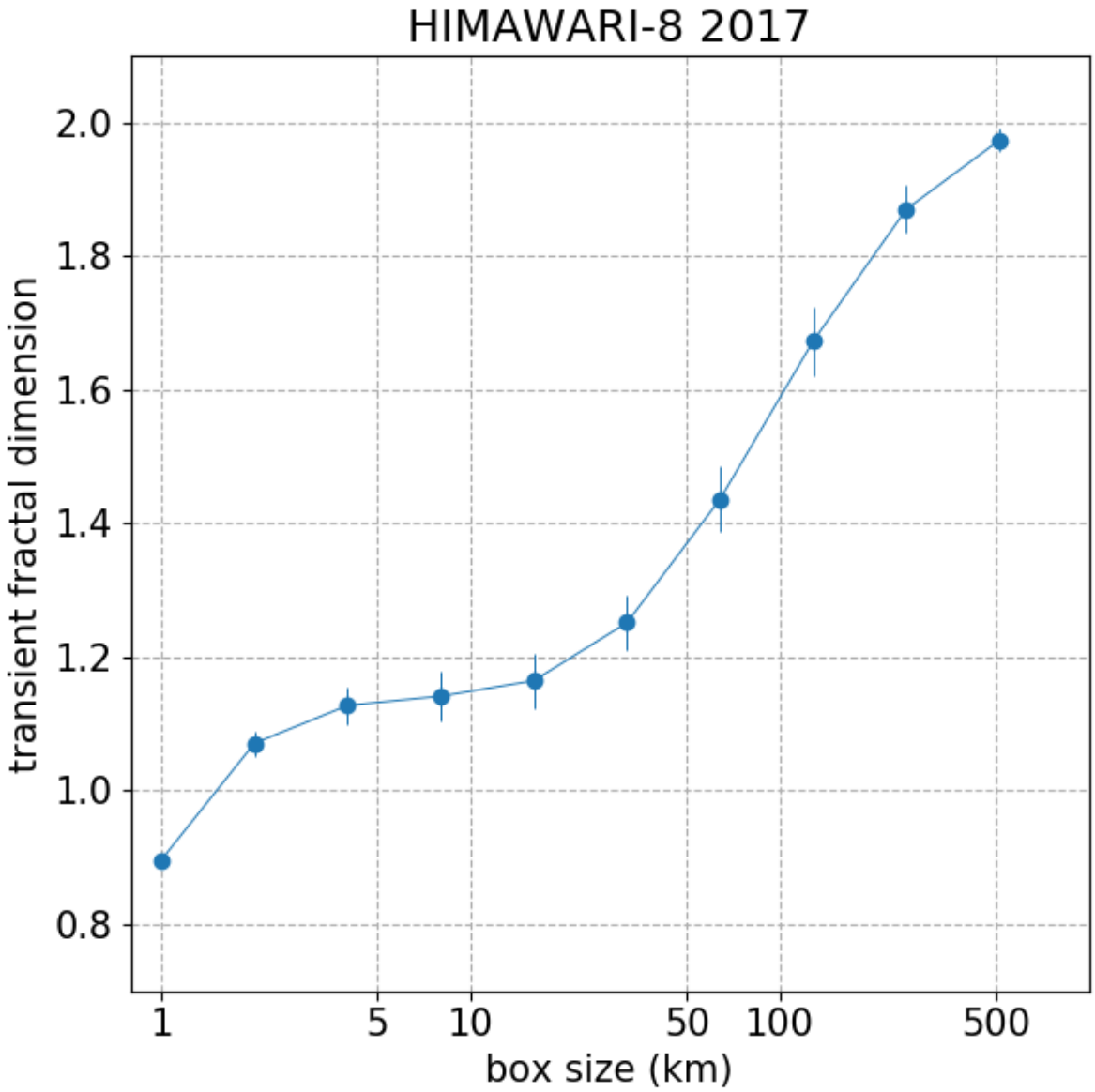

©2019. Japan Geoscience Union. All Right Reserved.

Large-scale deformation of tropical cloud band in the ITCZ detected in NICAM simulations

*Noriyuki Nishi[1], Atsushi Hamada[4], Yohei Yamada[2], Tomoe Nasuno[2], Reona Satoh[5], Masaki Satoh[3]

1. Faculty of Science, Fukuoka Universtiy, 2. JAMSTEC, 3. AORI, University of Tokyo, 4. Graduate School of Science and Engineering for Education, University of Toyama, 5. Graduate School of Science, Fukuoka University

Over the central/eastern tropical Pacific, the Inter Tropical Convergence Zone (ITCZ) is detected in the northern side of the equator. In the ITCZ, we can sometimes observe drastic deformation of the cloud bands elongated zonally with several thousand-kilometer scale. The initial stage of the band, which is composed of deep convective systems, expands meridionally and separates into two or three parallel cirrus bands that keep alive one or two days (Hamada et al., 2013, JMSJ). These separation events cannot be well described in the objective analysis datasets, probably due to lack of the observations over the open ocean; investigation of their mechanism with the analysis data is difficult. In order to study their mechanism, we attempted to use the numerical simulation results of global cloud system resolving model NICAM (Satoh et al. 2014, Progress in Earth and Planetary Science) to find similar events in them. If we can find separation events in the results, we can examine the mechanism with many physical parameters including wind, various kinds of hydrometeors. We have already analyzed several numerical experiment results for different periods, resolution and physical schemes.

We found a similar separation event in an output of the simulation for one year from June 2004 and horizontal resolution 3.5 km. We examined the life cycle of the cirrus bands after separation. One interesting point is on the height of the cirrus clouds in the separated bands. The simulated cirrus clouds in the bands lie in the 13-14 km height level, while the height of the maximum meridional wind that contributes to the meridional movement of the cirrus bands is about 12 km. This difference of the heights means that the cirrus clouds were not just advected by meridional wind but were possibly developed in the course of the separation.

The trigger of zonally simultaneous separation of a long band is another our interest. Inertial instability may be a candidate since vertical exchange of zonal momentum by deep convection would occur in an original band and result in the large meridional shear of the zonal wind in the upper troposphere. We tried to confirm necessary condition for inertial instability by calculating geostrophic vorticity, following the general procedure. However, the position of the bands is too close to the equator (3-7N) to establish geostrophic relationship, and the spatial pattern of the geostrophic vorticity is too noisy to analyze. Therefore, we instead calculate simple absolute vorticity. We found that the absolute vorticity around the separated bands was almost negative. It suggests the possibility of the inertial (or similar kind of) instability.

We are now analyzing another numerical experiment including four kinds of runs using a cloud scheme with different cloud parameter settings. In the real atmosphere, a separation event occurred on 16-17 June 2008 at the just east of the date line. The event can be simulated in all of four runs at 36 hours from the initial time. It suggests that the basic mechanism of the separation is not sensitive to the detail of cloud systems. By analyzing the dynamical fields of these outputs, we are trying to find the key mechanisms to trigger the meridional separation of the cloud bands.

©2019. Japan Geoscience Union. All Right Reserved.

Keywords: tropics, ITCZ, cirrus

©2019. Japan Geoscience Union. All Right Reserved.

Improvement of single-moment bulk microphysics for super-cooled water clouds over the Southern Ocean in NICAM using Joint simulator and double-moment microphysics

*Woosub Roh[1], Tatsuya Seiki[2], Masaki Satoh[1], Tempei Hashino[3]

1. AORI, the university of Tokyo, 2. JAMSTEC, 3. Kochi university of technology

It is important to evaluate and improve the cloud properties in global non-hydrostatic models like a Nonhydrostatic ICosahedral Atmospheric Model (NICAM, Satoh et al. 2014) using observation data. One of the methods is a radiance-based evaluation using satellite data and a satellite simulator (here Joint simulator, Hashino et al. 2013), which avoids making different settings of the microphysics between retrieval algorithms and NICAM.

One of the challenging issues is an evaluation of mixed-phase clouds, which consist of water vapor, ice particles, and supercooled water droplets. It is known one of the main reasons why climate models reveal large errors about the reflection of solar radiation over the Southern Ocean and Arctic.

This study is an evaluation and improvement of mixed-phase clouds over the Southern Ocean in NICAM using a Cloud-Aerosol Lidar and Infrared Pathfinder Satellite Observation (CALIPSO) and a satellite simulator. We evaluated thermodynamics phase of mixed phases clouds over the Southern Ocean in a regional version of NICAM between 45˚S to 65˚S and 170˚E to 170˚W following Yoshida et al. (2010) method. We found underestimation of supercooled water clouds in our single moment scheme. We improved the single moment microphysics scheme using a double moment microphysics and a single column model. We also investigate the impact of microphysics scheme on moisture distributions and the size of cloud systems.

Keywords: microphysics, CALIPSO, Satellite simulator

©2019. Japan Geoscience Union. All Right Reserved.

High-cloud property responses to SST change: sensitivity study using a global nonhydrostatic model

*Tomoki Ohno[1], Masaki Satoh[2]

1. Japan Agency for Marine-Earth Science and Technology, 2. Atmosphere and Ocean Research Institute, The University of Tokyo

Since it has been recognized that the uncertainty of cloud feedback is one of main contributors to the intermodel spread of climate sensitivity, the reduction of the uncertainties associated with cloud response to global warming has been one of central issues for robust projections and predictions of climate variability and change. High clouds have large impacts on the Earth’ s radiative energy budget, and the uncertainty of their response to climate change is known as one of large sources of the climate sensitivity spread although several possible hypotheses to predict the response have been proposed. As the radiation-cloud interaction plays a crucial role in the determination of life time of high clouds, the improvement of the understanding of cloud property responses to global warming helps the reduction of climate-sensitivity variability associated with the high-clouds feedback.

In order to investigate the cloud-property response to climate change, we conducted simulations with RCE configurations using a high-resolution nonhydrostatic global circulation model (the Nonhydrostatic Icosahedral Atmospheric Model; NICAM) with the earth-like sphere for simplifying the problem. Sea surface temperatures (SSTs) are fixed at 300K and 304K and a double-moment bulk scheme are used without cumulus parameterization scheme.

We found that high cloud amount increases with SST increase, as consistent with the previous NICAM studies. It was also determined that the change in particularly optically thin clouds whose optical thicknesses were <3 was dominant, and such thin clouds tended to have large particle sizes. These suggests that the slow evaporative property of ice phase clouds and their representability can play one of key roles in the uncertainty of the high-cloud amount change in global warming.

Keywords: cloud property responses, cloud feedback, climate change

©2019. Japan Geoscience Union. All Right Reserved.

Effects of different cloud overlapping parameters on simulated total cloud fraction over the globe and East Asian region

*bo hai Wang[1], hua Zhang[2]

1. Institute of Atmospheric Physics, Chinese Academy of Sciences, 2. State Key Laboratory of Severe Weather, Chinese Academy of Meteorological Sciences

The cloud overlapping parameter (vertical decorrelation length, L_{cf}) from CloudSat/CALIPSO is implemented in Beijing Climate Center’ s GCM (BCC_AGCM2.0) to reduce the uncertainly in radiation field. Comparing the climate simulation results obtained by using the constant L_{cf} of 2 km with those using the above retrieved L_{cf}, it is found that the total cloud fraction simulation has been obviously improved by using the satellite-based L_{cf}. The error of global mean total cloud fraction between simulations and CERES (Clouds and the Earth's Radiant Energy System) satellite data is decreased by 1.6% in both the winter and summer, of which the positive deviation of total cloud amount at tropical convection area and the negative deviation in subtropical region both are significantly reduced. These improvements are helpful for better simulation of energy budget differences between different regions. In East Asia, using the satellite-based L_{cf} can decrease the error of average total cloud fraction (compared to the CERES) by 1.8% (1.4%) in the winter (summer).Overall, using L_{cf} from CloudSat/CALIPSO satellite data can improve the simulation of total cloud fraction and thus obtain more accurate simulation of radiation field.

Keywords: Cloud overlapping parameter, Vertical decorrelation length, Total cloud fraction

©2019. Japan Geoscience Union. All Right Reserved.

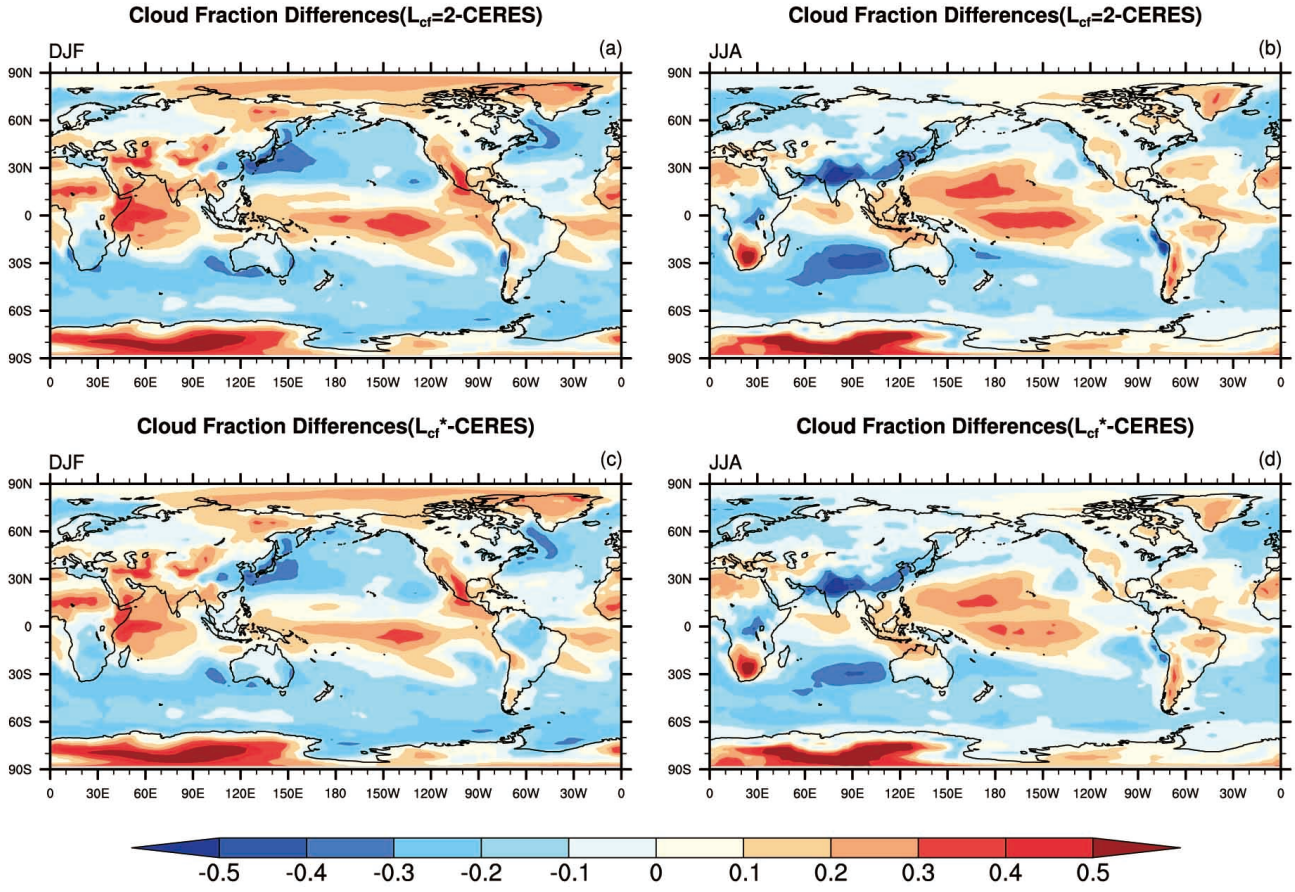

©2019. Japan Geoscience Union. All Right Reserved.

[E] Poster | A (Atmospheric and Hydrospheric Sciences)：A-AS Atmospheric Sciences, Meteorology & Atmospheric Environment

Tue. May 28, 2019 5:15 PM - 6:30 PM JST | Tue. May 28, 2019 8:15 AM - 9:30 AM UTC | Poster Hall International Exhibition Hall8, Makuhari Messe_6

[A-AS03] Large-scale moisture and organized cloud systems

convener:Hiroaki Miura(The University of Tokyo), Atsushi Hamada(University of Toyama), Satoru Yokoi(Japan Agency for Marine-Earth Science and Technology), Masaki Satoh(Atmosphere and Ocean Research Institute, The University of Tokyo)

Water vapor plays a significant role in regulating the global atmospheric circulation, especially in the troposphere. The overturning circulation is directly driven by the longwave radiative cooling of water vapor and the latent heating/cooling through microphysical processes to balance it. This global circulation is composed of diverse atmospheric phenomena with various spatial and temporal scales. Developments of some significant turbulent motions such as 3D isotropic turbulence in clouds, stratocumulus and cumulus convection, squall lines and tropical cyclones, and the Madden-Julian oscillation, are essentially associated with moisture anomaly in each scale. Moisture is accumulated relatively slowly in larger horizontal scales, but is consumed relatively quickly in smaller ones. This significant scale gaps between the accumulation and consumption may be one of the causes of the long-lasting difficulty in developing the theory of the moist atmosphere. The aim of this session is to share the recent researches about the relationships between moisture and organized cloud systems in wider spatial and temporal scales to enhance collaborations between modeling, observational, and theoretical approaches in tackling this challenging task. Research results relating to the Years of the Maritime Continent (YMC) and Radiative-Convective Equilibrium Model Intercomparison Project (RCEMPI) are welcome.

[AAS03-P01] Numerical investigation on the shape, terminal velocity, and drag coefficient of a small raindrop by the improved immersed boundary method

*Ong Chia Rui[1], Hiroaki Miura[1] (1.The University of Tokyo)

[AAS03-P02] **A diagnostic study of water vapor during an extreme precipitation event in Yili river valleyA diagnostic study of water vapor during an extreme precipitation event in Yili river valley**

*Jing LiU[1], Yushu Zhou[2], Lianmei Yang[1] (1.Institute of Desert Meteorology,CMA, 2.Institute of Atmospheric Physics,CAS)

[AAS03-P03] **The Study on the Characteristics of Weather and Cloud Types in the Summer and Winter Seasons of the South China Sea**

*Jou Ping Hou[1], Bo-Shiou Wei[1], Li-Zhen Su[1] (1.Chung Cheng Institute of Technology)

[AAS03-P04] **Linkages between the South and East Asian Monsoon water vapor transport during boreal summer**

*Yong Liu[1] (1.Institute of Atmospheric Physics, Beijing , China)

[AAS03-P05] Interannual Modulation of the Local Hadley Circulation on Clouds, Radiation and Diagnostic Fields over the Western North Pacific

*Xinyue Wang[1], Hironobu Iwabuchi[1] (1.Tohoku Univ.)

[AAS03-P06] Seasonal and Regional Variation of Diurnal Cycle of Rainfall over Java Island and the Surrounding Area

*Madam Taqiyya Maulana[1], Takeshi Yamazaki[1] (1.Tohoku University)

[AAS03-P07] **Study on atmospheric circulation characteristics of precipitation anomalies in arid region of Central Asia**

*Lianmei Yang[1], Xuefeng Guan[1] (1.Institute of Desert Meteorology, China Meteorological Administration,)

[AAS03-P08] Mechanisms for northward propagation of boreal summer intraseasonal oscillation

*Kanta Nakae[1], Masaki Satoh[1], Daisuke Takasuka[1] (1.Atmosphere and Ocean Research Institute, The University of Tokyo)

[AAS03-P09] Fractality in the perimeter of tropical clouds observed by Himawari-8 or simulated by a high-resolution model

*Takuya Jinno[1] (1.Graduate School of Science, The University of Tokyo)

[AAS03-P10] **Large-scale deformation of tropical cloud band in the ITCZ detected in NICAM simulations**

*Noriyuki Nishi[1], Atsushi Hamada[4], Yohei Yamada[2], Tomoe Nasuno[2], Reona Satoh[5], Masaki Satoh[3] (1.Faculty of Science, Fukuoka Universtiy, 2.JAMSTEC, 3.AORI, University of Tokyo, 4.Graduate School of Science and Engineering for Education, University of Toyama, 5.Graduate School of Science, Fukuoka University)

[AAS03-P11] **Improvement of single-moment bulk microphysics for super-cooled water clouds over the Southern Ocean in NICAM using Joint simulator and double-moment microphysics**

*Woosub Roh[1], Tatsuya Seiki[2], Masaki Satoh[1], Tempei Hashino[3] (1.AORI, the university of Tokyo, 2.JAMSTEC, 3.Kochi university of technology)

[AAS03-P12] High-cloud property responses to SST change: sensitivity study using a global nonhydrostatic model

*Tomoki Ohno[1], Masaki Satoh[2] (1.Japan Agency for Marine-Earth Science and Technology, 2.Atmosphere and Ocean Research Institute, The University of Tokyo)

[AAS03-P13] Effects of different cloud overlapping parameters on simulated total cloud fraction over the globe and East Asian region

*bo hai Wang[1], hua Zhang[2] (1.Institute of Atmospheric Physics, Chinese Academy of Sciences, 2.State Key Laboratory of Severe Weather, Chinese Academy of Meteorological Sciences)

Numerical investigation on the shape, terminal velocity, and drag coefficient of a small raindrop by the improved immersed boundary method

*Ong Chia Rui[1], Hiroaki Miura[1]

1. The University of Tokyo

The cloud microphysical processes play a crucial part in controlling the water cycle, cloud formation, and radiation transfer in the atmosphere. These process are parameterized in a numerical weather prediction model by empirical formulae. In particular, empirical formulae for the prediction of the terminal velocity, drag coefficient, and shape of a free-falling water droplet are used widely in the parameterizations. Despite that the model accuracy is sensitive to the microphysics parameterizations to a considerable extent, these formulae are only verified by experiments which are conducted at room temperature and standard atmospheric pressure or linear theories in an ideal condition. The validity of the parameterizations is therefore questionable under general conditions and the accuracy of the numerical prediction may be affected.
In this work, a new numerical tool, the immersed boundary method, is proposed as an alternative way to investigate the terminal velocity, drag coefficient, and shape of an axisymmetric free-falling raindrop. This improved immersed boundary method for water droplet simulations is applied to verify those commonly used empirical formulae under different conditions. The largest size of the free-falling raindrop in this work is 0.5 mm. To first verify the reliability and robustness of this new method the terminal velocity and drag coefficient obtained from axisymmetric raindrop simulations at standard pressure and temperature fit well with the experimental data. Further simulation results of an axisymmetric free-falling raindrop of diameters of 0.025, 0.01, and 0.5 mm at different altitudes assuming a fixed lapse rate show that the variation of the shape of the raindrop is negligibly small, and there is a significant discrepancy between the numerical results and some of the widely used empirical formulae. The discrepancy is larger at higher altitudes for small raindrops. This is because of the assumption of the fixed drag coefficient in the derivation of those empirical formulae. A new parameterization with better accuracy for terminal velocity aloft of raindrops with diameter smaller than 0.5 mm is proposed. A further sensitivity test of a 0.5 mm free-falling axisymmetric raindrop with different surface tension coefficients are performed and the numerical results suggest that the change in the shape and terminal velocity is negligible with respect to aerosols.

Keywords: Cloud Microphysis, Immersed boundary method, Terminal velocity

©2019. Japan Geoscience Union. All Right Reserved.

A diagnostic study of water vapor during an extreme precipitation event in Yili river valleyA diagnostic study of water vapor during an extreme precipitation event in Yili river valley

*Jing LiU[1], Yushu Zhou[2], Lianmei Yang[1]

1. Institute of Desert Meteorology,CMA, 2. Institute of Atmospheric Physics,CAS

An extreme precipitation events was happened during 31 July to 1 August, 2016 at Yili river valley which multi-stations breakthrough extreme precipitation’ s value. Based on calculation of water vapor transport stream function and the non-divergent (rotational) components, potential function and divergent (irrotational) components, the water vapor transport budget and water vapor transport trajectories for the Yili river valley using the conventional detection,1° x 1° NCEP/NCAR reanalysis, HYSPLIT model based on Lagrangian method, Ground-based GPS observation precipitable water vapor data(GPS-PWV) , the large-scale water vapor transport and convergence characteristics were analyzed during the heavy rainfall period. The results showed that: (1) The Indian, the Pacific and the Atlantic ocean all contributed to the water supply during the heavy rain period, and Indian summer monsoon circulation, the south China sea summer monsoon circulation at low latitudes and Atlantic ocean’ s east airflow at mid-latitude were constituted the water vapor transmission channel, which the Indian Ocean southwest water vapor transport mainly concentrated in the lower troposphere, and middle troposphere water vapor transport was given priority to the west flow of the Atlantic ocean and low trough itself; the valley was in the convergence area of water vapor flux during the heavy rain, and the convergence and uplift of the terrain to the West opening caused vertical motion development provided a favorable dynamic convergence mechanism for the occurrence of local heavy rain.(2) The 3000 m water vapor transmission trajectory included the westward and eastward path at bottom layer and the northward path at middle troposphere as complement of water vapor for the lower troposphere through the vertical motion, the southward path at lower troposphere which water vapor come from the Arabian sea,and the mid-latitude water vapor transport of the westward path was the most powerful ; The 5000 m water vapor transmission trajectory was dominated by the westward path and the low trough itself;(3) During the precipitation period, the water vapor was concentrated in the lower troposphere which transported to the upper level through vertical movement, and the water vapor was positive at the middle and upper layers contrasted with negative at the lower layer. south boundary of water vapor inflow was rapidly increasing at the lower layer while the middle and higher layer water vapor inflow derived from the western boundary during the heavy rainfall period;(4)Yili river valley GPS-PWV jumped caused by the southwest airflow front of low trough before the rainfall happened and steadily maintain the high value influenced by India southwest monsoon during the heavy rainfall period. The large-scale water vapor transport convergence enhancement corresponding local GPS-PWV increased, suggested that the water vapor supply in local heavy rain event was at least associated with the water vapor transport and convergence of hemisphere scale.

Keywords: torrential rain, transfer of water vapor, lagrange trajectory, ground-based GPS

©2019. Japan Geoscience Union. All Right Reserved.

The Study on the Characteristics of Weather and Cloud Types in the Summer and Winter Seasons of the South China Sea

*Jou Ping Hou[1], Bo-Shiou Wei[1], Li-Zhen Su[1]

1. Chung Cheng Institute of Technology

The South China Sea is vast with a tropical maritime climate near the equator and a subtropical climate in the north. Therefore, although it is winter, there are still deep convective and strong precipitation systems in the South China Sea. In summer, thermal convection is strong, sometimes typhoons pass; Dongsha Island and Taiping Island are located in the north and south of the South China Sea. The weather in the region is bound to be significantly affected by various weather systems in the South China Sea. We selected the winter of December 2017 and the summer of June 2018 to study it. The Dongsha Island and Taiping Island areas were subjected to research on the northeast monsoon and tropical convection. The dual island observation and satellite data were combined with numerical models to analyze the mutual interaction between the thermal and dynamic processes in the South China Sea. To enhance the understanding of the weather evolution mechanism in the South China Sea, in order to further clarify the various cloud-phase characteristics of the monsoon circulation and thermal convection in the South China Sea. The results show that the change of northeast monsoon intensity obviously affects the interaction of air-sea in the South China Sea, enhances the intensity of precipitation, and changes the amount and height of the stratus cumulus in the sea. In addition, the northeast monsoon circulation may interact with the surrounding terrain of the South China Sea, thus induces local deep convection. In the summer, the southwest monsoon will be enhanced and thermal convection is very strong. The intensity and life cycle of the typhoon can be maintained when it passes this area.

Keywords: Dongsha Island, Taiping Island, Air-Sea interaction, Deep Convection

©2019. Japan Geoscience Union. All Right Reserved.

Linkages between the South and East Asian Monsoon water vapor transport during boreal summer

*Yong Liu[1]

1. Institute of Atmospheric Physics, Beijing , China

This study provides a water vapor transport (WVT) perspective on the linkages between the South and East Asian summer monsoons (SASM and EASM) and indicates two robustly coupled modes of the vertical integrated WVT (VIWVT) over the two monsoons that accounts for above 90% of the total squared covariance fraction. The first coupled mode (SVD1 mode) depicts a meridional linkage between the meridional dipole VIWVT anomalies over both the SASM and EASM. While the second coupled mode (SVD2 mode) illustrates a zonal connection of an anomalous cyclonic/anticyclone VIWVT over the SASM and a zonal wave-like VIWVT over the EASM. The SVD1 mode is linked through the anomalous subtropical High over the western North Pacific (WNPSH) and primarily associated with the transition phase of El Niñ o/La Niña (ENSO) and simultaneous Indian Ocean Basin mode (IOBM) SST warming/cooling. The meridional connection of the VIWVT in the SVD1 mode experienced a clear intensification since the late-1970s that may be attributed to the strengthened impacts of the ENSO/IOBM on the EASM and SASM after the late-1970s. The SVD2 mode is connected by the Circumglobal teleconnection (CGT) pattern and related to the developing phase of ENSO and summer north Atlantic tripole (NAT) SST anomalies. The zonal VIWVT connection in SVD2 mode is strongly modulated by the SASM-CGT connections and reveals significant weakening since the late-1970s but re-intensifies after the early-1990s. This may be associated with the weakened ENSO-SASM relationship after the late-1970s and interdecadal decreasing of the all Indian summer rainfall since the early-1990s.

Keywords: Water vapor transport, South and East Asian summer monsoon, linkage, interdecadal change

©2019. Japan Geoscience Union. All Right Reserved.

Interannual Modulation of the Local Hadley Circulation on Clouds, Radiation and Diagnostic Fields over the Western North Pacific

*Xinyue Wang[1], Hironobu Iwabuchi[1]

1. Tohoku Univ.

Variation of the local Hadley cell (HC) northern boundary over the western North Pacific, and its interannual imprints on the tropospheric clouds and atmospheric fields are examined with observation and reanalysis data for the winter season from December 1982 to February 2016. The poleward shift of the local HC subsiding edge is marked by anomalous rising motion, large-scale decreased static stability, and corresponding increases of the midlevel cloud amount over the climatological sinking zone around 30N. These responses primarily locate over the continental and coastal areas instead of the open oceans. Concomitant with the increasing cloud fraction, a net negative top-of-atmosphere radiation anomaly is identified, and the main contributor is suggested to be the cumulus congestus, whose top pressures are in a range of 440–680 hPa, and optical thicknesses in a range of 23–60. Interactions between this specific cloud type and the vertical moist instability, and their constrains on the precipitation field is further discussed.

Keywords: Regional Hadley cell, Cloud and radiation, Precipitation pattern

©2019. Japan Geoscience Union. All Right Reserved.

Seasonal and Regional Variation of Diurnal Cycle of Rainfall over Java Island and the Surrounding Area

*Madam Taqiyya Maulana[1], Takeshi Yamazaki[1]

1. Tohoku University

The seasonality and regional variability of diurnal cycle of rainfall (DCR) over Java Island and the surrounding area (coastal region of the Java Sea and the Indian Ocean) are analyzed through satellite observations. This study focus on the area where the studies of the seasonality of DCR over Indonesian Maritime Continent (IMC) are still limited. The DCR is a prominent phenomenon over IMC which is important for aviation industry and related to heavy precipitation events that cause hydro-meteorological disasters.

In this study, **we investigate seasonal and regional variation of DCR (the phase and the amplitude)** through satellite observations. High resolution (spatial and temporal) rainfall estimate is needed to capture feature of DCR over the study area which is difficult to obtain from ground observation. We **mainly employ the high-resolution dataset of Global Satellite Mapping of Precipitation (GSMaP) reanalysis (GSMaP_RNL) and near real time (GSMaP_NRT).** The analysis of DCR seasonal variability is based on investigation throughout boreal winter (December-January-February), boreal spring (March-April-May), boreal summer (June-July-August), and boreal autumn (September-October-November) from 2008-2018 (GSMaP_NRT) and 2009-2014 (GSMaP_RNL).

The results show that hourly data of GSMaP_RNL and GSMaP_NRT with 0.1˚ spatial resolution are able to depict the detailed features of the seasonality and regional variability of DCRover Java Island and surrounding areas. **The comparison between GSMaP_RNL and GSMaP_NRT shows that GSMaP_NRT represents significant time lag of DCR phase over off shore region. GSMaP_NRT shows that the offshore region of the Java Sea is dominated by noon-afternoon rainfall while GSMaP_RNL shows morning rainfall.** However, both of GSMaP_RNL and GSMaP_NRT show similar pattern on phase and amplitude of DCR. Phase of DCR indicates the time when maximum rainfall occurs, while amplitudes indicates the magnitude of DCR. In general, both of GSMaP_RNL and GSMaP_NRT composites, show that the land region with wider landmass area (West Java and western part of East Java) is dominated by evening phase while narrow landmass area (Central Java and eastern part of Java Island) is dominated by late afternoon phase. A large magnitude of the DCR is concentrated inland. The Java Sea has a higher amplitude of DCR compared to the Indian Ocean and the coastal region. The amplitude over the coastal region of the Indian Ocean is higher than over the Indian Ocean and the coastal area of the Java Sea.

Both of rainfall estimates capture inhomogeneous seasonal shifting phase of DCR over this region. The remarkable seasonal shifting phase occurs along the coastal area of the Java Sea. Though, phase shifting over inland of a wide landmass area and the coastal region of the Indian Ocean is not significant. Inhomogeneous seasonal shifting phase of DCR indicated interactions between local circulations, which affected by the topography (e.g. terrain and shape of the coastline), and large circulations (background wind, synoptic conditions, etc.). The analysis of wind profile from reanalysis data confirms the seasonal change of interactions between large and small circulations that caused seasonal shifting phase of DCR.

Keywords: Diurnal cycle of rainfall (DCR), Seasonal variability, Regional variability, Shifting Phase, GSMaP

©2019. Japan Geoscience Union. All Right Reserved.

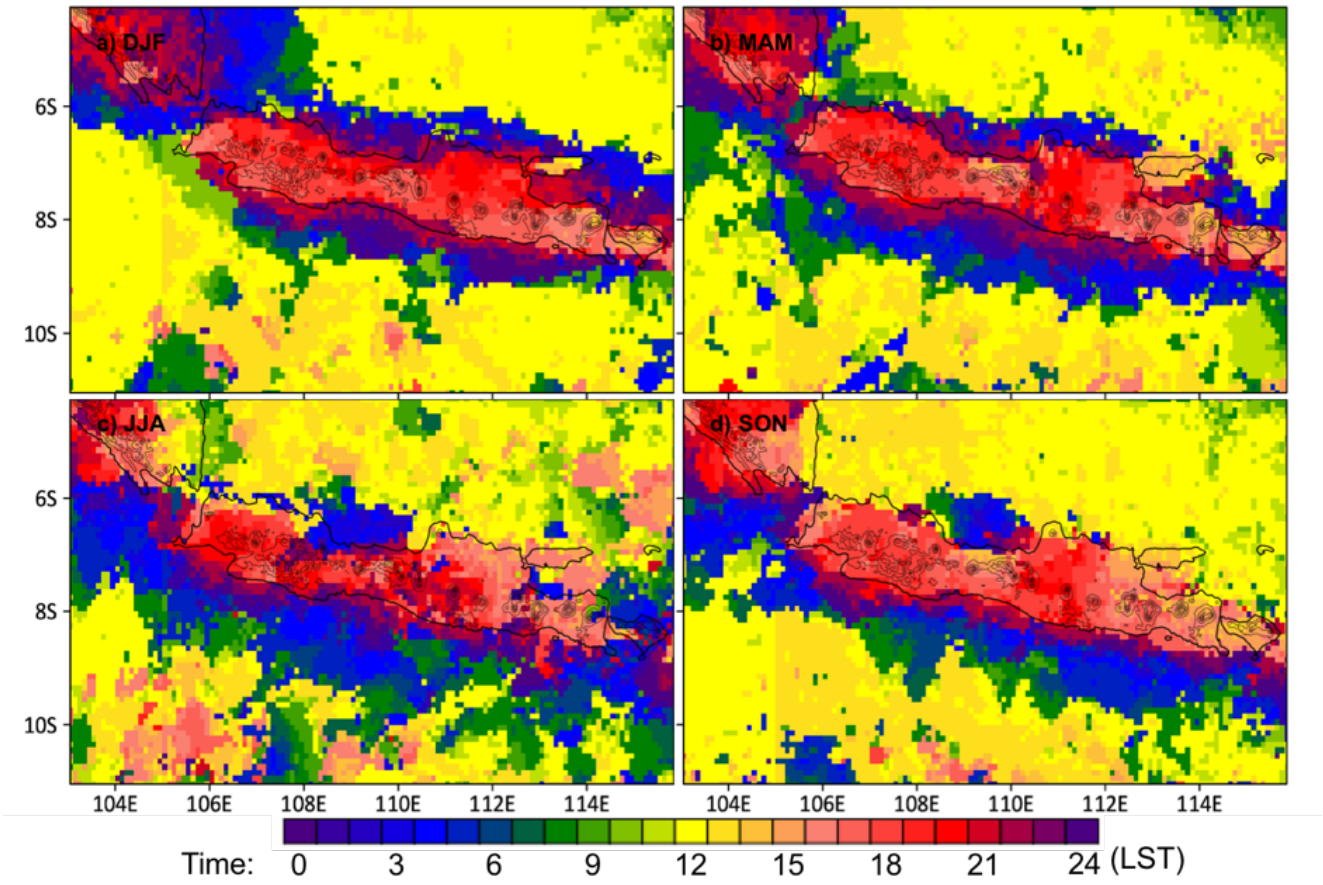

©2019. Japan Geoscience Union. All Right Reserved.

Study on atmospheric circulation characteristics of precipitation anomalies in arid region of Central Asia

*Lianmei Yang[1], Xuefeng Guan[1]

1. Institute of Desert Meteorology, China Meteorological Administration,

As climate transition zone between Mediterranean climate region and East Asian monsoon region, arid region of Central Asia (including five Central Asian countries and Xinjiang province of China) which is influenced by high, middle and low latitude circulations has different synoptic-climatic characteristics from that of Europe and East Asia while its climate characteristics also varies greatly within the region. Central Asia has unique and complicated topography and ecosystem patterns like deserts, oasis, glaciers and basins, forming a highly representative meteorological disaster-breeding environment under the influence of multiple-background, multiple-factor and multiple-scale. This area has abundant solar-heat energy, large evaporation and dramatic temperature changes. Besides, its precipitation is scarce and has extremely uneven distribution with high value in the western and middle parts of Tianshan Mountains. Over the last one hundred years, Central Asia has experienced a warm and wet trend. Central Asia low value system together with the high, middle and low latitude circulation systems linked by West Asia westerly jet stream have contributed to the interdecadal and interannual variations of precipitation in Xinjiang. However, due to the insufficient construction of integrated meteorological observation network, the studies concerning regional featured circulation system, regularity and mechanism of disastrous weathers, high resolution regional numerical model, impacts of land-atmosphere interaction on regional weather and climate change prediction are still inadequate. Correspondingly, to carry out those studies has essential scientific significance and strategic value for the sustainable social and economic development in Silk Road Economic Belt.

Keywords: Arid region of Central Asia, synoptic-climatic characteristics, precipitation anomaly, atmospheric circulation, water vapor

©2019. Japan Geoscience Union. All Right Reserved.

Mechanisms for northward propagation of boreal summer intraseasonal oscillation

*Kanta Nakae[1], Masaki Satoh[1], Daisuke Takasuka[1]

1. Atmosphere and Ocean Research Institute, The University of Tokyo

The 20-90-day Intraseasonal Oscillation (ISO) is one of the dominant modes of tropical variability. In boreal summer northward propagation (NP), which occurs on ISO time scales, originates near the equator and extends to India and western North Pacific Ocean. Understanding the NP of the boreal summer ISO (BSISO) is of vital importance to extended-range weather prediction. Hence, several mechanisms of the NP have been examined. However, they are still incompletely understood. The purpose of this study is to investigate the importance of vertical shear and sea surface temperature (SST) for the NP of the BSISO. In order to obtain a basic structure of the BSISO, we have conducted JJA-perpetual experiments using the Non-hydrostatic Icosahedral Atmospheric Model (NICAM) with a 56-km horizontal mesh.
Although the perpetual experiment has strong Indian monsoon over Arabian sea due to the bias of surface temperature on land, it is found that the NP of the BSISO from Indian Ocean (IO) has two abovementioned mechanisms. One warm SST anomaly north of convection destabilize the lower troposphere, while another tilted vertical shear can generate positive barotropic vorticity to the north of convection. In order to assess the effect of the former mechanism, we made an experiment using fix SST (SSTFIX) obtained from CTL experiment. SSTFIX experiment reproduces the NP of the BSISO from IO, although the amplitude became lower. Therefore, it suggests that the NP of the BSISO from IO doesn’t need warm SST anomaly. To Improve the bias related to basic state like vertical shear, we conducted an experiment using nudging method for surface temperature on land (LNDADJ). In LNDADJ experiment the NP of the BSISO from IO isn’t reproduced due to reduction of column water vapor over Bay of Bengal. Thus, tilted vertical shear can just begin the NP. On the other hand, it is suggested that the NP needs SST and column water vapor to maintain its strength.

Keywords: Boreal summer intraseasonal oscillation, Asian monsoon, Northward propagation

©2019. Japan Geoscience Union. All Right Reserved.

Fractality in the perimeter of tropical clouds observed by Himawari-8 or simulated by a high-resolution model

*Takuya Jinno[1]

1. Graduate School of Science, The University of Tokyo

Cloud clusters show a wide variety of shape and size, and their spatial pattern is often taken up as a typical example of fractal. However, the methods of studying fractal are in an early stage of development. In this study, we conducted fractal analysis on the perimeter of tropical clouds using satellite observation and cloud-resolving simulation of sub-kilometer resolution. We evaluated fractal dimension as a function of spatial scale (transient fractal dimension) and quantified the characteristic spatial scale of the pattern from the scale where self-similarity breaks down. From the observational data from HIMAWARI-8, It is shown that the self-similarity of the cloud perimeter persists only in the spatial scale range from 2 km up to 30 km. The limit of the self-similarity is suggested to be the characteristic scale of the pattern formation of tropical clouds. The cloud-resolving simulation data with NICAM also shows finite-size self-similarity. However, the profile of the transient fractal dimension changed with integration time far more rapidly than HIMAWARI-8 observation, and it lost its self-similarity at the end of the 48-hour simulation. This process is suggested to reflect the increase of stratiform cloud in the upper-troposphere as an adjustment to the transition of spatial resolution.

Keywords: fractal, HIMAWARI-8, cloud-resolving model

©2019. Japan Geoscience Union. All Right Reserved.

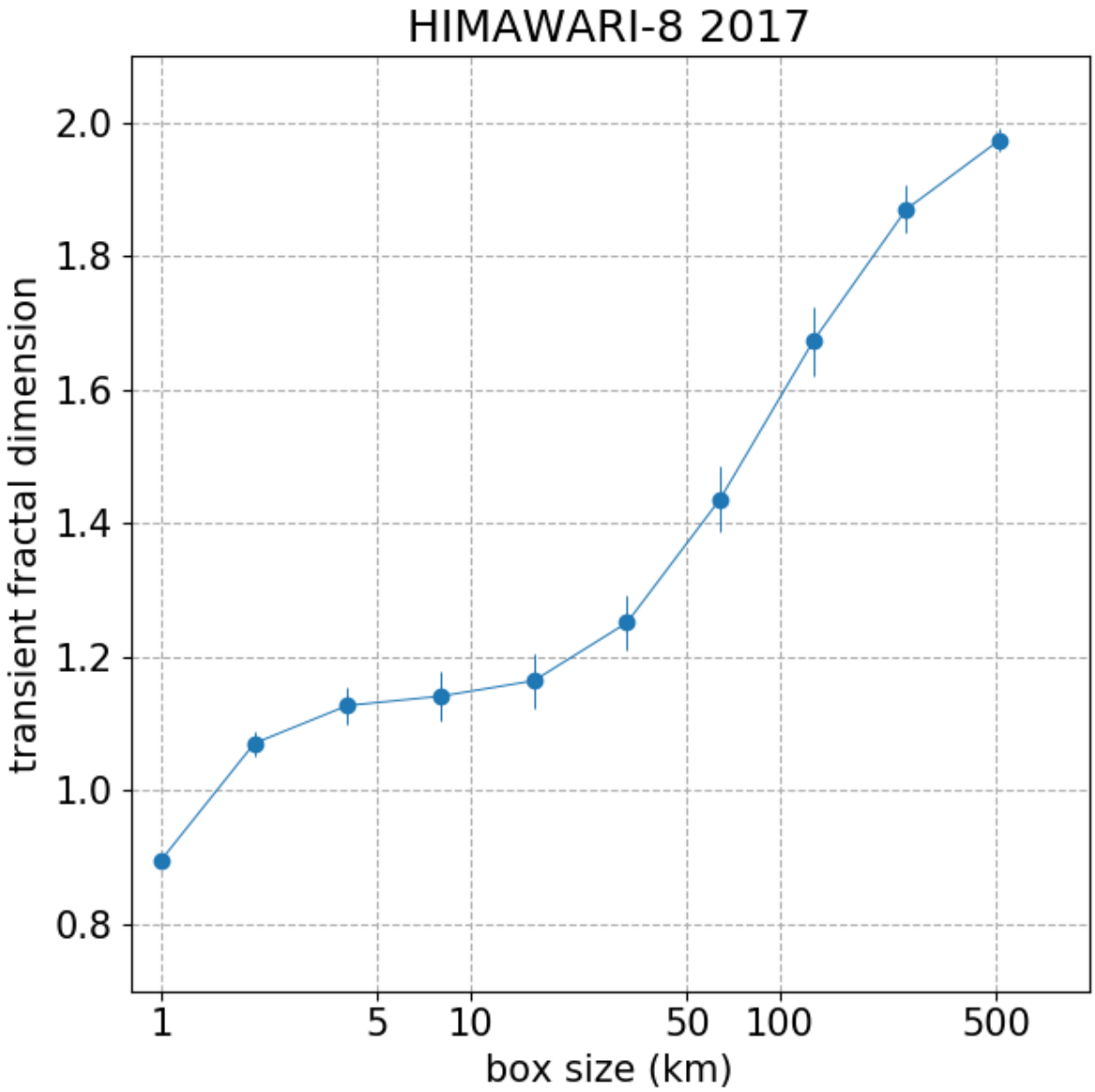

©2019. Japan Geoscience Union. All Right Reserved.

Large-scale deformation of tropical cloud band in the ITCZ detected in NICAM simulations

*Noriyuki Nishi[1], Atsushi Hamada[4], Yohei Yamada[2], Tomoe Nasuno[2], Reona Satoh[5], Masaki Satoh[3]

1. Faculty of Science, Fukuoka Universtiy, 2. JAMSTEC, 3. AORI, University of Tokyo, 4. Graduate School of Science and Engineering for Education, University of Toyama, 5. Graduate School of Science, Fukuoka University

Over the central/eastern tropical Pacific, the Inter Tropical Convergence Zone (ITCZ) is detected in the northern side of the equator. In the ITCZ, we can sometimes observe drastic deformation of the cloud bands elongated zonally with several thousand-kilometer scale. The initial stage of the band, which is composed of deep convective systems, expands meridionally and separates into two or three parallel cirrus bands that keep alive one or two days (Hamada et al., 2013, JMSJ). These separation events cannot be well described in the objective analysis datasets, probably due to lack of the observations over the open ocean; investigation of their mechanism with the analysis data is difficult. In order to study their mechanism, we attempted to use the numerical simulation results of global cloud system resolving model NICAM (Satoh et al. 2014, Progress in Earth and Planetary Science) to find similar events in them. If we can find separation events in the results, we can examine the mechanism with many physical parameters including wind, various kinds of hydrometeors. We have already analyzed several numerical experiment results for different periods, resolution and physical schemes.

We found a similar separation event in an output of the simulation for one year from June 2004 and horizontal resolution 3.5 km. We examined the life cycle of the cirrus bands after separation. One interesting point is on the height of the cirrus clouds in the separated bands. The simulated cirrus clouds in the bands lie in the 13-14 km height level, while the height of the maximum meridional wind that contributes to the meridional movement of the cirrus bands is about 12 km. This difference of the heights means that the cirrus clouds were not just advected by meridional wind but were possibly developed in the course of the separation.

The trigger of zonally simultaneous separation of a long band is another our interest. Inertial instability may be a candidate since vertical exchange of zonal momentum by deep convection would occur in an original band and result in the large meridional shear of the zonal wind in the upper troposphere. We tried to confirm necessary condition for inertial instability by calculating geostrophic vorticity, following the general procedure. However, the position of the bands is too close to the equator (3-7N) to establish geostrophic relationship, and the spatial pattern of the geostrophic vorticity is too noisy to analyze. Therefore, we instead calculate simple absolute vorticity. We found that the absolute vorticity around the separated bands was almost negative. It suggests the possibility of the inertial (or similar kind of) instability.

We are now analyzing another numerical experiment including four kinds of runs using a cloud scheme with different cloud parameter settings. In the real atmosphere, a separation event occurred on 16-17 June 2008 at the just east of the date line. The event can be simulated in all of four runs at 36 hours from the initial time. It suggests that the basic mechanism of the separation is not sensitive to the detail of cloud systems. By analyzing the dynamical fields of these outputs, we are trying to find the key mechanisms to trigger the meridional separation of the cloud bands.

©2019. Japan Geoscience Union. All Right Reserved.

Keywords: tropics, ITCZ, cirrus

©2019. Japan Geoscience Union. All Right Reserved.

Improvement of single-moment bulk microphysics for super-cooled water clouds over the Southern Ocean in NICAM using Joint simulator and double-moment microphysics

*Woosub Roh[1], Tatsuya Seiki[2], Masaki Satoh[1], Tempei Hashino[3]

1. AORI, the university of Tokyo, 2. JAMSTEC, 3. Kochi university of technology

It is important to evaluate and improve the cloud properties in global non-hydrostatic models like a Nonhydrostatic ICosahedral Atmospheric Model (NICAM, Satoh et al. 2014) using observation data. One of the methods is a radiance-based evaluation using satellite data and a satellite simulator (here Joint simulator, Hashino et al. 2013), which avoids making different settings of the microphysics between retrieval algorithms and NICAM.

One of the challenging issues is an evaluation of mixed-phase clouds, which consist of water vapor, ice particles, and supercooled water droplets. It is known one of the main reasons why climate models reveal large errors about the reflection of solar radiation over the Southern Ocean and Arctic.

This study is an evaluation and improvement of mixed-phase clouds over the Southern Ocean in NICAM using a Cloud-Aerosol Lidar and Infrared Pathfinder Satellite Observation (CALIPSO) and a satellite simulator. We evaluated thermodynamics phase of mixed phases clouds over the Southern Ocean in a regional version of NICAM between 45˚S to 65˚S and 170˚E to 170˚W following Yoshida et al. (2010) method. We found underestimation of supercooled water clouds in our single moment scheme. We improved the single moment microphysics scheme using a double moment microphysics and a single column model. We also investigate the impact of microphysics scheme on moisture distributions and the size of cloud systems.

Keywords: microphysics, CALIPSO, Satellite simulator

©2019. Japan Geoscience Union. All Right Reserved.

High-cloud property responses to SST change: sensitivity study using a global nonhydrostatic model

*Tomoki Ohno[1], Masaki Satoh[2]

1. Japan Agency for Marine-Earth Science and Technology, 2. Atmosphere and Ocean Research Institute, The University of Tokyo

Since it has been recognized that the uncertainty of cloud feedback is one of main contributors to the intermodel spread of climate sensitivity, the reduction of the uncertainties associated with cloud response to global warming has been one of central issues for robust projections and predictions of climate variability and change. High clouds have large impacts on the Earth’ s radiative energy budget, and the uncertainty of their response to climate change is known as one of large sources of the climate sensitivity spread although several possible hypotheses to predict the response have been proposed. As the radiation-cloud interaction plays a crucial role in the determination of life time of high clouds, the improvement of the understanding of cloud property responses to global warming helps the reduction of climate-sensitivity variability associated with the high-clouds feedback.

In order to investigate the cloud-property response to climate change, we conducted simulations with RCE configurations using a high-resolution nonhydrostatic global circulation model (the Nonhydrostatic Icosahedral Atmospheric Model; NICAM) with the earth-like sphere for simplifying the problem. Sea surface temperatures (SSTs) are fixed at 300K and 304K and a double-moment bulk scheme are used without cumulus parameterization scheme.

We found that high cloud amount increases with SST increase, as consistent with the previous NICAM studies. It was also determined that the change in particularly optically thin clouds whose optical thicknesses were <3 was dominant, and such thin clouds tended to have large particle sizes. These suggests that the slow evaporative property of ice phase clouds and their representability can play one of key roles in the uncertainty of the high-cloud amount change in global warming.

Keywords: cloud property responses, cloud feedback, climate change

©2019. Japan Geoscience Union. All Right Reserved.

Effects of different cloud overlapping parameters on simulated total cloud fraction over the globe and East Asian region

*bo hai Wang[1], hua Zhang[2]

1. Institute of Atmospheric Physics, Chinese Academy of Sciences, 2. State Key Laboratory of Severe Weather, Chinese Academy of Meteorological Sciences

The cloud overlapping parameter (vertical decorrelation length, L_{cf}) from CloudSat/CALIPSO is implemented in Beijing Climate Center’ s GCM (BCC_AGCM2.0) to reduce the uncertainly in radiation field. Comparing the climate simulation results obtained by using the constant L_{cf} of 2 km with those using the above retrieved L_{cf}, it is found that the total cloud fraction simulation has been obviously improved by using the satellite-based L_{cf}. The error of global mean total cloud fraction between simulations and CERES (Clouds and the Earth's Radiant Energy System) satellite data is decreased by 1.6% in both the winter and summer, of which the positive deviation of total cloud amount at tropical convection area and the negative deviation in subtropical region both are significantly reduced. These improvements are helpful for better simulation of energy budget differences between different regions. In East Asia, using the satellite-based L_{cf} can decrease the error of average total cloud fraction (compared to the CERES) by 1.8% (1.4%) in the winter (summer).Overall, using L_{cf} from CloudSat/CALIPSO satellite data can improve the simulation of total cloud fraction and thus obtain more accurate simulation of radiation field.

Keywords: Cloud overlapping parameter, Vertical decorrelation length, Total cloud fraction

©2019. Japan Geoscience Union. All Right Reserved.

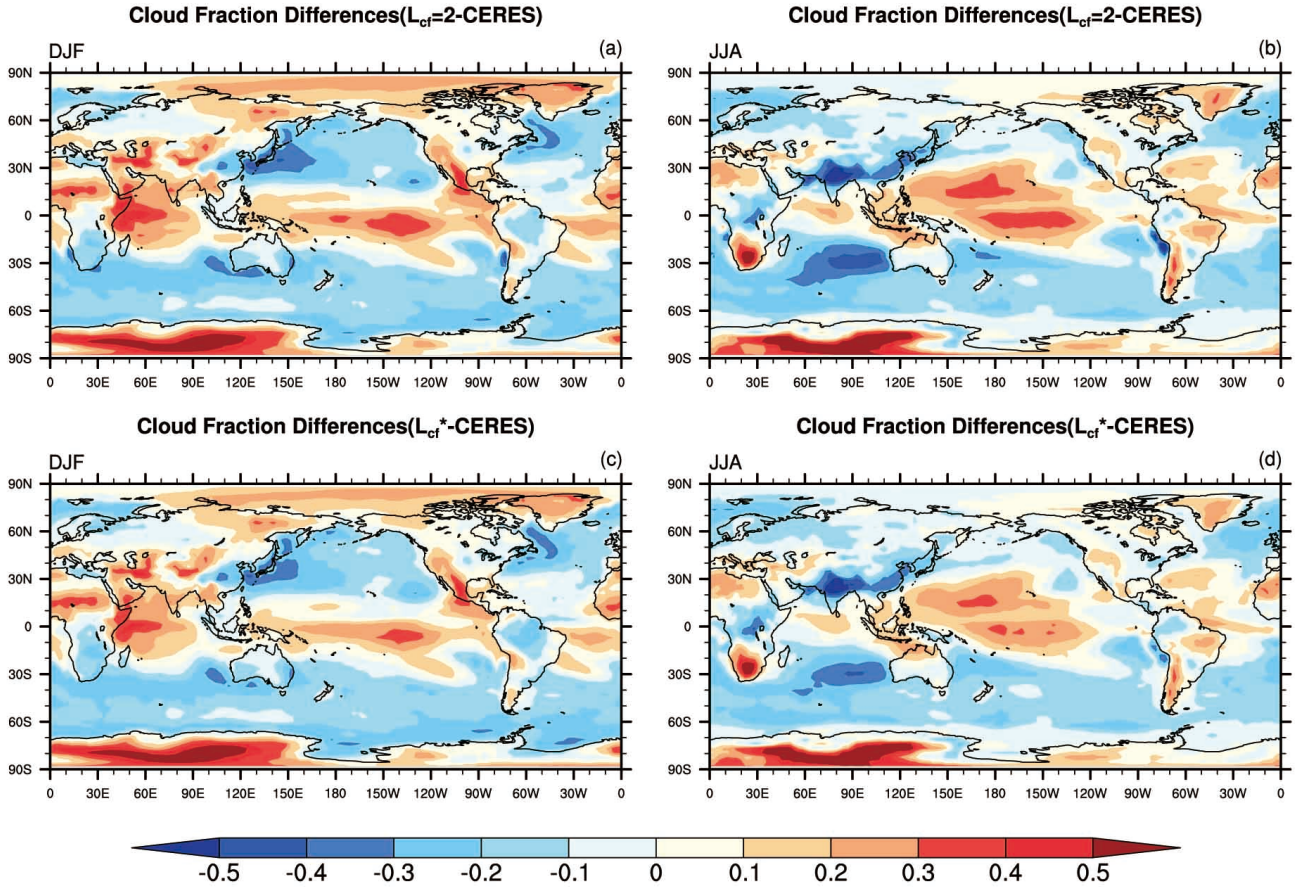

©2019. Japan Geoscience Union. All Right Reserved.

[E] Poster | A (Atmospheric and Hydrospheric Sciences)：A-CG Complex & General

Tue. May 28, 2019 10:45 AM - 12:15 PM JST | Tue. May 28, 2019 1:45 AM - 3:15 AM UTC | Poster Hall International Exhibition Hall8, Makuhari Messe_3

[A-CG32] Global Carbon Cycle Observation and Analysis

convener:Kazuhito Ichii(Chiba University), Prabir Patra(Research Institute for Global Change, JAMSTEC), Forrest M. Hoffman(Oak Ridge National Laboratory), Makoto Saito(National Institute of Environmental Studies)

The landmark Paris Agreement under the United Nations Framework Convention on Climate Change (UNFCCC) aims at reduction of greenhouse gases (GHGs) emission to keep the global warming below 2 degC. As per the agreement the nationally determined commitments (NDCs) and their progresses should be carefully monitored and verified by international bodies. The emission verification will be based on observation of the time evolution of greenhouse gases and model-based estimations of emissions from time to time.

In recent years, the number of observations and new techniques to monitor GHGs budget have been increasing. The improvements includes observational platforms for monitoring atmospheric GHGs, national or regional emission inventories, top-down models (e.g. atmospheric inverse models), and bottom-up models (e.g. process-based models). However, due to uncertainties in modeling and sparse observation network, high uncertainty exists in GHGs sources/sinks estimations at global and regional scales. These uncertainties lead to large variations in future projection of GHG budgets and climate changes.

The purpose of the session is to discuss state-of-the-art techniques for estimations of GHGs (e.g. CO2, CH4, N2O) budget at global and regional scales. The topic includes natural and anthropogenic processes, various methodologies (e.g. in-situ observation, aircraft monitoring, remote sensing, modeling), and various targets (e.g. atmosphere, terrestrial, and ocean), various spatial and temporal coverage (e.g. regional to global scales and past-present-future). Improved estimates of emissions from land use change, forest fires, and other anthropogenic sources (urban developments and thermal power station etc.) are also of interest. We also welcome discussions for designs and plans for future studies targeting city and country scale emission estimations using sophisticated modeling tools.

[ACG32-P01] Regional budgets of 3 major greenhouse gases using inverse modelling of atmospheric data

*Prabir Patra[1], Naveen Chandra[1], Jagat Bisht[1] (1.Japan Agency for Marine-Earth Science and Technology (JAMSTEC))

[ACG32-P02] Analysis of hot summer in 2018

*Kazutaka Murakami[1], Kazuhito Ichii[1,2], Yukio Yoshida[1], Haruki Oshio[1], Makoto Saito[1] (1.National Institute for Environmental Studies, 2.Chiba University)

[ACG32-P03] Updated Data-Driven GPP and NEE Estimation Using Machine Learning Algorithms with Remote Sensing and Flux Data

*Zhiyan Liu[1], Kazuhito Ichii[1], Yusuke Hayasi[1], Riku Kawase[1], Masahito Ueyama[2], Yuji Kominami[3] (1.Chiba University, 2.Osaka Prefecture University, 3.Forest Research and Management Organization)

[ACG32-P04] Response of a Bornean Rainforest to the Climatic Changes imposed by ENSO during 2009-2016

*Julie Karine Michelon[1], Tomo'omi Kumagai[2,3], Tetsuya Hiyama[3], Hatsuki Fujinami[3], Kazuho Matsumoto[4], Tomonori Kume[5], Takami Saito[6] (1.Graduate School of Environmental Studies, Nagoya University, 2.Graduate School of Agricultural and Life Sciences, The University of Tokyo, 3.Institute for Space-Earth Environmental Research, Nagoya University, 4.Faculty of Agriculture, University of the Ryukyus, 5.Faculty of Agriculture, Kyushu University, 6.Forest Research and Management Organization)

[ACG32-P05] Monitoring and Evaluating CO2 Flux in the Grassland Areas of Mongolia

*Qinxue Wang[1], Tomohiro Okadera[1], Deni Eer[1], Masataka Watanabe[2], Tomohiro Shishime[2], Akihiro Oba[2], Ochirbat Batkhishig[3] (1.National Institute for Environmental Studies, 2.Research and Development Initiative, Chuo University, 3.Institute of Geography and Geoecology, Mongolian Academy of Sciences)

[ACG32-P06] Data-driven monitoring of terrestrial carbon cycle in Mongolia

*ZAYA MART[1], Zhiyan Liu[1], Riku Kawase[1], Kazuhito Ichii[1] (1.Chiba University)

Regional budgets of 3 major greenhouse gases using inverse modelling of atmospheric data

*Prabir Patra[1], Naveen Chandra[1], Jagat Bisht[1]

1. Japan Agency for Marine-Earth Science and Technology (JAMSTEC)

Atmospheric observations of greenhouse gases provide accurate record the changes in their abundance in the Earth's environments, and it has now been well established that the increase in greenhouse gases concentrations is causing the rise in the mean surface air temperature. Using atmospheric chemistry-transport models (ACTM), along with the concentration measurements, we can estimate the sources and sinks of the chemical species. Using MIROC4-ACTM at JAMSTEC, we estimated regional sources and sinks of carbon dioxide (CO2), methane (CH4) and nitrous oxide (N2O) over the period of 1996 to 2016. This will help global stocktake every 5 years, as a independent estimate, when the coutries report their progress on nationally determined contributions (NDCs) under the Paris Agreement and their ammendments, overseen by the UNFCCC.

Keywords: Inverse modelling, Greenhouse gases sources and sinks, Paris Agreement and NDCs

©2019. Japan Geoscience Union. All Right Reserved.

Analysis of hot summer in 2018

*Kazutaka Murakami[1], Kazuhito Ichii[1,2], Yukio Yoshida[1], Haruki Oshio[1], Makoto Saito[1]

1. National Institute for Environmental Studies, 2. Chiba University

Global averaged temperature in 2018 was considerably higher than normal year. Probably it is the fourth highest in the past. Especially, it was memorable that East Asia, Europe, and the southwestern part of the United States were hit by record heat waves in this summer. It is important for the ecological resilience to investigate how much such extreme weather damages the terrestrial ecosystem and how will it change after that. In this study, we analyzed the effect of this extremely high temperature on terrestrial vegetation using satellite remote sensing data. First, we investigated the high temperature area using MODIS land surface temperature (LST) product. Then, focusing on these high LST areas, we analyzed the impact to satellite observed Solar Induced Fluorescence (SIF) that closely related to a photosynthetic activity. As a result, it was found that the LST of 2018 in the East Asia (Japan, Korea and North Korea) was the highest during 2002 - 2018 years. And it also indicated abnormal high LST regions from Germany to northern Europe. Analysis of SIF data showed a positive decline in Europe but did not show a clear trend in Asia. In addition, similar trends were seen from other satellite vegetation indices, and it was found that the terrestrial vegetation shows different responses in both areas affected by the same hot summer.

Keywords: 2018 summer, heat wave, satellite observation, SIF

©2019. Japan Geoscience Union. All Right Reserved.

Updated Data-Driven GPP and NEE Estimation Using Machine Learning Algorithms with Remote Sensing and Flux Data

*Zhiyan Liu[1], Kazuhito Ichii[1], Yusuke Hayasi[1], Riku Kawase[1], Masahito Ueyama[2], Yuji Kominami[3]

1. Chiba University, 2. Osaka Prefecture University, 3. Forest Research and Management Organization

Abstract

Data-driven approach is effective for understanding and up-scaling observation network data of terrestrial carbon fluxes. Recently, the expansion of observation network, the improvement of remote sensing products and more application of machine learning on natural science make it more possible. In this study, we estimated two important parameters of terrestrial ecosystem, terrestrial gross primary productivity (GPP) and net ecosystem exchange (NEE) through re-assessment of previous approaches [Ichii et al. 2017; Kondo et al. 2015]. We tested multiple combinations of input parameters with lagged effect, additional new input parameters and the updated MODIS datasets (Collection C6). Besides, we selected 3 typical machine learning methods (Random Forest, RF; Support Vector Regression, SVR; Artificial Neural Network, ANN) as data-driven method and compare the estimation from 3 different types of machine learning model. The site-level analysis shows that use of the new version data and the time-lagged improved the model performance. Finally, we compared our new estimation of GPP and NEE with several terrestrial models output and other available datasets and we found our new results show better consistency with them. This shows our estimation provides a good benchmark for understanding spatio-temporal variability in terrestrial GPP and NEE.

Acknowledgement

This research was financially supported by the Environment Research and Technology Development Fund (2-1701) of the Environmental Restoration and Conservation Agency of Japan.

Keywords: Terrestrial Carbon Cycle, MODIS Collection6, Data-driven, time-lag effect

©2019. Japan Geoscience Union. All Right Reserved.

Response of a Bornean Rainforest to the Climatic Changes imposed by ENSO during 2009-2016

*Julie Karine Michelon[1], Tomo'omi Kumagai[2,3], Tetsuya Hiyama[3], Hatsuki Fujinami[3], Kazuho Matsumoto[4], Tomonori Kume[5], Takami Saito[6]

1. Graduate School of Environmental Studies, Nagoya University, 2. Graduate School of Agricultural and Life Sciences, The University of Tokyo, 3. Institute for Space-Earth Environmental Research, Nagoya University, 4. Faculty of Agriculture, University of the Ryukyus, 5. Faculty of Agriculture, Kyushu University, 6. Forest Research and Management Organization

Tropical rainforests belong to the most important biomes, as they are one of the largest terrestrial carbon sink and also a consequent source of latent energy. Furthermore, they will be among the first ecosystems to undergo climatic changes in the near future. Understanding how they will response to those changes is essential. El Niño-Southern Oscillation (ENSO) is an opportunity to study ecosystem response under real climatic change conditions.

Transpiration (Tr), net ecosystem exchange (NEE) and heat fluxes were measured with an eddy covariance system in a natural rainforest in Sarawak, Malaysia. Meteorological and soil moisture observations were also conducted. This region does not have phase-locked dry periods, and seasonal variations of both air temperature and solar radiation are small. However, it is directly impacted by ENSO events. During the study period, from November 2009 to December 2016, two events were selected : La Niña 2010-2011 and El Niño 2014-2016. Normal conditions were assumed as a third "neutral" period. Comparisons of measured flux and meteorological drivers between the three periods were carried out, and analysis of environmental controls, as canopy conductance (g_c) were made.

Precipitation and air temperature were significantly different between the three periods. While the water cycle (latent heat flux, Tr, g_c) responded immediately to the changes imposed by La Niña, the enhancement of the ecosystem respiration balanced the gross primary production gain, resulting into a NEE similar to neutral conditions. Conversely, the NEE during El Niño was significantly smaller than during neutral, when the water cycle seemed not impacted. However, further observations of this late rainforest response evolution showed that, during the first part of El Niño, Tr and g_c increased while CO_2 flux reduced. Then, during the second part, the trend reversed : CO_2 flux increased and Tr, as well as g_c, reduced. This may indicate a time lag between the meteorological drivers (precipitation and air temperature) changes imposed by El Niño and the ecosystem response (H_2O and CO_2 fluxes). The response delay may be caused by the rainforest tendency to poorly regulate its water use, being a particular moist environment. As for the response itself, it may be triggered by the depletion of the soil water content.

Those results imply that considering the length of El Niño and the ecosystem response trigger are important to understand and model bornean rainforest fluxes under future climatic scenario.

Keywords: Borneo, Rainforest, ENSO, NEE, Transpiration

©2019. Japan Geoscience Union. All Right Reserved.

Monitoring and Evaluating CO2 Flux in the Grassland Areas of Mongolia

*Qinxue Wang[1], Tomohiro Okadera[1], Deni Eer[1], Masataka Watanabe[2], Tomohiro Shishime[2], Akihiro Oba[2], Ochirbat Batkhishig[3]

1. National Institute for Environmental Studies, 2. Research and Development Initiative, Chuo University, 3. Institute of Geography and Geoecology, Mongolian Academy of Sciences

For verification of data products of the Greenhouse Gas Observing Satellite (GOSAT), in this study, we monitored and evaluated CO2 flux, that is, the absorption and emission of CO2 by ecosystems in the grasslands of Mongolia by the eddy correlation method. Two flux towers were established in 2015 at the Nalaikh site near Ulaanbaatar City and the Hustai site with less influence of cities, respectively. The CO2 analyzers installed on the towers were calibrated every year by using the standard gas imported from Japan. Up to now, about 4-year monitoring data have been accumulated since 2015. The data analysis shows that the CO2 absorption was larger than emissions at both sites, which indicated that the ecosystem at both sites are carbon sinks. The annual mean value of the CO2 absorption at the Nalaikh site was about 2.66 μmol m^{-2} s^{-1} and the emission was about 1.53 μmol m^{-2} s^{-1}, but the absorption at the Hustai site was about 2.11 μmol m^{-2} s^{-1}, and the emission was about 1.37 μmol m^{-2} s^{-1} (Figure 1). Generally, the net CO2 absorption at the Nalaikh site (0.76 μmol m^{-2} s^{-1}) was found to be larger than that at the Hustai site (0.36 μmol m^{-2} s^{-1}).

To compare the GOSAT L4B data with the ground observation at both sites, we extracted the monthly mean value of CO2 absorption/emission from the grid data of GOSAT during 2009-2015 and compared with the observed data. We found that although the seasonal changing pattern and fluctuation range are similar, the CO2 emission derived by GOSAT were larger than absorption, which suggested that the steppe ecosystems at both sites are the carbon sources. However, the ground observations showed that the CO2 absorption at both sites was larger than emission, which suggested that the grassland ecosystems at both sites are carbon sinks (Figure 2). It is essential for us to find the reasons of this difference in the future.

Finally, to evaluate the spatiotemporal distribution of carbon absorption and emission in the whole country, we have developed a carbon budget model considering the influence of grazing density. The primary simulation results showed that the percentage of carbon loss by grazing (CLG) accounted for 19-38% of the net ecosystem production (NEP) in the Nalaikh area around the city of Ulaanbaatar, where the grazing density was 1.5-2.3 sheep/ha during 2012-2016. On the other hand, CLG accounted for only 7-20% of NEP in the Hustai area away from the city, where the grazing density was only 0.4-0.6 sheep/ha (Figure 3). The result implied that the carbon budget was greatly influenced by animal husbandry near cities, where the grazing density is large. The monitoring cameras installed at both sites show that the biomass inside and outside the fence was greatly influenced by the ingestion of livestock.

This study was funded by “the Project to implement MRV and related technological improvements contributing to the Joint Crediting Mechanism (JCM) in Mongolia”, Ministry of the Environment, Japan.

Keywords: Carbon flux, Grassland ecosystem, The Greenhouse Gases Observing Satellite (GOSAT)

©2019. Japan Geoscience Union. All Right Reserved.

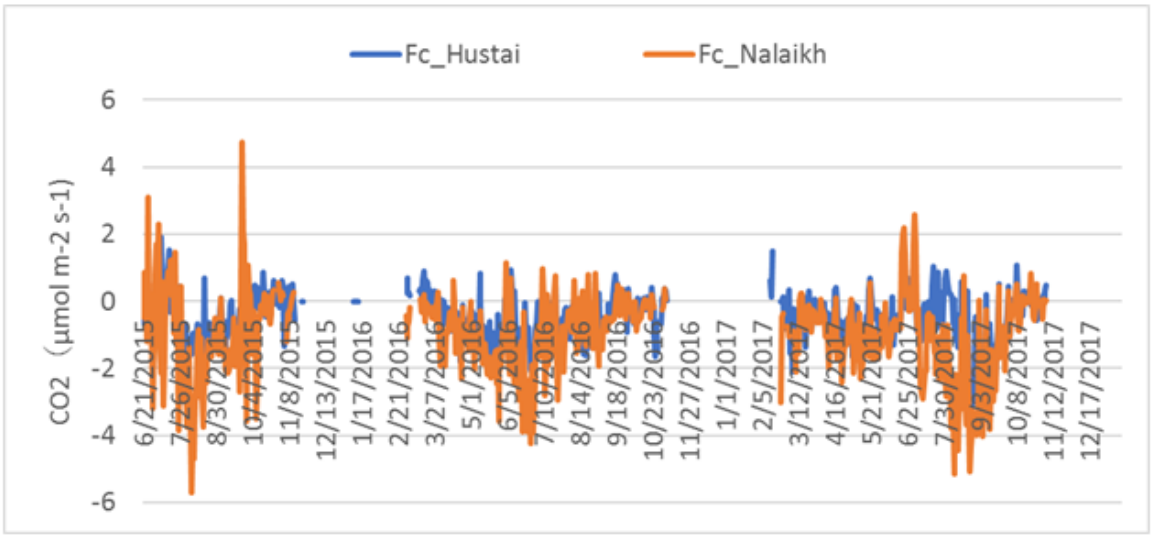

Figure 1 Comparison of CO2 flux observed at Nalaikh Site and Hustai Site

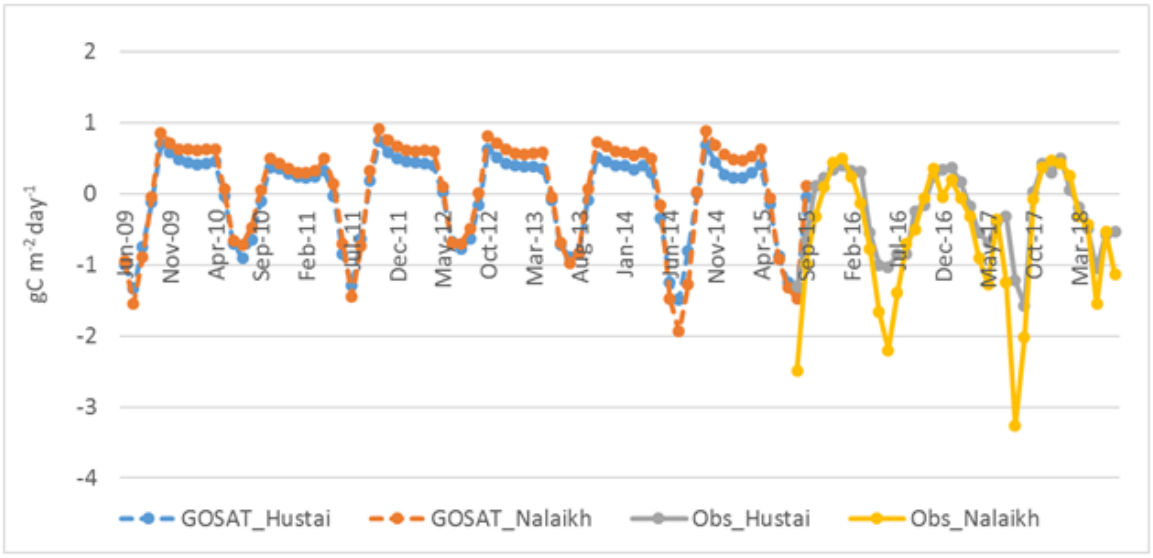

Figure 2 Comparison of GOSAT L4B and observations at Nalaikh Site and Hustai Site

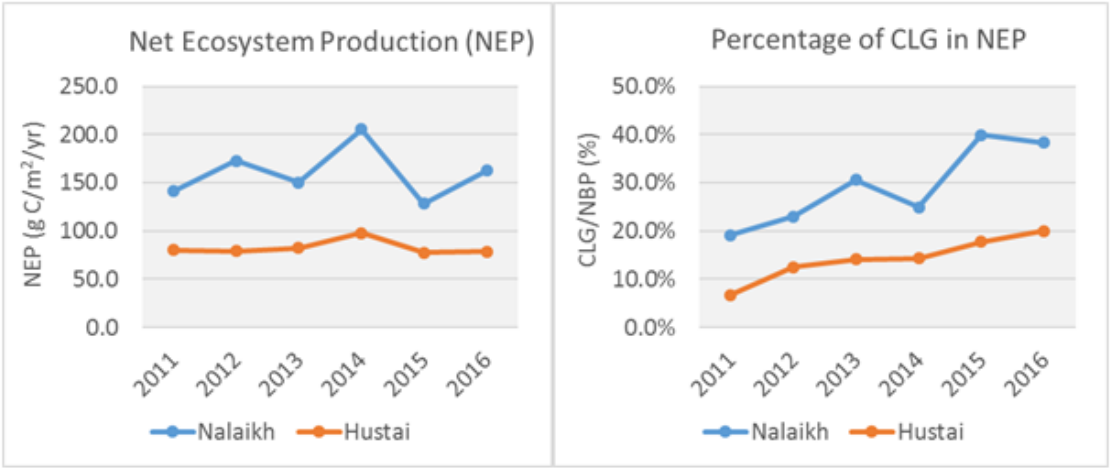

Figure 3 Impact of livestock grazing on NEP at Nalaikh Site and Hustai Site

©2019. Japan Geoscience Union. All Right Reserved.

Data-driven monitoring of terrestrial carbon cycle in Mongolia

*ZAYA MART[1], Zhiyan Liu[1], Riku Kawase[1], Kazuhito Ichii[1]

1. Chiba University

Mongolia has been experiencing both climate changes and anthropogenic environmental changes. Therefore, it is important to monitor environmental changes. In particular, more and more observation-based data sets are available, and synthesis analysis using these multiple observation-based data sets are essential.

We analyzed changes in the terrestrial environmental environment in Mongolia from the 1980s to 2010s. We focused on two different temporal periods, the 1980s to 2010s and 2000 to 2015. As for the first period (1980s to 2010s), we used NOAA AVHRR data sets, observed climate data sets for the analysis. As for the second period (1980s to 2010s), we used multiple remote sensing data sets (e.g. Terra MODIS), empirically upscaled CO2 flux products, and outputs from terrestrial ecosystem models. We will show and discuss the estimated terrestrial environmental changes in Mongolia at the conference.

Keywords: climate change, terrestrial environments, carbon cycle

©2019. Japan Geoscience Union. All Right Reserved.

[E] Poster | A (Atmospheric and Hydrospheric Sciences)：A-CG Complex & General

Tue. May 28, 2019 5:15 PM - 6:30 PM JST | Tue. May 28, 2019 8:15 AM - 9:30 AM UTC | Poster Hall International Exhibition Hall8, Makuhari Messe_13

[A-CG32] Global Carbon Cycle Observation and Analysis

convener:Kazuhito Ichii(Chiba University), Prabir Patra(Research Institute for Global Change, JAMSTEC), Forrest M. Hoffman(Oak Ridge National Laboratory), Makoto Saito(National Institute of Environmental Studies)

The landmark Paris Agreement under the United Nations Framework Convention on Climate Change (UNFCCC) aims at reduction of greenhouse gases (GHGs) emission to keep the global warming below 2 degC. As per the agreement the nationally determined commitments (NDCs) and their progresses should be carefully monitored and verified by international bodies. The emission verification will be based on observation of the time evolution of greenhouse gases and model-based estimations of emissions from time to time.

In recent years, the number of observations and new techniques to monitor GHGs budget have been increasing. The improvements includes observational platforms for monitoring atmospheric GHGs, national or regional emission inventories, top-down models (e.g. atmospheric inverse models), and bottom-up models (e.g. process-based models). However, due to uncertainties in modeling and sparse observation network, high uncertainty exists in GHGs sources/sinks estimations at global and regional scales. These uncertainties lead to large variations in future projection of GHG budgets and climate changes.

The purpose of the session is to discuss state-of-the-art techniques for estimations of GHGs (e.g. CO2, CH4, N2O) budget at global and regional scales. The topic includes natural and anthropogenic processes, various methodologies (e.g. in-situ observation, aircraft monitoring, remote sensing, modeling), and various targets (e.g. atmosphere, terrestrial, and ocean), various spatial and temporal coverage (e.g. regional to global scales and past-present-future). Improved estimates of emissions from land use change, forest fires, and other anthropogenic sources (urban developments and thermal power station etc.) are also of interest. We also welcome discussions for designs and plans for future studies targeting city and country scale emission estimations using sophisticated modeling tools.

[ACG32-P01] Regional budgets of 3 major greenhouse gases using inverse modelling of atmospheric data

*Prabir Patra[1], Naveen Chandra[1], Jagat Bisht[1] (1.Japan Agency for Marine-Earth Science and Technology (JAMSTEC))

[ACG32-P02] Analysis of hot summer in 2018

*Kazutaka Murakami[1], Kazuhito Ichii[1,2], Yukio Yoshida[1], Haruki Oshio[1], Makoto Saito[1] (1.National Institute for Environmental Studies, 2.Chiba University)

[ACG32-P03] Updated Data-Driven GPP and NEE Estimation Using Machine Learning Algorithms with Remote Sensing and Flux Data

*Zhiyan Liu[1], Kazuhito Ichii[1], Yusuke Hayasi[1], Riku Kawase[1], Masahito Ueyama[2], Yuji Kominami[3] (1.Chiba University, 2.Osaka Prefecture University, 3.Forest Research and Management Organization)

[ACG32-P04] Response of a Bornean Rainforest to the Climatic Changes imposed by ENSO during 2009-2016

*Julie Karine Michelon[1], Tomo'omi Kumagai[2,3], Tetsuya Hiyama[3], Hatsuki Fujinami[3], Kazuho Matsumoto[4], Tomonori Kume[5], Takami Saito[6] (1.Graduate School of Environmental Studies, Nagoya University, 2.Graduate School of Agricultural and Life Sciences, The University of Tokyo, 3.Institute for Space-Earth Environmental Research, Nagoya University, 4.Faculty of Agriculture, University of the Ryukyus, 5.Faculty of Agriculture, Kyushu University, 6.Forest Research and Management Organization)

[ACG32-P05] Monitoring and Evaluating CO2 Flux in the Grassland Areas of Mongolia

*Qinxue Wang[1], Tomohiro Okadera[1], Deni Eer[1], Masataka Watanabe[2], Tomohiro Shishime[2], Akihiro Oba[2], Ochirbat Batkhishig[3] (1.National Institute for Environmental Studies, 2.Research and Development Initiative, Chuo University, 3.Institute of Geography and Geoecology, Mongolian Academy of Sciences)

[ACG32-P06] Data-driven monitoring of terrestrial carbon cycle in Mongolia

*ZAYA MART[1], Zhiyan Liu[1], Riku Kawase[1], Kazuhito Ichii[1] (1.Chiba University)

Regional budgets of 3 major greenhouse gases using inverse modelling of atmospheric data

*Prabir Patra[1], Naveen Chandra[1], Jagat Bisht[1]

1. Japan Agency for Marine-Earth Science and Technology (JAMSTEC)

Atmospheric observations of greenhouse gases provide accurate record the changes in their abundance in the Earth's environments, and it has now been well established that the increase in greenhouse gases concentrations is causing the rise in the mean surface air temperature. Using atmospheric chemistry-transport models (ACTM), along with the concentration measurements, we can estimate the sources and sinks of the chemical species. Using MIROC4-ACTM at JAMSTEC, we estimated regional sources and sinks of carbon dioxide (CO2), methane (CH4) and nitrous oxide (N2O) over the period of 1996 to 2016. This will help global stocktake every 5 years, as a independent estimate, when the coutries report their progress on nationally determined contributions (NDCs) under the Paris Agreement and their ammendments, overseen by the UNFCCC.

Keywords: Inverse modelling, Greenhouse gases sources and sinks, Paris Agreement and NDCs

©2019. Japan Geoscience Union. All Right Reserved.

Analysis of hot summer in 2018

*Kazutaka Murakami[1], Kazuhito Ichii[1,2], Yukio Yoshida[1], Haruki Oshio[1], Makoto Saito[1]

1. National Institute for Environmental Studies, 2. Chiba University

Global averaged temperature in 2018 was considerably higher than normal year. Probably it is the fourth highest in the past. Especially, it was memorable that East Asia, Europe, and the southwestern part of the United States were hit by record heat waves in this summer. It is important for the ecological resilience to investigate how much such extreme weather damages the terrestrial ecosystem and how will it change after that. In this study, we analyzed the effect of this extremely high temperature on terrestrial vegetation using satellite remote sensing data. First, we investigated the high temperature area using MODIS land surface temperature (LST) product. Then, focusing on these high LST areas, we analyzed the impact to satellite observed Solar Induced Fluorescence (SIF) that closely related to a photosynthetic activity. As a result, it was found that the LST of 2018 in the East Asia (Japan, Korea and North Korea) was the highest during 2002 - 2018 years. And it also indicated abnormal high LST regions from Germany to northern Europe. Analysis of SIF data showed a positive decline in Europe but did not show a clear trend in Asia. In addition, similar trends were seen from other satellite vegetation indices, and it was found that the terrestrial vegetation shows different responses in both areas affected by the same hot summer.

Keywords: 2018 summer, heat wave, satellite observation, SIF

©2019. Japan Geoscience Union. All Right Reserved.

Updated Data-Driven GPP and NEE Estimation Using Machine Learning Algorithms with Remote Sensing and Flux Data

*Zhiyan Liu[1], Kazuhito Ichii[1], Yusuke Hayasi[1], Riku Kawase[1], Masahito Ueyama[2], Yuji Kominami[3]

1. Chiba University, 2. Osaka Prefecture University, 3. Forest Research and Management Organization

Abstract

Data-driven approach is effective for understanding and up-scaling observation network data of terrestrial carbon fluxes. Recently, the expansion of observation network, the improvement of remote sensing products and more application of machine learning on natural science make it more possible. In this study, we estimated two important parameters of terrestrial ecosystem, terrestrial gross primary productivity (GPP) and net ecosystem exchange (NEE) through re-assessment of previous approaches [Ichii et al. 2017; Kondo et al. 2015]. We tested multiple combinations of input parameters with lagged effect, additional new input parameters and the updated MODIS datasets (Collection C6). Besides, we selected 3 typical machine learning methods (Random Forest, RF; Support Vector Regression, SVR; Artificial Neural Network, ANN) as data-driven method and compare the estimation from 3 different types of machine learning model. The site-level analysis shows that use of the new version data and the time-lagged improved the model performance. Finally, we compared our new estimation of GPP and NEE with several terrestrial models output and other available datasets and we found our new results show better consistency with them. This shows our estimation provides a good benchmark for understanding spatio-temporal variability in terrestrial GPP and NEE.

Acknowledgement

This research was financially supported by the Environment Research and Technology Development Fund (2-1701) of the Environmental Restoration and Conservation Agency of Japan.

Keywords: Terrestrial Carbon Cycle, MODIS Collection6, Data-driven, time-lag effect

©2019. Japan Geoscience Union. All Right Reserved.

Response of a Bornean Rainforest to the Climatic Changes imposed by ENSO during 2009-2016

*Julie Karine Michelon[1], Tomo'omi Kumagai[2,3], Tetsuya Hiyama[3], Hatsuki Fujinami[3], Kazuho Matsumoto[4], Tomonori Kume[5], Takami Saito[6]

1. Graduate School of Environmental Studies, Nagoya University, 2. Graduate School of Agricultural and Life Sciences, The University of Tokyo, 3. Institute for Space-Earth Environmental Research, Nagoya University, 4. Faculty of Agriculture, University of the Ryukyus, 5. Faculty of Agriculture, Kyushu University, 6. Forest Research and Management Organization

Tropical rainforests belong to the most important biomes, as they are one of the largest terrestrial carbon sink and also a consequent source of latent energy. Furthermore, they will be among the first ecosystems to undergo climatic changes in the near future. Understanding how they will response to those changes is essential. El Niño-Southern Oscillation (ENSO) is an opportunity to study ecosystem response under real climatic change conditions.

Transpiration (Tr), net ecosystem exchange (NEE) and heat fluxes were measured with an eddy covariance system in a natural rainforest in Sarawak, Malaysia. Meteorological and soil moisture observations were also conducted. This region does not have phase-locked dry periods, and seasonal variations of both air temperature and solar radiation are small. However, it is directly impacted by ENSO events. During the study period, from November 2009 to December 2016, two events were selected : La Niña 2010-2011 and El Niño 2014-2016. Normal conditions were assumed as a third "neutral" period. Comparisons of measured flux and meteorological drivers between the three periods were carried out, and analysis of environmental controls, as canopy conductance (g_c) were made.

Precipitation and air temperature were significantly different between the three periods. While the water cycle (latent heat flux, Tr, g_c) responded immediately to the changes imposed by La Niña, the enhancement of the ecosystem respiration balanced the gross primary production gain, resulting into a NEE similar to neutral conditions. Conversely, the NEE during El Niño was significantly smaller than during neutral, when the water cycle seemed not impacted. However, further observations of this late rainforest response evolution showed that, during the first part of El Niño, Tr and g_c increased while CO_2 flux reduced. Then, during the second part, the trend reversed : CO_2 flux increased and Tr, as well as g_c, reduced. This may indicate a time lag between the meteorological drivers (precipitation and air temperature) changes imposed by El Niño and the ecosystem response (H_2O and CO_2 fluxes). The response delay may be caused by the rainforest tendency to poorly regulate its water use, being a particular moist environment. As for the response itself, it may be triggered by the depletion of the soil water content.

Those results imply that considering the length of El Niño and the ecosystem response trigger are important to understand and model bornean rainforest fluxes under future climatic scenario.

Keywords: Borneo, Rainforest, ENSO, NEE, Transpiration

©2019. Japan Geoscience Union. All Right Reserved.

Monitoring and Evaluating CO2 Flux in the Grassland Areas of Mongolia

*Qinxue Wang[1], Tomohiro Okadera[1], Deni Eer[1], Masataka Watanabe[2], Tomohiro Shishime[2], Akihiro Oba[2], Ochirbat Batkhishig[3]

1. National Institute for Environmental Studies, 2. Research and Development Initiative, Chuo University, 3. Institute of Geography and Geoecology, Mongolian Academy of Sciences

For verification of data products of the Greenhouse Gas Observing Satellite (GOSAT), in this study, we monitored and evaluated CO2 flux, that is, the absorption and emission of CO2 by ecosystems in the grasslands of Mongolia by the eddy correlation method. Two flux towers were established in 2015 at the Nalaikh site near Ulaanbaatar City and the Hustai site with less influence of cities, respectively. The CO2 analyzers installed on the towers were calibrated every year by using the standard gas imported from Japan. Up to now, about 4-year monitoring data have been accumulated since 2015. The data analysis shows that the CO2 absorption was larger than emissions at both sites, which indicated that the ecosystem at both sites are carbon sinks. The annual mean value of the CO2 absorption at the Nalaikh site was about 2.66 μmol m^{-2} s^{-1} and the emission was about 1.53 μmol m^{-2} s^{-1}, but the absorption at the Hustai site was about 2.11 μmol m^{-2} s^{-1}, and the emission was about 1.37 μmol m^{-2} s^{-1} (Figure 1). Generally, the net CO2 absorption at the Nalaikh site (0.76 μmol m^{-2} s^{-1}) was found to be larger than that at the Hustai site (0.36 μmol m^{-2} s^{-1}).

To compare the GOSAT L4B data with the ground observation at both sites, we extracted the monthly mean value of CO2 absorption/emission from the grid data of GOSAT during 2009-2015 and compared with the observed data. We found that although the seasonal changing pattern and fluctuation range are similar, the CO2 emission derived by GOSAT were larger than absorption, which suggested that the steppe ecosystems at both sites are the carbon sources. However, the ground observations showed that the CO2 absorption at both sites was larger than emission, which suggested that the grassland ecosystems at both sites are carbon sinks (Figure 2). It is essential for us to find the reasons of this difference in the future.

Finally, to evaluate the spatiotemporal distribution of carbon absorption and emission in the whole country, we have developed a carbon budget model considering the influence of grazing density. The primary simulation results showed that the percentage of carbon loss by grazing (CLG) accounted for 19-38% of the net ecosystem production (NEP) in the Nalaikh area around the city of Ulaanbaatar, where the grazing density was 1.5-2.3 sheep/ha during 2012-2016. On the other hand, CLG accounted for only 7-20% of NEP in the Hustai area away from the city, where the grazing density was only 0.4-0.6 sheep/ha (Figure 3). The result implied that the carbon budget was greatly influenced by animal husbandry near cities, where the grazing density is large. The monitoring cameras installed at both sites show that the biomass inside and outside the fence was greatly influenced by the ingestion of livestock.

This study was funded by “the Project to implement MRV and related technological improvements contributing to the Joint Crediting Mechanism (JCM) in Mongolia”, Ministry of the Environment, Japan.

Keywords: Carbon flux, Grassland ecosystem, The Greenhouse Gases Observing Satellite (GOSAT)

©2019. Japan Geoscience Union. All Right Reserved.

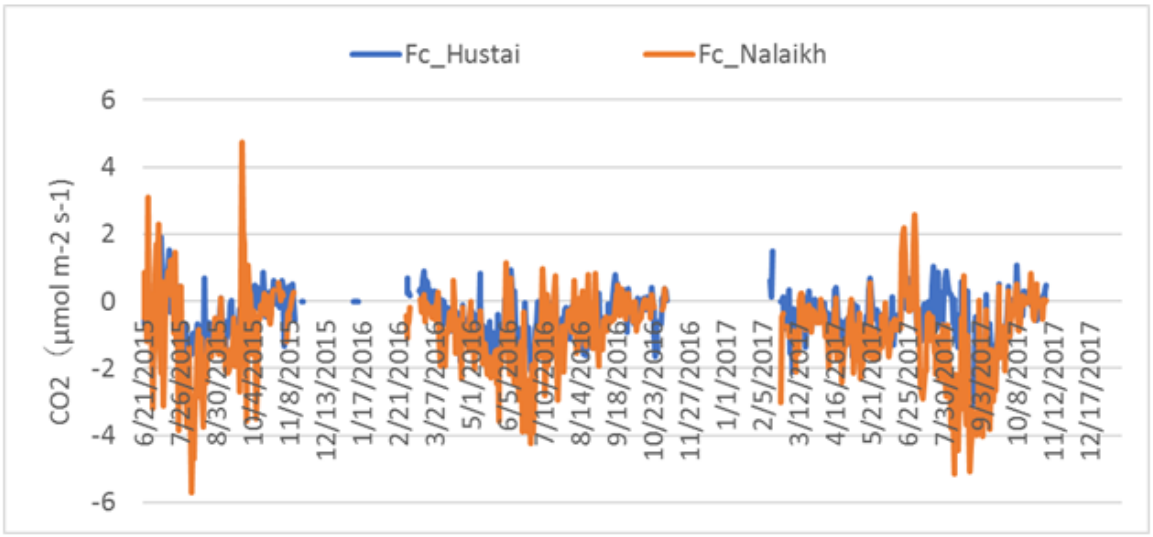

Figure 1 Comparison of CO2 flux observed at Nalaikh Site and Hustai Site

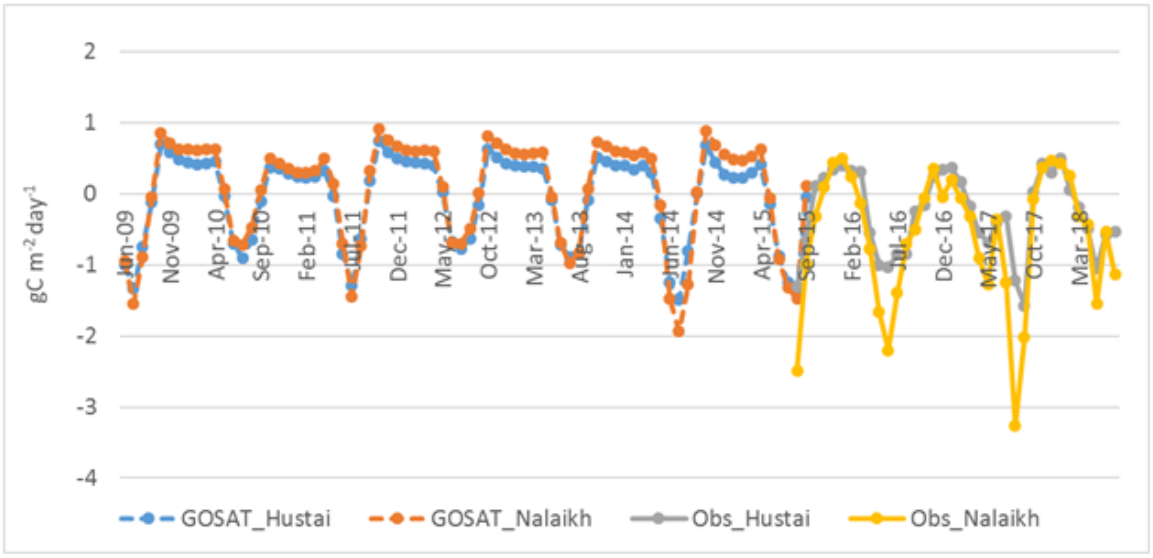

Figure 2 Comparison of GOSAT L4B and observations at Nalaikh Site and Hustai Site

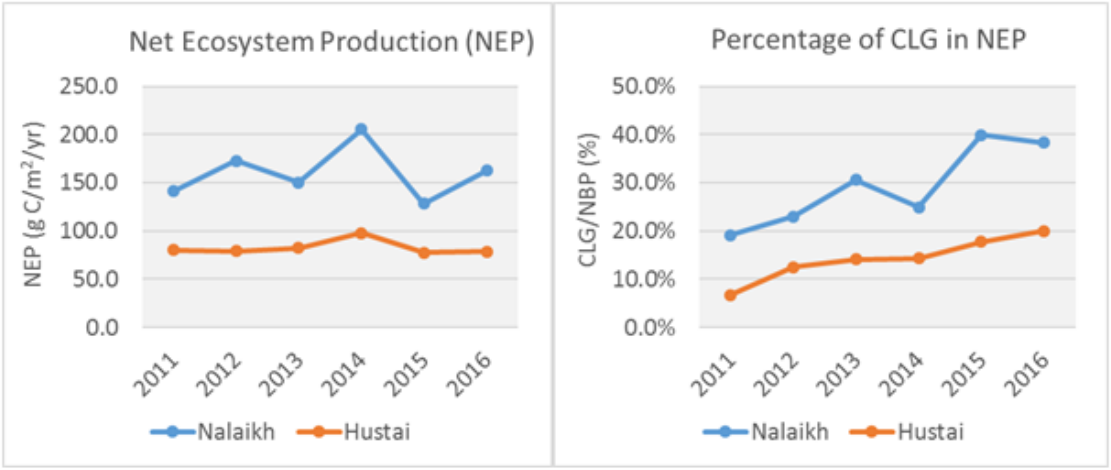

Figure 3 Impact of livestock grazing on NEP at Nalaikh Site and Hustai Site

©2019. Japan Geoscience Union. All Right Reserved.

Data-driven monitoring of terrestrial carbon cycle in Mongolia

*ZAYA MART[1], Zhiyan Liu[1], Riku Kawase[1], Kazuhito Ichii[1]

1. Chiba University

Mongolia has been experiencing both climate changes and anthropogenic environmental changes. Therefore, it is important to monitor environmental changes. In particular, more and more observation-based data sets are available, and synthesis analysis using these multiple observation-based data sets are essential.

We analyzed changes in the terrestrial environmental environment in Mongolia from the 1980s to 2010s. We focused on two different temporal periods, the 1980s to 2010s and 2000 to 2015. As for the first period (1980s to 2010s), we used NOAA AVHRR data sets, observed climate data sets for the analysis. As for the second period (1980s to 2010s), we used multiple remote sensing data sets (e.g. Terra MODIS), empirically upscaled CO2 flux products, and outputs from terrestrial ecosystem models. We will show and discuss the estimated terrestrial environmental changes in Mongolia at the conference.

Keywords: climate change, terrestrial environments, carbon cycle

©2019. Japan Geoscience Union. All Right Reserved.

[E] Poster | H (Human Geosciences)：H-DS Disaster geosciences

Tue. May 28, 2019 3:30 PM - 5:00 PM JST | Tue. May 28, 2019 6:30 AM - 8:00 AM UTC | Poster Hall International Exhibition Hall8, Makuhari Messe_12

[H-DS09] Landslides and related phenomena

convener:Masahiro Chigira(Disaster Prevention Research Institute, Kyoto University), Gonghui Wang(Disaster Prevention Research Institute, Kyoto University), Fumitoshi Imaizumi(Faculty of Agriculture, Shizuoka University)

Mass movements, such as landslides, rockfalls, and debris flows, have been occurring extensively in a large number of countries, causing heavy damage. In order to understand them and mitigate induced disasters, we invite contributions that report and discuss on mass movements and related phenomena, focusing on improved understanding of their characteristics; new insights into landslide mechanisms; the development of new approaches to monitoring; novel approaches to behavior forecasting and prediction; studies of successful landslide management; and the development of methods for hazard and risk evaluation. In particular, papers about recent landslide hazards, induced by 2017 northern Kyushu rainstorm, 2018 Osaka earthquake, 2018 western Japan rainstorm, and 2018 Hokkaido earthquake are welcome.

[HDS09-P01] **Fluidized landslides triggered by the liquefaction of subsurface volcanic deposits during the 2018 Iburi–Tobu earthquake, Hokkaido**

*Jun Kameda[1], Hiro Kamiya[2], Hirokazu Masumoto[1], Tomonori Morisaki[1], Toru Hiratsuka[2], Chisaki Inaoi (1.Department of Natural History Sciences, Graduate School of Science, Hokkaido University, 2.Department of Earth and Planetary Sciences, School of Science, Hokkaido University)

[HDS09-P02] A comparison between the acoustic signals and seismic signals generated during a dam-break test

★Invited Papers

*Zheng-yi Feng[1], Hao-yang Huang[1], Chia-Ming Chuang[1] (1.Department of Soil and Water Conservation, National Chung Hsing University, Taichung, Taiwan)

[HDS09-P03] Evaluation of factors of safety and landslide risk for a watershed by Scoops3D

*Zheng-yi Feng[1], Chia-Ming Chuang[1], Hao-yang Huang[1] (1.Department of Soil and Water Conservation, National Chung Hsing University, Taichung, Taiwan)

[HDS09-P04] **Fuzzy Clustering Algorithms for Establishing Landslide Susceptibility Map**

*Pei-hsun Tsai[1], Syuan-yi Wang[1], Jie-shin Cheng[1] (1.Chaoyang University of Technology)

[HDS09-P05] **A Study on Landslides and Debris Flows Susceptibility Mapping Using Unmanned Aerial Vehicles**

*Sheng-Jia Liu[1] (1.qwepoi13@gmail.com)

[HDS09-P06] Largescale landslide induced by AD1586 Tensho-Earthquake in Gifu Prefecture, central Japan

*Takahiro Kurimoto[1], Yoshihiko Kariya[2], Kuniyasu Mokudai[3], Ryuji Yamada[4], Takashi Kimura[4] (1.Undergraduate Senshu University, 2.Department of Geography, Senshu University, 3.Japan Geoservice Incorporated, 4.National Research Institute for Earth Science and Disaster Resilience)

[HDS09-P07] Failure Probability of Lushan Landslide, Taiwan

*Wei-Ting Lin[1], Kuang-Tsung Chang[1] (1.National Chung Hsing University)

[HDS09-P08] Interpretation of landslide surface deformation in Kali Gandaki River watershed, Nepal using ALOS-2/PALSAR-2 InSAR image

*Hiroshi, P. Sato[1] (1.College of Humanities and Sciences, Nihon University)

[HDS09-P09] A depth-integrated model for granular flows on the transition of different bed conditions

*Ling-Yi Hsu[1], Chi-Yao Hung[1] (1.National Chung Hsing University)

[HDS09-P10] A viscous granular flow experiment with new refractive index matching material

*Tsai-Jung Lin[1], Chi-Yao Hung[1] (1.National Chung Hsing University)

[HDS09-P11] Sandbox experiments of submarine landslide caused by water film in low permeability layer

*Shogo Kawakita[1], Daisuke Asahina[2], Keiji Kitajima[3], Mitsukazu Nakanishi[3] (1.Graduate School of Science & Technology, Nihon Univ., 2.National Institute of Advanced Industrial Science and Technology, 3.College of Science & Technology, Nihon Univ.)

[HDS09-P12] **Study on Creep Properties of Sand and Cemented Sand**

*JIN-YI YU[1], KUANG-TSUNG CHANG[1] (1.National Chung Hsing University)

[HDS09-P13] The effects of seepage force and the Poisson's ratio on slope stability

*Hirokazu Fukui[1], Tomomi Terajima[2] (1.Graduate school of Science, Kyoto University, 2.Disaster Prevention Research Institute, Kyoto University)

[HDS09-P14] Study on the factors of seepage erosion

*Szu-Wei Fu[1], Kuang-Tsung Chang[1] (1.National Chung Hsing University)

[HDS09-P15] Deformation of slope models with different orientations of weak planes

*taeyuan tseng[1], Kuang-Tsung Chang[1] (1.National Chung Hsing University)

Fluidized landslides triggered by the liquefaction of subsurface volcanic deposits during the 2018 Iburi–Tobu earthquake, Hokkaido

*Jun Kameda[1], Hiro Kamiya[2], Hirokazu Masumoto[1], Tomonori Morisaki[1], Toru Hiratsuka[2], Chisaki Inaoi

1. Department of Natural History Sciences, Graduate School of Science, Hokkaido University, 2. Department of Earth and Planetary Sciences, School of Science, Hokkaido University

The Iburi–Tobu earthquake of M_w = 6.7 occurred at 3:07 AM (local time) on 6 September 2018, in southern Hokkaido, Japan. The earthquake caused power cuts and destroyed distribution networks across Hokkaido, creating widespread disruption. A total of 41 people were killed during the earthquake, with most of these (36 people) perishing in landslides near the epicenter. The hills in southwestern Hokkaido are widely covered by volcanic deposits, derived from the repeated eruptions of nearby volcanoes such as Tarumai, Eniwa, and Shikotsu (e.g., Nakagawa et al., 2018). On 4 September, Typhoon Jebi caused heavy rainfall in this area, which likely soaked and weakened the volcanic soils. Subsequent earthquake ground motion (with a maximum intensity of 7 on the intensity scale of Japan Meteorology Agency; Japan Meteorology Agency, 2018) may have triggered sudden whole-slope failures. The total number of the present landslides was ~6000 (Yamagishi and Yamazaki, 2018), and most of the recorded landslides are shallow and show features characteristic of fluidized landslides, such as long runouts of debris on a flat depositional area.
To investigate the mechanism generating the landslides triggered by the Iburi–Tobu earthquake, we conducted a field survey at a typical landslide in the Tomisato area of Atsuma, and we found a distinctive occurrence of liquefaction in the field, which could be a precursive condition for the generation of the fluidized landslides triggered by the earthquake. In the scarp of the landslide, an altered halloysite-bearing volcanic layer is observed at a level almost coincident with the sliding surface. The layer is intensely undulating and can be divided into an upper clay-rich layer and a lower pumice-rich layer, suggesting that the altered layer had liquefied as a result of the strong coseismic ground motion. The layer had been soaked by heavy rainfall just one day before the earthquake and could have liquefied by interstitial fluid pressurization, producing a weak and slippery plane, resulting in the catastrophic landslides in this area.

Keywords: fluidized landslide, 2018 Iburi–Tobu earthquake, halloysite

©2019. Japan Geoscience Union. All Right Reserved.

A comparison between the acoustic signals and seismic signals generated during a dam-break test

*Zheng-yi Feng[1], Hao-yang Huang[1], Chia-Ming Chuang[1]

1. Department of Soil and Water Conservation, National Chung Hsing University, Taichung, Taiwan

Natural events, such as landslide, sediment transport, flooding, etc., usually release energy to produce acoustic waves and seismic waves. Acoustic wave is transmitted through air and seismic wave is transmitted through geologic structure. Therefore, the characteristics of acoustic waves and the seismic waves induced by these events should be different. This study focus on the differences in the acoustic signals and seismic signals during a dam-break test performed by the authors. We built a model dam and slope in a creek for the test. We filled the dam with water and caused it to overflow. The overflow water caused the downward erosion of the dam. The flood due to the dam-break eroded the toe of the model slope causing the slope to collapse locally. We set up microphones to collect acoustic signals and installed accelerometers to collect vertical seismic signals generated by the flood and collapse events during the test. During the test we also used unmanned aerial vehicle (UAV) to continuously take photos for the collapsed areas for making the digital surface model (DSM) of the slope to analyze the volumes of the collapsed materials. We used Hilbert-Huang Transform (HHT) to obtain the time-frequency spectra for the acoustic signals and seismic signals. From the spectra, we compared the energy and frequency content of the two kinds of signals and their differences. The results show that the acoustic signal showing earlier indication of overtopping than that of the seismic signal. In addition, the acoustic and seismic signals generated during the flood can correspond to each other. The collapse events of the slope during the flood can be investigated also by examining the time-frequency spectrum of the seismic signal. Usually the signals of the collapse events can be distinguished from the flooding signals.

Keywords: dam break, landslide, slope, acoustic signal, seismic signal, flood

©2019. Japan Geoscience Union. All Right Reserved.

Evaluation of factors of safety and landslide risk for a watershed by Scoops3D

*Zheng-yi Feng[1], Chia-Ming Chuang[1], Hao-yang Huang[1]

1. Department of Soil and Water Conservation, National Chung Hsing University, Taichung, Taiwan

In this study, the Scoops3D code (USGS, 2015) is used to analyze the three-dimensional stability of the slopes in a watershed in Taiwan. To perform Scoops3D it requires the inputs such as digital elevation model (DEM), geological materials, groundwater level, earthquake, etc. The code calculates the minimum factor of safety (F.S.) and the associated potential failure volumes by using three-dimensional limit equilibrium method. We performed a comprehensive analysis of slope stability for the research areas using the Scoops3D code. The ArcMap software was used to present the F.S. that are less than unity as a 2D contoured map. We can observe this contoured map to understand the overall slope stability of the studied watershed. We perform a parametrical study by set three different sizes of sliding volume, “large”, “medium” and “small”, for evaluating the risk of landslide for the three different volume sizes.

Keywords: Landslide, Scoops3D, Factor of safety, Risk

©2019. Japan Geoscience Union. All Right Reserved.

Fuzzy Clustering Algorithms for Establishing Landslide Susceptibility Map

*Pei-hsun Tsai[1], Syuan-yi Wang[1], Jie-shin Cheng[1]

1. Chaoyang University of Technology

In recent years, the rainfall distribution is not uniform because of extreme weather events, the occurrence frequency of heavy rain increases. Coupled with steep terrain and complicated geological condition, so that the slope often occurred landslide when typhoon or heavy rain. Landslide susceptibility map delineates the potential zones for landslide occurrence. To develop the landslide model, we used several independent data layers that are recognized as effective factors in landslide occurrence, including slope, aspect, shear strength of rock or soil, dip and dip direction of stratum, and distance to road. All data layers were converted to raster layers with a 30 m ×30 m cell size. A total of 231336 cells were derived in study area. For assessing landslide susceptibility spatially, this study used fuzzy c-means clustering algorithm to classify the aforementioned data set in the study area into six clusters. Each cluster has similar natural environmental conditions and collapse situation. It is helpful to establish the monitoring management system and it can be applied to an early warning system in the landslide. Results of validation show that this model can accurately predict the occurrence of new landslides.

Keywords: Landslide susceptibility map, Fuzzy c-means , Clustering algorithm

©2019. Japan Geoscience Union. All Right Reserved.

A Study on Landslides and Debris Flows Susceptibility Mapping Using Unmanned Aerial Vehicles

*Sheng-Jia Liu[1]

1. qwepoi13@gmail.com

The geology of Taiwan is generally vulnerable due to the natural adverse conditions such as younger strata, steep topography, active orogeny, frequent seismic activity, weathering and erosion, frequent typhoons, high rainfall, etc. Furthermore, the human factors like immature law and regulations, the weak execution, and improper land use and development also play an important role in reducing the slope stability. These factors to some degree worsen the slope conditions, lead to a more frequent natural disaster and cause the loss of life and property.

In order to effectively evaluate the landslide susceptibility and map the high risk areas, the Soil and Water Conservation Bureau of Taiwan Executive Yuan (SWCB) provides an assessment method for assessing the risk level of landslide susceptibility by selecting the combinations of impact factors that may trigger landslides. However, the accuracy and efficiency of data acquisitions, in a conventional way, for the assessment method are still limited.
With the advantages of UAVs, the digital image with high resolutions for a wider area without terrain restrictions can be obtained efficiently. Its applications have become more widespread, from battlefield detections and communications to forest management and mapping. This study utilizes the latest Dynamic Post-Processing Motion (PPK) positioning system to capture high-resolution image data from a chosen site in the northern part of Taiwan. The terrain information was extracted from aerial images using Pix4Dmapper with aerial triangulation techniques, thus the external direction of each image and the camera's internal direction parameters can be obtained, the point cloud data can be matched automatically, and a digital surface mode can be established. Further, a three-dimensional model with topographic map and landslide susceptibility evaluations can be established and performed by comparing with historical data and monitoring the slope conditions. A modified assessment method is proposed using the three factors (slope, the volume of soil and rock accumulations, and rainfall) to assess the landslide susceptibility of the study area. The evaluations made by the proposed method are in agreement with the SWCB method. The results from this study can be used in slope management and precaution, and rescue and recovery.

Keywords: UAVs, landslides, debris flows, susceptibility evaluation

©2019. Japan Geoscience Union. All Right Reserved.

Largescale landslide induced by AD1586 Tensho-Earthquake in Gifu Prefecture, central Japan

*Takahiro Kurimoto[1], Yoshihiko Kariya[2], Kuniyasu Mokudai[3], Ryuji Yamada[4], Takashi Kimura[4]

1. Undergraduate Senshu University, 2. Department of Geography, Senshu University, 3. Japan Geoservice Incorporated, 4. National Research Institute for Earth Science and Disaster Resilience

On the basis of field investigation and topographic analysis by using GIS, we clarified the geological and geomorphological features of a large-scale landslide (V=2.2×10^7 m^3) called Mizore Landslide (ML) in Gujo City of Gifu Prefecture, central Japan. According to old documents, it is thought to ML was caused by AD1586 Tensho earthquake (generated from the Shokawa fault zone close to the ML and estimated M=7 to 8). However, there are few studies on geomorphological and geological basis. The main results are as follows: a) The ML holds a set of three head scarps and three landslide bodies both showing multiple activities of slope movement; b) The ML shows unique sedimentological and geomorphological characteristics such as a jigsaw crack structure in landslide deposits and hummocks and depressions upon the ground surface of the landslide bodies; c) Both involved buried soils in the landslide deposits and fossil wood logs in the dammed lake deposits enable us to date the landslide events; d) According to those ^{14}C dates of soils and logs, the latest landslide event is thought to occur in the period from cal AD1436 to 1650; e) The latest landslide event would be triggered by AD1586 Tensho earthquake. AD1596 Keicho-Fushimi earthquake occurred around Kyoto is a candidate event for further consideration.

Keywords: AD1586 Tensho-earthquake, Large-scale landslide, Shokawa fault zone, Dammed lake

©2019. Japan Geoscience Union. All Right Reserved.

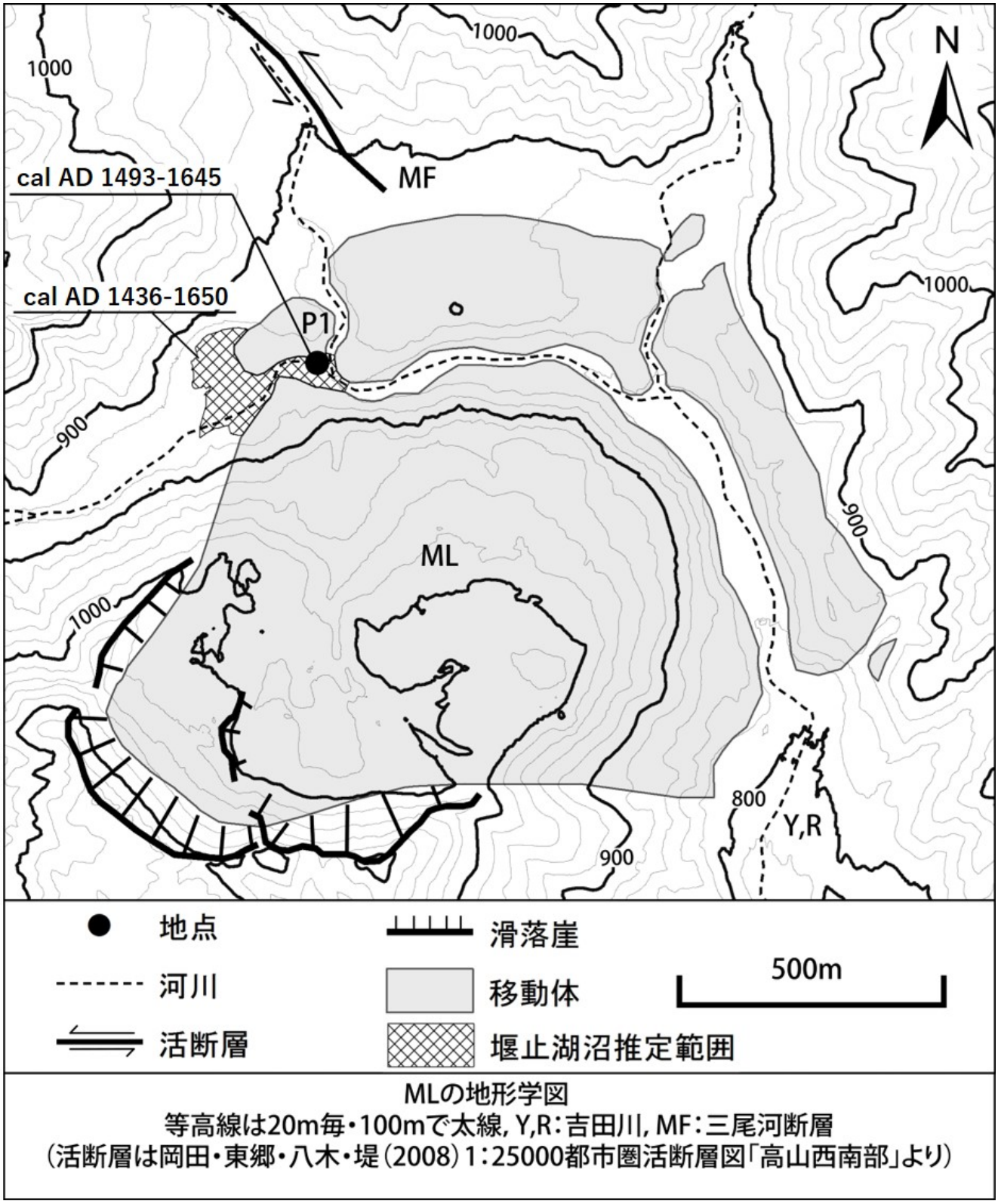

MLの地形学図
等高線は20m毎・100mで太線, Y,R:吉田川, MF:三尾河断層
(活断層は岡田・東郷・八木・堤(2008)1:25000都市圏活断層図「高山西南部」より)

©2019. Japan Geoscience Union. All Right Reserved.

Failure Probability of Lushan Landslide, Taiwan

*Wei-Ting Lin[1], Kuang-Tsung Chang[1]

1. National Chung Hsing University

The Lushan landslide located in the middle of Taiwan, has slid and damaged the road due to typhoons or heavy rainfalls for recent decades. It’ s seriously affecting the safety of life and property of the Lushan Hot Spring Tourist Area and local residents in the lower slope. In order to understand the probability of failure (Pf) of Lushan landslide, we built a numerical model by Plaxis2D, which is validated by the monitoring data of the 2009 typhoon Morakot. However, due to the lack of complete parameter data, uncertainties exist and may affect the simulation result of the collapse. With the back calculated friction angle (∅) and cohesion (c) from Plaxis2D, we used the Monte Carlo Simulation (MCS) to consider the friction angle and the cohesion of sliding body as random variables with uncertainty. The results are statistically analyzed to obtain the Probability Density Function (PDF) of the two parameters. Based on the parameter settings above, with the designed rainfall events at 24hr, 48hr and 72hr rainfall duration and 10, 25, 50, 100 and 200 years of recurrence interval, we calculate the factor of safety (SF) of the Lushan landslide in these 18 simulated rainfall events. Finally, we can obtain the distribution of factor of safety (SF) and probability of failure (Pf) of the Lushan landslide in different rainfall durations and recurrence intervals.

Keywords: probability of failure, Monte Carlo Simulation, uncertainty

©2019. Japan Geoscience Union. All Right Reserved.

Interpretation of landslide surface deformation in Kali Gandaki River watershed, Nepal using ALOS-2/PALSAR-2 InSAR image

*Hiroshi, P. Sato[1]

1. College of Humanities and Sciences, Nihon University

Previous studies have revealed and mapped glacial landform, fluvial terraces, and landslide landform in Thakkohla-Muktinath region, between Kagbeni and Ghasa along Kali Gandaki River, Nepal. And many attentions were paid to detect landslides that brock channels in the region, especially after Gorkha earthquake (25 Apr 2015; Mw7.8). Therefore, I tried to interpret landslide surface deformation on mountain slopes in Kali Gandaki River watershed after the earthquake, using Synthetic Aperture Radar interferometry (InSAR) image. The number of produced InSAR images was six, which is master image/slave image in order from ALOS-2/PALSAR-2 data, 08Oct2015/17Dec2015, 08Oct2015/30Nov2017, 25Feb2016/06Oct2016, 30Nov2017/24Jan2019, 08Mar2018/24Jan2019 and 31May2018/24Jan2019. In these InSAR images clear precursory landslide surface deformation was not interpreted on mountain slopes facing main stream of Kali Gandaki River. However, whose tributary watershed; i.e., Myagdi River watershed gave some landslide surface deformations (e.g., in 83.3983E, 28.4842N) clearly interpreted in the InSAR image of 08Oct2015/17Dec2015, which was relatively better coherence than the rest five images.

Keywords: SAR, earthquake, landslide, interpretation

©2019. Japan Geoscience Union. All Right Reserved.

A depth-integrated model for granular flows on the transition of different bed conditions

*Ling-Yi Hsu[1], Chi-Yao Hung[1]

1. National Chung Hsing University

The different basal boundary conditions profoundly affected the flow behavior of debris flow. However, it is hard to have a general and straightforward model to describe the flow profile switching from different bed conditions. In this study, we purpose a new depth-averaged model to simulate the dense granular flow transition between the rigid and mobile bed. The model is based on mass conservation, momentum conservation, and kinetic energy conservation. We apply the linearized mu(I) rheology to describe granular deformation and assume Coulomb friction along the sidewalls. By incorporating the basal shear rate term into the equations, the theory can balance the extra force from rigid bed friction force. To check the model approach, we conducted an equilibrium and non-equilibrium heap flow experiments using the narrow see-saw channel, which can be tilted to different angles between runs or during flows. To compare the experimental results with the theory, the flow fields are monitored using high-speed video and particle-tracking velocimetry.

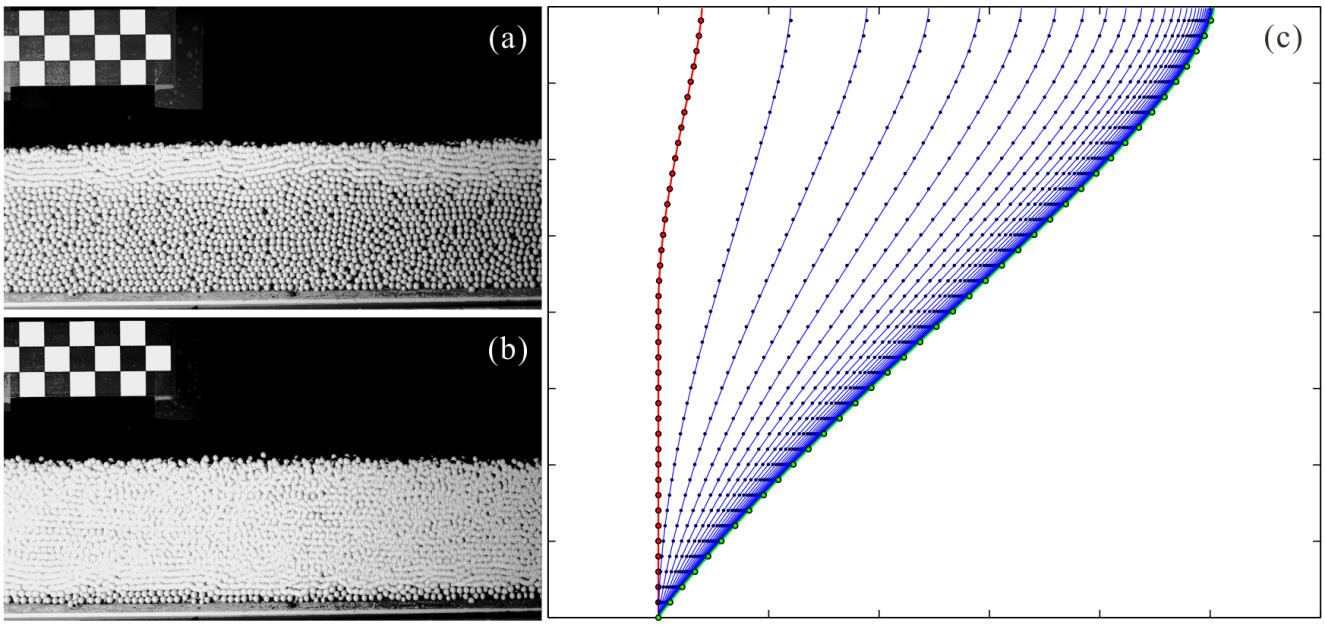

Fig.1 Experimental longexpousre image (a) over deposition bed; (b) over rigid bed; and (c) the transition velocity profile of theory prediction.

©2019. Japan Geoscience Union. All Right Reserved.

A viscous granular flow experiment with new refractive index matching material

*Tsai-Jung Lin[1], Chi-Yao Hung[1]

1. National Chung Hsing University

Entrainment rate at base controls how far the debris flow can travel and how large the debris flow becomes. Flow rheology of Refractive Index Matching (RIM) material are generally limited by the mono-particle properties (such as polymethyl methacrylate/liquid para-cymene etc.). In this study, a new RIM material (polyacrylamide polymer/18% Methanol solution) having a wide range of particle size distribution and viscosity (Fig. 1L) are purposed to visualize and measure the erosion process of mobile bed dam break experiments. Various rheology models may be formed by the different ratio of particle size. To improve the contrast between the particle phase and the liquid phase, a dye is used to make the particles bright under laser illumination. By varying the dye concentration, the entraining/detraining processes are easily distinguished (Fig. 1R). Granular motion is captured through a high-speed camera and Particle Tracking Velocimetry (PTV) method. Finally, an empirical relationship between the rheology and the entraining/ detraining process is developed.

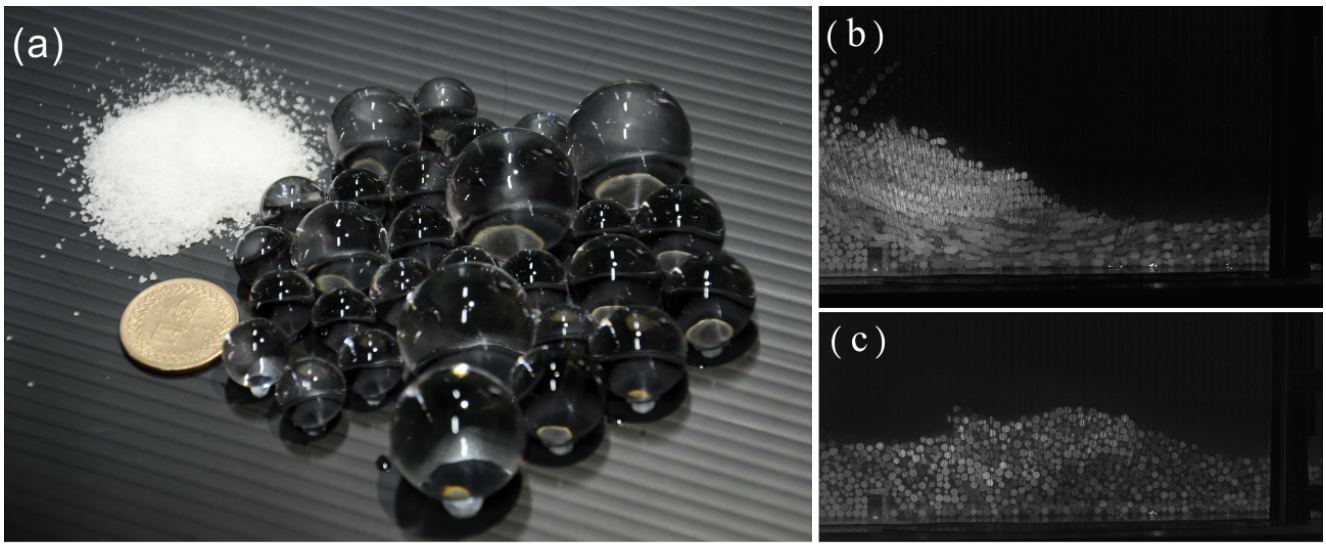

Fig.1 Experimental image (a)wide range of particle size; (b)longexposure image of dam break occurrence; (c)particles with different concentration of dye.

©2019. Japan Geoscience Union. All Right Reserved.

Sandbox experiments of submarine landslide caused by water film in low permeability layer

*Shogo Kawakita[1], Daisuke Asahina[2], Keiji Kitajima[3], Mitsukazu Nakanishi[3]

1. Graduate School of Science & Technology, Nihon Univ., 2. National Institute of Advanced Industrial Science and Technology, 3. College of Science & Technology, Nihon Univ.

Submarine landslides can be serious geohazards since they potentially cause tsunamis and damage seafloor infrastructure. Submarine landslides can be larger in scale than landslides on land. Direct measurements/observations of submarine landslides at deep seafloor still remain a challenging task. Kokusho et al. (2000) proposed a water film effect and its mechanism on lateral flow with less frictional resistance to explain a driving force of large-scale submarine landslides

In this study, we conducted laboratory experiments to understand the relationship between sand liquefaction and lateral flow by water film, and investigate the influence of water film formation on lateral flow of upper layer. In general, it is difficult to observe the formations of liquefaction and lateral flow at the same time. This is because sand particles of sloping layer model start to move when vibration is applied, and inclination disappears before liquefaction. To solve this problem, we devised a mechanism to prevent the flow of the lower layer by providing a weir plate in inside the soil tank. This mechanism enables to distinguish and observe the movement of sand by the liquefaction and the lateral flow by the water film.

The results obtained in this study clearly show three stages: first, the lower layer was liquefied; then pore water was stored below the low permeability layer; and finally, the lateral flow was occurred by the water film effect. The experimental results show that there was no clear correlation between the increase in the angle of sloping layer and the travel distance or the maximum flow velocity. We also discuss the relationship between the layer angle and the location of sand boil. The location where sand soiling occurred moved to the upper side of the slope as the layer angle become larger.

[Reference]

Kokusho, T.: Mechanism for water film generation and lateral flow in liquefied sand layer, Soils and Foundations, Vol.40, No.5, p 99-111, 2000.

Keywords: Submarine Landslides, Pore Water Pressure, Water Film, Lateral Flow

©2019. Japan Geoscience Union. All Right Reserved.

Study on Creep Properties of Sand and Cemented Sand

*JIN-YI YU[1], KUANG-TSUNG CHANG[1]

1. National Chung Hsing University

In this study, we investigated the effects of creep on sand and cemented sand, using triaxial test. Sand represents a non-cohesive material, while cemented sand represents a brittle material. Before the failure of specimens, the deviator stress was fixed and the cyclic mean stress was applied to study the influence of creep on the materials. According to the test results, the axial strain accumulation of sand caused by creep is less, and the peak strength is larger than that of the monotonic loading when the axial loading is resumed. For cemented sand, creep causes microcracks inside the specimens, gradually forming a failure surface. When the axial strain accumulation is large enough, the reapplication of the axial loading shows a reduction of peak strength. We conclude that the influence of creep on non-cohesive material (sand) is limited, whereas creep can reduce the strength of the brittle material (cemented sand) and even cause failure.

Keywords: creep, triaxial test, sand, cemented sand, strength, failure

©2019. Japan Geoscience Union. All Right Reserved.

The effects of seepage force and the Poisson’s ratio on slope stability

*Hirokazu Fukui[1], Tomomi Terajima[2]

1. Graduate school of Science, Kyoto University, 2. Disaster Prevention Research Institute, Kyoto University

To predict accurately the timing of shallow landslide occurrence, we need to consider the direction and magnitude of seepage force and earth pressure. A model sandy slope (L: 9m, W:1m, H:4m) was used to measure the hydraulic gradient and seepage force with the tensiometers under the artificial rainfall of 80mm/h. We incorporated not only the seepage force but also the Poisson’s ratio into conventional slope stability analysis by the limit equilibrium method. As a result, the calculated timing of shallow landslide occurrence was almost agree with the timing of that in the experiment and also more accurate than the timing calculated by the Spenser method which took into account the magnitude and moment equilibrium of the force. These results imply that, based on both monitoring at fields and conducting more experiments by a real-size model slope, we need to verify the effects of seepage force and earth pressure as the important factors causing rainfall-induced slope instability.

Keywords: process-based model, Seepage force, the Poisson's ratio, Shallow landslide, Sandy model slope

©2019. Japan Geoscience Union. All Right Reserved.

Study on the factors of seepage erosion

*Szu-Wei Fu[1], Kuang-Tsung Chang[1]

1. National Chung Hsing University

The causes of many slope disasters are often related to the seepage behaviors of soil. For instance, groundwater seepage may cause internal erosion of the soil. The soil particles are taken away by seepage water to form void or pipe. In addition , the earth pressure leads to the collapse of the overlying soil.

In this study, we designed a set of apparatus that can add confining pressure to the outside of the specimen. In order to simulate the situation of sand in slopes, we investigated the critical seepage velocity of sands caused by seepage erosion failure under different confining pressure, with different particle size distributions, sizes of outflow, etc. Then a failure criterion for seepage erosion is developed based on the drag equation in fluid dynamics and confirm with experimental data.

The results show that the critical seepage velocity at failure is affected by the particle size distributions, sizes of outflow and the confining pressure. The theoretical results are compared well to the experimental data.

Keywords: seepage erosion, Drag equation

©2019. Japan Geoscience Union. All Right Reserved.

Deformation of slope models with different orientations of weak planes

*taeyuan tseng[1], Kuang-Tsung Chang[1]

1. National Chung Hsing University

Weak planes influence failure and deformation of slopes. We conducted experiments to simulate slopes of different orientations of weak planes, including cataclinal and analcinal slopes with 30˚ and 60˚ inclination angles of weak planes. We stacked artificial bricks to make small-sized slope models. The artificial bricks were made of gypsum, sand, cement and water with different weight proportion. In view of the scaling law, the artificial bricks were made less strength than natural rocks. The slope models were weakened under rainfall, resulting in deformation and final collapse. The slope deformation processes were photographed by a camera, and the displacement vector fields were analyzed using the Particle Image Velocimetry (PIV). The deformation and accumulated displacements were compared between slopes of different orientations of weak planes.

Keywords: cataclinal slope, analcinal slopes, rainfall, Particle Image Velocimetry (PIV), weak planes, deformation

©2019. Japan Geoscience Union. All Right Reserved.

[E] Poster | H (Human Geosciences)：H-DS Disaster geosciences

Tue. May 28, 2019 5:15 PM - 6:30 PM JST | Tue. May 28, 2019 8:15 AM - 9:30 AM UTC | Poster Hall International Exhibition Hall8, Makuhari Messe_20

[H-DS09] Landslides and related phenomena

convener:Masahiro Chigira(Disaster Prevention Research Institute, Kyoto University), Gonghui Wang(Disaster Prevention Research Institute, Kyoto University), Fumitoshi Imaizumi(Faculty of Agriculture, Shizuoka University)

Mass movements, such as landslides, rockfalls, and debris flows, have been occurring extensively in a large number of countries, causing heavy damage. In order to understand them and mitigate induced disasters, we invite contributions that report and discuss on mass movements and related phenomena, focusing on improved understanding of their characteristics; new insights into landslide mechanisms; the development of new approaches to monitoring; novel approaches to behavior forecasting and prediction; studies of successful landslide management; and the development of methods for hazard and risk evaluation. In particular, papers about recent landslide hazards, induced by 2017 northern Kyushu rainstorm, 2018 Osaka earthquake, 2018 western Japan rainstorm, and 2018 Hokkaido earthquake are welcome.

[HDS09-P01] **Fluidized landslides triggered by the liquefaction of subsurface volcanic deposits during the 2018 Iburi–Tobu earthquake, Hokkaido**

*Jun Kameda[1], Hiro Kamiya[2], Hirokazu Masumoto[1], Tomonori Morisaki[1], Toru Hiratsuka[2], Chisaki Inaoi (1.Department of Natural History Sciences, Graduate School of Science, Hokkaido University, 2.Department of Earth and Planetary Sciences, School of Science, Hokkaido University)

[HDS09-P02] A comparison between the acoustic signals and seismic signals generated during a dam-break test

★Invited Papers

*Zheng-yi Feng[1], Hao-yang Huang[1], Chia-Ming Chuang[1] (1.Department of Soil and Water Conservation, National Chung Hsing University, Taichung, Taiwan)

[HDS09-P03] Evaluation of factors of safety and landslide risk for a watershed by Scoops3D

*Zheng-yi Feng[1], Chia-Ming Chuang[1], Hao-yang Huang[1] (1.Department of Soil and Water Conservation, National Chung Hsing University, Taichung, Taiwan)

[HDS09-P04] **Fuzzy Clustering Algorithms for Establishing Landslide Susceptibility Map**

*Pei-hsun Tsai[1], Syuan-yi Wang[1], Jie-shin Cheng[1] (1.Chaoyang University of Technology)

[HDS09-P05] **A Study on Landslides and Debris Flows Susceptibility Mapping Using Unmanned Aerial Vehicles**

*Sheng-Jia Liu[1] (1.qwepoi13@gmail.com)

[HDS09-P06] Largescale landslide induced by AD1586 Tensho-Earthquake in Gifu Prefecture, central Japan

*Takahiro Kurimoto[1], Yoshihiko Kariya[2], Kuniyasu Mokudai[3], Ryuji Yamada[4], Takashi Kimura[4] (1.Undergraduate Senshu University, 2.Department of Geography, Senshu University, 3.Japan Geoservice Incorporated, 4.National Research Institute for Earth Science and Disaster Resilience)

[HDS09-P07] Failure Probability of Lushan Landslide, Taiwan

*Wei-Ting Lin[1], Kuang-Tsung Chang[1] (1.National Chung Hsing University)

[HDS09-P08] Interpretation of landslide surface deformation in Kali Gandaki River watershed, Nepal using ALOS-2/PALSAR-2 InSAR image

*Hiroshi, P. Sato[1] (1.College of Humanities and Sciences, Nihon University)

[HDS09-P09] A depth-integrated model for granular flows on the transition of different bed conditions

*Ling-Yi Hsu[1], Chi-Yao Hung[1] (1.National Chung Hsing University)

[HDS09-P10] A viscous granular flow experiment with new refractive index matching material

*Tsai-Jung Lin[1], Chi-Yao Hung[1] (1.National Chung Hsing University)

[HDS09-P11] Sandbox experiments of submarine landslide caused by water film in low permeability layer

*Shogo Kawakita[1], Daisuke Asahina[2], Keiji Kitajima[3], Mitsukazu Nakanishi[3] (1.Graduate School of Science & Technology, Nihon Univ., 2.National Institute of Advanced Industrial Science and Technology, 3.College of Science & Technology, Nihon Univ.)

[HDS09-P12] **Study on Creep Properties of Sand and Cemented Sand**

*JIN-YI YU[1], KUANG-TSUNG CHANG[1] (1.National Chung Hsing University)

[HDS09-P13] The effects of seepage force and the Poisson's ratio on slope stability

*Hirokazu Fukui[1], Tomomi Terajima[2] (1.Graduate school of Science, Kyoto University, 2.Disaster Prevention Research Institute, Kyoto University)

[HDS09-P14] Study on the factors of seepage erosion

*Szu-Wei Fu[1], Kuang-Tsung Chang[1] (1.National Chung Hsing University)

[HDS09-P15] Deformation of slope models with different orientations of weak planes

*taeyuan tseng[1], Kuang-Tsung Chang[1] (1.National Chung Hsing University)

Fluidized landslides triggered by the liquefaction of subsurface volcanic deposits during the 2018 Iburi–Tobu earthquake, Hokkaido

*Jun Kameda[1], Hiro Kamiya[2], Hirokazu Masumoto[1], Tomonori Morisaki[1], Toru Hiratsuka[2], Chisaki Inaoi

1. Department of Natural History Sciences, Graduate School of Science, Hokkaido University, 2. Department of Earth and Planetary Sciences, School of Science, Hokkaido University

The Iburi–Tobu earthquake of M_w = 6.7 occurred at 3:07 AM (local time) on 6 September 2018, in southern Hokkaido, Japan. The earthquake caused power cuts and destroyed distribution networks across Hokkaido, creating widespread disruption. A total of 41 people were killed during the earthquake, with most of these (36 people) perishing in landslides near the epicenter. The hills in southwestern Hokkaido are widely covered by volcanic deposits, derived from the repeated eruptions of nearby volcanoes such as Tarumai, Eniwa, and Shikotsu (e.g., Nakagawa et al., 2018). On 4 September, Typhoon Jebi caused heavy rainfall in this area, which likely soaked and weakened the volcanic soils. Subsequent earthquake ground motion (with a maximum intensity of 7 on the intensity scale of Japan Meteorology Agency; Japan Meteorology Agency, 2018) may have triggered sudden whole-slope failures. The total number of the present landslides was ~6000 (Yamagishi and Yamazaki, 2018), and most of the recorded landslides are shallow and show features characteristic of fluidized landslides, such as long runouts of debris on a flat depositional area.
To investigate the mechanism generating the landslides triggered by the Iburi–Tobu earthquake, we conducted a field survey at a typical landslide in the Tomisato area of Atsuma, and we found a distinctive occurrence of liquefaction in the field, which could be a precursive condition for the generation of the fluidized landslides triggered by the earthquake. In the scarp of the landslide, an altered halloysite-bearing volcanic layer is observed at a level almost coincident with the sliding surface. The layer is intensely undulating and can be divided into an upper clay-rich layer and a lower pumice-rich layer, suggesting that the altered layer had liquefied as a result of the strong coseismic ground motion. The layer had been soaked by heavy rainfall just one day before the earthquake and could have liquefied by interstitial fluid pressurization, producing a weak and slippery plane, resulting in the catastrophic landslides in this area.

Keywords: fluidized landslide, 2018 Iburi–Tobu earthquake, halloysite

©2019. Japan Geoscience Union. All Right Reserved.

A comparison between the acoustic signals and seismic signals generated during a dam-break test

*Zheng-yi Feng[1], Hao-yang Huang[1], Chia-Ming Chuang[1]

1. Department of Soil and Water Conservation, National Chung Hsing University, Taichung, Taiwan

Natural events, such as landslide, sediment transport, flooding, etc., usually release energy to produce acoustic waves and seismic waves. Acoustic wave is transmitted through air and seismic wave is transmitted through geologic structure. Therefore, the characteristics of acoustic waves and the seismic waves induced by these events should be different. This study focus on the differences in the acoustic signals and seismic signals during a dam-break test performed by the authors. We built a model dam and slope in a creek for the test. We filled the dam with water and caused it to overflow. The overflow water caused the downward erosion of the dam. The flood due to the dam-break eroded the toe of the model slope causing the slope to collapse locally. We set up microphones to collect acoustic signals and installed accelerometers to collect vertical seismic signals generated by the flood and collapse events during the test. During the test we also used unmanned aerial vehicle (UAV) to continuously take photos for the collapsed areas for making the digital surface model (DSM) of the slope to analyze the volumes of the collapsed materials. We used Hilbert-Huang Transform (HHT) to obtain the time-frequency spectra for the acoustic signals and seismic signals. From the spectra, we compared the energy and frequency content of the two kinds of signals and their differences. The results show that the acoustic signal showing earlier indication of overtopping than that of the seismic signal. In addition, the acoustic and seismic signals generated during the flood can correspond to each other. The collapse events of the slope during the flood can be investigated also by examining the time-frequency spectrum of the seismic signal. Usually the signals of the collapse events can be distinguished from the flooding signals.

Keywords: dam break, landslide, slope, acoustic signal, seismic signal, flood

©2019. Japan Geoscience Union. All Right Reserved.

Evaluation of factors of safety and landslide risk for a watershed by Scoops3D

*Zheng-yi Feng[1], Chia-Ming Chuang[1], Hao-yang Huang[1]

1. Department of Soil and Water Conservation, National Chung Hsing University, Taichung, Taiwan

In this study, the Scoops3D code (USGS, 2015) is used to analyze the three-dimensional stability of the slopes in a watershed in Taiwan. To perform Scoops3D it requires the inputs such as digital elevation model (DEM), geological materials, groundwater level, earthquake, etc. The code calculates the minimum factor of safety (F.S.) and the associated potential failure volumes by using three-dimensional limit equilibrium method. We performed a comprehensive analysis of slope stability for the research areas using the Scoops3D code. The ArcMap software was used to present the F.S. that are less than unity as a 2D contoured map. We can observe this contoured map to understand the overall slope stability of the studied watershed. We perform a parametrical study by set three different sizes of sliding volume, “large”, “medium” and “small”, for evaluating the risk of landslide for the three different volume sizes.

Keywords: Landslide, Scoops3D, Factor of safety, Risk

©2019. Japan Geoscience Union. All Right Reserved.

Fuzzy Clustering Algorithms for Establishing Landslide Susceptibility Map

*Pei-hsun Tsai[1], Syuan-yi Wang[1], Jie-shin Cheng[1]

1. Chaoyang University of Technology

In recent years, the rainfall distribution is not uniform because of extreme weather events, the occurrence frequency of heavy rain increases. Coupled with steep terrain and complicated geological condition, so that the slope often occurred landslide when typhoon or heavy rain. Landslide susceptibility map delineates the potential zones for landslide occurrence. To develop the landslide model, we used several independent data layers that are recognized as effective factors in landslide occurrence, including slope, aspect, shear strength of rock or soil, dip and dip direction of stratum, and distance to road. All data layers were converted to raster layers with a 30 m ×30 m cell size. A total of 231336 cells were derived in study area. For assessing landslide susceptibility spatially, this study used fuzzy c-means clustering algorithm to classify the aforementioned data set in the study area into six clusters. Each cluster has similar natural environmental conditions and collapse situation. It is helpful to establish the monitoring management system and it can be applied to an early warning system in the landslide. Results of validation show that this model can accurately predict the occurrence of new landslides.

Keywords: Landslide susceptibility map, Fuzzy c-means , Clustering algorithm

©2019. Japan Geoscience Union. All Right Reserved.

A Study on Landslides and Debris Flows Susceptibility Mapping Using Unmanned Aerial Vehicles

*Sheng-Jia Liu[1]

1. qwepoi13@gmail.com

The geology of Taiwan is generally vulnerable due to the natural adverse conditions such as younger strata, steep topography, active orogeny, frequent seismic activity, weathering and erosion, frequent typhoons, high rainfall, etc. Furthermore, the human factors like immature law and regulations, the weak execution, and improper land use and development also play an important role in reducing the slope stability. These factors to some degree worsen the slope conditions, lead to a more frequent natural disaster and cause the loss of life and property.

In order to effectively evaluate the landslide susceptibility and map the high risk areas, the Soil and Water Conservation Bureau of Taiwan Executive Yuan (SWCB) provides an assessment method for assessing the risk level of landslide susceptibility by selecting the combinations of impact factors that may trigger landslides. However, the accuracy and efficiency of data acquisitions, in a conventional way, for the assessment method are still limited.
With the advantages of UAVs, the digital image with high resolutions for a wider area without terrain restrictions can be obtained efficiently. Its applications have become more widespread, from battlefield detections and communications to forest management and mapping. This study utilizes the latest Dynamic Post-Processing Motion (PPK) positioning system to capture high-resolution image data from a chosen site in the northern part of Taiwan. The terrain information was extracted from aerial images using Pix4Dmapper with aerial triangulation techniques, thus the external direction of each image and the camera's internal direction parameters can be obtained, the point cloud data can be matched automatically, and a digital surface mode can be established. Further, a three-dimensional model with topographic map and landslide susceptibility evaluations can be established and performed by comparing with historical data and monitoring the slope conditions. A modified assessment method is proposed using the three factors (slope, the volume of soil and rock accumulations, and rainfall) to assess the landslide susceptibility of the study area. The evaluations made by the proposed method are in agreement with the SWCB method. The results from this study can be used in slope management and precaution, and rescue and recovery.

Keywords: UAVs, landslides, debris flows, susceptibility evaluation

©2019. Japan Geoscience Union. All Right Reserved.

Largescale landslide induced by AD1586 Tensho-Earthquake in Gifu Prefecture, central Japan

*Takahiro Kurimoto[1], Yoshihiko Kariya[2], Kuniyasu Mokudai[3], Ryuji Yamada[4], Takashi Kimura[4]

1. Undergraduate Senshu University, 2. Department of Geography, Senshu University, 3. Japan Geoservice Incorporated, 4. National Research Institute for Earth Science and Disaster Resilience

On the basis of field investigation and topographic analysis by using GIS, we clarified the geological and geomorphological features of a large-scale landslide (V=2.2×10^7 m^3) called Mizore Landslide (ML) in Gujo City of Gifu Prefecture, central Japan. According to old documents, it is thought to ML was caused by AD1586 Tensho earthquake (generated from the Shokawa fault zone close to the ML and estimated M=7 to 8). However, there are few studies on geomorphological and geological basis. The main results are as follows: a) The ML holds a set of three head scarps and three landslide bodies both showing multiple activities of slope movement; b) The ML shows unique sedimentological and geomorphological characteristics such as a jigsaw crack structure in landslide deposits and hummocks and depressions upon the ground surface of the landslide bodies; c) Both involved buried soils in the landslide deposits and fossil wood logs in the dammed lake deposits enable us to date the landslide events; d) According to those ^{14}C dates of soils and logs, the latest landslide event is thought to occur in the period from cal AD1436 to 1650; e) The latest landslide event would be triggered by AD1586 Tensho earthquake. AD1596 Keicho-Fushimi earthquake occurred around Kyoto is a candidate event for further consideration.

Keywords: AD1586 Tensho-earthquake, Large-scale landslide, Shokawa fault zone, Dammed lake

©2019. Japan Geoscience Union. All Right Reserved.

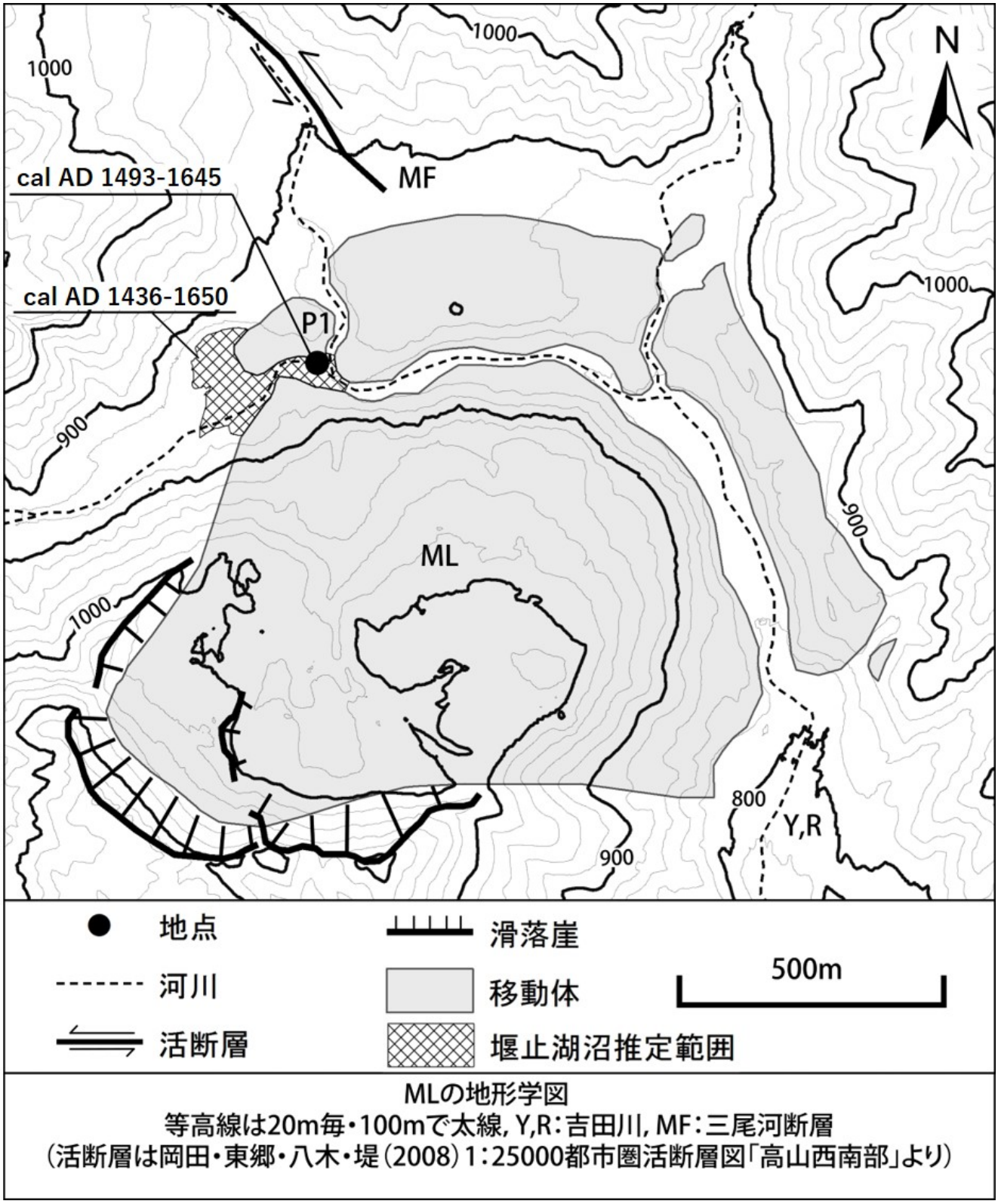

MLの地形学図
等高線は20m毎・100mで太線, Y,R:吉田川, MF:三尾河断層
(活断層は岡田・東郷・八木・堤(2008)1:25000都市圏活断層図「高山西南部」より)

©2019. Japan Geoscience Union. All Right Reserved.

Failure Probability of Lushan Landslide, Taiwan

*Wei-Ting Lin[1], Kuang-Tsung Chang[1]

1. National Chung Hsing University

The Lushan landslide located in the middle of Taiwan, has slid and damaged the road due to typhoons or heavy rainfalls for recent decades. It’ s seriously affecting the safety of life and property of the Lushan Hot Spring Tourist Area and local residents in the lower slope. In order to understand the probability of failure (Pf) of Lushan landslide, we built a numerical model by Plaxis2D, which is validated by the monitoring data of the 2009 typhoon Morakot. However, due to the lack of complete parameter data, uncertainties exist and may affect the simulation result of the collapse. With the back calculated friction angle (∅) and cohesion (c) from Plaxis2D, we used the Monte Carlo Simulation (MCS) to consider the friction angle and the cohesion of sliding body as random variables with uncertainty. The results are statistically analyzed to obtain the Probability Density Function (PDF) of the two parameters. Based on the parameter settings above, with the designed rainfall events at 24hr, 48hr and 72hr rainfall duration and 10, 25, 50, 100 and 200 years of recurrence interval, we calculate the factor of safety (SF) of the Lushan landslide in these 18 simulated rainfall events. Finally, we can obtain the distribution of factor of safety (SF) and probability of failure (Pf) of the Lushan landslide in different rainfall durations and recurrence intervals.

Keywords: probability of failure, Monte Carlo Simulation, uncertainty

©2019. Japan Geoscience Union. All Right Reserved.

Interpretation of landslide surface deformation in Kali Gandaki River watershed, Nepal using ALOS-2/PALSAR-2 InSAR image

*Hiroshi, P. Sato[1]

1. College of Humanities and Sciences, Nihon University

Previous studies have revealed and mapped glacial landform, fluvial terraces, and landslide landform in Thakkohla-Muktinath region, between Kagbeni and Ghasa along Kali Gandaki River, Nepal. And many attentions were paid to detect landslides that brock channels in the region, especially after Gorkha earthquake (25 Apr 2015; Mw7.8). Therefore, I tried to interpret landslide surface deformation on mountain slopes in Kali Gandaki River watershed after the earthquake, using Synthetic Aperture Radar interferometry (InSAR) image. The number of produced InSAR images was six, which is master image/slave image in order from ALOS-2/PALSAR-2 data, 08Oct2015/17Dec2015, 08Oct2015/30Nov2017, 25Feb2016/06Oct2016, 30Nov2017/24Jan2019, 08Mar2018/24Jan2019 and 31May2018/24Jan2019. In these InSAR images clear precursory landslide surface deformation was not interpreted on mountain slopes facing main stream of Kali Gandaki River. However, whose tributary watershed; i.e., Myagdi River watershed gave some landslide surface deformations (e.g., in 83.3983E, 28.4842N) clearly interpreted in the InSAR image of 08Oct2015/17Dec2015, which was relatively better coherence than the rest five images.

Keywords: SAR, earthquake, landslide, interpretation

©2019. Japan Geoscience Union. All Right Reserved.

A depth-integrated model for granular flows on the transition of different bed conditions

*Ling-Yi Hsu[1], Chi-Yao Hung[1]

1. National Chung Hsing University

The different basal boundary conditions profoundly affected the flow behavior of debris flow. However, it is hard to have a general and straightforward model to describe the flow profile switching from different bed conditions. In this study, we purpose a new depth-averaged model to simulate the dense granular flow transition between the rigid and mobile bed. The model is based on mass conservation, momentum conservation, and kinetic energy conservation. We apply the linearized mu(I) rheology to describe granular deformation and assume Coulomb friction along the sidewalls. By incorporating the basal shear rate term into the equations, the theory can balance the extra force from rigid bed friction force. To check the model approach, we conducted an equilibrium and non-equilibrium heap flow experiments using the narrow see-saw channel, which can be tilted to different angles between runs or during flows. To compare the experimental results with the theory, the flow fields are monitored using high-speed video and particle-tracking velocimetry.

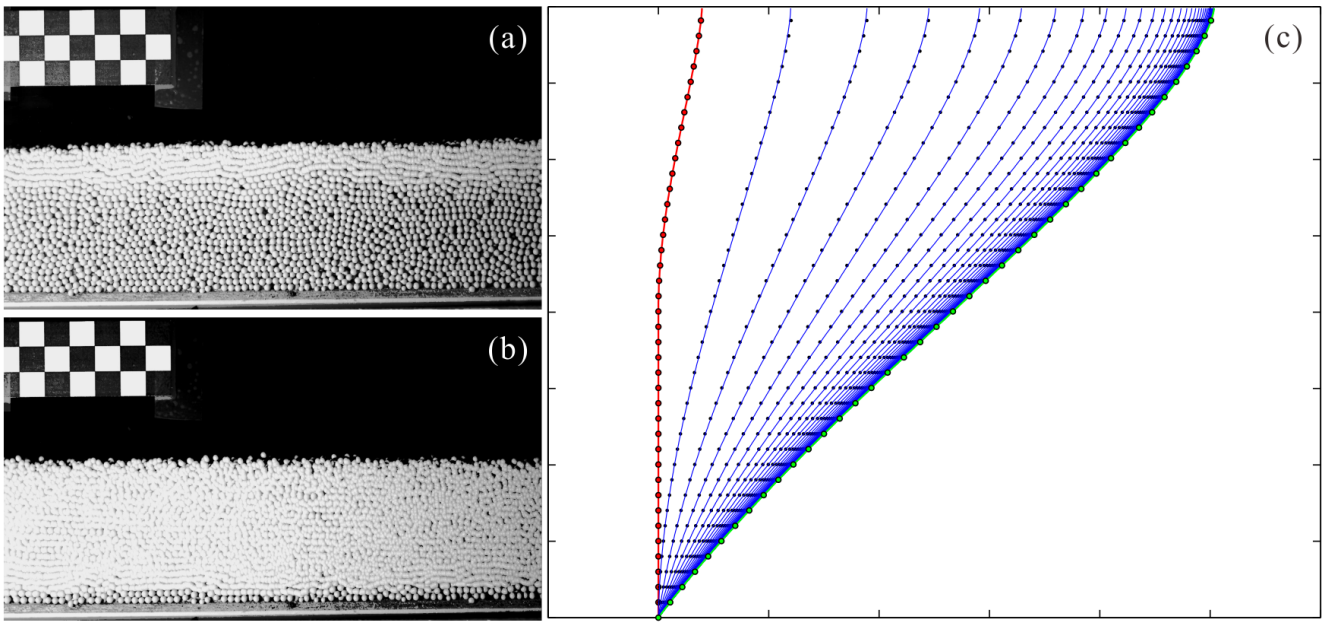

Fig.1 Experimental longexpousre image (a) over deposition bed; (b) over rigid bed; and (c) the transition velocity profile of theory prediction.

©2019. Japan Geoscience Union. All Right Reserved.

A viscous granular flow experiment with new refractive index matching material

*Tsai-Jung Lin[1], Chi-Yao Hung[1]

1. National Chung Hsing University

Entrainment rate at base controls how far the debris flow can travel and how large the debris flow becomes. Flow rheology of Refractive Index Matching (RIM) material are generally limited by the mono-particle properties (such as polymethyl methacrylate/liquid para-cymene etc.). In this study, a new RIM material (polyacrylamide polymer/18% Methanol solution) having a wide range of particle size distribution and viscosity (Fig. 1L) are purposed to visualize and measure the erosion process of mobile bed dam break experiments. Various rheology models may be formed by the different ratio of particle size. To improve the contrast between the particle phase and the liquid phase, a dye is used to make the particles bright under laser illumination. By varying the dye concentration, the entraining/detraining processes are easily distinguished (Fig. 1R). Granular motion is captured through a high-speed camera and Particle Tracking Velocimetry (PTV) method. Finally, an empirical relationship between the rheology and the entraining/ detraining process is developed.

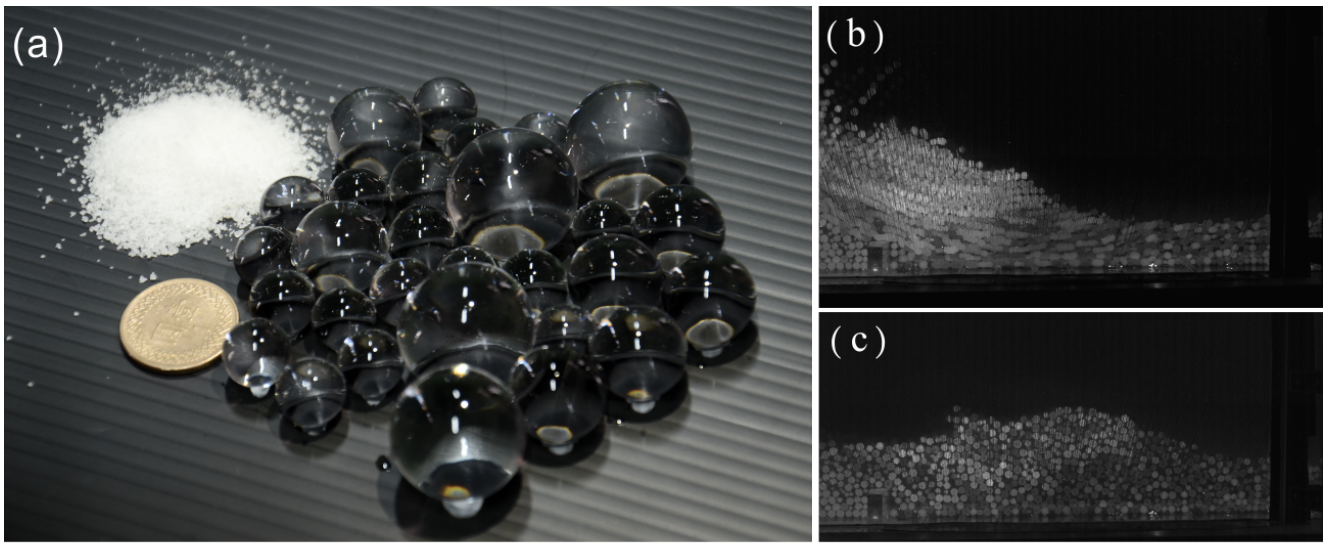

Fig.1 Experimental image (a)wide range of particle size; (b)longexposure image of dam break occurrence; (c)particles with different concentration of dye.

©2019. Japan Geoscience Union. All Right Reserved.

Sandbox experiments of submarine landslide caused by water film in low permeability layer

*Shogo Kawakita[1], Daisuke Asahina[2], Keiji Kitajima[3], Mitsukazu Nakanishi[3]

1. Graduate School of Science & Technology, Nihon Univ., 2. National Institute of Advanced Industrial Science and Technology, 3. College of Science & Technology, Nihon Univ.

Submarine landslides can be serious geohazards since they potentially cause tsunamis and damage seafloor infrastructure. Submarine landslides can be larger in scale than landslides on land. Direct measurements/observations of submarine landslides at deep seafloor still remain a challenging task. Kokusho et al. (2000) proposed a water film effect and its mechanism on lateral flow with less frictional resistance to explain a driving force of large-scale submarine landslides

In this study, we conducted laboratory experiments to understand the relationship between sand liquefaction and lateral flow by water film, and investigate the influence of water film formation on lateral flow of upper layer. In general, it is difficult to observe the formations of liquefaction and lateral flow at the same time. This is because sand particles of sloping layer model start to move when vibration is applied, and inclination disappears before liquefaction. To solve this problem, we devised a mechanism to prevent the flow of the lower layer by providing a weir plate in inside the soil tank. This mechanism enables to distinguish and observe the movement of sand by the liquefaction and the lateral flow by the water film.

The results obtained in this study clearly show three stages: first, the lower layer was liquefied; then pore water was stored below the low permeability layer; and finally, the lateral flow was occurred by the water film effect. The experimental results show that there was no clear correlation between the increase in the angle of sloping layer and the travel distance or the maximum flow velocity. We also discuss the relationship between the layer angle and the location of sand boil. The location where sand soiling occurred moved to the upper side of the slope as the layer angle become larger.

[Reference]

Kokusho, T.: Mechanism for water film generation and lateral flow in liquefied sand layer, Soils and Foundations, Vol.40, No.5, p 99-111, 2000.

Keywords: Submarine Landslides, Pore Water Pressure, Water Film, Lateral Flow

©2019. Japan Geoscience Union. All Right Reserved.

Study on Creep Properties of Sand and Cemented Sand

*JIN-YI YU[1], KUANG-TSUNG CHANG[1]

1. National Chung Hsing University

In this study, we investigated the effects of creep on sand and cemented sand, using triaxial test. Sand represents a non-cohesive material, while cemented sand represents a brittle material. Before the failure of specimens, the deviator stress was fixed and the cyclic mean stress was applied to study the influence of creep on the materials. According to the test results, the axial strain accumulation of sand caused by creep is less, and the peak strength is larger than that of the monotonic loading when the axial loading is resumed. For cemented sand, creep causes microcracks inside the specimens, gradually forming a failure surface. When the axial strain accumulation is large enough, the reapplication of the axial loading shows a reduction of peak strength. We conclude that the influence of creep on non-cohesive material (sand) is limited, whereas creep can reduce the strength of the brittle material (cemented sand) and even cause failure.

Keywords: creep, triaxial test, sand, cemented sand, strength, failure

©2019. Japan Geoscience Union. All Right Reserved.

The effects of seepage force and the Poisson’s ratio on slope stability

*Hirokazu Fukui[1], Tomomi Terajima[2]

1. Graduate school of Science, Kyoto University, 2. Disaster Prevention Research Institute, Kyoto University

To predict accurately the timing of shallow landslide occurrence, we need to consider the direction and magnitude of seepage force and earth pressure. A model sandy slope (L: 9m, W:1m, H:4m) was used to measure the hydraulic gradient and seepage force with the tensiometers under the artificial rainfall of 80mm/h. We incorporated not only the seepage force but also the Poisson’s ratio into conventional slope stability analysis by the limit equilibrium method. As a result, the calculated timing of shallow landslide occurrence was almost agree with the timing of that in the experiment and also more accurate than the timing calculated by the Spenser method which took into account the magnitude and moment equilibrium of the force. These results imply that, based on both monitoring at fields and conducting more experiments by a real-size model slope, we need to verify the effects of seepage force and earth pressure as the important factors causing rainfall-induced slope instability.

Keywords: process-based model, Seepage force, the Poisson's ratio, Shallow landslide, Sandy model slope

©2019. Japan Geoscience Union. All Right Reserved.

Study on the factors of seepage erosion

*Szu-Wei Fu[1], Kuang-Tsung Chang[1]

1. National Chung Hsing University

The causes of many slope disasters are often related to the seepage behaviors of soil. For instance, groundwater seepage may cause internal erosion of the soil. The soil particles are taken away by seepage water to form void or pipe. In addition , the earth pressure leads to the collapse of the overlying soil.

In this study, we designed a set of apparatus that can add confining pressure to the outside of the specimen. In order to simulate the situation of sand in slopes, we investigated the critical seepage velocity of sands caused by seepage erosion failure under different confining pressure, with different particle size distributions, sizes of outflow, etc. Then a failure criterion for seepage erosion is developed based on the drag equation in fluid dynamics and confirm with experimental data.

The results show that the critical seepage velocity at failure is affected by the particle size distributions, sizes of outflow and the confining pressure. The theoretical results are compared well to the experimental data.

Keywords: seepage erosion, Drag equation

©2019. Japan Geoscience Union. All Right Reserved.

Deformation of slope models with different orientations of weak planes

*taeyuan tseng[1], Kuang-Tsung Chang[1]

1. National Chung Hsing University

Weak planes influence failure and deformation of slopes. We conducted experiments to simulate slopes of different orientations of weak planes, including cataclinal and analcinal slopes with 30˚ and 60˚ inclination angles of weak planes. We stacked artificial bricks to make small-sized slope models. The artificial bricks were made of gypsum, sand, cement and water with different weight proportion. In view of the scaling law, the artificial bricks were made less strength than natural rocks. The slope models were weakened under rainfall, resulting in deformation and final collapse. The slope deformation processes were photographed by a camera, and the displacement vector fields were analyzed using the Particle Image Velocimetry (PIV). The deformation and accumulated displacements were compared between slopes of different orientations of weak planes.

Keywords: cataclinal slope, analcinal slopes, rainfall, Particle Image Velocimetry (PIV), weak planes, deformation

©2019. Japan Geoscience Union. All Right Reserved.

[E] Poster | H (Human Geosciences)：H-TT Technology & Techniques

Tue. May 28, 2019 3:30 PM - 5:00 PM JST | Tue. May 28, 2019 6:30 AM - 8:00 AM UTC | Poster Hall International Exhibition Hall8, Makuhari Messe_13

[H-TT18] Development and application of environmental traceability methods

convener:Ichiro Tayasu(Research Institute for Humanity and Nature), Nobuhito Ohte(Department of Social Informatics, Graduate School of Informatics, Kyoto University), Gabriel J Bowen(University of Utah)

Modern society uses almost all the elements present in the natural world. Although there have long been calls for the sustainable use of the resources that provide these elements and the building of human societies that are in harmony with the environment, the survival of the human race is increasingly at risk as a result of qualitative changes to the environment as a whole. Implementation by the society of methodologies for diagnosing and tracking these various elements of the natural environment and their relationships with humans are now required.
Elements cycle within and among the Earth system spheres, human society and the human body. Information on the concentrations and stable isotopes of elements is powerful tool for tracing this cycling and has been applied in studies of atmosphere-hydrosphere circulation, ecological systems, and the life, health and history of humans. We propose a session to discuss development and applications of environmental traceability methods toward the goal of establishing traceability in natural and human systems.
We encourage the presentation of research integrating isotopic information in various disciplines, such as geochemistry, hydrology, ecology, geology, mineralogy, anthropology, food science, and forensics. Studies applying "Isoscapes", maps of spatial isotopic variation, in addition to traditional database-based approaches, are strongly encouraged.

[HTT18-P01] Isotopic study on seasonal nitrogen dynamics at Lake Biwa

*Takaaki Ishibashi[1], Ken'ichi Osaka[1], Keisuke Koba[2], Takashi Nakamura[3], Kei Nishida[3] (1.Department of ecosystem study, University of Shiga Prefecture, 2.Center for Ecological Research, Kyoto University, 3.International Research Center for River Basin Environment, University of YAMANASHI)

[HTT18-P02] Relationship between residence time, water quality, and stable isotopes of spring water and groundwater in coastal area of Fukushima prefecture

*Shiho Yabusaki[1], Kazuyoshi Asai[2] (1. Research Institute for Humanity and Nature・Faculty of Symbiotic Systems Science, Fukushima University, 2.Geo Science Laboratory)

[HTT18-P03] Applicability evaluation of CIA due to river and lake

*yusuke hataya[1], SEIKI KAWAGOE[1], Shiho Yabusaki[2], KEN Suzuki[1] (1.fukushima university, 2.Research Institute for Humanity and Nature)

[HTT18-P04] Chemical property analysis of short time scale to determine snowfall source

*Suzuki hiromichi[1], SEIKI KAWAGOE[1], SHO ADACHI[1], Shiho Yabusaki[2] (1.Fukushima University, 2.Research Institute for Humanity and Nature)

[HTT18-P05] Analyzing the origin of surface water in the Saijo Plain, Japan, based on the antimony concentration in the water

*Minoru TOKUMASU[1,2], Ki-Cheol SHIN[3], Yoshihiro YAMADA[4] (1.The United Graduate School of Agricultural Sciences, Ehime University, 2.Saijo City, 3.The Research Institute for Humanity and Nature (RIHN) , 4.Kagawa University, Faculty of Agriculture)

[HTT18-P06] Basic kinetic study on stable isotope ratios of nitrogen compounds: a case study for groundwater in the Kathmandu Valley, Nepal

*Ken Yokozawa[1,2], Kei Nishida[1,3], Takashi Nakamura[1,3], Ken'ichi Osaka[4] (1.University of Yamanashi, 2.Special Graduate Program on River Basin Environmental Science,, 3.ICRE, 4.Department of ecosystem study Univercity of Shiga prefecture)

[HTT18-P07] Usefulness of strontium isotope composition for determining the geographical origin of wasabi and potato

*Takafumi Kamitani[1], Ki-Cheol Shin[2], Sachiko Nakamura[1], Rika Koda[1], Tomoya Oka[1], Noriaki Fushimi[1], Yasuhide Muranaka[1] (1.Shizuoka Institute of Environment and Hygiene, 2.Research Institute for Humanity and Nature)

[HTT18-P08] Reconstruction of sea surface temperature and salinity for the Medieval Climatic Anomaly using a long-lived fossil coral collected at Ishigaki Island, southwestern Japan

*Osamu Abe[1], Maki Morimoto[2], Ryuji Asami[3], Takeshi Nakatsuka[1,4] (1.Graduate School of Environmental Studies, Nagoya University, 2.School of Education, Gifu University, 3.Graduate School of Science, Tohoku University, 4.Research Institute for Humanity and Nature)

[HTT18-P09] Development of the analytical method for sulfur isotope in SO_2 gas

*Masaaki Takahashi[1], Hiroyuki Sase[1], Tsuyoshi Ohizumi[1] (1.Asia Center for Air Pollution Research)

[HTT18-P10] Zinc isotope analysis on human tooth enamel samples to reconstruct diet of the Jomon period.

*Soichiro Kusaka[1], Ki-Cheol Shin[2] (1.Tokai Univ., 2.Research Institute for Humanity and Nature)

[HTT18-P11] Zinc stable isotope analysis of environmental reference materials

*Ki-Cheol Shin[1] (1.Research Institute for Humanity and Nature)

Isotopic study on seasonal nitrogen dynamics at Lake Biwa

*Takaaki Ishibashi[1], Ken'ichi Osaka[1], Keisuke Koba[2], Takashi Nakamura[3], Kei Nishida[3]

1. Department of ecosystem study, University of Shiga Prefecture, 2. Center for Ecological Research, Kyoto University, 3. International Research Center for River Basin Environment, University of YAMANASHI

To clarify nitrogen dynamics in Lake Biwa, we measured the concentrations of nitrogen compounds and their nitrogen stable isotopic ratios in 14 depths in north basin of Lake Biwa. In the lake, particulate nitrogen (PN), such as phytoplankton, is generally decomposed to dissolved nitrogen (DN); in order of dissolved organic nitrogen (DON), ammonia nitrogen (NH_4^+) and nitrate nitrogen (NO_3^-). These dissolved nitrogen compounds are taken up by phytoplankton again, and the nitrogen circulation in the lake is established. To predict the water quality in future, it is necessary to understand the nitrogen cycle in the lake, as well as nutrient load to the lake.

In this study, we collected lake water sample at 14 depths in north basin of Lake Biwa (water depth is 90 m) in 1-2 months interval. The lake waster sample was analyzed for the concentration of PN, PC, DN, NO_3^-, NO_2^- and NH_4^+, $d^{15}N$ of PN, DN and NO_3^-.

NO_3^- concentration was lower in the surface layer (0-20m), and higher in the deep layer (20-90m) during the stratification period, whereas NO_3^- concentration was constant in all layers during the circulation period. PN concentration also increased in the surface layer from April to June, decreased sharply in July. These indicate that phytoplankton which grew on the surface layer from April to June used NO_3^-, thereafter, NO_3^- was depleted after June, then, phytoplankton decreased after July respectively. On the other hand, NO_3^- concentration is considered to be increased by decomposition of the precipitated PN from surface layer. It is considered that the NO_3^- concentration became constant in all layers because of mixing of deep layer and the surface layer.

The weighted average $d^{15}N_{DN}$, $d^{15}N_{NO3}$ in the unit water columns decreased about 3‰ in the circulation period, in the circulation period, then, increased during the stratification period. The decrease of $d^{15}N_{DN}$, $d^{15}N_{NO3}$ at the water column during circulation period can not be explained by mixing of deep layer and the surface layer. We will discuss the mechanisms of $d^{15}N_{DN}$, $d^{15}N_{NO3}$ decrease during circulation period in the presentation.

Keywords: nitrogen dynamics, nitrogen isotope, seasonality

©2019. Japan Geoscience Union. All Right Reserved.

Relationship between residence time, water quality, and stable isotopes of spring water and groundwater in coastal area of Fukushima prefecture

*Shiho Yabusaki[1], Kazuyoshi Asai[2]

1. Research Institute for Humanity and Nature・Faculty of Symbiotic Systems Science, Fukushima University, 2. Geo Science Laboratory

After the Great East Japan Earthquake occurred, the investigation near the coast area in northern part of Fukushima prefecture has been carried out to clarify the groundwater flow and residence time in this area. The measuring of EC, pH, water temperature, ORP and sampling of groundwater, spring water and river water have been carried out several times at Shinchi town, Soma city, Minamisoma city, Namie town, Okuma town, Iitate village and Date city since September in 2012. The inorganic ions, stable isotopes of oxygen and hydrogen, trace elements were analyzed for all samples by using the IC (ICS-3000), CRDS (Picarro L2130-i) and ICP-MS (Agilent 7500cx). For estimating the residence time, tritium concentration, CFCs and SF_6 measurements were made in several samples.

The water quality of river water and shallow groundwater indicates mainly Ca-HCO_3 type. In the part of the flooded area by a tsunami, the water quality of shallow groundwater and spring water is Na-Cl type. The Ca-SO_4 type and mixed type were also confirmed in some sites. In the case of deep groundwater, the water quality shows the Na-HCO_3 type and Ca-HCO_3 type. The concentration of Fe, Mn and Al were relatively high in some parts of deep groundwater. It is considered that the origin of these trace elements is soil.

The stable isotopes of oxygen and hydrogen ($\delta^{18}O$ and δD) in river water of Niida river, Mano river and Kamimano river indicate altitude effect. Because the stable isotopes in deep groundwater is relatively low, it is anticipated the recharge are of deep groundwater is about 300 m higher than that of shallow groundwater. It is expected that the recharge area of deep groundwater is around the Abukuma Mountains.

The average residence time of deep groundwater and spring water which indicate the Na-HCO_3 type is about 60 to 70 years. On the other hand, the average residence time of shallow groundwater which indicate the Ca-HCO_3 type is less than 10 years.

The information of groundwater flow is useful for considering the groundwater use with revival of the coastal area. We will continue the investigation of coastal area and make clear the groundwater flow system.

Keywords: Minamisoma city, Fukushima prefecture, CFCs・SF6, residence time, water quality, stable isotopes, groundwater flow

©2019. Japan Geoscience Union. All Right Reserved.

Applicability evaluation of CIA due to river and lake

*yusuke hataya[1], SEIKI KAWAGOE[1], Shiho Yabusaki[2], KEN Suzuki[1]

1. fukushima university, 2. Research Institute for Humanity and Nature

Water resources management must be further attention because extreme weather condition generate to predict climate change. However, a water area have the various regional characteristics. Therefore a universal way may not also be able to indicate the effect management. If categorized basin tool is developing to obtain characteristic, it is possible to choose suitable management technique in water areas. We tried to develop database to manage basin as chemical and geographical information. In this research, Water factors (Chemical condition, land use condition, soil condition and geological condition) between basins (rivers and reservoirs) were compared to develop data base. Especially, we applied to Chemical Index of Alteration (CIA) as chemical condition factor. As results, It was possible to obtain the basin area scale to apply CIA.

Keywords: CIA, water resource, Numerical geographic information

©2019. Japan Geoscience Union. All Right Reserved.

Chemical property analysis of short time scale to determine snowfall source

*Suzuki hiromichi[1], SEIKI KAWAGOE[1], SHO ADACHI[1], Shiho Yabusaki[2]

1. Fukushima University, 2. Research Institute for Humanity and Nature

Occurrence of the strange weather phenomenon is predicted from the current state depending on climate change. To ask this influence, we have to advance the match which raises the future predictability. And, we have to mark a phenomenon of the current state detail. This study targets to obtain chemically snow environment. The aim of this study was to analyse and predict the stable water isotopic composition of the snow cover at specific basin (Agano river). In addition, the dependence of short time step isotopic composition of the entire snow cover was analysed. Snow in 3 catchments was sampled at the end of the accumulation period from December 2016 to April 2018. The observed variability of short time step isotopic composition of the snow cover was analysed chemical verification. Especially, basin The Inawashiro-Lake north side of the northern upstream region indicated the low chemical feature (Suzuki et al 2018). I'm working on the investigation analysis to grasp the chemical special quality of the snow event of the short time scale at present based on this result (2016-2018). It was that a chemical analysis makes the sample which sampled and acquired it by each day the time of a snowfall at Fukushima, Hibara and Yonezawa located in an upstream region in a basin, and we tried to follow up a snowfall origin of the short time scale.

As results, a strong pressure pattern of southern high and northern low could admit January 22nd-the 25th, the result obtained from the result of analysis also reacted to the weather situation sensitively. And influence of a characteristic snowfall origin was admitted at 3 spots. The difference in the spatial time lags was done clearly.

Keywords: d-excess value, isotope, short time scale

©2019. Japan Geoscience Union. All Right Reserved.

Analyzing the origin of surface water in the Saijo Plain, Japan, based on the antimony concentration in the water

*Minoru TOKUMASU[1,2], Ki-Cheol SHIN[3], Yoshihiro YAMADA[4]

1. The United Graduate School of Agricultural Sciences, Ehime University, 2. Saijo City, 3. The Research Institute for Humanity and Nature (RIHN) , 4. Kagawa University, Faculty of Agriculture

1. Introduction

The flow of river water in many medium and small rivers is managed for water use and flood control. However, it is almost impossible to understand how the water taken from the rivers circulates throughout a basin. The source of water in the Saijo Plain in Ehime Prefecture is from the Kamo River surface water flow, shallow groundwater (unconfined ground water), and deep groundwater (confined ground water). Therefore, it is necessary to quantitatively clarify the source of water for sustainable water use. In this study, we tried to quantify the origin of river water in the plain based on the concentration of some chemical elements. In particular, antimony (Sb) was used as the main trace element because of large differences in its concentration between the water sources.

2. Materials and Methods

On November 25 and 26, 2017, during the non-irrigation period and on the 27th and 28th of July, 2018, during the irrigation period, surface water was collected at a total of 43 sites on small and medium rivers and waterways in the Saijo Plain. Multi-element analysis was carried out on the collected water using ICP-MS 7500 cx.

3. Results and Discussion

There was a large difference in the concentration of Sb among the sites. The highest concentration was found in the water from the Ichino River (Stn. 2) at 113 (2017) and 158 μg/L (2018). There was once an antimony mine in the Ichino River basin, so high concentrations of the element in the river water can be regarded as reflecting the influence of the geology. In the main stream of the Kamo River before joining the Ichinose River (Stn. 1), the Sb concentration was as low as 0.2 μg/L, and after the junction of the two rivers (Stn. 3), the concentration increased to 4.3 (2017) and 7.2 μg/L (2018). The concentration was 4.2 (2017) and 7.2 μg/L (2018) at Stn. 4 of the Kamo River, 11.6 (2017) and 11.7 μg/L (2018) in the unconfined ground water (average of Stns. 13, 14, 15), and 0.4 (2017) and 0.5 μg/L (2018) in the confined ground water (average of Stns. 28, 29, 40, 41, 43). The concentration of Si was 2.7 (2017) and 3.2 mg/L (2018) at Stn. 4 of the Kamo River, 3.4 (2017) and 2.9 mg/L (2018) in the unconfined ground water (average of Stns. 13, 14, 15), and 4.1 (2017) and 3.9 mg/L (2018) in the confined ground water (average of Stns. 28, 29, 40, 41, 43).
The ratio of water origin at each survey site was estimated using the above three sources as end members. In the upstream area, the irrigation water taken from the Kamo River occupied most of the surface water. In the middlestream area, the ratio of water taken from the rivers was smaller, and the contribution of

©2019. Japan Geoscience Union. All Right Reserved.

unconfined ground water exceeded 80%. In the downstream area, the confined ground water contribution exceeded 40% at many sites. In the Saijo Plain, the water origins are different in the upstream, middlestream, and downstream areas, where the contribution of irrigation water is small overall, and the contribution of the confined ground water is large.

©2019. Japan Geoscience Union. All Right Reserved.

Basic kinetic study on stable isotope ratios of nitrogen compounds: a case study for groundwater in the Kathmandu Valley, Nepal

*Ken Yokozawa[1,2], Kei Nishida[1,3], Takashi Nakamura[1,3], Ken'ichi Osaka[4]

1. University of Yamanashi, 2. Special Graduate Program on River Basin Environmental Science,, 3. ICRE, 4. Department of ecosystem study Univercity of Shiga prefecture

Groundwater is a valuable source of water in developing countries where water demand is increasing with population increase. At the same time, nitrogen contamination by industrial wastewater, domestic wastewater and agricultural activities has been reported. In underground environments, it is not unusual to identify sources of contamination since the forms and the concentrations of nitrogen compounds vary at different water flow or microbial metabolism. Stable isotopic analysis is one of the effective methods to detail the variations. However, the isotope value is also greatly affected by environmental conditions, and the theoretical enforcement for describing the variation of the isotope value is needed. In this study, we aimed to quantitatively understand and identify the factors of mixing and isotopic fractionation that determine the stable isotope ratio with a case study on groundwater contamination in the Kathmandu Valley, Nepal.

The data used for the analysis was obtained from the groundwater survey of the Kathmandu Valley conducted from September 2014 to August 2018. Based on the stable isotope ratios of nitrogen and oxygen of nitrate, the contamination patterns were roughly categorized. The mixing line and the denitrification line were prepared based on the dynamic fractionation for the stable isotope ratios of nitrate nitrogen, and the spatial distribution of denitrification-related samples was examined on the map. In addition, assuming that the reactants exist sufficiently and homogeneously in the system, an equilibrium fractionation model was formulated by combining nitrification and denitrification for oxygen stable isotope ratios of nitrate and water. The range of the model parameters were determined by using the measured data from the filed survey, the influence of each process on the stable oxygen isotope ratio of nitrate was quantified.

The result showed that the nitrate in shallow groundwater partially originated from the atmospheric source through infiltration of rainwater. A characteristic of denitrification was observed, which was initiated and proceeded over the valley. Additionally, the correspondent isotopic fractionation differed at the location and the season, particularly controlled by ammonia oxidation, nitrite reduction and oxygen exchange between nitrite and water.

Keywords: groundwater , nitrogen and oxygen stable isotope ratios, nitrification, denitrification, mixing, fractionation

©2019. Japan Geoscience Union. All Right Reserved.

Usefulness of strontium isotope composition for determining the geographical origin of wasabi and potato

*Takafumi Kamitani[1], Ki-Cheol Shin[2], Sachiko Nakamura[1], Rika Koda[1], Tomoya Oka[1], Noriaki Fushimi[1], Yasuhide Muranaka[1]

1. Shizuoka Institute of Environment and Hygiene, 2. Research Institute for Humanity and Nature

Originally, the use of strontium isotope ratios ($^{87}Sr/^{86}Sr$) was restricted to geology and petrology, but they have been used as a particularly effective tracer of geographical food origin, as plants reflect the strontium isotope composition of the regionally based rock, soil, and water. This study aims to evaluate the usefulness of $^{87}Sr/^{86}Sr$ for determining the geographical origin of wasabi (Japanese horseradish) and potato, which are specialty crops in Shizuoka Prefecture, Japan.

Wasabi is cultivated in springs and streams located at the top of rivers, where dissolved element and isotopic compositions in water would reflect the geological characteristics without the effects of atmospheric deposition and human activity. We collected wasabi and water samples from 40 locations of major production areas in Japan: Shizuoka, Iwate, Nagano, Tokyo, and Shimane. These samples were subjected to trace elements and $^{87}Sr/^{86}Sr$ analyses. The $^{87}Sr/^{86}Sr$ values differed, based on the geological characteristics of their site locations, and the value of wasabi was well accorded with that of water in the same location. The wasabi samples collected from Izu Peninsula and Mt. Fuji regions in Shizuoka, where young volcanic rocks such as Quaternary basalts are distributed, had low $^{87}Sr/^{86}Sr$ (below 0.7040), whereas those from Nagano and Tokyo, where older rocks such as Mesozoic granites and accretionary complex are distributed, showed higher ratios (over 0.7095). We conclude that $^{87}Sr/^{86}Sr$ value of wasabi allowed us to distinguish the production area clearly.

On the other hand, the $^{87}Sr/^{86}Sr$ values of crops cultivated in the field are considered to be partly affected by precipitation and fertilizer. Therefore we conducted field survey and planter test for potato in Shizuoka. Field survey was conducted at Mishima, in eastern part of Shizuoka prefecture, and at Mikatahara, in western part of it, and $^{87}Sr/^{86}Sr$ of potato and soil exchangeable fraction were compared. As a result, there was a correlation between potato and soil in $^{87}Sr/^{86}Sr$, although the effects of precipitation and fertilizer were observed. The planter test suggests that the influence of fertilizer on $^{87}Sr/^{86}Sr$ varies depending on the amount of exchangeable Sr contained in the original soil.

Keywords: geographical origin, strontium isotope ratio, wasabi, potato, Shizuoka

©2019. Japan Geoscience Union. All Right Reserved.

Reconstruction of sea surface temperature and salinity for the Medieval Climatic Anomaly using a long-lived fossil coral collected at Ishigaki Island, southwestern Japan

*Osamu Abe[1], Maki Morimoto[2], Ryuji Asami[3], Takeshi Nakatsuka[1,4]

1. Graduate School of Environmental Studies, Nagoya University, 2. School of Education, Gifu University, 3. Graduate School of Science, Tohoku University, 4. Research Institute for Humanity and Nature

The period between 950 and 1250CE is called as the Medieval Climate Anomaly (MCA; Masson-Delmotte et al., 2013), at the time when the warmer climate seemed dominant globally (Bradley et al., 2003). Recent investigations based on the proxy record such as tree-ring widths, speleothems, ice cores, and historical documents indicated that a significant climate change occurred during the latter half of the 10th century. Mann et al. (2009) found that an increase of the average air temperature in the northern hemisphere at the late 10c. coincided with an increase of sea surface temperature at northern subpolar oceans. Yan et al. (2011) indicated that atmospheric environments in the equatorial Pacific shifted from the La Nina like condition to the El Nino like condition around 1000CE. In East Asia, Zhang et al. (2008) and Ge et al. (2013) described that the activity of East Asian Summer Monsoon (EASM) had been enhanced during the late 10c., then the climate in China shifted to warmer and wetter. Whereas Lie et al. (2014) showed that the EASM had been weakened during the 11th century. In addition, the climate in southern China was reported as relatively dry (Chen et al., 2015).

These studies demonstrated that a large climatic shift occurred around 1000CE, however, most of them have relied on records collected on land. There is little long-term high-resolution marine record during the MCA.

We reconstructed sea surface temperature (SST) and salinity with a temporal resolution of one month for 300 years using a long-lived fossil coral collected at Ishigaki Island, southwestern Japan. Based on the U/Th dating in the youngest part of the coral skeletons as well as the band counting, this coral sample had lived between 845 and 1130CE, largely covered the MCA period. Skeletal Sr/Ca and oxygen isotopic composition were analyzed for about 4,000 samples.

The empirical equations between Sr/Ca and water temperature; between oxygen isotopic composition of coral skeleton and seawater, and water temperature, were established using the present coral records, observed water temperature and oxygen isotopic composition of seawater. With these equations and the relationship between seawater salinity and oxygen isotopic composition, proposed by Abe et al. (2009), SST and seawater salinity from 845 to 1130CE were reconstructed from the fossil coral Sr/Ca and oxygen isotopic composition.

Through the entire period, average summer and winter SSTs were 2 and 1 deg. C higher than the present, respectively. In addition, SST increased significantly after 1040CE; 0.9 for the annual average, 0.7 for summer and 1.1 for winter. Salinity also increased after 990CE; 0.8 all for the annual average, summer and winter. Salinity was significantly higher through the entire period than the present, however, its absolute value seems unconfirmed yet.

©2019. Japan Geoscience Union. All Right Reserved.

Increasing SST and salinity found in this study during ca. 1000 and 1130CE were consistent with the weakening of EASM during the 11th and 12th centuries shown by Liu et al. (2014). They argued the weakening occurred as a consequence of weakening of the solar activity and the decrease of SST at the western Pacific warm pool. In this study region, the decrease of precipitation during the Baiu period induced the increase of salinity as well as local SST increase due to the decrease of the cloud cover. Our results were also consistent with the warming of China in the late 10c. (Ge et al., 2013), and a drier condition in southern China (Chen et al., 2015).

The periodicity of SST and salinity based on the spectral analysis will be discussed in the presentation.

Keywords: Coral annual bands, Medieval Climate Anomaly

©2019. Japan Geoscience Union. All Right Reserved.

Development of the analytical method for sulfur isotope in SO_2 gas

*Masaaki Takahashi[1], Hiroyuki Sase[1], Tsuyoshi Ohizumi[1]

1. Asia Center for Air Pollution Research

1. Introduction

Sulfur is a major source of acid deposition. Usually sulfur is emitted as SO_2 and it is oxidized to SO_4^{2-} in atmosphere. S isotopic analysis of water and particulate samples were conducted in many studies. But gaseous SO_2 was rarely used for isotopic study. Isotopic ratio of SO_2 is strongly influenced by emission source near the sampling point. Because most of SO_2 emitted far from sampling point is oxidized to SO_4^{2-} during transportation. It is possible to distinguish domestic emission from transboundary emission. Moreover, dry deposition processes of SO_2 and particulate SO_4^{2-} and their interactions with tree canopy could be discussed more precisely. Isotopic analysis of SO_2 is considered as a powerful method to investigate the behavior of S in the atmosphere and ecosystems. We studied about the analytical method for S isotope in SO_2.

2. Method

(1) Equipment

SO_2 concentration in Japan is very low (e.g. annual 0.02ppb at Sado). We need to collect air sample at least $1m^3$ that is the amount we can obtain 1.2mg of $BaSO_4$ precipitation enough for isotopic analysis. High volume air sampler is generally used to collect around $1m^3$ of air sample. It uses filter, so we examined filter collection of SO_2 by K_2CO_3 filter generally used to collect SO_2 in filter-pack method.

(2) Filters

We used quarts filter for particulate SO_4^{2-} and K_2CO_3 filter for gaseous SO_2 next to it. K_2CO_3 filter is made on the basis of EANET manual. But to get enough flow rate for high volume air sampler, the size of K_2CO_3 filter is larger (20×26 cm, same size with quarts filter) than the manual and already dried before sampling.

(3) Flow rate/leak test

Under flow rate 100~400 L/min in this system, we confirmed weather sampling can be carried out stably. And we checked leak using two K_2CO_3 filters.

(4) Sample treatment

©2019. Japan Geoscience Union. All Right Reserved.

On the basis of EANET manual, the sample was extracted with 0.05% H_2O_2aq and filtered. Then 2N HCl was added and concentrated to remove CO_3^{2-}. Next 1%(w/w)$BaCl_2$ was added. We filtered forming $BaSO_4$ precipitation. We examined the method to get $BaSO_4$ precipitation and to remove the components from K_2CO_3 filter.

3. Results

(1) Sampling and sample treatment

Sampling could be conducted under flow rate 100~400 L/min. Sampling efficiency was about 80%..

Several conditions to get $BaSO_4$ precipitation ware examined, it could be gotten by the method as below.

Filter was cut and ultrasonic extracted with 0.05% H_2O_2aq 30 minutes and filtered. 2.5 ml of 2N HCl was added and concentrated to around 10 ml. Then 1 ml of heated 1 %(w/w) $BaCl_2$ was added under pH 4~6. Next evaporated all solvent and added 10 ml of water. $BaSO_4$ precipitation was observed. After put for one night, the precipitation was separated by centrifuge 3,600 rpm for 10 minutes and we removed the solvent. The precipitation was washed twice by 10 ml of water and filtered. At last the filter was ashed for four hours in muffle furnace in 800 ℃ .

(2) Actual analysis

We used two K_2CO_3 filters and collected 2160.2 m^3 of air sample under flow rate 300 L/min. 3.80 mg of particular SO_4^{2-} and 0.89 mg (first) and 0.14 mg (second) of SO_4^{2-} from SO_2 were obtained. $\delta^{34}S$ of particular SO_4^{2-} was 8.64 ‰and that of SO_2 from the first filter was -1.54 ‰. The amount of precipitation from second filter was not enough for isotopic analysis. This difference was caused by effect of sea salt mainly. But nss- $\delta^{34}S$ of particular SO_4^{2-} was 4.78 ‰. It was still higher than SO_2. It suggested that nss- SO_4^{2-} contains both transboundary SO_4^{2-} and domestic SO_4^{2-}. According to the relevant literature, domestic SO_2 may have negative isotopic values because of imported oil from Middle East. Considering that this sampling was carried out in January, possible effect of transboundary SO_2 with higher isotopic values should also be taken into account for source identification of the collected SO_2.
We would like to discuss at the conference with the latest data.

Keywords: sulfur isotope, SO2 gas

©2019. Japan Geoscience Union. All Right Reserved.

Zinc isotope analysis on human tooth enamel samples to reconstruct diet of the Jomon period.

*Soichiro Kusaka[1], Ki-Cheol Shin[2]

1. Tokai Univ., 2. Research Institute for Humanity and Nature

This study investigates zinc isotope ratios in tooth enamels of human skeletal remains of the Jomon period in Japan. Carbon and nitrogen isotope analysis on bone collagen were traditionary used to reconstruct diet and trophic levels on prehistoric people. The progress of isotope measurements using MC-ICP-MS enables us to analyze isotope ratios of zinc and other metals. Some researches report that the zinc isotope ratios of animals reflect dietary sources and vary according to trophic levels. This study newly develops zinc isotope analysis on human tooth enamels. The zinc isotope analysis has great potential to reconstruct dietary information from inorganic materials of archaeological bones or fossils.

The material used in this study is SRM1400 (bone ash), six samples of human tooth enamels from the Yoshigo and Inariyama shell mounds of Aichi prefecture, and faunal remains (six deer enamels, three boar enamels, six marine fish bones, and six modern plant leaves). Zinc was purified from these samples using anion exchange resin. Zinc isotope ratios were measured by MC-ICP-MS with the zinc standard solution of AA-ETH. The mass bias was corrected with Cu standard solution added to all standards and samples. The zinc isotope ratios of SRM1400 showed similar value with the value previously reported. The difference of zinc isotope ratios between washed and unwashed samples with acetic acids were very small, suggesting no significant diagenetic alteration. The deer and marine fish samples showed the value expected from their dietary ecology. The zinc isotope ratios of Jomon skeletal remains was higher than those of plants, but lower than deer and marine fish. This result indicates that sources of zinc for humans were terrestrial and marine meat as well as terrestrial plants.

Keywords: Zinc Isotope, Jomon period, Human skeletal remains

©2019. Japan Geoscience Union. All Right Reserved.

Zinc stable isotope analysis of environmental reference materials

*Ki-Cheol Shin[1]

1. Research Institute for Humanity and Nature

Zinc has atomic number 30 and atomic mass 65.39. It is a trace element of terrestrial rocks and widely distributed throughout the lithosphere and biosphere. It is chalcophile features and has rich coordination chemistry, participates in a large number of important biological compounds and reactions. The zinc plays an important role as an essential trace metal in all living systems from bacteria to humans. Zn has five stable isotopes ^{64}Zn, ^{66}Zn, ^{67}Zn, ^{68}Zn, and ^{70}Zn. Their isotopic fractionation could provide valuable information about environmental processes, especially in biological processes.

With the advent of multi-collector ICP-MS, it is possible to measure the precise value of ^{66}Zn/^{64}Zn in Zn solution. To promote the environmental stable isotope traceability, RIHN is desired to determine the isotope ratios of zinc for environmental reference materials with high precision and accuracy, rapidness, and convenience.

Here, I report a simple and efficient method for zinc isotope analysis. The various environmental samples over 20 types were used for the study. All samples have purified with an anion exchange resin to separated Zn and Fe at a time. Zinc isotope ratios were measured by MC-ICP-MS (NEPTUNE plus) with AA-ETH, which is a new zinc isotopic standard solution reported by Archer et al. (2017). The mass bias correction conducted with Cu standard solution (NIST SRM 976).

Keywords: stable isotope , Zinc, environmental reference materials

©2019. Japan Geoscience Union. All Right Reserved.

[E] Poster | H (Human Geosciences)：H-TT Technology & Techniques

Tue. May 28, 2019 5:15 PM - 6:30 PM JST | Tue. May 28, 2019 8:15 AM - 9:30 AM UTC | Poster Hall International Exhibition Hall8, Makuhari Messe_23

[H-TT18] Development and application of environmental traceability methods

convener:Ichiro Tayasu(Research Institute for Humanity and Nature), Nobuhito Ohte(Department of Social Informatics, Graduate School of Informatics, Kyoto University), Gabriel J Bowen(University of Utah)

Modern society uses almost all the elements present in the natural world. Although there have long been calls for the sustainable use of the resources that provide these elements and the building of human societies that are in harmony with the environment, the survival of the human race is increasingly at risk as a result of qualitative changes to the environment as a whole. Implementation by the society of methodologies for diagnosing and tracking these various elements of the natural environment and their relationships with humans are now required.
Elements cycle within and among the Earth system spheres, human society and the human body. Information on the concentrations and stable isotopes of elements is powerful tool for tracing this cycling and has been applied in studies of atmosphere-hydrosphere circulation, ecological systems, and the life, health and history of humans. We propose a session to discuss development and applications of environmental traceability methods toward the goal of establishing traceability in natural and human systems.
We encourage the presentation of research integrating isotopic information in various disciplines, such as geochemistry, hydrology, ecology, geology, mineralogy, anthropology, food science, and forensics. Studies applying "Isoscapes", maps of spatial isotopic variation, in addition to traditional database-based approaches, are strongly encouraged.

[HTT18-P01] Isotopic study on seasonal nitrogen dynamics at Lake Biwa

*Takaaki Ishibashi[1], Ken'ichi Osaka[1], Keisuke Koba[2], Takashi Nakamura[3], Kei Nishida[3] (1.Department of ecosystem study, University of Shiga Prefecture, 2.Center for Ecological Research, Kyoto University, 3.International Research Center for River Basin Environment, University of YAMANASHI)

[HTT18-P02] Relationship between residence time, water quality, and stable isotopes of spring water and groundwater in coastal area of Fukushima prefecture

*Shiho Yabusaki[1], Kazuyoshi Asai[2] (1. Research Institute for Humanity and Nature・Faculty of Symbiotic Systems Science, Fukushima University, 2.Geo Science Laboratory)

[HTT18-P03] Applicability evaluation of CIA due to river and lake

*yusuke hataya[1], SEIKI KAWAGOE[1], Shiho Yabusaki[2], KEN Suzuki[1] (1.fukushima university, 2.Research Institute for Humanity and Nature)

[HTT18-P04] Chemical property analysis of short time scale to determine snowfall source

*Suzuki hiromichi[1], SEIKI KAWAGOE[1], SHO ADACHI[1], Shiho Yabusaki[2] (1.Fukushima University, 2.Research Institute for Humanity and Nature)

[HTT18-P05] Analyzing the origin of surface water in the Saijo Plain, Japan, based on the antimony concentration in the water

*Minoru TOKUMASU[1,2], Ki-Cheol SHIN[3], Yoshihiro YAMADA[4] (1.The United Graduate School of Agricultural Sciences, Ehime University, 2.Saijo City, 3.The Research Institute for Humanity and Nature (RIHN) , 4.Kagawa University, Faculty of Agriculture)

[HTT18-P06] Basic kinetic study on stable isotope ratios of nitrogen compounds: a case study for groundwater in the Kathmandu Valley, Nepal

*Ken Yokozawa[1,2], Kei Nishida[1,3], Takashi Nakamura[1,3], Ken'ichi Osaka[4] (1.University of Yamanashi, 2.Special Graduate Program on River Basin Environmental Science,, 3.ICRE, 4.Department of ecosystem study Univercity of Shiga prefecture)

[HTT18-P07] Usefulness of strontium isotope composition for determining the geographical origin of wasabi and potato

*Takafumi Kamitani[1], Ki-Cheol Shin[2], Sachiko Nakamura[1], Rika Koda[1], Tomoya Oka[1], Noriaki Fushimi[1], Yasuhide Muranaka[1] (1.Shizuoka Institute of Environment and Hygiene, 2.Research Institute for Humanity and Nature)

[HTT18-P08] Reconstruction of sea surface temperature and salinity for the Medieval Climatic Anomaly using a long-lived fossil coral collected at Ishigaki Island, southwestern Japan

*Osamu Abe[1], Maki Morimoto[2], Ryuji Asami[3], Takeshi Nakatsuka[1,4] (1.Graduate School of Environmental Studies, Nagoya University, 2.School of Education, Gifu University, 3.Graduate School of Science, Tohoku University, 4.Research Institute for Humanity and Nature)

[HTT18-P09] Development of the analytical method for sulfur isotope in SO_2 gas

*Masaaki Takahashi[1], Hiroyuki Sase[1], Tsuyoshi Ohizumi[1] (1.Asia Center for Air Pollution Research)

[HTT18-P10] Zinc isotope analysis on human tooth enamel samples to reconstruct diet of the Jomon period.

*Soichiro Kusaka[1], Ki-Cheol Shin[2] (1.Tokai Univ., 2.Research Institute for Humanity and Nature)

[HTT18-P11] Zinc stable isotope analysis of environmental reference materials

*Ki-Cheol Shin[1] (1.Research Institute for Humanity and Nature)

Isotopic study on seasonal nitrogen dynamics at Lake Biwa

*Takaaki Ishibashi[1], Ken'ichi Osaka[1], Keisuke Koba[2], Takashi Nakamura[3], Kei Nishida[3]

1. Department of ecosystem study, University of Shiga Prefecture, 2. Center for Ecological Research, Kyoto University, 3. International Research Center for River Basin Environment, University of YAMANASHI

To clarify nitrogen dynamics in Lake Biwa, we measured the concentrations of nitrogen compounds and their nitrogen stable isotopic ratios in 14 depths in north basin of Lake Biwa. In the lake, particulate nitrogen (PN), such as phytoplankton, is generally decomposed to dissolved nitrogen (DN); in order of dissolved organic nitrogen (DON), ammonia nitrogen (NH_4^+) and nitrate nitrogen (NO_3^-). These dissolved nitrogen compounds are taken up by phytoplankton again, and the nitrogen circulation in the lake is established. To predict the water quality in future, it is necessary to understand the nitrogen cycle in the lake, as well as nutrient load to the lake.

In this study, we collected lake water sample at 14 depths in north basin of Lake Biwa (water depth is 90 m) in 1-2 months interval. The lake waster sample was analyzed for the concentration of PN, PC, DN, NO_3^-, NO_2^- and NH_4^+, $d^{15}N$ of PN, DN and NO_3^-.

NO_3^- concentration was lower in the surface layer (0-20m), and higher in the deep layer (20-90m) during the stratification period, whereas NO_3^- concentration was constant in all layers during the circulation period. PN concentration also increased in the surface layer from April to June, decreased sharply in July. These indicate that phytoplankton which grew on the surface layer from April to June used NO_3^-, thereafter, NO_3^- was depleted after June, then, phytoplankton decreased after July respectively. On the other hand, NO_3^- concentration is considered to be increased by decomposition of the precipitated PN from surface layer. It is considered that the NO_3^- concentration became constant in all layers because of mixing of deep layer and the surface layer.

The weighted average $d^{15}N_{DN}$, $d^{15}N_{NO3}$ in the unit water columns decreased about 3‰ in the circulation period, in the circulation period, then, increased during the stratification period. The decrease of $d^{15}N_{DN}$, $d^{15}N_{NO3}$ at the water column during circulation period can not be explained by mixing of deep layer and the surface layer. We will discuss the mechanisms of $d^{15}N_{DN}$, $d^{15}N_{NO3}$ decrease during circulation period in the presentation.

Keywords: nitrogen dynamics, nitrogen isotope, seasonality

©2019. Japan Geoscience Union. All Right Reserved.

Relationship between residence time, water quality, and stable isotopes of spring water and groundwater in coastal area of Fukushima prefecture

*Shiho Yabusaki[1], Kazuyoshi Asai[2]

1. Research Institute for Humanity and Nature・Faculty of Symbiotic Systems Science, Fukushima University, 2. Geo Science Laboratory

After the Great East Japan Earthquake occurred, the investigation near the coast area in northern part of Fukushima prefecture has been carried out to clarify the groundwater flow and residence time in this area. The measuring of EC, pH, water temperature, ORP and sampling of groundwater, spring water and river water have been carried out several times at Shinchi town, Soma city, Minamisoma city, Namie town, Okuma town, Iitate village and Date city since September in 2012. The inorganic ions, stable isotopes of oxygen and hydrogen, trace elements were analyzed for all samples by using the IC (ICS-3000), CRDS (Picarro L2130-i) and ICP-MS (Agilent 7500cx). For estimating the residence time, tritium concentration, CFCs and SF_6 measurements were made in several samples.

The water quality of river water and shallow groundwater indicates mainly Ca-HCO_3 type. In the part of the flooded area by a tsunami, the water quality of shallow groundwater and spring water is Na-Cl type. The Ca-SO_4 type and mixed type were also confirmed in some sites. In the case of deep groundwater, the water quality shows the Na-HCO_3 type and Ca-HCO_3 type. The concentration of Fe, Mn and Al were relatively high in some parts of deep groundwater. It is considered that the origin of these trace elements is soil.

The stable isotopes of oxygen and hydrogen ($\delta^{18}O$ and δD) in river water of Niida river, Mano river and Kamimano river indicate altitude effect. Because the stable isotopes in deep groundwater is relatively low, it is anticipated the recharge are of deep groundwater is about 300 m higher than that of shallow groundwater. It is expected that the recharge area of deep groundwater is around the Abukuma Mountains.

The average residence time of deep groundwater and spring water which indicate the Na-HCO_3 type is about 60 to 70 years. On the other hand, the average residence time of shallow groundwater which indicate the Ca-HCO_3 type is less than 10 years.

The information of groundwater flow is useful for considering the groundwater use with revival of the coastal area. We will continue the investigation of coastal area and make clear the groundwater flow system.

Keywords: Minamisoma city, Fukushima prefecture, CFCs・SF6, residence time, water quality, stable isotopes, groundwater flow

©2019. Japan Geoscience Union. All Right Reserved.

Applicability evaluation of CIA due to river and lake

*yusuke hataya[1], SEIKI KAWAGOE[1], Shiho Yabusaki[2], KEN Suzuki[1]

1. fukushima university, 2. Research Institute for Humanity and Nature

Water resources management must be further attention because extreme weather condition generate to predict climate change. However, a water area have the various regional characteristics. Therefore a universal way may not also be able to indicate the effect management. If categorized basin tool is developing to obtain characteristic, it is possible to choose suitable management technique in water areas. We tried to develop database to manage basin as chemical and geographical information. In this research, Water factors (Chemical condition, land use condition, soil condition and geological condition) between basins (rivers and reservoirs) were compared to develop data base. Especially, we applied to Chemical Index of Alteration (CIA) as chemical condition factor. As results, It was possible to obtain the basin area scale to apply CIA.

Keywords: CIA, water resource, Numerical geographic information

©2019. Japan Geoscience Union. All Right Reserved.

Chemical property analysis of short time scale to determine snowfall source

*Suzuki hiromichi[1], SEIKI KAWAGOE[1], SHO ADACHI[1], Shiho Yabusaki[2]

1. Fukushima University, 2. Research Institute for Humanity and Nature

Occurrence of the strange weather phenomenon is predicted from the current state depending on climate change. To ask this influence, we have to advance the match which raises the future predictability. And, we have to mark a phenomenon of the current state detail. This study targets to obtain chemically snow environment. The aim of this study was to analyse and predict the stable water isotopic composition of the snow cover at specific basin (Agano river). In addition, the dependence of short time step isotopic composition of the entire snow cover was analysed. Snow in 3 catchments was sampled at the end of the accumulation period from December 2016 to April 2018. The observed variability of short time step isotopic composition of the snow cover was analysed chemical verification. Especially, basin The Inawashiro-Lake north side of the northern upstream region indicated the low chemical feature (Suzuki et al 2018). I'm working on the investigation analysis to grasp the chemical special quality of the snow event of the short time scale at present based on this result (2016-2018). It was that a chemical analysis makes the sample which sampled and acquired it by each day the time of a snowfall at Fukushima, Hibara and Yonezawa located in an upstream region in a basin, and we tried to follow up a snowfall origin of the short time scale.

As results, a strong pressure pattern of southern high and northern low could admit January 22nd-the 25th, the result obtained from the result of analysis also reacted to the weather situation sensitively. And influence of a characteristic snowfall origin was admitted at 3 spots. The difference in the spatial time lags was done clearly.

Keywords: d-excess value, isotope, short time scale

©2019. Japan Geoscience Union. All Right Reserved.

Analyzing the origin of surface water in the Saijo Plain, Japan, based on the antimony concentration in the water

*Minoru TOKUMASU[1,2], Ki-Cheol SHIN[3], Yoshihiro YAMADA[4]

1. The United Graduate School of Agricultural Sciences, Ehime University, 2. Saijo City, 3. The Research Institute for Humanity and Nature (RIHN) , 4. Kagawa University, Faculty of Agriculture

1. Introduction

The flow of river water in many medium and small rivers is managed for water use and flood control. However, it is almost impossible to understand how the water taken from the rivers circulates throughout a basin. The source of water in the Saijo Plain in Ehime Prefecture is from the Kamo River surface water flow, shallow groundwater (unconfined ground water), and deep groundwater (confined ground water). Therefore, it is necessary to quantitatively clarify the source of water for sustainable water use. In this study, we tried to quantify the origin of river water in the plain based on the concentration of some chemical elements. In particular, antimony (Sb) was used as the main trace element because of large differences in its concentration between the water sources.

2. Materials and Methods

On November 25 and 26, 2017, during the non-irrigation period and on the 27th and 28th of July, 2018, during the irrigation period, surface water was collected at a total of 43 sites on small and medium rivers and waterways in the Saijo Plain. Multi-element analysis was carried out on the collected water using ICP-MS 7500 cx.

3. Results and Discussion

There was a large difference in the concentration of Sb among the sites. The highest concentration was found in the water from the Ichino River (Stn. 2) at 113 (2017) and 158 μg/L (2018). There was once an antimony mine in the Ichino River basin, so high concentrations of the element in the river water can be regarded as reflecting the influence of the geology. In the main stream of the Kamo River before joining the Ichinose River (Stn. 1), the Sb concentration was as low as 0.2 μg/L, and after the junction of the two rivers (Stn. 3), the concentration increased to 4.3 (2017) and 7.2 μg/L (2018). The concentration was 4.2 (2017) and 7.2 μg/L (2018) at Stn. 4 of the Kamo River, 11.6 (2017) and 11.7 μg/L (2018) in the unconfined ground water (average of Stns. 13, 14, 15), and 0.4 (2017) and 0.5 μg/L (2018) in the confined ground water (average of Stns. 28, 29, 40, 41, 43). The concentration of Si was 2.7 (2017) and 3.2 mg/L (2018) at Stn. 4 of the Kamo River, 3.4 (2017) and 2.9 mg/L (2018) in the unconfined ground water (average of Stns. 13, 14, 15), and 4.1 (2017) and 3.9 mg/L (2018) in the confined ground water (average of Stns. 28, 29, 40, 41, 43).
The ratio of water origin at each survey site was estimated using the above three sources as end members. In the upstream area, the irrigation water taken from the Kamo River occupied most of the surface water. In the middlestream area, the ratio of water taken from the rivers was smaller, and the contribution of

©2019. Japan Geoscience Union. All Right Reserved.

unconfined ground water exceeded 80%. In the downstream area, the confined ground water contribution exceeded 40% at many sites. In the Saijo Plain, the water origins are different in the upstream, middlestream, and downstream areas, where the contribution of irrigation water is small overall, and the contribution of the confined ground water is large.

©2019. Japan Geoscience Union. All Right Reserved.

Basic kinetic study on stable isotope ratios of nitrogen compounds: a case study for groundwater in the Kathmandu Valley, Nepal

*Ken Yokozawa[1,2], Kei Nishida[1,3], Takashi Nakamura[1,3], Ken'ichi Osaka[4]

1. University of Yamanashi, 2. Special Graduate Program on River Basin Environmental Science,, 3. ICRE, 4. Department of ecosystem study Univercity of Shiga prefecture

Groundwater is a valuable source of water in developing countries where water demand is increasing with population increase. At the same time, nitrogen contamination by industrial wastewater, domestic wastewater and agricultural activities has been reported. In underground environments, it is not unusual to identify sources of contamination since the forms and the concentrations of nitrogen compounds vary at different water flow or microbial metabolism. Stable isotopic analysis is one of the effective methods to detail the variations. However, the isotope value is also greatly affected by environmental conditions, and the theoretical enforcement for describing the variation of the isotope value is needed. In this study, we aimed to quantitatively understand and identify the factors of mixing and isotopic fractionation that determine the stable isotope ratio with a case study on groundwater contamination in the Kathmandu Valley, Nepal.

The data used for the analysis was obtained from the groundwater survey of the Kathmandu Valley conducted from September 2014 to August 2018. Based on the stable isotope ratios of nitrogen and oxygen of nitrate, the contamination patterns were roughly categorized. The mixing line and the denitrification line were prepared based on the dynamic fractionation for the stable isotope ratios of nitrate nitrogen, and the spatial distribution of denitrification-related samples was examined on the map. In addition, assuming that the reactants exist sufficiently and homogeneously in the system, an equilibrium fractionation model was formulated by combining nitrification and denitrification for oxygen stable isotope ratios of nitrate and water. The range of the model parameters were determined by using the measured data from the filed survey, the influence of each process on the stable oxygen isotope ratio of nitrate was quantified.

The result showed that the nitrate in shallow groundwater partially originated from the atmospheric source through infiltration of rainwater. A characteristic of denitrification was observed, which was initiated and proceeded over the valley. Additionally, the correspondent isotopic fractionation differed at the location and the season, particularly controlled by ammonia oxidation, nitrite reduction and oxygen exchange between nitrite and water.

Keywords: groundwater , nitrogen and oxygen stable isotope ratios, nitrification, denitrification, mixing, fractionation

©2019. Japan Geoscience Union. All Right Reserved.

Usefulness of strontium isotope composition for determining the geographical origin of wasabi and potato

*Takafumi Kamitani[1], Ki-Cheol Shin[2], Sachiko Nakamura[1], Rika Koda[1], Tomoya Oka[1], Noriaki Fushimi[1], Yasuhide Muranaka[1]

1. Shizuoka Institute of Environment and Hygiene, 2. Research Institute for Humanity and Nature

Originally, the use of strontium isotope ratios ($^{87}Sr/^{86}Sr$) was restricted to geology and petrology, but they have been used as a particularly effective tracer of geographical food origin, as plants reflect the strontium isotope composition of the regionally based rock, soil, and water. This study aims to evaluate the usefulness of $^{87}Sr/^{86}Sr$ for determining the geographical origin of wasabi (Japanese horseradish) and potato, which are specialty crops in Shizuoka Prefecture, Japan.

Wasabi is cultivated in springs and streams located at the top of rivers, where dissolved element and isotopic compositions in water would reflect the geological characteristics without the effects of atmospheric deposition and human activity. We collected wasabi and water samples from 40 locations of major production areas in Japan: Shizuoka, Iwate, Nagano, Tokyo, and Shimane. These samples were subjected to trace elements and $^{87}Sr/^{86}Sr$ analyses. The $^{87}Sr/^{86}Sr$ values differed, based on the geological characteristics of their site locations, and the value of wasabi was well accorded with that of water in the same location. The wasabi samples collected from Izu Peninsula and Mt. Fuji regions in Shizuoka, where young volcanic rocks such as Quaternary basalts are distributed, had low $^{87}Sr/^{86}Sr$ (below 0.7040), whereas those from Nagano and Tokyo, where older rocks such as Mesozoic granites and accretionary complex are distributed, showed higher ratios (over 0.7095). We conclude that $^{87}Sr/^{86}Sr$ value of wasabi allowed us to distinguish the production area clearly.

On the other hand, the $^{87}Sr/^{86}Sr$ values of crops cultivated in the field are considered to be partly affected by precipitation and fertilizer. Therefore we conducted field survey and planter test for potato in Shizuoka. Field survey was conducted at Mishima, in eastern part of Shizuoka prefecture, and at Mikatahara, in western part of it, and $^{87}Sr/^{86}Sr$ of potato and soil exchangeable fraction were compared. As a result, there was a correlation between potato and soil in $^{87}Sr/^{86}Sr$, although the effects of precipitation and fertilizer were observed. The planter test suggests that the influence of fertilizer on $^{87}Sr/^{86}Sr$ varies depending on the amount of exchangeable Sr contained in the original soil.

Keywords: geographical origin, strontium isotope ratio, wasabi, potato, Shizuoka

©2019. Japan Geoscience Union. All Right Reserved.

Reconstruction of sea surface temperature and salinity for the Medieval Climatic Anomaly using a long-lived fossil coral collected at Ishigaki Island, southwestern Japan

*Osamu Abe[1], Maki Morimoto[2], Ryuji Asami[3], Takeshi Nakatsuka[1,4]

1. Graduate School of Environmental Studies, Nagoya University, 2. School of Education, Gifu University, 3. Graduate School of Science, Tohoku University, 4. Research Institute for Humanity and Nature

The period between 950 and 1250CE is called as the Medieval Climate Anomaly (MCA; Masson-Delmotte et al., 2013), at the time when the warmer climate seemed dominant globally (Bradley et al., 2003). Recent investigations based on the proxy record such as tree-ring widths, speleothems, ice cores, and historical documents indicated that a significant climate change occurred during the latter half of the 10th century. Mann et al. (2009) found that an increase of the average air temperature in the northern hemisphere at the late 10c. coincided with an increase of sea surface temperature at northern subpolar oceans. Yan et al. (2011) indicated that atmospheric environments in the equatorial Pacific shifted from the La Nina like condition to the El Nino like condition around 1000CE. In East Asia, Zhang et al. (2008) and Ge et al. (2013) described that the activity of East Asian Summer Monsoon (EASM) had been enhanced during the late 10c., then the climate in China shifted to warmer and wetter. Whereas Lie et al. (2014) showed that the EASM had been weakened during the 11th century. In addition, the climate in southern China was reported as relatively dry (Chen et al., 2015).

These studies demonstrated that a large climatic shift occurred around 1000CE, however, most of them have relied on records collected on land. There is little long-term high-resolution marine record during the MCA.

We reconstructed sea surface temperature (SST) and salinity with a temporal resolution of one month for 300 years using a long-lived fossil coral collected at Ishigaki Island, southwestern Japan. Based on the U/Th dating in the youngest part of the coral skeletons as well as the band counting, this coral sample had lived between 845 and 1130CE, largely covered the MCA period. Skeletal Sr/Ca and oxygen isotopic composition were analyzed for about 4,000 samples.

The empirical equations between Sr/Ca and water temperature; between oxygen isotopic composition of coral skeleton and seawater, and water temperature, were established using the present coral records, observed water temperature and oxygen isotopic composition of seawater. With these equations and the relationship between seawater salinity and oxygen isotopic composition, proposed by Abe et al. (2009), SST and seawater salinity from 845 to 1130CE were reconstructed from the fossil coral Sr/Ca and oxygen isotopic composition.

Through the entire period, average summer and winter SSTs were 2 and 1 deg. C higher than the present, respectively. In addition, SST increased significantly after 1040CE; 0.9 for the annual average, 0.7 for summer and 1.1 for winter. Salinity also increased after 990CE; 0.8 all for the annual average, summer and winter. Salinity was significantly higher through the entire period than the present, however, its absolute value seems unconfirmed yet.

©2019. Japan Geoscience Union. All Right Reserved.

Increasing SST and salinity found in this study during ca. 1000 and 1130CE were consistent with the weakening of EASM during the 11th and 12th centuries shown by Liu et al. (2014). They argued the weakening occurred as a consequence of weakening of the solar activity and the decrease of SST at the western Pacific warm pool. In this study region, the decrease of precipitation during the Baiu period induced the increase of salinity as well as local SST increase due to the decrease of the cloud cover. Our results were also consistent with the warming of China in the late 10c. (Ge et al., 2013), and a drier condition in southern China (Chen et al., 2015).

The periodicity of SST and salinity based on the spectral analysis will be discussed in the presentation.

Keywords: Coral annual bands, Medieval Climate Anomaly

©2019. Japan Geoscience Union. All Right Reserved.

Development of the analytical method for sulfur isotope in SO_2 gas

*Masaaki Takahashi[1], Hiroyuki Sase[1], Tsuyoshi Ohizumi[1]

1. Asia Center for Air Pollution Research

1. Introduction

Sulfur is a major source of acid deposition. Usually sulfur is emitted as SO_2 and it is oxidized to SO_4^{2-} in atmosphere. S isotopic analysis of water and particulate samples were conducted in many studies. But gaseous SO_2 was rarely used for isotopic study. Isotopic ratio of SO_2 is strongly influenced by emission source near the sampling point. Because most of SO_2 emitted far from sampling point is oxidized to SO_4^{2-} during transportation. It is possible to distinguish domestic emission from transboundary emission. Moreover, dry deposition processes of SO_2 and particulate SO_4^{2-} and their interactions with tree canopy could be discussed more precisely. Isotopic analysis of SO_2 is considered as a powerful method to investigate the behavior of S in the atmosphere and ecosystems. We studied about the analytical method for S isotope in SO_2.

2. Method

(1) Equipment

SO_2 concentration in Japan is very low (e.g. annual 0.02ppb at Sado). We need to collect air sample at least $1m^3$ that is the amount we can obtain 1.2mg of $BaSO_4$ precipitation enough for isotopic analysis. High volume air sampler is generally used to collect around $1m^3$ of air sample. It uses filter, so we examined filter collection of SO_2 by K_2CO_3 filter generally used to collect SO_2 in filter-pack method.

(2) Filters

We used quarts filter for particulate SO_4^{2-} and K_2CO_3 filter for gaseous SO_2 next to it. K_2CO_3 filter is made on the basis of EANET manual. But to get enough flow rate for high volume air sampler, the size of K_2CO_3 filter is larger (20×26 cm, same size with quarts filter) than the manual and already dried before sampling.

(3) Flow rate/leak test

Under flow rate 100~400 L/min in this system, we confirmed weather sampling can be carried out stably. And we checked leak using two K_2CO_3 filters.

(4) Sample treatment

©2019. Japan Geoscience Union. All Right Reserved.

On the basis of EANET manual, the sample was extracted with 0.05% H_2O_2aq and filtered. Then 2N HCl was added and concentrated to remove CO_3^{2-}. Next 1%(w/w)$BaCl_2$ was added. We filtered forming $BaSO_4$ precipitation. We examined the method to get $BaSO_4$ precipitation and to remove the components from K_2CO_3 filter.

3. Results

(1) Sampling and sample treatment

Sampling could be conducted under flow rate 100~400 L/min. Sampling efficiency was about 80%..

Several conditions to get $BaSO_4$ precipitation ware examined, it could be gotten by the method as below.

Filter was cut and ultrasonic extracted with 0.05% H_2O_2aq 30 minutes and filtered. 2.5 ml of 2N HCl was added and concentrated to around 10 ml. Then 1 ml of heated 1 %(w/w) $BaCl_2$ was added under pH 4~6. Next evaporated all solvent and added 10 ml of water. $BaSO_4$ precipitation was observed. After put for one night, the precipitation was separated by centrifuge 3,600 rpm for 10 minutes and we removed the solvent. The precipitation was washed twice by 10 ml of water and filtered. At last the filter was ashed for four hours in muffle furnace in 800 ℃ .

(2) Actual analysis

We used two K_2CO_3 filters and collected 2160.2 m^3 of air sample under flow rate 300 L/min. 3.80 mg of particular SO_4^{2-} and 0.89 mg (first) and 0.14 mg (second) of SO_4^{2-} from SO_2 were obtained. $\delta^{34}S$ of particular SO_4^{2-} was 8.64 ‰and that of SO_2 from the first filter was -1.54 ‰. The amount of precipitation from second filter was not enough for isotopic analysis. This difference was caused by effect of sea salt mainly. But nss- $\delta^{34}S$ of particular SO_4^{2-} was 4.78 ‰. It was still higher than SO_2. It suggested that nss- SO_4^{2-} contains both transboundary SO_4^{2-} and domestic SO_4^{2-}. According to the relevant literature, domestic SO_2 may have negative isotopic values because of imported oil from Middle East. Considering that this sampling was carried out in January, possible effect of transboundary SO_2 with higher isotopic values should also be taken into account for source identification of the collected SO_2.
We would like to discuss at the conference with the latest data.

Keywords: sulfur isotope, SO2 gas

©2019. Japan Geoscience Union. All Right Reserved.

Zinc isotope analysis on human tooth enamel samples to reconstruct diet of the Jomon period.

*Soichiro Kusaka[1], Ki-Cheol Shin[2]

1. Tokai Univ., 2. Research Institute for Humanity and Nature

This study investigates zinc isotope ratios in tooth enamels of human skeletal remains of the Jomon period in Japan. Carbon and nitrogen isotope analysis on bone collagen were traditionary used to reconstruct diet and trophic levels on prehistoric people. The progress of isotope measurements using MC-ICP-MS enables us to analyze isotope ratios of zinc and other metals. Some researches report that the zinc isotope ratios of animals reflect dietary sources and vary according to trophic levels. This study newly develops zinc isotope analysis on human tooth enamels. The zinc isotope analysis has great potential to reconstruct dietary information from inorganic materials of archaeological bones or fossils.

The material used in this study is SRM1400 (bone ash), six samples of human tooth enamels from the Yoshigo and Inariyama shell mounds of Aichi prefecture, and faunal remains (six deer enamels, three boar enamels, six marine fish bones, and six modern plant leaves). Zinc was purified from these samples using anion exchange resin. Zinc isotope ratios were measured by MC-ICP-MS with the zinc standard solution of AA-ETH. The mass bias was corrected with Cu standard solution added to all standards and samples. The zinc isotope ratios of SRM1400 showed similar value with the value previously reported. The difference of zinc isotope ratios between washed and unwashed samples with acetic acids were very small, suggesting no significant diagenetic alteration. The deer and marine fish samples showed the value expected from their dietary ecology. The zinc isotope ratios of Jomon skeletal remains was higher than those of plants, but lower than deer and marine fish. This result indicates that sources of zinc for humans were terrestrial and marine meat as well as terrestrial plants.

Keywords: Zinc Isotope, Jomon period, Human skeletal remains

©2019. Japan Geoscience Union. All Right Reserved.

Zinc stable isotope analysis of environmental reference materials

*Ki-Cheol Shin[1]

1. Research Institute for Humanity and Nature

Zinc has atomic number 30 and atomic mass 65.39. It is a trace element of terrestrial rocks and widely distributed throughout the lithosphere and biosphere. It is chalcophile features and has rich coordination chemistry, participates in a large number of important biological compounds and reactions. The zinc plays an important role as an essential trace metal in all living systems from bacteria to humans. Zn has five stable isotopes ^{64}Zn, ^{66}Zn, ^{67}Zn, ^{68}Zn, and ^{70}Zn. Their isotopic fractionation could provide valuable information about environmental processes, especially in biological processes.

With the advent of multi-collector ICP-MS, it is possible to measure the precise value of ^{66}Zn/^{64}Zn in Zn solution. To promote the environmental stable isotope traceability, RIHN is desired to determine the isotope ratios of zinc for environmental reference materials with high precision and accuracy, rapidness, and convenience.

Here, I report a simple and efficient method for zinc isotope analysis. The various environmental samples over 20 types were used for the study. All samples have purified with an anion exchange resin to separated Zn and Fe at a time. Zinc isotope ratios were measured by MC-ICP-MS (NEPTUNE plus) with AA-ETH, which is a new zinc isotopic standard solution reported by Archer et al. (2017). The mass bias correction conducted with Cu standard solution (NIST SRM 976).

Keywords: stable isotope , Zinc, environmental reference materials

©2019. Japan Geoscience Union. All Right Reserved.

[E] Poster | H (Human Geosciences)：H-CG Complex & General

Tue. May 28, 2019 1:45 PM - 3:15 PM JST | Tue. May 28, 2019 4:45 AM - 6:15 AM UTC | Poster Hall International Exhibition Hall8, Makuhari Messe_6

[H-CG28] Implementing Integrated Research for Sustainable Future

convener:Yukio Himiyama(Emeritus Professor, Hokkaido University of Education), Akihiko Kondoh(Center for Environmental Remote Sensing, Chiba University), Takeshi Sakurai(Graduate School of Agricultural and Life Sciences, The University of Tokyo), Kenichi Abe(Research Institute for Humanity and Nature)

The world global environmental studies are being re-organized in the framework of Future Earth, which is considered to be an important driver to achieve the Sustainable Development Goals (SDGs) set by UN in 2015. Geoscience, which has traditionally been concerned about the dynamic nature and phenomena of the Earth, including lithosphere, hydrosphere, atmosphere and biosphere, is now increasingly committed to human sphere and human dimensions of global change, assuming unique roles in Future Earth and the SDGs. The session is intended to discuss the crucial issues related with them, particularly in reference to such SDGs as good health and well-being, quality education, clean water and sanitation, sustainable cities and communities, climate action, life below water and life on land. Those interested in Future Earth, SDGs, and ESD (Education for Sustainable Development) particularly those who have already started or are about to start related projects, or are interested in Future Earth Knowledge-Action Networks (KANs), such as Ocean, Food-Water-Energy Nexus, Health, Disasters, Cities, Natural Assets, will find this Session an ideal place to present his/her research results, to exchange information and ideas, and to seek new collaborative relations with other research groups and even with partners in the society.

[HCG28-P01] Ground Motion Instrumentation Network and Earthquake Early Warning System for Uttarakhand

*Pankaj Kumar[1,2], Ashok - Kumar[1,2], Ajay - Gairola[1,2] (1.Indian Institute of Technology Roorkee, India, 2.Earthquake Early Warning Laboratory, Centre of Excellence in Disaster Mitigation & Management, IIT Roorkee)

[HCG28-P02] Linking Socioeconomic and Geographical Model to Analyze Land Use Changes in the Jakarta - Bandung Mega Urban Regions

*Didit Okta Pribadi[1,2] (1.Center for Regional Systems Analysis, Planning and Development (CrestPent) - IPB University, 2.Research Center for Plant Conservation and Botanic Gardens - Indonesian Institute of Sciences)

[HCG28-P03] Development of an Integrated Model for Evaluation of Pasture Carrying Capacity and its Vulnerability based on Water Resources in Arid and Semi-arid Regions-----A Case Study in Mongolia

★Invited Papers

*Qinxue Wang[1], Tomohiro Okadera[1], Tadanobu Nakayama[1], Deni Eer[1], Ochirbat Batkhishig[2], Dorjgotov Battogtokh[2], Uudus Bayasaikhan[3] (1.National Institute for Environmental Studies, 2.Institute of Geography and Geoecology, Mongolian Academy of Sciences, 3.School of Arts and Sciences, National University of Mongolia)

[HCG28-P04] Influence of land use histories on vegetation and ecosystem services of restored wetlands in Tumen River basin, China

*CAO GUANGLAN[1], Kazuaki Tsuchiya[1], Weihong Zhu[2], OKURO TOSHIYA[1] (1.The University of Tokyo, 2.Yanbian University)

[HCG28-P05] The spatial flow of freshwater ecosystem services: A case study of Tumen River watershed

*JIAN ZHANG[1], Shizuka hashimoto[1], Kazuaki Tsuchiya[1], Weihong Zhu[2], OKURO TOSHIYA[1] (1.The University of Tokyo, 2.Yanbian University)

Ground Motion Instrumentation Network and Earthquake Early Warning System for Uttarakhand

*Pankaj Kumar[1,2], Ashok - Kumar[1,2], Ajay - Gairola[1,2]

1. Indian Institute of Technology Roorkee, India, 2. Earthquake Early Warning Laboratory, Centre of Excellence in Disaster Mitigation & Management, IIT Roorkee

An Earthquake Early Warning System (EEWS) has been developed by Indian institute of Technology Roorkee (IIT Roorkee) for Uttarakhand, a Himalayan province of India. The region behind to set up first EEWS in India for Uttarakhand is that the main central thrust (MCT) and main boundary thrust (MBT) passes through it and central seismic gap exists in its region and seismologist envisaged a big earthquake will hit this region in near future. Under this project, 155 accelerometers have been installed in 53,483 km^2 area in the Himalayan part of Uttarakhand. These accelerometers are installed on the ground floor of government owned offices of Bharat Sanchar Nigam Limited (BSNL) mobile towers and State Wide Area Network (SWAN) available in the province. The average station to station distance is kept between 10 to 20 km which ensure the triggering of more than 6 accelerometers if an earthquake of magnitude greater than 6 triggers in the region. The data is streamed at the central server located in Earthquake Early Warning Laboratory at Centre of Excellence in Disaster Mitigation & Management in IIT Roorkee through private network of BSNL and SWAN on 24 ×7 basis. The location of installed accelerometers and their streaming at the Earthquake Early Warning Laboratory is shown in figure 1. Whole system is automatic and the early warning parameter is peak displacement (Pd). When an earthquake of magnitude greater than 6 will strike in the instrumented region an earthquake warning will be issued to public through the sirens. The early warning sirens are installed in the public offices, government buildings, schools, colleges of the two major cities, Dehradun and Haldwani, and all 13 district emergency operation center of the province. After hearing, earthquake alarm, people can take necessary precautionary measures. This paper presents the details of instrumentation and working of the EEWS.

Fig 1. Installed accelerometers are shown in Uttarakhand’ s map. MCT and MBT passes through the Himalayan province. Streaming of the data from accelerometer to central server at EEW laboratory is shown in the snapshot.

Keywords: Instrumentation, Accelerometers, Seismic gap, EEWS, Sirens

©2019. Japan Geoscience Union. All Right Reserved.

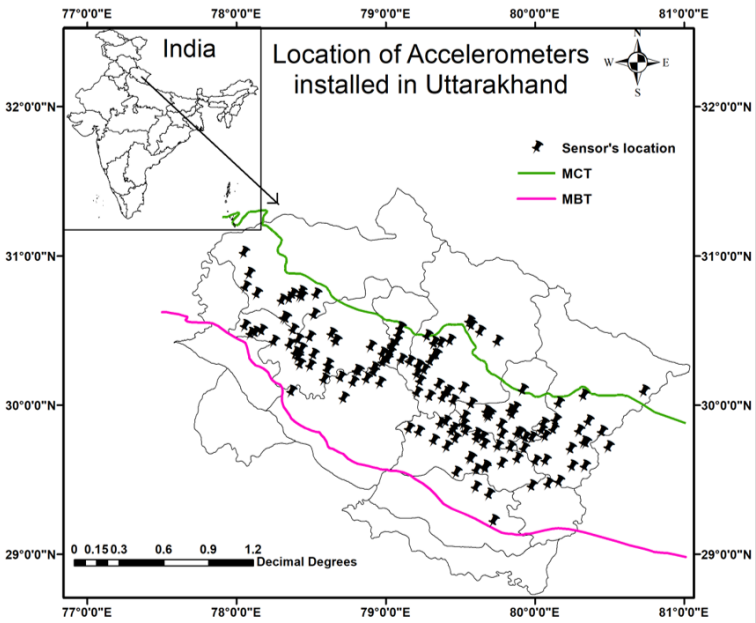

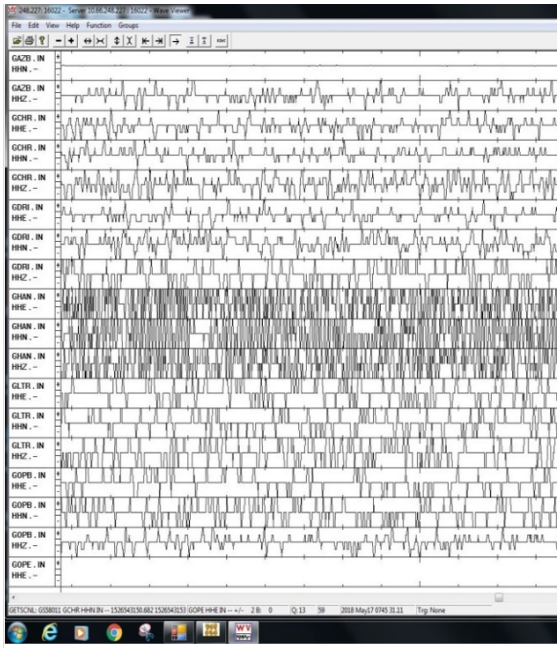

©2019. Japan Geoscience Union. All Right Reserved.

Linking Socioeconomic and Geographical Model to Analyze Land Use Changes in the Jakarta - Bandung Mega Urban Regions

*Didit Okta Pribadi[1,2]

1. Center for Regional Systems Analysis, Planning and Development (CrestPent) - IPB University, 2. Research Center for Plant Conservation and Botanic Gardens - Indonesian Institute of Sciences

Continuing rapid urbanization has led to escalating socio-economic and physical interaction between two adjacent megacities in Indonesia namely Jakarta and Bandung megacity. Physically, enhancing the connection over time has formed urban corridors that stimulate rapid land use changes as well as the expansion of urban-rural land use mixture in the vast area between the two big cities. As land use composition is essential to achieve urban sustainability, modelling land use changes is required as a tool for decision makers to assess the sustainability of different urban form. Nowadays, land use changes model has been rapidly developed owing to increasing computation capacity which is capable of incorporating previous trend of land use changes (e.g. Markov Chain), spatial correlation (e.g. Cellular Automata), and related driving factors (e.g. Logistic Regression or Neural Network) within the model. However, this model is too focused on geographical aspect, while lacking to consider socio-economic factors which spatially might have distinctive properties such as spatial heterogeneity, spatial network, and spatial multiplier effect. This paper aims to combine socioeconomic and geographical factors to analyze complex and dynamic land use systems as found in Jakarta-Bandung Megacity corridors. Land Change Modeler (LCM) from Idrisi Tersset software as a combination of Neural Network and CA-Markov model would be enhanced by incorporating socioeconomic aspects analyzed by GWR (Geographical Weighted Regression) for detecting spatial heterogeneity, gravity model for analyzing spatial network, and spatial autocorrelation model (SAM) for defining spatial multiplier effect. This model would be compared to the results of LCM as a single approach. A new model is suggested as an enhanced approach to understand multiple factors that influence land use changes in Jakarta-Bandung megacity corridors, thus more comprehensive policies can be formulated.

Keywords: Urbanization, Socioeconomic model, Geographical Model, Land Use Changes, Jakarta-Bandung Mega Urban Regions

©2019. Japan Geoscience Union. All Right Reserved.

Development of an Integrated Model for Evaluation of Pasture Carrying Capacity and its Vulnerability based on Water Resources in Arid and Semi-arid Regions------A Case Study in Mongolia

*Qinxue Wang[1], Tomohiro Okadera[1], Tadanobu Nakayama[1], Deni Eer[1], Ochirbat Batkhishig[2], Dorjgotov Battogtokh[2], Uudus Bayasaikhan[3]

1. National Institute for Environmental Studies, 2. Institute of Geography and Geoecology, Mongolian Academy of Sciences, 3. School of Arts and Sciences, National University of Mongolia

Arid and semi-arid regions cover 41% of the global land area and near 2 billion people (34.7%) live there, where fragile environment is getting more vulnerable due to climate change and human activities. Pasture carrying capacity and its vulnerability can be recognized as the integrated indicators for SDGs in arid and semi-arid regions. Our previous study revealed that climate change in past few decades caused the obvious degradation of permafrost, the water deficit of land-surface, and then the decrease of pasture productivity and carrying capacity. However, beside climate change, land use/cover changes caused by human activities such as urbanization, cultivation and mining industry may also have a large influence on pasture carrying capacity. In such regions, it is essential for us to develop some indicators to be used for sustainable management of pasture ecosystems.

In this study, we have developed an integrated model based on water resources to evaluate the pasture Carrying Capacity (CC), Grazing Pressure (GP) and Vulnerability Index (VI) under the influences of both climate change and land use/cover changes, such as urbanization, cultivation and mining & so on (Figure 1). The input data include the pasture net primary production, land use, gradient of slope and grazing density, etc. In order to evaluate the impact of land use/cover changes, we applied the model to four target areas: urban area (Ulaanbaatar City) and steppe area (Altanbulag Soum) in semi-arid regions of northern Mongolia and mining area (Khanbogd Soum) and desert (Manlai Soum) in arid regions of southern Mongolia, and the estimated result was shown in Figure 2, which indicates:

Carrying Capacity (CC): steppe area > urban area > desert area > mining area
Grazing Pressure (GP): urban area > steppe area > mining area > desert area
Vulnerability Index (VI): urban area > mining area > desert area > steppe area

We also applied the model to the Soum level in Mongolia and found that the areas with high vulnerability expanded rapidly, especially in central Mongolia in last decades. We are now trying to use the model to do sensitivity analysis to parameters, such as water accessibility, harvest index and so on, to be able to evaluate the efficiency of adaptation strategies, such as well construction for enhancing groundwater usage, forage plantation for enhancing harvest index and so on.

Keywords: Pasture Carrying Capacity, Environmental Vulnerability, Arid and Semi-arid Regions, Water Resources

©2019. Japan Geoscience Union. All Right Reserved.

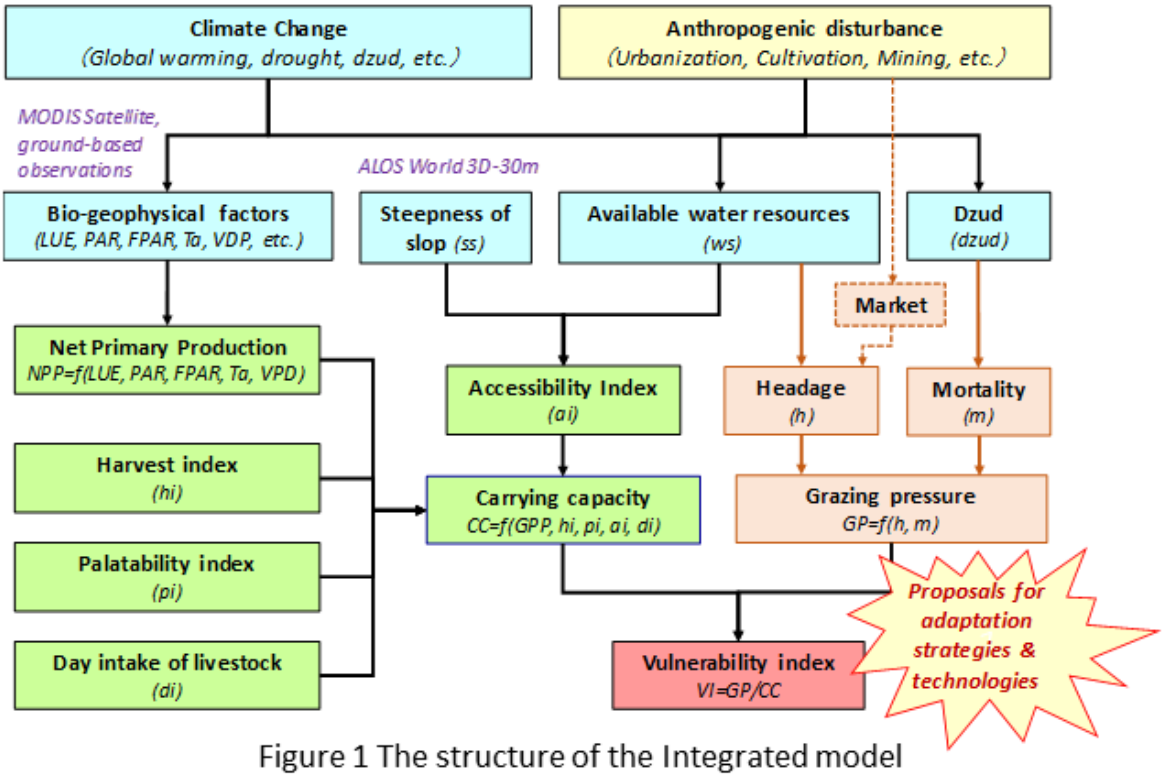

Figure 1 The structure of the Integrated model

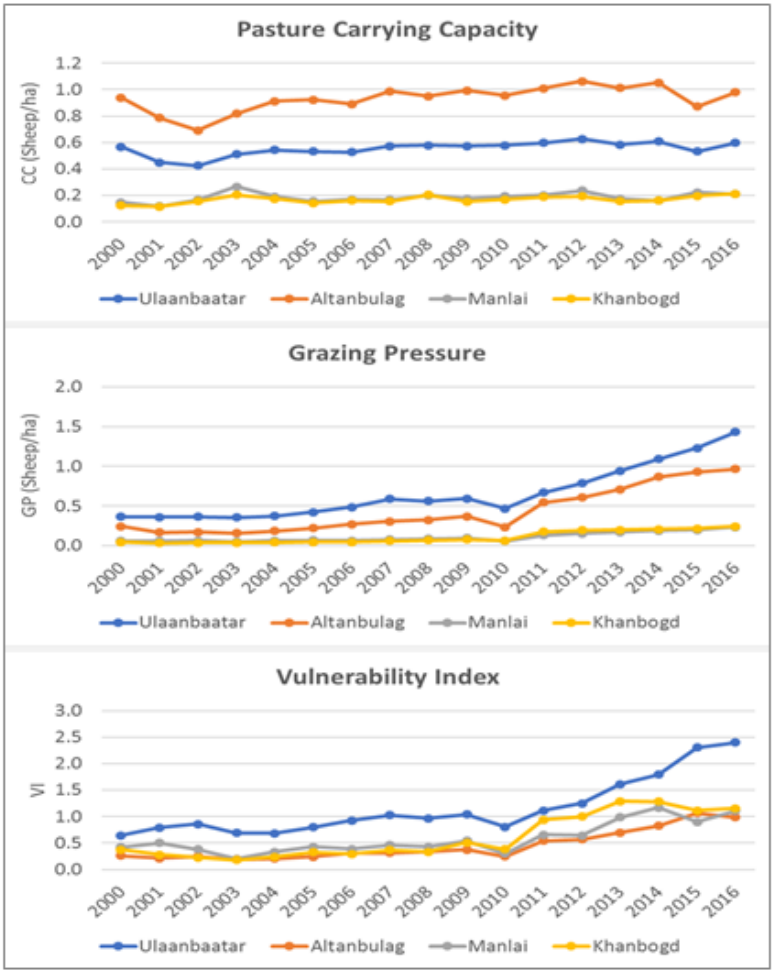

Figure 2 Evaluated pasture CC and VI in four target areas

©2019. Japan Geoscience Union. All Right Reserved.

Influence of land use histories on vegetation and ecosystem services of restored wetlands in Tumen River basin, China

*CAO GUANGLAN[1], Kazuaki Tsuchiya[1], Weihong Zhu[2], OKURO TOSHIYA[1]

1. The University of Tokyo, 2. Yanbian University

Wetlands are among the world’ s most productive and valuable ecosystems. They are important habitats for a variety of flora and fauna, and are vital ecosystems that provide diverse services. They not only are essential for ecological functions such as maintaining biodiversity, controlling floods, and removing pollutants, but also serve necessary economic functions in rice and fish production, transport, and hydropower energy. Despite this, they have suffered a loss of 54%–57% of their area worldwide, which continues under pressures from agriculture, urban expansion, industrialization, and resource extraction. Conservation and restoration of wetland ecosystems is important issues for conservation biodiversity and sustainable use of ecosystem services. In this study, we focus on the lower of Tumen River, Northeast China where the wetlands decreased dramatically because of reclamation. Our objective was to determine the influence of land use and management histories on vegetation structure and ecosystem services and future analyse their associations with environmental factors. The results of this study are of great significance to the impact of management measures on wetland ecosystems, as well as the analysis and evaluation of vegetation restoration.

Keywords: land use histories, vegetation dynamics, wetland restoration, ecosystem services

©2019. Japan Geoscience Union. All Right Reserved.

The spatial flow of freshwater ecosystem services: A case study of Tumen River watershed

*JIAN ZHANG[1], Shizuka hashimoto[1], Kazuaki Tsuchiya[1], Weihong Zhu[2], OKURO TOSHIYA[1]

1. The University of Tokyo, 2. Yanbian University

Freshwater is widely regarded as the most essential natural resource underpinning the well-being of human society, and while scientists translate it into ecosystem services' valuable processes, the supply of clean freshwater has the highest value among various provisioning services. However, due to the land-use intensification and projected warming climate, an increasing likelihood of persistent drought condition, and inadequate conservation, freshwater scarcity issues continue to gain urgency in science and policies. The fusion of the concept of ecosystem services with natural resources management nowadays represents a new conservation paradigm, but still faces notable limitations. Some scientists, noticing the occurrence of spatial mismatch between the supply and demand of ecosystem services, put forward the concept of ecosystem services flow to deal with the problem. Ecosystem services flow research brings out a spatio-temporal connection between the supply and demand, and an deepened understanding about when ,where, and how those benefits were enjoyed. Many papers also suggested that studies at landscape scale may offer a better understanding of ecosystem processes, ecosystem functions, ecosystem services and link them from one to another, as landscape patterns have long been discussed as tools for explaining numerous ecological consequences. In 2017, the annual meeting of IALE in USA as well emphasized the pressing need of integrating landscape patterns to ecosystem services. Thus the study attempt to conduct an analysis of freshwater ecosystem services flow in an intact watershed with the combination of landscape ecology theories. The conceptual framework and progress of this study will be introduced.

Keywords: freshwater ecosystem services, services flow, andscape pattern, watershed

©2019. Japan Geoscience Union. All Right Reserved.

[E] Poster | H (Human Geosciences)：H-CG Complex & General

Tue. May 28, 2019 5:15 PM - 6:30 PM JST | Tue. May 28, 2019 8:15 AM - 9:30 AM UTC | Poster Hall International Exhibition Hall8, Makuhari Messe_25

[H-CG28] Implementing Integrated Research for Sustainable Future

convener:Yukio Himiyama(Emeritus Professor, Hokkaido University of Education), Akihiko Kondoh(Center for Environmental Remote Sensing, Chiba University), Takeshi Sakurai(Graduate School of Agricultural and Life Sciences, The University of Tokyo), Kenichi Abe(Research Institute for Humanity and Nature)

The world global environmental studies are being re-organized in the framework of Future Earth, which is considered to be an important driver to achieve the Sustainable Development Goals (SDGs) set by UN in 2015. Geoscience, which has traditionally been concerned about the dynamic nature and phenomena of the Earth, including lithosphere, hydrosphere, atmosphere and biosphere, is now increasingly committed to human sphere and human dimensions of global change, assuming unique roles in Future Earth and the SDGs. The session is intended to discuss the crucial issues related with them, particularly in reference to such SDGs as good health and well-being, quality education, clean water and sanitation, sustainable cities and communities, climate action, life below water and life on land. Those interested in Future Earth, SDGs, and ESD (Education for Sustainable Development) particularly those who have already started or are about to start related projects, or are interested in Future Earth Knowledge-Action Networks (KANs), such as Ocean, Food-Water-Energy Nexus, Health, Disasters, Cities, Natural Assets, will find this Session an ideal place to present his/her research results, to exchange information and ideas, and to seek new collaborative relations with other research groups and even with partners in the society.

[HCG28-P01] Ground Motion Instrumentation Network and Earthquake Early Warning System for Uttarakhand

*Pankaj Kumar[1,2], Ashok - Kumar[1,2], Ajay - Gairola[1,2] (1.Indian Institute of Technology Roorkee, India, 2.Earthquake Early Warning Laboratory, Centre of Excellence in Disaster Mitigation & Management, IIT Roorkee)

[HCG28-P02] Linking Socioeconomic and Geographical Model to Analyze Land Use Changes in the Jakarta - Bandung Mega Urban Regions

*Didit Okta Pribadi[1,2] (1.Center for Regional Systems Analysis, Planning and Development (CrestPent) - IPB University, 2.Research Center for Plant Conservation and Botanic Gardens - Indonesian Institute of Sciences)

[HCG28-P03] Development of an Integrated Model for Evaluation of Pasture Carrying Capacity and its Vulnerability based on Water Resources in Arid and Semi-arid Regions-----A Case Study in Mongolia

★Invited Papers

*Qinxue Wang[1], Tomohiro Okadera[1], Tadanobu Nakayama[1], Deni Eer[1], Ochirbat Batkhishig[2], Dorjgotov Battogtokh[2], Uudus Bayasaikhan[3] (1.National Institute for Environmental Studies, 2.Institute of Geography and Geoecology, Mongolian Academy of Sciences, 3.School of Arts and Sciences, National University of Mongolia)

[HCG28-P04] Influence of land use histories on vegetation and ecosystem services of restored wetlands in Tumen River basin, China

*CAO GUANGLAN[1], Kazuaki Tsuchiya[1], Weihong Zhu[2], OKURO TOSHIYA[1] (1.The University of Tokyo, 2.Yanbian University)

[HCG28-P05] The spatial flow of freshwater ecosystem services: A case study of Tumen River watershed

*JIAN ZHANG[1], Shizuka hashimoto[1], Kazuaki Tsuchiya[1], Weihong Zhu[2], OKURO TOSHIYA[1] (1.The University of Tokyo, 2.Yanbian University)

Ground Motion Instrumentation Network and Earthquake Early Warning System for Uttarakhand

*Pankaj Kumar[1,2], Ashok - Kumar[1,2], Ajay - Gairola[1,2]

1. Indian Institute of Technology Roorkee, India, 2. Earthquake Early Warning Laboratory, Centre of Excellence in Disaster Mitigation & Management, IIT Roorkee

An Earthquake Early Warning System (EEWS) has been developed by Indian institute of Technology Roorkee (IIT Roorkee) for Uttarakhand, a Himalayan province of India. The region behind to set up first EEWS in India for Uttarakhand is that the main central thrust (MCT) and main boundary thrust (MBT) passes through it and central seismic gap exists in its region and seismologist envisaged a big earthquake will hit this region in near future. Under this project, 155 accelerometers have been installed in 53,483 km^2 area in the Himalayan part of Uttarakhand. These accelerometers are installed on the ground floor of government owned offices of Bharat Sanchar Nigam Limited (BSNL) mobile towers and State Wide Area Network (SWAN) available in the province. The average station to station distance is kept between 10 to 20 km which ensure the triggering of more than 6 accelerometers if an earthquake of magnitude greater than 6 triggers in the region. The data is streamed at the central server located in Earthquake Early Warning Laboratory at Centre of Excellence in Disaster Mitigation & Management in IIT Roorkee through private network of BSNL and SWAN on 24 ×7 basis. The location of installed accelerometers and their streaming at the Earthquake Early Warning Laboratory is shown in figure 1. Whole system is automatic and the early warning parameter is peak displacement (Pd). When an earthquake of magnitude greater than 6 will strike in the instrumented region an earthquake warning will be issued to public through the sirens. The early warning sirens are installed in the public offices, government buildings, schools, colleges of the two major cities, Dehradun and Haldwani, and all 13 district emergency operation center of the province. After hearing, earthquake alarm, people can take necessary precautionary measures. This paper presents the details of instrumentation and working of the EEWS.

Fig 1. Installed accelerometers are shown in Uttarakhand’ s map. MCT and MBT passes through the Himalayan province. Streaming of the data from accelerometer to central server at EEW laboratory is shown in the snapshot.

Keywords: Instrumentation, Accelerometers, Seismic gap, EEWS, Sirens

©2019. Japan Geoscience Union. All Right Reserved.

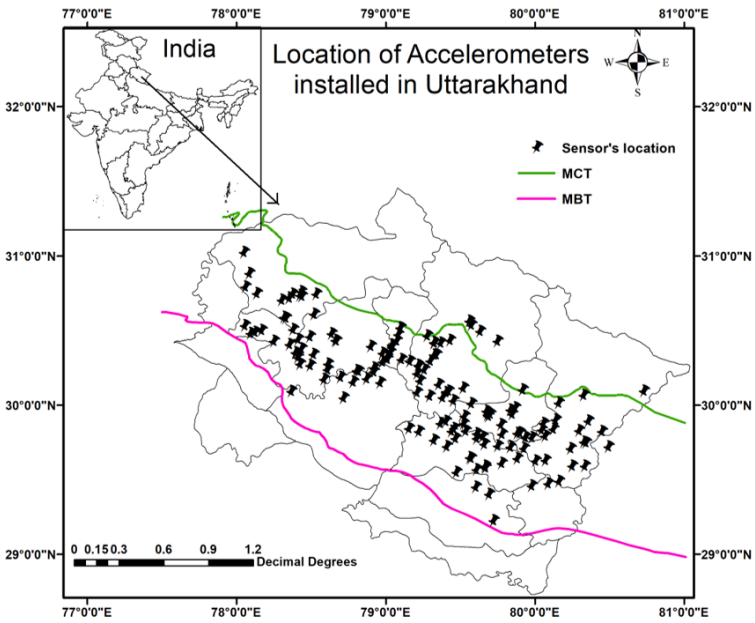

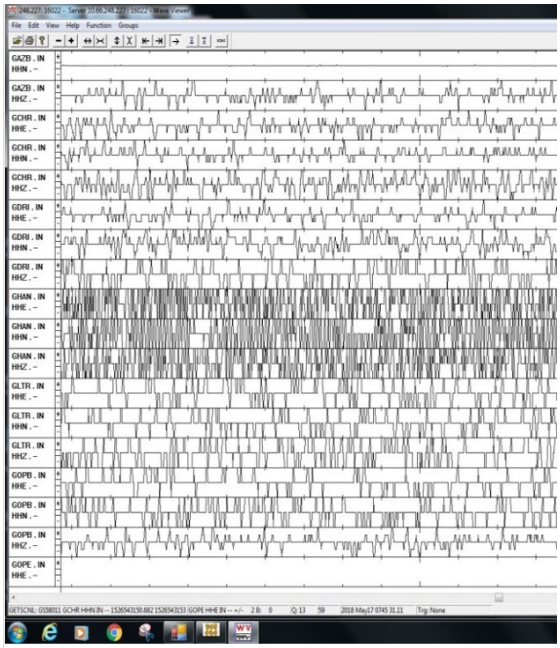

©2019. Japan Geoscience Union. All Right Reserved.

Linking Socioeconomic and Geographical Model to Analyze Land Use Changes in the Jakarta - Bandung Mega Urban Regions

*Didit Okta Pribadi[1,2]

1. Center for Regional Systems Analysis, Planning and Development (CrestPent) - IPB University, 2. Research Center for Plant Conservation and Botanic Gardens - Indonesian Institute of Sciences

Continuing rapid urbanization has led to escalating socio-economic and physical interaction between two adjacent megacities in Indonesia namely Jakarta and Bandung megacity. Physically, enhancing the connection over time has formed urban corridors that stimulate rapid land use changes as well as the expansion of urban-rural land use mixture in the vast area between the two big cities. As land use composition is essential to achieve urban sustainability, modelling land use changes is required as a tool for decision makers to assess the sustainability of different urban form. Nowadays, land use changes model has been rapidly developed owing to increasing computation capacity which is capable of incorporating previous trend of land use changes (e.g. Markov Chain), spatial correlation (e.g. Cellular Automata), and related driving factors (e.g. Logistic Regression or Neural Network) within the model. However, this model is too focused on geographical aspect, while lacking to consider socio-economic factors which spatially might have distinctive properties such as spatial heterogeneity, spatial network, and spatial multiplier effect. This paper aims to combine socioeconomic and geographical factors to analyze complex and dynamic land use systems as found in Jakarta-Bandung Megacity corridors. Land Change Modeler (LCM) from Idrisi Tersset software as a combination of Neural Network and CA-Markov model would be enhanced by incorporating socioeconomic aspects analyzed by GWR (Geographical Weighted Regression) for detecting spatial heterogeneity, gravity model for analyzing spatial network, and spatial autocorrelation model (SAM) for defining spatial multiplier effect. This model would be compared to the results of LCM as a single approach. A new model is suggested as an enhanced approach to understand multiple factors that influence land use changes in Jakarta-Bandung megacity corridors, thus more comprehensive policies can be formulated.

Keywords: Urbanization, Socioeconomic model, Geographical Model, Land Use Changes, Jakarta-Bandung Mega Urban Regions

©2019. Japan Geoscience Union. All Right Reserved.

Development of an Integrated Model for Evaluation of Pasture Carrying Capacity and its Vulnerability based on Water Resources in Arid and Semi-arid Regions------A Case Study in Mongolia

*Qinxue Wang[1], Tomohiro Okadera[1], Tadanobu Nakayama[1], Deni Eer[1], Ochirbat Batkhishig[2], Dorjgotov Battogtokh[2], Uudus Bayasaikhan[3]

1. National Institute for Environmental Studies, 2. Institute of Geography and Geoecology, Mongolian Academy of Sciences, 3. School of Arts and Sciences, National University of Mongolia

Arid and semi-arid regions cover 41% of the global land area and near 2 billion people (34.7%) live there, where fragile environment is getting more vulnerable due to climate change and human activities. Pasture carrying capacity and its vulnerability can be recognized as the integrated indicators for SDGs in arid and semi-arid regions. Our previous study revealed that climate change in past few decades caused the obvious degradation of permafrost, the water deficit of land-surface, and then the decrease of pasture productivity and carrying capacity. However, beside climate change, land use/cover changes caused by human activities such as urbanization, cultivation and mining industry may also have a large influence on pasture carrying capacity. In such regions, it is essential for us to develop some indicators to be used for sustainable management of pasture ecosystems.

In this study, we have developed an integrated model based on water resources to evaluate the pasture Carrying Capacity (CC), Grazing Pressure (GP) and Vulnerability Index (VI) under the influences of both climate change and land use/cover changes, such as urbanization, cultivation and mining & so on (Figure 1). The input data include the pasture net primary production, land use, gradient of slope and grazing density, etc. In order to evaluate the impact of land use/cover changes, we applied the model to four target areas: urban area (Ulaanbaatar City) and steppe area (Altanbulag Soum) in semi-arid regions of northern Mongolia and mining area (Khanbogd Soum) and desert (Manlai Soum) in arid regions of southern Mongolia, and the estimated result was shown in Figure 2, which indicates:

Carrying Capacity (CC): steppe area > urban area > desert area > mining area
Grazing Pressure (GP): urban area > steppe area > mining area > desert area
Vulnerability Index (VI): urban area > mining area > desert area > steppe area

We also applied the model to the Soum level in Mongolia and found that the areas with high vulnerability expanded rapidly, especially in central Mongolia in last decades. We are now trying to use the model to do sensitivity analysis to parameters, such as water accessibility, harvest index and so on, to be able to evaluate the efficiency of adaptation strategies, such as well construction for enhancing groundwater usage, forage plantation for enhancing harvest index and so on.

Keywords: Pasture Carrying Capacity, Environmental Vulnerability, Arid and Semi-arid Regions, Water Resources

©2019. Japan Geoscience Union. All Right Reserved.

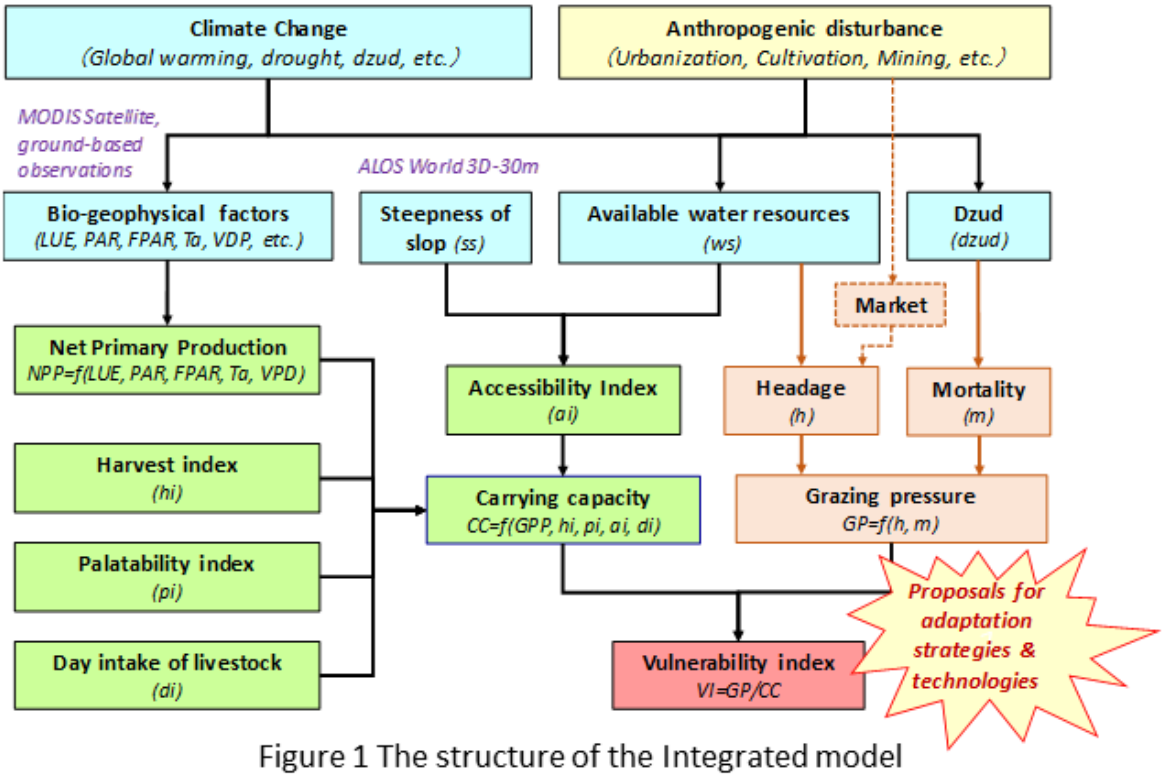

Figure 1 The structure of the Integrated model

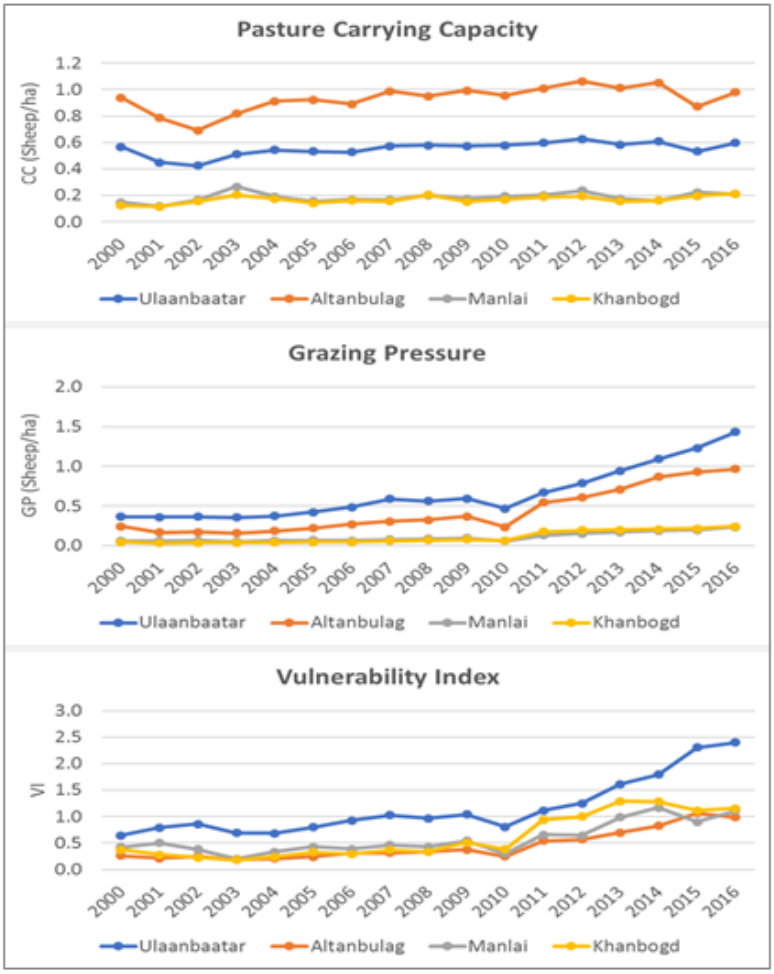

Figure 2 Evaluated pasture CC and VI in four target areas

©2019. Japan Geoscience Union. All Right Reserved.

Influence of land use histories on vegetation and ecosystem services of restored wetlands in Tumen River basin, China

*CAO GUANGLAN[1], Kazuaki Tsuchiya[1], Weihong Zhu[2], OKURO TOSHIYA[1]

1. The University of Tokyo, 2. Yanbian University

Wetlands are among the world’ s most productive and valuable ecosystems. They are important habitats for a variety of flora and fauna, and are vital ecosystems that provide diverse services. They not only are essential for ecological functions such as maintaining biodiversity, controlling floods, and removing pollutants, but also serve necessary economic functions in rice and fish production, transport, and hydropower energy. Despite this, they have suffered a loss of 54%–57% of their area worldwide, which continues under pressures from agriculture, urban expansion, industrialization, and resource extraction. Conservation and restoration of wetland ecosystems is important issues for conservation biodiversity and sustainable use of ecosystem services. In this study, we focus on the lower of Tumen River, Northeast China where the wetlands decreased dramatically because of reclamation. Our objective was to determine the influence of land use and management histories on vegetation structure and ecosystem services and future analyse their associations with environmental factors. The results of this study are of great significance to the impact of management measures on wetland ecosystems, as well as the analysis and evaluation of vegetation restoration.

Keywords: land use histories, vegetation dynamics, wetland restoration, ecosystem services

©2019. Japan Geoscience Union. All Right Reserved.

The spatial flow of freshwater ecosystem services: A case study of Tumen River watershed

*JIAN ZHANG[1], Shizuka hashimoto[1], Kazuaki Tsuchiya[1], Weihong Zhu[2], OKURO TOSHIYA[1]

1. The University of Tokyo, 2. Yanbian University

Freshwater is widely regarded as the most essential natural resource underpinning the well-being of human society, and while scientists translate it into ecosystem services' valuable processes, the supply of clean freshwater has the highest value among various provisioning services. However, due to the land-use intensification and projected warming climate, an increasing likelihood of persistent drought condition, and inadequate conservation, freshwater scarcity issues continue to gain urgency in science and policies. The fusion of the concept of ecosystem services with natural resources management nowadays represents a new conservation paradigm, but still faces notable limitations. Some scientists, noticing the occurrence of spatial mismatch between the supply and demand of ecosystem services, put forward the concept of ecosystem services flow to deal with the problem. Ecosystem services flow research brings out a spatio-temporal connection between the supply and demand, and an deepened understanding about when ,where, and how those benefits were enjoyed. Many papers also suggested that studies at landscape scale may offer a better understanding of ecosystem processes, ecosystem functions, ecosystem services and link them from one to another, as landscape patterns have long been discussed as tools for explaining numerous ecological consequences. In 2017, the annual meeting of IALE in USA as well emphasized the pressing need of integrating landscape patterns to ecosystem services. Thus the study attempt to conduct an analysis of freshwater ecosystem services flow in an intact watershed with the combination of landscape ecology theories. The conceptual framework and progress of this study will be introduced.

Keywords: freshwater ecosystem services, services flow, andscape pattern, watershed

©2019. Japan Geoscience Union. All Right Reserved.

[E] Poster | S (Solid Earth Sciences)：S-SS Seismology

Tue. May 28, 2019 3:30 PM - 5:00 PM JST | Tue. May 28, 2019 6:30 AM - 8:00 AM UTC | Poster Hall International Exhibition Hall8, Makuhari Messe_16

[S-SS06] Nankai Trough Seismogenic Zone Experiment: Logging and sampling the seismogenic megathrust

convener:Kyuichi Kanagawa(Graduate School of Science, Chiba University), Demian M Saffer(Pennsylvania State University), Masataka Kinoshita(Earthquake Research Institute, University of Tokyo)

The Nankai Trough Seismogenic Zone Experiment (NanTroSEIZE) is a multidisciplinary investigation of fault mechanics and seismogenesis along the megathrust at the Nankai Trough subduction zone, and includes reflection and refraction seismic imaging, direct sampling by drilling, in situ measurements, and long-term monitoring in conjunction with laboratory and numerical modeling studies. During the past 12 IODP expeditions off Kii Peninsula since 2007, 15 sites have been drilled by D/V "Chikyu" down to depths from 100s of meters to more than 3000 meters below seafloor, where the inner and outer wedge of the Nankai margin has been logged and sampled extensively, and three state-of-the-art real-time downhole observatories are now in operation. The final NanTroSEIZE expedition aiming to log and sample the seismogenic megathrust at ~5200 meters below seafloor is now ongoing from October, 2018 to March, 2019.
In this session, we expect presentations not only on scientific outcomes from the past NanTroSEIZE expeditions, but also on the exciting preliminary results of the final NanTroSEIZE expedition. We welcome presentations on, but are not limited to, seismic imaging, borehole logging and monitoring, chemical analyses of pore water and mud gas, lithology, structures, physical properties and laboratory experiments of cuttings and core samples, and theoretical and numerical modeling.

[SSS06-P01] Crustal structure in the Nankai Trough seismogenic zone based on renewed depth images and seismic attribute analysis

*Kazuya Shiraishi[1], Yasuhiro Yamada[1], Masataka Kinoshita[2], Gaku Kimura[3] (1.Japan Agency for Marine-Earth Science and Technology, 2.Earthquake Research Institute, The University of Tokyo, 3.Tokyo University of Marine Science and Technology)

[SSS06-P02] Along-strike variations in protothrust zone characteristics at the Nankai Trough subduction margin

*Hannah Tilley[1], Gregory F Moore[1], Mikiya Yamashita[2], Shuichi Kodaira[2] (1.University of Hawaii at Manoa, 2.JAMSTEC)

[SSS06-P03] Temporal change in seismic velocity in the Nankai subduction zone from cross-correlation analysis of ambient noise

*Tatsunori Ikeda[1], Takeshi Tsuji[1] (1.Kyushu University)

[SSS06-P04] Strength profile of the Nankai accretionary prism evaluated from drilling parameters

★Invited Papers

*Yohei Hamada[1], Manami Kitamura[2], Takehiro Hirose[1], Yasuhiro Yamada[1], Yoshinori Sanada[1], Takamitsu Sugihara[1], Saneatsu Saito[1], KYAW MOE[1] (1.Japan Agency for Marine-Earth Science and Technology, 2.National Institute of Advanced Industrial Science andTechnology)

[SSS06-P05] Paleotemperature anomalies deduced from thermal-maturity parameters within the décollement, off Cape of Muroto, Japan

*Nana Kamiya[1,2], Takehiro Hirose[2], Yuzuru Yamamoto[2], Yohei Hamada[2], Stephen A Bowden[3], Man-Yin Tsang[4], Kiho Yang[5], Satoshi Tonai[6], Weiren Lin[1,2] (1.Graduate School of Engineering, Kyoto University, 2.JAMSTEC, 3.University of Aberdeen, 4.University of Toronto, 5.Yonsei University, 6.Kochi University)

[SSS06-P06] Modelling thermal maturity of an accretionary wedge

Utsav Mannu[2], *Masataka Kinoshita[1], Taras Gerya[3] (1.Earthquake Research Institute, University of Tokyo, 2.Department of Earth and Climate Science, IISER Pune, 3.Institute of Geophysics, ETH Zürich)

Crustal structure in the Nankai Trough seismogenic zone based on renewed depth images and seismic attribute analysis

*Kazuya Shiraishi[1], Yasuhiro Yamada[1], Masataka Kinoshita[2], Gaku Kimura[3]

1. Japan Agency for Marine-Earth Science and Technology, 2. Earthquake Research Institute, The University of Tokyo, 3. Tokyo University of Marine Science and Technology

To better understand geological structure in the Nankai Trough seismogenic zone, we investigate deformations in the accretionary prism based on renewed depth images and seismic attribute analyses. We reprocessed subareas of the Kumano-nada 3D MCS data acquired in 2006: 25 km x 12 km area including IODP C0002 site in Phase 1 (2015-2016) and 20 km x 12 km area including IODP C0006 site in Phase 2 (2017-2018). We also reprocessed 2D MCS data along a 50-km line crossing C0002 site in NW-SE direction, which was selected from a 2D survey ODKM03 in 2003 with a longer streamer cable (6 km) than streamer cables of the 3D survey (4.5 km). Quality improvement of reflection signals was achieved by applying recent broadband processing and advanced process to attenuate noise and multiple reflections. Depth domain reflection images were obtained after applying new pre-stack depth migration methods. Then, we calculated several seismic attributes from the 3D reflection image volumes, such as coherence and structure dips which are useful to interpret structural features.
As a result of our investigation, deformed structure within the inner accreted sediments and its relation with the megathrust fault are clearer than before. Anticlines are identified just below the Kumano forearc basin and fragmented reflections can be seen below the anticlines. Characteristic patterns of folds can be recognized on the horizontal section of the coherence cube, which are corresponding to the anticlines on the vertical sections. These reflection features imply development of fold structures due to thrust faults with branched minor faults. In the reprocessed 2D section, curved reflectors with stepwise displacement are imaged in the region of 4 - 6 km depth. These reflectors may represent multiple thrust faults with back-thrusts, and the thrust faults are consistent with the structural features in the 3D images. The detachments of the thrust faults seem to converge to wavy points on the megathrust fault surface. Furthermore, details of deformation and fracture in the outer accretionary prism are imaged clearer than the previous images. Lithological boundaries with displacement along imbricated thrusts can be traced beyond the fault, and conjugate faults due to horizontal compression which cut the in-sequence thrusts are recognized on the horizontal section from superimposed view of the coherence and dip angles. Reflectors within underthrusted sediments beneath the imbricated thrust layer are clearly imaged. Some of the reflectors can be identified as parts of detachment of the thrust faults. The topographic relief of the oceanic crust should be considered when the deformed structures in the overburden sediments and distribution of décollement are revisited.

Acknowledgements:
This research is supported by JSPS KAKENHI (JP15H05717).

Keywords: Nankai Trough seismogenic zone, crustal structure, reflection seismic, seismic attribute

©2019. Japan Geoscience Union. All Right Reserved.

Along-strike variations in protothrust zone characteristics at the Nankai Trough subduction margin

*Hannah Tilley[1], Gregory F Moore[1], Mikiya Yamashita[2], Shuichi Kodaira[2]

1. University of Hawaii at Manoa, 2. JAMSTEC

Protothrust zones (PTZs) are assumed to control the development of new frontal thrusts at subduction zones. PTZs are areas of incipient thrust faulting between the deformation front and the frontal thrust. However, limited resolution of previous seismic studies has hindered the study of their role in subduction accretion. New high-resolution seismic reflection surveys enabled detailed analysis of the PTZ along the Nankai Trough, SE Japan. Seventeen multichannel seismic reflection lines were collected perpendicular to the trench axis between Cape Ashizuri and Cape Muroto using a 1200m long, 192 channel hydrophone cable and a 380 in^3 (5.24L) cluster airgun array. These lines were processed using pre-stack depth migration. PTZs only existed where a turbidite sequence was present beneath the trench wedge. The PTZs consisted of closely spaced, sub-parallel protothrusts that decreased in spacing and increased in length landward. Where the turbidites were truncated by basement topography, there was a transitional PTZ heterogeneous protothrusts and small displacement thrust faults. We hypothesize that elevated pore pressures due to the low permeability hemipelagic sediment inhibit the formation of PTZs and favor small displacement thrusts in a narrow trench wedge. Conversely, turbidite layers within the hemipelagic sediment allow drainage and reduce the pore pressure. This increases the effective stress and shear strength on faults, resulting in strain localizing protothrusts. This implies that the changes in pore pressure imposed by differences in the sediment permeability control the style of deformation in the trench wedge and consequently, the geometry of the accretionary wedge.

Keywords: Nankai Trough, Protothrust Zone, Subduction zone

©2019. Japan Geoscience Union. All Right Reserved.

Temporal change in seismic velocity in the Nankai subduction zone from cross-correlation analysis of ambient noise

*Tatsunori Ikeda[1], Takeshi Tsuji[1]

1. Kyushu University

To investigate the temporal variation of stress or strain in the Nankai subduction zone, we estimated the temporal variation of seismic velocity by using cross-correlations of ambient noise in the frequency range 0.7–2.0 Hz, which was dominated by ACR waves, recorded by the DONET offshore seismic network from 1 October 2014 to 30 November 2017. The 1 April 2016 Off-Mie earthquake (M_W 5.9) and its aftershocks occurred beneath the seismic network.

Our results document a clear decrease in seismic velocity at the time of the earthquake. These coseismic velocity drops were correlated with peak ground velocities at each station, suggesting that dynamic stress changes due to strong ground motions are a primary factor in coseismic velocity variations. Differences in the sensitivity of seismic velocity changes to peak ground velocity may reflect subsurface conditions at each station, such as geological structures and effective pressure conditions. We also observed a long-term increase in seismic velocities, independent of the 2016 earthquake, that may reflect tectonic strain accumulation around the Nankai subduction zone. After removing the long-term trend, we found that the coseismic velocity drops had not completely recovered by the end of the observation period, possibly indicating nonlinear effects of the 2016 earthquake. Our results suggest that ambient noise cross-correlation might be used to monitor the stress state in the Nankai accretionary prism in offshore environments, which would contribute to a better understanding of earthquake processes.

Keywords: Nankai Trough, 2016 Off-Mie earthquake, monitoring, ambient noise, seismic interferometry

©2019. Japan Geoscience Union. All Right Reserved.

Strength profile of the Nankai accretionary prism evaluated from drilling parameters

*Yohei Hamada[1], Manami Kitamura[2], Takehiro Hirose[1], Yasuhiro Yamada[1], Yoshinori Sanada[1], Takamitsu Sugihara[1], Saneatsu Saito[1], KYAW MOE[1]

1. Japan Agency for Marine-Earth Science and Technology, 2. National Institute of Advanced Industrial Science andTechnology

In-situ rock strength with depth under the ground/seafloor is a critical parameter for various studies in geology and seismology. The measurements on rock/core samples, however, hardly have been done with success due to lack of drilled cores and sufficient knowledge about the in situ conditions. We proposed a new indicator of the strength, equivalent strength (EST) developing previous mechanical parameter (Mechanical specific energy: Teal, 1964) from the oil industry, which is converted only from drilling performance parameters such as drillstring rotational torque, bit depth and drillstring rotational per minute. The data processing was applied to the data taken from International Ocean Discovery Program (IODP) expeditions in the Nankai Trough (sites C0002 and C0023). The depth profiles of the EST at Site C0002 are drawn from 0 to 3000 meter-below-seafloor (mbsf), across the forearc basin and the accretionary prism, and the values of the calculated EST are consistent with compressive strength measured on core samples under estimated in situ stress conditions in laboratory. The high (~20 MPa) EST in the forearc basin sediments corresponds to the high $CaCO_3$ content indicating the carbonate is cementing the shallow formation. The EST did not show a significant increase at the forearc basin–accretionary prism boundary, however clearly increased within the prism, ca. below 1500 mbsf. This result may indicate that even the shallow accretionary prism has been strengthened by horizontal compression derived from plate subduction. At the site C0023, where the toe of the accretionary prism area off Cape Muroto, the EST trend increases with depth and suddenly changes between 600–650 mbsf, 840–870 mbsf, and 1120 ~ mbsf, corresponding to tuff0rich zone, top of the subducting sediments and the basement igneous rocks, respectively. This EST trend shows good agreement with P-wave velocity curve measured on core samples. The EST decreases from ~20 MPa to 5 MPa below the frontal decollement with sharp negative peak. This low-EST zone probably indicate the existence of excess fluid pressure.

Keywords: The Nankai Trough, Equivalent strength, Nankai Trough SeismogenicZone Experiment, T-Limit of the Deep Biosphere off Muroto

©2019. Japan Geoscience Union. All Right Reserved.

Paleotemperature anomalies deduced from thermal-maturity parameters within the décollement, off Cape of Muroto, Japan

*Nana Kamiya[1,2], Takehiro Hirose[2], Yuzuru Yamamoto[2], Yohei Hamada[2], Stephen A Bowden[3], Man-Yin Tsang[4], Kiho Yang[5], Satoshi Tonai[6], Weiren Lin[1,2]

1. Graduate School of Engineering, Kyoto University, 2. JAMSTEC, 3. University of Aberdeen, 4. University of Toronto, 5. Yonsei University, 6. Kochi University

Heat flow is characteristically high at the toe of the Nankai accretionary prism, off cape Muroto, and this is considered to be a consequence of the subduction of a hot and active ridge (e.g. Yamano et al., 2003). Despite present-day heat flow being known, how heat has changed over time in this area remains uncertain and is poorly constrained. To address this question, we have investigated palaeotemperatures using thermal maturity parameters measured on cores collected during IODP Expedition 370. Paleotemperature data were evaluated within the context of present-day heat flow and expected changes in temperature with respect to depth; e.g., numerical constraint whether present-day temperatures are too hot or cold to explain thermal maturity measurements, and whether there are anomalies with respect to depth. This is particularly important for Expedition 370 (T-limits) which selected the Muroto-site (Site C0023) because of its high heat flow and the chance this offers to investigate the habitability of the deep biosphere with respect to the temperature. Site C0023 is located 120 km from Cape Muroto, and is in the protothrust-zone of the Nankai accretionary prism. The hole encountered the décollement at 758-795 mbsf, and present-day temperatures were measured down to ~350 mbsf. Vitrinite reflectance was used to estimate maximum paleotemperatures and to look for thermal anomalies. The vitrinite reflectance increases with depth from 0.2 to 0.6 % from 200 to 700 mbsf, typical of conventional burial metamorphism, but changes little from 700 to 1000 mbsf (values stay about 0.6 %). There is a notable high value at 1090 mbsf (about 1%). There are anomalously high values of both vitrinite reflectance and sterane and hopane biomarker data at about 800 mbsf. For heating durations of 400, 4000, 40000 and 400000 years, and assuming thermal maturation using the EasyVit model of Burnham and Sweeny (1990), temperatures of 40~140 ℃ can explain data between 200 to 750 mbsf. To match measurements of vitrinite reflectance at 750 mbsf, a maximum paleotemperature of 140 ℃ is required. At 1090 mbsf, temperatures as high as ~200 ℃ could be needed. The difference between the paleo- and present-day temperatures is the notably the greatest at the décollement, strongly suggesting an elevated heat flow at some time. A heating duration of 400 years, an elevated a heat flow of 130 ±90 mW/m^2 and a temperature > 150 ℃ can explain the observations on the vitrinite reflectance. Considering the scales of space and time of thermal advection, a high-temperature fluid along the décollement zone is our currently preferred explanation.

Keywords: Muroto, Décollement, Paleotemperature anomalies

©2019. Japan Geoscience Union. All Right Reserved.

Modelling thermal maturity of an accretionary wedge

Utsav Mannu[2], *Masataka Kinoshita[1], Taras Gerya[3]

1. Earthquake Research Institute, University of Tokyo, 2. Department of Earth and Climate Science, IISER Pune, 3. Institute of Geophysics, ETH Zürich

In accretionary margins, the estimation of peak heating through the thermal maturity of organic material reveals differentiated deformational pathways in the adjoining sections of the wedge. As the thermal maturity of the deformed structures is a function of both the geothermal gradient and the duration of time it has been exposed to different gradients, the distribution of vitrinite reflectance (the measure of thermal maturity) in the wedge does not necessarily reveal the temporal deformational pathway of the individual pockets. As a result, the different portions of the accretionary wedge exhibit different correlations between the thermal maturity and a unique deformational pathway. These different correlations can be explored through the means of geodynamic modelling which can then be used in the field to ascertain a more holistic picture of deformation in an accretionary wedge. Therefore, in this study, we use a 2D plate subduction thermomechanical model, to simulate formation of accretionary wedge and the track the evolution of the vitrinite reflectance in the accretionary wedge.

Keywords: thermal maturity, accretionary wedge, numerical simulation

©2019. Japan Geoscience Union. All Right Reserved.

[E] Poster | S (Solid Earth Sciences)：S-SS Seismology

Tue. May 28, 2019 5:15 PM - 6:30 PM JST | Tue. May 28, 2019 8:15 AM - 9:30 AM UTC | Poster Hall International Exhibition Hall8, Makuhari Messe_28

[S-SS06] Nankai Trough Seismogenic Zone Experiment: Logging and sampling the seismogenic megathrust

convener:Kyuichi Kanagawa(Graduate School of Science, Chiba University), Demian M Saffer(Pennsylvania State University), Masataka Kinoshita(Earthquake Research Institute, University of Tokyo)

The Nankai Trough Seismogenic Zone Experiment (NanTroSEIZE) is a multidisciplinary investigation of fault mechanics and seismogenesis along the megathrust at the Nankai Trough subduction zone, and includes reflection and refraction seismic imaging, direct sampling by drilling, in situ measurements, and long-term monitoring in conjunction with laboratory and numerical modeling studies. During the past 12 IODP expeditions off Kii Peninsula since 2007, 15 sites have been drilled by D/V "Chikyu" down to depths from 100s of meters to more than 3000 meters below seafloor, where the inner and outer wedge of the Nankai margin has been logged and sampled extensively, and three state-of-the-art real-time downhole observatories are now in operation. The final NanTroSEIZE expedition aiming to log and sample the seismogenic megathrust at ~5200 meters below seafloor is now ongoing from October, 2018 to March, 2019.
In this session, we expect presentations not only on scientific outcomes from the past NanTroSEIZE expeditions, but also on the exciting preliminary results of the final NanTroSEIZE expedition. We welcome presentations on, but are not limited to, seismic imaging, borehole logging and monitoring, chemical analyses of pore water and mud gas, lithology, structures, physical properties and laboratory experiments of cuttings and core samples, and theoretical and numerical modeling.

[SSS06-P01] Crustal structure in the Nankai Trough seismogenic zone based on renewed depth images and seismic attribute analysis

*Kazuya Shiraishi[1], Yasuhiro Yamada[1], Masataka Kinoshita[2], Gaku Kimura[3] (1.Japan Agency for Marine-Earth Science and Technology, 2.Earthquake Research Institute, The University of Tokyo, 3.Tokyo University of Marine Science and Technology)

[SSS06-P02] Along-strike variations in protothrust zone characteristics at the Nankai Trough subduction margin

*Hannah Tilley[1], Gregory F Moore[1], Mikiya Yamashita[2], Shuichi Kodaira[2] (1.University of Hawaii at Manoa, 2.JAMSTEC)

[SSS06-P03] Temporal change in seismic velocity in the Nankai subduction zone from cross-correlation analysis of ambient noise

*Tatsunori Ikeda[1], Takeshi Tsuji[1] (1.Kyushu University)

[SSS06-P04] Strength profile of the Nankai accretionary prism evaluated from drilling parameters

★Invited Papers

*Yohei Hamada[1], Manami Kitamura[2], Takehiro Hirose[1], Yasuhiro Yamada[1], Yoshinori Sanada[1], Takamitsu Sugihara[1], Saneatsu Saito[1], KYAW MOE[1] (1.Japan Agency for Marine-Earth Science and Technology, 2.National Institute of Advanced Industrial Science andTechnology)

[SSS06-P05] Paleotemperature anomalies deduced from thermal-maturity parameters within the décollement, off Cape of Muroto, Japan

*Nana Kamiya[1,2], Takehiro Hirose[2], Yuzuru Yamamoto[2], Yohei Hamada[2], Stephen A Bowden[3], Man-Yin Tsang[4], Kiho Yang[5], Satoshi Tonai[6], Weiren Lin[1,2] (1.Graduate School of Engineering, Kyoto University, 2.JAMSTEC, 3.University of Aberdeen, 4.University of Toronto, 5.Yonsei University, 6.Kochi University)

[SSS06-P06] Modelling thermal maturity of an accretionary wedge

Utsav Mannu[2], *Masataka Kinoshita[1], Taras Gerya[3] (1.Earthquake Research Institute, University of Tokyo, 2.Department of Earth and Climate Science, IISER Pune, 3.Institute of Geophysics, ETH Zürich)

Crustal structure in the Nankai Trough seismogenic zone based on renewed depth images and seismic attribute analysis

*Kazuya Shiraishi[1], Yasuhiro Yamada[1], Masataka Kinoshita[2], Gaku Kimura[3]

1. Japan Agency for Marine-Earth Science and Technology, 2. Earthquake Research Institute, The University of Tokyo, 3. Tokyo University of Marine Science and Technology

To better understand geological structure in the Nankai Trough seismogenic zone, we investigate deformations in the accretionary prism based on renewed depth images and seismic attribute analyses. We reprocessed subareas of the Kumano-nada 3D MCS data acquired in 2006: 25 km x 12 km area including IODP C0002 site in Phase 1 (2015-2016) and 20 km x 12 km area including IODP C0006 site in Phase 2 (2017-2018). We also reprocessed 2D MCS data along a 50-km line crossing C0002 site in NW-SE direction, which was selected from a 2D survey ODKM03 in 2003 with a longer streamer cable (6 km) than streamer cables of the 3D survey (4.5 km). Quality improvement of reflection signals was achieved by applying recent broadband processing and advanced process to attenuate noise and multiple reflections. Depth domain reflection images were obtained after applying new pre-stack depth migration methods. Then, we calculated several seismic attributes from the 3D reflection image volumes, such as coherence and structure dips which are useful to interpret structural features.
As a result of our investigation, deformed structure within the inner accreted sediments and its relation with the megathrust fault are clearer than before. Anticlines are identified just below the Kumano forearc basin and fragmented reflections can be seen below the anticlines. Characteristic patterns of folds can be recognized on the horizontal section of the coherence cube, which are corresponding to the anticlines on the vertical sections. These reflection features imply development of fold structures due to thrust faults with branched minor faults. In the reprocessed 2D section, curved reflectors with stepwise displacement are imaged in the region of 4 - 6 km depth. These reflectors may represent multiple thrust faults with back-thrusts, and the thrust faults are consistent with the structural features in the 3D images. The detachments of the thrust faults seem to converge to wavy points on the megathrust fault surface. Furthermore, details of deformation and fracture in the outer accretionary prism are imaged clearer than the previous images. Lithological boundaries with displacement along imbricated thrusts can be traced beyond the fault, and conjugate faults due to horizontal compression which cut the in-sequence thrusts are recognized on the horizontal section from superimposed view of the coherence and dip angles. Reflectors within underthrusted sediments beneath the imbricated thrust layer are clearly imaged. Some of the reflectors can be identified as parts of detachment of the thrust faults. The topographic relief of the oceanic crust should be considered when the deformed structures in the overburden sediments and distribution of décollement are revisited.

Acknowledgements:
This research is supported by JSPS KAKENHI (JP15H05717).

Keywords: Nankai Trough seismogenic zone, crustal structure, reflection seismic, seismic attribute

©2019. Japan Geoscience Union. All Right Reserved.

Along-strike variations in protothrust zone characteristics at the Nankai Trough subduction margin

*Hannah Tilley[1], Gregory F Moore[1], Mikiya Yamashita[2], Shuichi Kodaira[2]

1. University of Hawaii at Manoa, 2. JAMSTEC

Protothrust zones (PTZs) are assumed to control the development of new frontal thrusts at subduction zones. PTZs are areas of incipient thrust faulting between the deformation front and the frontal thrust. However, limited resolution of previous seismic studies has hindered the study of their role in subduction accretion. New high-resolution seismic reflection surveys enabled detailed analysis of the PTZ along the Nankai Trough, SE Japan. Seventeen multichannel seismic reflection lines were collected perpendicular to the trench axis between Cape Ashizuri and Cape Muroto using a 1200m long, 192 channel hydrophone cable and a 380 in^3 (5.24L) cluster airgun array. These lines were processed using pre-stack depth migration. PTZs only existed where a turbidite sequence was present beneath the trench wedge. The PTZs consisted of closely spaced, sub-parallel protothrusts that decreased in spacing and increased in length landward. Where the turbidites were truncated by basement topography, there was a transitional PTZ heterogeneous protothrusts and small displacement thrust faults. We hypothesize that elevated pore pressures due to the low permeability hemipelagic sediment inhibit the formation of PTZs and favor small displacement thrusts in a narrow trench wedge. Conversely, turbidite layers within the hemipelagic sediment allow drainage and reduce the pore pressure. This increases the effective stress and shear strength on faults, resulting in strain localizing protothrusts. This implies that the changes in pore pressure imposed by differences in the sediment permeability control the style of deformation in the trench wedge and consequently, the geometry of the accretionary wedge.

Keywords: Nankai Trough, Protothrust Zone, Subduction zone

©2019. Japan Geoscience Union. All Right Reserved.

Temporal change in seismic velocity in the Nankai subduction zone from cross-correlation analysis of ambient noise

*Tatsunori Ikeda[1], Takeshi Tsuji[1]

1. Kyushu University

To investigate the temporal variation of stress or strain in the Nankai subduction zone, we estimated the temporal variation of seismic velocity by using cross-correlations of ambient noise in the frequency range 0.7–2.0 Hz, which was dominated by ACR waves, recorded by the DONET offshore seismic network from 1 October 2014 to 30 November 2017. The 1 April 2016 Off-Mie earthquake (M_W 5.9) and its aftershocks occurred beneath the seismic network.

Our results document a clear decrease in seismic velocity at the time of the earthquake. These coseismic velocity drops were correlated with peak ground velocities at each station, suggesting that dynamic stress changes due to strong ground motions are a primary factor in coseismic velocity variations. Differences in the sensitivity of seismic velocity changes to peak ground velocity may reflect subsurface conditions at each station, such as geological structures and effective pressure conditions. We also observed a long-term increase in seismic velocities, independent of the 2016 earthquake, that may reflect tectonic strain accumulation around the Nankai subduction zone. After removing the long-term trend, we found that the coseismic velocity drops had not completely recovered by the end of the observation period, possibly indicating nonlinear effects of the 2016 earthquake. Our results suggest that ambient noise cross-correlation might be used to monitor the stress state in the Nankai accretionary prism in offshore environments, which would contribute to a better understanding of earthquake processes.

Keywords: Nankai Trough, 2016 Off-Mie earthquake, monitoring, ambient noise, seismic interferometry

©2019. Japan Geoscience Union. All Right Reserved.

Strength profile of the Nankai accretionary prism evaluated from drilling parameters

*Yohei Hamada[1], Manami Kitamura[2], Takehiro Hirose[1], Yasuhiro Yamada[1], Yoshinori Sanada[1], Takamitsu Sugihara[1], Saneatsu Saito[1], KYAW MOE[1]

1. Japan Agency for Marine-Earth Science and Technology, 2. National Institute of Advanced Industrial Science andTechnology

In-situ rock strength with depth under the ground/seafloor is a critical parameter for various studies in geology and seismology. The measurements on rock/core samples, however, hardly have been done with success due to lack of drilled cores and sufficient knowledge about the in situ conditions. We proposed a new indicator of the strength, equivalent strength (EST) developing previous mechanical parameter (Mechanical specific energy: Teal, 1964) from the oil industry, which is converted only from drilling performance parameters such as drillstring rotational torque, bit depth and drillstring rotational per minute. The data processing was applied to the data taken from International Ocean Discovery Program (IODP) expeditions in the Nankai Trough (sites C0002 and C0023). The depth profiles of the EST at Site C0002 are drawn from 0 to 3000 meter-below-seafloor (mbsf), across the forearc basin and the accretionary prism, and the values of the calculated EST are consistent with compressive strength measured on core samples under estimated in situ stress conditions in laboratory. The high (~20 MPa) EST in the forearc basin sediments corresponds to the high $CaCO_3$ content indicating the carbonate is cementing the shallow formation. The EST did not show a significant increase at the forearc basin–accretionary prism boundary, however clearly increased within the prism, ca. below 1500 mbsf. This result may indicate that even the shallow accretionary prism has been strengthened by horizontal compression derived from plate subduction. At the site C0023, where the toe of the accretionary prism area off Cape Muroto, the EST trend increases with depth and suddenly changes between 600–650 mbsf, 840–870 mbsf, and 1120 ~ mbsf, corresponding to tuff0rich zone, top of the subducting sediments and the basement igneous rocks, respectively. This EST trend shows good agreement with P-wave velocity curve measured on core samples. The EST decreases from ~20 MPa to 5 MPa below the frontal decollement with sharp negative peak. This low-EST zone probably indicate the existence of excess fluid pressure.

Keywords: The Nankai Trough, Equivalent strength, Nankai Trough SeismogenicZone Experiment, T-Limit of the Deep Biosphere off Muroto

©2019. Japan Geoscience Union. All Right Reserved.

Paleotemperature anomalies deduced from thermal-maturity parameters within the décollement, off Cape of Muroto, Japan

*Nana Kamiya[1,2], Takehiro Hirose[2], Yuzuru Yamamoto[2], Yohei Hamada[2], Stephen A Bowden[3], Man-Yin Tsang[4], Kiho Yang[5], Satoshi Tonai[6], Weiren Lin[1,2]

1. Graduate School of Engineering, Kyoto University, 2. JAMSTEC, 3. University of Aberdeen, 4. University of Toronto, 5. Yonsei University, 6. Kochi University

Heat flow is characteristically high at the toe of the Nankai accretionary prism, off cape Muroto, and this is considered to be a consequence of the subduction of a hot and active ridge (e.g. Yamano et al., 2003). Despite present-day heat flow being known, how heat has changed over time in this area remains uncertain and is poorly constrained. To address this question, we have investigated palaeotemperatures using thermal maturity parameters measured on cores collected during IODP Expedition 370. Paleotemperature data were evaluated within the context of present-day heat flow and expected changes in temperature with respect to depth; e.g., numerical constraint whether present-day temperatures are too hot or cold to explain thermal maturity measurements, and whether there are anomalies with respect to depth. This is particularly important for Expedition 370 (T-limits) which selected the Muroto-site (Site C0023) because of its high heat flow and the chance this offers to investigate the habitability of the deep biosphere with respect to the temperature. Site C0023 is located 120 km from Cape Muroto, and is in the protothrust-zone of the Nankai accretionary prism. The hole encountered the décollement at 758-795 mbsf, and present-day temperatures were measured down to ~350 mbsf. Vitrinite reflectance was used to estimate maximum paleotemperatures and to look for thermal anomalies. The vitrinite reflectance increases with depth from 0.2 to 0.6 % from 200 to 700 mbsf, typical of conventional burial metamorphism, but changes little from 700 to 1000 mbsf (values stay about 0.6 %). There is a notable high value at 1090 mbsf (about 1%). There are anomalously high values of both vitrinite reflectance and sterane and hopane biomarker data at about 800 mbsf. For heating durations of 400, 4000, 40000 and 400000 years, and assuming thermal maturation using the EasyVit model of Burnham and Sweeny (1990), temperatures of 40~140 ℃ can explain data between 200 to 750 mbsf. To match measurements of vitrinite reflectance at 750 mbsf, a maximum paleotemperature of 140 ℃ is required. At 1090 mbsf, temperatures as high as ~200 ℃ could be needed. The difference between the paleo- and present-day temperatures is the notably the greatest at the décollement, strongly suggesting an elevated heat flow at some time. A heating duration of 400 years, an elevated a heat flow of 130 ±90 mW/m^2 and a temperature > 150 ℃ can explain the observations on the vitrinite reflectance. Considering the scales of space and time of thermal advection, a high-temperature fluid along the décollement zone is our currently preferred explanation.

Keywords: Muroto, Décollement, Paleotemperature anomalies

©2019. Japan Geoscience Union. All Right Reserved.

Modelling thermal maturity of an accretionary wedge

Utsav Mannu[2], *Masataka Kinoshita[1], Taras Gerya[3]

1. Earthquake Research Institute, University of Tokyo, 2. Department of Earth and Climate Science, IISER Pune, 3. Institute of Geophysics, ETH Zürich

In accretionary margins, the estimation of peak heating through the thermal maturity of organic material reveals differentiated deformational pathways in the adjoining sections of the wedge. As the thermal maturity of the deformed structures is a function of both the geothermal gradient and the duration of time it has been exposed to different gradients, the distribution of vitrinite reflectance (the measure of thermal maturity) in the wedge does not necessarily reveal the temporal deformational pathway of the individual pockets. As a result, the different portions of the accretionary wedge exhibit different correlations between the thermal maturity and a unique deformational pathway. These different correlations can be explored through the means of geodynamic modelling which can then be used in the field to ascertain a more holistic picture of deformation in an accretionary wedge. Therefore, in this study, we use a 2D plate subduction thermomechanical model, to simulate formation of accretionary wedge and the track the evolution of the vitrinite reflectance in the accretionary wedge.

Keywords: thermal maturity, accretionary wedge, numerical simulation

©2019. Japan Geoscience Union. All Right Reserved.

[E] Poster | S (Solid Earth Sciences)：S-MP Mineralogy & Petrology

Tue. May 28, 2019 10:45 AM - 12:15 PM JST | Tue. May 28, 2019 1:45 AM - 3:15 AM UTC | Poster Hall International Exhibition Hall8, Makuhari Messe_7

[S-MP29] Oceanic and Continental Subduction Processes

convener:REHMAN Ur Hafiz(Department of Earth and Environmental Sciences, Graduate School of Science and Engineering, Kagoshima University), Tatsuki Tsujimori(Tohoku University), Chin-Ho Tsai(Department of Natural Resources and Environmental Studies, National Dong Hwa University), Kazuaki Okamoto(Faculty of Education, Saitama University)

This JpGU-AGU joint session aims at bringing earth scientists from Japan and overseas to present their research related to the processes of oceanic and continent subduction, continent-continent collisions, metamorphism of crustal rocks, formation of the oceanic/continental arcs, and accretion/ tectonic erosion of material along subduction boundaries.

Topics such as role of the fore- and back-arcs in the subduction zones, process of accretion of volcaniclastic and terrigenous sediments along the subduction/collision boundaries, deformation and metamorphism of subducted crust, and exhumation will be the main focus of the session.

In addition to the above mentioned topics, our focus for the10th anniversary of this international session will be towards our understanding and progress on the ultrahigh-pressure/temperature metamorphic terranes in the world.

Exchange of ideas among geoscientists applying different approaches on problems related to the theme of the session are most welcome.

[SMP29-P01] Zircon U-Pb ages of metasedimentary rocks in the Hakogase (Hida Marginal) area, Fukui Prefecture.

*Atsushi MIYASHITA[1], Tatsuki Tsujimori[2], Daniel Pastor-Galán[3], Yi Keewook[4] (1.Seikei University, 2.Tohoku University, 3.Salamanca University, 4.Korea Basic Science Institue)

[SMP29-P02] Late Permian to Early Triassic back-arc type volcanism in the southern Mongolia volcano-plutonic belt of the Central Asian Orogenic Belt: Implication for timing of the final closure of the Palaeo-Asian Ocean

*Takeshi Imayama[1], Yoichiro Koh[2], Kazumasa Aoki[3], Mototaka Saneyoshi[4], Koshi Yagi[5], Shogo Aoki[4], Yoshihiro Sawada[6], Chiaki Ikawa[5], Tomoya Terada[4], Shinobu Ishigaki[4], Shin Toyoda[3], Khishigjav Tsogtbaatar[7], Buuvei Mainbayar[7] (1.Research Institute of Natural Sciences, Okayama University of Science, 2.Graduate School of Environmental Science, Hokkaido University, 3.Faculty of Science, Okayama University of Science, 4.Faculty of Biosphere - Geosphere Science, Okayama University of Science, 5.Hiruzen Institute for Geology and Chronology, 6.Emeritus Professor of Shimane University, 7.Institute of Paleontology and Geology, Mongolian Academy of Sciences)

[SMP29-P03] Mantle dynamics of slab breakoff constrained from the temporal change of the melting depth estimated from the Cumulate Member of the Ordovician Hayachine-Miyamori Ophiolite

*Takafumi Kimura[1], Kazuhito Ozawa[1] (1.Department of Earth and Planetary Science, The University of Tokyo)

[SMP29-P04] **Evidence of HIMU seamount on the Farallon Plate: Application of *in-situ* Sr-Pb isotope analysis to Franciscan lawsonite-bearing metagreywacke**

*Tomomi Hara[1], Tatsuki Tsujimori[1], Jun-Ichi Kimura[2] (1.Tohoku University, 2.Japan Agency for Marine-Earth Science and Technology)

[SMP29-P05] Boron isotope variations of antigorite serpentinites associated with high-pressure metamorphic rocks: A case study in the Itoigawa–Omi area of the Hida-Gaien Belt, Japan

*Chinatsu Yamada[1], Tatsuki Tsujimori[1], King Chang[2], Jun-Ichi Kimura[2] (1.Tohoku University, 2.Japan Aegency for Marine-Earth Science and Technology)

[SMP29-P06] **Study of zircons structures from the Miocene Shibi-san Granodiorite, Kagoshima Prefecture, Japan**

*Nakabayashi Marimo[1], REHMAN Ur Hafiz[1] (1.Kagoshima University)

[SMP29-P07] **Experimental modeling of eclogite and C-O-H fluid interaction in the subduction zones**

*Nadezda Chertkova[1], Shigeru Yamashita[2], Hiroaki Ohfuji[1], Tetsuo Irifune[1], Hirokazu Kadobayashi[1], Yoshitaka Yamamoto[3] (1.Ehime University, Geodynamics Research Center, 2.Okayama University, Institute for Planetary Materials, 3.National Institute of Advanced Industrial Science and Technology)

[SMP29-P08] Microfabrics of omphacite and garnet in eclogite from the Lanterman Range, northern Victoria Land, Antarctica

*Daeyeong Kim[1], Taehwan Kim[2], Jungmin Kim[3] (1.Division of Polar-Earth Sciences, Korea Polar Research Institute, 2.School of Earth and Environmental Sciences, Seoul National University, 3.Earth and Environmental Sciences, Korea University)

[SMP29-P09] Primordial Apatite from Ophiolite in Taiwan

*Nobuaki Niitsuma[1], Reishi Takashima[2], Yuan Hsi Lee[3] (1.Institute of Geosciences,Shizuoka University, 2.Tohoku University Museum, 3.National Chung-Cheng University, Taiwan)

[SMP29-P10] The evolution of the Cretaceous Jinan Basin in South Korea and the age and tectonic setting for the volcanic rocks in it

*Seung Hwan LEE[1], Chang Whan Oh[1] (1.Department of earth and environmental sciences Chonbuk national university)

[SMP29-P11] GEOCHORONOLOGY AND PETROCHEMISTREY OF LATE PALEOZOIC MAGMATIC ROCKS OF THE MANDAKH AREA, SOUTHEAST MONGOLIA

*Undarmaa Batsaikhan[1], Noriyoshi Tsuchiya[1], Masaoki Uno[1], Yukio Isozaki[2], Uyanga Bold[2], Hikaru Sawada[2] (1.Graduate School of Environmental Studies, Tohoku University, 2.Graduate School of Arts and Sciences The University of Tokyo)

[SMP29-P12] Feedbacks Offshore the Cascadia Margin

*Joan S Gomberg[1] (1.USGS Earthquake Science Center)

Zircon U-Pb ages of metasedimentary rocks in the Hakogase (Hida Marginal) area, Fukui Prefecture.

*Atsushi MIYASHITA[1], Tatsuki Tsujimori[2], Daniel Pastor-Galán[3], Yi Keewook[4]

1. Seikei University, 2. Tohoku University, 3. Salamanca University, 4. Korea Basic Science Institue

Combined chronological study using detrital zircon U-Pb dating and phengite K-Ar dating enables to understand the tectonic evolution of the high *P/T* metamorphic belt. The youngest age of detrital zircon U-Pb ages of psamites in the Hida marginal metamorphic rocks (HMMR = Renge belt) approximate its depositional ages (Tsutsumi et al., 2009). The closure temperature of the phengite K-Ar ages are controlled by deformation and recrystallization during exhumation of the metamorphic rocks(Itaya and Tsujimori, 2015). Therefore, the gap between the youngest age of detrital zircons and phengite K-Ar ages are the age difference between subuduction and uplift of metamorphics.
The Hakogase (Nigure-gawa, Kuzuryu, Fukui Prefecture) metamorphic rocks belong to HMMR member as the olistolith in the Cretaceous Tedori Group. It consists mainly pelites with small amount of basites and mables. The main index mineral assemblage of metasediments are garnet + chlorite, and the phenigite K-Ar ages are 287.8 - 283.6 Ma (Kunugiza et al., 2004). Relic Lawsonite was also found in the basaites and psamites (Miyakawa, 1982).
The detrital Zircons U-Pb ages in the two pelites are obtained by the SHRIMP II of KBSI. The youngest U-Pb ages of detrital zircons are 307Ma. The gap of the sedimentation between uplift of the Hakogase metamorphics is estimated 20 Ma. This value means the migration speed of the HMMR metamorphic rocks are 1/10 of plate motion. This rapid migration speed is common for the high *P/T* metamorphic rocks.

Keywords: high P/T metamorphic rocks, Zircon U-Pb ages, Phengite K-Ar ages

©2019. Japan Geoscience Union. All Right Reserved.

Late Permian to Early Triassic back-arc type volcanism in the southern Mongolia volcano-plutonic belt of the Central Asian Orogenic Belt: Implication for timing of the final closure of the Palaeo-Asian Ocean

*Takeshi Imayama[1], Yoichiro Koh[2], Kazumasa Aoki[3], Mototaka Saneyoshi[4], Koshi Yagi[5], Shogo Aoki[4], Yoshihiro Sawada[6], Chiaki Ikawa[5], Tomoya Terada[4], Shinobu Ishigaki[4], Shin Toyoda[3], Khishigjav Tsogtbaatar[7], Buuvei Mainbayar[7]

1. Research Institute of Natural Sciences, Okayama University of Science, 2. Graduate School of Environmental Science, Hokkaido University, 3. Faculty of Science, Okayama University of Science, 4. Faculty of Biosphere - Geosphere Science, Okayama University of Science, 5. Hiruzen Institute for Geology and Chronology, 6. Emeritus Professor of Shimane University, 7. Institute of Paleontology and Geology, Mongolian Academy of Sciences

The timing of final subduction and closure of the Palaeo-Asian Ocean is still controversial in the eastern segments of the Central Asian Orogenic Belt (CAOB). A more detailed understanding is needed with respect to the formation of volcanic rocks and sediments associated with the final closure of the Palaeo-Asian Ocean in southern Mongolia. We investigated alkali series volcanic rocks newly discovered in the southern Mongolia volcano-plutonic belt of the CAOB and classified as basalt, basaltic trachyandesite, andesite, trachyandesite, and trachyte, mainly showing andesitic-dacitic compositions. In Harker diagrams, the TiO_2, FeO, MnO, Al_2O_3, CaO, and MgO contents generally decrease with increasing SiO_2, representing a series of differentiated volcanic rocks. The primitive mantle-normalized trace element spider diagram is characterized by incompatible element-rich patterns and negative Nb anomalies. The tectonic discrimination diagrams show that the volcanic rocks were formed by arc-related volcanism rather than within-plate volcanism. K-Ar dating of feldspars from six volcanic rocks yields ages ranging from 270 to 239 Ma, indicating that andesitic and dacitic magmatism occurred during this period. These geochemical and geochronological data indicate that the differentiated volcanic rocks intruding middle to late Palaeozoic volcanic sediments were formed by back-arc type subduction ca. 270–240 Ma. Based on detrital zircon U-Pb ages, the terrigenous sandstones underlain by the volcanic sediments record a maximum depositional age of Late Triassic (ca. 220–200 Ma) and include a main cluster of Early Devonian ages (ca. 410–390 Ma), possibly derived from the Devonian-Carboniferous arc complex observed surrounding this study area. These results from the volcanic and sedimentary rocks in this study, combined with investigations in previous studies, imply that subduction beneath the eastern segments of the CAOB to consume the Palaeo-Asian Ocean continued until Late Permian to Early Triassic.

Keywords: Palaeo-Asian Ocean, southern Mongolia, Central Asian Orogenic Belt, back-arc type volcanism

©2019. Japan Geoscience Union. All Right Reserved.

Mantle dynamics of slab breakoff constrained from the temporal change of the melting depth estimated from the Cumulate Member of the Ordovician Hayachine-Miyamori Ophiolite

*Takafumi Kimura[1], Kazuhito Ozawa[1]

1. Department of Earth and Planetary Science, The University of Tokyo

Slab breakoff, detachment of oceanic lithosphere highly expected during arc-continent collision, is one of the important mechanisms inducing passive upwelling of the asthenosphere and magma generation in arc environments [1]. In order to better understand the mantle dynamics of slab breakoff, we need to use continuous geological record with high time resolution. In this study, we have extracted a record of temporal change of the magma generation depth from cumulates in an Ordovician arc ophiolite at a time resolution of several tens of million years.
The Hayachine-Miyamori Ophiolite, northern Japan, is one of the Ordovician ophiolite formed in an arc environment [2]. The ultramafic member was built up by three main magmatic stages, which are recorded in three rock units: Tectonite Member, Cumulate Member, and ultramafic dikes, in the order of formation ages. The last two units in the entire evolution of the ophiolite is explained by decompressional melting of sub-slab mantle triggered by slab breakoff [2][3]. The melting depth of an ultramafic magma solidified as dikes in the Cumulate Member is estimated to be ~170km [3]. Our recent field study clarified a large-scale stratification characterized by alternation of wehrlite-dominant and dunite-dominant layers in the Cumulate Member. Each layer has a thickness from several meters to ~1 km and, the total thickness attains ~3km. Moreover, we succeeded in specifying the strike and plunge of the gravity field to be ~N48°E and ~20°NE during the cumulate formation from field information and westward stratigraphic younging [4].
We estimated the temporal change of generation depth of parent magmas of the Cumulate Member by garnet signature in heavy rare earth elements (HREEs) as depth proxy. The information may constrain the mantle dynamics during the slab breakoff. We examined stratigraphic variation of HREE ratio at the core of clinopyroxenes over the thickness of ~2km in the Cumulate Member. The obtained variation of the Dy/Lu increases from ~12.9 to ~16.5 with increasing the stratigraphic height. We estimated the extent of melting in the garnet stability field increasing from ~50 to ~90% of the total melting by applying an open-system fractional melting model to reproduce the Dy/Lu variation.
We also estimated the time scale of formation of the Cumulate Member by using cm –10cm scale heterogeneity recorded in contact zone of intruded magma and the host. The profile of Mg# of olivine in xenoliths of the Tectonite Member occurring at the bottom of the Cumulate Member shows that the cooling time is less than several tens of million years [5]. The dunite of the Cumulate Member contacting the ultramafic dike shows a systematic decrease of Mg# from 90 to 86.8 over the distance of 54 mm towards the contact. We calculated the time scale of subsolidus diffusional exchange between the dunite and dike and obtained several tens of million years at ~1000℃. The host was kept at a high temperature when the dikes intruded because of the absence of chilled margin. We thus estimated time scale of formation of the Cumulate Member to be < several tens of million years.
We propose the following tectonic model in the Ordovician northern Japan on the basis of the above result. The slab breakoff took place at the depth slightly deeper than the boundary of spinel and garnet stability fields (~80 km) and induced counter flow and adiabatic melting of the sub-slab mantle. The melting depth deepened down to ~170 km on the time scale of several tens of million years, which corresponds to the time scale to complete the slab breakoff. The sinking velocity of the slab is more than

©2019. Japan Geoscience Union. All Right Reserved.

a few millimeters per year.

[1]: Davies et al., 1995. [2]: Ozawa et al., 2015. [3],[4]: Kimura et al., 2017, 2018, JpGU abstract. [5]: Ozawa, 1983.

Keywords: slab breakoff, arc ophiolite, cumulate

©2019. Japan Geoscience Union. All Right Reserved.

Evidence of HIMU seamount on the Farallon Plate: Application of *in-situ* Sr-Pb isotope analysis to Franciscan lawsonite-bearing metagreywacke

*Tomomi Hara[1], Tatsuki Tsujimori[1], Jun-Ichi Kimura[2]

1. Tohoku University, 2. Japan Agency for Marine-Earth Science and Technology

Since bulk isotopic composition of oceanic basalt is susceptible to element remobilization during alteration process, there is a risk of causing misread of geochemical signatures from bulk metabasaltic rocks in subduction complex. As Hara et al. (2018) demonstrated, however, *in-situ* Sr-Pb isotope analysis of lawsonite in high-pressure metabasaltic rocks has a great potential for tracing the geochemical signatures reflecting the igneous protolith. In this study, we have applied the method to lawsonite in metasedimentary rocks to explore clastic components of a trench-fill sediment. A jadeite-bearing Franciscan metagreywacke from Pacheco Pass area, east-central Diablo Range, California Coast Ranges was selected for geochemical reconnaissance.

Lawsonites in the Franciscan metagreywacke record a high initial Pb isotope ratios ($^{206}Pb/^{204}Pb$ = 18.74–19.66, $^{207}Pb/^{204}Pb$ = 15.58–15.70 and $^{208}Pb/^{204}Pb$ = 38.41–39.34). This Pb-isotope signature suggests that a protolith of the metagreywacke have contained a debris derived from a HIMU-type basalt. Considering the maximum depositional age of the metagreywacke at ~102 Ma, the underflow of the Farallon Plate beneath continental crust of the North American Plate would have carried a HIMU seamount to a Franciscan trench.

Our study has demonstrated the potential application of 'lawsonitology' as sedimentary provenance analyses for metamorphosed accretionary complex. Moreover, the results would manifest that Pb isotopic signature of ancient oceanic basalt can be detectable from Ca-Al silicate mineral, such as lawsonite, epidote and pumpellyite, in metamorphic rocks.

Keywords: Lawsonite, Sr-Pb isotope, LA-MC-ICPMS, HIMU, Metasediment

©2019. Japan Geoscience Union. All Right Reserved.

Boron isotope variations of antigorite serpentinites associated with high-pressure metamorphic rocks: A case study in the Itoigawa–Omi area of the Hida-Gaien Belt, Japan

*Chinatsu Yamada[1], Tatsuki Tsujimori[1], King Chang[2], Jun-Ichi Kimura[2]

1. Tohoku University, 2. Japan Aegency for Marine-Earth Science and Technology

Boron isotope study of serpentinites in the Franciscan Complex using an ablation volume correction (AVC) LA-MC-ICPMS discriminates two groups (Yamada et al., 2018 JpGU abstr.; Yamada et al. 2019, in press). Serpentinites associated with blueschists are characterized by lighter boron isotope than serpentinites without blueschist-facies rocks. The lighter boron isotope signature (< ~10 ‰) of blueschist-bearing serpentinites results from interaction with forearc slab fluids with low δ^{11}B in deeper depth. In order to evaluate the versatility of B isotopes and composition of high-pressure metamorphosed serpentinites, we investigated antigorite serpentinites associated with three different type of high-pressure metamorphic rocks in the Itoigawa–Omi area.

The investigated serpentinites can be grouped into two types based on the B isotopes. Antigorite serpentinite with blueschist- and eclogite-facies metamorphic rocks in the Yunotani Valley is characterized by moderate boron (12.5–48.4 $\mu g \cdot g^{-1}$) and lower δ^{11}B (+6.6 to +12.3‰ [mostly smaller than +8‰]; n= 10); Brucite-bearing antigorite serpentinite with barroisite-bearing mafic schist in the Kotaki-gawa River is characterized by very high boron (37.5 –302 $\mu g \cdot g^{-1}$) and lower δ^{11}B (+5.8 to +10.7‰ [mostly smaller than +8‰]; n= 10). In contrast, antigorite serpentinite with garnet amphibolite in the Omi-gawa River is characterized by a wide range of boron (9.1–145 $\mu g \cdot g^{-1}$) and relatively high δ^{11}B (+11.5 to + 14.8 ‰; n= 10).

Our preliminary reconnaissance shows significantly lower δ^{11}B (smaller than +8‰) in antigorite serpentinites of the 'Eclogite Unit' proposed by Tsujimori (2002). This trend is consistent with our earlier study in the Franciscan Complex. The antigorite serpentinites in the 'Eclogite Unit' might have been affected by a deep forearc slab fluids.

Keywords: Serpentinite, boron isotope, subduction zone

©2019. Japan Geoscience Union. All Right Reserved.

Study of zircons structures from the Miocene Shibi-san Granodiorite, Kagoshima Prefecture, Japan

*Nakabayashi Marimo[1], REHMAN Ur Hafiz[1]

1. Kagoshima University

The Miocene granodiorite body (zircon fission track age by Miyachi, 1985) of the Mount Shibi, Kagoshima prefecture is a lenticular stock that intrudes the Cretaceous sedimentary rocks of the Shimanto belt. Previous studies subdivided the granodiorite body into the Kusu-bae (core facies) and Hira-bae (marginal facies) types based on the changes in litho-facies and distinct chemical composition of biotite and amphibole (Yamamoto et al., 1988). We conducted field survey in the study area and found no clear contrasts to sub-divide the body, instead it represents a single pluton with local chemical variation along the marginal portions. Based on detailed petrography, the entire body appears as homogeneous stock exhibiting identical mineral assemblage with no clear evidence that can mark the boundary between Kusu-bae and Hira-bae types. Moreover, to understand the processes of magmatic crystallization we investigated more than 600 zircon grains from about 8 samples for external (applying the zircon morphology method of Pupin, 1980) and internal morphology using the Cathodoluminescence imaging. Based on the Pupin’ s method, the deduced temperature range for the zircon crystallization was between 750 and 850℃. In addition, internal structures of zircon (CL images) showed oscillatory zoning with continuous growth domains and abundant apatite inclusions, suggesting the magma was fluid-rich and have been crystallized under relatively higher temperature. We also investigated zircons from the surrounding hornfels (Shimanto belt rocks) that were affected thermally due to the contact metamorphism. Zircons from the hornfels are completely different and rounded with different internal structures. Zircons from the so-called Kusu-bae and Hira-bae types are identical and suggest their crystallization from a single parental magma hence the pluton cannot be sub divisible.

References
Miyachi M. (1985). Fission track ages of some granitic rocks in Outer Zone ofKyushu, Japan. Journal of Mineralogical and Petrological Sciences 80, 406-409.
Pupin J. P. (1980). Zircon and granite petrology. Contribution to Mineralogy and Petrology 73, 207-220.
Yamamoto M., Oniwa N., Toyota K. (1988). Compositional Variation of the Shibi-san Granodioraite Body, Kagoshima Prefecture, Japan. Bulletin of the Kagoshima University Science Faculty 21, 35-49.

Keywords: zircon, granodiorite, crystal shape

©2019. Japan Geoscience Union. All Right Reserved.

Experimental modeling of eclogite and C-O-H fluid interaction in the subduction zones

*Nadezda Chertkova[1], Shigeru Yamashita[2], Hiroaki Ohfuji[1], Tetsuo Irifune[1], Hirokazu Kadobayashi[1], Yoshitaka Yamamoto[3]

1. Ehime University, Geodynamics Research Center, 2. Okayama University, Institute for Planetary Materials, 3. National Institute of Advanced Industrial Science and Technology

The presence of volatile components controls melting relationships in the subducting oceanic plate and the overlying mantle wedge, affecting their physical properties and seismic observables. The major volatile species in the mantle low oxygen fugacity environment are considered to be H_2O and CH_4, as estimated for mantle xenoliths and C-O-H fluid speciation in equilibrium with diamond [1,2]. Experimental studies with the direct monitoring of phase assemblages and melting relationships in the silicate systems with C-O-H components can shed light on the processes, which take place in the subduction zones, and provide important data for interpretation of observed physical parameters.
In this study, we employed *in situ* spectroscopic methods in combination with the diamond anvil cell (DAC) technique for investigation of C-O-H fluid behavior and its influence on phase relationships in the eclogite–5.75H_2O–CH_4 system at temperatures up to 1000 degree C and pressures exceeding 5 GPa. We designed a new cell assembly for Mao-type symmetric diamond anvil cell with large optical access to the sample in order to make it suitable for infrared and Raman measurements directly at high-pressure and high-temperature conditions. Mineral phase assemblages, observed during experiments, are consistent with those described in the dry system of the similar basaltic composition [3]. At the same time, miscibility between aqueous and carbonaceous components in the fluid phase coexisting with silicate minerals was confirmed at temperatures above 800 degree C and pressures above 3.2 GPa.

References

[1] Shirey, S.B., Cartigny, P., Frost, D.J., Keshav, S., Nestola, F., Nimis, P., Pearson, D.G., Sobolev, N.V. and Walter, M.J. (2013) *Rev. Mineral. Geochem.*, **75**, 355-421.
[2] Belonoshko, A. and Saxena, S. (1992) *Geochim. Cosmochim. Acta*, **56**, 3611-3626.
[3] Yasuda, A., Fujii, T. and Kurita, K. (1994) *J. Geophys. Res.: Solid Earth*, **99**, 9401-9414.

©2019. Japan Geoscience Union. All Right Reserved.

Microfabrics of omphacite and garnet in eclogite from the Lanterman Range, northern Victoria Land, Antarctica

*Daeyeong Kim[1], Taehwan Kim[2], Jungmin Kim[3]

1. Division of Polar-Earth Sciences, Korea Polar Research Institute, 2. School of Earth and Environmental Sciences, Seoul National University, 3. Earth and Environmental Sciences, Korea University

Layered structures in metamorphic rocks are sometimes crucial to occur strain localization then affect to seismic properties. We conducted microstructural analyses omphacite and garnet in foliated eclogite from the Lanterman Range, northern Victoria Land, Antarctica, to determine the influence of the layered structure on seismic observations in subduction zone. The analyzed eclogite, composed of layered garnet-rich and omphacite-rich layers, shows the low aspect ratios, similar angular distribution of long axes relative to the foliation, uniform grain size distribution, near-random crystallographic preferred orientations (CPOs), and misorientation angle distributions of garnet and opposite characteristics of omphacite in both layers. The results of fabric analyses are consistent with strain localization into omphacite or omphacite-rich layers rather than garnet or garnet-rich layers. Our results therefore demonstrate the importance of the layered structure in strain localization and in the development of the seismic anisotropies of subducting oceanic crust.

Keywords: Eclogite, EBSD, Layered structure

©2019. Japan Geoscience Union. All Right Reserved.

Primordial Apatite from Ophiolite in Taiwan

*Nobuaki Niitsuma[1], Reishi Takashima[2], Yuan Hsi Lee[3]

1. Institute of Geosciences,Shizuoka University, 2. Tohoku University Museum, 3. National Chung-Cheng University, Taiwan

Apatite is a common accessory mineral in igneous rocks. Because apatite has a wide range of trace element compositions as well as strong resistance to diagenetic alteration, the trace element composition of apatite has been used for tracing petrogenetic processes of plutonic bodies as well as the tephrochronology of Paleozoic tephras and Quaternary volcaniclastic deposits.

We studied trace element compositions of apatites from Ophiolite in Taiwan. The Ophiolite with mafic-ulatramafic rocks (150811-14) expose along the anticlinal axes of the metamorphic belts in Backbone Range of Taiwan, and exotic gabbro block (MA-15B) in chaotic deposits of Lichi Melange, in the southern end of Longitudinal Valley, in East Taiwan.

Lee (2015 JpGU; Chen et al., 2017 Tectonics) reported that zircon ages of Ophiolites in Taiwan are concentrated to 15 Ma, which should relate with termination of spreading in South China Sea and Shikoku & Parece Vela Basin just before Japan Sea Opening, and large scale igneous activities in the Outer Zone of Southwest Japan just after Japan Sea Opening (Niitsuma & Lee, 2018 JpGU).

Fifteen and twelve apatite phenocrysts from samples of MA-15B and 150811-14 were analyzed for major and minor elements using a JEOL 8530F wavelength dispersive Electron Probe Micro Analyzer (Takashima et al., 2017 Quaternary Geochronology) in weight % as follow;
__major elements: P=17.956 +/-0.100, 17.926 +/-0.129
_____Ca=38.362 +/-0.329, 38.128 +/-0.273
_____F=1.082+/-0.151, 0.445+/-0.046
__trace elements: Cl<0.01, 0.04 Mg<0.01, 0.01 Mn<0.04, 0.05
_____Fe<0.03, 0.17 Ce<0.09, 0.05 Y<0.13, 0.04

The contents of trace elements are extremely low and we concluded the apatite might be primordial without any contaminations and petrogenetic effect, and crystallized directly in the magma above rifted mantle along the northwestern margin of West Philippine Basin just before Japan Sea Opening.

Keywords: Apatite, trace element , Ophiolite, Taiwan, Opening of Japan Sea

©2019. Japan Geoscience Union. All Right Reserved.

The evolution of the Cretaceous Jinan Basin in South Korea and the age and tectonic setting for the volcanic rocks in it

*Seung Hwan LEE[1], Chang Whan Oh[1]

1. Department of earth and environmental sciences Chonbuk national university

The Jinan Basin is one of the Cretaceous pull-apart basins in the South Korea. It locates along the Yongdong-Gwangju fault system and consists of non-marine sediments with volcanic and pyroclastic rocks. The sinistral strike slip movement which formed the Cretaceous pull apart basins was occurred by the collision between Siberian and Manchuria blocks at ca. 130~100Ma. LA-MC-ICPMS age dating on the zircons from sedimentary and igneous rocks indicates followings. The sedimentation in the Jinan Basin had started at least from 97.7Ma and continued until 89.47Ma. During the sedimentation, basaltic andesite extruded at 90-92 Ma and later rhyolitc and andesitic magma intruded the Jinan Basin at 90-89 Ma and 85-84 Ma respectively. Later the Jinan Basin uplifted to form Noryeong mountain range due to the compression which was related with dextral strike slip fault movement. This fault movement is expected to be caused by the collision between Indian plate and Eurasian plate at ca. 55~25Ma. AFT(Apatite Fission Track) age from sediments in the Jinan Basin is approximately 68Ma. Due to the formation of Noryeong mountain range, the *Coreoleuciscus splendidus* was differentiated into two species, these two species of *Coreoleuciscus splendidus* have the same ancestors at around 38Ma. These data indicate that the Noryeong mountain range including the Jinan Basin are expected to have uplifted at around 68-38Ma. Rhyolitic volcanic rocks in and around the Jinan Basin are plotted on the VAG (Volcanic Arc Granite) field and basaltic to intermediated volcanic rocks are plotted on the CAB (Calc-Alkaline Basalt) and WPB (WIthin Plate Basalt) fields in the tectonic discrimination diagrams. There was a roll back of subduction zone toward Pacific ocean at ca. 100 Ma. These data suggest that the igneous rocks in the Jinan Basin formed by the mantle upwelling due to extension caused by the roll back of subduction zone. The upwelling asthenospheric mantle supplied heat which caused the felsic magma by the melting of the lithospheric mantle and crust which had been contaminated by crustal material supplied from subducting sediment or ocean before roll back of the subduction zone. The upwelling asthenospheric mantle was also melted to form basaltic magma. The deep faults formed by sinistral strike slip movement around the Jinan Basin at the Cretaceous, gave the path toward surface for the magma at deep depth.

Keywords: Jinan Basin, pull-apart basin, Igneous rock, Cretaceous

©2019. Japan Geoscience Union. All Right Reserved.

(a) ca. 97 ~90 Ma.

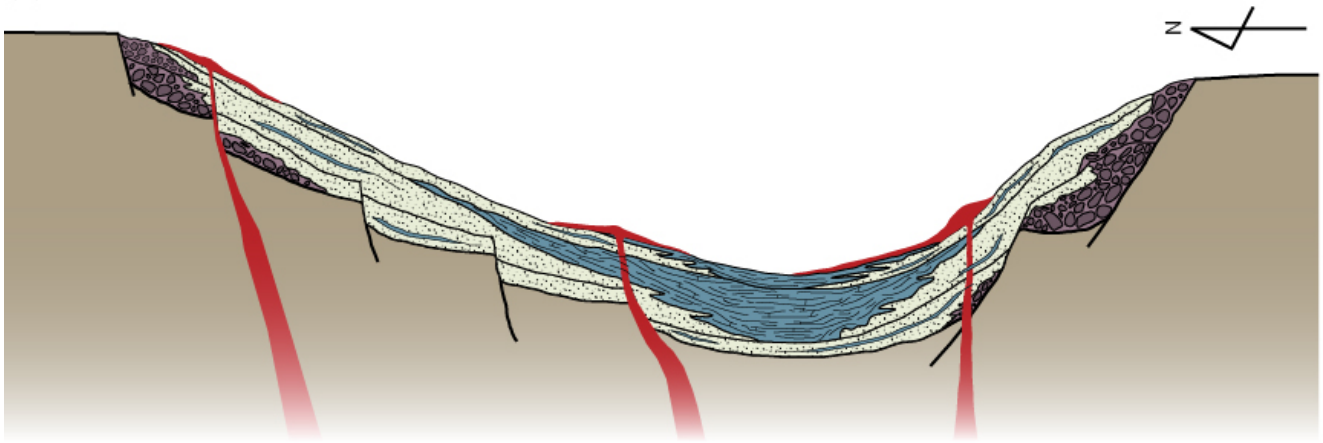

Deposition of lower part sedimentary rocks in the Jinan Basin (97~92 Ma) with extrusion of basaltic andesite (92~90 Ma)

(b) ca. 90 ~89 Ma.

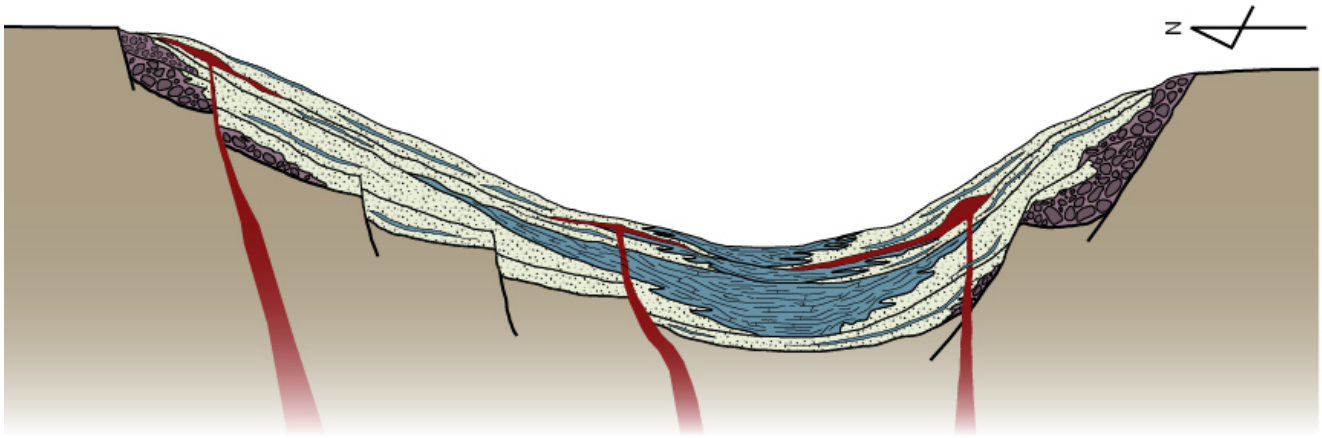

Deposition of upper part sedimentary rocks on the lower part sedimentary rocks and basaltic andesite extrusive volcanic rocks

(c) ca. 89 ~84 Ma.

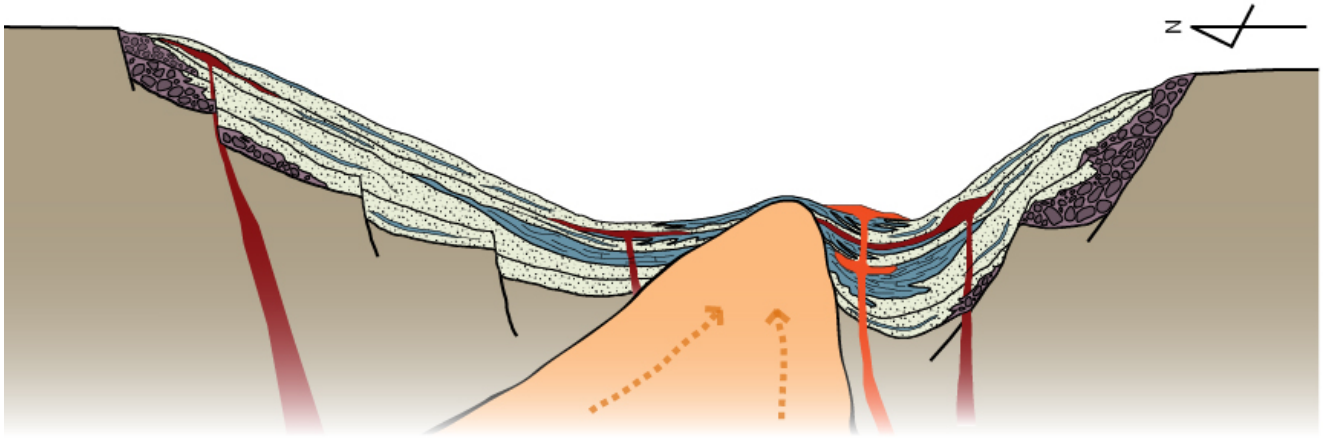

Intrusion and extrusion of rhyolite (ca. 89Ma) with late intrusion of andesitic volcanic rocks (ca. 84Ma)

Intrusive andesitic volcanic rocks
Rhyolite
Basalt and basaltic andesite
Conglomerate
Sandstone
Shale or mudstone

©2019. Japan Geoscience Union. All Right Reserved.

©2019. Japan Geoscience Union. All Right Reserved.

GEOCHORONOLOGY AND PETROCHEMISTREY OF LATE PALEOZOIC MAGMATIC ROCKS OF THE MANDAKH AREA, SOUTHEAST MONGOLIA

*Undarmaa Batsaikhan[1], Noriyoshi Tsuchiya[1], Masaoki Uno[1], Yukio Isozaki[2], Uyanga Bold[2], Hikaru Sawada[2]

1. Graduate School of Environmental Studies, Tohoku University, 2. Graduate School of Arts and Sciences The University of Tokyo

The southeast Mongolia has become a major survey area for unraveling the Paleozoic tectonic evolution because Mongolia occupies the central part of the CAOB which is enormous and composed of a multiplicity of terranes including ancient island and continental arcs, ophiolites, passive continental margins, Precambrian continental blocks and high-T/low-P metamorphic zones and where porphyry Cu deposits occur. The late Paleozoic magmatic rocks are widely distributed in the Mandakh area which is located in the Curvansaikhan and Manlai terrains, in the southeast Mongolia. We will discuss petrochemical features, mineral assemblage and new geochronological constrain of magmatic rocks in the Mandakh area. Furthermore, we compared petrochemical characteristics of the Mandakh area with Tampakan deposit (Philippines), Cerro Colorado deposit (Chili) and negative criteria of Cu deposits (Japan) in order to characterize potential of the porphyry copper deposit in Mandakh area.

The Mandakh area’ s igneous rocks the geochemical features are calc-alkaline, magnetite-series, I type and similar to adakite type. The Devonian intrusive rocks comprised of syenite and syenogranite, while the Carboniferous intrusive rocks consist of granodiorite, monzodiorite, quartz-monzonite and hornblende granite. Devonian magmatic rocks are more alkali in composition. Although Devonian and Carboniferous igneous rocks in the Mandakh area are a little different each other, these igneous rocks are possibility copper deposits as suggested by petrochemical comparisions with bonanza copper deposits in the world.

Keywords: Petrochemistry, Geochoronology, Southeastern Mongolia, Porphyry Copper deposits

©2019. Japan Geoscience Union. All Right Reserved.

Feedbacks Offshore the Cascadia Margin

*Joan S Gomberg[1]

1. USGS Earthquake Science Center

A growing body of evidence from the Cascadia subduction zone in the U.S. Pacific Northwest suggests that there are significant feedbacks among the offshore upper-plate material properties, geologic and geomorphic structures, seismic shaking, sediment redistribution, and mega-thrust slip behaviors. Analyses of seafloor seismic data show that the thick accretionary wedge sediments amplify and prolong shaking by low-frequency seismic waves and attenuate high frequencies (Gomberg, 2018). This strong contrast in shaking feeds back into reshaping the sediments, by controlling where they are likely to be destabilized and redistributed by shaking. Analyses of submarine landslide morphology and numerical modeling of slope strength suggest that different feedbacks, perhaps related to shaking-induced sediment compaction, may actually make sediments stronger (ten Brink et al., 2016; Scholz et al., 2016). Understanding of these contrasting influences in turn feeds into interpretations of turbidites as proxies for paleo-earthquakes, and hazard assessments based on earthquake recurrence models derived from them; for example, regions with greater numbers of turbidites may reflect permanent features of the shaking that are more suitable to trigger failure, but may be interpreted as indicative of a greater rate of earthquakes. Abrupt strike-perpendicular changes in shaking characteristics, apparent along most of the length of the margin, coincide with sharp gradients in topography and structure along the edge of the continental shelf. This same apparent boundary along the shelf-edge also coincides with concentrations of methane bubble plumes, with gas characteristics indicative of origins within the accretionary prism. One explanation is that the shelf is bounded by faults that connect with the megathrust and act as conduits for gas extrusion, some of which may connect with the megathrust directly or indirectly. This suggests another feedback, as structural changes promote or are caused by faulting, which itself permits pore pressure changes that modify the potential for additional faulting. Taken together, the aforementioned correlations and others observed between areas of non-volcanic tremor with gravity lows, crustal faulting patterns, and marginal basins, imply feedbacks between processes along the megathrust and upper plate structure (Wells et al., 2017). To reduce the degree of speculation about some of these feedbacks, several major experiments are planned and underway. These experiments, to be summarized in this presentation, will image the margin structure with sufficient resolution to identify and characterize faults, map changes in material properties, and more, along nearly the entire length of the Cascadia margin.

Gomberg, J. (2018). Cascadia onshore- offshore site response, submarine sediment mobilization, and earthquake recurrence. Journal of Geophysical Research: Solid Earth, 123, 1381–1404. https://doi.org/10.1002/2017JB014985
Johnson, H. P., Miller, U. K., Salmi, M. S., & Solomon, E. A. (2015). Analysis of bubble plume distributions to evaluate methane hydrate decomposition on the continental slope. Geochemistry, Geophysics, Geosystems, 16, 3825–3839. https://doi.org/10.1002/2015GC005955
Scholz, N. A., Riedel, M., Urlaub, M., Spence, G. D., & Hyndman, R. D. (2016). Submarine landslides offshore Vancouver Island along the northern Cascadia margin, British Columbia: Why preconditioning is likely required to trigger slope failure. Geo-Marine Letters, 36(5), 323–337. https://doi.org/10.1007/s00367-016-0452-8
ten Brink, U. S., Andrews, B. D., & Miller, N. C. (2016). Seismicity and sedimentation rate effects on submarine slope stability. Geology, 44(7), 563–566. https://doi.org/10.1130/G37866.1
Wells, R.E., R.J. Blakely, A.G. Wech, P.A. McCrory, and A. Michael (2017). Cascadia subduction tremor

©2019. Japan Geoscience Union. All Right Reserved.

muted by crustal faults, Geology, 45(6), 515-518, doi:10.1130/G38835.1

©2019. Japan Geoscience Union. All Right Reserved.

[E] Poster | S (Solid Earth Sciences)：S-MP Mineralogy & Petrology

Tue. May 28, 2019 5:15 PM - 6:30 PM JST | Tue. May 28, 2019 8:15 AM - 9:30 AM UTC | Poster Hall International Exhibition Hall8, Makuhari Messe_32

[S-MP29] Oceanic and Continental Subduction Processes

convener:REHMAN Ur Hafiz(Department of Earth and Environmental Sciences, Graduate School of Science and Engineering, Kagoshima University), Tatsuki Tsujimori(Tohoku University), Chin-Ho Tsai(Department of Natural Resources and Environmental Studies, National Dong Hwa University), Kazuaki Okamoto(Faculty of Education, Saitama University)

This JpGU-AGU joint session aims at bringing earth scientists from Japan and overseas to present their research related to the processes of oceanic and continent subduction, continent-continent collisions, metamorphism of crustal rocks, formation of the oceanic/continental arcs, and accretion/ tectonic erosion of material along subduction boundaries.

Topics such as role of the fore- and back-arcs in the subduction zones, process of accretion of volcaniclastic and terrigenous sediments along the subduction/collision boundaries, deformation and metamorphism of subducted crust, and exhumation will be the main focus of the session.

In addition to the above mentioned topics, our focus for the10th anniversary of this international session will be towards our understanding and progress on the ultrahigh-pressure/temperature metamorphic terranes in the world.

Exchange of ideas among geoscientists applying different approaches on problems related to the theme of the session are most welcome.

[SMP29-P01] Zircon U-Pb ages of metasedimentary rocks in the Hakogase (Hida Marginal) area, Fukui Prefecture.

*Atsushi MIYASHITA[1], Tatsuki Tsujimori[2], Daniel Pastor-Galán[3], Yi Keewook[4] (1.Seikei University, 2.Tohoku University, 3.Salamanca University, 4.Korea Basic Science Institue)

[SMP29-P02] Late Permian to Early Triassic back-arc type volcanism in the southern Mongolia volcano-plutonic belt of the Central Asian Orogenic Belt: Implication for timing of the final closure of the Palaeo-Asian Ocean

*Takeshi Imayama[1], Yoichiro Koh[2], Kazumasa Aoki[3], Mototaka Saneyoshi[4], Koshi Yagi[5], Shogo Aoki[4], Yoshihiro Sawada[6], Chiaki Ikawa[5], Tomoya Terada[4], Shinobu Ishigaki[4], Shin Toyoda[3], Khishigjav Tsogtbaatar[7], Buuvei Mainbayar[7] (1.Research Institute of Natural Sciences, Okayama University of Science, 2.Graduate School of Environmental Science, Hokkaido University, 3.Faculty of Science, Okayama University of Science, 4.Faculty of Biosphere - Geosphere Science, Okayama University of Science, 5.Hiruzen Institute for Geology and Chronology, 6.Emeritus Professor of Shimane University, 7.Institute of Paleontology and Geology, Mongolian Academy of Sciences)

[SMP29-P03] Mantle dynamics of slab breakoff constrained from the temporal change of the melting depth estimated from the Cumulate Member of the Ordovician Hayachine-Miyamori Ophiolite

*Takafumi Kimura[1], Kazuhito Ozawa[1] (1.Department of Earth and Planetary Science, The University of Tokyo)

[SMP29-P04] **Evidence of HIMU seamount on the Farallon Plate: Application of *in-situ* Sr-Pb isotope analysis to Franciscan lawsonite-bearing metagreywacke**

*Tomomi Hara[1], Tatsuki Tsujimori[1], Jun-Ichi Kimura[2] (1.Tohoku University, 2.Japan Agency for Marine-Earth Science and Technology)

[SMP29-P05] Boron isotope variations of antigorite serpentinites associated with high-pressure metamorphic rocks: A case study in the Itoigawa–Omi area of the Hida-Gaien Belt, Japan

*Chinatsu Yamada[1], Tatsuki Tsujimori[1], King Chang[2], Jun-Ichi Kimura[2] (1.Tohoku University, 2.Japan Aegency for Marine-Earth Science and Technology)

[SMP29-P06] **Study of zircons structures from the Miocene Shibi-san Granodiorite, Kagoshima Prefecture, Japan**

*Nakabayashi Marimo[1], REHMAN Ur Hafiz[1] (1.Kagoshima University)

[SMP29-P07] **Experimental modeling of eclogite and C-O-H fluid interaction in the subduction zones**

*Nadezda Chertkova[1], Shigeru Yamashita[2], Hiroaki Ohfuji[1], Tetsuo Irifune[1], Hirokazu Kadobayashi[1], Yoshitaka Yamamoto[3] (1.Ehime University, Geodynamics Research Center, 2.Okayama University, Institute for Planetary Materials, 3.National Institute of Advanced Industrial Science and Technology)

[SMP29-P08] Microfabrics of omphacite and garnet in eclogite from the Lanterman Range, northern Victoria Land, Antarctica

*Daeyeong Kim[1], Taehwan Kim[2], Jungmin Kim[3] (1.Division of Polar-Earth Sciences, Korea Polar Research Institute, 2.School of Earth and Environmental Sciences, Seoul National University, 3.Earth and Environmental Sciences, Korea University)

[SMP29-P09] Primordial Apatite from Ophiolite in Taiwan

*Nobuaki Niitsuma[1], Reishi Takashima[2], Yuan Hsi Lee[3] (1.Institute of Geosciences,Shizuoka University, 2.Tohoku University Museum, 3.National Chung-Cheng University, Taiwan)

[SMP29-P10] The evolution of the Cretaceous Jinan Basin in South Korea and the age and tectonic setting for the volcanic rocks in it

*Seung Hwan LEE[1], Chang Whan Oh[1] (1.Department of earth and environmental sciences Chonbuk national university)

[SMP29-P11] GEOCHORONOLOGY AND PETROCHEMISTREY OF LATE PALEOZOIC MAGMATIC ROCKS OF THE MANDAKH AREA, SOUTHEAST MONGOLIA

*Undarmaa Batsaikhan[1], Noriyoshi Tsuchiya[1], Masaoki Uno[1], Yukio Isozaki[2], Uyanga Bold[2], Hikaru Sawada[2] (1.Graduate School of Environmental Studies, Tohoku University, 2.Graduate School of Arts and Sciences The University of Tokyo)

[SMP29-P12] Feedbacks Offshore the Cascadia Margin

*Joan S Gomberg[1] (1.USGS Earthquake Science Center)

Zircon U-Pb ages of metasedimentary rocks in the Hakogase (Hida Marginal) area, Fukui Prefecture.

*Atsushi MIYASHITA[1], Tatsuki Tsujimori[2], Daniel Pastor-Galán[3], Yi Keewook[4]

1. Seikei University, 2. Tohoku University, 3. Salamanca University, 4. Korea Basic Science Institue

Combined chronological study using detrital zircon U-Pb dating and phengite K-Ar dating enables to understand the tectonic evolution of the high *P/T* metamorphic belt. The youngest age of detrital zircon U-Pb ages of psamites in the Hida marginal metamorphic rocks (HMMR = Renge belt) approximate its depositional ages (Tsutsumi et al., 2009). The closure temperature of the phengite K-Ar ages are controlled by deformation and recrystallization during exhumation of the metamorphic rocks(Itaya and Tsujimori, 2015). Therefore, the gap between the youngest age of detrital zircons and phengite K-Ar ages are the age difference between subuduction and uplift of metamorphics.
The Hakogase (Nigure-gawa, Kuzuryu, Fukui Prefecture) metamorphic rocks belong to HMMR member as the olistolith in the Cretaceous Tedori Group. It consists mainly pelites with small amount of basites and mables. The main index mineral assemblage of metasediments are garnet + chlorite, and the phenigite K-Ar ages are 287.8 - 283.6 Ma (Kunugiza et al., 2004). Relic Lawsonite was also found in the basaites and psamites (Miyakawa, 1982).
The detrital Zircons U-Pb ages in the two pelites are obtained by the SHRIMP II of KBSI. The youngest U-Pb ages of detrital zircons are 307Ma. The gap of the sedimentation between uplift of the Hakogase metamorphics is estimated 20 Ma. This value means the migration speed of the HMMR metamorphic rocks are 1/10 of plate motion. This rapid migration speed is common for the high *P/T* metamorphic rocks.

Keywords: high P/T metamorphic rocks, Zircon U-Pb ages, Phengite K-Ar ages

©2019. Japan Geoscience Union. All Right Reserved.

Late Permian to Early Triassic back-arc type volcanism in the southern Mongolia volcano-plutonic belt of the Central Asian Orogenic Belt: Implication for timing of the final closure of the Palaeo-Asian Ocean

*Takeshi Imayama[1], Yoichiro Koh[2], Kazumasa Aoki[3], Mototaka Saneyoshi[4], Koshi Yagi[5], Shogo Aoki[4], Yoshihiro Sawada[6], Chiaki Ikawa[5], Tomoya Terada[4], Shinobu Ishigaki[4], Shin Toyoda[3], Khishigjav Tsogtbaatar[7], Buuvei Mainbayar[7]

1. Research Institute of Natural Sciences, Okayama University of Science, 2. Graduate School of Environmental Science, Hokkaido University, 3. Faculty of Science, Okayama University of Science, 4. Faculty of Biosphere - Geosphere Science, Okayama University of Science, 5. Hiruzen Institute for Geology and Chronology, 6. Emeritus Professor of Shimane University, 7. Institute of Paleontology and Geology, Mongolian Academy of Sciences

The timing of final subduction and closure of the Palaeo-Asian Ocean is still controversial in the eastern segments of the Central Asian Orogenic Belt (CAOB). A more detailed understanding is needed with respect to the formation of volcanic rocks and sediments associated with the final closure of the Palaeo-Asian Ocean in southern Mongolia. We investigated alkali series volcanic rocks newly discovered in the southern Mongolia volcano-plutonic belt of the CAOB and classified as basalt, basaltic trachyandesite, andesite, trachyandesite, and trachyte, mainly showing andesitic-dacitic compositions. In Harker diagrams, the TiO_2, FeO, MnO, Al_2O_3, CaO, and MgO contents generally decrease with increasing SiO_2, representing a series of differentiated volcanic rocks. The primitive mantle-normalized trace element spider diagram is characterized by incompatible element-rich patterns and negative Nb anomalies. The tectonic discrimination diagrams show that the volcanic rocks were formed by arc-related volcanism rather than within-plate volcanism. K-Ar dating of feldspars from six volcanic rocks yields ages ranging from 270 to 239 Ma, indicating that andesitic and dacitic magmatism occurred during this period. These geochemical and geochronological data indicate that the differentiated volcanic rocks intruding middle to late Palaeozoic volcanic sediments were formed by back-arc type subduction ca. 270–240 Ma. Based on detrital zircon U-Pb ages, the terrigenous sandstones underlain by the volcanic sediments record a maximum depositional age of Late Triassic (ca. 220–200 Ma) and include a main cluster of Early Devonian ages (ca. 410–390 Ma), possibly derived from the Devonian-Carboniferous arc complex observed surrounding this study area. These results from the volcanic and sedimentary rocks in this study, combined with investigations in previous studies, imply that subduction beneath the eastern segments of the CAOB to consume the Palaeo-Asian Ocean continued until Late Permian to Early Triassic.

Keywords: Palaeo-Asian Ocean, southern Mongolia, Central Asian Orogenic Belt, back-arc type volcanism

©2019. Japan Geoscience Union. All Right Reserved.

Mantle dynamics of slab breakoff constrained from the temporal change of the melting depth estimated from the Cumulate Member of the Ordovician Hayachine-Miyamori Ophiolite

*Takafumi Kimura[1], Kazuhito Ozawa[1]

1. Department of Earth and Planetary Science, The University of Tokyo

Slab breakoff, detachment of oceanic lithosphere highly expected during arc-continent collision, is one of the important mechanisms inducing passive upwelling of the asthenosphere and magma generation in arc environments [1]. In order to better understand the mantle dynamics of slab breakoff, we need to use continuous geological record with high time resolution. In this study, we have extracted a record of temporal change of the magma generation depth from cumulates in an Ordovician arc ophiolite at a time resolution of several tens of million years.
The Hayachine-Miyamori Ophiolite, northern Japan, is one of the Ordovician ophiolite formed in an arc environment [2]. The ultramafic member was built up by three main magmatic stages, which are recorded in three rock units: Tectonite Member, Cumulate Member, and ultramafic dikes, in the order of formation ages. The last two units in the entire evolution of the ophiolite is explained by decompressional melting of sub-slab mantle triggered by slab breakoff [2][3]. The melting depth of an ultramafic magma solidified as dikes in the Cumulate Member is estimated to be ~170km [3]. Our recent field study clarified a large-scale stratification characterized by alternation of wehrlite-dominant and dunite-dominant layers in the Cumulate Member. Each layer has a thickness from several meters to ~1 km and, the total thickness attains ~3km. Moreover, we succeeded in specifying the strike and plunge of the gravity field to be ~N48°E and ~20°NE during the cumulate formation from field information and westward stratigraphic younging [4].
We estimated the temporal change of generation depth of parent magmas of the Cumulate Member by garnet signature in heavy rare earth elements (HREEs) as depth proxy. The information may constrain the mantle dynamics during the slab breakoff. We examined stratigraphic variation of HREE ratio at the core of clinopyroxenes over the thickness of ~2km in the Cumulate Member. The obtained variation of the Dy/Lu increases from ~12.9 to ~16.5 with increasing the stratigraphic height. We estimated the extent of melting in the garnet stability field increasing from ~50 to ~90% of the total melting by applying an open-system fractional melting model to reproduce the Dy/Lu variation.
We also estimated the time scale of formation of the Cumulate Member by using cm –10cm scale heterogeneity recorded in contact zone of intruded magma and the host. The profile of Mg# of olivine in xenoliths of the Tectonite Member occurring at the bottom of the Cumulate Member shows that the cooling time is less than several tens of million years [5]. The dunite of the Cumulate Member contacting the ultramafic dike shows a systematic decrease of Mg# from 90 to 86.8 over the distance of 54 mm towards the contact. We calculated the time scale of subsolidus diffusional exchange between the dunite and dike and obtained several tens of million years at ~1000℃. The host was kept at a high temperature when the dikes intruded because of the absence of chilled margin. We thus estimated time scale of formation of the Cumulate Member to be < several tens of million years.
We propose the following tectonic model in the Ordovician northern Japan on the basis of the above result. The slab breakoff took place at the depth slightly deeper than the boundary of spinel and garnet stability fields (~80 km) and induced counter flow and adiabatic melting of the sub-slab mantle. The melting depth deepened down to ~170 km on the time scale of several tens of million years, which corresponds to the time scale to complete the slab breakoff. The sinking velocity of the slab is more than

©2019. Japan Geoscience Union. All Right Reserved.

a few millimeters per year.

[1]: Davies et al., 1995. [2]: Ozawa et al., 2015. [3],[4]: Kimura et al., 2017, 2018, JpGU abstract. [5]: Ozawa, 1983.

Keywords: slab breakoff, arc ophiolite, cumulate

©2019. Japan Geoscience Union. All Right Reserved.

Evidence of HIMU seamount on the Farallon Plate: Application of *in-situ* Sr-Pb isotope analysis to Franciscan lawsonite-bearing metagreywacke

*Tomomi Hara[1], Tatsuki Tsujimori[1], Jun-Ichi Kimura[2]

1. Tohoku University, 2. Japan Agency for Marine-Earth Science and Technology

Since bulk isotopic composition of oceanic basalt is susceptible to element remobilization during alteration process, there is a risk of causing misread of geochemical signatures from bulk metabasaltic rocks in subduction complex. As Hara et al. (2018) demonstrated, however, *in-situ* Sr-Pb isotope analysis of lawsonite in high-pressure metabasaltic rocks has a great potential for tracing the geochemical signatures reflecting the igneous protolith. In this study, we have applied the method to lawsonite in metasedimentary rocks to explore clastic components of a trench-fill sediment. A jadeite-bearing Franciscan metagreywacke from Pacheco Pass area, east-central Diablo Range, California Coast Ranges was selected for geochemical reconnaissance.

Lawsonites in the Franciscan metagreywacke record a high initial Pb isotope ratios ($^{206}Pb/^{204}Pb$ = 18.74–19.66, $^{207}Pb/^{204}Pb$ = 15.58–15.70 and $^{208}Pb/^{204}Pb$ = 38.41–39.34). This Pb-isotope signature suggests that a protolith of the metagreywacke have contained a debris derived from a HIMU-type basalt. Considering the maximum depositional age of the metagreywacke at ~102 Ma, the underflow of the Farallon Plate beneath continental crust of the North American Plate would have carried a HIMU seamount to a Franciscan trench.

Our study has demonstrated the potential application of 'lawsonitology' as sedimentary provenance analyses for metamorphosed accretionary complex. Moreover, the results would manifest that Pb isotopic signature of ancient oceanic basalt can be detectable from Ca-Al silicate mineral, such as lawsonite, epidote and pumpellyite, in metamorphic rocks.

Keywords: Lawsonite, Sr-Pb isotope, LA-MC-ICPMS, HIMU, Metasediment

©2019. Japan Geoscience Union. All Right Reserved.

Boron isotope variations of antigorite serpentinites associated with high-pressure metamorphic rocks: A case study in the Itoigawa–Omi area of the Hida-Gaien Belt, Japan

*Chinatsu Yamada[1], Tatsuki Tsujimori[1], King Chang[2], Jun-Ichi Kimura[2]

1. Tohoku University, 2. Japan Aegency for Marine-Earth Science and Technology

Boron isotope study of serpentinites in the Franciscan Complex using an ablation volume correction (AVC) LA-MC-ICPMS discriminates two groups (Yamada et al., 2018 JpGU abstr.; Yamada et al. 2019, in press). Serpentinites associated with blueschists are characterized by lighter boron isotope than serpentinites without blueschist-facies rocks. The lighter boron isotope signature (< ~10 ‰) of blueschist-bearing serpentinites results from interaction with forearc slab fluids with low δ^{11}B in deeper depth. In order to evaluate the versatility of B isotopes and composition of high-pressure metamorphosed serpentinites, we investigated antigorite serpentinites associated with three different type of high-pressure metamorphic rocks in the Itoigawa–Omi area.

The investigated serpentinites can be grouped into two types based on the B isotopes. Antigorite serpentinite with blueschist- and eclogite-facies metamorphic rocks in the Yunotani Valley is characterized by moderate boron (12.5–48.4 $\mu g \cdot g^{-1}$) and lower δ^{11}B (+6.6 to +12.3‰ [mostly smaller than +8‰]; n= 10); Brucite-bearing antigorite serpentinite with barroisite-bearing mafic schist in the Kotaki-gawa River is characterized by very high boron (37.5 –302 $\mu g \cdot g^{-1}$) and lower δ^{11}B (+5.8 to +10.7‰ [mostly smaller than +8‰]; n= 10). In contrast, antigorite serpentinite with garnet amphibolite in the Omi-gawa River is characterized by a wide range of boron (9.1–145 $\mu g \cdot g^{-1}$) and relatively high δ^{11}B (+11.5 to + 14.8 ‰; n= 10).

Our preliminary reconnaissance shows significantly lower δ^{11}B (smaller than +8‰) in antigorite serpentinites of the 'Eclogite Unit' proposed by Tsujimori (2002). This trend is consistent with our earlier study in the Franciscan Complex. The antigorite serpentinites in the 'Eclogite Unit' might have been affected by a deep forearc slab fluids.

Keywords: Serpentinite, boron isotope, subduction zone

©2019. Japan Geoscience Union. All Right Reserved.

Study of zircons structures from the Miocene Shibi-san Granodiorite, Kagoshima Prefecture, Japan

*Nakabayashi Marimo[1], REHMAN Ur Hafiz[1]

1. Kagoshima University

The Miocene granodiorite body (zircon fission track age by Miyachi, 1985) of the Mount Shibi, Kagoshima prefecture is a lenticular stock that intrudes the Cretaceous sedimentary rocks of the Shimanto belt. Previous studies subdivided the granodiorite body into the Kusu-bae (core facies) and Hira-bae (marginal facies) types based on the changes in litho-facies and distinct chemical composition of biotite and amphibole (Yamamoto et al., 1988). We conducted field survey in the study area and found no clear contrasts to sub-divide the body, instead it represents a single pluton with local chemical variation along the marginal portions. Based on detailed petrography, the entire body appears as homogeneous stock exhibiting identical mineral assemblage with no clear evidence that can mark the boundary between Kusu-bae and Hira-bae types. Moreover, to understand the processes of magmatic crystallization we investigated more than 600 zircon grains from about 8 samples for external (applying the zircon morphology method of Pupin, 1980) and internal morphology using the Cathodoluminescence imaging. Based on the Pupin’ s method, the deduced temperature range for the zircon crystallization was between 750 and 850℃. In addition, internal structures of zircon (CL images) showed oscillatory zoning with continuous growth domains and abundant apatite inclusions, suggesting the magma was fluid-rich and have been crystallized under relatively higher temperature. We also investigated zircons from the surrounding hornfels (Shimanto belt rocks) that were affected thermally due to the contact metamorphism. Zircons from the hornfels are completely different and rounded with different internal structures. Zircons from the so-called Kusu-bae and Hira-bae types are identical and suggest their crystallization from a single parental magma hence the pluton cannot be sub divisible.

References
Miyachi M. (1985). Fission track ages of some granitic rocks in Outer Zone ofKyushu, Japan. Journal of Mineralogical and Petrological Sciences 80, 406-409.
Pupin J. P. (1980). Zircon and granite petrology. Contribution to Mineralogy and Petrology 73, 207-220.
Yamamoto M., Oniwa N., Toyota K. (1988). Compositional Variation of the Shibi-san Granodioraite Body, Kagoshima Prefecture, Japan. Bulletin of the Kagoshima University Science Faculty 21, 35-49.

Keywords: zircon, granodiorite, crystal shape

©2019. Japan Geoscience Union. All Right Reserved.

Experimental modeling of eclogite and C-O-H fluid interaction in the subduction zones

*Nadezda Chertkova[1], Shigeru Yamashita[2], Hiroaki Ohfuji[1], Tetsuo Irifune[1], Hirokazu Kadobayashi[1], Yoshitaka Yamamoto[3]

1. Ehime University, Geodynamics Research Center, 2. Okayama University, Institute for Planetary Materials, 3. National Institute of Advanced Industrial Science and Technology

The presence of volatile components controls melting relationships in the subducting oceanic plate and the overlying mantle wedge, affecting their physical properties and seismic observables. The major volatile species in the mantle low oxygen fugacity environment are considered to be H_2O and CH_4, as estimated for mantle xenoliths and C-O-H fluid speciation in equilibrium with diamond [1,2]. Experimental studies with the direct monitoring of phase assemblages and melting relationships in the silicate systems with C-O-H components can shed light on the processes, which take place in the subduction zones, and provide important data for interpretation of observed physical parameters.
In this study, we employed *in situ* spectroscopic methods in combination with the diamond anvil cell (DAC) technique for investigation of C-O-H fluid behavior and its influence on phase relationships in the eclogite–5.75H_2O–CH_4 system at temperatures up to 1000 degree C and pressures exceeding 5 GPa. We designed a new cell assembly for Mao-type symmetric diamond anvil cell with large optical access to the sample in order to make it suitable for infrared and Raman measurements directly at high-pressure and high-temperature conditions. Mineral phase assemblages, observed during experiments, are consistent with those described in the dry system of the similar basaltic composition [3]. At the same time, miscibility between aqueous and carbonaceous components in the fluid phase coexisting with silicate minerals was confirmed at temperatures above 800 degree C and pressures above 3.2 GPa.

References

[1] Shirey, S.B., Cartigny, P., Frost, D.J., Keshav, S., Nestola, F., Nimis, P., Pearson, D.G., Sobolev, N.V. and Walter, M.J. (2013) *Rev. Mineral. Geochem.*, **75**, 355-421.
[2] Belonoshko, A. and Saxena, S. (1992) *Geochim. Cosmochim. Acta*, **56**, 3611-3626.
[3] Yasuda, A., Fujii, T. and Kurita, K. (1994) *J. Geophys. Res.: Solid Earth*, **99**, 9401-9414.

©2019. Japan Geoscience Union. All Right Reserved.

Microfabrics of omphacite and garnet in eclogite from the Lanterman Range, northern Victoria Land, Antarctica

*Daeyeong Kim[1], Taehwan Kim[2], Jungmin Kim[3]

1. Division of Polar-Earth Sciences, Korea Polar Research Institute, 2. School of Earth and Environmental Sciences, Seoul National University, 3. Earth and Environmental Sciences, Korea University

Layered structures in metamorphic rocks are sometimes crucial to occur strain localization then affect to seismic properties. We conducted microstructural analyses omphacite and garnet in foliated eclogite from the Lanterman Range, northern Victoria Land, Antarctica, to determine the influence of the layered structure on seismic observations in subduction zone. The analyzed eclogite, composed of layered garnet-rich and omphacite-rich layers, shows the low aspect ratios, similar angular distribution of long axes relative to the foliation, uniform grain size distribution, near-random crystallographic preferred orientations (CPOs), and misorientation angle distributions of garnet and opposite characteristics of omphacite in both layers. The results of fabric analyses are consistent with strain localization into omphacite or omphacite-rich layers rather than garnet or garnet-rich layers. Our results therefore demonstrate the importance of the layered structure in strain localization and in the development of the seismic anisotropies of subducting oceanic crust.

Keywords: Eclogite, EBSD, Layered structure

©2019. Japan Geoscience Union. All Right Reserved.

Primordial Apatite from Ophiolite in Taiwan

*Nobuaki Niitsuma[1], Reishi Takashima[2], Yuan Hsi Lee[3]

1. Institute of Geosciences,Shizuoka University, 2. Tohoku University Museum, 3. National Chung-Cheng University, Taiwan

Apatite is a common accessory mineral in igneous rocks. Because apatite has a wide range of trace element compositions as well as strong resistance to diagenetic alteration, the trace element composition of apatite has been used for tracing petrogenetic processes of plutonic bodies as well as the tephrochronology of Paleozoic tephras and Quaternary volcaniclastic deposits.

We studied trace element compositions of apatites from Ophiolite in Taiwan. The Ophiolite with mafic-ulatramafic rocks (150811-14) expose along the anticlinal axes of the metamorphic belts in Backbone Range of Taiwan, and exotic gabbro block (MA-15B) in chaotic deposits of Lichi Melange, in the southern end of Longitudinal Valley, in East Taiwan.

Lee (2015 JpGU; Chen et al., 2017 Tectonics) reported that zircon ages of Ophiolites in Taiwan are concentrated to 15 Ma, which should relate with termination of spreading in South China Sea and Shikoku & Parece Vela Basin just before Japan Sea Opening, and large scale igneous activities in the Outer Zone of Southwest Japan just after Japan Sea Opening (Niitsuma & Lee, 2018 JpGU).

Fifteen and twelve apatite phenocrysts from samples of MA-15B and 150811-14 were analyzed for major and minor elements using a JEOL 8530F wavelength dispersive Electron Probe Micro Analyzer (Takashima et al., 2017 Quaternary Geochronology) in weight % as follow;
__major elements: P=17.956 +/-0.100, 17.926 +/-0.129
_____Ca=38.362 +/-0.329, 38.128 +/-0.273
_____F=1.082+/-0.151, 0.445+/-0.046
__trace elements: Cl<0.01, 0.04 Mg<0.01, 0.01 Mn<0.04, 0.05
_____Fe<0.03, 0.17 Ce<0.09, 0.05 Y<0.13, 0.04

The contents of trace elements are extremely low and we concluded the apatite might be primordial without any contaminations and petrogenetic effect, and crystallized directly in the magma above rifted mantle along the northwestern margin of West Philippine Basin just before Japan Sea Opening.

Keywords: Apatite, trace element , Ophiolite, Taiwan, Opening of Japan Sea

©2019. Japan Geoscience Union. All Right Reserved.

The evolution of the Cretaceous Jinan Basin in South Korea and the age and tectonic setting for the volcanic rocks in it

*Seung Hwan LEE[1], Chang Whan Oh[1]

1. Department of earth and environmental sciences Chonbuk national university

The Jinan Basin is one of the Cretaceous pull-apart basins in the South Korea. It locates along the Yongdong-Gwangju fault system and consists of non-marine sediments with volcanic and pyroclastic rocks. The sinistral strike slip movement which formed the Cretaceous pull apart basins was occurred by the collision between Siberian and Manchuria blocks at ca. 130~100Ma. LA-MC-ICPMS age dating on the zircons from sedimentary and igneous rocks indicates followings. The sedimentation in the Jinan Basin had started at least from 97.7Ma and continued until 89.47Ma. During the sedimentation, basaltic andesite extruded at 90-92 Ma and later rhyolitc and andesitic magma intruded the Jinan Basin at 90-89 Ma and 85-84 Ma respectively. Later the Jinan Basin uplifted to form Noryeong mountain range due to the compression which was related with dextral strike slip fault movement. This fault movement is expected to be caused by the collision between Indian plate and Eurasian plate at ca. 55~25Ma. AFT(Apatite Fission Track) age from sediments in the Jinan Basin is approximately 68Ma. Due to the formation of Noryeong mountain range, the *Coreoleuciscus splendidus* was differentiated into two species, these two species of *Coreoleuciscus splendidus* have the same ancestors at around 38Ma. These data indicate that the Noryeong mountain range including the Jinan Basin are expected to have uplifted at around 68-38Ma. Rhyolitic volcanic rocks in and around the Jinan Basin are plotted on the VAG (Volcanic Arc Granite) field and basaltic to intermediated volcanic rocks are plotted on the CAB (Calc-Alkaline Basalt) and WPB (WIthin Plate Basalt) fields in the tectonic discrimination diagrams. There was a roll back of subduction zone toward Pacific ocean at ca. 100 Ma. These data suggest that the igneous rocks in the Jinan Basin formed by the mantle upwelling due to extension caused by the roll back of subduction zone. The upwelling asthenospheric mantle supplied heat which caused the felsic magma by the melting of the lithospheric mantle and crust which had been contaminated by crustal material supplied from subducting sediment or ocean before roll back of the subduction zone. The upwelling asthenospheric mantle was also melted to form basaltic magma. The deep faults formed by sinistral strike slip movement around the Jinan Basin at the Cretaceous, gave the path toward surface for the magma at deep depth.

Keywords: Jinan Basin, pull-apart basin, Igneous rock, Cretaceous

©2019. Japan Geoscience Union. All Right Reserved.

(a) ca. 97 ~90 Ma.

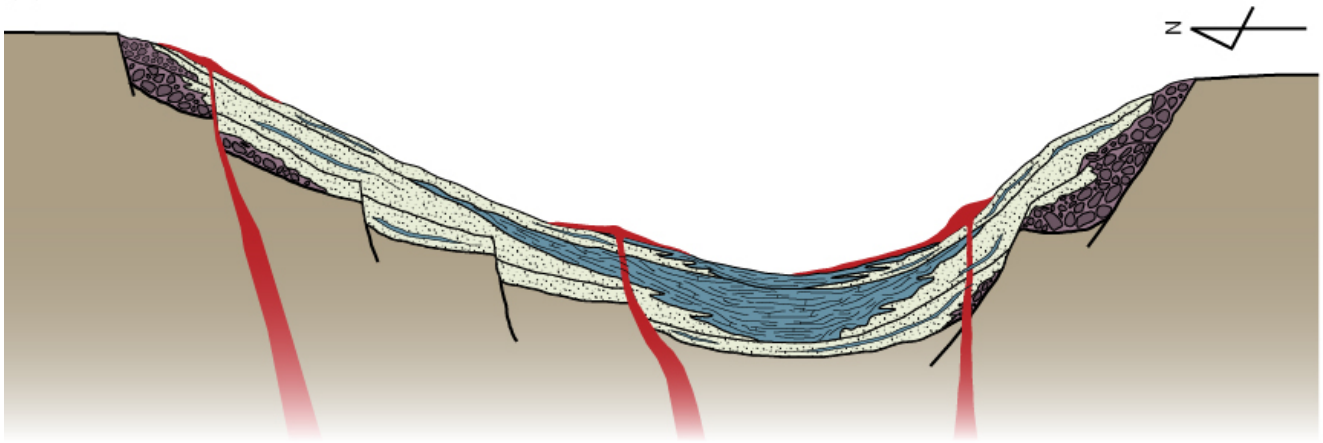

Deposition of lower part sedimentary rocks in the Jinan Basin (97~92 Ma) with extrusion of basaltic andesite (92~90 Ma)

(b) ca. 90 ~89 Ma.

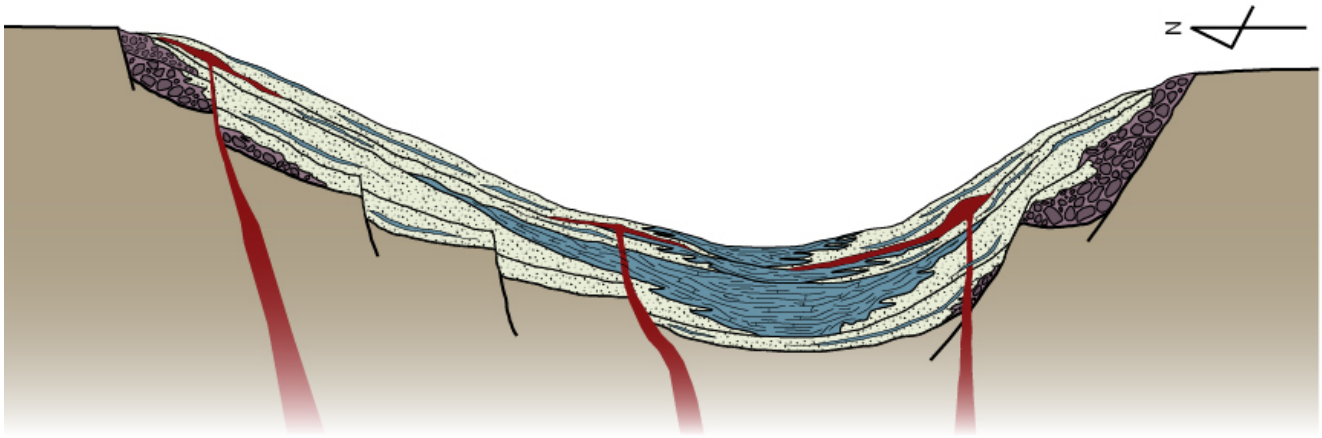

Deposition of upper part sedimentary rocks on the lower part sedimentary rocks and basaltic andesite extrusive volcanic rocks

(c) ca. 89 ~84 Ma.

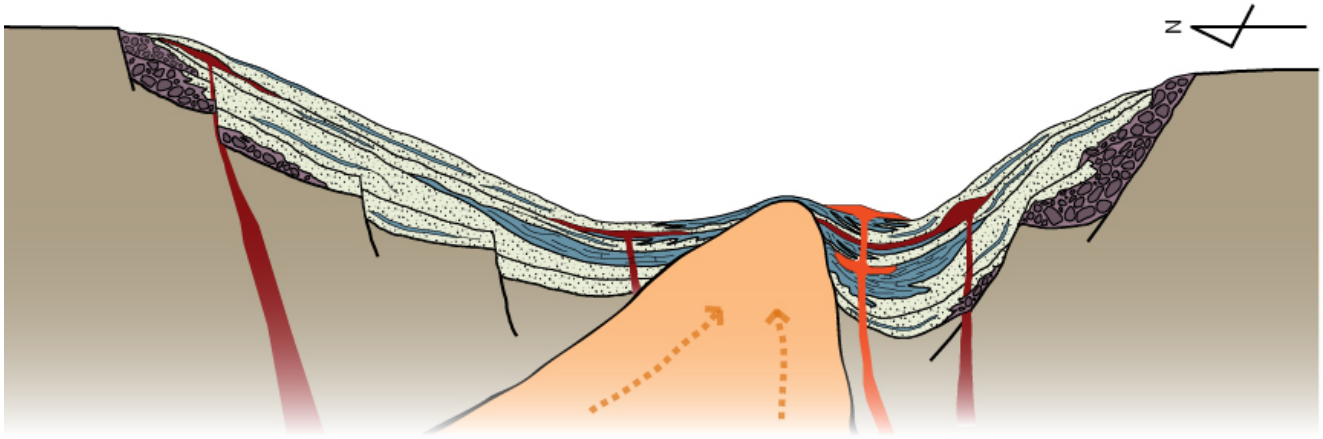

Intrusion and extrusion of rhyolite (ca. 89Ma) with late intrusion of andesitic volcanic rocks (ca. 84Ma)

Intrusive andesitic volcanic rocks
Rhyolite
Basalt and basaltic andesite
Conglomerate
Sandstone
Shale or mudstone

©2019. Japan Geoscience Union. All Right Reserved.

©2019. Japan Geoscience Union. All Right Reserved.

GEOCHORONOLOGY AND PETROCHEMISTREY OF LATE PALEOZOIC MAGMATIC ROCKS OF THE MANDAKH AREA, SOUTHEAST MONGOLIA

*Undarmaa Batsaikhan[1], Noriyoshi Tsuchiya[1], Masaoki Uno[1], Yukio Isozaki[2], Uyanga Bold[2], Hikaru Sawada[2]

1. Graduate School of Environmental Studies, Tohoku University, 2. Graduate School of Arts and Sciences The University of Tokyo

The southeast Mongolia has become a major survey area for unraveling the Paleozoic tectonic evolution because Mongolia occupies the central part of the CAOB which is enormous and composed of a multiplicity of terranes including ancient island and continental arcs, ophiolites, passive continental margins, Precambrian continental blocks and high-T/low-P metamorphic zones and where porphyry Cu deposits occur. The late Paleozoic magmatic rocks are widely distributed in the Mandakh area which is located in the Curvansaikhan and Manlai terrains, in the southeast Mongolia. We will discuss petrochemical features, mineral assemblage and new geochronological constrain of magmatic rocks in the Mandakh area. Furthermore, we compared petrochemical characteristics of the Mandakh area with Tampakan deposit (Philippines), Cerro Colorado deposit (Chili) and negative criteria of Cu deposits (Japan) in order to characterize potential of the porphyry copper deposit in Mandakh area.

The Mandakh area’ s igneous rocks the geochemical features are calc-alkaline, magnetite-series, I type and similar to adakite type. The Devonian intrusive rocks comprised of syenite and syenogranite, while the Carboniferous intrusive rocks consist of granodiorite, monzodiorite, quartz-monzonite and hornblende granite. Devonian magmatic rocks are more alkali in composition. Although Devonian and Carboniferous igneous rocks in the Mandakh area are a little different each other, these igneous rocks are possibility copper deposits as suggested by petrochemical comparisions with bonanza copper deposits in the world.

Keywords: Petrochemistry, Geochoronology, Southeastern Mongolia, Porphyry Copper deposits

©2019. Japan Geoscience Union. All Right Reserved.

Feedbacks Offshore the Cascadia Margin

*Joan S Gomberg[1]

1. USGS Earthquake Science Center

A growing body of evidence from the Cascadia subduction zone in the U.S. Pacific Northwest suggests that there are significant feedbacks among the offshore upper-plate material properties, geologic and geomorphic structures, seismic shaking, sediment redistribution, and mega-thrust slip behaviors. Analyses of seafloor seismic data show that the thick accretionary wedge sediments amplify and prolong shaking by low-frequency seismic waves and attenuate high frequencies (Gomberg, 2018). This strong contrast in shaking feeds back into reshaping the sediments, by controlling where they are likely to be destabilized and redistributed by shaking. Analyses of submarine landslide morphology and numerical modeling of slope strength suggest that different feedbacks, perhaps related to shaking-induced sediment compaction, may actually make sediments stronger (ten Brink et al., 2016; Scholz et al., 2016). Understanding of these contrasting influences in turn feeds into interpretations of turbidites as proxies for paleo-earthquakes, and hazard assessments based on earthquake recurrence models derived from them; for example, regions with greater numbers of turbidites may reflect permanent features of the shaking that are more suitable to trigger failure, but may be interpreted as indicative of a greater rate of earthquakes. Abrupt strike-perpendicular changes in shaking characteristics, apparent along most of the length of the margin, coincide with sharp gradients in topography and structure along the edge of the continental shelf. This same apparent boundary along the shelf-edge also coincides with concentrations of methane bubble plumes, with gas characteristics indicative of origins within the accretionary prism. One explanation is that the shelf is bounded by faults that connect with the megathrust and act as conduits for gas extrusion, some of which may connect with the megathrust directly or indirectly. This suggests another feedback, as structural changes promote or are caused by faulting, which itself permits pore pressure changes that modify the potential for additional faulting. Taken together, the aforementioned correlations and others observed between areas of non-volcanic tremor with gravity lows, crustal faulting patterns, and marginal basins, imply feedbacks between processes along the megathrust and upper plate structure (Wells et al., 2017). To reduce the degree of speculation about some of these feedbacks, several major experiments are planned and underway. These experiments, to be summarized in this presentation, will image the margin structure with sufficient resolution to identify and characterize faults, map changes in material properties, and more, along nearly the entire length of the Cascadia margin.

Gomberg, J. (2018). Cascadia onshore- offshore site response, submarine sediment mobilization, and earthquake recurrence. Journal of Geophysical Research: Solid Earth, 123, 1381–1404. https://doi.org/10.1002/2017JB014985
Johnson, H. P., Miller, U. K., Salmi, M. S., & Solomon, E. A. (2015). Analysis of bubble plume distributions to evaluate methane hydrate decomposition on the continental slope. Geochemistry, Geophysics, Geosystems, 16, 3825–3839. https://doi.org/10.1002/2015GC005955
Scholz, N. A., Riedel, M., Urlaub, M., Spence, G. D., & Hyndman, R. D. (2016). Submarine landslides offshore Vancouver Island along the northern Cascadia margin, British Columbia: Why preconditioning is likely required to trigger slope failure. Geo-Marine Letters, 36(5), 323–337. https://doi.org/10.1007/s00367-016-0452-8
ten Brink, U. S., Andrews, B. D., & Miller, N. C. (2016). Seismicity and sedimentation rate effects on submarine slope stability. Geology, 44(7), 563–566. https://doi.org/10.1130/G37866.1
Wells, R.E., R.J. Blakely, A.G. Wech, P.A. McCrory, and A. Michael (2017). Cascadia subduction tremor

©2019. Japan Geoscience Union. All Right Reserved.

muted by crustal faults, Geology, 45(6), 515-518, doi:10.1130/G38835.1

©2019. Japan Geoscience Union. All Right Reserved.

[E] Poster | S (Solid Earth Sciences)：S-MP Mineralogy & Petrology

Tue. May 28, 2019 10:45 AM - 12:15 PM JST | Tue. May 28, 2019 1:45 AM - 3:15 AM UTC | Poster Hall International Exhibition Hall8, Makuhari Messe_8

[S-MP30] Crust-Mantle Connections

convener:Yoshihiko Tamura(Research Institute for Marine Geodynamics, Japan Agency for Maine-Earth Science and Technology), Osamu Ishizuka(Geological Survey of Japan, AIST), Chris Conway(Geological Survey of Japan)

A paradigm of the solid Earth geochemical cycles is that the Earth's crust forms by melting of the Earth's upper peridotitic mantle. How divers is the spectrum of primary melts and which factors may contribute to its variations? What is the influence of crustal processing vs. primary magma diversity in creating the diversity of the Earth's crust? The session seeks to explore the crust-mantle connections at divergent and convergent plate boundaries, and oceanic island settings based on volcanology, petrology, geochemistry, geophysics, geochronology, and geodynamics studies.

[SMP30-P01] Secular evolution of proto-Izu-Bonin-Mariana arc volcanism: Constraints from statistical analysis of melt inclusion compositions

*Morihisa Hamada[1], Hikaru Iwamori[1,2], Philipp A. Brandl[3], Takayuki Ushikubo[4], Kenji Shimizu[4], Motoo Ito[4], He Li[5], Ivan P. Savov[6] (1.Department of Solid Earth Geochemistry, Japan Agency for Marine-Earth Science and Technology, 2.Earthquake Research Institute, University of Tokyo, 3.GEOMAR Helmholtz Centre for Ocean Research Kiel, 4.Kochi Institute for Core Sample Research, Japan Agency for Marine-Earth Science and Technology, 5.Institute of Oceanology, Chinese Academy of Sciences, 6.School of Earth and Environment, University of Leeds)

[SMP30-P02] The Jurassic magmatism of protoliths of Mikabu greenstones in SW Japan: zircon U-Pb dating and trace element analysis

*Hikaru Sawada[1], Yukio Isozaki[1], Shogo Aoki[3], Shuhei Sakata[2], Ryo Hasegawa[1], Yasuo Nakamura[1] (1.Department of General Systems Studies, the University of Tokyo, 2.Department of Chemistry, Gakushuin Universtiy, 3.Department of Applied Science, Okayama University of Science)

[SMP30-P03] Origin of variable CaO/Al_2O_3 in olivine-hosted melt inclusions from Kibblewhite Volcano, Kermadec Arc

*Yasuhiro Hirai[1], Yoshihiko Tamura[2], Kaj Hoernle[3], Christian Timm[4], Folkmar Hauff[3], Reinhard Werner[3], Takeshi Hanyu[2], Bogdan Vaglarov[2], Qing Chang[2], Takashi Miyazaki[2], Jun-Ichi Kimura[2] (1.Graduate School of Natural Science and Technology, Kanazawa University, Japan, 2.Japan Agency for Marine-Earth Science and Technology (JAMSTEC), Yokosuka, Kanagawa, Japan, 3.GEOMAR Helmholtz Centre for Ocean Research, Kiel, Germany, 4.GNS Science, Lower Hutt, New Zealand)

[SMP30-P04] Ankaramite from Doyo seamount in the Izu-Ogasawara arc: A precursor of continents?

*Yoshihiko Tamura[1], Tomoki Sato[1], Osamu Ishizuka[1,2], Takashi Miyazaki[1], Yasuhiro Hirai[1,3], Mami Takehara[4], Eri Sakamoto[5] (1.JAMSTEC, 2.AIST, 3.Kanazawa Univ., 4.NIPR, 5.NME)

[SMP30-P05] Different Moho reflections adjacent to Minami-Tori Shima and their petrologic origins

*Yoshihiko Tamura[1], Kentaro Kaneda[2], Gou Fujie[1], Akane Ohira[1], Eiichi TAKAZAWA[3], Georges Ceuleneer[4], Katsuyoshi Michibayashi[5], Tomoki Sato[1], Shuichi Kodaira[1], Seiichi Miura[1] (1.Japan Agency for Maine-Earth Science and Technology, 2.Japan Coast Guard, 3.Niigata University, 4.Universite de Toulouse, 5.Nagoya University)

[SMP30-P06] Melt-rock interaction in plagioclase peridotites from the southern Palawan Ophiolite, Philippines

*FLORENCE ANNETTE CRUSPERO LABIS[1], BETCHAIDA D PAYOT[1], GABRIEL THEOPHILUS V VALERA[1], JULIUS A PASCO[1], JESLEY MEI A DYCOCO[1] (1.UNIVERSITY OF THE PHILIPPINES)

[SMP30-P07] Intra-oceanic arc magma genesis: a case study from Havre volcano, Kermadec arc

*Chris Conway[1], Kenichiro Tani[2] (1.Geological Survey of Japan, 2.National Museum of Nature and Science)

Secular evolution of proto-Izu-Bonin-Mariana arc volcanism: Constraints from statistical analysis of melt inclusion compositions

*Morihisa Hamada[1], Hikaru Iwamori[1,2], Philipp A. Brandl[3], Takayuki Ushikubo[4], Kenji Shimizu[4], Motoo Ito[4], He Li[5], Ivan P. Savov[6]

1. Department of Solid Earth Geochemistry, Japan Agency for Marine-Earth Science and Technology, 2. Earthquake Research Institute, University of Tokyo, 3. GEOMAR Helmholtz Centre for Ocean Research Kiel, 4. Kochi Institute for Core Sample Research, Japan Agency for Marine-Earth Science and Technology, 5. Institute of Oceanology, Chinese Academy of Sciences, 6. School of Earth and Environment, University of Leeds

International Ocean Discovery Program (IODP) Expedition 351 'Izu–Bonin–Mariana (IBM) Arc Origins' drilled Site U1438, situated in the north-western margin of the Philippine Sea, into volcaniclastic sediments of the proto-IBM arc. Brandl *et al.* (2017, *Earth and Planetary Science Letters*) have analysed the major, trace and volatile elements of 304 melt inclusions hosted in fresh silicate minerals to unveil the magmatic evolution of the proto-IBM arc between 30 and 40 Ma, when the arc volcanism matured following subduction initiation at 52 Ma. Brandl *et al.* (2017) concluded that: (1) volcanism of the proto-IBM arc shifted from calc-alkaline affinity to tholeiitic affinity over time; and (2) such compositional shift is linked to both the volcanic productivity and the maturation of an evolving island arc. To better integrate the composition of melt inclusions with the magmatic evolution of the proto-IBM arc, this study extends the dataset of Brandl *et al.* (2017) by: (1) additional analysis of volatiles (H_2O, S, F and Cl) and P_2O_5 for 47 carefully selected melt inclusions by Secondary Ion Mass Spectrometry (SIMS); and (2) statistical analysis on the composition of 237 representative melt inclusions covering the full time range (30–40 Ma) of the dataset. Based on statistical analysis of the melt inclusion compositions and by considering trace element compositions and volatile concentrations, we can confidently distinguish five main clusters of melt inclusion compositions which can be further separated into a total of nine sub-clusters. Among the nine sub-clusters, we identified three major magma types: (1) medium-K enriched magmas which form a tholeiitic trend (30–38 Ma); (2) less-depleted medium-K melts which form a calc-alkaline trend (35–39 Ma); and (3) low-K depleted magmas which form a calc-alkaline trend (35–40 Ma). We demonstrate that: (1) volcanism of calc-alkaline depleted magmas lasted until 35 Ma; (2) the volcanism of calc-alkaline depleted magmas and that of more enriched normal arc magmas (tholeiitic and calc-alkaline affinities) overlap between 35 and 38–39 Ma and; (iii) the volcanism of normal arc magmas became predominant thereafter at the proto-IBM arc. Such identification of three major magma types is distinct from that of Brandl *et al.* (2017), in which less-depleted medium-K calc-alkaline magmas amd depleted low-K calc-alkaline gammas were not distinguished. We infer that depleted source mantle had been replaced by enriched mantle due to mantle convection beneath the proto-IBM arc from >40 Ma to 35 Ma. Statistical analysis is a useful tool to partition a mixture of multivariable dataset, such as datasets of melt inclusion compositions, into several distinct groups and potentially reconstruct their geological evolution.

Keywords: Amami Sankaku Basin, International Ocean Discovery Ptrogram, Izu-Bonin-Mariana arc, Melt inclusion, Statistical analysis, Volatiles

©2019. Japan Geoscience Union. All Right Reserved.

The Jurassic magmatism of protoliths of Mikabu greenstones in SW Japan: zircon U-Pb dating and trace element analysis

*Hikaru Sawada[1], Yukio Isozaki[1], Shogo Aoki[3], Shuhei Sakata[2], Ryo Hasegawa[1], Yasuo Nakamura[1]

1. Department of General Systems Studies, the University of Tokyo, 2. Department of Chemistry, Gakushuin Universtiy, 3. Department of Applied Science, Okayama University of Science

The Mikabu greenstones, incorporated with the Cretaceous high P/T-type Sanbagawa metamorphic belt in SW Japan, are accreted fragments of an oceanic plateau. We identified a Late Jurassic igneous age for the protoliths of the Mikabu greenstones in the eastern Kii Peninsula, by measuring U-Pb age and trace element composition (REE, Y, Sc, Nb, Ta, Hf, U, Th) of zircon grains with an Agilent 8800 single-collector triple quadrupole ICPMS coupled to a NWR-213 laser-ablation system. The U-Pb ages have a weighted average of 154.6 ±1.6 Ma (the Kimmeridgian, Late Jurassic) with an overlap within 2-sigma error. The igneous age is slightly younger than the previously reported radiolarian ages (Middle Jurassic) of deep-sea pelagic chert associated with the Mikabu greenstones. The age difference between them suggests that mafic magmas intruded pelagic deep-sea sediments on the pre-existing oceanic lithosphere. Trace element composition further indicates that the dated zircon grains are more similar to those in oceanic crusts than in granitic continental crusts, and the host mafic magma of the zircon grains was derived from depleted mantle like the mid-oceanic ridge-type source, rather than fertile mantle sources like Hawaii and Iceland. As rocks from the Shatsky Rise in the modern NW Pacific Ocean have similar age and compositional characteristics, this study concluded that the protoliths of the Mikabu greenstones had formed a part of an oceanic plateau, which was generated by the Late Jurassic intra-oceanic plate mafic magmatism in the ancient Pacific Ocean.

Keywords: Mikabu greenstones, zircon, Jurassic, oceanic plateau, U-Pb age, trace element

©2019. Japan Geoscience Union. All Right Reserved.

Origin of variable CaO/Al_2O_3 in olivine-hosted melt inclusions from Kibblewhite Volcano, Kermadec Arc

*Yasuhiro Hirai[1], Yoshihiko Tamura[2], Kaj Hoernle[3], Christian Timm[4], Folkmar Hauff[3], Reinhard Werner[3], Takeshi Hanyu[2], Bogdan Vaglarov[2], Qing Chang[2], Takashi Miyazaki[2], Jun-Ichi Kimura[2]

1. Graduate School of Natural Science and Technology, Kanazawa University, Japan, 2. Japan Agency for Marine-Earth Science and Technology (JAMSTEC), Yokosuka, Kanagawa, Japan, 3. GEOMAR Helmholtz Centre for Ocean Research, Kiel, Germany, 4. GNS Science, Lower Hutt, New Zealand

During R/V SONNE expedition SO-255 mafic basaltic to magnesian andesitic lavas containing melt inclusion hosting forsteritic olivines ($Fo_{90.3–92.4}$) were recovered from Kibblewhite Volcano, southern Kermadec Arc. The re-homogenized melt inclusions have compositions similar to primitive basalt (49.6–52.0 wt.% SiO_2; 12.7–15.9 wt.% MgO). Their CaO/Al_2O_3 values, however, range from 0.9 to 1.6, which cannot be explained by melting of lherzolite. Moreover, CaO/Al_2O_3 values in the melt inclusions correlate negatively with Ni contents of their host olivines suggesting that the high CaO/Al_2O_3 values result from interaction between mafic melts and subarc lithospheric mantle. Prior to the interaction the mafic magma must have had high Ni contents and low CaO/Al_2O_3 values, thus they crystallized high Ni olivines trapping low CaO/Al_2O_3 melt inclusions. During the interaction the olivines crystallized from the mafic magmas and its latent heat assimilated pyroxenes from the surrounding lithospheric mantle. This assimilation of pyroxenes allowed the Ni content of the melt to decrease and CaO/Al_2O_3 to increase while buffering the the Mg-number of the mafic magmas during the ascent. Thus, magmas during and after the interaction could crystallize low Ni olivines bearing high CaO/Al_2O_3 melt inclusions.

Keywords: Subduction zone, Kermadec Arc, Kibblewhite Volcano, SO-255, Olivine-hosted melt inclusion

©2019. Japan Geoscience Union. All Right Reserved.

Ankaramite from Doyo seamount in the Izu-Ogasawara arc: A precursor of continents?

*Yoshihiko Tamura[1], Tomoki Sato[1], Osamu Ishizuka[1,2], Takashi Miyazaki[1], Yasuhiro Hirai[1,3], Mami Takehara[4], Eri Sakamoto[5]

1. JAMSTEC, 2. AIST, 3. Kanazawa Univ., 4. NIPR, 5. NME

Izu-Ogasawara-Mariana (IOM) system of arcs (also known as the Izu-Bonin-Mariana arc system) is a typical oceanic arc produced by subduction of the Pacific Plate beneath the Philippine Sea Plate. Volcanoes along the southern segment of the Izu-Ogasawara arc are underlain by thin crust (10-20 km). According to the hypothesis presented by Tamura *et al.* (2016), rising mantle diapirs stall near the base of the oceanic crust at depths controlled by the thickness of the overlying crust. Where the crust is thin, melting occurs at relatively low pressures in the mantle wedge producing andesitic magmas. Andesites erupted from Nishinoshima that were produced in the recent history of the volcano have been generated by olivine fractionation of primary andesitic magmas (Tamura *et al.*, 2019).

To further examine this hypothesis, we have dived Doyo Seamount by using manned submersible SHINKAI 6500 to sample primitive magmas from the volcano, which is located about 50 km north of Nishinoshima and is underlain by thinner curst (15 km) compared to Nishinoshima. Doyo Seamount is located approximately 900 km south of Tokyo at 27˚41’ N, 140˚48’ E in the Ogasawara Arc. The seamount attained an elevation of ~400 m below sea level (mbsl) and its submarine flanks extend to the depth of 3,200 mbsl. The basal dimeter of the volcano is about 30 km. The deeper parts of this large submarine edifice have yet to be explored. Primitive lavas tend to erupt in the deeper parts of submarine volcanoes at the depth of ~2,000 m. Deeper satellite vents are expected to erupt more primitive magmas compared to the main summit vents because primitive magmas could bypass the shallow magma chambers where crystal fractionation and magma mixing happen.

There is a small satellite cone about 11 km east of the summit of Doyo Seamount at the depth of ~3,000 m. A ridge extends on the flank of the volcano from the summit in the ENE direction to the depth of ~2,400 m. Thus, we tried to sample this satellite cone and the deeper part of the ridge. Interestingly, 13 samples out of all 21 samples, which we have recovered during this dive 6K#1519, are olivine-clinopyroxene basalts containing 20-40 % of very coarse clinopyroxene phenocrysts, which could be called ankaramite (Figure 1). Ankaramites are strongly vesiculated and their blocks have rough and rugged surface, which are different from smooth surface of basaltic pillow lavas. Some of ankaramite magmas might have had explosive eruptions at the depth of 2,000~3,000 m, which have resulted in volcaniclastic cones or brecciated lava flows.

Similar primitive and phenocryst-rich ankaramitic basalts were recovered from the old submarine knolls near Nishinoshima (Tamura et al., 2019). We suggested that lithospheric mantle was thicker before the development of Nishinoshima volcano (Figure 2). Primary basaltic magmas could have been generated at depth beneath the thicker lithospheric lid, and these magmas might have interacted with the lithospheric uppermost mantle during their ascent and have resulted in the unique ankaramite magmas (Figure 1). The temperature of the upper part of the mantle wedge increases with frequent passage of magmas through it, and continuous subduction beneath it will drench the whole mantle wedge, thus, the thickness of the lithosphere will decrease and approach the thickness of the curst in mature arcs. Doyo Seamount could represent the early stage of Nishinoshima volcano, and thus, ankaramite magma is deemed to be a

©2019. Japan Geoscience Union. All Right Reserved.

precursor of andesitic magmas.

References

Tamura et al. (2016). Advent of continents: A new hypothesis. *Scientific Reports* **6,** 33517.
Tamura et al. (2019). Nishinoshima volcano in the Ogasawara Arc: New continent from the ocean? *Island Arc* **28,** e12285.

Keywords: ankaramite, andesite, continent, oceanic arc, lithosphere, mantle wedge

©2019. Japan Geoscience Union. All Right Reserved.

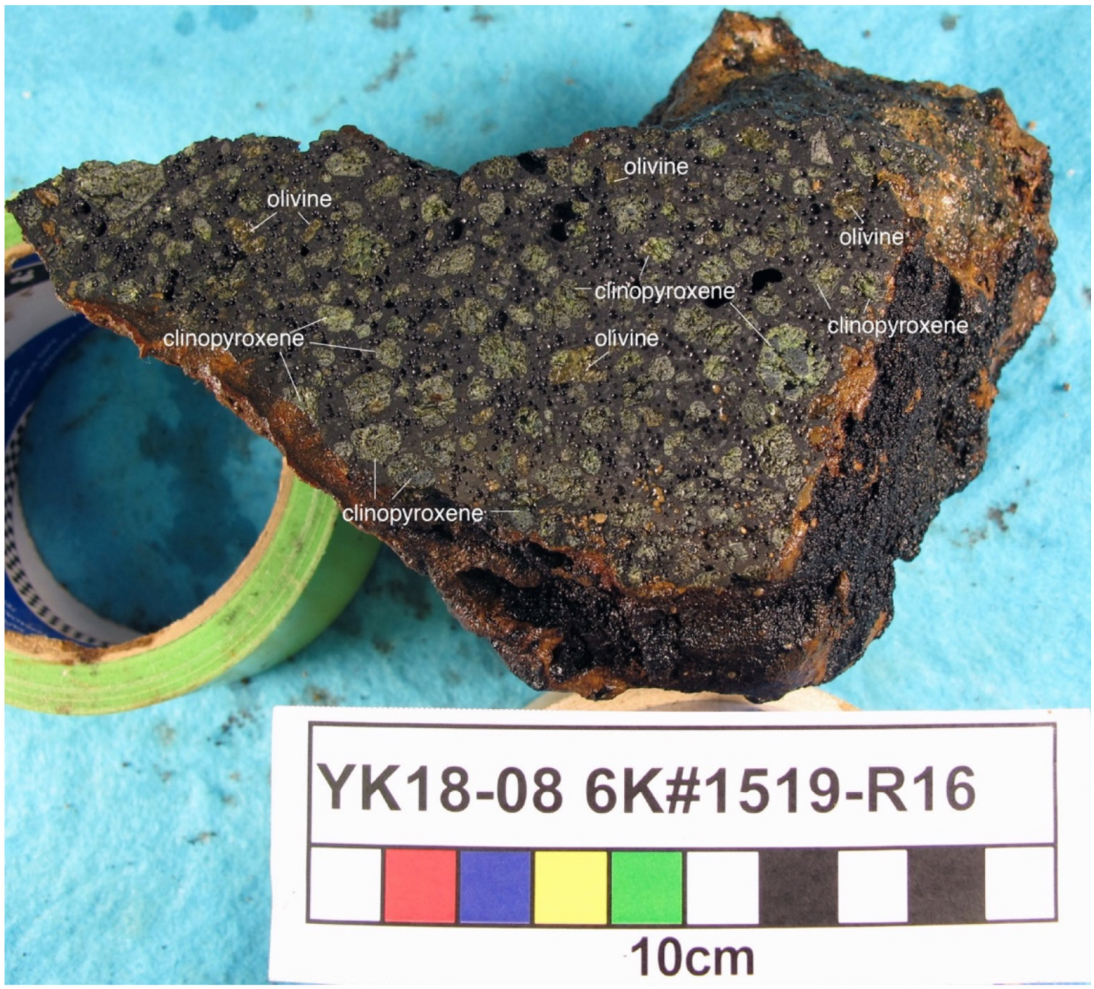

Figure 1. Ankaramite recovered from Doyo Seamount.

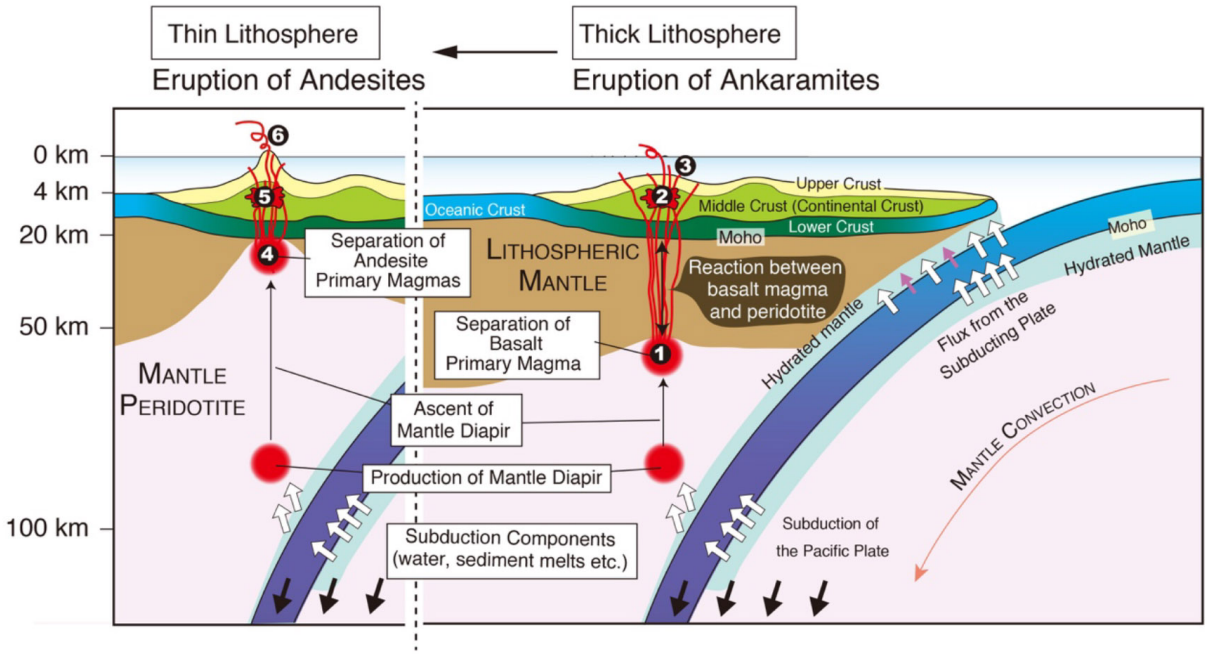

Figure 2. Schematic diagrams showing the genesis of andesite and ankaramite magmas in the Ogasawara arc.

©2019. Japan Geoscience Union. All Right Reserved.

Different Moho reflections adjacent to Minami-Tori Shima and their petrologic origins

*Yoshihiko Tamura[1], Kentaro Kaneda[2], Gou Fujie[1], Akane Ohira[1], Eiichi TAKAZAWA[3], Georges Ceuleneer[4], Katsuyoshi Michibayashi[5], Tomoki Sato[1], Shuichi Kodaira[1], Seiichi Miura[1]

1. Japan Agency for Maine-Earth Science and Technology, 2. Japan Coast Guard, 3. Niigata University, 4. Universite de Toulouse, 5. Nagoya University

It is the common knowledge that Moho is the boundary between the crust and mantle, which was discovered by and named after Croatian seismologist Mohorovičić. We have shown that Moho is not the crust-mantle boundary and presented a new hypothesis about the origin of Moho based on seismological and petrological observations (Tamura et al., EGU2018-11069-2; JpGU2018 SMP36-05; AGCC2018 abstract volume590; Tamura et al., in preparation). Direct drilling and sampling of Moho could be the best scenario to examine the hypothesis. However, IODP drillings of basaltic crust could estimate the petrologic origins of the crust-mantle boundary far below the seafloor, which could be useful to examine the hypothesis of formation of Moho.

Kaneda et al. (2010) conducted seismic surveys across the Marcus-Wake seamount chain near Minami-Tori Shima, which is the Japanese easternmost and one and only island on the Pacific Plate. They found contrasting seafloor in the north and south of the seamount chain, which were referred to the northern and southern basins (Figure 1). Average water depths in the northern and southern basins are about 5900 m and 5700 m, respectively. Magnetic anomalies suggest Jurassic ages of M32 (159 Ma) and M42 (167 Ma) for the northern and southern basins, respectively. The southern basin has the clear Moho reflections, which are characteristically sharp, single, flat, and continuous, and of large amplitude, but in the northern basin, Moho reflections are extremely weak or even absent. Interestingly, the crust of the southern basin has a constant thickness of 7.5-8.0 km, but the crust of the northern basin shows a constant thickness of 6 km, 1.5-2 km thinner than that of the northern basin.The correlation between Moho reflections and crustal thicknesses have been generally observed in other seismic profiles (e.g. Ohira et al., 2017).

The boundary between mantle peridotite and layered gabbro from the lower oceanic crust in the Oman ophiolite consists of a dunitic transition zone (DTZ), mostly made of olivine + scattered Cr-spinel. The thickness of DTZ ranges from a few meters to a few hundred meters. When mantle melts under hydrous conditions, the liquidus field of forsterite expands relative to that of enstatite and enstatite melts incongruently to produce dunites and andesitic melts.

We present here a new hypothesis that (1) accidental influx of seawater at the mid-ocean ridges results in hydrous melting of mantle peridotite just beneath the crust and produces thick dunite at the crust-mantle boundaries, (2) the thick dunite represents reflective Moho, and (3) this additional hydrous melting of shallowest mantle increases the thickness of oceanic crust.

Although the andesitic melts, which are the outgrowth of dunites, would be mixed with dominant basaltic melts extracted from the deeper parts of melting column of MORB, there must be systematic and significant differences between crustal materials with Moho and those without Moho. Comparative drillings of oceanic crust in the northern and southern basins for future IODP expeditions will reveal the differences of basalts and examine the models for Moho.

©2019. Japan Geoscience Union. All Right Reserved.

Keywords: Moho, Minami-Tori Shima, dunite, mantle, crust, basalt

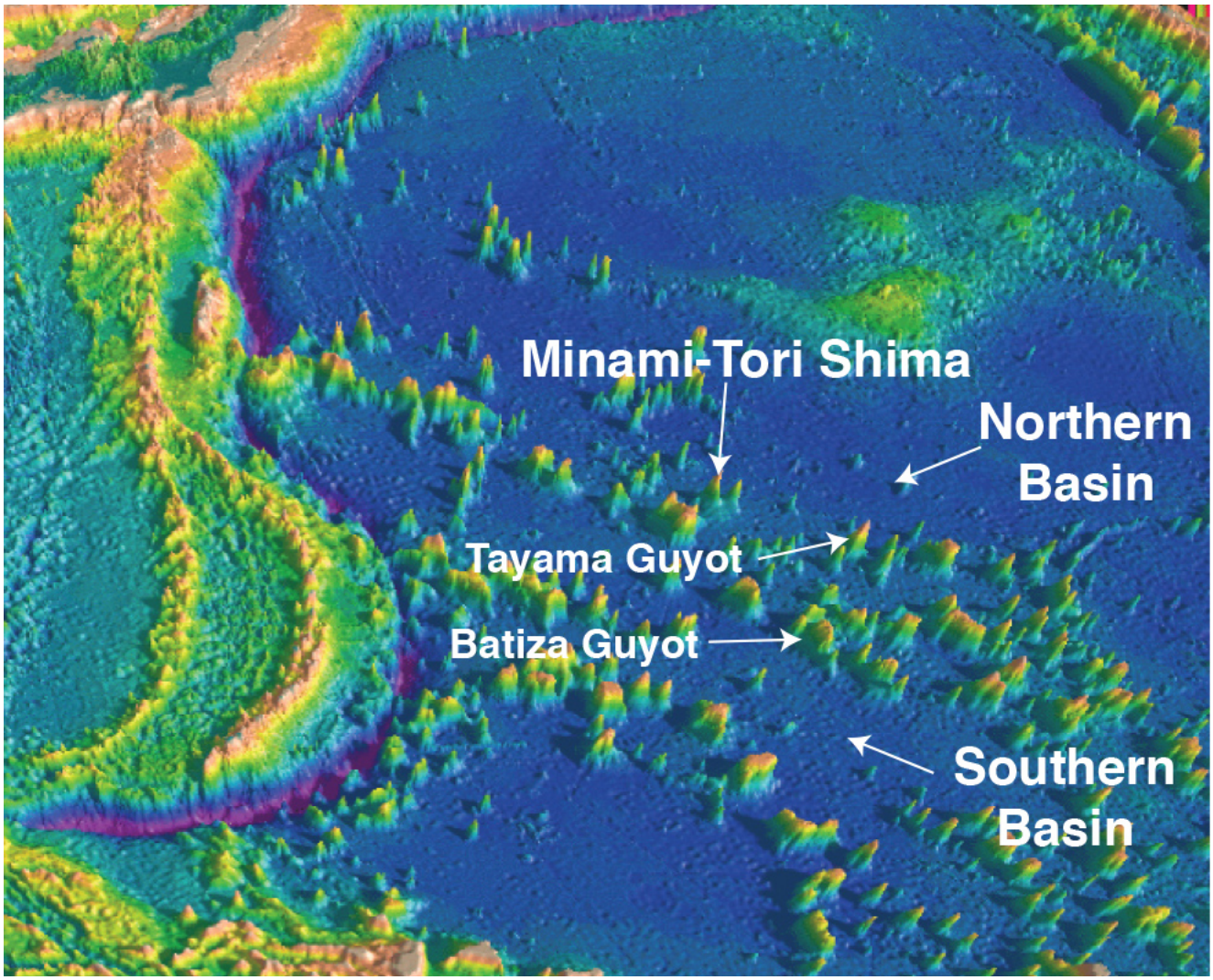

©2019. Japan Geoscience Union. All Right Reserved.

Melt-rock interaction in plagioclase peridotites from the southern Palawan Ophiolite, Philippines

*FLORENCE ANNETTE CRUSPERO LABIS[1], BETCHAIDA D PAYOT[1], GABRIEL THEOPHILUS V VALERA[1], JULIUS A PASCO[1], JESLEY MEI A DYCOCO[1]

1. UNIVERSITY OF THE PHILIPPINES

This work presents new petrographic and geochemical data on the plagioclase peridotites and the spinel harzburgites of the mantle section of the southern Palawan Ophiolite. The plagioclase peridotites show peculiar textures evident of melt-rock interaction as indicated by: (1) interstitial clinopyroxene and subhedral orthopyroxene around plagioclase, and (2) plagioclase blebs within the peridotite matrix. The spinel harzburgites display protogranular to porphyroclastic textures and dominantly composed of olivine, orthopyroxene, and small amounts of clinopyroxene and spinel. These minerals show kink banding and bent lamellae which are indicative of plastic deformation. Major element geochemistry of the spinel harzburgites reveals high Cr# (0.53-0.78) and Mg# (0.40-0.51) in spinel, and high NiO wt.% (0.40-0.43) and Fo contents (89.9-90.5) in olivine reflecting residual origin. Their geochemical composition is comparable to the residual peridotites in arc settings. Consequently, the plagioclase peridotites have lower Mg# (0.23-0.34) and relatively high Cr# (0.60-0.61) in spinel, as well as lower Fo (83.3-85.9) contents in olivine. Spinel and clinopyroxene in the plagioclase peridotites have higher TiO_2 contents compared with those of the spinel harzburgites. Clinopyroxene in plagioclase peridotites are marked by strong depletion in LREE and flat MREE to HREE with significant negative Eu and Sr anomalies. In contrast, the spinel harzburgites have lower REE abundances which suggest higher degrees of partial melting. We propose that the spinel harzburgites of the southern Palawan Ophiolite are residual peridotites formed by high degrees of partial melting above a subduction zone and were subsequently infiltrated by melts leading to the formation of the plagioclase peridotites.

Keywords: Palawan Ophiolite, plagioclase peridotites, melt-rock interaction

©2019. Japan Geoscience Union. All Right Reserved.

Intra-oceanic arc magma genesis: a case study from Havre volcano, Kermadec arc

*Chris Conway[1], Kenichiro Tani[2]

1. Geological Survey of Japan, 2. National Museum of Nature and Science

The Kermadec intra-oceanic arc comprises 33 active arc front volcanoes along its ~1200 km length, which represent key targets for studying the formation of Earth’ s crust. The discovery of numerous submarine caldera volcanoes and dacitic to rhyolitic pumice deposits from this setting has prompted new models for the genesis of intra-oceanic silicic arc magmas. A detailed investigation of the 2012 eruption of rhyolite pumice and lava at Havre volcano has provided a valuable opportunity to test these models. Moreover, the retrieval of older volcanic deposits from the edifice has given critical context for studying magma genesis throughout the lifetime of the volcano. Here we present whole-rock, mineral and glass major and trace element data for volcanic rock samples collected from Havre volcano. The samples, which span a compositional range from basalt to rhyolite, display several key features that support arguments against the derivation of silicic magmas primarily through crustal anatexis: (1) the range of sample compositions fit along coherent crystal fractionation trends; (2) low-MgO aphyric andesites fill the gap within the general bimodality of eruptive products from the Kermadec arc; and (3) there is a scarcity of tonalitic xenoliths. These features favour crystal fractionation over crustal anatexis as the dominant process for generating the compositional diversity seen at Havre volcano.

Keywords: rhyolite, magma genesis, Havre volcano

©2019. Japan Geoscience Union. All Right Reserved.

[E] Poster | S (Solid Earth Sciences)：S-MP Mineralogy & Petrology

Tue. May 28, 2019 5:15 PM - 6:30 PM JST | Tue. May 28, 2019 8:15 AM - 9:30 AM UTC | Poster Hall International Exhibition Hall8, Makuhari Messe_33

[S-MP30] Crust-Mantle Connections

convener:Yoshihiko Tamura(Research Institute for Marine Geodynamics, Japan Agency for Maine-Earth Science and Technology), Osamu Ishizuka(Geological Survey of Japan, AIST), Chris Conway(Geological Survey of Japan)

A paradigm of the solid Earth geochemical cycles is that the Earth's crust forms by melting of the Earth's upper peridotitic mantle. How divers is the spectrum of primary melts and which factors may contribute to its variations? What is the influence of crustal processing vs. primary magma diversity in creating the diversity of the Earth's crust? The session seeks to explore the crust-mantle connections at divergent and convergent plate boundaries, and oceanic island settings based on volcanology, petrology, geochemistry, geophysics, geochronology, and geodynamics studies.

[SMP30-P01] Secular evolution of proto-Izu-Bonin-Mariana arc volcanism: Constraints from statistical analysis of melt inclusion compositions

*Morihisa Hamada[1], Hikaru Iwamori[1,2], Philipp A. Brandl[3], Takayuki Ushikubo[4], Kenji Shimizu[4], Motoo Ito[4], He Li[5], Ivan P. Savov[6] (1.Department of Solid Earth Geochemistry, Japan Agency for Marine-Earth Science and Technology, 2.Earthquake Research Institute, University of Tokyo, 3.GEOMAR Helmholtz Centre for Ocean Research Kiel, 4.Kochi Institute for Core Sample Research, Japan Agency for Marine-Earth Science and Technology, 5.Institute of Oceanology, Chinese Academy of Sciences, 6.School of Earth and Environment, University of Leeds)

[SMP30-P02] The Jurassic magmatism of protoliths of Mikabu greenstones in SW Japan: zircon U-Pb dating and trace element analysis

*Hikaru Sawada[1], Yukio Isozaki[1], Shogo Aoki[3], Shuhei Sakata[2], Ryo Hasegawa[1], Yasuo Nakamura[1] (1.Department of General Systems Studies, the University of Tokyo, 2.Department of Chemistry, Gakushuin Universtiy, 3.Department of Applied Science, Okayama University of Science)

[SMP30-P03] Origin of variable CaO/Al_2O_3 in olivine-hosted melt inclusions from Kibblewhite Volcano, Kermadec Arc

*Yasuhiro Hirai[1], Yoshihiko Tamura[2], Kaj Hoernle[3], Christian Timm[4], Folkmar Hauff[3], Reinhard Werner[3], Takeshi Hanyu[2], Bogdan Vaglarov[2], Qing Chang[2], Takashi Miyazaki[2], Jun-Ichi Kimura[2] (1.Graduate School of Natural Science and Technology, Kanazawa University, Japan, 2.Japan Agency for Marine-Earth Science and Technology (JAMSTEC), Yokosuka, Kanagawa, Japan, 3.GEOMAR Helmholtz Centre for Ocean Research, Kiel, Germany, 4.GNS Science, Lower Hutt, New Zealand)

[SMP30-P04] Ankaramite from Doyo seamount in the Izu-Ogasawara arc: A precursor of continents?

*Yoshihiko Tamura[1], Tomoki Sato[1], Osamu Ishizuka[1,2], Takashi Miyazaki[1], Yasuhiro Hirai[1,3], Mami Takehara[4], Eri Sakamoto[5] (1.JAMSTEC, 2.AIST, 3.Kanazawa Univ., 4.NIPR, 5.NME)

[SMP30-P05] Different Moho reflections adjacent to Minami-Tori Shima and their petrologic origins

*Yoshihiko Tamura[1], Kentaro Kaneda[2], Gou Fujie[1], Akane Ohira[1], Eiichi TAKAZAWA[3], Georges Ceuleneer[4], Katsuyoshi Michibayashi[5], Tomoki Sato[1], Shuichi Kodaira[1], Seiichi Miura[1] (1.Japan Agency for Maine-Earth Science and Technology, 2.Japan Coast Guard, 3.Niigata University, 4.Universite de Toulouse, 5.Nagoya University)

[SMP30-P06] Melt-rock interaction in plagioclase peridotites from the southern Palawan Ophiolite, Philippines

*FLORENCE ANNETTE CRUSPERO LABIS[1], BETCHAIDA D PAYOT[1], GABRIEL THEOPHILUS V VALERA[1], JULIUS A PASCO[1], JESLEY MEI A DYCOCO[1] (1.UNIVERSITY OF THE PHILIPPINES)

[SMP30-P07] Intra-oceanic arc magma genesis: a case study from Havre volcano, Kermadec arc

*Chris Conway[1], Kenichiro Tani[2] (1.Geological Survey of Japan, 2.National Museum of Nature and Science)

Secular evolution of proto-Izu-Bonin-Mariana arc volcanism: Constraints from statistical analysis of melt inclusion compositions

*Morihisa Hamada[1], Hikaru Iwamori[1,2], Philipp A. Brandl[3], Takayuki Ushikubo[4], Kenji Shimizu[4], Motoo Ito[4], He Li[5], Ivan P. Savov[6]

1. Department of Solid Earth Geochemistry, Japan Agency for Marine-Earth Science and Technology, 2. Earthquake Research Institute, University of Tokyo, 3. GEOMAR Helmholtz Centre for Ocean Research Kiel, 4. Kochi Institute for Core Sample Research, Japan Agency for Marine-Earth Science and Technology, 5. Institute of Oceanology, Chinese Academy of Sciences, 6. School of Earth and Environment, University of Leeds

International Ocean Discovery Program (IODP) Expedition 351 'Izu–Bonin–Mariana (IBM) Arc Origins' drilled Site U1438, situated in the north-western margin of the Philippine Sea, into volcaniclastic sediments of the proto-IBM arc. Brandl *et al.* (2017, *Earth and Planetary Science Letters*) have analysed the major, trace and volatile elements of 304 melt inclusions hosted in fresh silicate minerals to unveil the magmatic evolution of the proto-IBM arc between 30 and 40 Ma, when the arc volcanism matured following subduction initiation at 52 Ma. Brandl *et al.* (2017) concluded that: (1) volcanism of the proto-IBM arc shifted from calc-alkaline affinity to tholeiitic affinity over time; and (2) such compositional shift is linked to both the volcanic productivity and the maturation of an evolving island arc. To better integrate the composition of melt inclusions with the magmatic evolution of the proto-IBM arc, this study extends the dataset of Brandl *et al.* (2017) by: (1) additional analysis of volatiles (H_2O, S, F and Cl) and P_2O_5 for 47 carefully selected melt inclusions by Secondary Ion Mass Spectrometry (SIMS); and (2) statistical analysis on the composition of 237 representative melt inclusions covering the full time range (30–40 Ma) of the dataset. Based on statistical analysis of the melt inclusion compositions and by considering trace element compositions and volatile concentrations, we can confidently distinguish five main clusters of melt inclusion compositions which can be further separated into a total of nine sub-clusters. Among the nine sub-clusters, we identified three major magma types: (1) medium-K enriched magmas which form a tholeiitic trend (30–38 Ma); (2) less-depleted medium-K melts which form a calc-alkaline trend (35–39 Ma); and (3) low-K depleted magmas which form a calc-alkaline trend (35–40 Ma). We demonstrate that: (1) volcanism of calc-alkaline depleted magmas lasted until 35 Ma; (2) the volcanism of calc-alkaline depleted magmas and that of more enriched normal arc magmas (tholeiitic and calc-alkaline affinities) overlap between 35 and 38–39 Ma and; (iii) the volcanism of normal arc magmas became predominant thereafter at the proto-IBM arc. Such identification of three major magma types is distinct from that of Brandl *et al.* (2017), in which less-depleted medium-K calc-alkaline magmas amd depleted low-K calc-alkaline gammas were not distinguished. We infer that depleted source mantle had been replaced by enriched mantle due to mantle convection beneath the proto-IBM arc from >40 Ma to 35 Ma. Statistical analysis is a useful tool to partition a mixture of multivariable dataset, such as datasets of melt inclusion compositions, into several distinct groups and potentially reconstruct their geological evolution.

Keywords: Amami Sankaku Basin, International Ocean Discovery Ptrogram, Izu-Bonin-Mariana arc, Melt inclusion, Statistical analysis, Volatiles

©2019. Japan Geoscience Union. All Right Reserved.

The Jurassic magmatism of protoliths of Mikabu greenstones in SW Japan: zircon U-Pb dating and trace element analysis

*Hikaru Sawada[1], Yukio Isozaki[1], Shogo Aoki[3], Shuhei Sakata[2], Ryo Hasegawa[1], Yasuo Nakamura[1]

1. Department of General Systems Studies, the University of Tokyo, 2. Department of Chemistry, Gakushuin Universtiy, 3. Department of Applied Science, Okayama University of Science

The Mikabu greenstones, incorporated with the Cretaceous high P/T-type Sanbagawa metamorphic belt in SW Japan, are accreted fragments of an oceanic plateau. We identified a Late Jurassic igneous age for the protoliths of the Mikabu greenstones in the eastern Kii Peninsula, by measuring U-Pb age and trace element composition (REE, Y, Sc, Nb, Ta, Hf, U, Th) of zircon grains with an Agilent 8800 single-collector triple quadrupole ICPMS coupled to a NWR-213 laser-ablation system. The U-Pb ages have a weighted average of 154.6 ±1.6 Ma (the Kimmeridgian, Late Jurassic) with an overlap within 2-sigma error. The igneous age is slightly younger than the previously reported radiolarian ages (Middle Jurassic) of deep-sea pelagic chert associated with the Mikabu greenstones. The age difference between them suggests that mafic magmas intruded pelagic deep-sea sediments on the pre-existing oceanic lithosphere. Trace element composition further indicates that the dated zircon grains are more similar to those in oceanic crusts than in granitic continental crusts, and the host mafic magma of the zircon grains was derived from depleted mantle like the mid-oceanic ridge-type source, rather than fertile mantle sources like Hawaii and Iceland. As rocks from the Shatsky Rise in the modern NW Pacific Ocean have similar age and compositional characteristics, this study concluded that the protoliths of the Mikabu greenstones had formed a part of an oceanic plateau, which was generated by the Late Jurassic intra-oceanic plate mafic magmatism in the ancient Pacific Ocean.

Keywords: Mikabu greenstones, zircon, Jurassic, oceanic plateau, U-Pb age, trace element

©2019. Japan Geoscience Union. All Right Reserved.

Origin of variable CaO/Al_2O_3 in olivine-hosted melt inclusions from Kibblewhite Volcano, Kermadec Arc

*Yasuhiro Hirai[1], Yoshihiko Tamura[2], Kaj Hoernle[3], Christian Timm[4], Folkmar Hauff[3], Reinhard Werner[3], Takeshi Hanyu[2], Bogdan Vaglarov[2], Qing Chang[2], Takashi Miyazaki[2], Jun-Ichi Kimura[2]

1. Graduate School of Natural Science and Technology, Kanazawa University, Japan, 2. Japan Agency for Marine-Earth Science and Technology (JAMSTEC), Yokosuka, Kanagawa, Japan, 3. GEOMAR Helmholtz Centre for Ocean Research, Kiel, Germany, 4. GNS Science, Lower Hutt, New Zealand

During R/V SONNE expedition SO-255 mafic basaltic to magnesian andesitic lavas containing melt inclusion hosting forsteritic olivines ($Fo_{90.3–92.4}$) were recovered from Kibblewhite Volcano, southern Kermadec Arc. The re-homogenized melt inclusions have compositions similar to primitive basalt (49.6–52.0 wt.% SiO_2; 12.7–15.9 wt.% MgO). Their CaO/Al_2O_3 values, however, range from 0.9 to 1.6, which cannot be explained by melting of lherzolite. Moreover, CaO/Al_2O_3 values in the melt inclusions correlate negatively with Ni contents of their host olivines suggesting that the high CaO/Al_2O_3 values result from interaction between mafic melts and subarc lithospheric mantle. Prior to the interaction the mafic magma must have had high Ni contents and low CaO/Al_2O_3 values, thus they crystallized high Ni olivines trapping low CaO/Al_2O_3 melt inclusions. During the interaction the olivines crystallized from the mafic magmas and its latent heat assimilated pyroxenes from the surrounding lithospheric mantle. This assimilation of pyroxenes allowed the Ni content of the melt to decrease and CaO/Al_2O_3 to increase while buffering the the Mg-number of the mafic magmas during the ascent. Thus, magmas during and after the interaction could crystallize low Ni olivines bearing high CaO/Al_2O_3 melt inclusions.

Keywords: Subduction zone, Kermadec Arc, Kibblewhite Volcano, SO-255, Olivine-hosted melt inclusion

©2019. Japan Geoscience Union. All Right Reserved.

Ankaramite from Doyo seamount in the Izu-Ogasawara arc: A precursor of continents?

*Yoshihiko Tamura[1], Tomoki Sato[1], Osamu Ishizuka[1,2], Takashi Miyazaki[1], Yasuhiro Hirai[1,3], Mami Takehara[4], Eri Sakamoto[5]

1. JAMSTEC, 2. AIST, 3. Kanazawa Univ., 4. NIPR, 5. NME

Izu-Ogasawara-Mariana (IOM) system of arcs (also known as the Izu-Bonin-Mariana arc system) is a typical oceanic arc produced by subduction of the Pacific Plate beneath the Philippine Sea Plate. Volcanoes along the southern segment of the Izu-Ogasawara arc are underlain by thin crust (10-20 km). According to the hypothesis presented by Tamura *et al.* (2016), rising mantle diapirs stall near the base of the oceanic crust at depths controlled by the thickness of the overlying crust. Where the crust is thin, melting occurs at relatively low pressures in the mantle wedge producing andesitic magmas. Andesites erupted from Nishinoshima that were produced in the recent history of the volcano have been generated by olivine fractionation of primary andesitic magmas (Tamura *et al.*, 2019).

To further examine this hypothesis, we have dived Doyo Seamount by using manned submersible SHINKAI 6500 to sample primitive magmas from the volcano, which is located about 50 km north of Nishinoshima and is underlain by thinner curst (15 km) compared to Nishinoshima. Doyo Seamount is located approximately 900 km south of Tokyo at 27˚41’ N, 140˚48’ E in the Ogasawara Arc. The seamount attained an elevation of ~400 m below sea level (mbsl) and its submarine flanks extend to the depth of 3,200 mbsl. The basal dimeter of the volcano is about 30 km. The deeper parts of this large submarine edifice have yet to be explored. Primitive lavas tend to erupt in the deeper parts of submarine volcanoes at the depth of ~2,000 m. Deeper satellite vents are expected to erupt more primitive magmas compared to the main summit vents because primitive magmas could bypass the shallow magma chambers where crystal fractionation and magma mixing happen.

There is a small satellite cone about 11 km east of the summit of Doyo Seamount at the depth of ~3,000 m. A ridge extends on the flank of the volcano from the summit in the ENE direction to the depth of ~2,400 m. Thus, we tried to sample this satellite cone and the deeper part of the ridge. Interestingly, 13 samples out of all 21 samples, which we have recovered during this dive 6K#1519, are olivine-clinopyroxene basalts containing 20-40 % of very coarse clinopyroxene phenocrysts, which could be called ankaramite (Figure 1). Ankaramites are strongly vesiculated and their blocks have rough and rugged surface, which are different from smooth surface of basaltic pillow lavas. Some of ankaramite magmas might have had explosive eruptions at the depth of 2,000~3,000 m, which have resulted in volcaniclastic cones or brecciated lava flows.

Similar primitive and phenocryst-rich ankaramitic basalts were recovered from the old submarine knolls near Nishinoshima (Tamura et al., 2019). We suggested that lithospheric mantle was thicker before the development of Nishinoshima volcano (Figure 2). Primary basaltic magmas could have been generated at depth beneath the thicker lithospheric lid, and these magmas might have interacted with the lithospheric uppermost mantle during their ascent and have resulted in the unique ankaramite magmas (Figure 1). The temperature of the upper part of the mantle wedge increases with frequent passage of magmas through it, and continuous subduction beneath it will drench the whole mantle wedge, thus, the thickness of the lithosphere will decrease and approach the thickness of the curst in mature arcs. Doyo Seamount could represent the early stage of Nishinoshima volcano, and thus, ankaramite magma is deemed to be a

©2019. Japan Geoscience Union. All Right Reserved.

precursor of andesitic magmas.

References

Tamura et al. (2016). Advent of continents: A new hypothesis. *Scientific Reports* **6,** 33517.
Tamura et al. (2019). Nishinoshima volcano in the Ogasawara Arc: New continent from the ocean? *Island Arc* **28,** e12285.

Keywords: ankaramite, andesite, continent, oceanic arc, lithosphere, mantle wedge

©2019. Japan Geoscience Union. All Right Reserved.

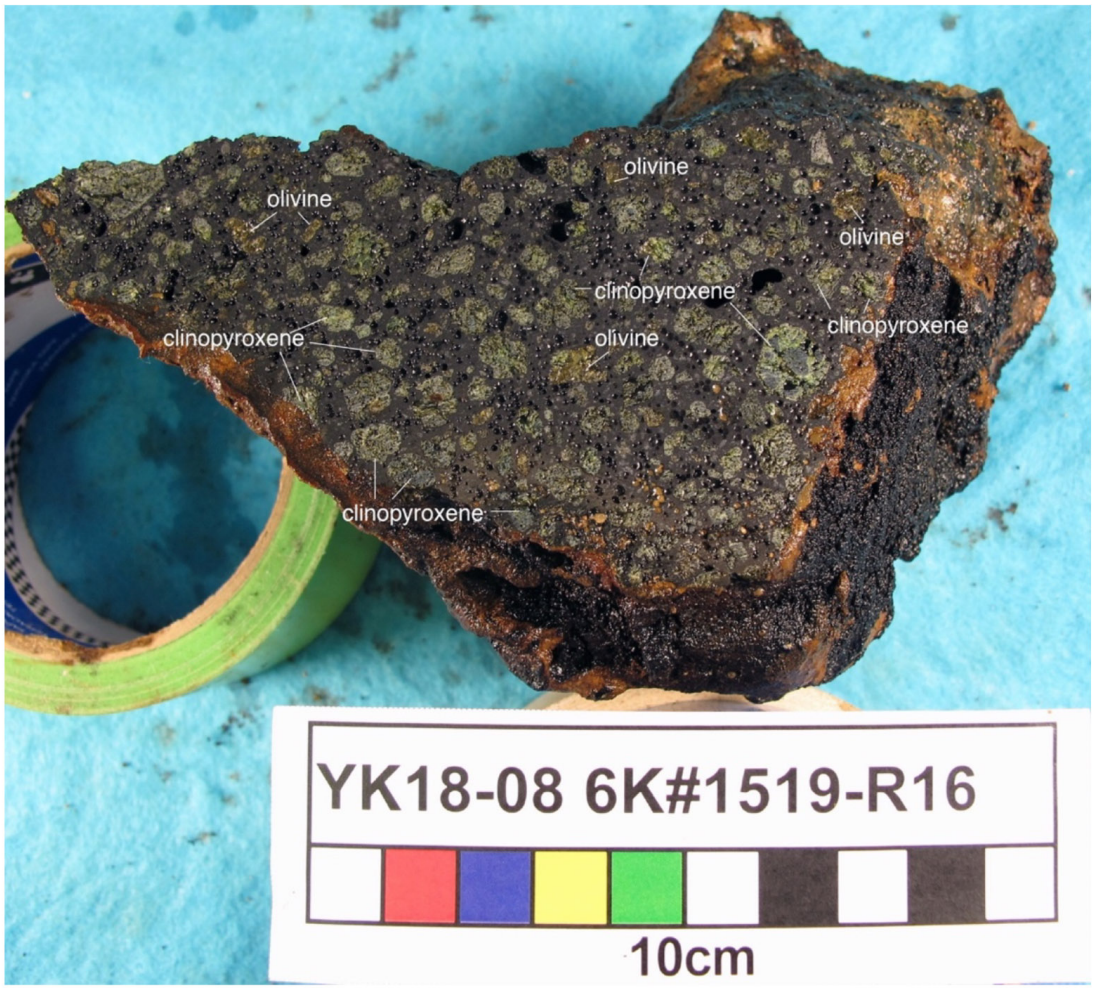

Figure 1. Ankaramite recovered from Doyo Seamount.

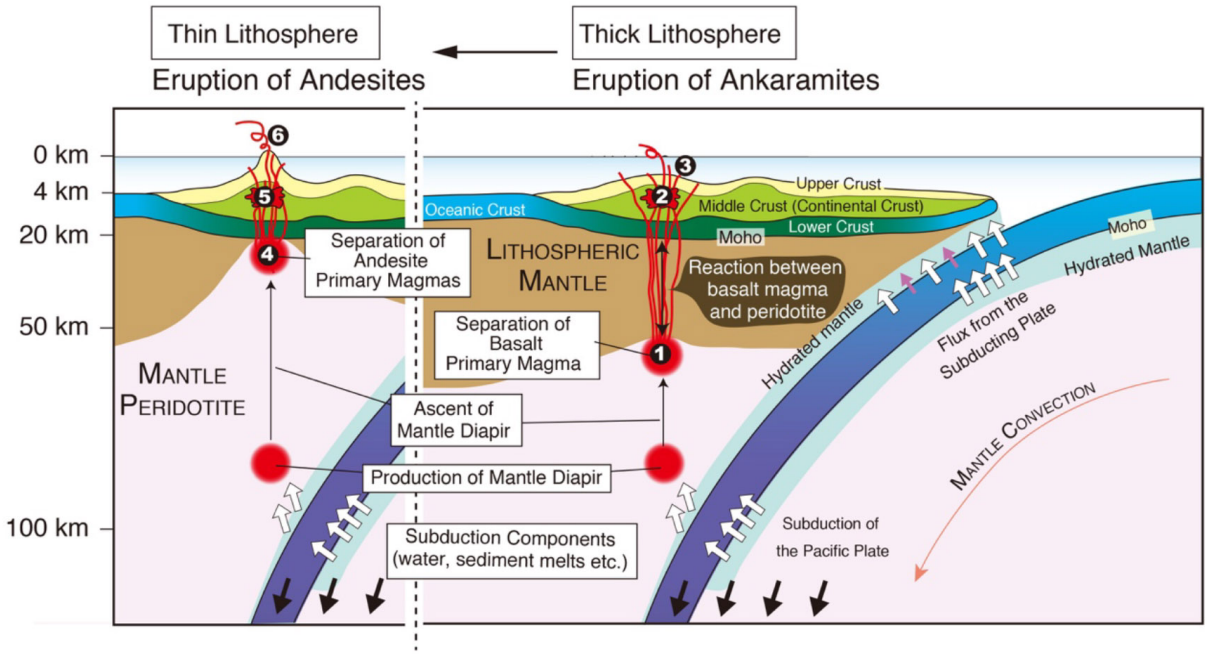

Figure 2. Schematic diagrams showing the genesis of andesite and ankaramite magmas in the Ogasawara arc.

©2019. Japan Geoscience Union. All Right Reserved.

Different Moho reflections adjacent to Minami-Tori Shima and their petrologic origins

*Yoshihiko Tamura[1], Kentaro Kaneda[2], Gou Fujie[1], Akane Ohira[1], Eiichi TAKAZAWA[3], Georges Ceuleneer[4], Katsuyoshi Michibayashi[5], Tomoki Sato[1], Shuichi Kodaira[1], Seiichi Miura[1]

1. Japan Agency for Maine-Earth Science and Technology, 2. Japan Coast Guard, 3. Niigata University, 4. Universite de Toulouse, 5. Nagoya University

It is the common knowledge that Moho is the boundary between the crust and mantle, which was discovered by and named after Croatian seismologist Mohorovičić. We have shown that Moho is not the crust-mantle boundary and presented a new hypothesis about the origin of Moho based on seismological and petrological observations (Tamura et al., EGU2018-11069-2; JpGU2018 SMP36-05; AGCC2018 abstract volume590; Tamura et al., in preparation). Direct drilling and sampling of Moho could be the best scenario to examine the hypothesis. However, IODP drillings of basaltic crust could estimate the petrologic origins of the crust-mantle boundary far below the seafloor, which could be useful to examine the hypothesis of formation of Moho.

Kaneda et al. (2010) conducted seismic surveys across the Marcus-Wake seamount chain near Minami-Tori Shima, which is the Japanese easternmost and one and only island on the Pacific Plate. They found contrasting seafloor in the north and south of the seamount chain, which were referred to the northern and southern basins (Figure 1). Average water depths in the northern and southern basins are about 5900 m and 5700 m, respectively. Magnetic anomalies suggest Jurassic ages of M32 (159 Ma) and M42 (167 Ma) for the northern and southern basins, respectively. The southern basin has the clear Moho reflections, which are characteristically sharp, single, flat, and continuous, and of large amplitude, but in the northern basin, Moho reflections are extremely weak or even absent. Interestingly, the crust of the southern basin has a constant thickness of 7.5-8.0 km, but the crust of the northern basin shows a constant thickness of 6 km, 1.5-2 km thinner than that of the northern basin.The correlation between Moho reflections and crustal thicknesses have been generally observed in other seismic profiles (e.g. Ohira et al., 2017).

The boundary between mantle peridotite and layered gabbro from the lower oceanic crust in the Oman ophiolite consists of a dunitic transition zone (DTZ), mostly made of olivine + scattered Cr-spinel. The thickness of DTZ ranges from a few meters to a few hundred meters. When mantle melts under hydrous conditions, the liquidus field of forsterite expands relative to that of enstatite and enstatite melts incongruently to produce dunites and andesitic melts.

We present here a new hypothesis that (1) accidental influx of seawater at the mid-ocean ridges results in hydrous melting of mantle peridotite just beneath the crust and produces thick dunite at the crust-mantle boundaries, (2) the thick dunite represents reflective Moho, and (3) this additional hydrous melting of shallowest mantle increases the thickness of oceanic crust.

Although the andesitic melts, which are the outgrowth of dunites, would be mixed with dominant basaltic melts extracted from the deeper parts of melting column of MORB, there must be systematic and significant differences between crustal materials with Moho and those without Moho. Comparative drillings of oceanic crust in the northern and southern basins for future IODP expeditions will reveal the differences of basalts and examine the models for Moho.

©2019. Japan Geoscience Union. All Right Reserved.

Keywords: Moho, Minami-Tori Shima, dunite, mantle, crust, basalt

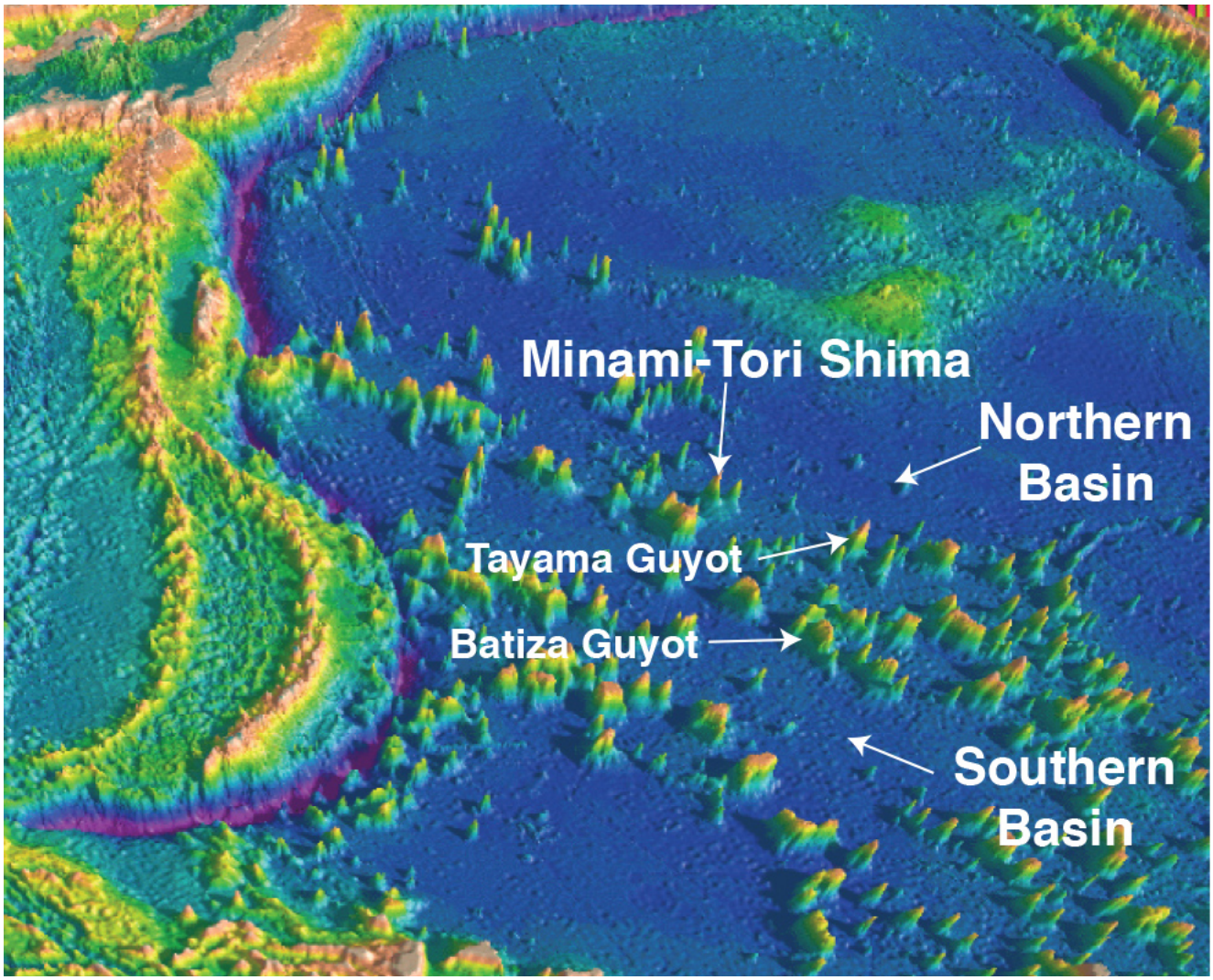

©2019. Japan Geoscience Union. All Right Reserved.

Melt-rock interaction in plagioclase peridotites from the southern Palawan Ophiolite, Philippines

*FLORENCE ANNETTE CRUSPERO LABIS[1], BETCHAIDA D PAYOT[1], GABRIEL THEOPHILUS V VALERA[1], JULIUS A PASCO[1], JESLEY MEI A DYCOCO[1]

1. UNIVERSITY OF THE PHILIPPINES

This work presents new petrographic and geochemical data on the plagioclase peridotites and the spinel harzburgites of the mantle section of the southern Palawan Ophiolite. The plagioclase peridotites show peculiar textures evident of melt-rock interaction as indicated by: (1) interstitial clinopyroxene and subhedral orthopyroxene around plagioclase, and (2) plagioclase blebs within the peridotite matrix. The spinel harzburgites display protogranular to porphyroclastic textures and dominantly composed of olivine, orthopyroxene, and small amounts of clinopyroxene and spinel. These minerals show kink banding and bent lamellae which are indicative of plastic deformation. Major element geochemistry of the spinel harzburgites reveals high Cr# (0.53-0.78) and Mg# (0.40-0.51) in spinel, and high NiO wt.% (0.40-0.43) and Fo contents (89.9-90.5) in olivine reflecting residual origin. Their geochemical composition is comparable to the residual peridotites in arc settings. Consequently, the plagioclase peridotites have lower Mg# (0.23-0.34) and relatively high Cr# (0.60-0.61) in spinel, as well as lower Fo (83.3-85.9) contents in olivine. Spinel and clinopyroxene in the plagioclase peridotites have higher TiO_2 contents compared with those of the spinel harzburgites. Clinopyroxene in plagioclase peridotites are marked by strong depletion in LREE and flat MREE to HREE with significant negative Eu and Sr anomalies. In contrast, the spinel harzburgites have lower REE abundances which suggest higher degrees of partial melting. We propose that the spinel harzburgites of the southern Palawan Ophiolite are residual peridotites formed by high degrees of partial melting above a subduction zone and were subsequently infiltrated by melts leading to the formation of the plagioclase peridotites.

Keywords: Palawan Ophiolite, plagioclase peridotites, melt-rock interaction

©2019. Japan Geoscience Union. All Right Reserved.

Intra-oceanic arc magma genesis: a case study from Havre volcano, Kermadec arc

*Chris Conway[1], Kenichiro Tani[2]

1. Geological Survey of Japan, 2. National Museum of Nature and Science

The Kermadec intra-oceanic arc comprises 33 active arc front volcanoes along its ~1200 km length, which represent key targets for studying the formation of Earth’ s crust. The discovery of numerous submarine caldera volcanoes and dacitic to rhyolitic pumice deposits from this setting has prompted new models for the genesis of intra-oceanic silicic arc magmas. A detailed investigation of the 2012 eruption of rhyolite pumice and lava at Havre volcano has provided a valuable opportunity to test these models. Moreover, the retrieval of older volcanic deposits from the edifice has given critical context for studying magma genesis throughout the lifetime of the volcano. Here we present whole-rock, mineral and glass major and trace element data for volcanic rock samples collected from Havre volcano. The samples, which span a compositional range from basalt to rhyolite, display several key features that support arguments against the derivation of silicic magmas primarily through crustal anatexis: (1) the range of sample compositions fit along coherent crystal fractionation trends; (2) low-MgO aphyric andesites fill the gap within the general bimodality of eruptive products from the Kermadec arc; and (3) there is a scarcity of tonalitic xenoliths. These features favour crystal fractionation over crustal anatexis as the dominant process for generating the compositional diversity seen at Havre volcano.

Keywords: rhyolite, magma genesis, Havre volcano

©2019. Japan Geoscience Union. All Right Reserved.

[E] Poster | S (Solid Earth Sciences)：S-MP Mineralogy & Petrology

Tue. May 28, 2019 3:30 PM - 5:00 PM JST | Tue. May 28, 2019 6:30 AM - 8:00 AM UTC | Poster Hall International Exhibition Hall8, Makuhari Messe_18

[S-MP31] Supercontinents and Crustal Evolution

convener:Madhusoodhan Satish-Kumar(Department of Geology, Faculty of Science, Niigata University), Tomokazu Hokada(National Institute of Polar Research), Krishnan Sajeev(Centre for Earth Sciences, Indian Institute of Science), Yasuhito Osanai(Division of Evolution of Earth Environments, Faculty of Social and Cultural Studies, Kyushu University)

Supercontinent formation and dispersion has been enigmatic in the Earth's history. Eurasia is one such current supercontinent and incredible progress in the understanding of its geological evolution has been achieved in the past decade. Earlier supercontinents in the Earth's history such as Gondwana (0.5 Ga), Rodinia (1.0 Ga), Columbia/Nuna (2.0 Ga), Kenorland (2.5 Ga) and Vaalbara (3.1 Ga), have been the focus of several studies, however limited information on older supercontinents has restricted an understanding of their tectonic evolution. In this session, we invite authors around the world to present new data as well as review existing results on the continental scale crustal processes and tectonic evolution that are associated with supercontinent formation and breakup events in the Earth's history. The well-studied Eurasia and Gondwana supercontinents are of particular focus. Topics of interest include, but not restricted to, extremes in metamorphism, P-T-d-t evolution, magmatism, and the role of fluids. We hope to provide a platform for scientific discussions that will enlighten our understanding of the physical and chemical processes in the continental crust that records episodes of orogenesis that contributed to the formation and evolution of supercontinents.

[SMP31-P01] Re-examination of metamorphic and geochronologic events in Rayner Complex and Western Rayner Complex in Antarctica

*Tomokazu Hokada[1,2], Sotaro Baba[3], Atsushi Kamei[4], Ippei Kitano[5], Kenji Horie[1,2], Yoshikuni Hiroi[1,6], Yoichi Motoyoshi[1,2], Mami Takehara[1], Kazuyuki Shiraishi[1] (1.National Institute of Polar Research, 2.The Graduate University for Advanced Studies (SOKENDAI), 3.University of the Ryukyus, 4.Shimane University, 5.Kyushu University, 6.Chiba University)

[SMP31-P02] Composition of constituent minerals in corona-bearing and -free mafic gneisses from the Lützow-Holm Complex at Skallen, East Antarctica

*Yuki Mori[1], Takeshi Ikeda[2] (1.Department of Earth and Planetary Sciences, Graduate School of Sciences, Kyushu University, 2.Department of Earth and Planetary Sciences, Faculty of Sciences, Kyushu University)

[SMP31-P03] “Pseudo-concordance” of U-Pb system in zircon at Harvey Nunatak, Napier Complex, East Antarctica

*Mami Takehara[1] (1.National Institute of Polar Research)

[SMP31-P04] Rapid UHT metamorphism and exhumation of the Lützow-Holm Complex in Antarctica

*Yoshikuni Hiroi[1], Tomokazu Hokada[2], Tatsuro Adachi[3], Yasuhito Osanai[3], Yoichi Motoyoshi[2], Kazuyuki Shiraishi[2] (1.Chiba Univ, 2.National Institute of Polar Research, 3.Kyushu University)

[SMP31-P05] Tectonic History of Hiroo Complex and its implication inpaleo-Kuril Arc evolution

*Sreehari Lakshmanan[1], Tsuyoshi Toyoshima[2], Futoshi Nanayama[3] (1.Graduate School of Science and Technology, Niigata University, Niigata, Japan, 2.Department of Geology, Faculty of Science, Niigata Univ. , 3.Geological Survey of Japan, AIST)

[SMP31-P06] Behaviour of C, O, Sr, Nd and Pb isotopes in high-grade metacarbonate rocks

*Madhusoodhan Satish-Kumar[1], Akari Imura[1], Momoko Shirakawa[2], Gen Shimoda[3], Kosuke T. Goto[3], M A Sanjeewa P K Malaviarachchi[4] (1.Department of Geology, Faculty of Science, Niigata University, 2.Graduate School of Science and Technology, Niigata University, 3.Geological Survey of Japan, 4.University of Peradeniya, Sri Lanka)

Re-examination of metamorphic and geochronologic events in Rayner Complex and Western Rayner Complex in Antarctica

*Tomokazu Hokada[1,2], Sotaro Baba[3], Atsushi Kamei[4], Ippei Kitano[5], Kenji Horie[1,2], Yoshikuni Hiroi[1,6], Yoichi Motoyoshi[1,2], Mami Takehara[1], Kazuyuki Shiraishi[1]

1. National Institute of Polar Research, 2. The Graduate University for Advanced Studies (SOKENDAI), 3. University of the Ryukyus, 4. Shimane University, 5. Kyushu University, 6. Chiba University

Enderby Land in Antarctica comprises of Neoproterozoic-Cambrian (c.650-500 Ma) high-grade metamorphic terranes that constituting Gondwana supercontinent (e.g., Shiraishi et al., 2008). Easternmost part is “Western Rayner Complex” of which granulite-facies and partly UHT metamorphism (Motoyoshi et al., 1994, 1995) and 2400-1000 Ma protolith and 540-520 Ma metamorphic ages were reported (Shiraishi et al., 1997). Neighboring “Rayner Complex” is characterized by >2500-1000 Ma protolith and 980-910 Ma granulite-facies metamorphic ages. Boundary between the Rayner and the Western Rayner Complex has been not clearly defined until when Horie et al. (2016) obtained 934-894 Ma SHIRMP zircon U-Pb ages from Mt. Lira, Condon Hills and Mt. Yuzhnaya regions with minor 590-570 Ma zircons from Mt. Yuzhnaya. Hiroi (unpublished data) also demonstrated contrasting metamorphic P-T evolution among the Mt. Lira, Condon Hills and Mt. Yuzhnaya regions.

JARE-58 (2016-2017) geology team made a short visit and sampling at a small nunatak of west of Mt. Yuzhnaya, a small nunatak of east of Forefinger Point, and Point Widdows in order to assess the relationship between the Rayner and the Western Rayner Complexes. We will report and discuss the update of the characteristic features of the Rayner and the Western Rayner Complexes.

Keywords: Antarctica, Gondwana, Supercontinent, metamorphism, geochronology

©2019. Japan Geoscience Union. All Right Reserved.

Composition of constituent minerals in corona-bearing and -free mafic gneisses from the Lützow-Holm Complex at Skallen, East Antarctica

*Yuki Mori[1], Takeshi Ikeda[2]

1. Department of Earth and Planetary Sciences, Graduate School of Sciences, Kyushu University, 2. Department of Earth and Planetary Sciences, Faculty of Sciences, Kyushu University

Corona is one of the non-equilibrium microstructures and has been employed to infer pressure-temperature path of the metamorphic rocks. The corona around garnet is common in mafic to ultramafic gneisses in the Lützow-Holm Complex (LHC) of East Antarctica (e.g., Hiroi et al., 1991). However, not every garnet in mafic to ultramafic gneisses accompanies the corona. In our ongoing study to reveal the controlling factors of presence and absence of the corona, we compare the composition of garnet and hornblende of the corona-bearing (no. I-223) and -free (no. I-232) mafic gneisses from Skallen.

The metamorphic grade of the complex increases progressively from the upper amphibolite facies to granulite facies toward the southwest, and the LHC is divided into three zones referred to as the amphibolite-facies zone, transitional zone, and granulite-facies zone (Hiroi et al., 1991). Recent studies have revealed that both transitional and granulite-facies zones had undergone high temperatures that exceed 800 ˚C (e.g., Iwamura et al, 2013; Kawakami et al., 2016). Skallen is an exposure located in the granulite-facies zone.

The constituent minerals in the matrix of the studied samples are almost same (garnet, hornblende, plagioclase with minor amounts of clinopyroxene and orthopyroxene), but I-223 further contains biotite. The microstructure and chemical composition of I-223 is as follows. The garnet grain is coarse (15 mm in diameter) and surrounded by a symplectitic corona composed of orthopyroxene and plagioclase. Garnet is clearly divided into two domains of Ca-rich core (Xgrs=0.23) and Ca-poor rim (Xgrs=0.18). X_{Mg} [=Mg/(Mg+Fe)] increases toward rim from 0.22 to 0.27, and that in the outer part of the rim decreases toward the boundary between the garnet and the corona from 0.27 to 0.22. The Ca-poor rim of the garnet includes irregular-shaped nanogranite composed of quartz, biotite, plagioclase, and K-feldspar. Hornblende is brown to brownish-green and polygonal. The X_{Mg} of the hornblende is 0.46-0.50. Matrix plagioclase often shows antiperthite intergrowing An50 plagioclase with Or96 K-feldspar. The coronal plagioclase has higher anorthite content (An80) than that in the matrix (An50). The microstructure and chemical composition of I-232 is as follows. The garnet grain is coarse (10 mm long) and elongated. The garnet and the hornblende define foliation of the rock. The hornblende is brown to pale brown. The composition of garnet gradually changes from core (Alm52Prp31Grs14Sps3) to rim (Alm52Prp28Grs17Sps3). The X_{Mg} in the hornblende varies from 0.60-0.70, and the composition is heterogeneous even in one grain. Most part of plagioclase is An45, and some parts of rim of the plagioclase have higher anorthite content of 70.

The garnet and hornblende in the corona-bearing gneiss have lower X_{Mg} than those in the corona-free gneiss. In addition, calcium content of the garnet and matrix plagioclase in the corona-bearing gneiss is higher than that in the corona-free gneiss. Therefore, we consider that bulk composition is one of the factors controlling the corona formation. The presence of nanogranite in the garnet surrounded by the corona suggests that partial melting and transport of the melt would cause the change of bulk composition in part.

©2019. Japan Geoscience Union. All Right Reserved.

Keywords: corona, garnet, nanogranite, Lützow-Holm Complex, Antarctica

©2019. Japan Geoscience Union. All Right Reserved.

“Pseudo-concordance” of U-Pb system in zircon at Harvey Nunatak, Napier Complex, East Antarctica

*Mami Takehara[1]

1. National Institute of Polar Research

U-Pb zircon dating has played a pivotal role in geochronology due to zircon’s high durability and high closure temperature. In addition, the paired decay scheme of two U isotopes allows us to verify the determined U-Pb zircon age. The Napier Complex in East Antarctica is well known because it preserves both of evidence of ultrahigh-temperature (UHT) metamorphism (e.g., Sheraton et al., 1987; Harley & Hensen 1990) and long Archaean crustal history from 3800 Ma to 2500 Ma (e.g., Harley & Black 1997). Previous researchers also reported the possibilities of the early Archean crust in the Napier Complex (e.g., Compston and Williams, 1982). Some previous researchers pointed out discordant U-Pb data including reverse discordance which was derived from the redistribution of radiogenic Pb isotopes in zircon in the Napier Complex samples (e.g., Kusiak et al., 2013). The some discordant U-Pb data looks concordant but actually reflect the Pb redistribution, namely “pseudo-concordance.” They suggest the redistribution of the radiogenic Pb isotopes in zircons was associated with the UHT metamorphism based on the Pb isotope mapping of the zircons. This report is critical for accurate U-Pb zircon geochronology in the UHT metamorphic region, such as the Napier Complex. Therefore, in this study, the zircons from the rock sample of the Napier Complex were characterized on the basis of the observation and trace-element contents, and the information was utilized for interpretation of the U-Pb data.
Zircons collected from a tonalitic gneiss (170223-2A-09) were first analyzed using sensitive high resolution ion-microprobes (SHRIMP IIe and SHRIMP IIe/AMC) at the National Institute of Polar Research, Japan. The sample was collected at the Harvey Nunatak, which is located close to Mt. Sones. The geochronological data from the Harvey Nunatak had never been reported. The sample was crushed by a high-voltage pulse power fragmentation device (Selfrag Lab) to preserve the external morphology of zircons and prevent contamination (Takehara et al., 2018). After pulverizing, the zircon grains were concentrated using conventional mineral separation techniques, including heavy liquid separation with methylene iodide and magnetic separation.
The zircon grains include fractures and slightly mineral inclusion based on the observation of transmitted light images by an optical microscope. BSE images show that some zircon grains have darker BSE-response domains, which suggests depletion of contents of Zr and Si during hydrothermal alteration of zircon. The zircons show typically high U contents (average is ~2500 ppm), and the U-Pb age from the high U zircons was corrected for the matrix effect derived from the high U contents according to the method by Williams & Hergt (2000) and White & Ireland (2012). It seems that the unaltered zircons show concordant data from about 2450 Ma to 2540 Ma with discordance (Disc.(%) = 1 −(206Pb/238U age)/(207Pb/206Pb age)} ×100 (e.g, Song et al., 1996)) ranges from -5 to +9%. On the other hand, trace element geochemistry of zircons does not support detritus protolith. In this presentation, the information of trace-element contents in zircons was utilized for the interpretation of U-Pb data and “pseudo-concordance.”

©2019. Japan Geoscience Union. All Right Reserved.

Rapid UHT metamorphism and exhumation of the Lützow-Holm Complex in Antarctica

*Yoshikuni Hiroi[1], Tomokazu Hokada[2], Tatsuro Adachi[3], Yasuhito Osanai[3], Yoichi Motoyoshi[2], Kazuyuki Shiraishi[2]

1. Chiba Univ, 2. National Institute of Polar Research, 3. Kyushu University

The Lützow-Holm Complex in Antarctica is a part of Neoproterozoic-Cambrian (c.650-500 Ma) collisional orogen to form Gondwana supercontinent. It is characterized by progressive metamorphism from upper amphibolite facies in the eastern part of the Prince Olav Coast to upper granulite facies in the southern Sôya Coast (e.g., Hiroi et al., 1991). UHT metamorphism is evidenced by such diagnostic mineral assemblages as Opx + Sil + Grt + Rt + Qz and Spr + Qz in Mg-Al-rich pelitic granulites in Rundvågshetta. Intimate intergrowths of Ky + Spr + Grt and Sil + Spr + Grt as well as andalusite-bearing falsite-nanogranite inclusions are included in the same porphyroblastic garnet, which is compositionally zoned, with Mg-rich core, Fe–Mn-rich rim, and core-to-rim oscillation of Ca. Integration of these new data with those previously documented leads to the inference of a rapid change in pressure–temperature conditions during regional UHT metamorphism in this part of the late Neoproterozoic to early Paleozoic ‘large and hot orogen’. Several lines of evidence indicate that partial melting and melt extraction took place even in mafic granulites of fragmented gabbro origin.

Keywords: Antarctica, Gondwana, Supercontinent, UHT metamorphism

©2019. Japan Geoscience Union. All Right Reserved.

Tectonic History of Hiroo Complex and its implication inpaleo-Kuril Arc evolution

*Sreehari Lakshmanan[1], Tsuyoshi Toyoshima[2], Futoshi Nanayama[3]

1. Graduate School of Science and Technology, Niigata University, Niigata, Japan, 2. Department of Geology, Faculty of Science, Niigata Univ. , 3. Geological Survey of Japan, AIST

Melanges records information about deformation history and tectonic events in plate margins and orogens and hence they are important in evolution of accretionary complexes [1]. Mélange facies rocks and brocken formations distributed in Nakanogawa Group of Hidaak Belt in Central Hokkaido is known as Hiroo Complex. We carried out detailed field mapping and structural studies on melange facies rocks distributed around Tachiiwa, Kamitoyoni and Daimaruyama region of Hiroo Complex. Four different deformation processes (D1,D2,D3 and D4) are identified from field to micro-scale observations. D1 event shear zones are wide and considerd as penitrative but D2, D3 and D4 shear zones observed in narrow deformation zones and considerd as less penitrative local events. D1 shearzones are identified as scaly fabric in mudstone and asymmetrically sheared sandstone clast distributed in it. This is similar to 'block in matrix' structure, typical of tectonic melange devoloped in accretionary complexes. D1 foliation trends in N-NNW direction. Tectonic evolution of theses rocks confirmed by pressure solution cleavage, composite planar fabrics (P-Y-R shear), asymmetrical folds and dip-parallel streching lineation. P-Y-R shear relation and other asymmetrical structures in both field and microscale observation shows east-side-up sense of movement. This shear sense suggest that major penetrative deformatoin phase in melange was connected to accretionary complex devolopment in paleo-Kuril-Arc region, where initial subduction was directed in N-S direction and later it rotated clockwise and attained its present position. D2, D3 and D4 events were recognized as dextral strike-slip movement, sinistral-strike-slip to oblique-slip movement and west-side-down movement sense respectively . Mega-micro scale observation of D2 and D3 events show the properties of cataclastic deformation and D4 event is that of fault gouge. Based on this D2, D3 and D4 events are considered as upper crustal or local deformation processes. We consider these are linked to post-melange deformation processes and related to final stages of devolopment of Hidaka Metamorphic Belt (HMB). Recent geochemical studies from Daimaruyama region and geochronological studies from Nakanogawa Group region points that Hiroo Complex was part of initiallly northward subducting Paleo-Kuril Arc region [2]. Through detailed strucural analysis, this study also confirms that Hiroo Complex was devoloped in accretionary complex of paleo- Kuril-Arc by an offscrapping mode of evolution. Later Hiroo Complex became part of Nakanogawa Group through a series of deformation processes asocciated with arc-arc colission between paleo-Kuril Arc and paleo-Japan Arc.
[1]A. Festa et al., 2012. Tectonophysics, 568, 7-24 [2] T.Yamasaki, F. Nanayama, 2018. Lithos. 302, 224-241

Keywords: Hiroo Complex, Paleo Kuri lArc, Mélange tectonics, Accretionary Complex, Nakanogawa Group

©2019. Japan Geoscience Union. All Right Reserved.

Behaviour of C, O, Sr, Nd and Pb isotopes in high-grade metacarbonate rocks

*Madhusoodhan Satish-Kumar[1], Akari Imura[1], Momoko Shirakawa[2], Gen Shimoda[3], Kosuke T. Goto[3], M A Sanjeewa P K Malaviarachchi[4]

1. Department of Geology, Faculty of Science, Niigata University, 2. Graduate School of Science and Technology, Niigata University, 3. Geological Survey of Japan, 4. University of Peradeniya, Sri Lanka

Tectonic environment of metasedimentary sequences deposit in orogenic belts is of importance in understanding the formation and evolution of supercontinents. In particular, chemically deposited carbonate rocks are supposed to hold key information of extinct paleo-oceans, since they are directly precipitated from seawater. In this study, we carried out a comprehensive trace and rare earth element analysis, carbon, oxygen, strontium, neodymium and lead isotope measurements in metacarbonate rocks from the Highland Complex, Sri Lanka. The isotopic systems studied have distinct residence and mixing time in seawater, and are also controlled by the input from surrounding continents. We present here the behaviour of each isotopic system with respect to different processes right from the deposition of carbonate from the seawater through diagenesis and then prograde and retrograde metamorphism. TheProterozoic basement of Sri Lanka is subdivided into four lithotectonic units, namely, the Highland Complex (HC), the Wanni Complex (WC), the Vijayan Complex (VC), and the Kadugannawa Complex (KC), based on Nd isotope model ages. The HC is mainly composed of metasedimentary rocks (granulite facies metaquartzites, metapelitic gneisses and metacarbonate rocks), whereas exposures of the WC and the VC are mainly metaigneous rocks. The metacarbonate rocks in the HC generally occur as layers parallel with other metasedimentary lithological units, and show a NE trend.

We measured oxygen and carbon isotope ratios to understand the effect of diagenetic to metamorphic alterations, which can be recognized in negative isotope shifts. In general, the metacarbonate rocks have positive oxygen isotopic composition comparable with the Proterozoic unmetamorphosed carbonates, suggesting that these rocks were not affected by external fluids during digenesis, dolomitization or metamorphism. However, some of the rock units have been affected by later fluid infiltration as seen in major shifts in oxygen isotopic composition. Negative shifts in both carbon and oxygen isotopes correspond to the metamorphic decarbonation reactions being prominent. Strontium isotope chemostratigraphy was applied for the selected samples with least signatures of alteration. The depositional ages show a younging direction of sedimentation from the Wanni-side to the Vijayan-side. In the case of Nd isotopes, the values correspond to variable mixing of continent derived and oceanic crust derived components during carbonate deposition. This is clearly depicted in the ε Sr vs. ε Nd cross-plots where typical seawater-rock mixing relationship in metacarbonate rocks associated with continents and oceanic crusts can be deduced.Pb isotopic composition of the metacarbonate rocks in Sri Lanka indicated significant differences within the HC; the Vijayan side is more radiogenic than that of Wanni side. This might be due to the difference of initial composition, as well as the relationship to depositional basin and seawater composition. We also observed very low U/Pb ratios, which are considered to have occurred due to the U-loss during metamorphic recrystallization.Thus, the Sr-Nd-Pb isotopic composition in metacarbonate rocks suggests interaction between the oceanic crust and carbonate rocks on the Wanni side whereas on the Vijayan side, carbonate sedimentation was accompanied by interaction with cratonic continental crust.Thus, by applying a multi-element isotope geochemical approach on metacarbonate rocks collected from continental collisional zones, and by comparing the data with basement rocks from various neighbouring Gondwana continents, regional affinities could be established.

©2019. Japan Geoscience Union. All Right Reserved.

Sr, Nd and Pb isotopic compositions provide important information about the depositional settings of sedimentary rocks and provide key information about the surrounding terrains of oceanic and continental affinities during the time of deposition. This can lead to a better understanding of paleo-tectonic settings of crustal fragments that assemble to form supercontinents.

Keywords: metacarbonates, Sr-Nd-Pb isotopes, Sri Lanka

©2019. Japan Geoscience Union. All Right Reserved.

[E] Poster | S (Solid Earth Sciences)：S-MP Mineralogy & Petrology

Tue. May 28, 2019 5:15 PM - 6:30 PM JST | Tue. May 28, 2019 8:15 AM - 9:30 AM UTC | Poster Hall International Exhibition Hall8, Makuhari Messe_34

[S-MP31] Supercontinents and Crustal Evolution

convener:Madhusoodhan Satish-Kumar(Department of Geology, Faculty of Science, Niigata University), Tomokazu Hokada(National Institute of Polar Research), Krishnan Sajeev(Centre for Earth Sciences, Indian Institute of Science), Yasuhito Osanai(Division of Evolution of Earth Environments, Faculty of Social and Cultural Studies, Kyushu University)

Supercontinent formation and dispersion has been enigmatic in the Earth's history. Eurasia is one such current supercontinent and incredible progress in the understanding of its geological evolution has been achieved in the past decade. Earlier supercontinents in the Earth's history such as Gondwana (0.5 Ga), Rodinia (1.0 Ga), Columbia/Nuna (2.0 Ga), Kenorland (2.5 Ga) and Vaalbara (3.1 Ga), have been the focus of several studies, however limited information on older supercontinents has restricted an understanding of their tectonic evolution. In this session, we invite authors around the world to present new data as well as review existing results on the continental scale crustal processes and tectonic evolution that are associated with supercontinent formation and breakup events in the Earth's history. The well-studied Eurasia and Gondwana supercontinents are of particular focus. Topics of interest include, but not restricted to, extremes in metamorphism, P-T-d-t evolution, magmatism, and the role of fluids. We hope to provide a platform for scientific discussions that will enlighten our understanding of the physical and chemical processes in the continental crust that records episodes of orogenesis that contributed to the formation and evolution of supercontinents.

[SMP31-P01] Re-examination of metamorphic and geochronologic events in Rayner Complex and Western Rayner Complex in Antarctica

*Tomokazu Hokada[1,2], Sotaro Baba[3], Atsushi Kamei[4], Ippei Kitano[5], Kenji Horie[1,2], Yoshikuni Hiroi[1,6], Yoichi Motoyoshi[1,2], Mami Takehara[1], Kazuyuki Shiraishi[1] (1.National Institute of Polar Research, 2.The Graduate University for Advanced Studies (SOKENDAI), 3.University of the Ryukyus, 4.Shimane University, 5.Kyushu University, 6.Chiba University)

[SMP31-P02] Composition of constituent minerals in corona-bearing and -free mafic gneisses from the Lützow-Holm Complex at Skallen, East Antarctica

*Yuki Mori[1], Takeshi Ikeda[2] (1.Department of Earth and Planetary Sciences, Graduate School of Sciences, Kyushu University, 2.Department of Earth and Planetary Sciences, Faculty of Sciences, Kyushu University)

[SMP31-P03] “Pseudo-concordance” of U-Pb system in zircon at Harvey Nunatak, Napier Complex, East Antarctica

*Mami Takehara[1] (1.National Institute of Polar Research)

[SMP31-P04] Rapid UHT metamorphism and exhumation of the Lützow-Holm Complex in Antarctica

*Yoshikuni Hiroi[1], Tomokazu Hokada[2], Tatsuro Adachi[3], Yasuhito Osanai[3], Yoichi Motoyoshi[2], Kazuyuki Shiraishi[2] (1.Chiba Univ, 2.National Institute of Polar Research, 3.Kyushu University)

[SMP31-P05] Tectonic History of Hiroo Complex and its implication inpaleo-Kuril Arc evolution

*Sreehari Lakshmanan[1], Tsuyoshi Toyoshima[2], Futoshi Nanayama[3] (1.Graduate School of Science and Technology, Niigata University, Niigata, Japan, 2.Department of Geology, Faculty of Science, Niigata Univ. , 3.Geological Survey of Japan, AIST)

[SMP31-P06] Behaviour of C, O, Sr, Nd and Pb isotopes in high-grade metacarbonate rocks

*Madhusoodhan Satish-Kumar[1], Akari Imura[1], Momoko Shirakawa[2], Gen Shimoda[3], Kosuke T. Goto[3], M A Sanjeewa P K Malaviarachchi[4] (1.Department of Geology, Faculty of Science, Niigata University, 2.Graduate School of Science and Technology, Niigata University, 3.Geological Survey of Japan, 4.University of Peradeniya, Sri Lanka)

Re-examination of metamorphic and geochronologic events in Rayner Complex and Western Rayner Complex in Antarctica

*Tomokazu Hokada[1,2], Sotaro Baba[3], Atsushi Kamei[4], Ippei Kitano[5], Kenji Horie[1,2], Yoshikuni Hiroi[1,6], Yoichi Motoyoshi[1,2], Mami Takehara[1], Kazuyuki Shiraishi[1]

1. National Institute of Polar Research, 2. The Graduate University for Advanced Studies (SOKENDAI), 3. University of the Ryukyus, 4. Shimane University, 5. Kyushu University, 6. Chiba University

Enderby Land in Antarctica comprises of Neoproterozoic-Cambrian (c.650-500 Ma) high-grade metamorphic terranes that constituting Gondwana supercontinent (e.g., Shiraishi et al., 2008). Easternmost part is “Western Rayner Complex” of which granulite-facies and partly UHT metamorphism (Motoyoshi et al., 1994, 1995) and 2400-1000 Ma protolith and 540-520 Ma metamorphic ages were reported (Shiraishi et al., 1997). Neighboring “Rayner Complex” is characterized by >2500-1000 Ma protolith and 980-910 Ma granulite-facies metamorphic ages. Boundary between the Rayner and the Western Rayner Complex has been not clearly defined until when Horie et al. (2016) obtained 934-894 Ma SHIRMP zircon U-Pb ages from Mt. Lira, Condon Hills and Mt. Yuzhnaya regions with minor 590-570 Ma zircons from Mt. Yuzhnaya. Hiroi (unpublished data) also demonstrated contrasting metamorphic P-T evolution among the Mt. Lira, Condon Hills and Mt. Yuzhnaya regions.

JARE-58 (2016-2017) geology team made a short visit and sampling at a small nunatak of west of Mt. Yuzhnaya, a small nunatak of east of Forefinger Point, and Point Widdows in order to assess the relationship between the Rayner and the Western Rayner Complexes. We will report and discuss the update of the characteristic features of the Rayner and the Western Rayner Complexes.

Keywords: Antarctica, Gondwana, Supercontinent, metamorphism, geochronology

©2019. Japan Geoscience Union. All Right Reserved.

Composition of constituent minerals in corona-bearing and -free mafic gneisses from the Lützow-Holm Complex at Skallen, East Antarctica

*Yuki Mori[1], Takeshi Ikeda[2]

1. Department of Earth and Planetary Sciences, Graduate School of Sciences, Kyushu University, 2. Department of Earth and Planetary Sciences, Faculty of Sciences, Kyushu University

Corona is one of the non-equilibrium microstructures and has been employed to infer pressure-temperature path of the metamorphic rocks. The corona around garnet is common in mafic to ultramafic gneisses in the Lützow-Holm Complex (LHC) of East Antarctica (e.g., Hiroi et al., 1991). However, not every garnet in mafic to ultramafic gneisses accompanies the corona. In our ongoing study to reveal the controlling factors of presence and absence of the corona, we compare the composition of garnet and hornblende of the corona-bearing (no. I-223) and -free (no. I-232) mafic gneisses from Skallen.

The metamorphic grade of the complex increases progressively from the upper amphibolite facies to granulite facies toward the southwest, and the LHC is divided into three zones referred to as the amphibolite-facies zone, transitional zone, and granulite-facies zone (Hiroi et al., 1991). Recent studies have revealed that both transitional and granulite-facies zones had undergone high temperatures that exceed 800 ˚C (e.g., Iwamura et al, 2013; Kawakami et al., 2016). Skallen is an exposure located in the granulite-facies zone.

The constituent minerals in the matrix of the studied samples are almost same (garnet, hornblende, plagioclase with minor amounts of clinopyroxene and orthopyroxene), but I-223 further contains biotite. The microstructure and chemical composition of I-223 is as follows. The garnet grain is coarse (15 mm in diameter) and surrounded by a symplectitic corona composed of orthopyroxene and plagioclase. Garnet is clearly divided into two domains of Ca-rich core (Xgrs=0.23) and Ca-poor rim (Xgrs=0.18). X_{Mg} [=Mg/(Mg+Fe)] increases toward rim from 0.22 to 0.27, and that in the outer part of the rim decreases toward the boundary between the garnet and the corona from 0.27 to 0.22. The Ca-poor rim of the garnet includes irregular-shaped nanogranite composed of quartz, biotite, plagioclase, and K-feldspar. Hornblende is brown to brownish-green and polygonal. The X_{Mg} of the hornblende is 0.46-0.50. Matrix plagioclase often shows antiperthite intergrowing An50 plagioclase with Or96 K-feldspar. The coronal plagioclase has higher anorthite content (An80) than that in the matrix (An50). The microstructure and chemical composition of I-232 is as follows. The garnet grain is coarse (10 mm long) and elongated. The garnet and the hornblende define foliation of the rock. The hornblende is brown to pale brown. The composition of garnet gradually changes from core (Alm52Prp31Grs14Sps3) to rim (Alm52Prp28Grs17Sps3). The X_{Mg} in the hornblende varies from 0.60-0.70, and the composition is heterogeneous even in one grain. Most part of plagioclase is An45, and some parts of rim of the plagioclase have higher anorthite content of 70.

The garnet and hornblende in the corona-bearing gneiss have lower X_{Mg} than those in the corona-free gneiss. In addition, calcium content of the garnet and matrix plagioclase in the corona-bearing gneiss is higher than that in the corona-free gneiss. Therefore, we consider that bulk composition is one of the factors controlling the corona formation. The presence of nanogranite in the garnet surrounded by the corona suggests that partial melting and transport of the melt would cause the change of bulk composition in part.

©2019. Japan Geoscience Union. All Right Reserved.

Keywords: corona, garnet, nanogranite, Lützow-Holm Complex, Antarctica

©2019. Japan Geoscience Union. All Right Reserved.

“Pseudo-concordance” of U-Pb system in zircon at Harvey Nunatak, Napier Complex, East Antarctica

*Mami Takehara[1]

1. National Institute of Polar Research

U-Pb zircon dating has played a pivotal role in geochronology due to zircon’s high durability and high closure temperature. In addition, the paired decay scheme of two U isotopes allows us to verify the determined U-Pb zircon age. The Napier Complex in East Antarctica is well known because it preserves both of evidence of ultrahigh-temperature (UHT) metamorphism (e.g., Sheraton et al., 1987; Harley & Hensen 1990) and long Archaean crustal history from 3800 Ma to 2500 Ma (e.g., Harley & Black 1997). Previous researchers also reported the possibilities of the early Archean crust in the Napier Complex (e.g., Compston and Williams, 1982). Some previous researchers pointed out discordant U-Pb data including reverse discordance which was derived from the redistribution of radiogenic Pb isotopes in zircon in the Napier Complex samples (e.g., Kusiak et al., 2013). The some discordant U-Pb data looks concordant but actually reflect the Pb redistribution, namely “pseudo-concordance.” They suggest the redistribution of the radiogenic Pb isotopes in zircons was associated with the UHT metamorphism based on the Pb isotope mapping of the zircons. This report is critical for accurate U-Pb zircon geochronology in the UHT metamorphic region, such as the Napier Complex. Therefore, in this study, the zircons from the rock sample of the Napier Complex were characterized on the basis of the observation and trace-element contents, and the information was utilized for interpretation of the U-Pb data.
Zircons collected from a tonalitic gneiss (170223-2A-09) were first analyzed using sensitive high resolution ion-microprobes (SHRIMP IIe and SHRIMP IIe/AMC) at the National Institute of Polar Research, Japan. The sample was collected at the Harvey Nunatak, which is located close to Mt. Sones. The geochronological data from the Harvey Nunatak had never been reported. The sample was crushed by a high-voltage pulse power fragmentation device (Selfrag Lab) to preserve the external morphology of zircons and prevent contamination (Takehara et al., 2018). After pulverizing, the zircon grains were concentrated using conventional mineral separation techniques, including heavy liquid separation with methylene iodide and magnetic separation.
The zircon grains include fractures and slightly mineral inclusion based on the observation of transmitted light images by an optical microscope. BSE images show that some zircon grains have darker BSE-response domains, which suggests depletion of contents of Zr and Si during hydrothermal alteration of zircon. The zircons show typically high U contents (average is ~2500 ppm), and the U-Pb age from the high U zircons was corrected for the matrix effect derived from the high U contents according to the method by Williams & Hergt (2000) and White & Ireland (2012). It seems that the unaltered zircons show concordant data from about 2450 Ma to 2540 Ma with discordance (Disc.(%) = 1 −(206Pb/238U age)/(207Pb/206Pb age)} ×100 (e.g, Song et al., 1996)) ranges from -5 to +9%. On the other hand, trace element geochemistry of zircons does not support detritus protolith. In this presentation, the information of trace-element contents in zircons was utilized for the interpretation of U-Pb data and “pseudo-concordance.”

©2019. Japan Geoscience Union. All Right Reserved.

Rapid UHT metamorphism and exhumation of the Lützow-Holm Complex in Antarctica

*Yoshikuni Hiroi[1], Tomokazu Hokada[2], Tatsuro Adachi[3], Yasuhito Osanai[3], Yoichi Motoyoshi[2], Kazuyuki Shiraishi[2]

1. Chiba Univ, 2. National Institute of Polar Research, 3. Kyushu University

The Lützow-Holm Complex in Antarctica is a part of Neoproterozoic-Cambrian (c.650-500 Ma) collisional orogen to form Gondwana supercontinent. It is characterized by progressive metamorphism from upper amphibolite facies in the eastern part of the Prince Olav Coast to upper granulite facies in the southern Sôya Coast (e.g., Hiroi et al., 1991). UHT metamorphism is evidenced by such diagnostic mineral assemblages as Opx + Sil + Grt + Rt + Qz and Spr + Qz in Mg-Al-rich pelitic granulites in Rundvågshetta. Intimate intergrowths of Ky + Spr + Grt and Sil + Spr + Grt as well as andalusite-bearing falsite-nanogranite inclusions are included in the same porphyroblastic garnet, which is compositionally zoned, with Mg-rich core, Fe–Mn-rich rim, and core-to-rim oscillation of Ca. Integration of these new data with those previously documented leads to the inference of a rapid change in pressure–temperature conditions during regional UHT metamorphism in this part of the late Neoproterozoic to early Paleozoic ‘large and hot orogen’. Several lines of evidence indicate that partial melting and melt extraction took place even in mafic granulites of fragmented gabbro origin.

Keywords: Antarctica, Gondwana, Supercontinent, UHT metamorphism

©2019. Japan Geoscience Union. All Right Reserved.

Tectonic History of Hiroo Complex and its implication inpaleo-Kuril Arc evolution

*Sreehari Lakshmanan[1], Tsuyoshi Toyoshima[2], Futoshi Nanayama[3]

1. Graduate School of Science and Technology, Niigata University, Niigata, Japan, 2. Department of Geology, Faculty of Science, Niigata Univ. , 3. Geological Survey of Japan, AIST

Melanges records information about deformation history and tectonic events in plate margins and orogens and hence they are important in evolution of accretionary complexes [1]. Mélange facies rocks and brocken formations distributed in Nakanogawa Group of Hidaak Belt in Central Hokkaido is known as Hiroo Complex. We carried out detailed field mapping and structural studies on melange facies rocks distributed around Tachiiwa, Kamitoyoni and Daimaruyama region of Hiroo Complex. Four different deformation processes (D1,D2,D3 and D4) are identified from field to micro-scale observations. D1 event shear zones are wide and considerd as penitrative but D2, D3 and D4 shear zones observed in narrow deformation zones and considerd as less penitrative local events. D1 shearzones are identified as scaly fabric in mudstone and asymmetrically sheared sandstone clast distributed in it. This is similar to 'block in matrix' structure, typical of tectonic melange devoloped in accretionary complexes. D1 foliation trends in N-NNW direction. Tectonic evolution of theses rocks confirmed by pressure solution cleavage, composite planar fabrics (P-Y-R shear), asymmetrical folds and dip-parallel streching lineation. P-Y-R shear relation and other asymmetrical structures in both field and microscale observation shows east-side-up sense of movement. This shear sense suggest that major penetrative deformatoin phase in melange was connected to accretionary complex devolopment in paleo-Kuril-Arc region, where initial subduction was directed in N-S direction and later it rotated clockwise and attained its present position. D2, D3 and D4 events were recognized as dextral strike-slip movement, sinistral-strike-slip to oblique-slip movement and west-side-down movement sense respectively . Mega-micro scale observation of D2 and D3 events show the properties of cataclastic deformation and D4 event is that of fault gouge. Based on this D2, D3 and D4 events are considered as upper crustal or local deformation processes. We consider these are linked to post-melange deformation processes and related to final stages of devolopment of Hidaka Metamorphic Belt (HMB). Recent geochemical studies from Daimaruyama region and geochronological studies from Nakanogawa Group region points that Hiroo Complex was part of initiallly northward subducting Paleo-Kuril Arc region [2]. Through detailed strucural analysis, this study also confirms that Hiroo Complex was devoloped in accretionary complex of paleo- Kuril-Arc by an offscrapping mode of evolution. Later Hiroo Complex became part of Nakanogawa Group through a series of deformation processes asocciated with arc-arc colission between paleo-Kuril Arc and paleo-Japan Arc.
[1]A. Festa et al., 2012. Tectonophysics, 568, 7-24 [2] T.Yamasaki, F. Nanayama, 2018. Lithos. 302, 224-241

Keywords: Hiroo Complex, Paleo Kuri lArc, Mélange tectonics, Accretionary Complex, Nakanogawa Group

©2019. Japan Geoscience Union. All Right Reserved.

Behaviour of C, O, Sr, Nd and Pb isotopes in high-grade metacarbonate rocks

*Madhusoodhan Satish-Kumar[1], Akari Imura[1], Momoko Shirakawa[2], Gen Shimoda[3], Kosuke T. Goto[3], M A Sanjeewa P K Malaviarachchi[4]

1. Department of Geology, Faculty of Science, Niigata University, 2. Graduate School of Science and Technology, Niigata University, 3. Geological Survey of Japan, 4. University of Peradeniya, Sri Lanka

Tectonic environment of metasedimentary sequences deposit in orogenic belts is of importance in understanding the formation and evolution of supercontinents. In particular, chemically deposited carbonate rocks are supposed to hold key information of extinct paleo-oceans, since they are directly precipitated from seawater. In this study, we carried out a comprehensive trace and rare earth element analysis, carbon, oxygen, strontium, neodymium and lead isotope measurements in metacarbonate rocks from the Highland Complex, Sri Lanka. The isotopic systems studied have distinct residence and mixing time in seawater, and are also controlled by the input from surrounding continents. We present here the behaviour of each isotopic system with respect to different processes right from the deposition of carbonate from the seawater through diagenesis and then prograde and retrograde metamorphism. TheProterozoic basement of Sri Lanka is subdivided into four lithotectonic units, namely, the Highland Complex (HC), the Wanni Complex (WC), the Vijayan Complex (VC), and the Kadugannawa Complex (KC), based on Nd isotope model ages. The HC is mainly composed of metasedimentary rocks (granulite facies metaquartzites, metapelitic gneisses and metacarbonate rocks), whereas exposures of the WC and the VC are mainly metaigneous rocks. The metacarbonate rocks in the HC generally occur as layers parallel with other metasedimentary lithological units, and show a NE trend.

We measured oxygen and carbon isotope ratios to understand the effect of diagenetic to metamorphic alterations, which can be recognized in negative isotope shifts. In general, the metacarbonate rocks have positive oxygen isotopic composition comparable with the Proterozoic unmetamorphosed carbonates, suggesting that these rocks were not affected by external fluids during digenesis, dolomitization or metamorphism. However, some of the rock units have been affected by later fluid infiltration as seen in major shifts in oxygen isotopic composition. Negative shifts in both carbon and oxygen isotopes correspond to the metamorphic decarbonation reactions being prominent. Strontium isotope chemostratigraphy was applied for the selected samples with least signatures of alteration. The depositional ages show a younging direction of sedimentation from the Wanni-side to the Vijayan-side. In the case of Nd isotopes, the values correspond to variable mixing of continent derived and oceanic crust derived components during carbonate deposition. This is clearly depicted in the ε Sr vs. ε Nd cross-plots where typical seawater-rock mixing relationship in metacarbonate rocks associated with continents and oceanic crusts can be deduced.Pb isotopic composition of the metacarbonate rocks in Sri Lanka indicated significant differences within the HC; the Vijayan side is more radiogenic than that of Wanni side. This might be due to the difference of initial composition, as well as the relationship to depositional basin and seawater composition. We also observed very low U/Pb ratios, which are considered to have occurred due to the U-loss during metamorphic recrystallization.Thus, the Sr-Nd-Pb isotopic composition in metacarbonate rocks suggests interaction between the oceanic crust and carbonate rocks on the Wanni side whereas on the Vijayan side, carbonate sedimentation was accompanied by interaction with cratonic continental crust.Thus, by applying a multi-element isotope geochemical approach on metacarbonate rocks collected from continental collisional zones, and by comparing the data with basement rocks from various neighbouring Gondwana continents, regional affinities could be established.

©2019. Japan Geoscience Union. All Right Reserved.

Sr, Nd and Pb isotopic compositions provide important information about the depositional settings of sedimentary rocks and provide key information about the surrounding terrains of oceanic and continental affinities during the time of deposition. This can lead to a better understanding of paleo-tectonic settings of crustal fragments that assemble to form supercontinents.

Keywords: metacarbonates, Sr-Nd-Pb isotopes, Sri Lanka

©2019. Japan Geoscience Union. All Right Reserved.

[E] Poster | S (Solid Earth Sciences)：S-CG Complex & General

Tue. May 28, 2019 3:30 PM - 5:00 PM JST | Tue. May 28, 2019 6:30 AM - 8:00 AM UTC | Poster Hall International Exhibition Hall8, Makuhari Messe_19

[S-CG49] Hard-Rock Drilling Science: From Continental to Deep Sea Drilling, and Oman Project

convener:Katsuyoshi Michibayashi(Department of Earth and Planetary Sciences, Nagoya University), Eiichi TAKAZAWA(Department of Geology, Faculty of Science, Niigata University), Norikatsu Akizawa(Department of Ocean Floor Geoscience, Atmosphere and Ocean Research Institute, The University of Tokyo)

The Oman Drilling Project (OmDP) has completed to drill numerous hard-rock cores within ancient oceanic lithosphere and the underlying subduction zone of the Samail ophiolite in Oman, with support from ICDP, IODP, Japan Society for the Promotion of Science, the Sloan Foundation's Deep Carbon Observatory, US, and European research agencies. Moreover, a number of IODP expeditions have focused on hard-rock drilling over the last several years including Expedition 352 in 2014, which drilled the volcanic sequence associated with subduction initiation in the Bonin fore-arc, Expedition 357, which drilled the Lost City hydrothermal field, Expedition 360, which drilled the lithosphere associated with ultraslow-spreading at the Southwest Indian Ridge in 2016, and Expedition 366, which drilled the serpentinite seamounts in the Mariana fore-arc. In this session, we invite presentations on the scientific results of hard-rock drilling at these and other sites. We also invite related presentations on oceanic lithosphere, island arc formation, and any other significant issue that could be addressed by future hard-rock drilling. This includes marine studies of oceanic lithosphere and on-land geological investigations of ophiolites, accreted arcs, and subduction complexes. The session is intended to be interdisciplinary, including the fields of geophysics, geochemistry, petrology, engineering, and biology.

[SCG49-P01] Permeability profile in the Oman Drilling Project inferred from resistivity measurements

*Ikuo Katayama[1], Keishi Okazaki[2], Natsue Abe[2], Ole Ivar Ulven[3], Gilbert Hong[4], Wenlu Zhu[5], Benoit Cordonnier[3], Kohei Hatakeyama[1], Yuya Akamatsu[1], Katsuyoshi Michibayashi[6], Marguerite Godard[7], Peter Kelemen[8], Science Party The Oman Drilling Project Phase 2 (1.Hiroshima University, 2.JAMSTEC, 3.University of Oslo, 4.Seoul National University, 5.University of Maryland, 6.Nagoya University, 7.Universitè Montpellier, 8.Columbia University)

[SCG49-P02] Relationship between alteration intensity and elastic wave velocity of gabbroic rocks from ICDP Hole CM1A, Oman Drilling Project Phase II

*Kosuke Kimura[1], Ikuo Katayama[1], Kohei Hatakeyama[1], Yuya Akamatsu[1], Natsue Abe[2], Keishi Okazaki[2], The Oman Drilling Project Phase II Science Party (1.Hiroshima University, 2.JAMSTEC)

[SCG49-P03] Physical property of the fossilized crust-mantle transition zone from ICDP Oman Drilling Project Hole CM1A and CM2B measured onboard D/V Chikyu

*Keishi Okazaki[1], Natsue Abe[1], Kohei Hatakeyama[2], Yuya Akamatsu[2], Ikuo Katayama[2], Eiichi TAKAZAWA[3], Damon A H Teagle[4], Peter B Kelemen[5], Jude Coggon[4], The Oman Drilling Project Phase 2 Science Party (1.Japan Agency for Marine-Earth Science and Technology, 2.Hiroshima University, 3.Niigata University, 4.University of Southampton, 5.Columbia University)

[SCG49-P04] Microstructures of lower crust gabbros from the Oman Ophiolite: Analyses of the drilled cores of the Oman Drilling Project

*Koki Iida[1], Takahiro Fudai[1], Susumu Umino[1], Yuki Kusano[2] (1.Kanazawa University, 2.Geological Survey of Japan)

[SCG49-P05] Olivine fabric and mineral compositions in the Maqsad area of the Samail massif, the southern Oman ophiolite

*Kaho Takahashi[1], Eiichi TAKAZAWA[2,3], Katsuyoshi Michibayashi[4], Kakihata Yuki[4], Ryoko Senda[5] (1.Graduate School of Science and Technology, Niigata University, 2.Department of Geology, Faculty of

Science, Niigata University, 3.JAMSTEC, 4.Nagoya University, 5.Kyushu University)

[SCG49-P06] The evolution of melt inclusions in podiform chromitite in Oman

*Yuan YAO[1], Eiichi TAKAZAWA[2,3], Oman Drilling Project Phase 2 Science Party (1.Graduate School of Sciences& Technology, Niigata University, Japan, 2.Department of Geology, Faculty of Science, Niigata University, Japan, 3.Research and Development Center for Ocean Drilling Science, JAMSTEC, Japan)

[SCG49-P07] Melt/fluid - rock reaction inferred from the Wadi Tayin mantle section in the southern Oman ophiolite

*Keisuke ISHII[1], Eiichi TAKAZAWA[2], Akihiro kuriyama[2], Kyouka Someya[2], Yoshihiko Tamura[3] (1.Graduate School of Science and Technology, Niigata University, 2.Department of Geology, Faculty of Science, Niigata University , 3.R&D Center for Ocean Drilling Science, Japan Agency for Marine-Earth Science and Technology)

[SCG49-P08] Numerical simulations for reaction-induced fracture formation of layered gabbro during hydration process

*Kazuki Yoshida[1], Hiroyuki Shimizu[2], Noriyoshi Tsuchiya[1], Atsushi Okamoto[1], Phase 2 Science Party Oman Drilling Project[3] (1.Tohoku university, 2.Geotechnical Analysis Group, Advanced Analysis Department, Civil Engineering Design Division, Kajima Corporation, 3.Oman Drilling Project Phase 2 Science Party)

[SCG49-P09] X-ray CT images of oceanic lithologies obtained on Oman Drilling Project drillcores during ChikyuOman 2017 and 2018

*Katsuyoshi Michibayashi[1], Peter B Kelemen[2], Margurette Godard[3], Eiichi TAKAZAWA[4], Damon A H Teagle[5], The Oman Drilling Project Science Party[6] (1.Department of Earth and Planetary Sciences, Nagoya University, 2.Columbia University, 3.Université Montpellier, 4.Niigata University, 5.Southampton University, 6.ICDP)

[SCG49-P10] Re-examination of the crystallization process of clinopyroxene oikocrysts in layered gabbros at Hess Deep Rift, EPR

*Akane Yasui[1], Takashi Hoshide[1] (1.Graduate School of International Resource Sciences, Akita University)

[SCG49-P11] Structural petrology of peridotites from the Kalaymyo ophiolite

*Kouhei Asano[1,2], Katsuyoshi Michibayashi[1], Jung-Woo Park[3] (1.Graduate School of Environmental Studies, Nagoya University, 2.Shizuoka University, 3.Seoul National University)

[SCG49-P12] Reevaluation of the origin of mafic layers in the Upper Zone of the Horoman Peridotite

*Yumeto KOGURE[1], Eiichi TAKAZAWA[1] (1.Department of Geology, Faculty of Science, Niigata University)

[SCG49-P13] A structural and petrological study of "Shibukawa ultramafic body" in the Sanbagawa belt, western Shizuoka, Japan

*Hikaru Shioya[1,2], Katsuyoshi Michibayashi[1], Ken-ichi Hirauchi[2] (1.Graduate School of Environmental Studies, Nagoya University, 2.Institute of Geosciences, Shizuoka University)

Permeability profile in the Oman Drilling Project inferred from resistivity measurements

*Ikuo Katayama[1], Keishi Okazaki[2], Natsue Abe[2], Ole Ivar Ulven[3], Gilbert Hong[4], Wenlu Zhu[5], Benoit Cordonnier[3], Kohei Hatakeyama[1], Yuya Akamatsu[1], Katsuyoshi Michibayashi[6], Marguerite Godard[7], Peter Kelemen[8], Science Party The Oman Drilling Project Phase 2

1. Hiroshima University, 2. JAMSTEC, 3. University of Oslo, 4. Seoul National University, 5. University of Maryland, 6. Nagoya University, 7. Universitè Montpellier, 8. Columbia University

Permeability is a key property that controls heat and chemical exchange in the oceanic lithosphere as well as microbial activity in the sub-seafloor. Although direct measurements of permeability were not made on board D/V Chikyu during analysis of cores from the Oman Drilling Project, we estimated permeability profiles based on onboard measurements of electrical resistivity. For each core sample, we measure its resistivity at nominally dry conditions to obtain the dry resistivity. We then saturate the sample with NaCl solution (3.5g/L) and repeat the resistivity measurements at brine-saturated conditions to obtain the wet resistivity. Owing to the conductive brine in the pore space, the wet resistivity is systematically lower than dry resistivity. Because the difference between dry and wet resistivity is predominantly controlled by the movement of dissolved ions in the brine that occupied the pore space, we can use the resistivity data to infer the volume fraction of pores that contribute to electrical transport (termed “transport porosity”). We apply the Hashin-Shtrikman upper bound to estimate transport porosity. The estimated transport porosity shows a positive correlation with bulk porosity measured on board (MAD analysis), but is approximately one order of magnitude lower. Using an empirical cubic law between transport porosity and permeability, we produce estimated permeability profiles for the crust-mantle transition zone and the serpentinized mantle sections in the Hole CM1A, BA1B, BA3A and BA4A. The results indicate, (1) the gabbro sequence exhibits a markedly lower permeability than the underlying mantle sequence, (2) serpentinized dunites have higher permeability compared to serpentinized harzburgites, and (3) the general variation of discrete sample permeability is correlated with fault zone and intervals with abundant fractures. These permeability structures are most likely modified by alteration and juxtapositions, and do not represent the in-situ profile of the oceanic lithosphere; but this technique can be applicable to infer on-board permeability in future hard rock drilling.

©2019. Japan Geoscience Union. All Right Reserved.

Relationship between alteration intensity and elastic wave velocity of gabbroic rocks from ICDP Hole CM1A, Oman Drilling Project Phase II

*Kosuke Kimura[1], Ikuo Katayama[1], Kohei Hatakeyama[1], Yuya Akamatsu[1], Natsue Abe[2], Keishi Okazaki[2], The Oman Drilling Project Phase II Science Party

1. Hiroshima University, 2. JAMSTEC

The mafic to ultramafic rocks suffer metamorphism and metasomatism by the seafloor hydrothermal activities. These alterations can influence the elastic wave velocity due to the change of mineral assemblages during the ocean floor metamorphism. However, most previous studies have measured the elastic wave velocity of relatively unaltered samples. In this study, we measured elastic wave velocity of the altered gabbro from the Semail ophiolite collected from the Oman Drilling Project Phase II in order to estimate the effect of ocean floor metamorphism on the elastic wave velocity.

Gabbro samples were collected from CM1A site that is reported to be a layered gabbro sequence. Total seven samples those have different alteration intensity were measured. We use intra-vessel deformation and fluid flow apparatus at Hiroshima University to measure elastic wave velocity under confining pressure up to 200 MPa. Elastic wave velocity was measured by the pulse transmission method, with the amplitude and the frequency of a trigger wave of 5 V and 2 MHz, respectively. After measurements under dry condition, measurements under wet conditions injecting pore water were performed (P_P = 10 MPa). Alteration intensity is recognized by the relative abundances of the secondary minerals.

On the basis of the petrography, alteration group could be divided into four types. First type is almost fresh, olivine altered to serpentine and chlorite partially with less green minerals present. Second type has saussuritized plagioclase dominantly and also some sample shows alteration of clinopyroxene to amphibole. In the third type amphibolitization of clinopyroxene is dominant, and also saussuritization of plagioclase occur. Fourth type is the most altered sample showing alteration halo along the veins. Almost of the minerals are changed to prehnite except a few relict clinopyroxene. This type has higher porosity than other types.

Sample density ranges from 2.77-3.08 g/cm^3, and porosity ranges from 0.02-0.22% except ca. 1% from halo alteration sample. Data from these samples show a trend that elastic wave velocities (V_P and V_S) increase with increasing the confining pressure from 20 to 200 MPa. V_P increases from 5.68-6.80 to 6.16-6.91 km/s, V_S slightly increases from 3.65-3.97 to 3.69-3.99 km/s and V_P/V_S is almost constant ranging between 1.56-1.86 to 1.64-1.88 under dry condition, and on the other hand, V_P increases from 6.08-6.82 to 6.31-6.93 km/s, V_S slightly increases from 3.64-3.98 to 3.69-4.00 km/s and V_P/V_S is almost constant 1.67-1.86 to 1.68-1.87 under fluid-saturated condition, respectively. This result is mostly consistent with the layered gabbro occur in a normal oceanic crust (e.g. White et al., 1992; Shinohara et al., 2008).

At 200 MPa and under dry condition, V_P moderately decreases with increase in alteration intensity. About 0.75 km/s decreases in response to the increase in alteration intensity from 10 to 80 %. Comparing dV_P (difference in calculated and measured values) from the back-calculated original mineral assemblages of gabbro and peridotite reveled that the decrease in dV_P for the former is less than the latter. Moreover, both the curves of V_P and impedance change cross-over each other for gabbro and peridotite after nearly 50% of alteration.

©2019. Japan Geoscience Union. All Right Reserved.

From the above results, we suggest that if both gabbro and peridotite suffer more than 50% alteration, reversal of seismic velocity and impedance occurs, which effectively would affect the determination of geophysical Moho.

Reference: White et al. (1992) J. Geophys. Res. 97, 19,683-19,715. Shinohara et al. (2008) Phys. Earth Plan. Inter., 170, 95-106. Christensen (2004) Inter. Geol. Rev., 46, 795-816.

Keywords: Oman ophiolite, Gabbroic rocks, Elastic Wave Velocity, alteration

©2019. Japan Geoscience Union. All Right Reserved.

Physical property of the fossilized crust-mantle transition zone from ICDP Oman Drilling Project Hole CM1A and CM2B measured onboard D/V Chikyu

*Keishi Okazaki[1], Natsue Abe[1], Kohei Hatakeyama[2], Yuya Akamatsu[2], Ikuo Katayama[2], Eiichi TAKAZAWA[3], Damon A H Teagle[4], Peter B Kelemen[5], Jude Coggon[4], The Oman Drilling Project Phase 2 Science Party

1. Japan Agency for Marine-Earth Science and Technology, 2. Hiroshima University, 3. Niigata University, 4. University of Southampton, 5. Columbia University

To understand physical properties of the oceanic crust and the mantle is fundamentally important to reveal the dynamics of plate tectonics, and the global circulations of H_2O and CO_2 fluids. We report results on physical property measurements of core samples from Oman Drilling Project (OmanDP) Holes CM1A and CM2B, which drilled from the lower igneous crust into the upper mantle in the Samail Ophiolite, Sultanate of Oman.

X-ray CT, bulk/grain density, porosity, magnetic susceptibility, P-wave velocity, electrical resistivity and thermal conductivity were measured onboard D/V Chikyu using whole-round cores and discrete samples for core sections from CM1A and CM2B.

The paleo-Moho in CM1A may not preserve the original structure due to minor faulting, possibly during obduction. The gabbro-dunite transition (paleo-Moho) in Hole CM1A is characterized by a sharp change in physical property data. For example, P-wave velocity decreases from ~6.7 km/s in the layered gabbro sequence to ~4.9 km/s in the MTZ. Low P-wave velocity and density (~2.6 g/cm^3) in serpentinized dunites reflect the fact that olivine in the dunites is almost completely serpentinized. Serpentinization could have occurred during hydrothermal alteration near the spreading ridge axis, during subduction of 100’s of km of oceanic crust and sediment beneath the ophiolite, during obduction onto the Arabian continental margin, and/or during present-day weathering. In contrast to the paleo-Moho, the boundary between the Crust-Mantle Transition (CMT) sequences (i.e., dunites and dunites with gabbro lenses) and the underlying, residual mantle harzburgites is somewhat gradual. P-wave velocity gradually increases from ~4.9 km/s for dunite in the CMT to ~5.5 km/s for harzburgite in the mantle sequence. The thickness of the CMT is 50–70 m in Holes CM1A and CM2B. We also report on correlations between physical properties, especially electrical conductivity and magnetic susceptibility, and the fault intensity and alteration intensity from the core descriptions.

Keywords: ophiolite, mantle, oceanic crust, moho

©2019. Japan Geoscience Union. All Right Reserved.

Microstructures of lower crust gabbros from the Oman Ophiolite: Analyses of the drilled cores of the Oman Drilling Project

*Koki Iida[1], Takahiro Fudai[1], Susumu Umino[1], Yuki Kusano[2]

1. Kanazawa University, 2. Geological Survey of Japan

Oman Drilling Project in 2016 to 2017 recovered 400 m long cores of layered gabbros at Site GT1 in the Wadi Tayin Massif of the Oman Ophiolilte. The purpose of this research is to describe microstructures of the layered gabbro core samples and to discuss the conditions of magmatic and hypersolidus deformation that operated in the lower crust beneath the Oman paleoridge.

Core samples were cut into slabs parallel to foliation and slabs normal to foliation and parallel to lineation, which were made into thin sections for microscopic observations. Structural fabrics and the relationships between crystal shapes and alliginment were described to identify magmatic and hypersolidus deformation structures.

Cored samples are predominantly olivine gabbros consisting of anhedral olivine, anhedral to subhedral clinopyroxene and subhedral to euhedral plagioclase. Grain size ranges from 0.5 mm to a few millimeters irrespective of mineral species.

The structures shown by the gabbros are classified into three regimes by temperature or the amount of melt present: Regime I, magmatic conditions without or minimal plastic deformation; regime Ⅱ, plastic deformation assisted by interstitial melt (Dunn, 2000); regime Ⅲ, near solidus deformation. Regime Ⅱ is identified by ameboid grain boundaries with no intracrystalline deformation and equigranular textures, resulted from decreasing internal strain energy by at high temperatures. The presence of melt is evidenced by the clear euhedral plagioclase rims with resorbed turbid cores as discussed below.

Regime I. Magmatic structures are identified as modal layering due to changes in mineral mode, no preferred orientation or shape-preferred orientation of clinopyroxene and plagioclase, poikilitic texture of olivine enclosing plagioclase laths and ophitic texture of clinopyroxene including plagioclase laths.

Regime II. The hypersolidus deformation structures overprint igneous structures: ameboid olivine with or without strain in the crystal, elongated olivine, and lenticular aggregates of olivine grains with an asymmetric quarter structure. Single clinopyroxene crystals show an asymmetric quarter structure like olivine aggregates. Ophitic clinopyroxenes consist of subgrains with slightly different orientations <10˚. Plagioclase shows deformation twin and undulose extinction. Equigranular fine-grained plagioclase with grain boundaries intersecting at 120˚ are common. Large plagioclases have a resorbed core with a wavy outline and are surrounded by euhedral rim.

Regime III. Subsolidus recrystallization includes buldging and grain boundary migration resulted in ameoboid grain boundaries of clinopyroxene. Undulose extinction and kinked twinning of plagioclase are observed.

It is well known that mid-ocean ridge basalt magma commonly crystallizes in the order of olivine, plagioclase and clinopyroxene, which is also true for the gabbros of the Oman Ophiolite (Adachi and Miyashita, 2003). Nevertheless, only plagioclase shows euhedral to subhedral shapes in the observed

©2019. Japan Geoscience Union. All Right Reserved.

layered gabbro core samples. Deformed olivine aggregates and clinopyroxene with quarter structures are embedded in plagioclase with equilibrium granoblastic textures and large euhedral plagioclases with resorbed turbid cores. Considering these textures combined with the mechanical strength of the three constituent minerals, these gabbros suffered deformation under the presence of melt, which assisted complete recovery of strain through recrystallization of fine-grained plagioclase and overgrowth of euhedral rims around magmatic plagioclase cores. Poikilitic olivine occurs through the hole, whereas ophitic Cpx occurs at 73 m and 220 m in depth. Most deformation structures of regime II are present irrespective to depth. The asymmetric structures of olivine and clinopyroxene were used to determine the relative sense of shear. Both dextral and sinistral sense of shear are observed within the same samples.

Keywords: Oman ophiolite, Oman Drilling Project , Layered gabbro , Foliated gabbro , Microstructures , Lower crust

©2019. Japan Geoscience Union. All Right Reserved.

Olivine fabric and mineral compositions in the Maqsad area of the Samail massif, the southern Oman ophiolite

*Kaho Takahashi[1], Eiichi TAKAZAWA[2,3], Katsuyoshi Michibayashi[4], Kakihata Yuki[4], Ryoko Senda[5]

1. Graduate School of Science and Technology, Niigata University, 2. Department of Geology, Faculty of Science, Niigata University, 3. JAMSTEC, 4. Nagoya University, 5. Kyushu University

In this study, we conducted structural and chemical analysis of oriented samples of 17 harzburgites and 4 dunites collected from the Maqsad area of Samail massif in the southern Oman ophiolite. We investigated the degree of partial melting and the mantle-melt reaction with relation to mantle diapir structure.

The crystallographic preferred orientation (CPO) of olivine grains were measured in highly polished XZ thin sections using a scanning electron microscope equipped with an electron-back scatter diffraction system at Shizuoka University. After plotting the results in the Vp Flinn plot expanded for olivine fabric types [1,2], the fabric type of peridotites in this study are summarized as follows. The distribution of A type is limited in the southeastern part where the diapir structure has been identified [3], whereas D type is dominant in the peripheral part of the diapir. Minor amounts of AG type and E type are also observed in the peripheral part. From these, the olivine in the southeastern part (diapir area) of this study area is likely to have been deformed under high temperature whereas the peripheral part was deformed at slightly lower temperature. The CPOs of olivine in both areas do not show any influence from the presence of H2O except for only one sample with E type CPO. Moreover, strong alignment of [100] to the vertical orientation was observed in the southeastern part (diapir area) of this study area. Since vertical mantle flow has been estimated in this diapir area, our results are consistent with the previous study [3,4].

The Cr# (=Cr/[Cr+Al] atomic ratio) of spinel in the harzburgites and dunites are as high as 0.55-0.58 in the central part of the southeastern part (diapir area) and along the paleo-ridge axis running in the NW - SE direction [3,4]. On the other hand, the Cr# of spinel in the peripheral part is 0.41-0.55 indicating slightly less depleted than in the central part. In addition, the REE abundance of clinopyroxenes in the central part of the diapir area is lower than in the peripheral part being consistent with the distribution of spinel Cr#.

We consider that the upwelling rate in the southeastern part (diapir area) may have been greater than the peripheral part possibly due to higher temperature in the focused vertical mantle flow. This model is consistent with the distribution of the Cr# of spinel: the degree of melting was greater in the diapir area where Cr# of spinel are higher than the peripheral part. The strongly focused pipe-like model for axis location [3,5] is well fitted by our observations in this study.

[1] Karato et al., 2008, Ann. Rev. Earth Planet. Sci., 36, 59-95. [2] Michibayashi, 2015, J. Geography, 124, 397-409. [3] Jousselin et al., 1998, JGR, 103, 18153-18170. [4] Nicolas et al., 2000, Marine Geophys. Res., 21, 147-179. [5] Nicolas and Boudier, 1995, JGR, 100, 6179-6197.

Keywords: Oman ophiolite, crystalographic preferred orientation, olivine, fabric, peridotite, mantle flow

©2019. Japan Geoscience Union. All Right Reserved.

The evolution of melt inclusions in podiform chromitite in Oman

*Yuan YAO[1], Eiichi TAKAZAWA[2,3], Oman Drilling Project Phase 2 Science Party

1. Graduate School of Sciences& Technology, Niigata University, Japan, 2. Department of Geology, Faculty of Science, Niigata University, Japan, 3. Research and Development Center for Ocean Drilling Science, JAMSTEC, Japan

Melt inclusions are tiny inclusions which trapped in the host magmatic minerals. After trapping, the host mineral can be considered as a closed and isolated system (Roedder, 1984). Thus, melt inclusions behave as time capsules, which record the liquid line of descent of magmatic systems (Frezzotti, 2001). Therefore, melt inclusions can provide important information of the primary melts (Kent, 2008).

We studied the melt inclusions in chromite from a chromitite deposit mine in the north of Maqsad and the core sample from the Oman drilling project phase 2. The silicate inclusions range in diameter from 5 μm to 200 μm, contain pargasite, tremolite, aspidolite, high Cr# (=Cr/[Cr+Al] atomic ratio) chromite, diopside, enstatite, forsterite, grossular, albite, titanite, pentlandite, apatite, chlorite, wollastonite and serpentine. We found the high Cr# chromite occurs as lining of the inclusion, moreover the daughter minerals precipitated in the high Cr# chromite lining. Those phenomenon can be explained by the crystallization of chromite on the wall of inclusion. In addition, this is the first report about the necking down of melt inclusion in chromitite. The necking down of inclusions is an originally large, liquid-filled inclusion divided into smaller inclusions. If the necking down happens after the phase change of inclusion, the compositions of smaller inclusions probably are inhomogeneity. Last year, we conducted the high temperature homogenized experiments, the result showed that the homogenized quenching glass are heterogeneous. We consider the inhomogeneity of inclusions perhaps caused by the necking down. Based above all, we suggest the composition of homogenized inclusion can not represent the parental melt.

To summarize, we suggest before analysis and experiment of inclusions in chromite, the origin and the evolution of inclusions should be carefully studied.

Reference

Frezzotti, M. (2001). "Silicate-melt inclusions in magmatic rocks: applications to petrology." Lithos **55** (1-4): 273-299.
Kent, A. J. R. (2008). "Melt Inclusions in Basaltic and Related Volcanic Rocks." Reviews in Mineralogy and Geochemistry **69** (1): 273-331.
Roedder, E. (1984). Fluid inclusions, Walter de Gruyter GmbH & Co KG.

Keywords: melt inclusion, Oman, chromitite

©2019. Japan Geoscience Union. All Right Reserved.

Melt/fluid - rock reaction inferred from the Wadi Tayin mantle section in the southern Oman ophiolite

*Keisuke ISHII[1], Eiichi TAKAZAWA[2], Akihiro kuriyama[2], Kyouka Someya[2], Yoshihiko Tamura[3]

1. Graduate School of Science and Technology, Niigata University, 2. Department of Geology, Faculty of Science, Niigata University , 3. R&D Center for Ocean Drilling Science, Japan Agency for Marine-Earth Science and Technology

We report the petrology and the mineral compositions of peridotites from the Wadi Tayin massif in the southern Oman ophiolite [1-3] to investigate the influence of arc related magmatism during oceanic thrusting of the ophiolite. Harzburgites, dunites and a small number of lherzolite were systematically corrected along wadis to cover the mantle section from the boundary between lower crust and uppermost mantle namely “Moho” to the basal thrust. Spinel Cr# [=Cr/(Cr+Al) atomic ratio] of harzburgite varies from 0.22 to 0.58 similar to the range in abyssal peridotites [4]. Moreover, it gradually increases from the basal part to the Moho indicating the compositional variation expected for the residual mantle column formed at a mid ocean ridge. On the other hand, the spinel Cr# of dunite often exceeds 0.6 in the NW-SE striking shear zone in the middle part of the study area. The chondrite-normalized rare earth element (REE) patterns of clinopyroxenes in peridotites from the shear zone show a linear pattern that monotonously decreases from heavy REE to light REE (LREE). Calculated melt compositions in equilibrium with these clinopyroxenes are equivalent with the V2 (Type2) lava reported in the northern Oman ophiolite [5-6].

The plots in Cr# of spinel versus Ce/Yb ratio of clinopyroxenes show a linear trend with a positive correlation. It indicates that the LREE enrichment of clinopyroxene is associated with an increase in the degree of melting. Clinopyroxenes in the dunite from the shear zone are most significantly enriched in LREE to middle REE and have REE abundances being in equilibrium with the V2 lava. We consider that harzburgites were suffered from a flux melting by infiltration of H2O-rich fluid producing V2 lava. Comparing to the results from the northern massifs the linear trend in the diagram of Cr# of spinel versus Ce/Yb ratio of clinopyroxenes in the southern massif is obviously shifted toward lower in Cr#. It suggests that the infiltration of H2O-rich fluid may have started at early stage of melting in the Wadi Tayin massif relative to the northern massifs.

[1] Kelemen et al., 1995, Nature, 375, 747-753, [2] Godard al., 2000, EPSL, 180, 133-148, [3] HanghØj et al., 2010, J. Petrol., 51, 201-227, [4] Dick and Bullen, 1984, CMP, 86, 54-76, [5] Godard et al., 2003, G-cubed, 4, 8609, [6] Kusano et al., 2016, Chem. Geol., 449, 206-225.

Keywords: Oman ophiolite, Mantle section, Peridotite, Melt/rock reaction

©2019. Japan Geoscience Union. All Right Reserved.

Numerical simulations for reaction-induced fracture formation of layered gabbro during hydration process

*Kazuki Yoshida[1], Hiroyuki Shimizu[2], Noriyoshi Tsuchiya[1], Atsushi Okamoto[1], Phase 2 Science Party Oman Drilling Project[3]

1. Tohoku university, 2. Geotechnical Analysis Group, Advanced Analysis Department, Civil Engineering Design Division, Kajima Corporation, 3. Oman Drilling Project Phase 2 Science Party

Serpentinization of oceanic lithosphere is important for various geological processes, including magmatism and earthquake at subduction zone, and generation of hydrogen and hydrocarbon at seafloor. For understanding the extent of the water infiltration into mantle within the oceanic lithosphere, permeability of the lower crust is an important factor, since gabbro has low permeability at high confining pressure (Katayama et al., 2012). In natural olivine-bearing gabbro, serpentinization of olivine grains produced radial fractures within the plagioclase matrix, which can potentially enhance the permeability (Jamtveit et al., 2008). Based on the numerical simulations using discrete element method (DEM), Jamtveit et al. (2008) shows that fracture network is produced by the volume expansion of olivine grains during hydration. However, their model dos not treat the advective fluid flow explicitly, it is not clear how permeability evolves during such processes. In this study, inspired by the natural textures of olivine gabbro taken from CM1A-7A (Wazi Zeeb, Oman Drilling Project), we conducted the DEM simulation for understanding the feedback of the fluid flow –olivine hydration –fracturing to the layered gabbro, which consists of olivine-rich layer and olivine-poor layer alternately. In particular, we focus on the contrasting fracture patterns between olivine and plagioclase, the evolution and anisotropy of permeability produced by the reaction-induced fracturing within the layered gabbro.

We conducted the two-dimensional DEM model, and the details of the model follows Okamoto and Shimizu (2015) and Shimizu and Okamoto (2016). We consider a simple volume increasing hydration reaction ($A + H_2O \rightarrow B$; 50% volume increase), and the reaction rate is defined as a linear function of fluid pressure. In the model, advective fluid flow occurs through apertures between particles, in response to difference of fluid pressure of individual domains. The rock model is consist of reactive part (it can change from olivine to sperneitne) and non-reactive part (e.g., plagioclase and clnopyronene). The reaction rate constant and aperture width of matrix and fracture are defined based on the non-dimensional numbers based on Shimizu and Okamoto (2016).

Firstly, we conducted the simulations for the model in which a single olivine exists in non-reactive matrix. When fluid is supplied through matrix, hydration of olivine starts, which produces the mesh-like textures inside the olivine grain and radial cracks within the unreactive matrix, which is consistent with those observed in the gabbro sample from CM1A. Second, we conducted a case where several olivine grains exist in matrix. In this case, we found the formation of fracture network that connects among the olivine grains, and positive relationship between the reaction rate and permeability. Finally, we tested the case of the layered structure that consists of olivine-rich layer and olivine-absent layer, and that fluid flows in direction perpendicular to the layers. The results of the simulations reveals that the development of vertical fractures in both olivine-rich and non-reactive layers, whereas the horizontal fractures are only developed in the olivine-rich layers. These features of fracture orientation are consistent with the natural observations and indicate that he reaction-induced fracturing could significantly enhance the fluid infiltration through layered gabbro.

©2019. Japan Geoscience Union. All Right Reserved.

References

Katayama I, Terada T, Okazaki K, Tanikawa W (2012) Nat Geosci 5:731–734.

Jamtveit B., Malthe-Sørenssen A., Kostenko O., 2008. Earth Planet. Sci. Lett., 267, pp. 620-627

Okamoto,A.,Shimizu,H., 2015. Earth and Planetary Science Letters 415, 9–18.

Shimizu, H., Okamoto, A., 2016. Contributions to Mineralogy and Petrology, 171, 73.

Keywords: Oman Drilling Project, layered gabbro, permeability, Discrete Element Method, serpentinization

©2019. Japan Geoscience Union. All Right Reserved.

X-ray CT images of oceanic lithologies obtained on Oman Drilling Project drillcores during ChikyuOman 2017 and 2018

*Katsuyoshi Michibayashi[1], Peter B Kelemen[2], Margurette Godard[3], Eiichi TAKAZAWA[4], Damon A H Teagle[5], The Oman Drilling Project Science Party[6]

1. Department of Earth and Planetary Sciences, Nagoya University, 2. Columbia University, 3. Université Montpellier, 4. Niigata University, 5. Southampton University, 6. ICDP

The Oman Drilling Project (OmanDP) has drilled >3,200 meters of the Oman ophiolite during Phases 1 and 2 in Holes GT1A, GT2A, GT3A, BT1B, CM1A, CM2B, BA1B, BA3A and BA4A. All cores have been described on board D/V Chikyu during the summers of 2017 and 2018. X-ray computed tomography (X-ray CT) images were obtained on all cores as a routine part of the IODP measurement protocol onboard D/V Chikyu.

The X-ray CT scanner (Discovery CT 750HD, GE Medical Systems) scans and reconstructs an image of a 1.4 m section in 10 minutes and produces a series of scan images, each 0.625 mm thick. The X-ray source and detector are installed inside of the gantry opposite each other. The excitation voltage and current for X-ray tube are 140 kV and 100 mA, respectively. Core samples are scanned in the gantry with a scanning rate of 20 mm/sec. The distribution of attenuation values mapped to an individual slice comprises the raw data that are used for subsequent image processing. Successive two-dimensional (2D) slices of 512 x 512 pixels yield a representation of attenuation values in three-dimensional (3D) voxels of 512 x 512 by ~1600 in length. Data generated for each core consist of core-axis-normal planes (XY planes) of X-ray attenuation values with dimensions of 512 ×512 pixels in 9 cm ×9 cm cross-section, with a resolution of 0.176 mm/pixel.

As a consequence, we have >3,200 meters length of X-ray CT images from the dyke/gabbro transition zone to the gabbroic sequence to the mantle sequence to the basal thrust of the ophiolite. All X-ray CT images have been processed to match with individual photo images of the archive halves of the cores. The data are useful for assessing sample locations and quality. X-ray CT images can be used for 3D fabric analyses even after core has been cut in half and subsampled for other analyses.

Keywords: OmanDP, XCT, image

©2019. Japan Geoscience Union. All Right Reserved.

Re-examination of the crystallization process of clinopyroxene oikocrysts in layered gabbros at Hess Deep Rift, EPR

*Akane Yasui[1], Takashi Hoshide[1]

1. Graduate School of International Resource Sciences, Akita University

In the Hess Deep Rift, located about 60km east of the East Pacific Rise, the lower crustal gabbros which have been formed at the fast-spreading ridge are exposed. In the IODP Exp. 345, primitive layered gabbros were collected from the lower crust as mainly three drill cores (U1415 I, J, P; Gillis et al., 2014). From the U1415J, unique gabbroic rocks (troctolites) with poikilitic clinopyroxenes (oikocrysts) including many small plagioclase laths have been found (Maeda and Kaise, 2015, Abstracts of the Geological Society of Japan).

Recently, on the origins of clinopyroxene-oikocryst-bearing gabbroic rocks, the different hypotheses have been proposed by Leuthold et al. (2018) and Maeda and Kaise (2015).
Leuthold et al. (2018) proposed that initial olivine gabbros had been partially molten by the intrusion of a primitive melt and then clinopyroxene oikocrysts had crystallized from clinopyroxene-rich basaltic melts formed by the mixing between the partial melt and the primitive magma.
On the other hands, Maeda and Kaise (2015) proposed that clinopyroxenes have first crystallized from a primitive magma and after molten by the encounter with another primitive magma they have continued to grow further and then, the clinopyroxene rim has simultaneously crystallized with matrix olivine and plagioclase. Several hypotheses other than those above (e.g.,Tegner et al., 1995; Nicolas and Boudier., 2011) have been also proposed for the origin of the clinopyroxene oikocrysts in gabbroic rocks. The question is still open to discussion.
Therefore, I re-examine the process of clinopyroxene-oikocryst formation through the textural observation and chemical analysis of the constituent minerals for 8 samples of clinopyroxene-oikocryst-bearing gabbros from 3R, 5R, 7G, 8R and 15G of the U1415J core collected at the IODP Exp. 345.

The matrix part is troctolite consisting mainly of olivine (about 0.5 mm - 2 mm in size, amoeboidal, Fo85~) and plagioclase (about 1 mm in size, An#77-82). Spherical to ellipsoidal clinopyroxene oikocrysts (5-10 mm in size, Mg#85 to 88) is distributed in the matrix troctolite. In addition, clinopyroxene oikocrysts exhibit the following characteristics:

(1) Clinopyroxene oikocrysts basically do not contain any olivine crystals. Rarely, they contain aggregates of plagioclase and olivine.
(2) Orthopyroxene rims (about 100 μm thick, film-like, Mg#85-87) are observed only in matrix olivines (Fo85~) near the rim of the clinopyroxene oikocryst. The olivine crystals rimmed by orthopyroxene are shrinked.
(3) The decreases in Al and Cr contents towards the plagioclase chadacrysts are observed in clinopyroxene oikocrysts.
(4) In the core of the clinopyroxene oikocrysts, we can find parts with Mg# higher than the values which can be in the Fe/Mg equilibrium with olivine in the matrix troctolite.

The facts of (1) and (2) indicate that the assemblage of olivine and plagioclase had already existed when the clinopyroxene oikocrysts crystallized from the melt. In additions, these facts suggest that the melt which formed clinopyroxene oikocryst was in a reaction relationship with olivine. These interpretations

©2019. Japan Geoscience Union. All Right Reserved.

are consistent with the hypothesis of Leuthold et al. (2018).

Keywords: clinopyroxene oikocrysts, Hess Deep, troctolite, Magma mixing, MORB

©2019. Japan Geoscience Union. All Right Reserved.

Structural petrology of peridotites from the Kalaymyo ophiolite

*Kouhei Asano[1,2], Katsuyoshi Michibayashi[1], Jung-Woo Park[3]

1. Graduate School of Environmental Studies, Nagoya University, 2. Shizuoka University, 3. Seoul National University

The Kalaymyo ophiolite is located at Myanmar. The Kalaymyo ophiolite includes large peridotite massifs, where peridotites are commonly well preserved. In recent years, petrologic and geochemical studies have been carried out on the Kalaymyo peridotites. These results suggest that the Kalaymyo peridotites have been undergone melt-rock interactions. In this study, we used fourteen samples from outcrops and drill cores, and carried out analyses of crystal preferred orientations (CPOs) of olivine and of major elements of olivine and spinel. The samples show coarse-grained equigranular textures. The mineral compositions in spinel Cr# and olivine Mg# plot in the field of OSMA (olivine-spinel mantle array) indicate that these samples represent residual upper mantle rocks after partial melting. Spinel grains with Cr# higher than 0.3 have relatively high TiO_2 contents (0.10-0.20 wt.%). Because Ti is incompatible element, high spinel TiO_2 content suggests that these peridotites have experienced melt-rock interaction. There is a positive correlation between J-index and spinel Cr# in the samples. The correlation also has two trends: high and low positive relationships between J-index and spinel Cr#, respectively. Samples experienced melt-rock interaction belong to the low positive trend. It suggests that melt percolation by melt-rock interaction could have an impact on deformation, in particular on CPO development. We propose that melt-rock interaction was synchronous with deformation. It is noted that peridotites experienced melt-rock interaction are intensely located on a narrow range with respect to the elevation, indicating that the occurrence of melt-rock interaction was localized within the Kalaymyo ophiolite.

Keywords: Kalaymyo ophiolite, peridotite, melt-rock interaction, J-index

©2019. Japan Geoscience Union. All Right Reserved.

Reevaluation of the origin of mafic layers in the Upper Zone of the Horoman Peridotite

*Yumeto KOGURE[1], Eiichi TAKAZAWA[1]

1. Department of Geology, Faculty of Science, Niigata University

Horoman peridotite is situated at the southern tip of the Hidaka mountain range, spreads 8 km east-west, 10 km north-south, and has a layer thickness of 3,000 m. We reevaluated the origin of the mafic layer in the Upper Zone of the Horoman Peridotite. We studied Fumo section in the Upper Zone. This section has total thickness of 263 m and consists of plagioclase lherzolite, harzburgite and mafic layer. In the Fumo section, the mafic layer is only interlayered in the plagioclase lherzolite. In the Al2O3, CaO, and Na2O vs. MgO diagrams of whole rock compositions, the mafic layer is plotted on the extension of the linear composition trend indicated by plagioclase lherzolite and harzburgite. There are two types of mafic layer, one plotted in the vicinity of N-MORB and the other plotted in the vicinity of plagioclase lherzolite. The plagioclase lherzolites which have higher Al2O3, CaO, and Na2O and lower MgO contents than the Depleted MORB Mantle (DMM) [1] contain amphiboles whereas the other plagioclase lherzolite which has lower Al2O3, CaO, and Na2O contents and higher MgO content than the DMM do not contain amphibole. Chondrite-normalized whole rock rare earth element (REE) patterns of plagioclase lherzolites are flat from heavy REE to middle REE and show convex upward pattern with depletion in light REE. The mafic layers also show the similar pattern although the abundances of REE is much lower than N-MORB.

From these results, the mafic layers in the Fumo section do not have the composition of primary melt and is considered to be cumulate [2,3]. Also, in the whole rock FeO, TiO2 vs. MgO diagrams, the compositional trends suddenly bend at the most fertile plagioclase lherzolite and becomes depleted in FeO, TiO2 toward the thin mafic layers. On the extension of this bent trends reach to the composition of Cpx and plagioclase. The mafic layer in the Fumo section suggests the possibility that Cpx and plagioclase were crystallized from a melt penetrated into plagioclase lherzolite in a relatively low pressure where the combination of Cpx and plagioclase was stable.

[1] Workman and Hart, 2005, EPSL, 231, 53-72. [2] Shiotani and Niida, 1997, Memoir. Geol. Soc. Japan, 47, 123–137. [3] Takazawa et al., 1999, J. Petrol., 40, 1827-1851.

Keywords: Horoman Peridotite, mantle, mafic layer, orogenic lherzolite, Hidaka Metamorphic Belt

©2019. Japan Geoscience Union. All Right Reserved.

A structural and petrological study of "Shibukawa ultramafic body" in the Sanbagawa belt, western Shizuoka, Japan

*Hikaru Shioya[1,2], Katsuyoshi Michibayashi[1], Ken-ichi Hirauchi[2]

1. Graduate School of Environmental Studies, Nagoya University, 2. Institute of Geosciences, Shizuoka University

We studied an ultramafic body, which is named "Shibukawa ultramafic body" in this study, in the Sanbagawa belt located to the western Shizuoka, focusing on their primary mineral olivine to reveal its petrogenesis. Shibukawa ultramafic body is composed of dunites and wehlites, although the body was heavily weathered due to serpentinization. Yet, most of samples still contain olivine, spinel and a few amounts of clinopyroxene. The olivine crystal preferred orientations (CPOs) of this body were divided into two types: D type and single maxima type. The CPO intensities were relatively high in the north area, whereas those in the south area were relatively low. Considering the grain size distribution of olivine in the samples, the samples in the south area was weakly deformed as they preserve porphyroclastic olivine grains in the fine-grained matrix. In contrast, grain size reduction due to deformation has been completed in the north area. Olivine CPO patterns and major elements composition of both olivine and spinel indicate that the origin of this ultramafic body could be cumulate such as the Mikabu belt and is different from those of Shikoku mountains in the Sanbagawa belt.

Keywords: Sanbagawa belt, Mikabu belt, Cumulate, Ultramafic, Olivine fabrics, Dunite

©2019. Japan Geoscience Union. All Right Reserved.

[E] Poster | S (Solid Earth Sciences)：S-CG Complex & General

Tue. May 28, 2019 5:15 PM - 6:30 PM JST | Tue. May 28, 2019 8:15 AM - 9:30 AM UTC | Poster Hall International Exhibition Hall8, Makuhari Messe_35

[S-CG49] Hard-Rock Drilling Science: From Continental to Deep Sea Drilling, and Oman Project

convener:Katsuyoshi Michibayashi(Department of Earth and Planetary Sciences, Nagoya University), Eiichi TAKAZAWA(Department of Geology, Faculty of Science, Niigata University), Norikatsu Akizawa(Department of Ocean Floor Geoscience, Atmosphere and Ocean Research Institute, The University of Tokyo)

The Oman Drilling Project (OmDP) has completed to drill numerous hard-rock cores within ancient oceanic lithosphere and the underlying subduction zone of the Samail ophiolite in Oman, with support from ICDP, IODP, Japan Society for the Promotion of Science, the Sloan Foundation's Deep Carbon Observatory, US, and European research agencies. Moreover, a number of IODP expeditions have focused on hard-rock drilling over the last several years including Expedition 352 in 2014, which drilled the volcanic sequence associated with subduction initiation in the Bonin fore-arc, Expedition 357, which drilled the Lost City hydrothermal field, Expedition 360, which drilled the lithosphere associated with ultraslow-spreading at the Southwest Indian Ridge in 2016, and Expedition 366, which drilled the serpentinite seamounts in the Mariana fore-arc. In this session, we invite presentations on the scientific results of hard-rock drilling at these and other sites. We also invite related presentations on oceanic lithosphere, island arc formation, and any other significant issue that could be addressed by future hard-rock drilling. This includes marine studies of oceanic lithosphere and on-land geological investigations of ophiolites, accreted arcs, and subduction complexes. The session is intended to be interdisciplinary, including the fields of geophysics, geochemistry, petrology, engineering, and biology.

[SCG49-P01] Permeability profile in the Oman Drilling Project inferred from resistivity measurements

*Ikuo Katayama[1], Keishi Okazaki[2], Natsue Abe[2], Ole Ivar Ulven[3], Gilbert Hong[4], Wenlu Zhu[5], Benoit Cordonnier[3], Kohei Hatakeyama[1], Yuya Akamatsu[1], Katsuyoshi Michibayashi[6], Marguerite Godard[7], Peter Kelemen[8], Science Party The Oman Drilling Project Phase 2 (1.Hiroshima University, 2.JAMSTEC, 3.University of Oslo, 4.Seoul National University, 5.University of Maryland, 6.Nagoya University, 7.Universitè Montpellier, 8.Columbia University)

[SCG49-P02] Relationship between alteration intensity and elastic wave velocity of gabbroic rocks from ICDP Hole CM1A, Oman Drilling Project Phase II

*Kosuke Kimura[1], Ikuo Katayama[1], Kohei Hatakeyama[1], Yuya Akamatsu[1], Natsue Abe[2], Keishi Okazaki[2], The Oman Drilling Project Phase II Science Party (1.Hiroshima University, 2.JAMSTEC)

[SCG49-P03] Physical property of the fossilized crust-mantle transition zone from ICDP Oman Drilling Project Hole CM1A and CM2B measured onboard D/V Chikyu

*Keishi Okazaki[1], Natsue Abe[1], Kohei Hatakeyama[2], Yuya Akamatsu[2], Ikuo Katayama[2], Eiichi TAKAZAWA[3], Damon A H Teagle[4], Peter B Kelemen[5], Jude Coggon[4], The Oman Drilling Project Phase 2 Science Party (1.Japan Agency for Marine-Earth Science and Technology, 2.Hiroshima University, 3.Niigata University, 4.University of Southampton, 5.Columbia University)

[SCG49-P04] Microstructures of lower crust gabbros from the Oman Ophiolite: Analyses of the drilled cores of the Oman Drilling Project

*Koki Iida[1], Takahiro Fudai[1], Susumu Umino[1], Yuki Kusano[2] (1.Kanazawa University, 2.Geological Survey of Japan)

[SCG49-P05] Olivine fabric and mineral compositions in the Maqsad area of the Samail massif, the southern Oman ophiolite

*Kaho Takahashi[1], Eiichi TAKAZAWA[2,3], Katsuyoshi Michibayashi[4], Kakihata Yuki[4], Ryoko Senda[5] (1.Graduate School of Science and Technology, Niigata University, 2.Department of Geology, Faculty of

Science, Niigata University, 3.JAMSTEC, 4.Nagoya University, 5.Kyushu University)

[SCG49-P06] The evolution of melt inclusions in podiform chromitite in Oman

*Yuan YAO[1], Eiichi TAKAZAWA[2,3], Oman Drilling Project Phase 2 Science Party (1.Graduate School of Sciences& Technology, Niigata University, Japan, 2.Department of Geology, Faculty of Science, Niigata University, Japan, 3.Research and Development Center for Ocean Drilling Science, JAMSTEC, Japan)

[SCG49-P07] Melt/fluid - rock reaction inferred from the Wadi Tayin mantle section in the southern Oman ophiolite

*Keisuke ISHII[1], Eiichi TAKAZAWA[2], Akihiro kuriyama[2], Kyouka Someya[2], Yoshihiko Tamura[3] (1.Graduate School of Science and Technology, Niigata University, 2.Department of Geology, Faculty of Science, Niigata University , 3.R&D Center for Ocean Drilling Science, Japan Agency for Marine-Earth Science and Technology)

[SCG49-P08] Numerical simulations for reaction-induced fracture formation of layered gabbro during hydration process

*Kazuki Yoshida[1], Hiroyuki Shimizu[2], Noriyoshi Tsuchiya[1], Atsushi Okamoto[1], Phase 2 Science Party Oman Drilling Project[3] (1.Tohoku university, 2.Geotechnical Analysis Group, Advanced Analysis Department, Civil Engineering Design Division, Kajima Corporation, 3.Oman Drilling Project Phase 2 Science Party)

[SCG49-P09] X-ray CT images of oceanic lithologies obtained on Oman Drilling Project drillcores during ChikyuOman 2017 and 2018

*Katsuyoshi Michibayashi[1], Peter B Kelemen[2], Margurette Godard[3], Eiichi TAKAZAWA[4], Damon A H Teagle[5], The Oman Drilling Project Science Party[6] (1.Department of Earth and Planetary Sciences, Nagoya University, 2.Columbia University, 3.Université Montpellier, 4.Niigata University, 5.Southampton University, 6.ICDP)

[SCG49-P10] Re-examination of the crystallization process of clinopyroxene oikocrysts in layered gabbros at Hess Deep Rift, EPR

*Akane Yasui[1], Takashi Hoshide[1] (1.Graduate School of International Resource Sciences, Akita University)

[SCG49-P11] Structural petrology of peridotites from the Kalaymyo ophiolite

*Kouhei Asano[1,2], Katsuyoshi Michibayashi[1], Jung-Woo Park[3] (1.Graduate School of Environmental Studies, Nagoya University, 2.Shizuoka University, 3.Seoul National University)

[SCG49-P12] Reevaluation of the origin of mafic layers in the Upper Zone of the Horoman Peridotite

*Yumeto KOGURE[1], Eiichi TAKAZAWA[1] (1.Department of Geology, Faculty of Science, Niigata University)

[SCG49-P13] A structural and petrological study of "Shibukawa ultramafic body" in the Sanbagawa belt, western Shizuoka, Japan

*Hikaru Shioya[1,2], Katsuyoshi Michibayashi[1], Ken-ichi Hirauchi[2] (1.Graduate School of Environmental Studies, Nagoya University, 2.Institute of Geosciences, Shizuoka University)

Permeability profile in the Oman Drilling Project inferred from resistivity measurements

*Ikuo Katayama[1], Keishi Okazaki[2], Natsue Abe[2], Ole Ivar Ulven[3], Gilbert Hong[4], Wenlu Zhu[5], Benoit Cordonnier[3], Kohei Hatakeyama[1], Yuya Akamatsu[1], Katsuyoshi Michibayashi[6], Marguerite Godard[7], Peter Kelemen[8], Science Party The Oman Drilling Project Phase 2

1. Hiroshima University, 2. JAMSTEC, 3. University of Oslo, 4. Seoul National University, 5. University of Maryland, 6. Nagoya University, 7. Universitè Montpellier, 8. Columbia University

Permeability is a key property that controls heat and chemical exchange in the oceanic lithosphere as well as microbial activity in the sub-seafloor. Although direct measurements of permeability were not made on board D/V Chikyu during analysis of cores from the Oman Drilling Project, we estimated permeability profiles based on onboard measurements of electrical resistivity. For each core sample, we measure its resistivity at nominally dry conditions to obtain the dry resistivity. We then saturate the sample with NaCl solution (3.5g/L) and repeat the resistivity measurements at brine-saturated conditions to obtain the wet resistivity. Owing to the conductive brine in the pore space, the wet resistivity is systematically lower than dry resistivity. Because the difference between dry and wet resistivity is predominantly controlled by the movement of dissolved ions in the brine that occupied the pore space, we can use the resistivity data to infer the volume fraction of pores that contribute to electrical transport (termed “transport porosity”). We apply the Hashin-Shtrikman upper bound to estimate transport porosity. The estimated transport porosity shows a positive correlation with bulk porosity measured on board (MAD analysis), but is approximately one order of magnitude lower. Using an empirical cubic law between transport porosity and permeability, we produce estimated permeability profiles for the crust-mantle transition zone and the serpentinized mantle sections in the Hole CM1A, BA1B, BA3A and BA4A. The results indicate, (1) the gabbro sequence exhibits a markedly lower permeability than the underlying mantle sequence, (2) serpentinized dunites have higher permeability compared to serpentinized harzburgites, and (3) the general variation of discrete sample permeability is correlated with fault zone and intervals with abundant fractures. These permeability structures are most likely modified by alteration and juxtapositions, and do not represent the in-situ profile of the oceanic lithosphere; but this technique can be applicable to infer on-board permeability in future hard rock drilling.

©2019. Japan Geoscience Union. All Right Reserved.

Relationship between alteration intensity and elastic wave velocity of gabbroic rocks from ICDP Hole CM1A, Oman Drilling Project Phase II

*Kosuke Kimura[1], Ikuo Katayama[1], Kohei Hatakeyama[1], Yuya Akamatsu[1], Natsue Abe[2], Keishi Okazaki[2], The Oman Drilling Project Phase II Science Party

1. Hiroshima University, 2. JAMSTEC

The mafic to ultramafic rocks suffer metamorphism and metasomatism by the seafloor hydrothermal activities. These alterations can influence the elastic wave velocity due to the change of mineral assemblages during the ocean floor metamorphism. However, most previous studies have measured the elastic wave velocity of relatively unaltered samples. In this study, we measured elastic wave velocity of the altered gabbro from the Semail ophiolite collected from the Oman Drilling Project Phase II in order to estimate the effect of ocean floor metamorphism on the elastic wave velocity.

Gabbro samples were collected from CM1A site that is reported to be a layered gabbro sequence. Total seven samples those have different alteration intensity were measured. We use intra-vessel deformation and fluid flow apparatus at Hiroshima University to measure elastic wave velocity under confining pressure up to 200 MPa. Elastic wave velocity was measured by the pulse transmission method, with the amplitude and the frequency of a trigger wave of 5 V and 2 MHz, respectively. After measurements under dry condition, measurements under wet conditions injecting pore water were performed (P_P = 10 MPa). Alteration intensity is recognized by the relative abundances of the secondary minerals.

On the basis of the petrography, alteration group could be divided into four types. First type is almost fresh, olivine altered to serpentine and chlorite partially with less green minerals present. Second type has saussuritized plagioclase dominantly and also some sample shows alteration of clinopyroxene to amphibole. In the third type amphibolitization of clinopyroxene is dominant, and also saussuritization of plagioclase occur. Fourth type is the most altered sample showing alteration halo along the veins. Almost of the minerals are changed to prehnite except a few relict clinopyroxene. This type has higher porosity than other types.

Sample density ranges from 2.77-3.08 g/cm^3, and porosity ranges from 0.02-0.22% except ca. 1% from halo alteration sample. Data from these samples show a trend that elastic wave velocities (V_P and V_S) increase with increasing the confining pressure from 20 to 200 MPa. V_P increases from 5.68-6.80 to 6.16-6.91 km/s, V_S slightly increases from 3.65-3.97 to 3.69-3.99 km/s and V_P/V_S is almost constant ranging between 1.56-1.86 to 1.64-1.88 under dry condition, and on the other hand, V_P increases from 6.08-6.82 to 6.31-6.93 km/s, V_S slightly increases from 3.64-3.98 to 3.69-4.00 km/s and V_P/V_S is almost constant 1.67-1.86 to 1.68-1.87 under fluid-saturated condition, respectively. This result is mostly consistent with the layered gabbro occur in a normal oceanic crust (e.g. White et al., 1992; Shinohara et al., 2008).

At 200 MPa and under dry condition, V_P moderately decreases with increase in alteration intensity. About 0.75 km/s decreases in response to the increase in alteration intensity from 10 to 80 %. Comparing dV_P (difference in calculated and measured values) from the back-calculated original mineral assemblages of gabbro and peridotite reveled that the decrease in dV_P for the former is less than the latter. Moreover, both the curves of V_P and impedance change cross-over each other for gabbro and peridotite after nearly 50% of alteration.

©2019. Japan Geoscience Union. All Right Reserved.

From the above results, we suggest that if both gabbro and peridotite suffer more than 50% alteration, reversal of seismic velocity and impedance occurs, which effectively would affect the determination of geophysical Moho.

Reference: White et al. (1992) J. Geophys. Res. 97, 19,683-19,715. Shinohara et al. (2008) Phys. Earth Plan. Inter., 170, 95-106. Christensen (2004) Inter. Geol. Rev., 46, 795-816.

Keywords: Oman ophiolite, Gabbroic rocks, Elastic Wave Velocity, alteration

©2019. Japan Geoscience Union. All Right Reserved.

Physical property of the fossilized crust-mantle transition zone from ICDP Oman Drilling Project Hole CM1A and CM2B measured onboard D/V Chikyu

*Keishi Okazaki[1], Natsue Abe[1], Kohei Hatakeyama[2], Yuya Akamatsu[2], Ikuo Katayama[2], Eiichi TAKAZAWA[3], Damon A H Teagle[4], Peter B Kelemen[5], Jude Coggon[4], The Oman Drilling Project Phase 2 Science Party

1. Japan Agency for Marine-Earth Science and Technology, 2. Hiroshima University, 3. Niigata University, 4. University of Southampton, 5. Columbia University

To understand physical properties of the oceanic crust and the mantle is fundamentally important to reveal the dynamics of plate tectonics, and the global circulations of H_2O and CO_2 fluids. We report results on physical property measurements of core samples from Oman Drilling Project (OmanDP) Holes CM1A and CM2B, which drilled from the lower igneous crust into the upper mantle in the Samail Ophiolite, Sultanate of Oman.

X-ray CT, bulk/grain density, porosity, magnetic susceptibility, P-wave velocity, electrical resistivity and thermal conductivity were measured onboard D/V Chikyu using whole-round cores and discrete samples for core sections from CM1A and CM2B.

The paleo-Moho in CM1A may not preserve the original structure due to minor faulting, possibly during obduction. The gabbro-dunite transition (paleo-Moho) in Hole CM1A is characterized by a sharp change in physical property data. For example, P-wave velocity decreases from ~6.7 km/s in the layered gabbro sequence to ~4.9 km/s in the MTZ. Low P-wave velocity and density (~2.6 g/cm^3) in serpentinized dunites reflect the fact that olivine in the dunites is almost completely serpentinized. Serpentinization could have occurred during hydrothermal alteration near the spreading ridge axis, during subduction of 100’s of km of oceanic crust and sediment beneath the ophiolite, during obduction onto the Arabian continental margin, and/or during present-day weathering. In contrast to the paleo-Moho, the boundary between the Crust-Mantle Transition (CMT) sequences (i.e., dunites and dunites with gabbro lenses) and the underlying, residual mantle harzburgites is somewhat gradual. P-wave velocity gradually increases from ~4.9 km/s for dunite in the CMT to ~5.5 km/s for harzburgite in the mantle sequence. The thickness of the CMT is 50–70 m in Holes CM1A and CM2B. We also report on correlations between physical properties, especially electrical conductivity and magnetic susceptibility, and the fault intensity and alteration intensity from the core descriptions.

Keywords: ophiolite, mantle, oceanic crust, moho

©2019. Japan Geoscience Union. All Right Reserved.

Microstructures of lower crust gabbros from the Oman Ophiolite: Analyses of the drilled cores of the Oman Drilling Project

*Koki Iida[1], Takahiro Fudai[1], Susumu Umino[1], Yuki Kusano[2]

1. Kanazawa University, 2. Geological Survey of Japan

Oman Drilling Project in 2016 to 2017 recovered 400 m long cores of layered gabbros at Site GT1 in the Wadi Tayin Massif of the Oman Ophiolilte. The purpose of this research is to describe microstructures of the layered gabbro core samples and to discuss the conditions of magmatic and hypersolidus deformation that operated in the lower crust beneath the Oman paleoridge.

Core samples were cut into slabs parallel to foliation and slabs normal to foliation and parallel to lineation, which were made into thin sections for microscopic observations. Structural fabrics and the relationships between crystal shapes and alliginment were described to identify magmatic and hypersolidus deformation structures.

Cored samples are predominantly olivine gabbros consisting of anhedral olivine, anhedral to subhedral clinopyroxene and subhedral to euhedral plagioclase. Grain size ranges from 0.5 mm to a few millimeters irrespective of mineral species.

The structures shown by the gabbros are classified into three regimes by temperature or the amount of melt present: Regime I, magmatic conditions without or minimal plastic deformation; regime Ⅱ, plastic deformation assisted by interstitial melt (Dunn, 2000); regime Ⅲ, near solidus deformation. Regime Ⅱ is identified by ameboid grain boundaries with no intracrystalline deformation and equigranular textures, resulted from decreasing internal strain energy by at high temperatures. The presence of melt is evidenced by the clear euhedral plagioclase rims with resorbed turbid cores as discussed below.

Regime I. Magmatic structures are identified as modal layering due to changes in mineral mode, no preferred orientation or shape-preferred orientation of clinopyroxene and plagioclase, poikilitic texture of olivine enclosing plagioclase laths and ophitic texture of clinopyroxene including plagioclase laths.

Regime II. The hypersolidus deformation structures overprint igneous structures: ameboid olivine with or without strain in the crystal, elongated olivine, and lenticular aggregates of olivine grains with an asymmetric quarter structure. Single clinopyroxene crystals show an asymmetric quarter structure like olivine aggregates. Ophitic clinopyroxenes consist of subgrains with slightly different orientations <10˚. Plagioclase shows deformation twin and undulose extinction. Equigranular fine-grained plagioclase with grain boundaries intersecting at 120˚ are common. Large plagioclases have a resorbed core with a wavy outline and are surrounded by euhedral rim.

Regime III. Subsolidus recrystallization includes buldging and grain boundary migration resulted in ameoboid grain boundaries of clinopyroxene. Undulose extinction and kinked twinning of plagioclase are observed.

It is well known that mid-ocean ridge basalt magma commonly crystallizes in the order of olivine, plagioclase and clinopyroxene, which is also true for the gabbros of the Oman Ophiolite (Adachi and Miyashita, 2003). Nevertheless, only plagioclase shows euhedral to subhedral shapes in the observed

©2019. Japan Geoscience Union. All Right Reserved.

layered gabbro core samples. Deformed olivine aggregates and clinopyroxene with quarter structures are embedded in plagioclase with equilibrium granoblastic textures and large euhedral plagioclases with resorbed turbid cores. Considering these textures combined with the mechanical strength of the three constituent minerals, these gabbros suffered deformation under the presence of melt, which assisted complete recovery of strain through recrystallization of fine-grained plagioclase and overgrowth of euhedral rims around magmatic plagioclase cores. Poikilitic olivine occurs through the hole, whereas ophitic Cpx occurs at 73 m and 220 m in depth. Most deformation structures of regime II are present irrespective to depth. The asymmetric structures of olivine and clinopyroxene were used to determine the relative sense of shear. Both dextral and sinistral sense of shear are observed within the same samples.

Keywords: Oman ophiolite, Oman Drilling Project , Layered gabbro , Foliated gabbro , Microstructures , Lower crust

©2019. Japan Geoscience Union. All Right Reserved.

Olivine fabric and mineral compositions in the Maqsad area of the Samail massif, the southern Oman ophiolite

*Kaho Takahashi[1], Eiichi TAKAZAWA[2,3], Katsuyoshi Michibayashi[4], Kakihata Yuki[4], Ryoko Senda[5]

1. Graduate School of Science and Technology, Niigata University, 2. Department of Geology, Faculty of Science, Niigata University, 3. JAMSTEC, 4. Nagoya University, 5. Kyushu University

In this study, we conducted structural and chemical analysis of oriented samples of 17 harzburgites and 4 dunites collected from the Maqsad area of Samail massif in the southern Oman ophiolite. We investigated the degree of partial melting and the mantle-melt reaction with relation to mantle diapir structure.

The crystallographic preferred orientation (CPO) of olivine grains were measured in highly polished XZ thin sections using a scanning electron microscope equipped with an electron-back scatter diffraction system at Shizuoka University. After plotting the results in the Vp Flinn plot expanded for olivine fabric types [1,2], the fabric type of peridotites in this study are summarized as follows. The distribution of A type is limited in the southeastern part where the diapir structure has been identified [3], whereas D type is dominant in the peripheral part of the diapir. Minor amounts of AG type and E type are also observed in the peripheral part. From these, the olivine in the southeastern part (diapir area) of this study area is likely to have been deformed under high temperature whereas the peripheral part was deformed at slightly lower temperature. The CPOs of olivine in both areas do not show any influence from the presence of H2O except for only one sample with E type CPO. Moreover, strong alignment of [100] to the vertical orientation was observed in the southeastern part (diapir area) of this study area. Since vertical mantle flow has been estimated in this diapir area, our results are consistent with the previous study [3,4].

The Cr# (=Cr/[Cr+Al] atomic ratio) of spinel in the harzburgites and dunites are as high as 0.55-0.58 in the central part of the southeastern part (diapir area) and along the paleo-ridge axis running in the NW - SE direction [3,4]. On the other hand, the Cr# of spinel in the peripheral part is 0.41-0.55 indicating slightly less depleted than in the central part. In addition, the REE abundance of clinopyroxenes in the central part of the diapir area is lower than in the peripheral part being consistent with the distribution of spinel Cr#.

We consider that the upwelling rate in the southeastern part (diapir area) may have been greater than the peripheral part possibly due to higher temperature in the focused vertical mantle flow. This model is consistent with the distribution of the Cr# of spinel: the degree of melting was greater in the diapir area where Cr# of spinel are higher than the peripheral part. The strongly focused pipe-like model for axis location [3,5] is well fitted by our observations in this study.

[1] Karato et al., 2008, Ann. Rev. Earth Planet. Sci., 36, 59-95. [2] Michibayashi, 2015, J. Geography, 124, 397-409. [3] Jousselin et al., 1998, JGR, 103, 18153-18170. [4] Nicolas et al., 2000, Marine Geophys. Res., 21, 147-179. [5] Nicolas and Boudier, 1995, JGR, 100, 6179-6197.

Keywords: Oman ophiolite, crystalographic preferred orientation, olivine, fabric, peridotite, mantle flow

©2019. Japan Geoscience Union. All Right Reserved.

The evolution of melt inclusions in podiform chromitite in Oman

*Yuan YAO[1], Eiichi TAKAZAWA[2,3], Oman Drilling Project Phase 2 Science Party

1. Graduate School of Sciences& Technology, Niigata University, Japan, 2. Department of Geology, Faculty of Science, Niigata University, Japan, 3. Research and Development Center for Ocean Drilling Science, JAMSTEC, Japan

Melt inclusions are tiny inclusions which trapped in the host magmatic minerals. After trapping, the host mineral can be considered as a closed and isolated system (Roedder, 1984). Thus, melt inclusions behave as time capsules, which record the liquid line of descent of magmatic systems (Frezzotti, 2001). Therefore, melt inclusions can provide important information of the primary melts (Kent, 2008).

We studied the melt inclusions in chromite from a chromitite deposit mine in the north of Maqsad and the core sample from the Oman drilling project phase 2. The silicate inclusions range in diameter from 5 μm to 200 μm, contain pargasite, tremolite, aspidolite, high Cr# (=Cr/[Cr+Al] atomic ratio) chromite, diopside, enstatite, forsterite, grossular, albite, titanite, pentlandite, apatite, chlorite, wollastonite and serpentine. We found the high Cr# chromite occurs as lining of the inclusion, moreover the daughter minerals precipitated in the high Cr# chromite lining. Those phenomenon can be explained by the crystallization of chromite on the wall of inclusion. In addition, this is the first report about the necking down of melt inclusion in chromitite. The necking down of inclusions is an originally large, liquid-filled inclusion divided into smaller inclusions. If the necking down happens after the phase change of inclusion, the compositions of smaller inclusions probably are inhomogeneity. Last year, we conducted the high temperature homogenized experiments, the result showed that the homogenized quenching glass are heterogeneous. We consider the inhomogeneity of inclusions perhaps caused by the necking down. Based above all, we suggest the composition of homogenized inclusion can not represent the parental melt.

To summarize, we suggest before analysis and experiment of inclusions in chromite, the origin and the evolution of inclusions should be carefully studied.

Reference

Frezzotti, M. (2001). "Silicate-melt inclusions in magmatic rocks: applications to petrology." Lithos **55** (1-4): 273-299.
Kent, A. J. R. (2008). "Melt Inclusions in Basaltic and Related Volcanic Rocks." Reviews in Mineralogy and Geochemistry **69** (1): 273-331.
Roedder, E. (1984). Fluid inclusions, Walter de Gruyter GmbH & Co KG.

Keywords: melt inclusion, Oman, chromitite

©2019. Japan Geoscience Union. All Right Reserved.

Melt/fluid - rock reaction inferred from the Wadi Tayin mantle section in the southern Oman ophiolite

*Keisuke ISHII[1], Eiichi TAKAZAWA[2], Akihiro kuriyama[2], Kyouka Someya[2], Yoshihiko Tamura[3]

1. Graduate School of Science and Technology, Niigata University, 2. Department of Geology, Faculty of Science, Niigata University , 3. R&D Center for Ocean Drilling Science, Japan Agency for Marine-Earth Science and Technology

We report the petrology and the mineral compositions of peridotites from the Wadi Tayin massif in the southern Oman ophiolite [1-3] to investigate the influence of arc related magmatism during oceanic thrusting of the ophiolite. Harzburgites, dunites and a small number of lherzolite were systematically corrected along wadis to cover the mantle section from the boundary between lower crust and uppermost mantle namely “Moho” to the basal thrust. Spinel Cr# [=Cr/(Cr+Al) atomic ratio] of harzburgite varies from 0.22 to 0.58 similar to the range in abyssal peridotites [4]. Moreover, it gradually increases from the basal part to the Moho indicating the compositional variation expected for the residual mantle column formed at a mid ocean ridge. On the other hand, the spinel Cr# of dunite often exceeds 0.6 in the NW-SE striking shear zone in the middle part of the study area. The chondrite-normalized rare earth element (REE) patterns of clinopyroxenes in peridotites from the shear zone show a linear pattern that monotonously decreases from heavy REE to light REE (LREE). Calculated melt compositions in equilibrium with these clinopyroxenes are equivalent with the V2 (Type2) lava reported in the northern Oman ophiolite [5-6].

The plots in Cr# of spinel versus Ce/Yb ratio of clinopyroxenes show a linear trend with a positive correlation. It indicates that the LREE enrichment of clinopyroxene is associated with an increase in the degree of melting. Clinopyroxenes in the dunite from the shear zone are most significantly enriched in LREE to middle REE and have REE abundances being in equilibrium with the V2 lava. We consider that harzburgites were suffered from a flux melting by infiltration of H2O-rich fluid producing V2 lava. Comparing to the results from the northern massifs the linear trend in the diagram of Cr# of spinel versus Ce/Yb ratio of clinopyroxenes in the southern massif is obviously shifted toward lower in Cr#. It suggests that the infiltration of H2O-rich fluid may have started at early stage of melting in the Wadi Tayin massif relative to the northern massifs.

[1] Kelemen et al., 1995, Nature, 375, 747-753, [2] Godard al., 2000, EPSL, 180, 133-148, [3] HanghØj et al., 2010, J. Petrol., 51, 201-227, [4] Dick and Bullen, 1984, CMP, 86, 54-76, [5] Godard et al., 2003, G-cubed, 4, 8609, [6] Kusano et al., 2016, Chem. Geol., 449, 206-225.

Keywords: Oman ophiolite, Mantle section, Peridotite, Melt/rock reaction

©2019. Japan Geoscience Union. All Right Reserved.

Numerical simulations for reaction-induced fracture formation of layered gabbro during hydration process

*Kazuki Yoshida[1], Hiroyuki Shimizu[2], Noriyoshi Tsuchiya[1], Atsushi Okamoto[1], Phase 2 Science Party Oman Drilling Project[3]

1. Tohoku university, 2. Geotechnical Analysis Group, Advanced Analysis Department, Civil Engineering Design Division, Kajima Corporation, 3. Oman Drilling Project Phase 2 Science Party

Serpentinization of oceanic lithosphere is important for various geological processes, including magmatism and earthquake at subduction zone, and generation of hydrogen and hydrocarbon at seafloor. For understanding the extent of the water infiltration into mantle within the oceanic lithosphere, permeability of the lower crust is an important factor, since gabbro has low permeability at high confining pressure (Katayama et al., 2012). In natural olivine-bearing gabbro, serpentinization of olivine grains produced radial fractures within the plagioclase matrix, which can potentially enhance the permeability (Jamtveit et al., 2008). Based on the numerical simulations using discrete element method (DEM), Jamtveit et al. (2008) shows that fracture network is produced by the volume expansion of olivine grains during hydration. However, their model dos not treat the advective fluid flow explicitly, it is not clear how permeability evolves during such processes. In this study, inspired by the natural textures of olivine gabbro taken from CM1A-7A (Wazi Zeeb, Oman Drilling Project), we conducted the DEM simulation for understanding the feedback of the fluid flow –olivine hydration –fracturing to the layered gabbro, which consists of olivine-rich layer and olivine-poor layer alternately. In particular, we focus on the contrasting fracture patterns between olivine and plagioclase, the evolution and anisotropy of permeability produced by the reaction-induced fracturing within the layered gabbro.

We conducted the two-dimensional DEM model, and the details of the model follows Okamoto and Shimizu (2015) and Shimizu and Okamoto (2016). We consider a simple volume increasing hydration reaction ($A + H_2O \rightarrow B$; 50% volume increase), and the reaction rate is defined as a linear function of fluid pressure. In the model, advective fluid flow occurs through apertures between particles, in response to difference of fluid pressure of individual domains. The rock model is consist of reactive part (it can change from olivine to sperneitne) and non-reactive part (e.g., plagioclase and clnopyronene). The reaction rate constant and aperture width of matrix and fracture are defined based on the non-dimensional numbers based on Shimizu and Okamoto (2016).

Firstly, we conducted the simulations for the model in which a single olivine exists in non-reactive matrix. When fluid is supplied through matrix, hydration of olivine starts, which produces the mesh-like textures inside the olivine grain and radial cracks within the unreactive matrix, which is consistent with those observed in the gabbro sample from CM1A. Second, we conducted a case where several olivine grains exist in matrix. In this case, we found the formation of fracture network that connects among the olivine grains, and positive relationship between the reaction rate and permeability. Finally, we tested the case of the layered structure that consists of olivine-rich layer and olivine-absent layer, and that fluid flows in direction perpendicular to the layers. The results of the simulations reveals that the development of vertical fractures in both olivine-rich and non-reactive layers, whereas the horizontal fractures are only developed in the olivine-rich layers. These features of fracture orientation are consistent with the natural observations and indicate that he reaction-induced fracturing could significantly enhance the fluid infiltration through layered gabbro.

©2019. Japan Geoscience Union. All Right Reserved.

References

Katayama I, Terada T, Okazaki K, Tanikawa W (2012) Nat Geosci 5:731–734.

Jamtveit B., Malthe-Sørenssen A., Kostenko O., 2008. Earth Planet. Sci. Lett., 267, pp. 620-627

Okamoto,A.,Shimizu,H., 2015. Earth and Planetary Science Letters 415, 9–18.

Shimizu, H., Okamoto, A., 2016. Contributions to Mineralogy and Petrology, 171, 73.

Keywords: Oman Drilling Project, layered gabbro, permeability, Discrete Element Method, serpentinization

©2019. Japan Geoscience Union. All Right Reserved.

X-ray CT images of oceanic lithologies obtained on Oman Drilling Project drillcores during ChikyuOman 2017 and 2018

*Katsuyoshi Michibayashi[1], Peter B Kelemen[2], Margurette Godard[3], Eiichi TAKAZAWA[4], Damon A H Teagle[5], The Oman Drilling Project Science Party[6]

1. Department of Earth and Planetary Sciences, Nagoya University, 2. Columbia University, 3. Université Montpellier, 4. Niigata University, 5. Southampton University, 6. ICDP

The Oman Drilling Project (OmanDP) has drilled >3,200 meters of the Oman ophiolite during Phases 1 and 2 in Holes GT1A, GT2A, GT3A, BT1B, CM1A, CM2B, BA1B, BA3A and BA4A. All cores have been described on board D/V Chikyu during the summers of 2017 and 2018. X-ray computed tomography (X-ray CT) images were obtained on all cores as a routine part of the IODP measurement protocol onboard D/V Chikyu.

The X-ray CT scanner (Discovery CT 750HD, GE Medical Systems) scans and reconstructs an image of a 1.4 m section in 10 minutes and produces a series of scan images, each 0.625 mm thick. The X-ray source and detector are installed inside of the gantry opposite each other. The excitation voltage and current for X-ray tube are 140 kV and 100 mA, respectively. Core samples are scanned in the gantry with a scanning rate of 20 mm/sec. The distribution of attenuation values mapped to an individual slice comprises the raw data that are used for subsequent image processing. Successive two-dimensional (2D) slices of 512 x 512 pixels yield a representation of attenuation values in three-dimensional (3D) voxels of 512 x 512 by ~1600 in length. Data generated for each core consist of core-axis-normal planes (XY planes) of X-ray attenuation values with dimensions of 512 ×512 pixels in 9 cm ×9 cm cross-section, with a resolution of 0.176 mm/pixel.

As a consequence, we have >3,200 meters length of X-ray CT images from the dyke/gabbro transition zone to the gabbroic sequence to the mantle sequence to the basal thrust of the ophiolite. All X-ray CT images have been processed to match with individual photo images of the archive halves of the cores. The data are useful for assessing sample locations and quality. X-ray CT images can be used for 3D fabric analyses even after core has been cut in half and subsampled for other analyses.

Keywords: OmanDP, XCT, image

©2019. Japan Geoscience Union. All Right Reserved.

Re-examination of the crystallization process of clinopyroxene oikocrysts in layered gabbros at Hess Deep Rift, EPR

*Akane Yasui[1], Takashi Hoshide[1]

1. Graduate School of International Resource Sciences, Akita University

In the Hess Deep Rift, located about 60km east of the East Pacific Rise, the lower crustal gabbros which have been formed at the fast-spreading ridge are exposed. In the IODP Exp. 345, primitive layered gabbros were collected from the lower crust as mainly three drill cores (U1415 I, J, P; Gillis et al., 2014). From the U1415J, unique gabbroic rocks (troctolites) with poikilitic clinopyroxenes (oikocrysts) including many small plagioclase laths have been found (Maeda and Kaise, 2015, Abstracts of the Geological Society of Japan).

Recently, on the origins of clinopyroxene-oikocryst-bearing gabbroic rocks, the different hypotheses have been proposed by Leuthold et al. (2018) and Maeda and Kaise (2015).
Leuthold et al. (2018) proposed that initial olivine gabbros had been partially molten by the intrusion of a primitive melt and then clinopyroxene oikocrysts had crystallized from clinopyroxene-rich basaltic melts formed by the mixing between the partial melt and the primitive magma.
On the other hands, Maeda and Kaise (2015) proposed that clinopyroxenes have first crystallized from a primitive magma and after molten by the encounter with another primitive magma they have continued to grow further and then, the clinopyroxene rim has simultaneously crystallized with matrix olivine and plagioclase. Several hypotheses other than those above (e.g.,Tegner et al., 1995; Nicolas and Boudier., 2011) have been also proposed for the origin of the clinopyroxene oikocrysts in gabbroic rocks. The question is still open to discussion.
Therefore, I re-examine the process of clinopyroxene-oikocryst formation through the textural observation and chemical analysis of the constituent minerals for 8 samples of clinopyroxene-oikocryst-bearing gabbros from 3R, 5R, 7G, 8R and 15G of the U1415J core collected at the IODP Exp. 345.

The matrix part is troctolite consisting mainly of olivine (about 0.5 mm - 2 mm in size, amoeboidal, Fo85~) and plagioclase (about 1 mm in size, An#77-82). Spherical to ellipsoidal clinopyroxene oikocrysts (5-10 mm in size, Mg#85 to 88) is distributed in the matrix troctolite. In addition, clinopyroxene oikocrysts exhibit the following characteristics:

(1) Clinopyroxene oikocrysts basically do not contain any olivine crystals. Rarely, they contain aggregates of plagioclase and olivine.
(2) Orthopyroxene rims (about 100 μm thick, film-like, Mg#85-87) are observed only in matrix olivines (Fo85~) near the rim of the clinopyroxene oikocryst. The olivine crystals rimmed by orthopyroxene are shrinked.
(3) The decreases in Al and Cr contents towards the plagioclase chadacrysts are observed in clinopyroxene oikocrysts.
(4) In the core of the clinopyroxene oikocrysts, we can find parts with Mg# higher than the values which can be in the Fe/Mg equilibrium with olivine in the matrix troctolite.

The facts of (1) and (2) indicate that the assemblage of olivine and plagioclase had already existed when the clinopyroxene oikocrysts crystallized from the melt. In additions, these facts suggest that the melt which formed clinopyroxene oikocryst was in a reaction relationship with olivine. These interpretations

©2019. Japan Geoscience Union. All Right Reserved.

are consistent with the hypothesis of Leuthold et al. (2018).

Keywords: clinopyroxene oikocrysts, Hess Deep, troctolite, Magma mixing, MORB

©2019. Japan Geoscience Union. All Right Reserved.

Structural petrology of peridotites from the Kalaymyo ophiolite

*Kouhei Asano[1,2], Katsuyoshi Michibayashi[1], Jung-Woo Park[3]

1. Graduate School of Environmental Studies, Nagoya University, 2. Shizuoka University, 3. Seoul National University

The Kalaymyo ophiolite is located at Myanmar. The Kalaymyo ophiolite includes large peridotite massifs, where peridotites are commonly well preserved. In recent years, petrologic and geochemical studies have been carried out on the Kalaymyo peridotites. These results suggest that the Kalaymyo peridotites have been undergone melt-rock interactions. In this study, we used fourteen samples from outcrops and drill cores, and carried out analyses of crystal preferred orientations (CPOs) of olivine and of major elements of olivine and spinel. The samples show coarse-grained equigranular textures. The mineral compositions in spinel Cr# and olivine Mg# plot in the field of OSMA (olivine-spinel mantle array) indicate that these samples represent residual upper mantle rocks after partial melting. Spinel grains with Cr# higher than 0.3 have relatively high TiO_2 contents (0.10-0.20 wt.%). Because Ti is incompatible element, high spinel TiO_2 content suggests that these peridotites have experienced melt-rock interaction. There is a positive correlation between J-index and spinel Cr# in the samples. The correlation also has two trends: high and low positive relationships between J-index and spinel Cr#, respectively. Samples experienced melt-rock interaction belong to the low positive trend. It suggests that melt percolation by melt-rock interaction could have an impact on deformation, in particular on CPO development. We propose that melt-rock interaction was synchronous with deformation. It is noted that peridotites experienced melt-rock interaction are intensely located on a narrow range with respect to the elevation, indicating that the occurrence of melt-rock interaction was localized within the Kalaymyo ophiolite.

Keywords: Kalaymyo ophiolite, peridotite, melt-rock interaction, J-index

©2019. Japan Geoscience Union. All Right Reserved.

Reevaluation of the origin of mafic layers in the Upper Zone of the Horoman Peridotite

*Yumeto KOGURE[1], Eiichi TAKAZAWA[1]

1. Department of Geology, Faculty of Science, Niigata University

Horoman peridotite is situated at the southern tip of the Hidaka mountain range, spreads 8 km east-west, 10 km north-south, and has a layer thickness of 3,000 m. We reevaluated the origin of the mafic layer in the Upper Zone of the Horoman Peridotite. We studied Fumo section in the Upper Zone. This section has total thickness of 263 m and consists of plagioclase lherzolite, harzburgite and mafic layer. In the Fumo section, the mafic layer is only interlayered in the plagioclase lherzolite. In the Al2O3, CaO, and Na2O vs. MgO diagrams of whole rock compositions, the mafic layer is plotted on the extension of the linear composition trend indicated by plagioclase lherzolite and harzburgite. There are two types of mafic layer, one plotted in the vicinity of N-MORB and the other plotted in the vicinity of plagioclase lherzolite. The plagioclase lherzolites which have higher Al2O3, CaO, and Na2O and lower MgO contents than the Depleted MORB Mantle (DMM) [1] contain amphiboles whereas the other plagioclase lherzolite which has lower Al2O3, CaO, and Na2O contents and higher MgO content than the DMM do not contain amphibole. Chondrite-normalized whole rock rare earth element (REE) patterns of plagioclase lherzolites are flat from heavy REE to middle REE and show convex upward pattern with depletion in light REE. The mafic layers also show the similar pattern although the abundances of REE is much lower than N-MORB.

From these results, the mafic layers in the Fumo section do not have the composition of primary melt and is considered to be cumulate [2,3]. Also, in the whole rock FeO, TiO2 vs. MgO diagrams, the compositional trends suddenly bend at the most fertile plagioclase lherzolite and becomes depleted in FeO, TiO2 toward the thin mafic layers. On the extension of this bent trends reach to the composition of Cpx and plagioclase. The mafic layer in the Fumo section suggests the possibility that Cpx and plagioclase were crystallized from a melt penetrated into plagioclase lherzolite in a relatively low pressure where the combination of Cpx and plagioclase was stable.

[1] Workman and Hart, 2005, EPSL, 231, 53-72. [2] Shiotani and Niida, 1997, Memoir. Geol. Soc. Japan, 47, 123–137. [3] Takazawa et al., 1999, J. Petrol., 40, 1827-1851.

Keywords: Horoman Peridotite, mantle, mafic layer, orogenic lherzolite, Hidaka Metamorphic Belt

©2019. Japan Geoscience Union. All Right Reserved.

A structural and petrological study of "Shibukawa ultramafic body" in the Sanbagawa belt, western Shizuoka, Japan

*Hikaru Shioya[1,2], Katsuyoshi Michibayashi[1], Ken-ichi Hirauchi[2]

1. Graduate School of Environmental Studies, Nagoya University, 2. Institute of Geosciences, Shizuoka University

We studied an ultramafic body, which is named "Shibukawa ultramafic body" in this study, in the Sanbagawa belt located to the western Shizuoka, focusing on their primary mineral olivine to reveal its petrogenesis. Shibukawa ultramafic body is composed of dunites and wehlites, although the body was heavily weathered due to serpentinization. Yet, most of samples still contain olivine, spinel and a few amounts of clinopyroxene. The olivine crystal preferred orientations (CPOs) of this body were divided into two types: D type and single maxima type. The CPO intensities were relatively high in the north area, whereas those in the south area were relatively low. Considering the grain size distribution of olivine in the samples, the samples in the south area was weakly deformed as they preserve porphyroclastic olivine grains in the fine-grained matrix. In contrast, grain size reduction due to deformation has been completed in the north area. Olivine CPO patterns and major elements composition of both olivine and spinel indicate that the origin of this ultramafic body could be cumulate such as the Mikabu belt and is different from those of Shikoku mountains in the Sanbagawa belt.

Keywords: Sanbagawa belt, Mikabu belt, Cumulate, Ultramafic, Olivine fabrics, Dunite

©2019. Japan Geoscience Union. All Right Reserved.

[E] Poster | B (Biogeosciences)：B-CG Complex & General

Tue. May 28, 2019 3:30 PM - 5:00 PM JST | Tue. May 28, 2019 6:30 AM - 8:00 AM UTC | Poster Hall International Exhibition Hall8, Makuhari Messe_22

[B-CG06] Earth and Planetary Science Frontiers for Life and Global Environment

convener:Yoshinori Takano(Japan Agency for Marine-Earth Science and Technology (JAMSTEC)), Yohey Suzuki(Graduate School of Science, The University of Tokyo), Shingo Kato(RIKEN), Keisuke Fukushi(Institute of Nature & Environmental Technology, Kanazawa University)

Earth and planetary science is currently capable of sampling from four frontiers: space, polar regions, deep ocean and deep underground for the study of the origin and evolution of life. Next generation sequencing technology of nucleic acids and nanotechnology-driven innovation of solid characterizations are very powerful to expand our understanding of many fields of earth and planetary sciences. It is also important for us to be aware of global warming and climate change that dramatically affect biodiversity, biological activities and elemental cycling. The aim of this session is to cross the border of science sections to explore the frontiers of earth and planetary science.

[BCG06-P01] Dynamisms and characteristics of dissolved organic matter (DOM) in deep aquifer: A scope for deep biosphere

*Atsushi Urai[1,2], Yoshinori Takano[2], Naohiko Ohkouchi[2] (1.Department of Science and Technology, Graduate School of Medicine, Science and Technology, Shinshu University, 2.Department of Biogeochemistry, Japan Agency for Marine-Earth Science and Technology)

[BCG06-P02] Correlations of magnetosome-related genes in Nitrospirae genomes to magnetosome geometry and redox stratification in deep-sea environments

*Shinsaku Nakano[1], Shingo Kato[2], Mariko Kouduka[1], Toshitsugu Yamazaki[3], Yohey Suzuki[1] (1.Graduate School of Science, The University of Tokyo, 2.RIKEN, 3.Atmosphere and Ocean Research Institute, The University of Tokyo)

[BCG06-P03] Reconstruction of key ecological responses leading to the most recent dead zone formations in Japan Sea through ancient DNA metabarcodring

*Mariko Kouduka[1], Yohey Suzuki[1] (1.Department of Earth and Planetary Science, The University of Tokyo, 7-3-1 Hongo, Bunkyo-ku, Tokyo, Japan.)

[BCG06-P04] Search for microbial CH_4 production processes in lake sediments and surface water associated with cyanobacterial bloom

*Makoto Matsushita[1], Yoshinori Takano[1], Hiroyuki Imachi[1], Atsushi Urai[2], Ho-Dong Park[3], Hiroki Iwata[3], Naohiko Ohkouchi[1] (1.Japan Agency for Marine-Earth Science and Technology, 2.Department of Science and Technology, Graduate School of Medicine, Science and Technology, Shinshu University, 3.Department of Environmental Sciences, Faculty of Science, Shinshu University)

[BCG06-P05] Did life emerge in a deep-sea metal sulfide chimney? New insights from an archaeal genome and a nanoscale microbe-silicate assemblage

*Hinako Takamiya[1], Hiroki Mukai[2], Mariko Kouduka[1], Shingo Kato[4], Motoo Ito[3], Yohey Suzuki[1] (1.Earth and Planetary Science Graduate School of Science, The University of Tokyo , 2.National Institute of Advanced Industrial Science and Technology, 3.Kochi Institute for Core Sample Research JAMSTEC, 4.RIKEN)

[BCG06-P06] X-ray computed nano-tomography for visualizing microbial cells and their surrounding environments

*Yuki Morono[1], Go-Ichiro Uramoto[2,1], Kentaro Uesugi[3], Nobuhisa Takeuchi[3], Masayuki Uesugi[3], Kengo Kubota[4], Tatsuhiko Hoshino[1], Fumio Inagaki[1] (1.Japan Agency for Marine-Earth Science and Technology, 2.Kochi University, 3.Japan Synchrotron Radiation Research Institute, 4.Tohoku University)

[BCG06-P07] **Carbon signatures in amino acids during deep-sea anoxic methanotrophy**

*Yoshinori Takano[1] (1.Japan Agency for Marine-Earth Science and Technology (JAMSTEC))

Dynamisms and characteristics of dissolved organic matter (DOM) in deep aquifer: A scope for deep biosphere

*Atsushi Urai[1,2], Yoshinori Takano[2], Naohiko Ohkouchi[2]

1. Department of Science and Technology, Graduate School of Medicine, Science and Technology, Shinshu University, 2. Department of Biogeochemistry, Japan Agency for Marine-Earth Science and Technology

Dissolved organic matter (DOM) is generally derived from multiple sources and affected by complicated transformation and degradation reactions. In a general geochemical description of marine environments, high-molecular-weight DOM (HMW-DOM; >1 kDa) particularly represents a unique organic carbon pool, which is accompanied by considerable difference in the molecular and stable isotopic compositions from other organic components such as particulate organic matter (POM) and low-molecular-weight DOM (LMW-DOM; <1 kDa) (e.g., Benner et al., 1997).

To date, formation of DOM fraction and potential microbial interaction in deep aquifer have been particularly poorly understood on the context of prokaryotic ecology. We investigated the molecular composition of DOM fraction including LMW and HMW by an improved method (Urai et al., 2018). The filtered samples are tentatively defined by conventional size scales; macromolecular scale (100 mm >> 40 mm), POM (40 mm >> 0.6 mm), HMW-DOM(0.6 mm>>1kDa), and total-DOM (<0.6 mm). We also have a validation to distinguish the molecular signature between phototrophic primary producers (i.e., fossil molecules) and presently living benthic prokaryotes (i.e., modern molecules; cf. biological methanogenesis, Kaneko et al., 2014). We report a preliminary result of the feasibility study and discuss a perspective from the view of deep biosphere.

References:

Benner et al. Abundance, size distribution, and stable carbon and nitrogen isotopic compositions of marine organic matter isolated by tangential-flow ultrafiltration. Marine Chemistry 57, 243-263 (1997).

Kaneko et al. Quantitative analysis of coenzyme F430 in environmental samples: a new diagnostic tool for methanogenesis and anaerobic methane oxidation. Analytical Chemistry 86, 3633-3638 (2014).

Urai et al. Algal-derived 24-ethylcholesta-5, 22-dien-3β-ol (stigmasterol) is frequently found in high-molecular-weight dissolved organic matter (HMW-DOM) during summer in freshwater and brackish lakes. Geochemical Journal 52, e15-e20 (2018).

Keywords: HMW-DOM, sterol, carbon and hydrogen isotopic compositions, deep aquifer, methanogenesis

©2019. Japan Geoscience Union. All Right Reserved.

Correlations of magnetosome-related genes in Nitrospirae genomes to magnetosome geometry and redox stratification in deep-sea environments

*Shinsaku Nakano[1], Shingo Kato[2], Mariko Kouduka[1], Toshitsugu Yamazaki[3], Yohey Suzuki[1]

1. Graduate School of Science, The University of Tokyo, 2. RIKEN, 3. Atmosphere and Ocean Research Institute, The University of Tokyo

Biogenic magnetic particles are ubiquitously found in deep-sea sediments and important carriers of rock magnetism for reconstructing the Earth’ s past regarding sediment age and geomagnetic field. However, microorganisms responsible for the formation of magnetic particles are largely unknown in the deep-sea environment, because of the difficulty in sampling, cultivation, and magnetic separation of magnetotactic cells for single-cell genomics. In this study, deep-sea sediments from Japan Sea and a metal sulfide chimney from South Mariana Trough were subjected to magnetic separation and subsequent electron microscopic observations. Although teardrop-shaped magnetite (Fe_3O_4) particles without microbial cells and 16S rRNA gene sequences related to magnetotactic Nitrospirae species were previously obtained from Japan Sea sediments with a redox zonation enriched with dissolved Fe(II) (the iron boundary), no magnetotactic cells were observed after the magnetic separation. From the metal sulfide chimney, magnetotactic cells were observed with teardrop-shaped magnetite particles. Metagenomic analysis of the chimney sample revealed that contig sequences encoding genes involved in the formation of magnetosome, membrane-bound magnetic particles, were mostly affiliated within Nitrospirae based on sequence similarity. Previous studies have reported that magnetosome-related genes are clustered together as the magnetosome island (MAI) in known magnetotactic bacteria. However, those genes were scattered in a near-complete Nitrospirae genome reconstructed from the chimney sample. Although magnetotactic bacteria are generally considered to align magnetic particles into a chain for efficiently moving in a vertical redox zonation by orienting the cell along the geomagnetic filed, Nitrospirae-affiliated genes involved in chain formation were not found in the near-complete Nitrospirae genome from the chimney with a horizontal redox zonation. Comparative analysis of near-complete Nitrospirae genomes available from public databases revealed that the chain-related genes were found in the genomes from terrestrial deep aquifers and deep-sea sediments with a vertical redox zonation. As the Nitrospirae species associated with teardrop magnetite and the iron boundary in Japan Sea was closely related to Nitrospirae species with the chain-related genes, the presence of the chain-related genes appears to be correlated with a vertical redox zonation. In addition, our results suggest that the Nitrospirae species without MAI are responsible for the production of teardrop magnetite in deep-sea environment, and that teardrop magnetite is a paleoredox indicator especially for the iron boundary.

Keywords: magnetotactic bacteria, metal sulfide chimney, magnetofossil, remnant magnetization

©2019. Japan Geoscience Union. All Right Reserved.

Reconstruction of key ecological responses leading to the most recent dead zone formations in Japan Sea through ancient DNA metabarcodring

*Mariko Kouduka[1], Yohey Suzuki[1]

1. Department of Earth and Planetary Science, The University of Tokyo, 7-3-1 Hongo, Bunkyo-ku, Tokyo, Japan.

Semi-closed ocean basins are very sensitive to climate changes as recorded in frequent formations of sediments with clearly laminated layers, which was caused by the lack of O_2 available to benthic organisms. This is so-called “dead zone formation” and caused by water stagnation after channel closure and/or nutrient inflow through upwelling and channel opening. In contrast to the hydrologic causes, it remains poorly understood about organismal causes such as enhanced primary production and heterotrophic consumption of O_2. We investigated ancient eukaryotic DNA obtained from a thinly laminated layer deposited in the Japan Sea across the most recent global warming event after Younger Dryas (TL-1). Metabarcoding of 18S rRNA gene sequences clarified that across the transition from oxygenated to anoxic bottom water conditions, dominant protist populations shifted through five stages:

Stage1: Under oxygenated bottom conditions, the most dominant taxonomic group was Marine Stramenopiles Group 9 (MAST-9). MAST-9 encompasses diverse uncharacterized planktonic species, 18S rRNA gene sequences of which were detected from both anoxic and oxic water bodies in Pacific and Atlantic Oceans, Mediterranean Sea and South China Sea.

Stage 2: Before the onset of dead zone formation, the sharp decline of MAST-9 was accompanied with the expansion of marine diatom species of the genus Skeletonema, many members of which are known to be a cause of red tide around the world.

Stage 3: The dead zone formation was synchronized with the expansion of marine radiolarians of the order Chaunacanthida, the members of which are encrusted within $SrSO_4$.

Stage 4: Stages 2 was repeated, whereas the expansion of the Chaunacanthida radiolarians was not evident.

Stage 5: The uncharacterized MAST-9 that was dominant before the dead zone formation was gradually recovered towards oxygenated bottom conditions.

From these results, it is suspected that the expansion of Radiolaria species encrusted with $SrSO_4$ triggered dead zone formation by the accelerated downward transport of dead cells and subsequent heterotrophic consumption of O_2. From bioturbated sediment samples from a maximum depth of 31 mbsf with a depositional age of 100 ka, the Chaunacanthida sequences closely related to that from the laminated sediments have been previously detected.It is therefore suggested the record of the Chaunacanthida species can be reconstructed from sediments with great depth and age.

Keywords: global warming paleo-analogue, hypoxemia expansion, molecular paleoecologcail dynamics, biogeochemical cycling

©2019. Japan Geoscience Union. All Right Reserved.

©2019. Japan Geoscience Union. All Right Reserved.

Search for microbial CH_4 production processes in lake sediments and surface water associated with cyanobacterial bloom

*Makoto Matsushita[1], Yoshinori Takano[1], Hiroyuki Imachi[1], Atsushi Urai[2], Ho-Dong Park[3], Hiroki Iwata[3], Naohiko Ohkouchi[1]

1. Japan Agency for Marine-Earth Science and Technology, 2. Department of Science and Technology, Graduate School of Medicine, Science and Technology, Shinshu University, 3. Department of Environmental Sciences, Faculty of Science, Shinshu University

Methane (CH_4) is an important greenhouse gas and contributes substantial budget to global warming. Freshwater lakes are identified as one of the main CH_4 sources, as it is estimated that they contribute to 6-16% of natural CH_4 emissions [1]. The main part of CH_4 released from lakes is considered to be produced by methanogenic archaea in anoxic sediments as terminal step in the degradation of organic matter. The microbial CH_4 production in lake sediments has been mainly investigated by microbiological studies using culture-dependent methods and molecular analysis.

Microbial CH_4 production is still regarded by many as a process limited to anoxic environments. Nevertheless, over the past few decades, increasing evidence of CH_4 accumulation in oxygen-saturated lake and marine surface water has emerged [2]. To explain the enigmatic issues, it has been proposed that CH_4 production by methanogenic archaea takes place in anoxic microenvironments such as detritus and animals' gut. Alternatively, recent studies suggest that some bacteria break down methylphosphonate (MPn) or dimethylsulfoniopropionate (DMSP) and release CH_4 as a biogenic byproduct. These novel microbial CH_4 production processes may play a potential contribution to the total atmospheric carbon cycle.

Oxic CH_4 peaks have been found to be closely associated with phytoplankton dynamics across multiple lakes. Grossart *et al*. [3] found potentially methanogenic archaea associated with cyanobacteria such as *Aphanizomenon* and *Microcystis* in oxygenated surface water. Additionally, Berg *et al*. [4] showed that hydrogen produced during nitrogen fixation by cyanobacteria can be consumed by methanogenic archaea. These studies suggest the presence of a CH_4 production process by methanogenic archaea associated with cyanobacteria in lake surface water. However, it is unclear whether the CH_4 production is taking place in actual environments.

In this study, we investigated microbial CH_4 production in sediments and surface water of Lake Suwa in Nagano Prefecture, Japan, a typical hypertrophic shallow lake, using culture-independent methods. Especially, we focused on cyanobacterial bloom and tried to identify a CH_4 production process by methanogenic archaea associated with cyanobacteria. 16S rRNA gene analyses revealed the presence of methanogenic archaea closely related to the order *Methanobacteriales*, *Methanomicrobiales*, and *Methanosarcinales* in sediment core samples from 30 cm depth. On the other hand, 16S rRNA genes and *mcrA* genes of methanogenic archaea were not detected in bulk DNA from cyanobacterial bloom sample (mainly *Microcystis*)[5]. In order to estimate the potential for methanogenic archaea, we extracted Coenzyme F430, a biomarker for methanogenic archaea, from sediment and bloom samples and determined by using HPLC [6]. F430 was detected from sediment samples, but that from bloom sample was currently below detection limit (<1 pmol).

These results suggest that methanogenic archaea actively produce CH_4 in the sediments of Lake Suwa,

©2019. Japan Geoscience Union. All Right Reserved.

however, its contribution in oxygenated surface water seems to be small. We are currently conducting a more sensitive analysis of F430 using LC-MS/MS [6] with the pre-treatment procedure [7]. The analysis may identify the CH_4 production process by methanogenic archaea associated with cyanobacteria in the surface water. Although this study did not cover other CH_4 production processes such as MPn and DMSP decomposition, our results may also be applicable to estimate the *in situ* contribution of these novel CH_4 source.

Refs.
[1] Bastviken *et al.*, *Global Biogeochem. Cycles*, 18, GB4009 (2004). [2] Tang *et al.*, *Environ. Sci. Technol. Lett.*, 3, 227-233 (2016). [3] Grossart *et al. PNAS*, 108, 19657-19661 (2011). [4] Berg *et al. World J. Microbiol. Biotechnol.*, 30, 539-545 (2014). [5] Park *et al., Environ. Toxicol. Water Qual.*, 13, 61-72 (1998). [6] Kaneko *et al.*, *Anal. Chem.*, 86, 3633-3638 (2014). [7] Kaneko *et al., Geochem. J.,* 50, 453-460 (2016).

Keywords: Microbial methane production, Methane paradox, Freshwater lake, Methanogenic archaea, Cyanobacterial bloom

©2019. Japan Geoscience Union. All Right Reserved.

Did life emerge in a deep-sea metal sulfide chimney? New insights from an archaeal genome and a nanoscale microbe-silicate assemblage

*Hinako Takamiya[1], Hiroki Mukai[2], Mariko Kouduka[1], Shingo Kato[4], Motoo Ito[3], Yohey Suzuki[1]

1. Earth and Planetary Science Graduate School of Science, The University of Tokyo , 2. National Institute of Advanced Industrial Science and Technology, 3. Kochi Institute for Core Sample Research JAMSTEC, 4. RIKEN

Deep-sea hydrothermal activities have continued for 3.8 billion years on Earth. After the formation of metal sulfide chimneys from high-temperature fluid, their low-temperature interactions with ambient seawater potentially provide the cold, stable habitat for microbial life. In such a challenging habitat with metal toxicity, 16S rRNA gene sequences formerly affiliated within Deep-Sea Hydrothermal Vent Euryarchaeota Subtype 6 (DHVE6) and recently reclassified as Pacearchaeota are dominantly detected by 16S rRNA gene sequence analysis. However, the distribution and metabolic activities of Pacearchaeota in metal sulfide chimneys are largely unknown. In this study, a metal sulfide chimney collected from a deep-sea hydrothermal field in South Mariana Trough was subjected to genome-resolved metagenomics analysis. It was revealed that a near-complete Pacearchaeota genome has carbon metabolism genes involved in glycolysis and pentose phosphate pathway linked to nucleotide salvage pathway with light-independent CO_2incorporating ribulose bisphosphate carboxylase/oxygenase (RubisCO). By comparative analysis of Pacearchaeota genomes from deep-sea metal sulfide deposits and terrestrial subsurface aquifers, the carbon metabolism was commonly found with genes annotated for Cu detoxification. Based on the NanoSIMS ion imaging analysis, we found an evidence of a dense microbial colonization inside the chimney where the surface of chalcopyrite ($CuFeS_2$) was overlayered with a silica-bearing material enriched in CN, S and P. Our results explain the geographically and physicochemically diverse distributions of Pacearchaeota indicated by 16S rRNA gene sequence analysis as well as the predominance of Pacearchaeota in the metal sulfide chimney where energy sources from photosynthesis and hydrothermal fluid are limited. The carbon metabolism operated by Pacearchaeota in one of candidate environments for the origin of life could be relevant to that operated by primitive life on early Earth.

Keywords: hydrothermal vent, metagenomic analysis, extremophile ecology, origin of life, microbial carbon metabolism, Rock life detection

©2019. Japan Geoscience Union. All Right Reserved.

X-ray computed nano-tomography for visualizing microbial cells and their surrounding environments

*Yuki Morono[1], Go-Ichiro Uramoto[2,1], Kentaro Uesugi[3], Nobuhisa Takeuchi[3], Masayuki Uesugi[3], Kengo Kubota[4], Tatsuhiko Hoshino[1], Fumio Inagaki[1]

1. Japan Agency for Marine-Earth Science and Technology, 2. Kochi University, 3. Japan Synchrotron Radiation Research Institute, 4. Tohoku University

Recent developments of the X-ray computed tomography (CT) reaches to the spatial resolution of down to few tens of nanometers scale, which is enough to visualize single microbial cells, together with those distributions as well as its surrounding environments. In this study, we tried to visualize microbial cells in the environmental samples by using nanometer-scale X-ray CT.
We used anaerobic granular sludge and subseafloor sediments for the test samples. The X-ray CT analyses were conducted at beamlines of BL20XU and BL47XU in synchrotron radiation facility of Spring-8. The soft samples were either freeze-dried or embedded in the epoxy resin for the analysis. Since the high-spatial resolution observation of the X-ray CT analysis requires a higher density of X-ray per field, the samples often deformed during the analysis, which results in the failure of the 3D reconstruction of the data. Optimization of the resin, its polymerization condition, together with the stain of the cells by osmium tetroxide to put heavy element onto the microbial cells, we could successfully visualize single microbial cells in the samples. Also, the observations of the sample at the pre- and post-edge energies of the element (such as Os) enabled specific signal enhancement of osmium-stained cells.
The investigations of subseafloor biosphere have often based on destructive measurements. Although these analyses revealed the large-scale distribution of microbes along the chemical gradients, no previous attempt explored the spatial distribution of microbial cells at their size range. The visualization of microbes with its surrounding environments will give basic but critical information to understand the microbial in-situ ecophysiology.

Keywords: X-ray Computed Tomography, Subseafloor biosphere

©2019. Japan Geoscience Union. All Right Reserved.

Carbon signatures in amino acids during deep-sea anoxic methanotrophy

*Yoshinori Takano[1]

1. Japan Agency for Marine-Earth Science and Technology (JAMSTEC)

Microorganisms play a central role in both methane production and consumption in the global carbon cycle. Oceanic methane from global deep-sea sediment is largely consumed through microbially mediated sulfate-coupled oxidation, resulting in 13C-depleted cell biomass of anaerobic methanotrophic archaea (ANME). The general ecological importance of subseafloor ANME has been well recognized in the last two decades. However, the crucial biochemical pathways for the overall anaerobic oxidation of methane (AOM) still remain enigmatic. In the present study, methanotrophic pathways were analyzed to trace 13C-depleted amino acid biosynthesis in two clades of ANME (ANME-1 and ANME-2) from the Black Sea. Compound-specific analysis of ANME-dominated microbial mats showed a significant 13C-depletion trend in association with increasing carbon numbers in protein-derived amino acid families within the pyruvate family in the order of alanine, valine, isoleucine and leucine down to -114‰. This result indicates a stepwise elongation of 13C-depleted carbon during amino acid biosynthesis. The overall results suggest that intracellular protein amino acids and the most 13C-depleted signature of leucine, which has a specific branched-chain structure, are potentially propagated as isoprenoid precursor molecules into archaeal biosynthesis, resulting in the extremely 13C- and 14C-depleted nature of ANME cells in the deep microbial oasis.

References:
Takano, Y., Chikaraishi, Y., Imachi, H., Miyairi, Y., Ogawa, N.O., Kaneko, M., Yokoyama, Y., Kruger, M. and Ohkouchi, N. (2018) Insight into anaerobic methanotrophy from 13C/12C- amino acids and 14C/12C-ANME cells in seafloor microbial ecology. Scientific Reports, 8:14070, doi: 10.1038/s41598-018-31004-5.

Supplementary Information:
https://www.nature.com/articles/s41598-018-31004-5#article-info

Acknowledgments:
We thank Dr. R. Seifert and Prof. Dr. W. Michaelis (Univ. Hamburg) and the shipboard party of the R/V Meteor cruise (M72/1: Geochemical cycling and microbial life at active gas seeps). We also thank Y. Saito, Y. Sasaki (JAMSTEC) for technical support and Dr. Y. Takaki (JAMSTEC) for the discussion of genomic sequence. The study was supported in part by the Japan Society for the Promotion of Science (JSPS) and the Submarine Resources Research Project in JAMSTEC.

Keywords: Carbon signatures in ANMEs, Organic molecules, Anoxic methanotrophy

©2019. Japan Geoscience Union. All Right Reserved.

[E] Poster | B (Biogeosciences)：B-CG Complex & General

Tue. May 28, 2019 5:15 PM - 6:30 PM JST | Tue. May 28, 2019 8:15 AM - 9:30 AM UTC | Poster Hall International Exhibition Hall8, Makuhari Messe_40

[B-CG06] Earth and Planetary Science Frontiers for Life and Global Environment

convener:Yoshinori Takano(Japan Agency for Marine-Earth Science and Technology (JAMSTEC)), Yohey Suzuki(Graduate School of Science, The University of Tokyo), Shingo Kato(RIKEN), Keisuke Fukushi(Institute of Nature & Environmental Technology, Kanazawa University)

Earth and planetary science is currently capable of sampling from four frontiers: space, polar regions, deep ocean and deep underground for the study of the origin and evolution of life. Next generation sequencing technology of nucleic acids and nanotechnology-driven innovation of solid characterizations are very powerful to expand our understanding of many fields of earth and planetary sciences. It is also important for us to be aware of global warming and climate change that dramatically affect biodiversity, biological activities and elemental cycling. The aim of this session is to cross the border of science sections to explore the frontiers of earth and planetary science.

[BCG06-P01] Dynamisms and characteristics of dissolved organic matter (DOM) in deep aquifer: A scope for deep biosphere

*Atsushi Urai[1,2], Yoshinori Takano[2], Naohiko Ohkouchi[2] (1.Department of Science and Technology, Graduate School of Medicine, Science and Technology, Shinshu University, 2.Department of Biogeochemistry, Japan Agency for Marine-Earth Science and Technology)

[BCG06-P02] Correlations of magnetosome-related genes in Nitrospirae genomes to magnetosome geometry and redox stratification in deep-sea environments

*Shinsaku Nakano[1], Shingo Kato[2], Mariko Kouduka[1], Toshitsugu Yamazaki[3], Yohey Suzuki[1] (1.Graduate School of Science, The University of Tokyo, 2.RIKEN, 3.Atmosphere and Ocean Research Institute, The University of Tokyo)

[BCG06-P03] Reconstruction of key ecological responses leading to the most recent dead zone formations in Japan Sea through ancient DNA metabarcodring

*Mariko Kouduka[1], Yohey Suzuki[1] (1.Department of Earth and Planetary Science, The University of Tokyo, 7-3-1 Hongo, Bunkyo-ku, Tokyo, Japan.)

[BCG06-P04] Search for microbial CH_4 production processes in lake sediments and surface water associated with cyanobacterial bloom

*Makoto Matsushita[1], Yoshinori Takano[1], Hiroyuki Imachi[1], Atsushi Urai[2], Ho-Dong Park[3], Hiroki Iwata[3], Naohiko Ohkouchi[1] (1.Japan Agency for Marine-Earth Science and Technology, 2.Department of Science and Technology, Graduate School of Medicine, Science and Technology, Shinshu University, 3.Department of Environmental Sciences, Faculty of Science, Shinshu University)

[BCG06-P05] Did life emerge in a deep-sea metal sulfide chimney? New insights from an archaeal genome and a nanoscale microbe-silicate assemblage

*Hinako Takamiya[1], Hiroki Mukai[2], Mariko Kouduka[1], Shingo Kato[4], Motoo Ito[3], Yohey Suzuki[1] (1.Earth and Planetary Science Graduate School of Science, The University of Tokyo , 2.National Institute of Advanced Industrial Science and Technology, 3.Kochi Institute for Core Sample Research JAMSTEC, 4.RIKEN)

[BCG06-P06] X-ray computed nano-tomography for visualizing microbial cells and their surrounding environments

*Yuki Morono[1], Go-Ichiro Uramoto[2,1], Kentaro Uesugi[3], Nobuhisa Takeuchi[3], Masayuki Uesugi[3], Kengo Kubota[4], Tatsuhiko Hoshino[1], Fumio Inagaki[1] (1.Japan Agency for Marine-Earth Science and Technology, 2.Kochi University, 3.Japan Synchrotron Radiation Research Institute, 4.Tohoku University)

[BCG06-P07] **Carbon signatures in amino acids during deep-sea anoxic methanotrophy**

*Yoshinori Takano[1] (1.Japan Agency for Marine-Earth Science and Technology (JAMSTEC))

Dynamisms and characteristics of dissolved organic matter (DOM) in deep aquifer: A scope for deep biosphere

*Atsushi Urai[1,2], Yoshinori Takano[2], Naohiko Ohkouchi[2]

1. Department of Science and Technology, Graduate School of Medicine, Science and Technology, Shinshu University, 2. Department of Biogeochemistry, Japan Agency for Marine-Earth Science and Technology

Dissolved organic matter (DOM) is generally derived from multiple sources and affected by complicated transformation and degradation reactions. In a general geochemical description of marine environments, high-molecular-weight DOM (HMW-DOM; >1 kDa) particularly represents a unique organic carbon pool, which is accompanied by considerable difference in the molecular and stable isotopic compositions from other organic components such as particulate organic matter (POM) and low-molecular-weight DOM (LMW-DOM; <1 kDa) (e.g., Benner et al., 1997).

To date, formation of DOM fraction and potential microbial interaction in deep aquifer have been particularly poorly understood on the context of prokaryotic ecology. We investigated the molecular composition of DOM fraction including LMW and HMW by an improved method (Urai et al., 2018). The filtered samples are tentatively defined by conventional size scales; macromolecular scale (100 mm >> 40 mm), POM (40 mm >> 0.6 mm), HMW-DOM(0.6 mm>>1kDa), and total-DOM (<0.6 mm). We also have a validation to distinguish the molecular signature between phototrophic primary producers (i.e., fossil molecules) and presently living benthic prokaryotes (i.e., modern molecules; cf. biological methanogenesis, Kaneko et al., 2014). We report a preliminary result of the feasibility study and discuss a perspective from the view of deep biosphere.

References:

Benner et al. Abundance, size distribution, and stable carbon and nitrogen isotopic compositions of marine organic matter isolated by tangential-flow ultrafiltration. Marine Chemistry 57, 243-263 (1997).

Kaneko et al. Quantitative analysis of coenzyme F430 in environmental samples: a new diagnostic tool for methanogenesis and anaerobic methane oxidation. Analytical Chemistry 86, 3633-3638 (2014).

Urai et al. Algal-derived 24-ethylcholesta-5, 22-dien-3β-ol (stigmasterol) is frequently found in high-molecular-weight dissolved organic matter (HMW-DOM) during summer in freshwater and brackish lakes. Geochemical Journal 52, e15-e20 (2018).

Keywords: HMW-DOM, sterol, carbon and hydrogen isotopic compositions, deep aquifer, methanogenesis

©2019. Japan Geoscience Union. All Right Reserved.

Correlations of magnetosome-related genes in Nitrospirae genomes to magnetosome geometry and redox stratification in deep-sea environments

*Shinsaku Nakano[1], Shingo Kato[2], Mariko Kouduka[1], Toshitsugu Yamazaki[3], Yohey Suzuki[1]

1. Graduate School of Science, The University of Tokyo, 2. RIKEN, 3. Atmosphere and Ocean Research Institute, The University of Tokyo

Biogenic magnetic particles are ubiquitously found in deep-sea sediments and important carriers of rock magnetism for reconstructing the Earth’ s past regarding sediment age and geomagnetic field. However, microorganisms responsible for the formation of magnetic particles are largely unknown in the deep-sea environment, because of the difficulty in sampling, cultivation, and magnetic separation of magnetotactic cells for single-cell genomics. In this study, deep-sea sediments from Japan Sea and a metal sulfide chimney from South Mariana Trough were subjected to magnetic separation and subsequent electron microscopic observations. Although teardrop-shaped magnetite (Fe_3O_4) particles without microbial cells and 16S rRNA gene sequences related to magnetotactic Nitrospirae species were previously obtained from Japan Sea sediments with a redox zonation enriched with dissolved Fe(II) (the iron boundary), no magnetotactic cells were observed after the magnetic separation. From the metal sulfide chimney, magnetotactic cells were observed with teardrop-shaped magnetite particles. Metagenomic analysis of the chimney sample revealed that contig sequences encoding genes involved in the formation of magnetosome, membrane-bound magnetic particles, were mostly affiliated within Nitrospirae based on sequence similarity. Previous studies have reported that magnetosome-related genes are clustered together as the magnetosome island (MAI) in known magnetotactic bacteria. However, those genes were scattered in a near-complete Nitrospirae genome reconstructed from the chimney sample. Although magnetotactic bacteria are generally considered to align magnetic particles into a chain for efficiently moving in a vertical redox zonation by orienting the cell along the geomagnetic filed, Nitrospirae-affiliated genes involved in chain formation were not found in the near-complete Nitrospirae genome from the chimney with a horizontal redox zonation. Comparative analysis of near-complete Nitrospirae genomes available from public databases revealed that the chain-related genes were found in the genomes from terrestrial deep aquifers and deep-sea sediments with a vertical redox zonation. As the Nitrospirae species associated with teardrop magnetite and the iron boundary in Japan Sea was closely related to Nitrospirae species with the chain-related genes, the presence of the chain-related genes appears to be correlated with a vertical redox zonation. In addition, our results suggest that the Nitrospirae species without MAI are responsible for the production of teardrop magnetite in deep-sea environment, and that teardrop magnetite is a paleoredox indicator especially for the iron boundary.

Keywords: magnetotactic bacteria, metal sulfide chimney, magnetofossil, remnant magnetization

©2019. Japan Geoscience Union. All Right Reserved.

Reconstruction of key ecological responses leading to the most recent dead zone formations in Japan Sea through ancient DNA metabarcodring

*Mariko Kouduka[1], Yohey Suzuki[1]

1. Department of Earth and Planetary Science, The University of Tokyo, 7-3-1 Hongo, Bunkyo-ku, Tokyo, Japan.

Semi-closed ocean basins are very sensitive to climate changes as recorded in frequent formations of sediments with clearly laminated layers, which was caused by the lack of O_2 available to benthic organisms. This is so-called “dead zone formation” and caused by water stagnation after channel closure and/or nutrient inflow through upwelling and channel opening. In contrast to the hydrologic causes, it remains poorly understood about organismal causes such as enhanced primary production and heterotrophic consumption of O_2. We investigated ancient eukaryotic DNA obtained from a thinly laminated layer deposited in the Japan Sea across the most recent global warming event after Younger Dryas (TL-1). Metabarcoding of 18S rRNA gene sequences clarified that across the transition from oxygenated to anoxic bottom water conditions, dominant protist populations shifted through five stages:

Stage1: Under oxygenated bottom conditions, the most dominant taxonomic group was Marine Stramenopiles Group 9 (MAST-9). MAST-9 encompasses diverse uncharacterized planktonic species, 18S rRNA gene sequences of which were detected from both anoxic and oxic water bodies in Pacific and Atlantic Oceans, Mediterranean Sea and South China Sea.

Stage 2: Before the onset of dead zone formation, the sharp decline of MAST-9 was accompanied with the expansion of marine diatom species of the genus Skeletonema, many members of which are known to be a cause of red tide around the world.

Stage 3: The dead zone formation was synchronized with the expansion of marine radiolarians of the order Chaunacanthida, the members of which are encrusted within $SrSO_4$.

Stage 4: Stages 2 was repeated, whereas the expansion of the Chaunacanthida radiolarians was not evident.

Stage 5: The uncharacterized MAST-9 that was dominant before the dead zone formation was gradually recovered towards oxygenated bottom conditions.

From these results, it is suspected that the expansion of Radiolaria species encrusted with $SrSO_4$ triggered dead zone formation by the accelerated downward transport of dead cells and subsequent heterotrophic consumption of O_2. From bioturbated sediment samples from a maximum depth of 31 mbsf with a depositional age of 100 ka, the Chaunacanthida sequences closely related to that from the laminated sediments have been previously detected.It is therefore suggested the record of the Chaunacanthida species can be reconstructed from sediments with great depth and age.

Keywords: global warming paleo-analogue, hypoxemia expansion, molecular paleoecologcail dynamics, biogeochemical cycling

©2019. Japan Geoscience Union. All Right Reserved.

©2019. Japan Geoscience Union. All Right Reserved.

Search for microbial CH_4 production processes in lake sediments and surface water associated with cyanobacterial bloom

*Makoto Matsushita[1], Yoshinori Takano[1], Hiroyuki Imachi[1], Atsushi Urai[2], Ho-Dong Park[3], Hiroki Iwata[3], Naohiko Ohkouchi[1]

1. Japan Agency for Marine-Earth Science and Technology, 2. Department of Science and Technology, Graduate School of Medicine, Science and Technology, Shinshu University, 3. Department of Environmental Sciences, Faculty of Science, Shinshu University

Methane (CH_4) is an important greenhouse gas and contributes substantial budget to global warming. Freshwater lakes are identified as one of the main CH_4 sources, as it is estimated that they contribute to 6-16% of natural CH_4 emissions [1]. The main part of CH_4 released from lakes is considered to be produced by methanogenic archaea in anoxic sediments as terminal step in the degradation of organic matter. The microbial CH_4 production in lake sediments has been mainly investigated by microbiological studies using culture-dependent methods and molecular analysis.

Microbial CH_4 production is still regarded by many as a process limited to anoxic environments. Nevertheless, over the past few decades, increasing evidence of CH_4 accumulation in oxygen-saturated lake and marine surface water has emerged [2]. To explain the enigmatic issues, it has been proposed that CH_4 production by methanogenic archaea takes place in anoxic microenvironments such as detritus and animals' gut. Alternatively, recent studies suggest that some bacteria break down methylphosphonate (MPn) or dimethylsulfoniopropionate (DMSP) and release CH_4 as a biogenic byproduct. These novel microbial CH_4 production processes may play a potential contribution to the total atmospheric carbon cycle.

Oxic CH_4 peaks have been found to be closely associated with phytoplankton dynamics across multiple lakes. Grossart *et al*. [3] found potentially methanogenic archaea associated with cyanobacteria such as *Aphanizomenon* and *Microcystis* in oxygenated surface water. Additionally, Berg *et al*. [4] showed that hydrogen produced during nitrogen fixation by cyanobacteria can be consumed by methanogenic archaea. These studies suggest the presence of a CH_4 production process by methanogenic archaea associated with cyanobacteria in lake surface water. However, it is unclear whether the CH_4 production is taking place in actual environments.

In this study, we investigated microbial CH_4 production in sediments and surface water of Lake Suwa in Nagano Prefecture, Japan, a typical hypertrophic shallow lake, using culture-independent methods. Especially, we focused on cyanobacterial bloom and tried to identify a CH_4 production process by methanogenic archaea associated with cyanobacteria. 16S rRNA gene analyses revealed the presence of methanogenic archaea closely related to the order *Methanobacteriales*, *Methanomicrobiales*, and *Methanosarcinales* in sediment core samples from 30 cm depth. On the other hand, 16S rRNA genes and *mcrA* genes of methanogenic archaea were not detected in bulk DNA from cyanobacterial bloom sample (mainly *Microcystis*)[5]. In order to estimate the potential for methanogenic archaea, we extracted Coenzyme F430, a biomarker for methanogenic archaea, from sediment and bloom samples and determined by using HPLC [6]. F430 was detected from sediment samples, but that from bloom sample was currently below detection limit (<1 pmol).

These results suggest that methanogenic archaea actively produce CH_4 in the sediments of Lake Suwa,

©2019. Japan Geoscience Union. All Right Reserved.

however, its contribution in oxygenated surface water seems to be small. We are currently conducting a more sensitive analysis of F430 using LC-MS/MS [6] with the pre-treatment procedure [7]. The analysis may identify the CH_4 production process by methanogenic archaea associated with cyanobacteria in the surface water. Although this study did not cover other CH_4 production processes such as MPn and DMSP decomposition, our results may also be applicable to estimate the *in situ* contribution of these novel CH_4 source.

Refs.
[1] Bastviken *et al.*, *Global Biogeochem. Cycles*, 18, GB4009 (2004). [2] Tang *et al.*, *Environ. Sci. Technol. Lett.*, 3, 227-233 (2016). [3] Grossart *et al. PNAS*, 108, 19657-19661 (2011). [4] Berg *et al. World J. Microbiol. Biotechnol.*, 30, 539-545 (2014). [5] Park *et al., Environ. Toxicol. Water Qual.*, 13, 61-72 (1998). [6] Kaneko *et al.*, *Anal. Chem.*, 86, 3633-3638 (2014). [7] Kaneko *et al., Geochem. J.,* 50, 453-460 (2016).

Keywords: Microbial methane production, Methane paradox, Freshwater lake, Methanogenic archaea, Cyanobacterial bloom

©2019. Japan Geoscience Union. All Right Reserved.

Did life emerge in a deep-sea metal sulfide chimney? New insights from an archaeal genome and a nanoscale microbe-silicate assemblage

*Hinako Takamiya[1], Hiroki Mukai[2], Mariko Kouduka[1], Shingo Kato[4], Motoo Ito[3], Yohey Suzuki[1]

1. Earth and Planetary Science Graduate School of Science, The University of Tokyo , 2. National Institute of Advanced Industrial Science and Technology, 3. Kochi Institute for Core Sample Research JAMSTEC, 4. RIKEN

Deep-sea hydrothermal activities have continued for 3.8 billion years on Earth. After the formation of metal sulfide chimneys from high-temperature fluid, their low-temperature interactions with ambient seawater potentially provide the cold, stable habitat for microbial life. In such a challenging habitat with metal toxicity, 16S rRNA gene sequences formerly affiliated within Deep-Sea Hydrothermal Vent Euryarchaeota Subtype 6 (DHVE6) and recently reclassified as Pacearchaeota are dominantly detected by 16S rRNA gene sequence analysis. However, the distribution and metabolic activities of Pacearchaeota in metal sulfide chimneys are largely unknown. In this study, a metal sulfide chimney collected from a deep-sea hydrothermal field in South Mariana Trough was subjected to genome-resolved metagenomics analysis. It was revealed that a near-complete Pacearchaeota genome has carbon metabolism genes involved in glycolysis and pentose phosphate pathway linked to nucleotide salvage pathway with light-independent CO_2incorporating ribulose bisphosphate carboxylase/oxygenase (RubisCO). By comparative analysis of Pacearchaeota genomes from deep-sea metal sulfide deposits and terrestrial subsurface aquifers, the carbon metabolism was commonly found with genes annotated for Cu detoxification. Based on the NanoSIMS ion imaging analysis, we found an evidence of a dense microbial colonization inside the chimney where the surface of chalcopyrite ($CuFeS_2$) was overlayered with a silica-bearing material enriched in CN, S and P. Our results explain the geographically and physicochemically diverse distributions of Pacearchaeota indicated by 16S rRNA gene sequence analysis as well as the predominance of Pacearchaeota in the metal sulfide chimney where energy sources from photosynthesis and hydrothermal fluid are limited. The carbon metabolism operated by Pacearchaeota in one of candidate environments for the origin of life could be relevant to that operated by primitive life on early Earth.

Keywords: hydrothermal vent, metagenomic analysis, extremophile ecology, origin of life, microbial carbon metabolism, Rock life detection

©2019. Japan Geoscience Union. All Right Reserved.

X-ray computed nano-tomography for visualizing microbial cells and their surrounding environments

*Yuki Morono[1], Go-Ichiro Uramoto[2,1], Kentaro Uesugi[3], Nobuhisa Takeuchi[3], Masayuki Uesugi[3], Kengo Kubota[4], Tatsuhiko Hoshino[1], Fumio Inagaki[1]

1. Japan Agency for Marine-Earth Science and Technology, 2. Kochi University, 3. Japan Synchrotron Radiation Research Institute, 4. Tohoku University

Recent developments of the X-ray computed tomography (CT) reaches to the spatial resolution of down to few tens of nanometers scale, which is enough to visualize single microbial cells, together with those distributions as well as its surrounding environments. In this study, we tried to visualize microbial cells in the environmental samples by using nanometer-scale X-ray CT.
We used anaerobic granular sludge and subseafloor sediments for the test samples. The X-ray CT analyses were conducted at beamlines of BL20XU and BL47XU in synchrotron radiation facility of Spring-8. The soft samples were either freeze-dried or embedded in the epoxy resin for the analysis. Since the high-spatial resolution observation of the X-ray CT analysis requires a higher density of X-ray per field, the samples often deformed during the analysis, which results in the failure of the 3D reconstruction of the data. Optimization of the resin, its polymerization condition, together with the stain of the cells by osmium tetroxide to put heavy element onto the microbial cells, we could successfully visualize single microbial cells in the samples. Also, the observations of the sample at the pre- and post-edge energies of the element (such as Os) enabled specific signal enhancement of osmium-stained cells.
The investigations of subseafloor biosphere have often based on destructive measurements. Although these analyses revealed the large-scale distribution of microbes along the chemical gradients, no previous attempt explored the spatial distribution of microbial cells at their size range. The visualization of microbes with its surrounding environments will give basic but critical information to understand the microbial in-situ ecophysiology.

Keywords: X-ray Computed Tomography, Subseafloor biosphere

©2019. Japan Geoscience Union. All Right Reserved.

Carbon signatures in amino acids during deep-sea anoxic methanotrophy

*Yoshinori Takano[1]

1. Japan Agency for Marine-Earth Science and Technology (JAMSTEC)

Microorganisms play a central role in both methane production and consumption in the global carbon cycle. Oceanic methane from global deep-sea sediment is largely consumed through microbially mediated sulfate-coupled oxidation, resulting in 13C-depleted cell biomass of anaerobic methanotrophic archaea (ANME). The general ecological importance of subseafloor ANME has been well recognized in the last two decades. However, the crucial biochemical pathways for the overall anaerobic oxidation of methane (AOM) still remain enigmatic. In the present study, methanotrophic pathways were analyzed to trace 13C-depleted amino acid biosynthesis in two clades of ANME (ANME-1 and ANME-2) from the Black Sea. Compound-specific analysis of ANME-dominated microbial mats showed a significant 13C-depletion trend in association with increasing carbon numbers in protein-derived amino acid families within the pyruvate family in the order of alanine, valine, isoleucine and leucine down to -114‰. This result indicates a stepwise elongation of 13C-depleted carbon during amino acid biosynthesis. The overall results suggest that intracellular protein amino acids and the most 13C-depleted signature of leucine, which has a specific branched-chain structure, are potentially propagated as isoprenoid precursor molecules into archaeal biosynthesis, resulting in the extremely 13C- and 14C-depleted nature of ANME cells in the deep microbial oasis.

References:
Takano, Y., Chikaraishi, Y., Imachi, H., Miyairi, Y., Ogawa, N.O., Kaneko, M., Yokoyama, Y., Kruger, M. and Ohkouchi, N. (2018) Insight into anaerobic methanotrophy from 13C/12C- amino acids and 14C/12C-ANME cells in seafloor microbial ecology. Scientific Reports, 8:14070, doi: 10.1038/s41598-018-31004-5.

Supplementary Information:
https://www.nature.com/articles/s41598-018-31004-5#article-info

Acknowledgments:
We thank Dr. R. Seifert and Prof. Dr. W. Michaelis (Univ. Hamburg) and the shipboard party of the R/V Meteor cruise (M72/1: Geochemical cycling and microbial life at active gas seeps). We also thank Y. Saito, Y. Sasaki (JAMSTEC) for technical support and Dr. Y. Takaki (JAMSTEC) for the discussion of genomic sequence. The study was supported in part by the Japan Society for the Promotion of Science (JSPS) and the Submarine Resources Research Project in JAMSTEC.

Keywords: Carbon signatures in ANMEs, Organic molecules, Anoxic methanotrophy

©2019. Japan Geoscience Union. All Right Reserved.

[E] Poster | M (Multidisciplinary and Interdisciplinary)：M-IS Intersection

Tue. May 28, 2019 10:45 AM - 12:15 PM JST | Tue. May 28, 2019 1:45 AM - 3:15 AM UTC | Poster Hall International Exhibition Hall8, Makuhari Messe_10

[M-IS05] New technologies to monitor thunderstorm and severe weather activities

convener:Mitsuteru Sato(Department of Cosmoscience, Hokkaido University), Yukihiro Takahashi(Department of Cosmosciences, Graduate School of Science, Hokkaido University), Hisayuki Kubota(Hokkaido University), Kozo Yamashita(Ashikaga University, Department of Engineering.)

In order to predict the intensity development of severe weather, lightning and thunderstorm are markers of severe weather, often accompanied by precipitation, hail and strong winds that can create significant natural hazards, especially in disaster-prone area. Lightning is also a strong indicator of convection, and it becomes a key parameter to predict the intensity development of tropical cyclones (typhoons and hurricanes). As the climate warms in the first decades of the 21st century, the intensity and frequency of thunderstorms is projected to increase. The need for detecting and monitoring the development of thunderstorms and lightning activities on global, local, and regional scales is therefore clear and urgent.
This session seeks topics presenting new technologies to monitor thunderstorm and severe weather activities. In addition, observational and theoretical contributions on thunderstorm microphysics and dynamics, convective systems and tropical storms are welcome. Present patterns and distributions of lightning and extreme weather events derived from the ground-based networks and satellites, as well as forecasts of future trends, are also of interest. Lightning detecting and monitoring system performance and validation, and early-warning schemes are requested, either in operational or planning phase. The session will also highlight regional and global lightning and atmospheric electricity networks and invite contributions on technological innovations in this field.

[MIS05-P01] Study on monitoring of thunderstorm activity based on multiple electrostatic measurement

*Kozo Yamashita[1], Kakeru Kanno[1], Mitsuteru Sato[2], Yukihiro Takahashi[2] (1.Ashikaga Univ., 2.Hokkaido Univ.)

[MIS05-P02] **Contribution of Rainfall and Lightning Activities to the Fair Weather Electric Field Evaluated by 3D GEC Model**

*Kittanapat Bandholnopparat[1], Mitsuteru Sato[2], Yukihiro Takahashi[2], Toru Adachi[3], Masashi Kamogawa[5], Yasuhiro Minamoto[5], Akira Kadokura[6], Tomoo Ushio[4] (1.Department of Cosmosciences, Hokkaido University, Sapporo, Japan, 2.Faculty of Science, Hokkaido University, Sapporo, Japan, 3.Meteorological Research Institute, Tsukuba, Japan, 4.Department of Aerospace Engineering, Tokyo Metropolitan University, Hino, Japan, 5.Tokyo Gakugei University, Tokyo, Japan, 6.National Institute of Polar Research, Tokyo, Japan)

[MIS05-P03] A method for locating lightning discharges using tweek atmospherics

*Masafumi Kanno[1], Hiroyo Ohya[2], Kazuo Shiokawa[3], Hiroyuki Nakata[2], Toshiaki Takano[2] (1.Graduate School of Science and Engineering, Chiba University, 2.Graduate School of Engineering, Chiba University, 3.Institute for Space-Earth Environmental Research, Nagoya University)

[MIS05-P04] Monitoring for lightning activities and thunder cloud development over the Tokyo metropolitan area during the 2018 summer

*Jun-Ichi Hamada[1], Jun Matsumoto[1], Kozo Yamashita[2], Masashi Kamogawa[3], Yukihiro Takahashi[4] (1.Faculty of Urban Environmental Sciences, Tokyo Metropolitan University, 2.Department of Engineering, Ashikaga University, 3.Department of Physics, Tokyo Gakugei University, 4.Department of Cosmosciences, Graduate School of Science, Hokkaido University)

Study on monitoring of thunderstorm activity based on multiple electrostatic measurement

*Kozo Yamashita[1], Kakeru Kanno[1], Mitsuteru Sato[2], Yukihiro Takahashi[2]

1. Ashikaga Univ., 2. Hokkaido Univ.

Quantitative evaluation of thundercloud activity is essential for early detection and short-term forecast of severe weather events such as heavy rainfall, lightning stroke, downburst, and so on. In previous researches, lightning observation based on electromagnetic measurement has been focused on as an effective tool for nowcast of thunderstorm activity. Advanced lightning sensors have high sensitivity and makes it possible to detect whole lightning activity. Lightning discharge occurs as a result of vertical atmospheric convection which causes thunderstorm. Preceding studies pointed that lighting occurrence could be an indicator of vertical deep convection in storm region and severe thunderstorm intensity.

Ground-based measurement of electrostatic field has been also considered as an efficient way to detect electrification in thundercloud and monitor development of severe storm. In preceding studies, multiple electrostatic measurement has been examined to estimate charge amount in cloud. One of the difficulties for those studies is to understand correlation between electrostatic field on ground and charges in horizontally extended thunderstorm. In this study, methodology for quantitative evaluation of charge amount in cloud is developed. We newly construct multipoint electrostatic sensor network in Tochigi, Japan. In this region, isolated thunderstorm whose horizontal scale is about 10 km occurs. By analyzing Isolated thunderstorm, we can simplify the correlation between ground-based electrostatic field and charge in cloud. In this presentation, initial result of electrostatic measurement with multiple sensors is summarized.

Keywords: thunderstorm, electrostatic field, sensor network

©2019. Japan Geoscience Union. All Right Reserved.

Contribution of Rainfall and Lightning Activities to the Fair Weather Electric Field Evaluated by 3D GEC Model

*Kittanapat Bandholnopparat[1], Mitsuteru Sato[2], Yukihiro Takahashi[2], Toru Adachi[3], Masashi Kamogawa[5], Yasuhiro Minamoto[5], Akira Kadokura[6], Tomoo Ushio[4]

1. Department of Cosmosciences, Hokkaido University, Sapporo, Japan, 2. Faculty of Science, Hokkaido University, Sapporo, Japan, 3. Meteorological Research Institute, Tsukuba, Japan, 4. Department of Aerospace Engineering, Tokyo Metropolitan University, Hino, Japan, 5. Tokyo Gakugei University, Tokyo, Japan, 6. National Institute of Polar Research, Tokyo, Japan

Lightning and precipitation are the main current sources in the global atmospheric electric circuit (GEC). The lightning and precipitation currents maintain the electrical potential gap of ~250 kV between the ionosphere and the Earth’ s surface. However, the contribution of lightning current to the GEC is not well understood due to the difficulty of estimating the global occurrence number of intracloud (IC) discharges. In addition, it is difficult to quantitatively estimate the contribution of the global precipitation current to the GEC due to the difficulty of identifying the rain volume and its global distribution. The purposes of this study are to estimate the global occurrence number of IC discharges and to investigate the contribution of lightning and precipitation currents to the GEC. Firstly, the global Z-value map obtained by the JEM-GLIMS spaced-based mission and the cloud-to-ground (CG) lightning data obtained by the WWLLN were combined to estimate the occurrence number of the global IC discharges with the time resolution of 5 minutes and with the spatial resolution of 0.2º×0.2º. Then, the estimated occurrence number of the global IC and CG discharges and the precipitation data provided by the global precipitation measurement (GPM) project were used as the input parameters in a 3-dimensional model of the GEC, which we have newly developed. In this model, the average column resistance including the influence of the cloud coverage was assumed. Using this model, we estimated the total GEC current and the fair weather electric field at the Syowa station on March 16, July 20, and September 29, 2014. It is found that the average lightning and precipitation currents in the GEC were ~70 A and ~ 670 A, respectively. It is also found that the average fair weather electric field at the Syowa station is ~ 70 V/m. The absolute value of the estimated fair weather electric field is almost consistent with the observational data. From these results, the role of lightning current in the GEC is quantitatively evaluated, and we found that the upward current from thunderclouds to the ionosphere generated by lightning discharges is only 9% while that induced by the precipitation is ~91%.

©2019. Japan Geoscience Union. All Right Reserved.

A method for locating lightning discharges using tweek atmospherics

*Masafumi Kanno[1], Hiroyo Ohya[2], Kazuo Shiokawa[3], Hiroyuki Nakata[2], Toshiaki Takano[2]

1. Graduate School of Science and Engineering, Chiba University, 2. Graduate School of Engineering, Chiba University, 3. Institute for Space-Earth Environmental Research, Nagoya University

Locating accuracy for lightning discharges of world-wide lightning location (WWLLN) is high to be less than 10 km [Rodger et al., 2005], although the accuracy of horizontal propagation distance for tweek atmospherics is low to be ~60 km [Santolik and Kolmasova, 2017]. Tweek atmospherics are very low frequency (VLF)/extremely low frequency (ELF) waves radiated from lightning discharges, and propagate between the Earth surface and the bottom of the ionosphere for a long distance (several thousand kilometers). In this study, we improve the estimation method for the tweek propagation distance, and compare between the lightning location estimated from tweek propagation distance by intersection method with those from the WWLLN data and cloud images derived by the MTSAT-2 satellite. We used two wideband VLF data observed at Kagoshima (31.48˚N, 130.72˚E) and Moshiri (44.37˚N, 142.27˚E), Japan, at 12:20-12:22 UT, on 23 August, 2013. The main point of the improvement was modification for the width of window on dynamic spectra drawn by maximum entropy method. The accuracy of the estimation became higher and the error for the propagation distance became the half of the original estimation, by using narrow window for the beginning, and wide window for the end of the tweek signals. We estimated the lightning location by both automatic and manual methods. In the manual method, the estimated location of lightning for the two-minute data was in good agreement with thick clouds observed by the MTSAT-2 satellite. However, in the automatic method, the location of the lightning was in disagreement with cloud images, because the accuracy of triggered times were not sufficient due to overlapping tweeks or noises such like short pulses just before the tweeks. In the presentation, we discuss the estimation method for the lightning location in detail.

©2019. Japan Geoscience Union. All Right Reserved.

Monitoring for lightning activities and thunder cloud development over the Tokyo metropolitan area during the 2018 summer

*Jun-Ichi Hamada[1], Jun Matsumoto[1], Kozo Yamashita[2], Masashi Kamogawa[3], Yukihiro Takahashi[4]

1. Faculty of Urban Environmental Sciences, Tokyo Metropolitan University, 2. Department of Engineering, Ashikaga University, 3. Department of Physics, Tokyo Gakugei University, 4. Department of Cosmosciences, Graduate School of Science, Hokkaido University

In order to monitor lightning activities and development of thunder cloud, we have established an observational network with electromagnetic and electrostatic field measurements over the Tokyo metropolitan area since 2016. In the summer season of 2018, we observed atmospheric electrostatic field with the electric field monitor (BOLTEK ELF-100) at Hachioji campus of Tokyo Metropolitan University and the surrounding area. Lightning activities were measured with ELV-VLF band radio observation system at a few sites in the area. We also used the worldwide lightning location network (WWLLN) data to indicate temporal and spatial variations of lightning and the climatological characteristics over the area. Lightning observations showed clear intra-seasonal variations of lightning activities over the area during the summer. Significant lightning events at around Hachioji were observed in 6th, 13th, and 27th of August as a synoptic frontal system located in the north from Kanto area. The electrostatic field measurement at Hachioji detected frequent lightning events and developing/approaching of thunder cloud near the site in these days. At the presentation, we will introduce more detail observation results on thunder cloud developments based on the XRAIN (eXtended RAdar Information Network) observation data.

This work was partly supported by Japan Science and Technology Agency (JST) and Japan International Cooperation Agency (JICA) under SATREPS.

Keywords: Lightning, Heavy rainfall

©2019. Japan Geoscience Union. All Right Reserved.

[E] Poster | M (Multidisciplinary and Interdisciplinary) : M-IS Intersection

Tue. May 28, 2019 5:15 PM - 6:30 PM JST | Tue. May 28, 2019 8:15 AM - 9:30 AM UTC | Poster Hall International Exhibition Hall8, Makuhari Messe_42

[M-IS05] New technologies to monitor thunderstorm and severe weather activities

convener:Mitsuteru Sato(Department of Cosmoscience, Hokkaido University), Yukihiro Takahashi(Department of Cosmosciences, Graduate School of Science, Hokkaido University), Hisayuki Kubota(Hokkaido University), Kozo Yamashita(Ashikaga University, Department of Engineering.)

In order to predict the intensity development of severe weather, lightning and thunderstorm are markers of severe weather, often accompanied by precipitation, hail and strong winds that can create significant natural hazards, especially in disaster-prone area. Lightning is also a strong indicator of convection, and it becomes a key parameter to predict the intensity development of tropical cyclones (typhoons and hurricanes). As the climate warms in the first decades of the 21st century, the intensity and frequency of thunderstorms is projected to increase. The need for detecting and monitoring the development of thunderstorms and lightning activities on global, local, and regional scales is therefore clear and urgent.
This session seeks topics presenting new technologies to monitor thunderstorm and severe weather activities. In addition, observational and theoretical contributions on thunderstorm microphysics and dynamics, convective systems and tropical storms are welcome. Present patterns and distributions of lightning and extreme weather events derived from the ground-based networks and satellites, as well as forecasts of future trends, are also of interest. Lightning detecting and monitoring system performance and validation, and early-warning schemes are requested, either in operational or planning phase. The session will also highlight regional and global lightning and atmospheric electricity networks and invite contributions on technological innovations in this field.

[MIS05-P01] Study on monitoring of thunderstorm activity based on multiple electrostatic measurement

*Kozo Yamashita[1], Kakeru Kanno[1], Mitsuteru Sato[2], Yukihiro Takahashi[2] (1.Ashikaga Univ., 2.Hokkaido Univ.)

[MIS05-P02] Contribution of Rainfall and Lightning Activities to the Fair Weather Electric Field Evaluated by 3D GEC Model

*Kittanapat Bandholnopparat[1], Mitsuteru Sato[2], Yukihiro Takahashi[2], Toru Adachi[3], Masashi Kamogawa[5], Yasuhiro Minamoto[5], Akira Kadokura[6], Tomoo Ushio[4] (1.Department of Cosmosciences, Hokkaido University, Sapporo, Japan, 2.Faculty of Science, Hokkaido University, Sapporo, Japan, 3.Meteorological Research Institute, Tsukuba, Japan, 4.Department of Aerospace Engineering, Tokyo Metropolitan University, Hino, Japan, 5.Tokyo Gakugei University, Tokyo, Japan, 6.National Institute of Polar Research, Tokyo, Japan)

[MIS05-P03] A method for locating lightning discharges using tweek atmospherics

*Masafumi Kanno[1], Hiroyo Ohya[2], Kazuo Shiokawa[3], Hiroyuki Nakata[2], Toshiaki Takano[2] (1.Graduate School of Science and Engineering, Chiba University, 2.Graduate School of Engineering, Chiba University, 3.Institute for Space-Earth Environmental Research, Nagoya University)

[MIS05-P04] Monitoring for lightning activities and thunder cloud development over the Tokyo metropolitan area during the 2018 summer

*Jun-Ichi Hamada[1], Jun Matsumoto[1], Kozo Yamashita[2], Masashi Kamogawa[3], Yukihiro Takahashi[4] (1.Faculty of Urban Environmental Sciences, Tokyo Metropolitan University, 2.Department of Engineering, Ashikaga University, 3.Department of Physics, Tokyo Gakugei University, 4.Department of Cosmosciences, Graduate School of Science, Hokkaido University)

Study on monitoring of thunderstorm activity based on multiple electrostatic measurement

*Kozo Yamashita[1], Kakeru Kanno[1], Mitsuteru Sato[2], Yukihiro Takahashi[2]

1. Ashikaga Univ., 2. Hokkaido Univ.

Quantitative evaluation of thundercloud activity is essential for early detection and short-term forecast of severe weather events such as heavy rainfall, lightning stroke, downburst, and so on. In previous researches, lightning observation based on electromagnetic measurement has been focused on as an effective tool for nowcast of thunderstorm activity. Advanced lightning sensors have high sensitivity and makes it possible to detect whole lightning activity. Lightning discharge occurs as a result of vertical atmospheric convection which causes thunderstorm. Preceding studies pointed that lighting occurrence could be an indicator of vertical deep convection in storm region and severe thunderstorm intensity.

Ground-based measurement of electrostatic field has been also considered as an efficient way to detect electrification in thundercloud and monitor development of severe storm. In preceding studies, multiple electrostatic measurement has been examined to estimate charge amount in cloud. One of the difficulties for those studies is to understand correlation between electrostatic field on ground and charges in horizontally extended thunderstorm. In this study, methodology for quantitative evaluation of charge amount in cloud is developed. We newly construct multipoint electrostatic sensor network in Tochigi, Japan. In this region, isolated thunderstorm whose horizontal scale is about 10 km occurs. By analyzing Isolated thunderstorm, we can simplify the correlation between ground-based electrostatic field and charge in cloud. In this presentation, initial result of electrostatic measurement with multiple sensors is summarized.

Keywords: thunderstorm, electrostatic field, sensor network

©2019. Japan Geoscience Union. All Right Reserved.

Contribution of Rainfall and Lightning Activities to the Fair Weather Electric Field Evaluated by 3D GEC Model

*Kittanapat Bandholnopparat[1], Mitsuteru Sato[2], Yukihiro Takahashi[2], Toru Adachi[3], Masashi Kamogawa[5], Yasuhiro Minamoto[5], Akira Kadokura[6], Tomoo Ushio[4]

1. Department of Cosmosciences, Hokkaido University, Sapporo, Japan, 2. Faculty of Science, Hokkaido University, Sapporo, Japan, 3. Meteorological Research Institute, Tsukuba, Japan, 4. Department of Aerospace Engineering, Tokyo Metropolitan University, Hino, Japan, 5. Tokyo Gakugei University, Tokyo, Japan, 6. National Institute of Polar Research, Tokyo, Japan

Lightning and precipitation are the main current sources in the global atmospheric electric circuit (GEC). The lightning and precipitation currents maintain the electrical potential gap of ~250 kV between the ionosphere and the Earth’ s surface. However, the contribution of lightning current to the GEC is not well understood due to the difficulty of estimating the global occurrence number of intracloud (IC) discharges. In addition, it is difficult to quantitatively estimate the contribution of the global precipitation current to the GEC due to the difficulty of identifying the rain volume and its global distribution. The purposes of this study are to estimate the global occurrence number of IC discharges and to investigate the contribution of lightning and precipitation currents to the GEC. Firstly, the global Z-value map obtained by the JEM-GLIMS spaced-based mission and the cloud-to-ground (CG) lightning data obtained by the WWLLN were combined to estimate the occurrence number of the global IC discharges with the time resolution of 5 minutes and with the spatial resolution of 0.2º×0.2º. Then, the estimated occurrence number of the global IC and CG discharges and the precipitation data provided by the global precipitation measurement (GPM) project were used as the input parameters in a 3-dimensional model of the GEC, which we have newly developed. In this model, the average column resistance including the influence of the cloud coverage was assumed. Using this model, we estimated the total GEC current and the fair weather electric field at the Syowa station on March 16, July 20, and September 29, 2014. It is found that the average lightning and precipitation currents in the GEC were ~70 A and ~ 670 A, respectively. It is also found that the average fair weather electric field at the Syowa station is ~ 70 V/m. The absolute value of the estimated fair weather electric field is almost consistent with the observational data. From these results, the role of lightning current in the GEC is quantitatively evaluated, and we found that the upward current from thunderclouds to the ionosphere generated by lightning discharges is only 9% while that induced by the precipitation is ~91%.

©2019. Japan Geoscience Union. All Right Reserved.

A method for locating lightning discharges using tweek atmospherics

*Masafumi Kanno[1], Hiroyo Ohya[2], Kazuo Shiokawa[3], Hiroyuki Nakata[2], Toshiaki Takano[2]

1. Graduate School of Science and Engineering, Chiba University, 2. Graduate School of Engineering, Chiba University, 3. Institute for Space-Earth Environmental Research, Nagoya University

Locating accuracy for lightning discharges of world-wide lightning location (WWLLN) is high to be less than 10 km [Rodger et al., 2005], although the accuracy of horizontal propagation distance for tweek atmospherics is low to be ~60 km [Santolik and Kolmasova, 2017]. Tweek atmospherics are very low frequency (VLF)/extremely low frequency (ELF) waves radiated from lightning discharges, and propagate between the Earth surface and the bottom of the ionosphere for a long distance (several thousand kilometers). In this study, we improve the estimation method for the tweek propagation distance, and compare between the lightning location estimated from tweek propagation distance by intersection method with those from the WWLLN data and cloud images derived by the MTSAT-2 satellite. We used two wideband VLF data observed at Kagoshima (31.48˚N, 130.72˚E) and Moshiri (44.37˚N, 142.27˚E), Japan, at 12:20-12:22 UT, on 23 August, 2013. The main point of the improvement was modification for the width of window on dynamic spectra drawn by maximum entropy method. The accuracy of the estimation became higher and the error for the propagation distance became the half of the original estimation, by using narrow window for the beginning, and wide window for the end of the tweek signals. We estimated the lightning location by both automatic and manual methods. In the manual method, the estimated location of lightning for the two-minute data was in good agreement with thick clouds observed by the MTSAT-2 satellite. However, in the automatic method, the location of the lightning was in disagreement with cloud images, because the accuracy of triggered times were not sufficient due to overlapping tweeks or noises such like short pulses just before the tweeks. In the presentation, we discuss the estimation method for the lightning location in detail.

©2019. Japan Geoscience Union. All Right Reserved.

Monitoring for lightning activities and thunder cloud development over the Tokyo metropolitan area during the 2018 summer

*Jun-Ichi Hamada[1], Jun Matsumoto[1], Kozo Yamashita[2], Masashi Kamogawa[3], Yukihiro Takahashi[4]

1. Faculty of Urban Environmental Sciences, Tokyo Metropolitan University, 2. Department of Engineering, Ashikaga University, 3. Department of Physics, Tokyo Gakugei University, 4. Department of Cosmosciences, Graduate School of Science, Hokkaido University

In order to monitor lightning activities and development of thunder cloud, we have established an observational network with electromagnetic and electrostatic field measurements over the Tokyo metropolitan area since 2016. In the summer season of 2018, we observed atmospheric electrostatic field with the electric field monitor (BOLTEK ELF-100) at Hachioji campus of Tokyo Metropolitan University and the surrounding area. Lightning activities were measured with ELV-VLF band radio observation system at a few sites in the area. We also used the worldwide lightning location network (WWLLN) data to indicate temporal and spatial variations of lightning and the climatological characteristics over the area. Lightning observations showed clear intra-seasonal variations of lightning activities over the area during the summer. Significant lightning events at around Hachioji were observed in 6th, 13th, and 27th of August as a synoptic frontal system located in the north from Kanto area. The electrostatic field measurement at Hachioji detected frequent lightning events and developing/approaching of thunder cloud near the site in these days. At the presentation, we will introduce more detail observation results on thunder cloud developments based on the XRAIN (eXtended RAdar Information Network) observation data.

This work was partly supported by Japan Science and Technology Agency (JST) and Japan International Cooperation Agency (JICA) under SATREPS.

Keywords: Lightning, Heavy rainfall

©2019. Japan Geoscience Union. All Right Reserved.

[E] Poster | M (Multidisciplinary and Interdisciplinary)：M-GI General Geosciences, Information Geosciences & Simulations

Tue. May 28, 2019 3:30 PM - 5:00 PM JST | Tue. May 28, 2019 6:30 AM - 8:00 AM UTC | Poster Hall International Exhibition Hall8, Makuhari Messe_28

[M-GI29] Near Surface Investigation and Modeling for Groundwater Resources Assessment and Conservation

convener:Jui-Pin Tsai(National Cheng Kung University, Taiwan), Hwa-Lung Yu(National Taiwan University), Ching-Chung Cheng(National Chiao Tung University Taiwan), Jing-Sen Cai(China University of Geosciences)

Groundwater resources serve as a vital source for regional water supply under the climate change condition. However, improper use of the available groundwater resources leads to serious environmental disasters such as land subsidence or seawater intrusion. Therefore, groundwater management is a key issue for groundwater resources conservation. Before applying any management practice, it is essential to accurately assess the groundwater system in multi-scales. In this session, we focus on the issues associated with the application of near-surface investigation and modeling on groundwater resources assessment. We welcome studies related to numerical modeling, spatiotemporal modeling, data fusion, and field investigation using hydrogeological approaches, geophysical approaches, geochemical approaches, and remote sensing. We also welcome the studies associated with groundwater contamination transport and remediation, geothermal energy exchange, groundwater microorganisms, hot spring, volcanic hydrology, and environmental disasters evaluation and prevention. We especially encourage the pilot groundwater management studies that solve multi-scale and interdisciplinary problems.

[MGI29-P01] Modelling of self-potential signals associated with groundwater flows

*ayaka ishikawa[1], Katsumi Hattori[1] (1.chiba university)

[MGI29-P02] Estimating the Hydraulic Conductivity and Heat Capacity of the Aquifer between the River and Well Site Using Joint Inversion Approach

*Jui-Pin Tsai[1], Chin-Tsai Hsiao[4], Liang-Cheng Chang[2], You-Cheng Chen[2], Chun-Hung Chen[3], Yun-Ta Cheng[3], Jen-Hung Yu[3] (1.National Cheng Kung University, Taiwan , 2.National Chiao Tung University, Taiwan , 3.Water Resources Planning Institute, Water Resources Agency, Taiwan, 4.Department of Information Management, Chung Chou University of Science and Technology)

[MGI29-P03] Evaluation on Soil Permeability Using Electrical Resistant Tomography

*CHIHPING KUO[1], BONIAN SHEN[1], CHIHWEI HUANG[1], YUCHIAO LEE[1], SHENXIANG HUANG[1], YENLIN CHEN[1] (1.Department and Institute of Civil Engineering and Environmental Informatics, Minghsin University of Science and Technology)

[MGI29-P04] The Potential Study of Open Loop System Geothermal Heat Pump in Gifu City, Japan

*Randa Permanda[1], Tomoyuki Ohtani[2] (1.Department of Civil and Environmental Engineering, Gifu University, 2.Department of Civil Engineering, Gifu University)

[MGI29-P05] Application of TL-CHERT Smart Characterization Method to Investigate a Groundwater Contaminated Site

*Tzu-Pin Wang[1,2,5], Yao-Tsung Chen[3], Tien-Hsing Tung[3], Chih-Hung Cheng[2], Jie Wang[4] (1.NCU TW, 2.Geophysical Technology and Engineering Co.,Ltd. R.O.C, 3.Apollo Technology Co.,Ltd. R.O.C., 4.Department of Civil Engineering, Chien Hsin University of Science and Technology, Taoyuan City, Taiwan, 5.Disaster Reduction Research Center, Chien Hsin University of Science and Technology, Taoyuan City, Taiwan)

[MGI29-P06] Data Assimilation in Hydraulic Conductivity Identification using Bayesian Statistical Method

*Shih-Yang Cheng[1], Kuo-Chin Hsu[1] (1.National Cheng Kung Univ.)

[MGI29-P07] Groundwater recharge estimation by using empirical orthogonal function method

Hua-Ting Zeng [1], *Hwa-Lung Yu[1] (1. National Taiwan University)

[MGI29-P08] The Application of Drought Early Warning Index for Regional Hydrological Circumstance Analysis

*Chih Chao Ho[1], Ta Wei Chen[2] (1.Construction and Disaster Prevention Research Center, Feng Chia Univ., 2.Taiwan Hsin-Chu Irrigation Association)

Modelling of self-potential signals associated with groundwater flows

*ayaka ishikawa[1], Katsumi Hattori[1]

1. chiba university

Landslides triggered by rainfall are one of the most dangerous natural disasters which give the loss of lives and properties. Although the importance of the short-term forecast of landslides is widely accepted, it is not achieved. In this research, we pay attention to electro-magnetic approach for monitoring ground water condition under the slope. That is, we understand the processes of the landslide and develop the system for forecast to detect precursory signal through the electromagnetic changes. In this study, we apply the self-potential approach, which is related on electro-kinetic effects or streaming potential. We have conducted several flume tests and sandbox experiments and the results showed the repeatability of the phenomena or correlation between self-potential and ground water condition. Therefore, we will report the model and numerical computation for the sandbox experiment on injection in this presentation.

SP signals measured in the sandbox during pumping experiment are considered to be due to the electro-kinetic effects. The total current density j is $j=sE-l\mathrm{d}h/\mathrm{d}x_i$, where s (in S m^{-1}) is the electrical conductivity, E (in Vm^{-1}) is the electric field, l (in A Pa^{-1} m^{-1}) is the current coupling coefficient, and h (in m) is the hydraulic head. The variation of SP signals of the sandbox gives quasi-instantaneous information on changes of the hydraulic head. Therefore we consider this problem with quasi-static limit condition i.e. div j = 0. It leads $\mathrm{div}(s\,\mathrm{grad}\,phi)=-\mathrm{div}(l\,\mathrm{grad}\,h)$.Where phi (in V) is electric potential. In addition, we assume that s and l are uniform through the sandbox because we assume saturated condition. Finally, the solved equation is $s\mathrm{d}^2phi/dx_i^2=-l\mathrm{d}^2h/dx_i^2$. We simulated distribution of hydraulic head during pumping test using finite element method. Then, we modeled the SP generation.

Consequently, the variation of SP modeled and observed are generally consistent with each other. Therefore, we found that groundwater flows control the occurrence of SP in the sandbox experiment. However, in the detail of time variation, modeled SP differ from those of observed partly. We consider that heterogeneity of soil or necessary of 3D modeling could cause these discordances. Details will be shown in our presentation.

Keywords: self-potential, ground water flow, modelling

©2019. Japan Geoscience Union. All Right Reserved.

Estimating the Hydraulic Conductivity and Heat Capacity of the Aquifer between the River and Well Site Using Joint Inversion Approach

*Jui-Pin Tsai[1], Chin-Tsai Hsiao[4], Liang-Cheng Chang[2], You-Cheng Chen[2], Chun-Hung Chen[3], Yun-Ta Cheng[3], Jen-Hung Yu[3]

1. National Cheng Kung University, Taiwan , 2. National Chiao Tung University, Taiwan , 3. Water Resources Planning Institute, Water Resources Agency, Taiwan, 4. Department of Information Management, Chung Chou University of Science and Technology

This study continued to measure the water temperature and pressure at the riverbed, agricultural waterway, and groundwater monitoring well from Oct. to Nov. 2018. These observations were then used to estimate the hydraulic conductivity (K) and flux between the river and the aquifer of the well site. The water pressure data reveal that the correlation coefficient between river and groundwater level reaches 0.9 and that between the agricultural waterway and groundwater level is almost 0. This reveals that the groundwater head variation mainly affected by the river stage of the nearby river. The temperature data show that the groundwater temperature is correlated to the temperature of the river water and is uncorrelated to the air temperature. Accordingly, the temperature and head data of the groundwater and river water were used to estimate K and heat capacity of the aquifer between the river and well site using a joint inversion approach. The results show that the estimated K and heat capacity are 67.53 m ⁄ day and 4485000 J ⁄ (m^3–℃), respectively.

Keywords: Hydraulic conductivity, Soil heat capactiy , Joint inversion, Temperature, Groundwater head , Interaction between groundwater and river water

©2019. Japan Geoscience Union. All Right Reserved.

Evaluation on Soil Permeability Using Electrical Resistant Tomography

*CHIHPING KUO[1], BONIAN SHEN[1], CHIHWEI HUANG[1], YUCHIAO LEE[1], SHENXIANG HUANG[1], YENLIN CHEN[1]

1. Department and Institute of Civil Engineering and Environmental Informatics, Minghsin University of Science and Technology

The permeability of soil is used to adapt field constant head permeability test or variable head permeability test. The former test is suitable for soil with higher permeability like sand and gravels; the later test is suitable for soil with lower permeability like silt and clays. Both tests need in-situ drilling holes. The required operating time is usually about couple of hours. A widely used geophysical method, Electrical Resistant Tomography (ERT), is adapted here to evaluate the soil permeability. Two types of soil with different permeability were performed, and the results were compared with the result of same samples using traditional permeability test. The result showed that they were very close. The operating time of ERT for one soil was only less than one hour. The idea of evaluating soil permeability using ERT is proposed in this study.

Keywords: Soil Permeability, Electrical Resistant Tomography

主機設定 (107.10.31 攝於明學樓噴水池旁)

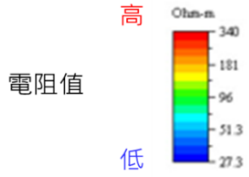

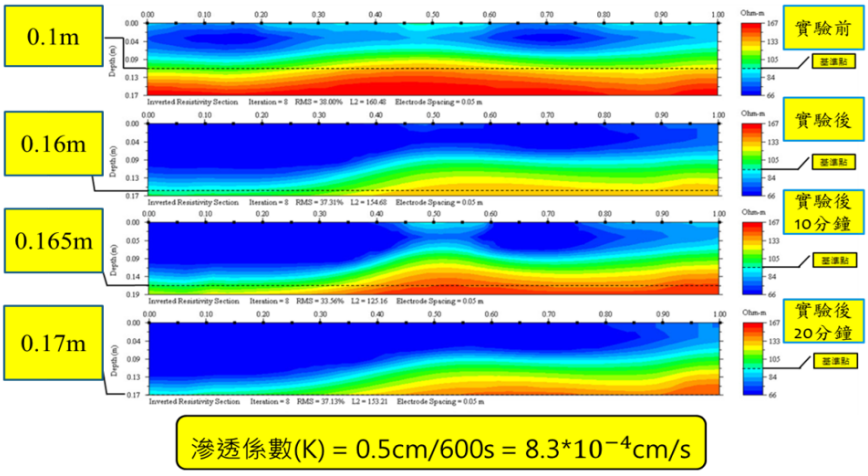

©2019. Japan Geoscience Union. All Right Reserved.

The Potential Study of Open Loop System Geothermal Heat Pump in Gifu City, Japan

*Randa Permanda[1], Tomoyuki Ohtani[2]

1. Department of Civil and Environmental Engineering, Gifu University, 2. Department of Civil Engineering, Gifu University

Geothermal heat pumps (GHPs) are considered to be one of the most energy efficient and environmentally friendly air-conditioning systems for temperate zones. In Japan, the expansive use of GHPs technology is finite, because of insufficient information on the advantages offered by the system and high installation cost. Therefore, the prediction of potential energy of GHPs at the first stage of installation is desirable. Open-loop system is one of GHPs types system which mostly depends on geological and hydrogeological parameter. This system interacts directly with ground and groundwater factor, because it uses groundwater as direct heat transfer medium through extraction and injection wells. Accordingly, groundwater flow with heat transfer is the most important factor that could affect the performance of open-loop GHPs system. Therefore groundwater flow system as well as distribution of subsurface temperature must be comprehended in detail. The aim of this study is to understand the distribution of groundwater flow and heat transport in study area from the simulation study using the program, FEFLOW. FEFLOW is a finite element code which can numerically simulate groundwater flow and heat transport. As the final result, the simulation model can be used to understand of open loop GHPs system in specified area.

The study area is an alluvial fan of the Nagara River, Gifu city, Japan. It is bounded by mountain ranges from north to northeast side and plain area remains. The Nagara River flows in the center of the plain. This alluvial fan is composed of sands and gravels and often intercalate thin fine sand and silt layers. Groundwater flow occur mainly in the Quaternary deposits, which are sand and gravel layers. Alluvial fans are recharge areas of groundwater and rapid groundwater flow are expected. The underground temperature in alluvial fan is affected by rapid groundwater flow recharged from a river. For assessment of potential energy of open loop GHPs, 3D model of groundwater flow with heat transport in Gifu city was developed using FEFLOW program. Model is constructed first by geological and hydrogeological data. The pre-existing geological columns and profile of study area were collected, which consisted of borehole and cross section data. Furthermore, pre-existing hydrogeological data which consist of groundwater table, underground temperature, and temperature of river water data in study area are also compiled to construct the simulation model. Boundary condition of groundwater flow system is defined by water table distribution. Bottom of the model is basement rock, treated as impermeable boundary and lateral sides are set as no flow boundaries. For boundary conditions of heat transport, top and bottom of the model are fixed by constant temperature boundaries, and lateral sides are as insulated. Based on constructed model, the simulation on groundwater flow with heat transport is performed. The effectiveness of heat transport and fluid flow are affected by material properties. Material properties were determined on the basis of formation types. Groundwater temperature were matched against observed temperatures, using the result of groundwater flow simulation. The observed underground temperatures in study area are fluctuated not only near surface but also in aquifer. This temperature change is resulted from lateral flow of the recharged groundwater. The calculated groundwater temperature will be adjusted until simulation result agreed with observed data from field. So that model can represent the groundwater flow system in alluvial fan of the Nagara River, Gifu city, Japan. For future plan, simulation model is used to investigate potential open loop GHPs system resulted from presence flowing groundwater in study area. This

©2019. Japan Geoscience Union. All Right Reserved.

simulation model is effective to predict the natural change of underground temperature, one main factor that affecting heat pumps efficiency.

Keywords: Geothermal heat pump, Groundwater flow, Heat transport, Open loop system, FEFLOW

©2019. Japan Geoscience Union. All Right Reserved.

Application of TL-CHERT Smart Characterization Method to Investigate a Groundwater Contaminated Site

*Tzu-Pin Wang[1,2,5], Yao-Tsung Chen[3], Tien-Hsing Tung[3], Chih-Hung Cheng[2], Jie Wang[4]

1. NCU TW, 2. Geophysical Technology and Engineering Co.,Ltd. R.O.C, 3. Apollo Technology Co.,Ltd. R.O.C., 4. Department of Civil Engineering, Chien Hsin University of Science and Technology, Taoyuan City, Taiwan, 5. Disaster Reduction Research Center, Chien Hsin University of Science and Technology, Taoyuan City, Taiwan

The Environmental Protection Administration in Taiwan effectively integrates Cross-Hole Electrical Resistivity Tomography (CHERT) into remediation planning in the anticipatory improvement project of sites with no polluter. During the reagent injection, Time-lapse Cross-Hole Electrical Resistivity (TL-CHERT) data are collected continuously. After data preprocessing and inversion algorithm, the ERT results are presented in images. 4D images could depict the main transmission range of reagent during the reagent injection, and further adjust or revise the second stage of remediation design. Therefore, CHERT could not only improve the remediation of complex groundwater contaminated sites, but also achieve the goal of precise surgical remediation. Besides, setting geophysical exploration equipment together with monitoring wells could greatly increase the use efficiency of the wells. Because groundwater contamination is usually a severe problem, a cross-professional cooperation is necessary. It is expected that this study will provide a worth case study for the survey application of similar contaminated site.

Keywords: CHERT, groundwater, pollution, resistiviy, geophysics, SCM

©2019. Japan Geoscience Union. All Right Reserved.

Data Assimilation in Hydraulic Conductivity Identification using Bayesian Statistical Method

*Shih-Yang Cheng[1], Kuo-Chin Hsu[1]

1. National Cheng Kung Univ.

Characterizing spatially heterogeneous hydraulic conductivity plays a crucial role in groundwater resources management and subsurface contaminant remediation. Since the direct measurements of hydraulic conductivity are sparse, the uncertainty is inherent in the estimated parameters. We propose decreasing the uncertainty by assimilating auxiliary data (electrical resistivity) with the direct data (hydraulic conductivity) using Bayesian statistical method. Different from classical geostatistical methods, both linear and nonlinear relations between the direct and auxiliary data can be considered in Bayesian statistical method. A synthetic example is designed to evaluate the method. Results show that the accuracy of hydraulic conductivity is improved through the Bayesian statistical method. Moreover, the effectiveness of auxiliary data in estimation error decrease is more significant when high correlation exists. However, the relation type has little influence on the accuracy. The estimation uncertainty quantified by variance is also compared. The uncertainty is inversely proportional to the amounts of auxiliary data and the correlation in both linear and nonlinear cases. The usefulness of auxiliary data in variance reduction is more obvious in linear cases. A systemic discussion of the sampling strategies of auxiliary data for improving hydraulic conductivity identification is also proposed.

Keywords: Data assimilation, Bayesian statistical method, Hydraulic conductivity, Nonlinear

©2019. Japan Geoscience Union. All Right Reserved.

Groundwater recharge estimation by using empirical orthogonal function method

Hua-Ting Zeng [1], *Hwa-Lung Yu[1]

1. National Taiwan University

Groundwater recharge estimation has been challenging due to the limited knowledge of the hyogeological heterogeneity. This issue is particularly important in the areas with high dependence on groundwater resources. This study proposed a data-driven approach along with a simple ODE model to estimate the groundwater recharge in our study area, Cho-shui river aquifer which is one of the most water-abundant aquifers in Taiwan; however, is suffered from the water overdraft. We analyzed the daily groundwater level observations during 2004-2010 from all wells across the entire study area. Based upon our proposed method, we identified two major recharge areas, i.e., proximal fan of the aquifer and Min-Chu basin at its upstream. The two areas obtained about 181.9 million and 78.8million tons of recharge water annually, resectively, in which about 131 million tons of water flowing from Min-Chu basin into Cho-shui aquifer annually. In summary, this study proposed a novel method for the groundwater recharge estimation.

Keywords: Groundwater, Recharge, EOF

©2019. Japan Geoscience Union. All Right Reserved.

The Application of Drought Early Warning Index for Regional Hydrological Circumstance Analysis

*Chih Chao Ho[1], Ta Wei Chen[2]

1. Construction and Disaster Prevention Research Center, Feng Chia Univ., 2. Taiwan Hsin-Chu Irrigation Association

Recently, rainfall become more unevenly both in special and temporal distribution caused by global climate change. The frequency of drought decrease from once every 17 years to once every 9 years. How to define warning signs of a drought and propose adaptive strategies is one of the key topic for water resources management. The drought can be divided into meteorological drought, agricultural drought and hydrological drought. The study tries to introduces difference Drought Early Warning Index, such as Standardized Precipitation Index, Standardized Groundwater Index, Normalized Difference Vegetation Index etc., to predict drought circumstance. The result can be a reference for development of drought early warning system.

Keywords: Standardized Precipitation Index, Standardized Groundwater Index, Normalized Difference Vegetation Index

©2019. Japan Geoscience Union. All Right Reserved.

[E] Poster | M (Multidisciplinary and Interdisciplinary)：M-GI General Geosciences, Information Geosciences & Simulations

Tue. May 28, 2019 5:15 PM - 6:30 PM JST | Tue. May 28, 2019 8:15 AM - 9:30 AM UTC | Poster Hall International Exhibition Hall8, Makuhari Messe_47

[M-GI29] Near Surface Investigation and Modeling for Groundwater Resources Assessment and Conservation

convener:Jui-Pin Tsai(National Cheng Kung University, Taiwan), Hwa-Lung Yu(National Taiwan University), Ching-Chung Cheng(National Chiao Tung University Taiwan), Jing-Sen Cai(China University of Geosciences)

Groundwater resources serve as a vital source for regional water supply under the climate change condition. However, improper use of the available groundwater resources leads to serious environmental disasters such as land subsidence or seawater intrusion. Therefore, groundwater management is a key issue for groundwater resources conservation. Before applying any management practice, it is essential to accurately assess the groundwater system in multi-scales. In this session, we focus on the issues associated with the application of near-surface investigation and modeling on groundwater resources assessment. We welcome studies related to numerical modeling, spatiotemporal modeling, data fusion, and field investigation using hydrogeological approaches, geophysical approaches, geochemical approaches, and remote sensing. We also welcome the studies associated with groundwater contamination transport and remediation, geothermal energy exchange, groundwater microorganisms, hot spring, volcanic hydrology, and environmental disasters evaluation and prevention. We especially encourage the pilot groundwater management studies that solve multi-scale and interdisciplinary problems.

[MGI29-P01] Modelling of self-potential signals associated with groundwater flows

*ayaka ishikawa[1], Katsumi Hattori[1] (1.chiba university)

[MGI29-P02] Estimating the Hydraulic Conductivity and Heat Capacity of the Aquifer between the River and Well Site Using Joint Inversion Approach

*Jui-Pin Tsai[1], Chin-Tsai Hsiao[4], Liang-Cheng Chang[2], You-Cheng Chen[2], Chun-Hung Chen[3], Yun-Ta Cheng[3], Jen-Hung Yu[3] (1.National Cheng Kung University, Taiwan , 2.National Chiao Tung University, Taiwan , 3.Water Resources Planning Institute, Water Resources Agency, Taiwan, 4.Department of Information Management, Chung Chou University of Science and Technology)

[MGI29-P03] Evaluation on Soil Permeability Using Electrical Resistant Tomography

*CHIHPING KUO[1], BONIAN SHEN[1], CHIHWEI HUANG[1], YUCHIAO LEE[1], SHENXIANG HUANG[1], YENLIN CHEN[1] (1.Department and Institute of Civil Engineering and Environmental Informatics, Minghsin University of Science and Technology)

[MGI29-P04] The Potential Study of Open Loop System Geothermal Heat Pump in Gifu City, Japan

*Randa Permanda[1], Tomoyuki Ohtani[2] (1.Department of Civil and Environmental Engineering, Gifu University, 2.Department of Civil Engineering, Gifu University)

[MGI29-P05] Application of TL-CHERT Smart Characterization Method to Investigate a Groundwater Contaminated Site

*Tzu-Pin Wang[1,2,5], Yao-Tsung Chen[3], Tien-Hsing Tung[3], Chih-Hung Cheng[2], Jie Wang[4] (1.NCU TW, 2.Geophysical Technology and Engineering Co.,Ltd. R.O.C, 3.Apollo Technology Co.,Ltd. R.O.C., 4.Department of Civil Engineering, Chien Hsin University of Science and Technology, Taoyuan City, Taiwan, 5.Disaster Reduction Research Center, Chien Hsin University of Science and Technology, Taoyuan City, Taiwan)

[MGI29-P06] Data Assimilation in Hydraulic Conductivity Identification using Bayesian Statistical Method

*Shih-Yang Cheng[1], Kuo-Chin Hsu[1] (1.National Cheng Kung Univ.)

[MGI29-P07] Groundwater recharge estimation by using empirical orthogonal function method

Hua-Ting Zeng [1], *Hwa-Lung Yu[1] (1. National Taiwan University)

[MGI29-P08] The Application of Drought Early Warning Index for Regional Hydrological Circumstance Analysis

*Chih Chao Ho[1], Ta Wei Chen[2] (1.Construction and Disaster Prevention Research Center, Feng Chia Univ., 2.Taiwan Hsin-Chu Irrigation Association)

Modelling of self-potential signals associated with groundwater flows

*ayaka ishikawa[1], Katsumi Hattori[1]

1. chiba university

Landslides triggered by rainfall are one of the most dangerous natural disasters which give the loss of lives and properties. Although the importance of the short-term forecast of landslides is widely accepted, it is not achieved. In this research, we pay attention to electro-magnetic approach for monitoring ground water condition under the slope. That is, we understand the processes of the landslide and develop the system for forecast to detect precursory signal through the electromagnetic changes. In this study, we apply the self-potential approach, which is related on electro-kinetic effects or streaming potential. We have conducted several flume tests and sandbox experiments and the results showed the repeatability of the phenomena or correlation between self-potential and ground water condition. Therefore, we will report the model and numerical computation for the sandbox experiment on injection in this presentation.

SP signals measured in the sandbox during pumping experiment are considered to be due to the electro-kinetic effects. The total current density j is $j=sE-l\mathrm{d}h/\mathrm{d}x_i$, where s (in S m^{-1}) is the electrical conductivity, E (in Vm^{-1}) is the electric field, l (in A Pa^{-1} m^{-1}) is the current coupling coefficient, and h (in m) is the hydraulic head. The variation of SP signals of the sandbox gives quasi-instantaneous information on changes of the hydraulic head. Therefore we consider this problem with quasi-static limit condition i.e. div j = 0. It leads $\mathrm{div}(s\,\mathrm{grad}\,phi)=-\mathrm{div}(l\,\mathrm{grad}\,h)$.Where phi (in V) is electric potential. In addition, we assume that s and l are uniform through the sandbox because we assume saturated condition. Finally, the solved equation is $s\mathrm{d}^2phi/dx_i^2=-l\mathrm{d}^2h/dx_i^2$. We simulated distribution of hydraulic head during pumping test using finite element method. Then, we modeled the SP generation.

Consequently, the variation of SP modeled and observed are generally consistent with each other. Therefore, we found that groundwater flows control the occurrence of SP in the sandbox experiment. However, in the detail of time variation, modeled SP differ from those of observed partly. We consider that heterogeneity of soil or necessary of 3D modeling could cause these discordances. Details will be shown in our presentation.

Keywords: self-potential, ground water flow, modelling

©2019. Japan Geoscience Union. All Right Reserved.

Estimating the Hydraulic Conductivity and Heat Capacity of the Aquifer between the River and Well Site Using Joint Inversion Approach

*Jui-Pin Tsai[1], Chin-Tsai Hsiao[4], Liang-Cheng Chang[2], You-Cheng Chen[2], Chun-Hung Chen[3], Yun-Ta Cheng[3], Jen-Hung Yu[3]

1. National Cheng Kung University, Taiwan , 2. National Chiao Tung University, Taiwan , 3. Water Resources Planning Institute, Water Resources Agency, Taiwan, 4. Department of Information Management, Chung Chou University of Science and Technology

This study continued to measure the water temperature and pressure at the riverbed, agricultural waterway, and groundwater monitoring well from Oct. to Nov. 2018. These observations were then used to estimate the hydraulic conductivity (K) and flux between the river and the aquifer of the well site. The water pressure data reveal that the correlation coefficient between river and groundwater level reaches 0.9 and that between the agricultural waterway and groundwater level is almost 0. This reveals that the groundwater head variation mainly affected by the river stage of the nearby river. The temperature data show that the groundwater temperature is correlated to the temperature of the river water and is uncorrelated to the air temperature. Accordingly, the temperature and head data of the groundwater and river water were used to estimate K and heat capacity of the aquifer between the river and well site using a joint inversion approach. The results show that the estimated K and heat capacity are 67.53 m ⁄ day and 4485000 J ⁄ (m^3–℃), respectively.

Keywords: Hydraulic conductivity, Soil heat capactiy , Joint inversion, Temperature, Groundwater head , Interaction between groundwater and river water

©2019. Japan Geoscience Union. All Right Reserved.

Evaluation on Soil Permeability Using Electrical Resistant Tomography

*CHIHPING KUO[1], BONIAN SHEN[1], CHIHWEI HUANG[1], YUCHIAO LEE[1], SHENXIANG HUANG[1], YENLIN CHEN[1]

1. Department and Institute of Civil Engineering and Environmental Informatics, Minghsin University of Science and Technology

The permeability of soil is used to adapt field constant head permeability test or variable head permeability test. The former test is suitable for soil with higher permeability like sand and gravels; the later test is suitable for soil with lower permeability like silt and clays. Both tests need in-situ drilling holes. The required operating time is usually about couple of hours. A widely used geophysical method, Electrical Resistant Tomography (ERT), is adapted here to evaluate the soil permeability. Two types of soil with different permeability were performed, and the results were compared with the result of same samples using traditional permeability test. The result showed that they were very close. The operating time of ERT for one soil was only less than one hour. The idea of evaluating soil permeability using ERT is proposed in this study.

Keywords: Soil Permeability, Electrical Resistant Tomography

主機設定 (107.10.31 攝於明學樓噴水池旁)

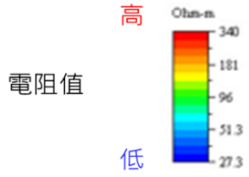

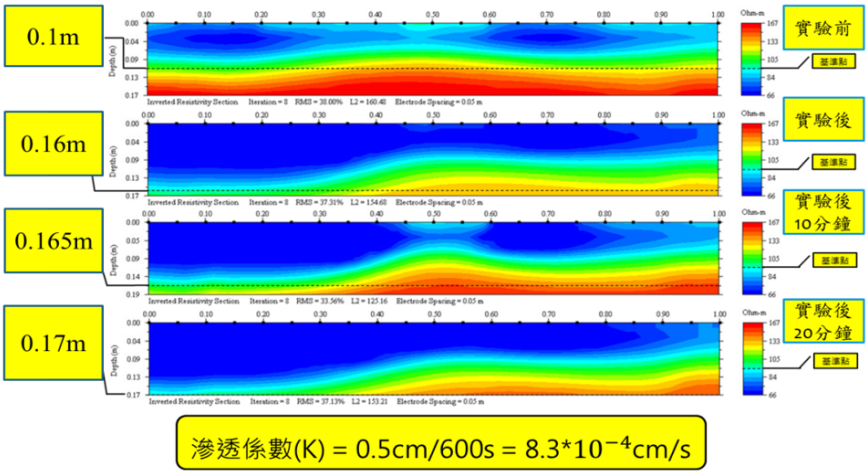

©2019. Japan Geoscience Union. All Right Reserved.

The Potential Study of Open Loop System Geothermal Heat Pump in Gifu City, Japan

*Randa Permanda[1], Tomoyuki Ohtani[2]

1. Department of Civil and Environmental Engineering, Gifu University, 2. Department of Civil Engineering, Gifu University

Geothermal heat pumps (GHPs) are considered to be one of the most energy efficient and environmentally friendly air-conditioning systems for temperate zones. In Japan, the expansive use of GHPs technology is finite, because of insufficient information on the advantages offered by the system and high installation cost. Therefore, the prediction of potential energy of GHPs at the first stage of installation is desirable. Open-loop system is one of GHPs types system which mostly depends on geological and hydrogeological parameter. This system interacts directly with ground and groundwater factor, because it uses groundwater as direct heat transfer medium through extraction and injection wells. Accordingly, groundwater flow with heat transfer is the most important factor that could affect the performance of open-loop GHPs system. Therefore groundwater flow system as well as distribution of subsurface temperature must be comprehended in detail. The aim of this study is to understand the distribution of groundwater flow and heat transport in study area from the simulation study using the program, FEFLOW. FEFLOW is a finite element code which can numerically simulate groundwater flow and heat transport. As the final result, the simulation model can be used to understand of open loop GHPs system in specified area.

The study area is an alluvial fan of the Nagara River, Gifu city, Japan. It is bounded by mountain ranges from north to northeast side and plain area remains. The Nagara River flows in the center of the plain. This alluvial fan is composed of sands and gravels and often intercalate thin fine sand and silt layers. Groundwater flow occur mainly in the Quaternary deposits, which are sand and gravel layers. Alluvial fans are recharge areas of groundwater and rapid groundwater flow are expected. The underground temperature in alluvial fan is affected by rapid groundwater flow recharged from a river. For assessment of potential energy of open loop GHPs, 3D model of groundwater flow with heat transport in Gifu city was developed using FEFLOW program. Model is constructed first by geological and hydrogeological data. The pre-existing geological columns and profile of study area were collected, which consisted of borehole and cross section data. Furthermore, pre-existing hydrogeological data which consist of groundwater table, underground temperature, and temperature of river water data in study area are also compiled to construct the simulation model. Boundary condition of groundwater flow system is defined by water table distribution. Bottom of the model is basement rock, treated as impermeable boundary and lateral sides are set as no flow boundaries. For boundary conditions of heat transport, top and bottom of the model are fixed by constant temperature boundaries, and lateral sides are as insulated. Based on constructed model, the simulation on groundwater flow with heat transport is performed. The effectiveness of heat transport and fluid flow are affected by material properties. Material properties were determined on the basis of formation types. Groundwater temperature were matched against observed temperatures, using the result of groundwater flow simulation. The observed underground temperatures in study area are fluctuated not only near surface but also in aquifer. This temperature change is resulted from lateral flow of the recharged groundwater. The calculated groundwater temperature will be adjusted until simulation result agreed with observed data from field. So that model can represent the groundwater flow system in alluvial fan of the Nagara River, Gifu city, Japan. For future plan, simulation model is used to investigate potential open loop GHPs system resulted from presence flowing groundwater in study area. This

©2019. Japan Geoscience Union. All Right Reserved.

simulation model is effective to predict the natural change of underground temperature, one main factor that affecting heat pumps efficiency.

Keywords: Geothermal heat pump, Groundwater flow, Heat transport, Open loop system, FEFLOW

©2019. Japan Geoscience Union. All Right Reserved.

Application of TL-CHERT Smart Characterization Method to Investigate a Groundwater Contaminated Site

*Tzu-Pin Wang[1,2,5], Yao-Tsung Chen[3], Tien-Hsing Tung[3], Chih-Hung Cheng[2], Jie Wang[4]

1. NCU TW, 2. Geophysical Technology and Engineering Co.,Ltd. R.O.C, 3. Apollo Technology Co.,Ltd. R.O.C., 4. Department of Civil Engineering, Chien Hsin University of Science and Technology, Taoyuan City, Taiwan, 5. Disaster Reduction Research Center, Chien Hsin University of Science and Technology, Taoyuan City, Taiwan

The Environmental Protection Administration in Taiwan effectively integrates Cross-Hole Electrical Resistivity Tomography (CHERT) into remediation planning in the anticipatory improvement project of sites with no polluter. During the reagent injection, Time-lapse Cross-Hole Electrical Resistivity (TL-CHERT) data are collected continuously. After data preprocessing and inversion algorithm, the ERT results are presented in images. 4D images could depict the main transmission range of reagent during the reagent injection, and further adjust or revise the second stage of remediation design. Therefore, CHERT could not only improve the remediation of complex groundwater contaminated sites, but also achieve the goal of precise surgical remediation. Besides, setting geophysical exploration equipment together with monitoring wells could greatly increase the use efficiency of the wells. Because groundwater contamination is usually a severe problem, a cross-professional cooperation is necessary. It is expected that this study will provide a worth case study for the survey application of similar contaminated site.

Keywords: CHERT, groundwater, pollution, resistiviy, geophysics, SCM

©2019. Japan Geoscience Union. All Right Reserved.

Data Assimilation in Hydraulic Conductivity Identification using Bayesian Statistical Method

*Shih-Yang Cheng[1], Kuo-Chin Hsu[1]

1. National Cheng Kung Univ.

Characterizing spatially heterogeneous hydraulic conductivity plays a crucial role in groundwater resources management and subsurface contaminant remediation. Since the direct measurements of hydraulic conductivity are sparse, the uncertainty is inherent in the estimated parameters. We propose decreasing the uncertainty by assimilating auxiliary data (electrical resistivity) with the direct data (hydraulic conductivity) using Bayesian statistical method. Different from classical geostatistical methods, both linear and nonlinear relations between the direct and auxiliary data can be considered in Bayesian statistical method. A synthetic example is designed to evaluate the method. Results show that the accuracy of hydraulic conductivity is improved through the Bayesian statistical method. Moreover, the effectiveness of auxiliary data in estimation error decrease is more significant when high correlation exists. However, the relation type has little influence on the accuracy. The estimation uncertainty quantified by variance is also compared. The uncertainty is inversely proportional to the amounts of auxiliary data and the correlation in both linear and nonlinear cases. The usefulness of auxiliary data in variance reduction is more obvious in linear cases. A systemic discussion of the sampling strategies of auxiliary data for improving hydraulic conductivity identification is also proposed.

Keywords: Data assimilation, Bayesian statistical method, Hydraulic conductivity, Nonlinear

©2019. Japan Geoscience Union. All Right Reserved.

Groundwater recharge estimation by using empirical orthogonal function method

Hua-Ting Zeng [1], *Hwa-Lung Yu[1]

1. National Taiwan University

Groundwater recharge estimation has been challenging due to the limited knowledge of the hyogeological heterogeneity. This issue is particularly important in the areas with high dependence on groundwater resources. This study proposed a data-driven approach along with a simple ODE model to estimate the groundwater recharge in our study area, Cho-shui river aquifer which is one of the most water-abundant aquifers in Taiwan; however, is suffered from the water overdraft. We analyzed the daily groundwater level observations during 2004-2010 from all wells across the entire study area. Based upon our proposed method, we identified two major recharge areas, i.e., proximal fan of the aquifer and Min-Chu basin at its upstream. The two areas obtained about 181.9 million and 78.8million tons of recharge water annually, resectively, in which about 131 million tons of water flowing from Min-Chu basin into Cho-shui aquifer annually. In summary, this study proposed a novel method for the groundwater recharge estimation.

Keywords: Groundwater, Recharge, EOF

©2019. Japan Geoscience Union. All Right Reserved.

The Application of Drought Early Warning Index for Regional Hydrological Circumstance Analysis

*Chih Chao Ho[1], Ta Wei Chen[2]

1. Construction and Disaster Prevention Research Center, Feng Chia Univ., 2. Taiwan Hsin-Chu Irrigation Association

Recently, rainfall become more unevenly both in special and temporal distribution caused by global climate change. The frequency of drought decrease from once every 17 years to once every 9 years. How to define warning signs of a drought and propose adaptive strategies is one of the key topic for water resources management. The drought can be divided into meteorological drought, agricultural drought and hydrological drought. The study tries to introduces difference Drought Early Warning Index, such as Standardized Precipitation Index, Standardized Groundwater Index, Normalized Difference Vegetation Index etc., to predict drought circumstance. The result can be a reference for development of drought early warning system.

Keywords: Standardized Precipitation Index, Standardized Groundwater Index, Normalized Difference Vegetation Index

©2019. Japan Geoscience Union. All Right Reserved.

[E] Poster | M (Multidisciplinary and Interdisciplinary) : M-ZZ Others

Tue. May 28, 2019 1:45 PM - 3:15 PM JST | Tue. May 28, 2019 4:45 AM - 6:15 AM UTC | Poster Hall International Exhibition Hall8, Makuhari Messe_10

[M-ZZ50] Governance for Trans-boundary Volcanic Disaster

convener:Mayumi Sakamoto(Graduate School of Disaster Resilience and Governance, University of Hyogo), Haruhisa Nakamichi(Sakurajima Volcano Research Center, Disaster Prevention Research Institute, Kyoto University), MASARU ARAKIDA(Asian Disaster Reduction Center)

Volcanic monitoring systems are developed and managed for the purpose to observe a specific volcanic activity in each country based on its own regulation. However, the experience of Icelandic volcano Eyjafjallajokull eruption in 2010 caused huge air traffic disturbances, and left large economic and social impact to international community. In order to reduce possible financial, environmental, health or social damages caused by trans-boundary volcanic disaster, it is important to develop international cooperative system to monitor and share the information of emission, dispersion or deposition of volcanic products. In this session, we discuss trans-boundary effect of volcanic eruption, and how to establish international collaborative mechanism from different research disciplines such as disaster management, volcanology, environmental politics or international law.

[MZZ50-P01] Governance for Trans-boundary Volcanic Disaster -a case of 2010 Eyjafjallajökull Eruption-

*Mayumi Sakamoto[1] (1.Graduate School of Disaster Resilience and Governance, University of Hyogo)

[MZZ50-P02] Regional Cooperation against Cross-border Disasters

*MASARU ARAKIDA[1] (1.Asian Disaster Reduction Center)

[MZZ50-P03] Issues of Japan's volcanic disaster prevention system as viewed from overseas alert systems

*Erika Ishimizu[1], Mayumi Sakamoto[1] (1.Graduate School of Disaster Resilience and Governance University of Hyogo)

Governance for Trans-boundary Volcanic Disaster -a case of 2010 Eyjafjallajökull Eruption-

*Mayumi Sakamoto[1]

1. Graduate School of Disaster Resilience and Governance, University of Hyogo

The volcanic eruption occurred in one country can trigger different effect in other country. The experience of 2010 Icelandic volcano Eyjafjallajökull eruption demonstrated the necessity of international governance for trans-boundary effect caused by eruption. In Iceland, national disaster response was effective to evacuate people from hazardous area and there were no humanitarian damages caused by eruption. However, the estimation of volcanic ash plumes and its dispersion caused huge international air traffic disruption or airport closure, and left large international economic and industrial impact. Followings are problems found through the 2010 eruption.
First, the necessity of international collaboration for observing atmospheric dispersion of volcanic ash. As for 2010 eruption, Icelandic Meteorological Agency (IMO) informed London Volcanic Ash Advisory Center (VAAC) which observes Iceland, about the plume height, ash content and other data. Based on the provided data, London VAAC predicted ash dispersion over Europe. However, there was no detailed discussion between IMO and London VAAC when and how often they communicate prior to eruption. It is important to update forecast using satellite imagery or observation of ashfalls in other countries.
Second, the necessity of immediate information sharing with both local and international medias. During the eruption, there was a huge need for information from international medias. A communication team, composed by professional communicator from various institutions gathered at the National Crisis Coordination and Command Center (NCCCC). Press conference were held and status reports were prepared and distributed. Such an international information sharing system should be discussed prior to disaster.
Disaster management systems are generally developed to respond hazard activity in each country based on its own regulation. However, 2010 experience showed there is no international agreement or regime to respond such a trans-boundary effect. Immediate crisis communication among hazard origin country, international institute and possibly affective country is required to reduce secondary effect, which shows importance or precautionary approaches for trans-boundary volcanic disaster.

Keywords: trans-boudary disaster, volcano, governance, Eyjafjallajökull

©2019. Japan Geoscience Union. All Right Reserved.

Regional Cooperation against Cross-border Disasters

*MASARU ARAKIDA[1]

1. Asian Disaster Reduction Center

Since affected area by disasters such as floods on international scale river, haize by forest fire, and volcanic ejectaare are recognized as no boundaries, there are many benefits of working together through regional cooperation. These include the sharing of best practices for handling major disasters, responding together on search and rescue efforts, and understanding and improving DRR through early warnings, the mutual exchange of information, joint education and training exercises, and joint assistance on disaster response.

Keywords: cross-border disaster, regional cooperation

©2019. Japan Geoscience Union. All Right Reserved.

Issues of Japan's volcanic disaster prevention system as viewed from overseas alert systems

*Erika Ishimizu[1], Mayumi Sakamoto[1]

1. Graduate School of Disaster Resilience and Governance University of Hyogo

Volcanic alert levels was introduced in Japan in 2007. Thereafter, the level was raised or lowered for several volcanoes, some volcanoes erupted and residents evacuated. Among them, the problem of exploiting volcanic alert levels for evacuation has become clear. In this research, by comparing Japan's warning system with overseas (the United States, Indonesia, New Zealand), we will examine the issues of Japanese volcanic disaster prevention system and future disaster prevention system.
In Japan, several institutions, such as universities and Japan Meteorological Agency (JMA), are conducting observations of volcanic activity. In the volcano where volcanic alert levels is introduced, JMA announces five levels of volcanic alert levels according to the activity of the volcano. Each municipality carries out basic disaster response such as issuance of evacuation information.
In the United States, the United States Geological Survey (USGS) will unite from the observation of a volcano to the announcement of an alarm (4 stages). Basic disaster response is handled by municipalities and counties. If requested, the state government responds, and if it is still difficult, FEMA is asked.
In Indonesia, the Center of Volcanology and Geological Hazard Mitigation (PVMBG) classify active volcanoes into three stages, ranging from A to C class, and is conducting observations. When the volcano becomes active, they present four levels of warning level. The basic disaster response such as the issuance of evacuation information is taken by the Regional Disaster Management Agency in Indonesia (BPBD), and the National Agency for Disaster Countermeasure (BNPB) supports this. If evacuation accompanied with level rise but the eruption does not occur, BNPB bears the expenses.
In New Zealand, GNS Science Corporation conducts observation of volcanic activity and issuance of alarm (6 stages).An evacuation information issuance is made by CDEM which is a collaboration body of local public bodies.
This presentation discusses issues of volcanic disaster prevention system in Japan and future disaster prevention system by comparing systems of each country.

Keywords: volcano, volcanic disaster prevention system , volcanic alert level

©2019. Japan Geoscience Union. All Right Reserved.

[E] Poster | M (Multidisciplinary and Interdisciplinary)：M-ZZ Others

Tue. May 28, 2019 5:15 PM - 6:30 PM JST | Tue. May 28, 2019 8:15 AM - 9:30 AM UTC | Poster Hall International Exhibition Hall8, Makuhari Messe_50

[M-ZZ50] Governance for Trans-boundary Volcanic Disaster

convener:Mayumi Sakamoto(Graduate School of Disaster Resilience and Governance, University of Hyogo), Haruhisa Nakamichi(Sakurajima Volcano Research Center, Disaster Prevention Research Institute, Kyoto University), MASARU ARAKIDA(Asian Disaster Reduction Center)

Volcanic monitoring systems are developed and managed for the purpose to observe a specific volcanic activity in each country based on its own regulation. However, the experience of Icelandic volcano Eyjafjallajokull eruption in 2010 caused huge air traffic disturbances, and left large economic and social impact to international community. In order to reduce possible financial, environmental, health or social damages caused by trans-boundary volcanic disaster, it is important to develop international cooperative system to monitor and share the information of emission, dispersion or deposition of volcanic products. In this session, we discuss trans-boundary effect of volcanic eruption, and how to establish international collaborative mechanism from different research disciplines such as disaster management, volcanology, environmental politics or international law.

[MZZ50-P01] Governance for Trans-boundary Volcanic Disaster -a case of 2010 Eyjafjallajökull Eruption-

*Mayumi Sakamoto[1] (1.Graduate School of Disaster Resilience and Governance, University of Hyogo)

[MZZ50-P02] Regional Cooperation against Cross-border Disasters

*MASARU ARAKIDA[1] (1.Asian Disaster Reduction Center)

[MZZ50-P03] Issues of Japan's volcanic disaster prevention system as viewed from overseas alert systems

*Erika Ishimizu[1], Mayumi Sakamoto[1] (1.Graduate School of Disaster Resilience and Governance University of Hyogo)

Governance for Trans-boundary Volcanic Disaster -a case of 2010 Eyjafjallajökull Eruption-

*Mayumi Sakamoto[1]

1. Graduate School of Disaster Resilience and Governance, University of Hyogo

The volcanic eruption occurred in one country can trigger different effect in other country. The experience of 2010 Icelandic volcano Eyjafjallajökull eruption demonstrated the necessity of international governance for trans-boundary effect caused by eruption. In Iceland, national disaster response was effective to evacuate people from hazardous area and there were no humanitarian damages caused by eruption. However, the estimation of volcanic ash plumes and its dispersion caused huge international air traffic disruption or airport closure, and left large international economic and industrial impact. Followings are problems found through the 2010 eruption.
First, the necessity of international collaboration for observing atmospheric dispersion of volcanic ash. As for 2010 eruption, Icelandic Meteorological Agency (IMO) informed London Volcanic Ash Advisory Center (VAAC) which observes Iceland, about the plume height, ash content and other data. Based on the provided data, London VAAC predicted ash dispersion over Europe. However, there was no detailed discussion between IMO and London VAAC when and how often they communicate prior to eruption. It is important to update forecast using satellite imagery or observation of ashfalls in other countries.
Second, the necessity of immediate information sharing with both local and international medias. During the eruption, there was a huge need for information from international medias. A communication team, composed by professional communicator from various institutions gathered at the National Crisis Coordination and Command Center (NCCCC). Press conference were held and status reports were prepared and distributed. Such an international information sharing system should be discussed prior to disaster.
Disaster management systems are generally developed to respond hazard activity in each country based on its own regulation. However, 2010 experience showed there is no international agreement or regime to respond such a trans-boundary effect. Immediate crisis communication among hazard origin country, international institute and possibly affective country is required to reduce secondary effect, which shows importance or precautionary approaches for trans-boundary volcanic disaster.

Keywords: trans-boudary disaster, volcano, governance, Eyjafjallajökull

©2019. Japan Geoscience Union. All Right Reserved.

Regional Cooperation against Cross-border Disasters

*MASARU ARAKIDA[1]

1. Asian Disaster Reduction Center

Since affected area by disasters such as floods on international scale river, haize by forest fire, and volcanic ejectaare are recognized as no boundaries, there are many benefits of working together through regional cooperation. These include the sharing of best practices for handling major disasters, responding together on search and rescue efforts, and understanding and improving DRR through early warnings, the mutual exchange of information, joint education and training exercises, and joint assistance on disaster response.

Keywords: cross-border disaster, regional cooperation

©2019. Japan Geoscience Union. All Right Reserved.

Issues of Japan's volcanic disaster prevention system as viewed from overseas alert systems

*Erika Ishimizu[1], Mayumi Sakamoto[1]

1. Graduate School of Disaster Resilience and Governance University of Hyogo

Volcanic alert levels was introduced in Japan in 2007. Thereafter, the level was raised or lowered for several volcanoes, some volcanoes erupted and residents evacuated. Among them, the problem of exploiting volcanic alert levels for evacuation has become clear. In this research, by comparing Japan's warning system with overseas (the United States, Indonesia, New Zealand), we will examine the issues of Japanese volcanic disaster prevention system and future disaster prevention system.
In Japan, several institutions, such as universities and Japan Meteorological Agency (JMA), are conducting observations of volcanic activity. In the volcano where volcanic alert levels is introduced, JMA announces five levels of volcanic alert levels according to the activity of the volcano. Each municipality carries out basic disaster response such as issuance of evacuation information.
In the United States, the United States Geological Survey (USGS) will unite from the observation of a volcano to the announcement of an alarm (4 stages). Basic disaster response is handled by municipalities and counties. If requested, the state government responds, and if it is still difficult, FEMA is asked.
In Indonesia, the Center of Volcanology and Geological Hazard Mitigation (PVMBG) classify active volcanoes into three stages, ranging from A to C class, and is conducting observations. When the volcano becomes active, they present four levels of warning level. The basic disaster response such as the issuance of evacuation information is taken by the Regional Disaster Management Agency in Indonesia (BPBD), and the National Agency for Disaster Countermeasure (BNPB) supports this. If evacuation accompanied with level rise but the eruption does not occur, BNPB bears the expenses.
In New Zealand, GNS Science Corporation conducts observation of volcanic activity and issuance of alarm (6 stages).An evacuation information issuance is made by CDEM which is a collaboration body of local public bodies.
This presentation discusses issues of volcanic disaster prevention system in Japan and future disaster prevention system by comparing systems of each country.

Keywords: volcano, volcanic disaster prevention system , volcanic alert level

©2019. Japan Geoscience Union. All Right Reserved.